# INVESTIGATION OF THE ROLE OF HAEMATOPOIETIC CELL KINASE IN NORMAL AND LEUKAEMIC HAEMATOPOIESIS

Thesis submitted to
**University College London**
for the Degree of
**Doctor of Philosophy**

by
**Emilie Aurelie Bureau**

Host laboratory:
Haematopoietic Stem Cell Laboratory
Cancer Research UK

Supervisor: Dr Dominique Bonnet





ProQuest LLC
789 East Eisenhower Parkway
P.O. Box 1346
Ann Arbor, MI 48106-1346

## Declaration of work presented

I, Emilie A. Bureau, confirm that the work presented in this thesis is my own. Where information has been derived from other sources, I confirm that this has been indicated in the thesis.

## Acknowledgements

I would like to thank my supervisor Dr Dominique Bonnet for giving me the opportunity to work in her laboratory on this very interesting project and for her critical help in managing the project and writing the PhD thesis.

I would like to acknowledge the members of my thesis committee, Pr Peter Parker, Dr Fiona Watt and Pr Nicholas Wright for their beneficial advice on conducting my PhD.

I would like to thank all the current and past members of the Haematopoietic Stem Cell Laboratory. They have been a great support all along the PhD and it has been a great pleasure to work in their company. Special thanks are going to Dr Bithiah Grace Jaganathan and Dr Fernando Anjos-Afonso for their valuable help, patience and support answering my numerous questions and to Christopher Ridler for correcting this manuscript.

I also would like to thank all my friends for their precious support all along the way; I would not have made it through without them.

Finally, I would like to thank my family for giving me the opportunity to be where I am now: at the end of a challenging experience, waiting for a new one to begin.

## Abstract

Acute myeloid leukaemia (AML) is characterised by an accumulation of immature blasts that fail to fully differentiate. Leukaemia is organised as a hierarchy, which is maintained by leukaemic stem cells (LSC). To identify molecular differences between normal haematopoietic stem cells (HSC) and LSC, we performed microarray analysis and found that haematopoietic cell kinase (HCK) is overexpressed in LSC. Thus, by knocking-down HCK in leukaemic cells or overexpressing it in stem cell enriched fractions, we should be able to evaluate its role in leukaemogenesis.

Since LSC are difficult to culture *in vitro*, we started to validate HCK silencing in leukaemic cell lines, Mono-mac-6 (MM6), U937 and Fujioka/P31, which highly express HCK. In all cell lines studied, no more than 50% silencing could be achieved, even when a short-hairpin anti-HCK was cloned into a lentiviral backbone to follow the long-term effect of HCK silencing. Decrease in kinase activity was confirmed using kinase assay and phospho-specific antibody recognising the activated HCK kinase. We show that HCK silencing does not affect the cell cycle, proliferation, differentiation or apoptosis of the cell lines. However, using methylcellulose assay, we observe a significant change in MM6 colony morphology caused by a decrease in their migration properties. Moreover, using phospho-flow cytometry, G-CSF and GM-CSF signal transduction towards STAT5 could be proven to occur via HCK in MM6, but not in Fujioka/P31 or U937 cells.

HSC enriched umbilical cord blood cells were also transduced with a lentivirus encoding p59HCK. Overexpression of p59HCK in these cells led to their enhanced erythroid differentiation at the expense of myeloid differentiation underlined by the activation of c-Raf, ERK and STAT5.

Overall, this study can be used as a preliminary set up for further investigation of the role of HCK in normal human stem cells and in primary AML samples *in vivo*.

## Individual contributions

Chapter III:

UCB and AML sample sorts: Dr Daniel Pearce and Dr Fernando Anjos-Afonso.

Affymetrix microarrays set up and analysis: Dr Kazem Zibara and Emilie Bureau.

Chapter VIII:

Myeloid and erythroid differentiation culture: Dr Bithiah Grace Jaganathan and Emilie Bureau.

## Abbreviation list

| Abbreviation | Meaning |
|---|---|
| 2% FCS: | PBS supplemented with 2% FCS |
| 293T-HEK cells: | Human embryonic kidney epithelial cells 293 expressing a large T antigen |
| ABL or v-abl: | Abelson murine leukemia viral oncogene homolog 1 |
| ACK1: | Activated Cdc42-associated kinase 1 |
| ADAM15: | A disintegrin and metallopeptidase domain 15 |
| ADD3: | Adducin 3 |
| AF1Q: | ALL1-fused gene from chromosome 1q |
| AF9: | ALL1 fused gene from chromosome 9 |
| AKAP13: | A kinase (PRKA) anchor protein 13 |
| Akt or AKT: | v-akt murine thymoma viral oncogene homolog |
| ALL: | Acute lymphoblastic leukaemia |
| AML: | Acute myeloid leukaemia |
| AML1: | Acute myeloid leukemia 1 |
| ANKRD12: | Ankyrin repeat domain 12 |
| ANP32E: | Acidic (leucine-rich) nuclear phosphoprotein 32 family, member E |
| APC: | Antigen-Presenting Cell |
| APC: | Allophycocyanin |
| APL: | Acute promylocytic leukaemia |
| ATP: | Adenosine tri-phosphate |
| ATRA: | All-trans retinoic acid |
| β2M: | Beta-2-microglobulin |
| BAALC: | Brain and acute leukemia, cytoplasmic |
| $Bclx_L$: | Basal cell lymphoma-extra large |
| BCR: | Break point cluster region |
| BCR: | B-Cell Receptor |
| BDT: | BigDye Terminator |
| BFU-E: | Blast forming unit-Erythrocyte |
| Blk: | B lymphoid tyrosine kinase |
| BM: | Bone marrow |
| bp: | Base pair |
| BRD2: | Bromodomain containing 2 |
| BSA: | Bovine serum albumin |
| C/EBPα or CEBPA: | CCAAT/enhancer binding protein (C/EBP) alpha |
| CAP350: | Centrosomal protein 350 |
| CBF: | Core binding factor |
| CBFA2: | Core binding factor A2 |
| CCND3: | CyclinD3 |

| | |
|---|---|
| CD: | Cluster of differentiation |
| Cdc42: | Cell division cycle 42 |
| cddB: | Cyclododecanone to dodecanoic diacid B |
| CDK: | Cyclin dependant kinase |
| cDNA: | Complementary desoxyribonucleic acid |
| CFAC assay: | Cobblestone area-forming cell assay |
| CFC assay: | Colony forming cell assay |
| CFU-E: | Colony forming unit-Erythroid |
| CFU-G: | Colony forming unit-Granulocyte |
| CFU-GEMM: | Colony forming unit-Granulocyte erythroid monocyte megakaryocyte |
| CFU-GM: | Colony forming unit-Granulocyte monocyte |
| CFU-M: | Colony forming unit-Monocyte |
| CHS1: | Chediak-Higashi syndrome 1 |
| CIP: | Calf Intestinal Phosphatase |
| c-KIT | v-kit Hardy-Zuckerman 4 feline sarcoma viral oncogene homolog |
| CLL: | Chronic lymphoid leukaemia |
| CLP: | Common lymphoid progenitor(s) |
| CML: | Chronic myeloid leukaemia |
| CMP: | Common myeloid progenitor(s) |
| CMV: | Cytomegalovirus |
| CNTF: | Ciliary neurotrophic factor |
| $CO_2$: | Carbon dioxyde |
| COS cells: | CV-1 (simian) in Origin carrying the SV40 genetic material (African Green Monkey Kidney Fibroblast Cell) |
| cPPT: | Central polypurine tract sequence |
| CR: | Complete remission |
| c-Raf or Raf: | v-raf-1 murine leukemia viral oncogene homolog 1 |
| CREB: | cAMP responsive element binding protein |
| CREBBP: | CREB binding protein |
| Crk: | v-crk sarcoma virus CT10 oncogene homolog |
| CRUK: | Cancer Research UK |
| Csk: | c-src tyrosine kinase |
| Ct: | Cycle threshold |
| CT: | Cardiotropin-1 |
| CTLA4: | Cytotoxic T-lymphocyte-associated protein 4 |
| CXCR4: | Chemokine (C-X-C motif) receptor 4 |
| DAP12: | DNAX-activating protein of molecular mass 12 kilodaltons |
| DAPI: | 4,6 -diamidino -2 -phenylindoiole |
| DC: | Dendritic Cell |
| DEK: | DEK oncogene (DNA binding) |
| DLEU2: | Deleted in lymphocytic leukaemia 2 (non-protein coding) |
| DMEM: | Dulbecco's Modified Eagle's Medium |
| DMSO: | Dimethyl-sulphoxide |

| | |
|---|---|
| DNA: | Deoxyribonucleic acid |
| dNTPs: | Desoxyribonucleotides |
| DOCK180: | Dedicator of cytokinesis 180 |
| DRD2: | Dopamine receptor D2 |
| DTT: | 1,4-Dithiothreitol |
| E2F: | E2F transcription factor |
| EDTA: | Ethylene diamine tetra-acetic acid |
| EGF: | Epidermal growth factor |
| eGFP: | Enhanced green fluorescent protein |
| EGTA: | Ethylene glycol tetraacetic acid |
| ELMO: | Engulfment and cell motility 1 |
| EmGFP | Emerald green fluorescent protein |
| ENL: | Eleven-nineteen leukaemia |
| EPO or Epo: | Erythropoietin |
| EpoR: | Erythropoietin receptor |
| ErbB: | Erythroblastic leukemia viral (v-erb-b) oncogene homolog |
| ERG: | v-ets erythroblastosis virus E26 oncogene homolog |
| ERK: | Extracellular signal-regulated kinases |
| ES cells: | Embryonic stem cells |
| ETO: | Eight twenty-one |
| EVI1: | Ecotropic viral integration site 1 |
| FAB: | French British American |
| FACS: | Fluorescence-activated cell sorting |
| FAK: | Focal adhesion kinase |
| FcR: | Receptors for the Fc portion of immunoglobulin antibodies |
| FCS: | Fetal calf serum |
| FGR or v-Fgr | Gardner-Rasheed feline sarcoma viral (v-fgr) oncogene homolog |
| FISH: | Fluorescent in situ hybridisation |
| FITC: | Fluorescein isothiocyanate |
| FLT3: | Fms-like tyrosine kinase 3 |
| Flt3-L: | Fms-like tyrosine kinase 3 ligand |
| FOXO3: | Forkhead box O3 |
| Fuji: | Fujioka/P31 |
| FYB: | FYN binding protein |
| Fyn: | FYN oncogene related to SRC, FGR, YES |
| FynB: | Fyn isoform highly expressed in the brain |
| FynT: | Fyn isoform mainly found in T-cells |
| g: | Grams |
| g: | Gravity |
| GAPDH: | Glyceraldehyde-3-phosphate dehydrogenase |
| GAS7: | Growth arrest specific 7 |
| GATA | Globin transcription factor 1 |
| G-CSF: | Granulocyte-colony stimulating factor |

| | |
|---|---|
| GFP: | Green fluorescent protein |
| GH: | Growth hormone |
| GH-R: | Growth hormone receptor |
| GLYA or Gly-A | Glycophorin A |
| GM-CSF: | Granulocyte-macrophage colony-stimulating factor |
| GMP: | Granulocyte/macrophage progenitor |
| Grb2: | Growth factor receptor-bound protein 2 |
| GTPase: | Guanine triphosphate hydrolase |
| GvH disease: | Graft versus host disease |
| GvL disease: | Graft versus leukaemia disease |
| H&E: | Haematoxilin and eosin |
| HCK or Hck: | Haematopoietic cell kinase |
| HDAC: | Histone deacetylase |
| HgCl2 | Mercuric chloride |
| HIST2H2AA: | Histone cluster 2, H2aa |
| HIV-1: | Human immunodeficiency virus 1 |
| HLF: | Hepatic leukemia factor |
| HOXA9: | Homeobox A9 |
| H-RAS: | v-Ha-ras Harvey rat sarcoma viral oncogene homolog |
| HSC: | Haematopoietic stem cell(s) |
| IFNAR: | Interferon alpha receptor |
| IFNγ: | Interferon gamma |
| IFNGR: | Interferon gamma receptor |
| IL: | Interleukin |
| IL6R: | Interleukin 6 receptor |
| IMDM: | Iscove's Modified Dulbecco's Medium |
| IRES: | Internal ribosome entry site |
| ITAM: | Immunoreceptor tyrosine-based activation motif |
| ITD: | Internal tandem duplication(s) |
| ITIM: | Immunoreceptor tyrosine-based inhibitory motif |
| JAK: | Janus kinases(s) |
| JNK: | c-Jun NH2-terminal kinase |
| JunB: | Jun B proto-oncogene |
| kbp: | Kilobase pair |
| kDa: | Kilodalton |
| KIR: | Killer inhibitory receptor(s) |
| K-RAS or KRAS: | v-Ki-ras2 Kirsten rat sarcoma viral oncogene homolog |
| KTLS: | c-Kit+/Thy1-/Lineage-/Sca1+ |
| KYNU: | Kynureninase (L-kynurenine hydrolase) |
| L: | Litre |
| LB: | Luria-Bertani |
| LCK or Lck: | Lymphocyte-specific protein tyrosine kinase |
| LEF1: | Lymphoid enhancer-binding factor 1 |

| | |
|---|---|
| Leu-cam: | Leucocyte cell adhesion molecules |
| LIF: | Leukaemia inhibitory factor |
| Lin: | Lineage |
| $Lin^-$: | Lineage negative |
| $Lin^+$: | Lineage positive |
| LPS: | Lipopolysaccharide |
| LSC: | Leukaemic Stem Cell(s) |
| LTC-IC: | Long term culture-initiating cell(s) |
| LYN or Lyn: | v-yes-1 Yamaguchi sarcoma viral related oncogene homolog |
| M: | Molar |
| Mac1: | Macrophage 1 |
| MAC30: | Meningioma-associated protein |
| MAPK: | Mitogen-activated protein kinase |
| MCS: | Multiple cloning site |
| M-CSF: | Macrophage colony-stimulating factor |
| MDS: | Myelodysplastic syndrome |
| MDS1: | Myelodysplastic syndrome 1 |
| MEF: | Murine embryonic fibroblast |
| MEK: | MAP kinase or ERK kinase |
| MEM: | Minimal Essential Medium (Eagle's) |
| MFI: | Mean fluorescence intensity |
| $Mg^{2+}$: | Magnesium ion |
| µg: | Micrograms |
| µL: | Microlitre |
| miRNA: | Micro RNA |
| MKL1: | Megakaryoblastic leukemia (translocation) 1 |
| mL: | Mililitre |
| MLL: | Mixed lineage leukaemia |
| MM6: | Mono-mac-6 |
| $Mn^{2+}$: | Manganese ion |
| MNC: | Mononuclear cell(s) |
| MOI: | Multiplicity of infection |
| Mono: | Mono-mac-6 |
| MOPS: | 3-(N-morpholino)propanesulphonic acid |
| MPD: | Myeloproliferative disease |
| MRC: | Medical Research Council |
| MRD: | Minimal residual disease |
| mTOR: | Mammalian target of rapamycin |
| MYH11: | Myosin heavy chain 11 |
| MYST3: | MYST histone acetyltransferase (monocytic leukemia) 3 |
| NaF: | Sodium Fluoride |
| NBS1: | Nijmegen breakage syndrome 1 (nibrin) |
| NEB: | New England Biolabs |

| | |
|---|---|
| Nef protein: | Negative factor protein |
| NF1: | Neurofibromin 1 |
| NFKBIA: | Nuclear factor of kappa light polypeptide gene enhancer in B-cells inhibitor alpha |
| NK cells: | Natural killer cell(s) |
| NK: | Normal karyotype |
| NKTR: | Natural killer-tumor recognition sequence |
| NOD: | Non-obese diabetic |
| NOG: | NOD/SCID/IL-2Rgamma |
| NPM1: | Nucleophosmin 1 |
| N-RAS or NRAS: | Neuroblastoma RAS viral (v-ras) oncogene homolog |
| n-Src: | Neuronal Src |
| NT: | Non-transfectd |
| NT: | Non-transduced |
| NTC: | Non-template control |
| NUP214: | Nucleoporin 214kDa |
| NUP98: | Nucleoporin 98kDa |
| NUSAP1: | Nucleolar and spindle associated protein 1 |
| OptiMEM: | Reduced serum medium modification of MEM |
| ORF: | Open reading frame |
| OSM: | Oncostatin M |
| ovHCK: | Overexpressing HCK |
| p120Cbl: | Cas-Br-M (murine) ecotropic retroviral transforming sequence |
| PAGE: | Polyacrylamide gel electrophoresis |
| PAK: | p21 protein (Cdc42/Rac)-activated kinase |
| PB: | Peripheral blood |
| PBS: | Phosphate buffered saline |
| PCNA: | Proliferating cell nuclear antigen |
| PCR: | Polymerase chain reaction |
| PD1: | Programmed cell death 1 |
| PDGF: | Platelet derived growth factor |
| PDGFR: | Platelet derived growth factor receptor |
| PE: | Phycoerythrin |
| PE-Cy7: | Phycoerythrin-cyanine dye Cy7 |
| PEI: | Polyethylenimine |
| PFA | Paraformaldehyde |
| PGK: | Phosphoglycerate kinase |
| pH1: | Promoter H1 |
| PI3K: | Phosphoinositide-3-kinase |
| PIAS: | Protein inhibitors of activated STATs |
| Pim1: | Proviral integration site 1 |
| PIR-B: | Paired-immunoglobulin like receptor-B |
| PML: | Promyelocytic leukaemia |

| | |
|---|---|
| PMN: | Polymorphonuclear leukocyte |
| PPII: | Polyproline type II |
| PRC1: | Protein regulator of cytokinesis 1 |
| PRL: | Prolactin |
| PTD: | Partial tandem duplication |
| PTEN: | Phosphatase and tensin homolog |
| PTK: | Protein tyrosine kinase |
| PTP1B: | Protein tyrosine phosphatase, non-receptor type 1 |
| PTPeC: | Cytosolic isoform of protein tyrosine phosphatase, receptor type, E |
| PTPN11: | Protein tyrosine phosphatase, non-receptor type 11 |
| PTP-PEST: | Protein Tyrosine Phosphatase PEST |
| PU.1: | PU box1 |
| qPCR: | Quantitative PCR |
| qRT-PCR: | Quantitative real-time PCR |
| -R: | Receptor |
| RA: | Retinoic acid |
| RA70: | src kinase associated phosphoprotein 2 |
| Rac: | ras-related C3 botulinum toxin substrate 1 (rho family, small GTP binding protein Rac1) |
| RACGAP1: | Rac GTPase activating protein 1 |
| Rap1: | Ras associated protein 1 |
| RARA or RARα: | Retinoic acid receptor alpha |
| Ras GTPase: | Ras guanine triphosphate hydrolase |
| RAS or Ras: | Rat sarcoma 2 viral oncogene homolog |
| RasGAP: | Ras GTPase activating protein |
| Rb: | Retinoblastoma |
| RBM15: | NA binding motif protein 15 |
| Rho: | Ras homolog gene family |
| RIPA: | Radio Immuno Precipitation Assay |
| RNA: | Ribonucleic acid |
| RNAi | RNA interference |
| rpm: | Revolutions per minute |
| RPMI: | Roswell Park Memorial Institute |
| RPN1: | Ribophorin I |
| RRM2: | Ribonucleotide reductase M2 polypeptide |
| RSV: | Rous sarcoma virus |
| RT: | Real time |
| RT: | Room temparature |
| RUNX1: | Runt related transcription factor 1 |
| RUNX1T1: | Runt-related transcription factor 1; translocated to, 1 (cyclin D-related) |
| SAP: | Shrimp alkaline phosphatase |
| Sca1: | Stem Cell Antigen-1 |
| SCF: | Stem Cell Factor |

| | |
|---|---|
| SCID: | Severe combined immunodeficiency |
| SCL: | Stem cell leukaemia |
| SDF1: | Stromal cell-derived factor-1 |
| SDS: | Sodium dodecylsulphate |
| Sffv: | Spleen focus forming virus |
| SFK: | Src family kinase(s) |
| sh: | Short hairpin |
| SH1: | Src homology 1 |
| SH2: | Src homology 2 |
| SH3: | Src homology 3 |
| SH4: | Src homology 4 |
| Shc: | SHC (Src homology 2 domain containing) transforming protein |
| shHCK: | Short hairpin ahti-HCK |
| SHIP1: | SH2-domain-containing inositol phosphatase 1 |
| Shp1 or SHP1: | SH2-domain-containing phosphatase 1 |
| Shp2 or SHP1: | SH2-domain-containing phosphatase 2 |
| SHPS-1: | Src homology 2 domain-containing phosphatase substrate-1 |
| SH-PTP1: | Src homology domain-containing protein tyrosine phosphatase |
| shRNA: | Short hairpin RNA |
| si: | siRNA |
| SIN: | Self-inactivating |
| siRNA: | Small interfereing RNA |
| SIRPa: | Signal-regulatory protein alpha |
| SLCO3A1: | Solute carrier organic anion transporter family, member 3A1 |
| SL-IC: | SCID leukaemia initiating cell(s) |
| SLP-76: | SH2 domain containing leukocyte protein of 76kDa |
| SOC: | Super Optimal Broth + catobolite repression |
| SOCS: | Supressors of cytokine signalling |
| SRC or c-Src: | v-src sarcoma (Schmidt-Ruppin A-2) viral oncogene homolog |
| SRC: | SCID repopulating cell(s) |
| STAT: | Signal transducer and activator of transcription |
| SUMO: | Small ubiquitin-like modifier |
| Syk: | Spleen tyrosine kinase |
| TAE: | Tris-acetate-EDTA |
| TBC1D16: | TBC1 domain family, member 16 |
| TBE: | Tris-borate-EDTA |
| TBS: | Tris buffered saline |
| TBST: | Tris buffered saline supplemented with 0.1% Tween |
| TCR: | T-Cell Receptor |
| TE: | Tris-EDTA |
| TEL(ETV6): | TEL oncogene (ETS variant 6) |
| Thy1: | Thy-1 cell surface antigen |
| TKD: | Tyrosine kinase domain |

| | |
|---|---|
| TNFβ: | Tumor necrosis factor-beta |
| TOP1: | Topoisomerase (DNA) I |
| TP53: | Tumor protein 53 |
| TPA: | 12-O-Tetradecanoyl-phorbol-13-acetate |
| TPO: | Thrombopoietin |
| TPR: | Translocated promoter region |
| TREM-2: | Triggering receptor expressed on myeloid cells 2 |
| TRIB1: | Tribbles homologue 2 |
| TRIM38: | Tripartite motif-containing 38 |
| TXNDC7: | Thioredoxin domain containing 7 (protein disulphideisomerase) |
| TYK2: | Tyrosine kinase 2 |
| TYROBP: | TYRO protein tyrosine kinase binding protein |
| UCB: | Umbilical cord blood |
| UCP2: | Uncoupling protein 2 (mitochondrial, proton carrier) |
| UK: | United Kingdom |
| UTR: | Untranslated region |
| UV: | Ultra violet |
| Vav: | vav guanine nucleotide exchange factor |
| VLA: | Very late antigen |
| WASP: | Wiskott-Aldrich syndrome protein |
| WHO: | World Health Organisation |
| WIP: | WASP-interacting protein |
| WPRE: | Woodchuck hepatitis virus posttranscriptional regulatory element |
| WT1: | Wilms Tumour 1 |
| XTT: | Tetrazolium salt |
| Yes or c-Yes: | v-yes Yamaguchi sarcoma viral oncogene homolog 1 |
| YFP: | Yellow fluorescent protein |
| Yrk: | Proto-oncogene tyrosine-protein kinase Yrk |
| ZAP70: | Zeta-chain (TCR) associated protein kinase 70kDa |
| ZNF216: | Zinc finger protein 216 |

## Table of contents

## List of figures

## List of tables

# Chapter I

# I Introduction

## 1. Acute Myeloid Leukaemia

### 1.1 AML: the disease

#### 1.1.1 Four main types of leukaemias

Leukaemia is a malignant bone marrow disease with blood infiltration characterised by the clonal expansion and proliferation of an abnormal precursor cell from either the lymphoid or myeloid lineage. Leukaemia accounts for approximately 3% of all cancers in the United Kingdom. Depending on the rapidity of the clinical progression of the disease, the leukaemia is defined as acute or chronic. The acute leukaemias, acute lymphoblastic and acute myeloid leukaemia (ALL and AML respectively), are characterised by a rapid onset of the disease and the accumulation of immature precursor cells in the bone marrow. The accumulation of these so called leukaemic blasts provokes a bone marrow failure resulting in cytopenia. The chronic leukaemias, chronic myeloid leukaemia and chronic lymphoid leukaemia (CML and CLL respectively) have a more sluggish course than acute leukaemias and are characterised by the proliferation of fully mature but abnormal cells (*Figure 0.1*).

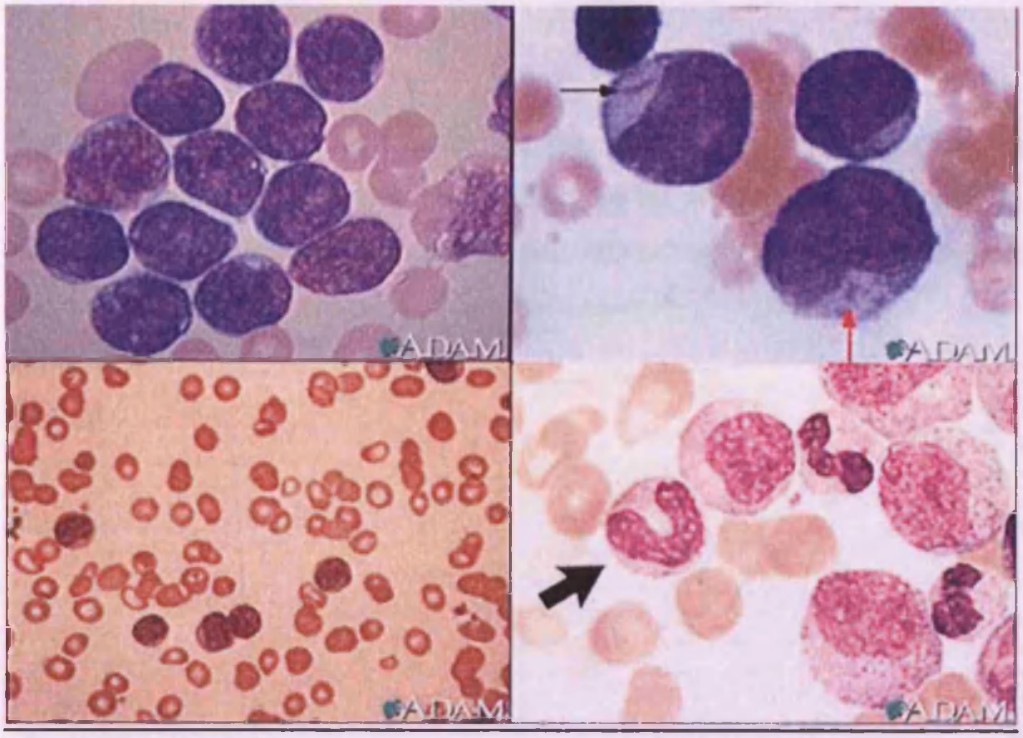

***Figure I.1:* Photomicrograph images of the four main classes of leukaemia.**
*Top Left: Acute Lymphocytic Leukaemia characterised by darkly stained lymphoblasts. Top Right: Acute Myeloblastic Leukaemia characterised by blasts with a prominent nucleoli (red arrow) and cytoplasmic granules (black arrows). Bottom Left: Chronic Lymphocytic Leukaemia characterised by predominantly small, mature lymphocytes. Bottom Right: Chronic Myelocytic Leukaemia characterised by predominantly normal-appearing cells with intermediate maturity. Images taken and edited from http://health.allrefer.com/.*

### 1.1.2 Incidence

Grouped together, leukaemias are the ninth most common cancer in men and tenth in women. However, leukaemia is the most common cancer of childhood. About a third of childhood malignancies are leukaemias, of which 80% are ALL, 15% are AML and around 5% are CML. In adults, CLL and AML are the most common leukaemias, representing 35% and 30% of the newly diagnosed cases respectively. ALL account for 12% of the cases and CML for 10% (source: www.leukemia-lymphoma.org).

### 1.1.3 Risk factors

Age is an important risk factor in the development of leukaemia. In childhood leukaemias, zero to four years old children are the most at risk to develop the disease. In adults, incidence is higher for people over 50 years old and increases exponentially from there. Gender is also a minor risk factor for leukaemia development with 5% more males being diagnosed with leukaemia than females. (http://info.cancerresearchuk.org/cancerSTAT/types/leukaemia/incidence/; *Figure I.2*). The focus of this study will be AML in adults, therefore symptoms, diagnosis, classification and remission rates will only be discussed for this particular cancer in the following sections.

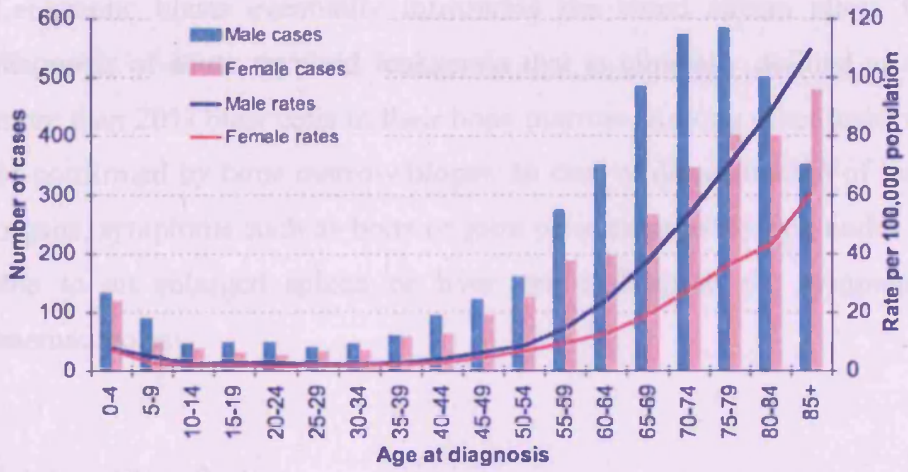


***Figure I.2:* Number of new cases and age specific incidence rates of leukaemias by sex (UK 2004).**

*Histogram bars showing the number of newly diagnosed cases in 2004 and graphic lines showing the specific incidence rate per 100,000 population in 2004 per age class and gender.*

Another important risk factor is the cytogenetic profile of the leukaemia, this criterium will also influence response to chemotherapy and will be discussed in section 1.1.5. In any case, an early diagnosis and treatment can improve remission rates, particularly in younger adults.

### 1.1.4 Symptoms and diagnosis of AML

Common symptoms experienced by the patient include fatigue, abnormal bleeding and bruising and increased susceptibility to infections. All those features are actually the manifestation of bone marrow failure caused by the accumulation of immature blasts in the bone marrow and are unrelated to the proliferative nature of the blast cells themselves. Indeed, leukaemia is originated by an impaired capacity of the bone marrow to properly produce mature haematopoietic cells that leads to cytopenias. The observed fatigue is therefore due to anaemia, which can also account for a possible shortness of breath. Thrombocytopenia causes the abnormal bleeding and bruising and neutropenia and leukopenia are the source of the vulnerability to infections.

Leukaemic blasts eventually infiltrating the blood stream allow for one of the first diagnosis of acute myeloid leukaemia that is clinically defined as a patient presenting more than 20% blast cells in their bone marrow. Among other tests, this diagnosis has to be confirmed by bone marrow biopsy. In case of dissemination of the blast cells to other organs, symptoms such as bone or joint pain, enlarged lymph nodes and abdominal pain due to an enlarged spleen or liver can add up to the symptoms of an abnormal haematopoiesis.

### 1.1.5 Classification

Traditionally, AMLs were classified based on the morphology of the blast cells found in the peripheral blood or the bone marrow of the patient. To this purpose, staining with the dyes haematoxilin and eosin (H&E staining), allowing a clear distinction between the volumes corresponding to the nucleus and the cytoplasm of the cells, gave the basis for the French American British (FAB) classification. The FAB classification comprises eight subclasses, M0 to M7, which, if superimposed on a normal haematopoietic tree, correspond to distinct blocks in differentiation (*Figure I.3*).

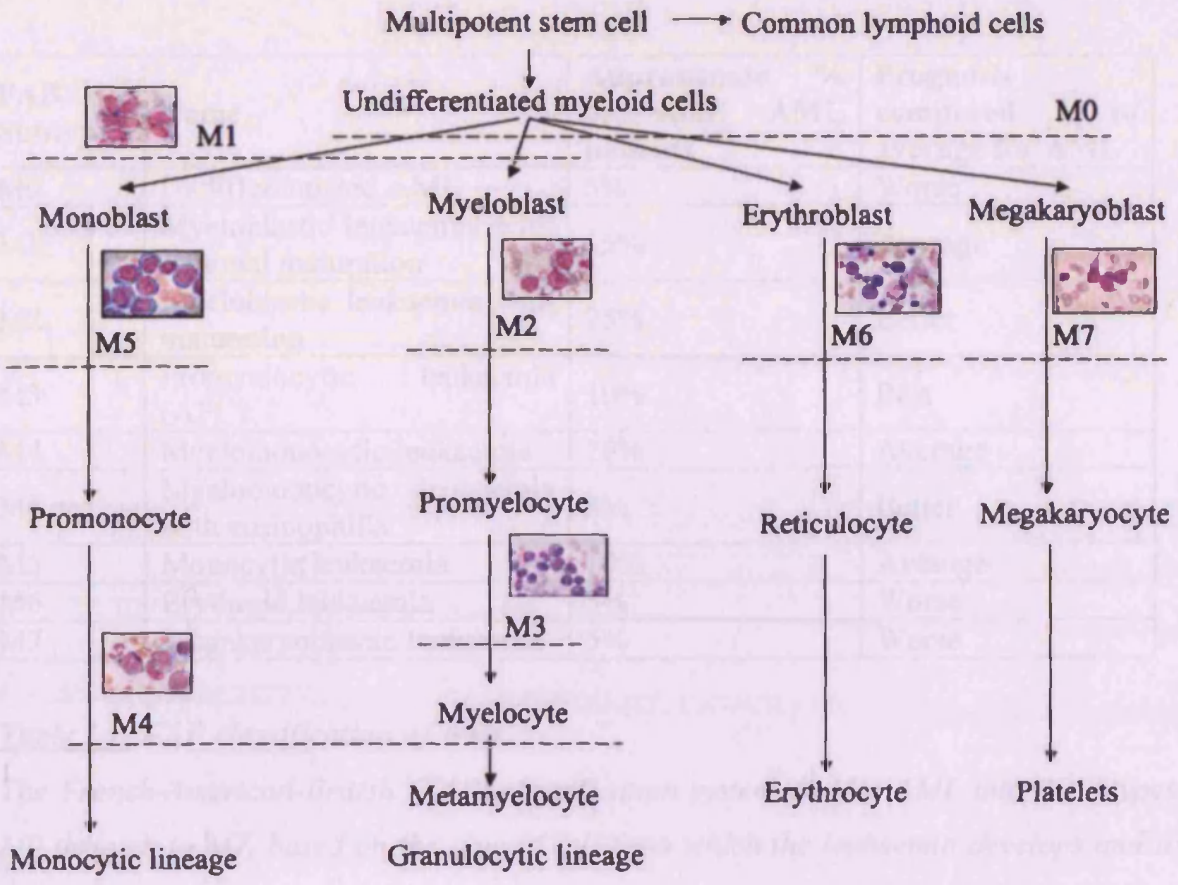


***Figure I.3:* Repartition of the eight FAB subclasses on the haematopoietic tree.**
*FAB M0 and M1 AML correspond to poorly differentiated cells. FAB M5 and M4 AML correspond to a block in the monocytic maturation process. FAB M2 and M3 AML correspond to a block in the granulocytic maturation process. FAB M6 AML correspond to a block in maturation of cells from the erythrocytic lineage while FAB M7 AML correspond to a block in maturation of cells from the megacaryocytic lineage.*

*Table I.1* indicates the frequency of occurrence of each subtype of AML as well as their prognosis. *Figure I.4* shows the morphology of the leukaemic blasts encountered in each FAB subclass. Different FAB types tend to have different prognosis outcomes, although this is based on the underlying genotype of the disease.

| FAB Subtype | Name | Approximate % of adult AML patients | Prognosis compared to average for AML |
|---|---|---|---|
| M0 | Undifferentiated AML | 5% | Worse |
| M1 | Myeloblastic leukaemia with minimal maturation | 15% | Average |
| M2 | Myeloblastic leukaemia with maturation | 25% | Better |
| M3 | Promyelocytic leukaemia (APL) | 10% | Best |
| M4 | Myelomonocytic leukaemia | 20% | Average |
| M4 eos | Myelomonocytic leukaemia with eosinophilia | 5% | Better |
| M5 | Monocytic leukaemia | 10% | Average |
| M6 | Erythroid leukaemia | 5% | Worse |
| M7 | Megakaryoblastic leukaemia | 5% | Worse |

***Table I.1:* FAB classification of AML.**

*The French-American-British (FAB) classification system divides AML into 8 subtypes, M0 through to M7, based on the type of cell from which the leukaemia develops and its degree of maturity. Diagnosis is made based on the phenotype of the cells. Different FAB types tend to have different prognosis outcomes, although this is based on the underlying genotype of the disease.*

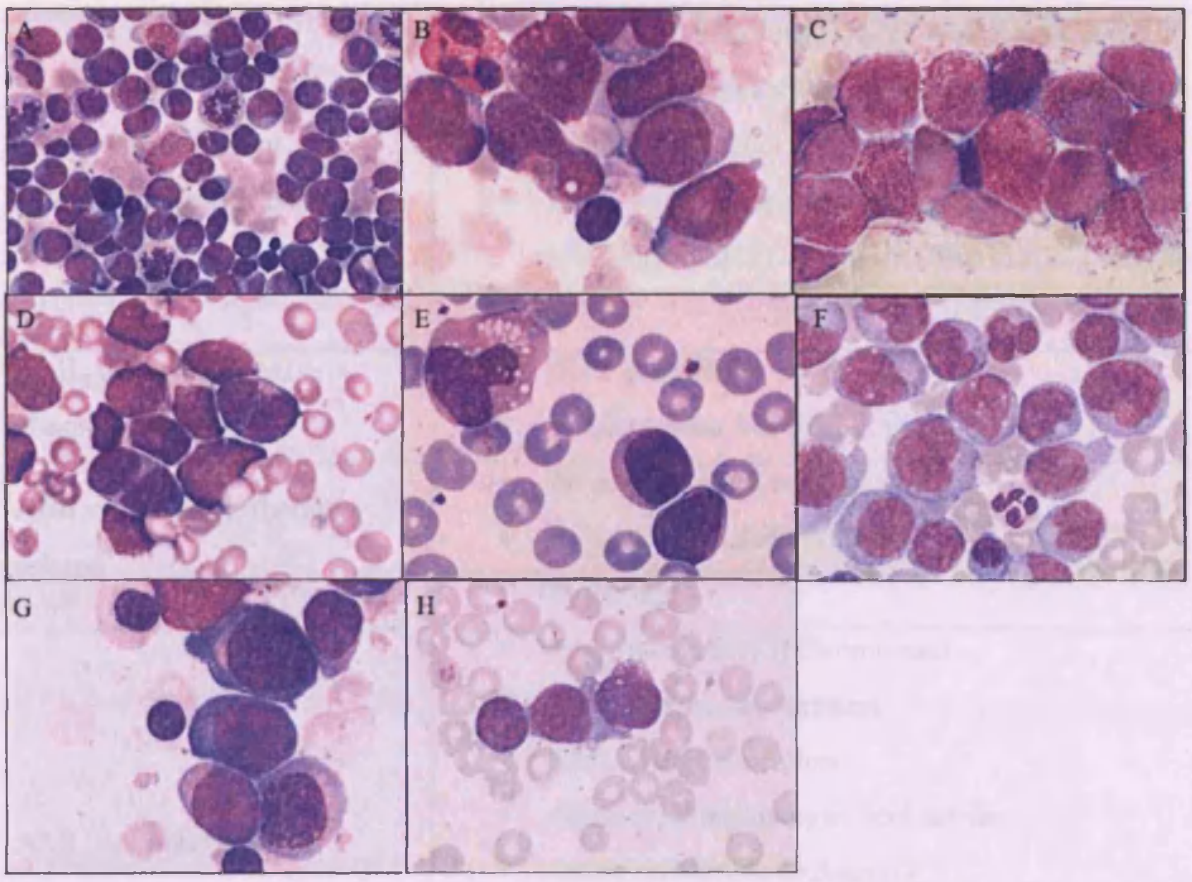


***Figure I.4:* AML blasts morphology according to the FAB classification.**

*(A) FAB M1 invasive myeloblasts (x10). (B) FAB M2 myeloid blasts with granular cytoplasm (x10). (C) FAB M3 large granular blasts (x100). (D) FAB M3 multi granular blasts (x100). (E) FAB M4 large myeloblast and two monocytes (x100). (F) FAB M5 large blasts with large cytoplasm and condensed chromatin (x100). (G) FAB M6 erythroblasts and monoblasts (x100). (H) FAB M7 megakaryocytic blasts (x100).*

Thus, the FAB classification system divides AML into 8 subtypes based on the type of cell from which the leukaemia develops and its degree of maturity. Although not completely obsolete, it has recently been replaced by the World Health Organisation (WHO) classification system which also takes into account more recent additional tools of diagnosis such as cytogenetics and the antecedents of the patient in terms of myelodysplastic syndrome (MDS) or chemotherapy (Harris *et al.*, 1999).

| | |
|---|---|
| AML with recurrent cytogenetic translocations | • AML with t(8;21)(q22;q22) AML1/CBFα-ETO<br>• Acute promyelocytic leukaemia: AML with t(15;17)(q22;q12) PML-RARα and variants<br>• AML with abnormal bone marrow eosinophils: inv(16)(p13;q22) and t(16;16)(p13;q22) CBFβ-MYH1 |
| AML with 11q23 MLL abnormalities | • With prior MDS<br>• Without prior MDS |
| AML with MDS, therapy related | • Alkalating agent related<br>• Epipodophyllotoxin related<br>• Other types |
| AML not otherwise categorised | • AML minimally differentiated<br>• AML without maturation<br>• AML with maturation<br>• Acute myelomonocytic leukaemia<br>• Acute monocytic leukaemia<br>• Acute erythroid leukaemia<br>• Acute megakaryocytic leukaemia<br>• Acute basophilic leukaemia<br>• Acute panmyelosis with myelofibrosis |

***Table I.2:* WHO classification (adapted from(Harris et al., 1999).**

*The current classification system for AML, developed by the WHO takes into account cytogenetics and attempts to provide more prognostic information about the disease.*

Cytogenetics is nowadays an important tool in diagnosis of leukaemias (Mrozek and Bloomfield, 2008). Indeed, about 65% of acute leukaemias are characterised by non-random chromosomal translocations and 45% of AML patients have a normal karyotype (Marcucci *et al.*, 2005b). The Philadelphia chromosome -the hallmark of CML- was discovered in 1960 and corresponds to the first chromosomal translocation to have been characterised. The subsequent intensive studies using fluorescent *in situ* hybridisation

(FISH) allowed for the identification of more than a hundred chromosomal abnormalities which have been proven to segregate AML in different prognosis groups: favourable, intermediate and poor (*Table I.3; Figure I.5*).

| Risk group | Abnormality | 5 year survival | Relapse rate |
|---|---|---|---|
| Favourable | t(8;21)<br>t(15;17)<br>inv(16) | 70% | 33% |
| Intermediate | Normal<br>+8<br>+21<br>+22<br>del(7q)<br>del(9q)<br>Abnormal 11q23<br>All other structural/ numerical abnormalities | 48% | 50% |
| Poor | -5<br>-7<br>del(5q)<br>Abnormal 3q<br>Complex | 15% | 78% |

***Table I.3:** AML cytogenetic risk groups (adapted from (Grimwade et al., 1998).*

*Hierarchical prognostic classification, derived taking into consideration the influence of additional cytogenetic abnormalities on outcome, and used for directing treatment approach in the current MRC AML 12 trial. The presence of certain genetic abnormalities indicates whether the AML will respond favourably or poorly to therapy. Prognosis may also be used to determine the nature of the therapy given, with more aggressive treatment for disease with adverse cytogenetics.*

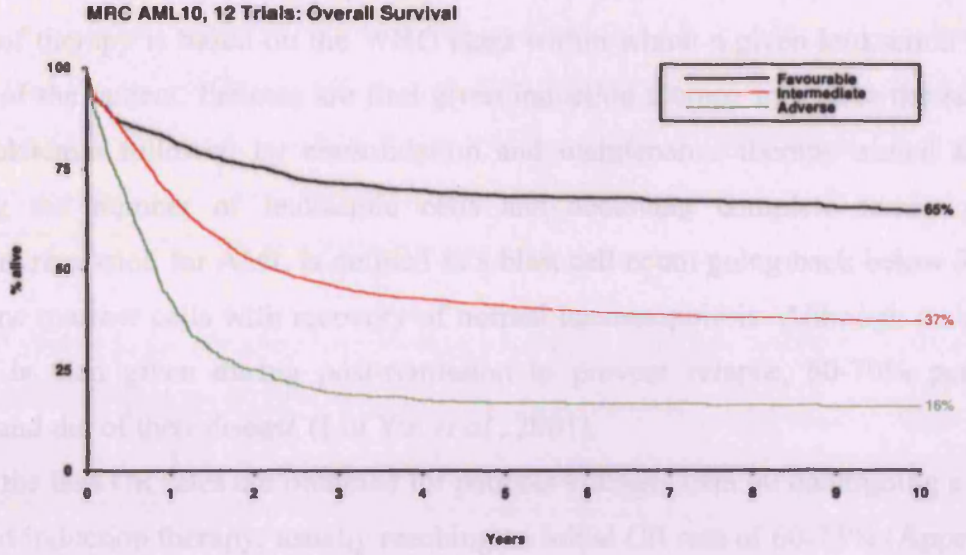


***Figure I.5:*** ***Overall survival of prognostic risk groups in de novo AML (adapted from (Grimwade et al., 1998)***

*Overall survival of patients with AML is highly influenced by the genetics behind the disease. In the MRC AML 10 and 12 trials, at 10 years, 65% of patients with favourable cytogenetics remained alive, 37% and 16% with intermediate and adverse cytogenetics survived for the same period of time respectively.*

A correlation between the age of the patient and the cytogenetic risk group has also been observed, with younger people having the tendency to develop leukaemia of the favourable group. Although AML with normal karyotype is classified within the intermediate prognosis group, recent research has shown that the presence of certain mutations can be used to further risk stratify. This point will be discussed in section 1.4.1 (Mrozek *et al.*, 2007b).

### 1.1.6 Therapies and their outcome

Choice of therapy is based on the WHO class within which a given leukaemia falls and the age of the patient. Patients are first given induction therapy to reduce the size of the bulk leukaemia followed by consolidation and maintenance therapy aimed at further reducing the number of leukaemic cells and achieving complete remission (CR). Complete remission for AML is defined as a blast cell count going back below 5% of the total bone marrow cells with recovery of normal haematopoiesis. Although maintenance therapy is then given during post-remission to prevent relapse, 60-70% patients do relapse and die of their disease (Liu Yin *et al.*, 2001).

Overall the best CR rates are obtained for patients younger than 60 undergoing a standard course of induction therapy, usually reaching an initial CR rate of 60-75% (Appelbaum *et al.*, 2001). Specifically patients with acute promyelocytic leukaemia (APL) achieve up to 80% CR rate based on the propensity of all-trans retinoic acid (ATRA) to induce differentiation of the AML FAB M3 leukaemic blasts (Warrell *et al.*, 1991). Thanks to intensive post remission therapy, the overall survival at 5 years subsequently exceeds 50% for patients with favourable cytogenetics. Patients from the intermediate risk group mostly undergo allogeneic haematopoietic stem cell transplantation if they match a suitable donor, while those without a suitable donor receive intensive post remission chemotherapy. Bone marrow transplantation increases the rate of successful therapies since it allows for the delivery of larger doses of chemotherapy to patients that could otherwise not be treated so well. However, it is only offered to rather fit patients since the conditioning treatment prior to transplantation is quite drastic. Despite potential graft versus host disease (GvH disease), allogeneic transplantation can also give rise to graft versus leukaemia effect (GvL effect) where donor immune cells kill residual leukaemic cells thus increasing the success of the therapy (Horowitz *et al.*, 1990). However, patients falling into the poor cytogenetic risk group, which are most often older people, hardly exceed 50% initial response to induction therapy and their overall survival at 5 years remains below 20%, regardless of the type of post remission therapy they undergo (Byrd *et al.*, 2002; Visani *et al.*, 2001). Therapy for these patients provides the greatest challenge to AML research since it shows that more targeted therapies are essentially

needed. Moreover, when dealing with older patients, therapies need to be less severe since these patients are unable to tolerate intensive chemotherapy (Stone *et al.*, 2004). In addition, the development of resistance to chemotherapy is becoming a major concern since it leads to less effective subsequent therapies in the case of relapsed leukaemias. Eventually the novel targeted therapies would generally not only benefit the older poor prognostic group but younger patients as well (Morgan and Reuter, 2006).

## 1.2 Normal haematopoiesis as a background for understanding leukaemia

### 1.2.1 Haematopoietic stem cells and haematopoietic hierarchy

AML being the result of an aberrant and malignant haematopoiesis, the normal haematopoietic hierarchy can be used as a background for understanding where leukaemias are originating.

The proportions of red and white blood cells in the normal blood are constantly maintained via a homeostatic process by the haematopoietic system. Since most mature haematopoietic cells are relatively short lived, they need to be replaced at a high rate. Indeed, between birth and death, the body of a human being is thought to produce approximately $10^{16}$ blood cells. The turnover of cells in the haematopoietic system in an average individual weighing 70kg is estimated to be $10^{12}$ cells per day, including 200 billion erythocytes and 70 billion neutrophilic leukocytes. This remarkable turnover is kept up by a small population of pluripotent haematopoietic stem cells (HSC), which have the peculiar capacity to be able to balance self-renewal versus differentiation into precursor cells, making them able to sustain the entire hierarchy of haematopoietic cells throughout the life of an individual (*Figure I.6*).

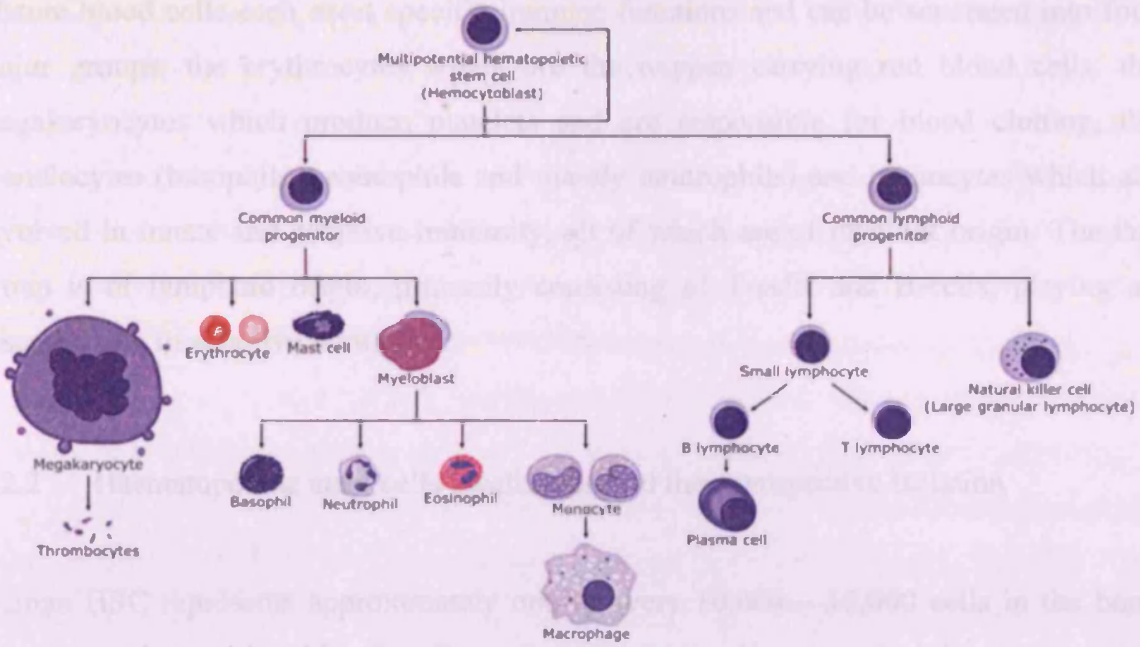


***Figure I.6:* Haematopoietic hierarchy (adapted from www.dentalarticles.com).**

*The variety of cells in normal blood is constantly being maintained by the haematopoietic system, a hierarchy of cells which is driven by the pluripotent haematopoietic stem cell which has the ability to self-renew and is able to produce all mature cells of the blood lineage. Common myeloid and lymphoid progenitors have limited self-renewal capacity and are restricted to differentiate into their specific lineages. As cells become increasingly differentiated, their ability to self-renew decreases as well.*

*In vivo*, HSC can give rise, by asymmetric division, to two daughter cells with different fates; one of them being identical to the original HSC and the other being able to differentiate into an immature, more committed, progenitor (Ho, 2005). In order to maintain a haematopoietic stem pool available throughout the lifetime of an individual without outgrowth of immature precursor cells, a tight regulation of HSC division is therefore necessary.

As cells become more differentiated, they progressively lose their ability to self-renew, get committed towards a specific lineage and ultimately acquire more specialised functions required for an efficient immune system. Common myeloid and lymphoid progenitors have limited self-renewal capacity and are restricted to differentiate into their specific lineages due to regulation of expression of specific sets of genes.

Mature blood cells each exert specific immune functions and can be separated into four major groups: the erythrocytes which are the oxygen carrying red blood cells, the megakaryocytes which produce platelets and are responsible for blood clotting, the granulocytes (basophils, eosinophils and mainly neutrophils) and monocytes which are involved in innate and adaptive immunity, all of which are of myeloid origin. The last group is of lymphoid origin, primarily consisting of T-cells and B-cells, playing an essential role in adaptive immunity.

### 1.2.2 Haematopoietic stem cells localisation and their prospective isolation

Human HSC represents approximately one in every 10,000 – 15,000 cells in the bone marrow and are devoid of cell surface markers characteristic of more mature haematopoietic cells (Kondo *et al.*, 2003). Their rarity and difficulty to access proned scientists to develop a variety of assays based on limited dilutions and cell surface marker depletion rather than on basic cell morphology or density. Although the development of assays for prospective isolation of stem cells is still ongoing, *in vivo* xenotransplantation models exploiting the property of stem cells being able to self-renew are nowadays the best way to know that true stem cells are being worked with. Over the years, assays becoming progressively more selective for stem cells, the definition of what stem cells are and the understanding of haematopoiesis have greatly improved. The various *in vitro* and *in vivo* assays used to specifically study progenitors, stem cells and self-renewal potential will be described below.

#### 1.2.2.1 *In vitro* assays

The first assays developed were *in vitro* assays trying to reproduce stimuli encountered by stem and progenitor cells *in vivo*. The colony forming cell assay (CFC assay) involves the seeding of haematopoietic cells into a semi-solid, methylcellulose based medium supplemented with a specific set of cytokines that promotes differentiation and proliferation of haematopoietic progenitor cells.

The long-term culture initiating cells assay (LTC-IC assay) involves the culture of haematopoietic cells with stromal feeder layers and a specific set of cytokines for a period of five weeks followed by a CFC assay. The LTC-IC assay is an attempt to recreate, *in vitro*, a niche environment specifically able to maintain cells with a more extensive proliferative ability, including the quiescent stem cells. These cells are able to form colonies, or cobblestone area, beneath the stromal layer and the subsequent assessment of progenitor formation by CFC assay allows for the retrospective evidence of successful stem cells maintenance and characterisation of their differentiation potential. Besides, committed cells and progenitors exhausting their proliferative potential within a few weeks are no longer part of the culture (Breems *et al.*, 1994; Ploemacher *et al.*, 1989). Although the LTC-IC assay gives access to more primitive cells than the CFC assay, it does not allow to study the full potential of the primitive cells maintained since it does not allow for the assessment of the lymphoid potential of the propagated cells. Other assays were therefore developed where initially growing cells in a lymphoid supportive environment followed by a switch to a myeloid supportive environment allowed for multilineage potential assessment (Hao *et al.*, 1998; Miller *et al.*, 1999).

Alltogether, these assays are used for study of both human and mouse haematopoiesis, relying each on a specific cocktail of murine or human cytokines. Although the CFC and LTC-IC assays narrow the window of analysis to study the proper haematopoietic stem cells, these assays remain limited by requirements for external stimulation by cytokines and growth on an adequately supporting stromal layer, which does not exactly replicate endogenous conditions. Indeed, the composition of the bone marrow includes not only stromal cells but also stromal stem cells, haematopoietic progenitor cells, mature and maturing red and white blood cells as well as megakaryocytes maturing into platelets. This dynamic environment is therefore far more complicated in terms of kinetics of cytokine production than the environment created in the *in vitro* assays. Observing growth of cells in an endogeneous microenvironment where they would receive the appropriate signals would consequently definitely help in overcoming these limitations.

### 1.2.2.2 *In vivo* assays

*In vivo* models were first developed for studying mouse haematopoiesis using transplantation models involving inbred mice. Transplantation of haematopoietic cells from mice into genetically similar mice allow the observation of the growth of primitive haematopoietic cells for a significant period of time (Morrison and Weissman, 1994; Osawa *et al.*, 1996; Spangrude *et al.*, 1988). Since similar transplantation models cannot be used to study human haematopoiesis, for obvious ethical reasons, the use of immunocompromised mouse models offers the possibility to study human haematopoietic cells in a xenotransplantation system.

Three types of models are being currently used which have differences in their permissivity for human cells engraftment. The severe combined immunodeficiency (SCID) mutation in mice causes a lack of functional T and B lymphocytes, therefore allowing cytokine stimulated human cells to develop in the marrows of these mice without immune rejection (Lapidot *et al.*, 1992). Human cells able to repopulate the bone marrow of SCID mice after an incubating period of 6 weeks are termed short term SCID repopulating cells (short term SRC) while the ones able to repopulate the bone marrow of SCID mice after an incubating period of 12 weeks are termed long term SCID repopulating cells (Dick *et al.*, 1997).

When mice with the SCID mutation are crossed with mice presenting a non-obese diabetic (NOD) phenotype, NOD/SCID mice in addition to a lack of functional T and B lymphocytes, show an impaired natural killer (NK) and antigen-presenting cell (APC) function, allowing the engraftment of human cells in these mice without the need for cytokine prestimulation (Cashman *et al.*, 1997; Larochelle *et al.*, 1996; Shultz *et al.*, 1995). Given ideal conditions, the NOD/SCID model can therefore support multilineage (B-cell and myeloid) engraftment for over 3 months and can also support secondary engraftment (Hogan *et al.*, 1997). Indeed secondary engraftment is to date the only assay proving the prospective isolation of a fraction of cells containing the true haematopoietic stem cells.

Crossing NOD/SCID mice with mice deficient for β2 microglobulin (giving rise to NOD/SCID/$\beta 2m^{-/-}$ mice) allows a higher engraftment efficiency for both primary and

secondary transplantation (Kollet *et al.*, 2000) while crossing NOD/SCID mice with mice deficient for interleukin-2Rγ (giving rise to NOD/SCID/IL-2Rγ$^{-/-}$, or NOG, mice) further improves the permissivity of the mice (Ito *et al.*, 2002). Both resulting mouse strains, NOD/SCID/β2m$^{-/-}$ and NOD/SCID/IL-2Rγ$^{-/-}$, are currently equally used for assessing the self-renewal, proliferation and differentiation of human haematopoietic stem cells.

#### 1.2.2.3 Cell surface phenotyping

The establishment of mouse xenotransplantation models revolutionised the stem cell field by allowing further progress to be made into isolating pure HSC. Since primitive human haematopoietic cells, including the HSC, do not express certain cell surface markers that are associated with mature blood cell types, they can be isolated based on the lack of expression of these "lineage markers" (Lin). Thus, immature 'Lineage negative' (Lin$^-$) cells can be distinguished from the more abundant differentiated 'Lineage positive' (Lin$^+$) cells (Wognum *et al.*, 2003).

In the search for a marker specific of human HSC, CD34 expression was identified as being restricted to HSC and early progenitors (Sutherland *et al.*, 1989). Combination of selection for CD34 expressing cells and injection into NOD/SCID mice led to the observation that CD34 is expressed on the majority of cells with *in vivo* repopulating potential, including the HSC and long term repopulating cells as well as early progenitors, but not on the majority of terminally differentiated cells. Thus, CD34$^+$ cells are routinely considered as enriched for HSC in the clinics.

In an attempt to further refine the selection of HSC, the CD38 marker has also been used for isolating HSC. Indeed SRC have been phenotyped as Lin$^-$/CD34$^+$/CD38$^-$ (Bhatia *et al.*, 1997). As a population highly enriched for multilineage repopulating cells, SRC are one of the most primitive populations of the haematopoietic hierarchy identified so far. This subset is generally considered to contain the HSC, although other studies have demonstrated that cells with long-term repopulating ability may additionally reside within a Lin$^-$/CD34$^-$ population (Bhatia *et al.*, 1998). The further development of more permissive murine models and extensive work on further refinement and characterisation

of specific markers on the surface of human HSC should allow for further refinement of the identity of human HSC.

Of note, an important body of work on HSC is carried out in inbred mice. Murine HSC display a different cell surface marker phenotype to human HSC. They are defined as KTLS (c-Kit$^+$/Thy1$^-$/Lin$^-$/Sca$^+$) (Morrison and Weissman, 1994) and are studied using the same *in vitro* and *in vivo* assays than human HSC using murine cytokines and stromal cells in *in vitro* assays.

## 1.3 Evidence of dysregulated normal haematopoiesis leading to AML

### 1.3.1 AML is a stem cell disease

Once the identity of the normal HSC was somewhat clarified, it was attractive to define if they could be giving rise to AML. The hypothesis that leukaemic stem cells (LSC) could derive from HSC was based on the fact that the leukaemic bulk mostly consists of immature cells with limited proliferative capacity. A cell with an extensive degree of proliferative ability must have therefore existed to give rise to and maintain the entire leukaemic bulk. As mentioned previously, HSC are able to self-renew or differentiate into a variety of specialised cells but also to mobilise out of the bone marrow into circulating blood, undergo apoptosis or remain in a quiescent state. This variety of functions made them an attractive target for generation of the LSC.

Such a cell with long-term proliferative ability has been identified in AML using the same assay as for the identification of normal HSC, the SCID assay (Lapidot *et al.*, 1994). The evidence that these SCID-leukaemia initiating cells (SL-IC) are haematopoietic stem cell has been demonstrated by the fact that, as for normal haematopoiesis, the leukaemic stem cell is not only able to repopulate the SCID mice bone marrow but is also able to generate a transplantable AML in the NOD/SCID mice, which exhibits the same characteristics than the original AML sample (Bonnet and Dick, 1997). Additionally both studies highlighted the fact that SL-IC share the same phenotype as SRC since they are Lin$^-$/CD34$^+$/CD38$^-$. Furthermore, it has also been

demonstrated that, like normal HSC, the majority of LSC exist in a quiescent state (Guan *et al.*, 2003), thereby allowing them to escape therapies which are usually directed towards rapidly dividing cells. The fact that LSC are not eliminated by chemotherapy would therefore explain the frequent relapses seen in AML patients.

However, recent publications have suggested that LSC could also reside within the $Lin^-/CD34^+/CD38^+$ fraction (Taussig *et al.*, 2008). Although this fraction of cells was initially thought to not contain any engrafting cells, pre-treatment of the recipient mice with immunosuppressive anti-CD122 antibodies was shown to allow for their engraftment (McKenzie *et al.*, 2005). In normal haematopoiesis, the $Lin^-/CD34^+/CD38^+$ fraction contains a long-term engrafting population that cannot give rise to secondary transplant (Hogan et al., 2002). In AML, some patient samples present long-term engrafting cells in the $Lin^-/CD34^+/CD38^-$ fraction, in the $Lin^-/CD34^+/CD38^+$ or in both fractions. It is not yet known if the $Lin^-/CD34^+/CD38^+$ fraction from AML samples can give rise to secondary transplants. This finding suggests that LSC could originate from a progenitor having acquired HSC properties or that cell surface marker expression is modified upon AML onset and cannot be readily compared to normal haematopoiesis. This last point still remains to be clarified.

Of note, identification of SL-IC pioneered the search for cancer stem cells in solid tumours. Since then breast, brain, prostate, colon and pancreatic cancers, as well as head and neck squamous cell carcinoma, multiple myeloma and melanoma have been shown to contain a cancer initiating cell (Al-Hajj *et al.*, 2003; Collins *et al.*, 2005; Dalerba *et al.*, 2007; Fang *et al.*, 2005; Li *et al.*, 2007; Matsui *et al.*, 2004; O'Brien *et al.*, 2007; Prince *et al.*, 2007; Ricci-Vitiani *et al.*, 2007; Singh *et al.*, 2004).

### 1.3.2 Leukaemic cells present chromosomal aberrations and gene specific mutations

It is now commonly acknowledged that cancer arises from an accumulation of genetic and epigenetic changes in oncogenes and tumour suppressor genes that free cells from the mechanisms that control normal cell proliferation. The idea that cancer is caused by a series of successive somatic mutations has been originally supported by the study of

cancers such as retinoblastoma, in which the age of incidence is consistent with the requirement of two mutations to completely remove the function of the Rb gene. Such studies have given rise to the 'two hits' model for cancer development (Hethcote and Knudson, 1978; Knudson, 2001). The fact that AML is a disease that primarily affects the elderly also supports the idea of damage accumulating over time. In AML such damage occurs in the form of chromosomal aberrations as well as gene specific mutations but rarely, unlike in solid tumours, as chromosomal amplification due to chromosome instability.

#### 1.3.2.1 Chromosomal aberrations

Chromosomal aberrations encountered in AML can be deletion, gain of chromosomes or translocations, which are routinely identified by FISH. Gene and chromosomal deletions may involve a small part of the chromosome, such as the short or long arm (eg 5q") or the loss of an entire chromosome (monosomy 7). Losses most commonly affect chromosomes 5, 6, 7, 11, 20 and Y. Gains are common in chromosomes 8, 12, 19, 21 and Y. While numerical changes in AML are not unusual, balanced translocations of chromosomes, where no material is gained or lost, are the most common chromosomal aberrations observed. To date, there have been approximately 300 balanced translocations described in AML (Mitelman *et al.*, 2008). In cancer in general, balanced translocations contributing to malignant change can arise via two main mechanisms: either by overexpression of a normal cellular gene due to the fusion of the promoter region from one gene to the protein coding region of another, or by the fusion of two genes to generate a chimeric gene that encodes a novel 'fusion protein'. In AML, balanced translocations exclusively result in fusion proteins (*Table I.4*). Of note, one given fusion protein can arise due to several different breakpoints usually located in the same region of the respective genes.

| Aberration | Fusion protein | Frequency (%) |
|---|---|---|
| t(8;21)(q22;q22) | RUNX1–RUNX1T1 | 4.3 |
| t(15;17)(q22;q21) | PML–RARA | 4.1 |
| der(11q23) | MLL fusions | 2.4 |
| inv(16)(p13q22) | CBFB–MYH11 | 2.3 |
| t(9;22)(q34;q11) | BCR–ABL1 | 0.7 |
| inv(3)(q21q26) | RPN1–EVI1 | 0.6 |
| t(6;9)(p22;q34) | DEK–NUP214 | 0.3 |
| t(1;22)(p13;q13) | RBM15–MKL1 | 0.2 |
| t(8;16)(p11;p13) | MYST3–CREBBP | 0.1 |
| t(7;11)(p15;p15) | NUP98–HOXA9 | <0.1 |

***Table I.4:*** ***The 10 most common balanced chromosomal aberrations in AML (Mitelman et al., 2007).***

Not all fusion protein partners have been characterised for all the different translocations identified in leukaemia, this is usually depending on the rarity of the translocation and the availability of chromosomal material to go beyond FISH and identify gene loci by PCR. Moreover, even if the identity and cellular function of the fusion partners are known, the role of the new chimeric protein is not always known. Fusion proteins can indeed act by a variety of mechanisms in AML.

Two well studied translocations are the t(9;22)(q34;q11) translocation in CML and the t(15;17)(q22;q21) translocation in FAB AML M3. As mentioned earlier, the t(9;22)(q34;q11) chromosomal rearrangement, also known as Philadelphia chromosome, was the first translocation to be characterised and results in the fusion of the genes *BCR* and *ABL*. This chimeric protein causes the tyrosine kinase activity of ABL to not be regulated anymore and the resulting constitutively active kinase provokes a deregulation of cell cycle control and resistance to apoptosis (Skorski, 2008). The t(15;17) translocation fuses the promyelocytic leukaemia gene *PML* on chromosome 15 to the retinoic acid receptor α gene, *RARα*, on chromosome 17. The resultant *PML-RARα*

fusion protein functions as a transcriptional repressor whereas the wild type *RARα* is an activator (Pandolfi, 2001). Additionally 11q23 aberrations involving MLL rearrangement, which represents one class of the WHO classification by themselves, are also quite well studied. More than 30 different fusion partners have been identified for this transcription factor. These partners can be cytoplasmic proteins (MLL-SEPT6; MLL-AF1Q) but are mostly transcription factors as well (MLL-GAS7, MLL-ENL, MLL-AF9 etc.). The resulting chimeric protein causes abnormal dimerisation of MLL, leading to aberrant maintenance of target gene expression, often resulting in a block in differentiation of haematopoietic cells (Mitterbauer-Hohendanner and Mannhalter, 2004; So and Cleary, 2004).

Although balanced translocations are often found in leukaemia, it is uncertain whether these translocations alone are sufficient to cause overt leukaemia. For instance, in CML, low levels of the *BCR-ABL* transcript are detectable in normal individuals indicating that while the translocation is important, it is not the only factor responsible for causing CML (Melo, 1996). Furthermore, two studies on identical twins harbouring the same *TEL(ETV6)-AML* translocation *in-utero* showed the twins to develop childhood ALL with variable latency periods before the onset of overt disease in one study (Ford *et al.*, 1998) and a twin being pre-leukaemic and the other twin developing B-ALL in the other study (Hong *et al.*, 2008). Such reports indicate that additional genetic events to the translocation are needed before the development of overt leukaemia.

#### 1.3.2.2 Normal karyotype AML and gene specific mutations

As mentioned previously, the 10 most common balanced translocations occur in approximately 15% of AMLs, the other rare recurrent balanced translocations are observed in only 5% of cases and numerical changes in chromosome number and complex abnormalities each contribute to approximately 10% of AMLs respectively (*Figure I.7*). Screening for mutations responsible for the development of the remaining 50% of AMLs with no detectable cytogenetic abnormalities has therefore been of great interest for the past few years. Trying to understand if these mutations are linked in any

sequential way is also essential since prognosis of patients with normal karyotype is greatly variable.

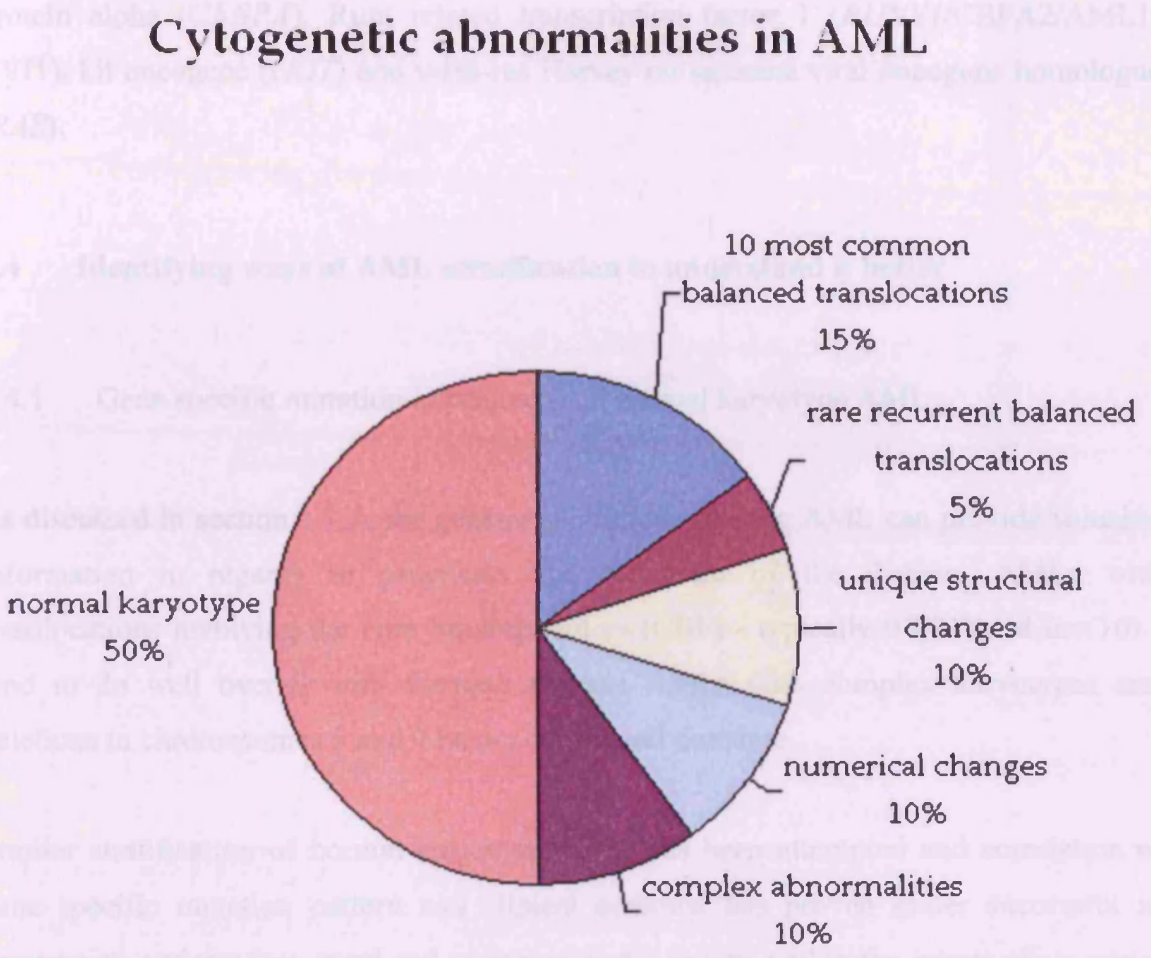


***Figure I.7:* Karyotype breakdown of AML.**

*Approximately 50% of AML have no cytogenetic abnormalities. The ten most common balanced translocations observed in AML are detectable in approximately 15% of cases. Rare recurrent balanced translocations, unique structural changes, numerical changes and complex abnormalities account for approximately 35% of AMLs.*

The completion of the human genome sequence has made every gene accessible to mutation analysis. Characterisation and study of gene specific mutations in AML revealed that they can alter both normal proliferation and differentiation of haematopoietic cells. Some mutations result in constitutive activation of tyrosine kinases

and their subsequent pathways while other mutations alter the function of transcription factors. Genes commonly mutated in AML include FMS-like tyrosine kinase 3 (*FLT3*), nucleophosmin (*NPM11*), mixed lineage leukaemia (*MLL*), CCAAT enhancer binding protein alpha (*CEBPA*), Runt related transcription factor 1 (*RUNX1*/CBFA2/AML1/ EVI1), kit oncogene (*cKIT*) and v-Ha-ras Harvey rat sarcoma viral oncogene homologue (*RAS*).

## 1.4 Identifying ways of AML stratification to understand it better

### 1.4.1 Gene specific mutation in prognosis of normal karyotype AML

As discussed in section 1.1.5, the genetic aberrations causing AML can provide valuable information in regards to prognosis and treatment of the disease. AMLs with translocations involving the core binding factors (CBF) - typically t(8;21) and inv(16) - tend to do well overall with therapy whereas AMLs with complex karyotypes and deletions in chromosomes 5 and 7 have poor overall outcome.

Similar stratification of normal karyotype AML has been attempted and correlation of gene specific mutation pattern and clinical outcome has proven rather successful in segregating patients into good and poor prognostic groups within the intermediate group (*Figure I.8* and (Mrozek *et al.*, 2007a)).

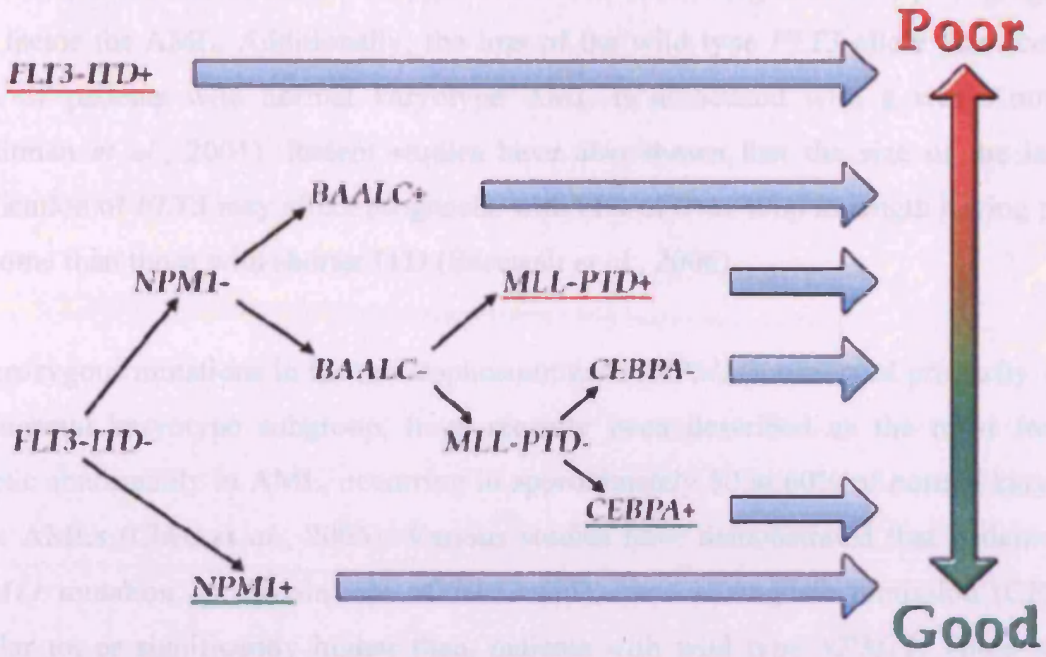


***Figure I.8:* Gene specific mutations pattern in normal karyotype AML as a prognostic tool (Mrozek et al., 2007b).**

*Despite having the same normal karyotype, adults with de novo NK AML are diverse in respect to their acquired gene mutations and gene expression changes. The presence of FLT3-ITD indicate poor prognosis. In the absence of FLT3-ITD, the presence of NPM11 mutations and CEBPA mutations are indications of favourable prognosis, while the presence of MLL-PTDs and high BAALC expression are indicators of poor prognosis.*

Indeed, *FLT3* has been found to be mutated in approximately one third of AML patients and has also been reported as mutated in ALL and MDS, making it one of the most frequently mutated genes in haematological malignancies. The FMS-like tyrosine kinase 3 *(FLT3),* encodes a membrane bound receptor tyrosine kinase, which is important in haematopoietic stem/progenitor cell survival and proliferation by signalling through the RAS pathway. *FLT3* mutations are either internal tandem duplications (ITD) of the juxtamembrane domain (30%) or point mutations usually involving the tyrosine kinase domain (TKD) (7%). Both types of mutation constitutively activate FLT3 (Small, 2006; Stirewalt and Radich, 2003) therefore specific inhibitors of FLT3 are being developed to be used as therapy for patients presenting such mutations (Hiddemann *et al.*, 2005).

*FLT3* ITD mutation in the heterozygous state has been recognized as a poor prognostic risk factor for AML. Additionally, the loss of the wild type *FLT3* allele that occurs in 10% of patients with normal karyotype AML is associated with a worse outcome (Whitman *et al.*, 2001). Recent studies have also shown that the size of the internal duplication of *FLT3* may affect prognosis, with ITD of over 40bp in length having poorer outcome than those with shorter ITD (Stirewalt *et al.*, 2006).

Heterozygous mutations in the nucleophosmin gene *(NPM11)*, observed primarily within the normal karyotype subgroup, have recently been described as the most frequent genetic abnormality in AML, occurring in approximately 50 to 60% of normal karyotype adult AMLs (Chen *et al.*, 2006). Various studies have demonstrated that patients with *NPM11* mutation, in the absence of *FLT3* ITD, have a complete remission (CR) rate similar to, or significantly higher than, patients with wild type *NPM11*. These studies have shown a statistical trend towards favourable outcome in event free survival and overall survival in patients with *NPM11* mutations (Boissel *et al.*, 2005; Dohner *et al.*, 2005; Schnittger *et al.*, 2005; Suzuki *et al.*, 2005).

In addition to being involved in numerous chromosomal translocations, MLL can also be found mutated in AML: partial tandem duplication in the *MLL* gene (*MLL* PTD) was the first molecular alteration shown to impact on the clinical outcome of NK AML. *MLL* PTD is detected in approximately 5 to 10% of cytogenetically normal adults with *de novo* AML and is associated with *FLT3* ITD (Dohner *et al.*, 2005). Patients with *MLL* PTDs have significantly shorter complete remission durations than patients without the mutation (Caligiuri *et al.*, 1998; Dohner *et al.*, 2002).

CCAAT enhancer binding protein alpha *(CEBPA)* is a transcription factor involved in myeloid differentiation and proliferation control. Mutations in *CEBPA* occur in approximately 15 to 20% of NK AMLs and are also associated with favourable prognosis (Bienz *et al.*, 2005; Frohling *et al.*, 2004). Mutations in this gene are an example that gene specific mutation can occur in normal karyotype AML as well as in addition to a chromosomal aberration. Indeed, favourable prognosis conferred by mutations in *CEBPA*

was initially demonstrated in patients in the intermediate cytogenetic risk category (Barjesteh van Waalwijk van Doorn-Khosrovani *et al.*, 2003; Preudhomme *et al.*, 2002) and later confirmed in patients with normal karyotype (Bienz *et al.*, 2005; Boissel *et al.*, 2005). Patients with mutations in *CEBPA* are also less likely to have concurrent poor prognostic mutations in *FLT3* and *MLL* PTDs (Frohling *et al.*, 2004).

The overexpression of specific genes in normal karyotype AML can also be used in prognosis, with overexpression of *BAALC*, *ERG*, and *WT1* all conferring poor prognosis (Bergmann *et al.*, 1997; Marcucci *et al.*, 2005a; Mrozek *et al.*, 2007b). Moreover, mutations in c-*KIT* and *TP53*, each occuring in 5 to 10% of cases of AML overall, have also been noticed preferably in one given prognosis cytogenetic group and predominate in patients with 'favourable' and 'poor risk' cytogenetics respectively (Beghini *et al.*, 2000; Stirewalt *et al.*, 2001). Similarly, mutations in *RUNX1* occur with higher incidence in patients with FAB type M0 or patients presenting with additional copies of chromosome 21 (Preudhomme *et al.*, 2000). Further studies on identification of mutations and correlation with chromosome abnormalities will help decipher any specific sequence of events required for the full onset of leukaemia.

### 1.4.2 Class I and class II mutations

Although AML appears to be a genetically heterogeneous disease, grouping mutations and chromosomal aberrations into broad categories based on their functional consequences is one way of simplifying the system. Frequently genetically heterogeneous mutations do target the same signal transduction and transcriptional pathways and therefore can be divided into groups. In an attempt to provide a more unified molecular way to explain how different mutations can generate essentially similar phenotypes, Gililland proposed a 'two-hit' model for leukaemogenesis (Dash and Gilliland, 2001; Gilliland, 2001). This is not to be confused with Knudson's two-hit model of cancer development mentioned earlier (Knudson, 2001).

myeloid disease such as activated *RAS, FLT3* and *c-KIT.* Although there are differe between individual tyrosine kinases, Class I mutation functions result in similariti activation of downstream effectors such as STAT, PI3K and RAS signalling pathway murine models, many of these mutations cause expansion of the stem cell pool ra than overt leukaemia (McCormack *et al.*, 2008).

| **Class I mutations** | **Class II mutations** |
|---|---|
| BCR-ABL | CBFβ-MYH11 |
| N-RAS | AML1-ETO |
| K-RAS | TEL(ETV6)-AML1 |
| c-KIT (exon 8 and Asp 816) | PML-RARα |
| FLT3 (ITD and Asp 835) | NUP98-HOXA9 |
| PTPN11 | PU.1 |
| NF1 | C/EBPα |
| TEL(ETV6)-PDGFRβ | AML1 |
| | AML1-AMP19 |

***Table I.5:* Class I and class II mutations in AML**

*Gilliland's "two hit hypothesis" postulates that the development of overt AML requir least one mutation from each class. Class I mutations offer a survival or prolifer advantage to the cell, whereas Class II mutations are involved in blocking differentia*

Class II mutations comprise chromosomal translocations and point mutations targ transcription factors and transcriptional co-activators, often involving the core bir factor complex (CBF complex). In many cases, Class II mutations result in a bloc differentiation pathways or apoptotic mechanisms, causing impaired haematopo differentiation. In murine models these genes cause myeloproliferation rather than

leukaemia (McCormack *et al.*, 2008). Evidence of two concomitant mutations coming each from one class has been reported in numerous studies (e.g FLT3 associates with PML-RARα but not with c-KIT or K-RAS; (Renneville *et al.*, 2008)) corroborating Gililland's two hit model where both a block in differentiation and a proliferative and/or survival advantage are necessary to result in leukaemic transformation.

Trying to fit each chromosomal aberration and gene specific mutation discovered in one of these two classes could help on with designing therapies based on the signalling pathway most likely to be dysregulated. FLT3 inhibitors, RAS pathway inhibitors and HDAC inhibitors are already being tested in clinical trials based on this rationale (Renneville *et al.*, 2008). Additionally routine screening for the presence of such well characterised mutations would help in monitoring the disease in patients with normal karyotype. Based on current large studies, the majority of AMLs have at least one genetic lesion described, however a proportion still remain with unknown genetic background. Also some mutations, such as NPM11, are well established as recurrent in leukaemia but are not known to be particularly involved in haematopoietic proliferation or differentiation. In such cases, a transgenic mouse model study can prove helpful. Indeed, transgenic mice heterozygous for NPM11 are shown to develop a haematological syndrome with features of a human myelodysplastic syndrome (Grisendi *et al.*, 2005) which, according to what has been found with other mouse models would classify NPM11 as a class II mutation and would indicate a role for NPM11 in haematopoietic differentiation. The fact that NPM11 associates with FLT3-ITD but not with CEBPA, would also support this hypothesis (Renneville *et al.*, 2008).

Finally, determining a sequence of genetic events would potentially help to prevent progression of AML. This can be done by comparing samples from patients diagnosed with MDS which progress into AML, comparing progression from chronic phase to blast crisis in CML or examining variation in type of mutations between presentation and relapse samples from the same AML patient. In each case, a mutation that is maintained throughout the course of the disease is likely to have occurred early in the leukaemogenic

process. Studying rare cases of familial AML can also help understanding leukaemogenesis.

Observation that acquisition of the *AML-ETO* translocation followed by the FLT3-ITD mutation led to the progression of MDS to AML (Pinheiro *et al.*, 2007) and that, in mouse models, the co-expression of pairs of genetic events such as the *BCR-ABL* and *AML1-EVI1* fusion proteins (Cuenco and Ren, 2004), or the *PML-RARA* translocation and an *FLT3* mutation (Kelly *et al.*, 2002) are necessary for the development of AML, indicate that class II mutations might precede class I mutations in the onset of leukaemogenesis.

## 1.5 Trying to generate leukaemic stem cells to understand their origin

Having identified AML as being organised as a hierarchy, thanks to the NOD/SCID model, and having acknowledged that chromosomal aberrations and mutations are causes or consequences of the disease, the exact way AML is generated still remains to be elucidated.

The fact that HSC remain in a quiescent state for a period of time, possibly as long as the lifetime of an individual, make them more likely to accumulate multiple mutations required for transformation to a malignant state. Alternatively, it could be possible that the LSC arises from a more restricted progenitor, or even a differentiated mature cell, which would first need to reacquire the ability to self-renew before becoming tumourigenic (*Figure I.9*). The later hypothesis requires many genetic abnormalities to occur, it is therefore more likely that AML represents aberrant haematopoiesis with the target cell for transformation lying within the HSC repertoire.

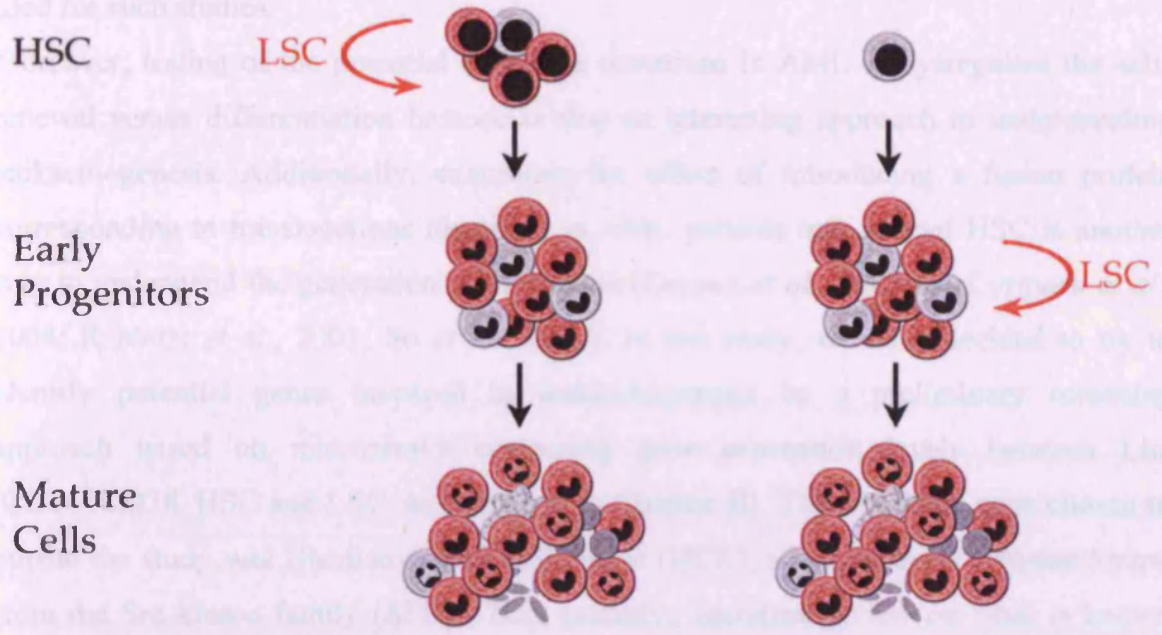


***Figure I.9:* The origin of the LSC.**

*The HSC is an attractive cell for the transformation into LSC, already having the ability to self-renew and having longevity, allowing enough time for the accumulation of genetic events required for transformation. However, the LSC could also arise from an early progenitor or mature cell that regains the ability to self-renew. Regardless of the site of origin, the bulk of the blast cells resulting would be the same.*

Although HSC and LSC are both quiescent, share the same surface marker phenotype and are capable to engraft NOD/SCID mice, LSC exhibit a dramatic increase in self-renewal ability over normal HSC while showing a block in differentiation. As mentioned earlier, this observation points out a major dysregulation of the balance between self-renewal and differentiation in HSC as an essential feature of leukaemogenesis. Thus, gaining understanding on how these processes are regulated in normal haematopoiesis is important for the understanding of how AML and other haematological malignancies are generated. Many studies have therefore been directed towards deciphering which genes regulate the decision of the HSC to follow either route during normal haematopoiesis. Various techniques such as knock-out and knock-in mice or overexpression and

downregulation of genes in HSC or other subsets of cells using viral vectors have been used for such studies.

Moreover, testing of the potential of known mutations in AML to dysregulate the self-renewal versus differentiation balance is also an interesting approach in understanding leukaemogenesis. Additionally, examining the effect of introducing a fusion protein corresponding to translocations identified in AML patients into normal HSC is another way to understand the generation of leukaemia (Drynan *et al.*, 2005; McCormack *et al.*, 2008; Rabbitts *et al.*, 2001; So *et al.*, 2003). In this study, we have decided to try to identify potential genes involved in leukaemogenesis by a preliminary screening approach based on microarrays comparing gene expression levels between $Lin^-$ /$CD34^+$/$CD38^-$ HSC and LSC, as described in Chapter III. The candidate gene chosen to pursue the study was Haematopoietic cell kinase (HCK), a non receptor tyrosine kinase from the Src kinase family (SFK) . Non exclusive literature review on what is known about SFK, cancer, haematopoiesis and leukaemogenesis will follow.

# 2. Src Family Kinases

## 2.1 SFK and cancer

### 2.1.1 v-src: the first oncogene from a big family

v-src was first discovered by Rous as a mutated gene captured in the genome of a retrovirus capable of causing sarcoma in chicken (Rous, 1911a; Rous, 1911b). Seven decades later the cellular homologue of v-Src, c-Src, was isolated (Stehelin *et al.*, 1976; Takeya *et al.*, 1982) and it was established that the gene encoded in the Rous sarcoma virus (RSV) genome, was coding for a protein with phosphorylation activity specifically directed towards tyrosine residues (Hunter and Sefton, 1980). It was then confirmed that this tyrosine kinase activity was required for RSV transformation (Sefton *et al.*, 1980; Shalloway *et al.*, 1981). Src was therefore not only ascertained as the first proto-oncogene but also as the first protein tyrosine kinase.

Three of the nine members of the Src kinase family were isolated as oncogenes before being identified as cellular genes. v-Yes is able to induce sarcoma in chicken (Hunter and Sefton, 1980) while v-Fgr induces sarcoma in cats (Naharro *et al.*, 1983). Fyn, Lyn, Hck, Lck and Blk were later cloned and classified as Src family kinases (SFK) based on sequence homology. Their implication in cancer is becoming more and more evident. Yrk is the most recently found member of the family and is only expressed in chicken (Sudol *et al.*, 1993).

### 2.1.2 SFK tissue specific expression

One or more SFK are expressed in one given cell type and tissue specific splice variants as well as alternative translation initiation products result in the existence of at least 16 Src-related gene products. Src, Fyn and Yes are ubiquitously expressed with increased

expression in specific tissues (Brown and Cooper, 1996). Src exists as three splice variants, c-Src and two n-Src, alternative splice variants with an additional exon exclusively expressed in neurons (Modafferi and Black, 1999). Fyn also exists as three splice variants: Fyn, FynT and FynB. FynT and FynB contain two different extra seventh exons in comparison to Fyn and are found exclusively in T-cells and in neurons respectively (Davidson *et al.*, 1992; Picard *et al.*, 2002). The other members of the family are solely found in the haematopoietic system with specific expression between the different cell types constituting the system (Varmus and Lowell, 1994). Lyn exists as two alternatively spliced isoforms that are co-expressed together and primarily found in B cells and monocytes (Yi *et al.*, 1991). The two isoforms from HCK are produced by the use of two different translation start codons and are found co-expressed in monocytes, neutrophils and immature B-cells (Lock *et al.*, 1991; Taguchi *et al.*, 2000). Lck is expressed in T-cells and Fgr in monocytes, natural killer cells and neutrophils; they both exist as one protein originating from one single transcript. *Figure I.10* shows the specific combination of SFK expressed at a definite level of expression by the different haematopoietic lineages (Corey and Anderson, 1999).

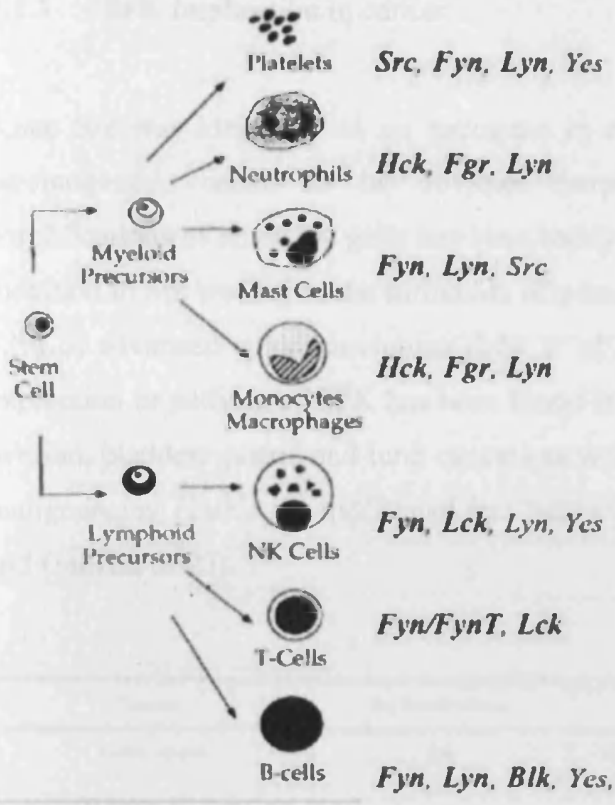


***Figure I.10:* Expression of src family kinases in haematopoietic cells.**

*Expression of SFK increases as cells differentiate into one particular lineage. Adapted from Cooper et al. (Cooper and Howell, 1993; Varmus and Lowell, 1994).*

It also has to be kept in mind, that SFK expression varies during haematopoiesis and cell differentiation. Evidence came first from differentiation studies of the HL-60 AML FAB M2 cell line: indeed monocytic differentiation induced by treatment with 12-O-tetradecanoyl-phorbol-13-acetate (TPA) leads to expression of Fyn and Lyn while treatment with 1,25-dihydroxyvitamin D3 leads to expression of Fgr and Lyn. On the other hand, granulocytic differentiation following treatment with retinoic acid (RA) leads to strong expression of Fgr and weak expression of Fyn and Lyn (Katagiri *et al.*, 1991). HCK appears only following terminal differentiation of HL60 to monocytes and is even more abundant in HL-60 terminally differentiated into granulocytes using DMSO (Quintrell *et al.*, 1987). This was further confirmed using other leukaemic cell lines (Willman *et al.*, 1991).

### 2.1.3 SFK implication in cancer

Since Src was identified as an oncogene in chicken, searching for a role of SFK in carcinogenesis seems to be obvious. Surprisingly mutations, rearrangements or amplifications of any SFK gene has been rarely observed in human cancer. Only a point mutation in Src leading to the formation of a truncated protein has been found to occur in 12% of advanced colon carcinoma (Irby *et al.*, 1999). However, an increase in protein expression or activity of SFK has been found in colorectal carcinoma, breast, pancreatic, ovarian, bladder, gastric and lung cancers as well as in brain tumours and haematopoietic malignancies (*Table I.6* and(Benati and Baldari, 2008; Irby and Yeatman, 2000; Summy and Gallick, 2003).

| Disease | Src family kinase | Defect |
|---|---|---|
| Colon cancer | Src | ↑ Expression and activity, truncated form |
| | Lck | Ectopic expression |
| | Yes | ↑ Kinase activity |
| Breast cancer | Src | ↑ Activity |
| | Yes | ↑ Expression and activity |
| | Fyn | ↑ Expression and activity |
| Small cell lung cancer | Src | ↑ Expression |
| | Lck | Ectopic expression |
| PET | Lck | Ectopic expression |
| | Src | ↑ Expression |
| CML | Hck | ↑ Activity |
| | Lyn | ↑ Activity |
| AML | Lck | ↑ Expression |
| ALL | Lck | ↑ Expression |
| B-CLL | Lck | Ectopic expression |

***Table I.6:*** ***Variation in SFK expression and activity related to cancers adapted from*****(Benati and Baldari, 2008).**

## 2.2 Src / SFK structure and folding

SFK are proteins of 52-60 kDa which share a conserved structural organisation consisting of six distinct functional domains: 1) The N-terminal Src homology 4 (SH4) domain, 2) the unique domain, 3) the SH3 domain, 4) the SH2 domain, 5) the catalytic domain, or SH1 domain, and 6) the C-terminal tail. *Figure I.11* shows the crystal structure of Src as a model for the general structure of SFK. Each domain has a specific role either in the membrane localisation or in the kinase activity regulation that will be described in the following paragraphs.

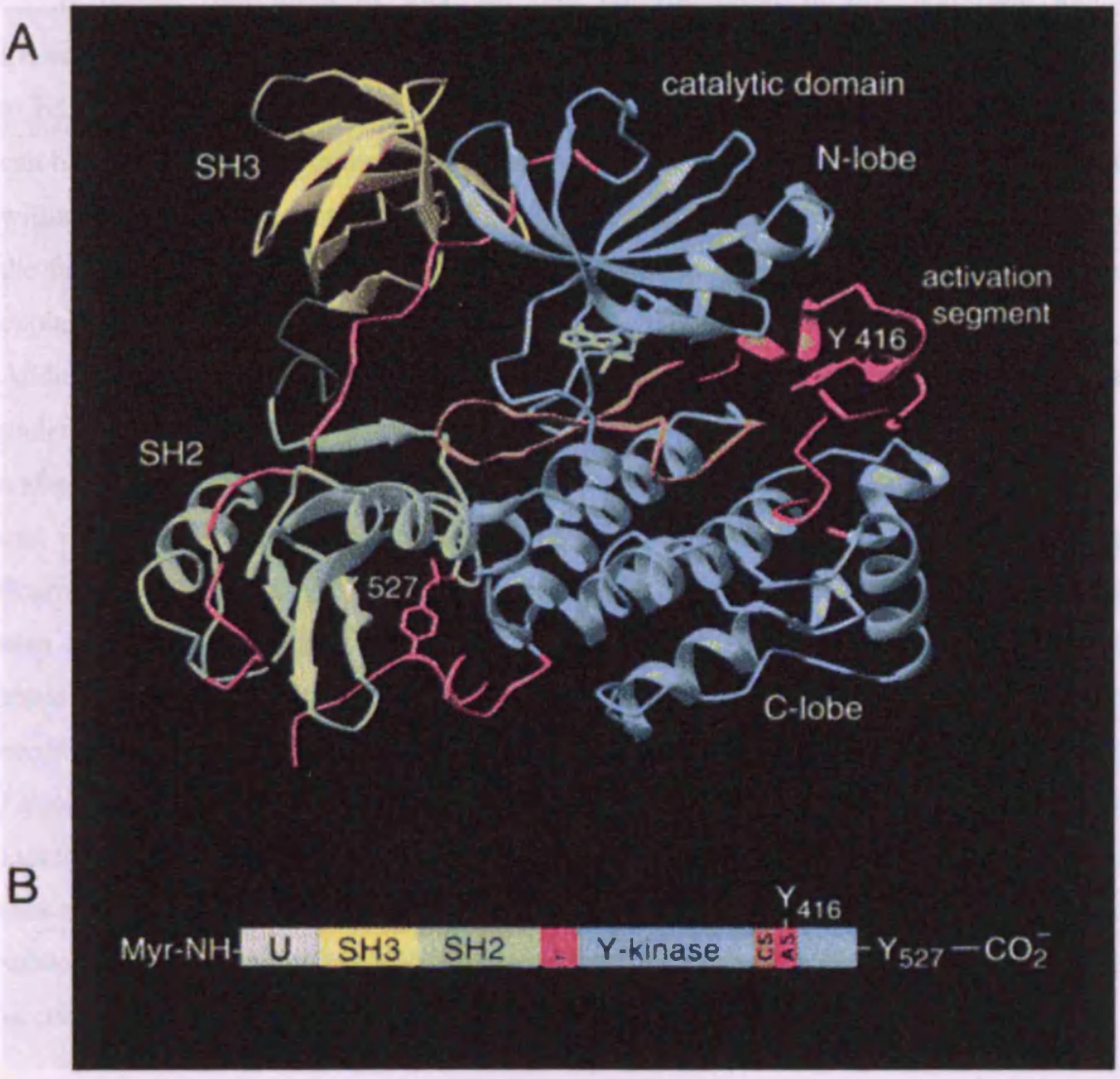


***Figure I.11:** Src family tyrosine kinase structure (Schindler et al., 1999).*

### 2.2.1 The SH4 domain is directing membrane localisation of SFK

SFK are cytoplasmic tyrosine kinases associated with either the plasma membrane or intracellular membranes such as the endoplasmic reticulum or the endosomes. Localisation to either compartment is dependent on the type of acyl modification undergone by the 10 to 15 amino acids SH4 domain. The first 7 to 10 amino acid residues serve as a recognition signal for an N-myristoyl transferase (Kaplan *et al.*, 1988; Pellman *et al.*, 1985) which catalyses the attachment of myristic acid to an invariant amino-terminal glycine residue following cleavage of the N-terminal methionine. Myristoylation occurs during translation of SFK on free polyribosomes in the cytoplasm and is irreversible (Buss *et al.*, 1984). This modification is necessary but not sufficient for SFK to be associated with the inner leaflet of the plasma membrane since myristoylated SFK can be also found in the cytoplasm (Levinson *et al.*, 1981). The presence of a lysine motif within the SH4 domain of most SFK contributes to their membrane targeting. Moreover the fact that several SFK share a common mechanism for membrane binding could also explain their functional redundancy (Silverman *et al.*, 1993).

Additionally to myristoylation, the SH4 domain of any SFK, except Src and Blk, can undergo posttranslational palmitoylation on conserved cystein residues at position 3 and/or 5. This reversible acylation occurs at the membrane on SFK already myristoylated and is required for targeting the proteins to lipid rafts (Robbins *et al.*, 1995; Shenoy-Scaria *et al.*, 1994). These specialised microenvironments within the plasma membrane, also known as calveolae, are enriched in glycosphingolipids, phosphoinositides and cholesterol as well as in distinctive integral membrane proteins and serve as signalling centres for the efficient integration of specific signals (Zajchowski and Robbins, 2002). Palmitoylation being reversible thanks to the action of palmitoylthioesterases (Linder and Deschenes, 2003), SFK might be relocalised to and from lipid rafts upon specific stimuli, thus establishing a mean of spacio-temporal regulation of SFK activation. Trimethylation subsequent to acylations has also been described for Fyn and is important for its function in cell adhesion and spreading (Liang *et al.*, 2004).

### 2.2.2 The unique domain confers specificity in cellular functions

The 50 to 70 amino acid long unique domain is highly divergent between the different SFK and is thought to confer specificity to each kinase by mediating interactions with specific receptors or cytoplasmic proteins. For instance the Lck unique domain mediates its interaction with CD4 and CD8α (Shaw *et al.*, 1989). Fyn and Lyn unique domains allow their association to T and B cell receptors (TCR and BCR) (Rudd *et al.*, 1993; Timson Gauen *et al.*, 1992).

### 2.2.3 Ligands with polyproline regions specifically bind to the SH3 domain

Src homology 3 domains (SH3 domains) are non-catalytic conserved domains that have been identified in many protein structures outside and including the SFK. The SH3 domain is approximately 50 amino acids long and confers specificity in protein-protein interactions through the recognition of short contiguous proline rich motifs that fold into a left-handed polyproline type II (PPII) helical conformation (Musacchio, 2002). The sequence requirements for SH3 ligands have been figured out by use of phage display and chemical combinatorial peptide libraries and the signature sequence of SH3 ligands has been found to be a PxxP motif (in which x represents any amino-acid) nestled into two conserved hydrophobic binding pockets (Cheadle *et al.*, 1994; Rickles *et al.*, 1994; Rickles *et al.*, 1995; Yu *et al.*, 1994). Flexibility in the amino acid composition outside of the proline rich motif allows for binding to different SH3 domains of specific proteins (Mongiovi *et al.*, 1999). Another mechanism that might govern ligand binding to SFK is phosphorylation of certain residues within the SH3 domain. This phenomenon has been reported for Src where, following PDGF receptor stimulation, SH3 domain phosphorylation occurs on its peptide binding surface and reduces its binding affinity for peptide ligands *in vitro* (Broome and Hunter, 1997). On the other hand, phosphorylation of the SH3 domain binding ligands themselves within the proline rich recognition site has also been reported and can affect the intensity of the protein-protein interaction (Wu *et al.*, 1998). It can be noticed that the two neuronal splice variants of Src, n-Src, differs

from c-Src by an insert of six or eleven amino acids in the SH3 domain (Brugge *et al.*, 1985; Martinez *et al.*, 1987). This insertion might biase their binding affinity towards a distinct set of substrates and render them more active than c-Src, probably because of a destabilisation of the inactive conformation (Levy and Brugge, 1989). Additionally to binding PxxP motif containing signalling proteins, in order to position SFK in a certain molecular environment, the SH3 domain plays an important role in the regulation of SFK activity via protein-protein interactions as well as via intramolecular contact. This point will be discussed in section 2.2.6. HIV-1 Nef (Saksela *et al.*, 1995), Ras GTPase activating protein (RasGAP), (Briggs *et al.*, 1995), a disintegrin and metallopeptidase domain 15 (ADAM15) (Poghosyan *et al.*, 2002), Wiskott-Aldrich syndrome protein (WASP), WASP-interacting protein (WIP), and engulfment and cell motility 1 (ELMO1) (Scott *et al.*, 2002), signal transducer and activator of transcription 3 (STAT3) (Schreiner *et al.*, 2002), activated Cdc42-associated kinase 1 (ACK1) (Yokoyama and Miller, 2003), the guanine nucleotide exchange factor C3G (Shivakrupa *et al.*, 2003) and p73 (Paliwal *et al.*, 2007) have been shown to be direct ligands for HCK SH3 domain, mostly by overexpression and interaction studies in Sf9 or COS cells.

### 2.2.4 Ligands with a specific phosphorylated tyrosine motif bind to the SH2 domain

Src homology 2 domains (SH2 domains) are also non-catalytic conserved domains that can be found in many protein structures outside and including the SFK and can be divided in four groups depending on the constitution of their consensus binding sequence (Pawson *et al.*, 2001; Songyang *et al.*, 1993). *Figure I.12* shows the main protein families containing SH2 domains, most of which are known to be direct interactors of SFK.

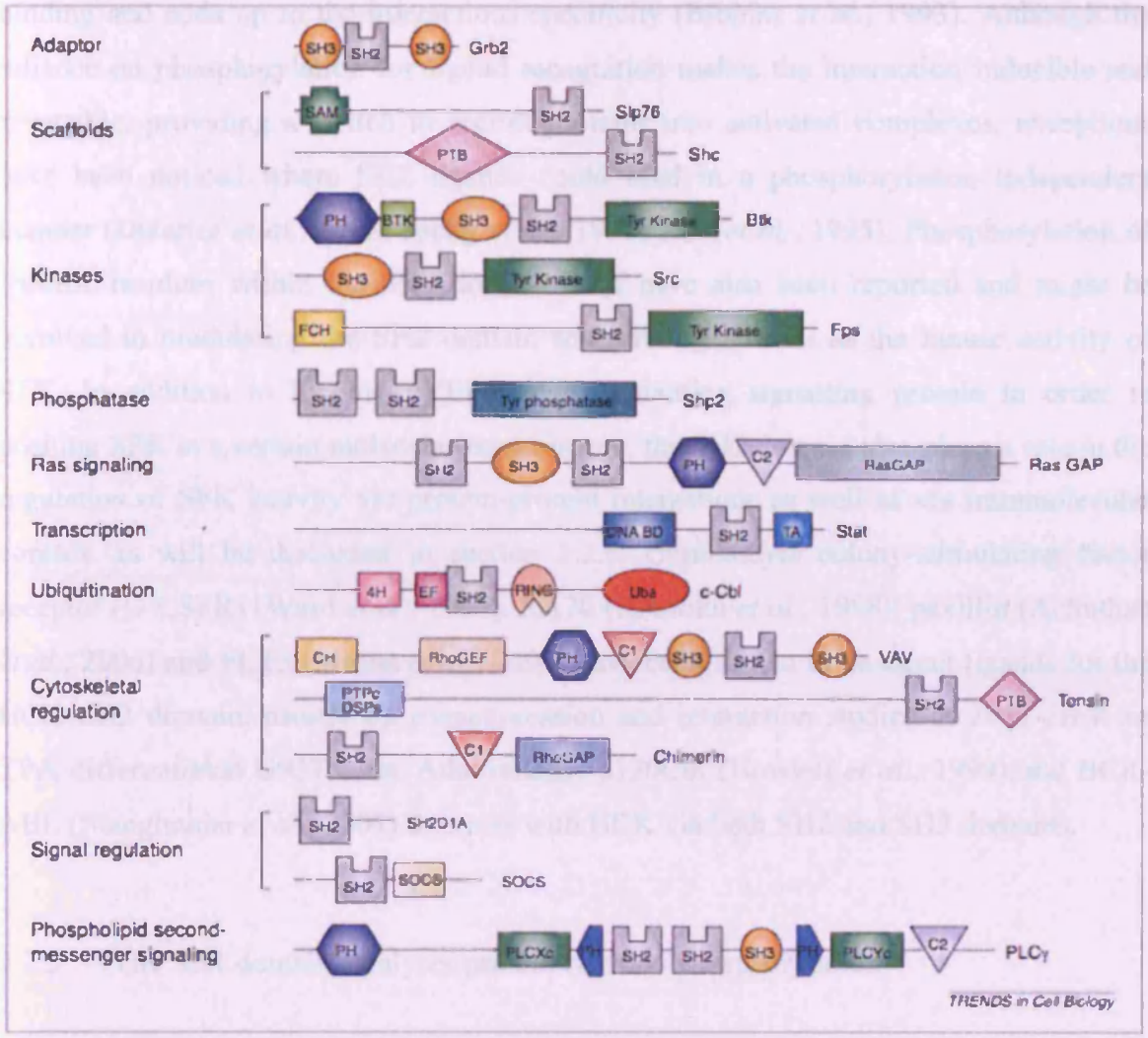


***Figure I.12:* Protein families containing SH2 and SH3 domains (Pawson et al., 2001).**

While SH3 domain interaction with a ligand is independent of posttranslational modification, interactions with the SH2 domain are phosphorylation dependent. The SFK SH2 domain belongs to group I SH2 domains and its consensus binding sequence has been identified as pYEEI. Group II to IV SH2 domains from other proteins select for different sequences with binding specifity being based on residues positioned C-terminal of the phosphorylated tyrosine, i.e . +1 through +6 (Songyang *et al.*, 1993). Mutation of a single critical residue can change the binding specificity of a SH2 domain from one group to the binding specificity of a SH2 domain from a different group, implicating a major change in ligand type and subsequent signal transduction cascade (Songyang *et al.*, 1995b). However, amino acids N-terminal to the phosphotyrosine are also involved in

binding and adds up to the interactions specificity (Bibbins *et al.*, 1993). Although the reliance on phosphorylation for ligand recognition makes the interaction inducible and reversible, providing a switch to recruit proteins into activated complexes, exceptions have been noticed where SH2 ligands could bind in a phosphorylation independent manner (Dutartre *et al.*, 1998; Joung *et al.*, 1996; Park *et al.*, 1995). Phosphorylation of specific residues within the SH2 domain itself have also been reported and might be involved in modulating the SH2 domain accessibility as well as the kinase activity of SFK. In addition to binding pYEEI motif containing signalling protein in order to position SFK in a certain molecular environment, the SH2 domain also plays a role in the regulation of SFK activity via protein-protein interactions as well as via intramolecular contact, as will be discussed in section 2.2.6. Granulocyte colony-stimulating factor receptor (G-CSFR) (Ward *et al.*, 1998), RA70 (Kouroku *et al.*, 1998), paxillin (Achuthan *et al.*, 2006) and FLT3 (Mitina *et al.*, 2007) have been shown to be direct ligands for the HCK SH2 domain, mostly by overexpression and interaction studies in 293T-HEK or TPA differentiated U937 cells. Additionally, p120Cbl (Howlett *et al.*, 1999) and BCR-ABL (Stanglmaier *et al.*, 2003) interacts with HCK via both SH2 and SH3 domains.

### 2.2.5 The SH1 domain catalyses protein tyrosine phosphorylation

The SH1 domain is the catalytic domain of the SFK and like for all eukaryotic protein kinases is shaped into a bilobal structure (Taylor *et al.*, 1993). The classic protein kinase conformation comprises a smaller N-terminal lobe connected by a flexible hinge region to a larger C-terminal lobe, with the active site located in the cleft inbetween the two lobes. The N-lobe is responsible for binding metal associated nucleotides. SFK being tyrosine kinases prefer $Mn2^+$ over $Mg2^+$ ions as co-factors *in vitro* (Hunter, 1989; Hunter and Cooper, 1985). A conserved lysine residue, K295 in c-Src and K290 in HCK, is present in the nucleotide binding pocket in the small lobe and co-ordinates the α- and β-phosphate groups of ATP. Mutation of this critical lysine residue results in the generation of an enzymatically inactive, or kinase dead, protein. The C-lobe is principally responsible for substrate binding and catalysis. The activation loop connecting the two

lobes contains an autophosphorylation site corresponding to Y416 in c-Src and to Y411 in HCK. Phosphorylation of this critical tyrosine, while not absolutely required for enzymatic activity, ensures maximal catalytic potential of SFK (Ferracini and Brugge, 1990). Affinity of substrate binding is dependent on recognition of certain tyrosines in a sequence specific context by certain residues in the activation loop itself (Laham *et al.*, 2000). The use of synthetic combinatorial peptide and phage display libraries have shown that different classes of tyrosine kinases preferentially bind to distinct sequences in their substrates (Nair *et al.*, 1995; Schmitz *et al.*, 1996; Songyang and Cantley, 1995; Songyang *et al.*, 1995a). It has actually been reported that distinct groups of protein tyrosine kinases phosphorylate peptidic motifs recognised by distinct groups of SH2 domain or can even phosphorylate motifs recognised by their own SH2 domain (Songyang *et al.*, 1995a). Catalytic domains are, however, autonomous from regulatory domains in terms of substrate/ligand specificity since fusion of the regulatory domains of EGF receptor ErbB to the catalytic domain of Src results in a chimeric protein inducing sarcoma formation (a Src property) without the leukaemogenic potential of ErbB (Chang *et al.*, 1995).

### 2.2.6 SFK folding and ligand interaction: a complex regulation of activity

Protein kinases are important molecular switches involved in the transmission of numerous cellular signals. As such, they must possess the inherent ability to alternate between catalytically active and catalytically inactive states. Point mutations and deletion studies suggested that such regulation was made possible by intramolecular interactions involving the SH2 and SH3 domains (Erpel *et al.*, 1995; Hirai and Varmus, 1990a; Hirai and Varmus, 1990b; O'Brien *et al.*, 1990; Reynolds *et al.*, 1992; Seidel-Dugan *et al.*, 1992; Veillette *et al.*, 1992). The C-terminal tail was also long known to have an influence on Src activity since the main difference between v-Src and c-Src resides in the fact that the C-terminal part of c-Src is replaced by a viral sequence in v-Src, rendering it sarcomagenic (Takeya *et al.*, 1981). Mutation studies revealed that tyrosine Y527 was a critical residue in restricting Src activity since its phosphorylation by the kinase Csk led

to suppression of fibroblast transformation by activated c-Src but not by v-Src or mutant Y527F (Sabe *et al.*, 1992). Additional mutations studies also suggested a link between Y527 regulatory phosphorylation and SH2 and/or SH3 domains presence since mutations in, or deletion of, either domain led to SFK activity even when Y527 was phosphorylated (Okada *et al.*, 1993; Superti-Furga *et al.*, 1993). Crystal structures of inactive c-Src and HCK confirmed that phosphorylated Y527 (Y522 in HCK) was physically interacting with the SH2 domain - reminding that SH2 domain typically interact with a phosphotyrosyl motif (Sicheri and Kuriyan, 1997; Sicheri *et al.*, 1997). However, this interaction is not obstructing the catalytic site directly, but rather positioning the SH2 domain on the other side of the molecule making contact with the C-terminal lobe of the kinase domain (as best visible on *Figure I.11*).

Comparing crystal structures of inactive SFK to the crystal structure of active Lck (Yamaguchi and Hendrickson, 1996) revealed that the intramolecular interactions within inactive SFK were actually more complicated than expected. As shown on the schematic representation of the close inactive conformation of SFK (*Figure I.13 B*), a linker region connecting the SH2 domain and the kinase domain adopts a left-handed polyproline type II conformation, typical motif recognised by the SH3 domain, providing the basis for a tripartite interaction between the SH3 domain, the linker and the back of the N-terminal lobe of the kinase domain (*Figure I.13 C*).

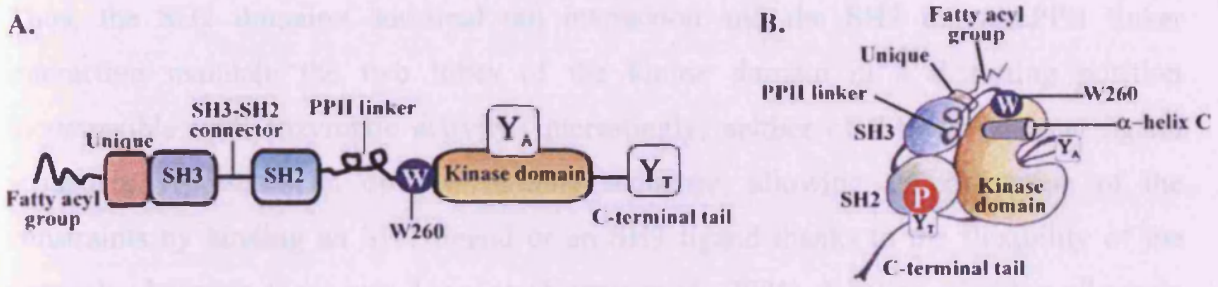

C.

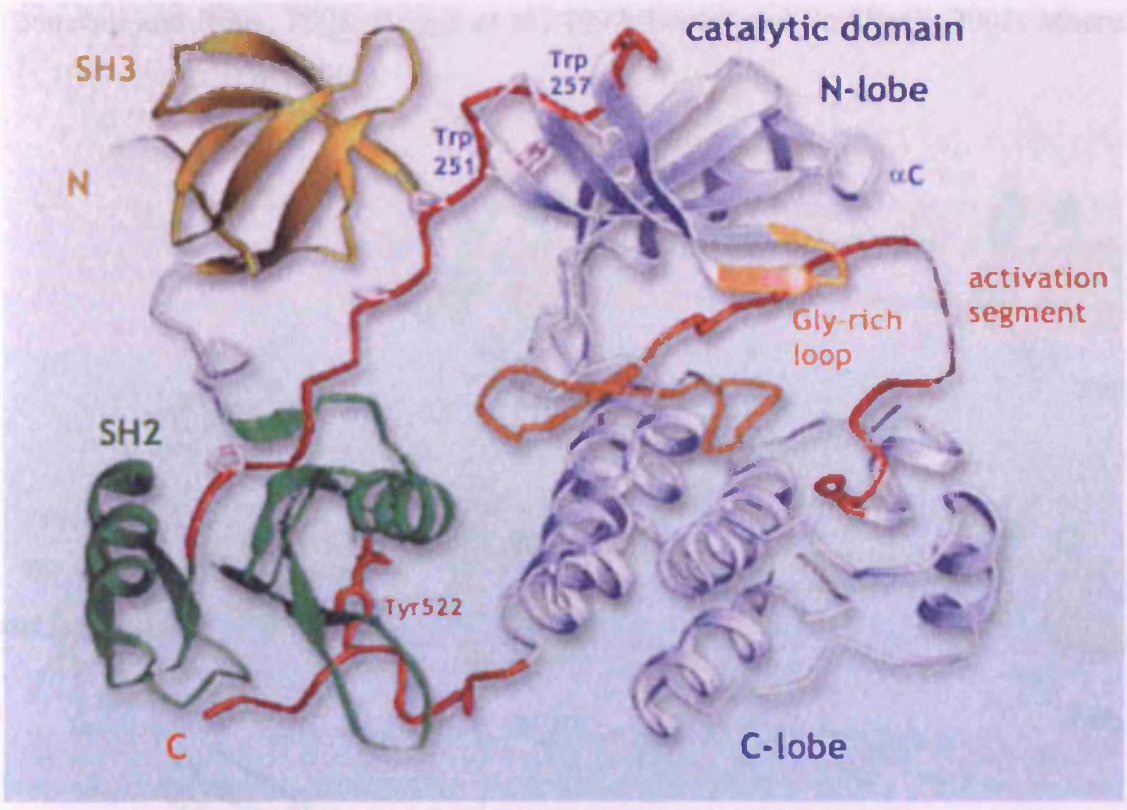


***Figure I.13:*** ***Crystal structure of HCK (Chong et al., 2005).***

*(A) Schematic representation of the hypothetical unfolded SFK. (B) Schematic representation of the close inactive conformation of SFK. (C) Crystal structure of HCK.*

Thus, the SH2 domain:C-terminal tail interaction and the SH3 domain:PPII linker interaction maintain the two lobes of the kinase domain in a distorting position incompatible with enzymatic activity. Interestingly, neither of the two internal ligand sequences represents an optimal binding sequence, allowing for disruption of the constraints by binding an SH2 ligand or an SH3 ligand thanks to the flexibility of the connector between these two domains (Young *et al.*, 2001). Binding of either allosteric effector, which exert higher binding affinity than the intramolecular sequences, or dephosphorylation of Y527 in the C-terminal tail allow for ultimate autophosphorylation of Y416 in the activation loop and adoption of a fully catalytically active conformation. It was first thought that dephosphorylation of Y527 was necessary for phosphorylation of Y416 to happen but a multitude of recent studies have proven that several intermediate

active states could lead to the ultimate fully active state as illustrated in *Figure I.14* (Banavali and Roux, 2008; Briggs *et al.*, 1997; Lerner and Smithgall, 2002; Moarefi *et al.*, 1997; Porter *et al.*, 2000).

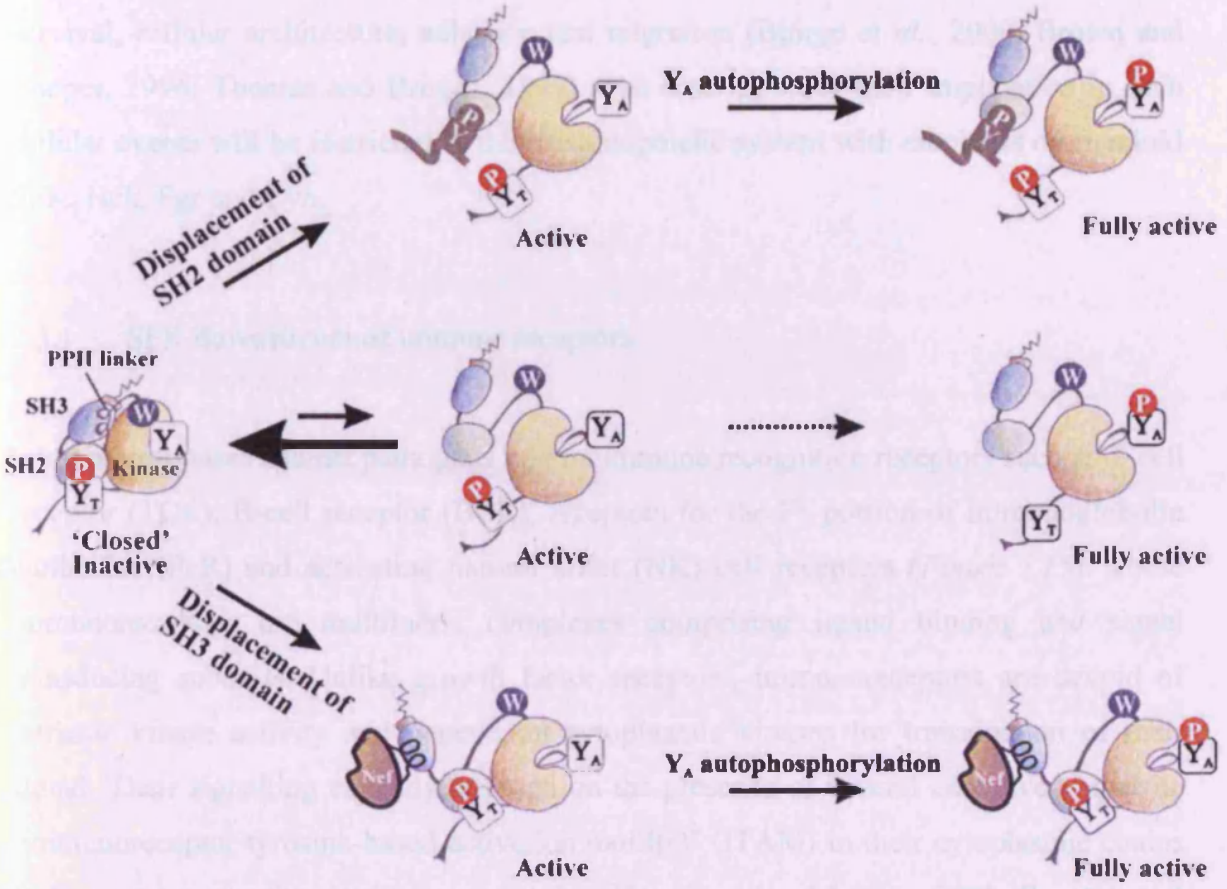


***Figure I.14:*** ***Possible interactions leading to change of conformation from a closed inactive state to an open fully active state of SFK (Chong et al., 2005).***

Of note, none of the crystal structures resolved to date include the SH4 and unique domains (Sicheri *et al.*, 1997; Xu *et al.*, 1997). Since the unique domain is divergent for each SFK, resolution of full length protein crystal structures might reveal that the regulations described previously may slightly differ inbetween SFK depending on the extent to which the N-terminal regions folding influences the reported conformation of the SH1, SH2 and SH3 domains.

## 2.3 Functions of SFK in the mature haematopoietic system

SFK are activated downstream of several cell surface receptors and have been implicated in mediating a variety of signals leading to changes in proliferation, differentiation, survival, cellular architecture, adhesion and migration (Bjorge *et al.*, 2000; Brown and Cooper, 1996; Thomas and Brugge, 1997). The description of their implication in such cellular events will be restricted to the haematopoietic system with emphasis on myeloid SFK, Hck, Fgr and Lyn.

### 2.3.1 SFK downstream of immune receptors

Immune responses against pathogens rely on immune recognition receptors such as T-cell receptor (TCR), B-cell receptor (BCR), receptors for the Fc portion of immunoglobulin antibodies (FcR) and activating natural killer (NK) cell receptors (*Figure I.15*). These immunoreceptors are multimeric complexes comprising ligand binding and signal transducing subunits. Unlike growth factor receptors, immunoreceptors are devoid of intrinsic kinase activity and depend on cytoplasmic kinases for transduction of their signal. Their signalling capacity is based on the presence of several conserved bipartite 'immunoreceptor tyrosine-based activation motif(s)' (ITAM) in their cytoplasmic chains or in receptor-associated adaptor molecules (Hamerman and Lanier, 2006; Ravetch and Lanier, 2000).

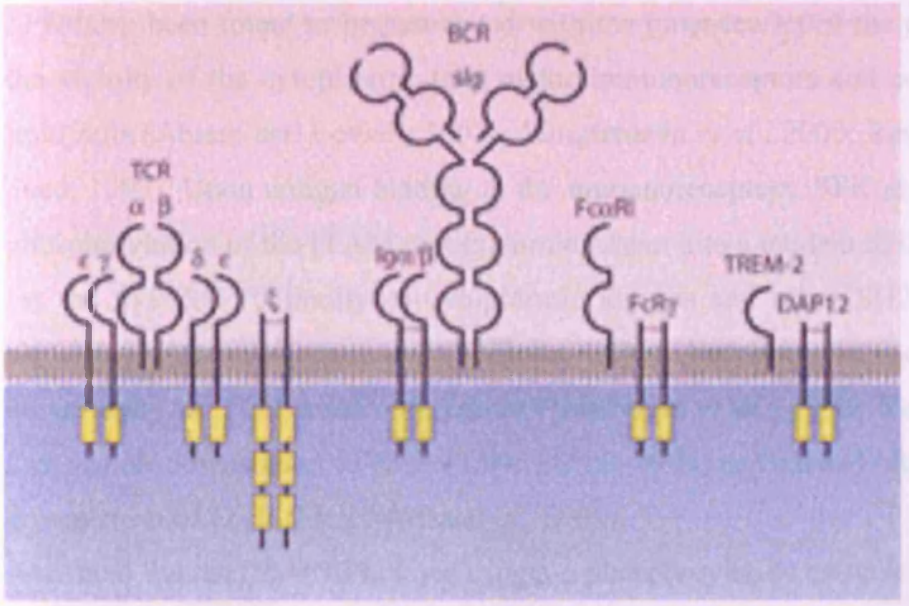


***Figure I.15:*** ***ITAM-bearing adaptors and immunoreceptors (Hamerman and Lanier, 2006).***

*The α and β chains of the T cell receptor (TCR) associate with the CD3 family of ITAM-containing adaptors. CD3δ, γ, and ε each contain one cytoplasmic ITAM and one extracellular Ig domain and are found exclusively in T-cells. CD3ζ displays three ITAMs and forms a disulphide-bonded homodimer. CD3ζ is also found in T-cells as well as in NK cells, where it associates with several activating NK receptors. The B cell receptor (BCR) is composed of surface immunoglobulin (sIg) associated with a disulphide-bonded heterodimer of Igα and Igβ, each of which contains one ITAM and one extracellular Ig domain similar to CD3δ, γ, and ε. Igα and Igβ are exclusively expressed in B-cells. The FcεRIγ (FcRγ) ITAM-containing adaptor is expressed in myeloid cells, B-cells, and NK cells and in some T-cells. FcεRIγ consists of a minimal extracellular domain with one cytoplasmic ITAM and forms a disulphide-bonded homodimer (of note, in some cells FcεRIγ forms a disulphide-bonded heterodimer with CD3ζ). FcεRIγ can associate with various receptors, including FcαRI (also known as CD89) depicted here. DAP12 has a structure and expression pattern similar to that of FcRγ. In myeloid cells and NK cells, DAP12 associates with various receptors, including TREM-2 depicted here.*

SFK have been found to be associated with the inner-leaflet of the plasma membrane in the vicinity of the cytoplasmic tails of the immunoreceptors and adaptors organised as lipid rafts (Abram and Lowell, 2007b; Ilangumaran *et al.*, 2000; Resh, 1996; Xavier and Seed, 1999). Upon antigen binding to the immunoreceptors, SFK are responsible for the phosphorylation of the ITAM motifs, turning them into a tandem SH2 ligand docking site for the Syk/ZAP70 family of cytoplasmic kinases and other SH2 domain containing signalling proteins (Latour and Veillette, 2001). For example, Lck and FynT signal downstream of TCR immunoreceptors (Gassmann *et al.*, 1992; Veillette *et al.*, 1988), Lyn signals downstream of BCR (Takata *et al.*, 1994) as well as FcR. Fgr and Hck signal downstream of FcγR (Fitzer-Attas *et al.*, 2000).
Activated Syk and ZAP70 kinases trigger a phosphorylation cascade implicating proteins such as SLP-76, phosphatidylinositol 3-kinase (PI3K), and Vav family members, leading to activation of MAPKs and actin cytoskeletal reorganisation. Specific cellular responses follow, e.g. proliferation and cytokine production for T-cells, proliferation and antibody secretion for B-cells and degranulation and respiratory burst for granulocytic cells.

SFK are also implicated in regulation of the immune response by phosphorylating 'immunoreceptor tyrosine-based inhibitory motif(s)' (ITIM) within the cytoplasmic tails of negative regulatory receptors such as CD22 in B-cells, killer inhibitory receptors (KIR) in NK and cytotoxic T-cells, FcγRIIB, PIR-B or SHPS-1/SIRPα in myeloid cells (Abram and Lowell, 2007a). Phosphorylated ITIM motifs serve as SH2 ligand docking site for phosphatases SHP1 and SHP2 (SH2-domain-containing phosphatase 1 and 2) or lipid phosphatase SHIP1 (SH2-domain-containing inositol phosphatase 1) depending on the cellular context. In turn, these phosphatases dephosphorylate phospho-ITAM and autophosphorylated SFK leading to immune signal attenuation (Abram and Lowell, 2007b).
Thus, immune signal transmission and immune response regulation are dependant on the specific composition of lipid rafts at the surface of a given haematopoietic cell bringing together immunoreceptors, ITAM-containing adaptors, SFK and ITIM-containing inhibitory receptors which would recruit Syk/ZAP70 kinases as transducers and phosphatases as inhibitors (*Table I.7*). The mechanism by which SFK and subsequently

ITIM-containing inhibitory receptors are clustered to lipid rafts is currently poorly understood.

| Cell type | Immunoreceptor | ITAM adaptor | SFK | Syk or ZAP70 kinase | ITIM containing inhibitory receptors |
|---|---|---|---|---|---|
| T-cells | TCR | CD3ζ | Lck | ZAP70 | CTLA4 (CD152), PD1(CD279) |
| B-cells | BCR | Ig α and β (CD79 a and b) | Lyn | Syk | FcγRIIB, CD22 |
| Myeloid cells | FcR | FcRγ chain | Hck/Fgr/ Lyn | Syk | PIR-B, SIRPα, FcγRIIB (CD32) |
| NK cells | NK-activating receptors | DAP12 | Lck | ZAP70/Syk | KIR (CD158) |

***Table I.7:* Composition of lipid rafts for signalling downstream of immunoreceptors (Abram and Lowell, 2007a).**

*Differential composition of lipid rafts downstream of T-cells, B-cells, myeloid cells and natural killer (NK) cells immunoreceptors.*

### 2.3.2 SFK downstream of cytokine receptors

Haematopoietic cells possess the particularity of proliferating or differentiating strictly upon external stimulation by soluble cytokines or upon cell-to-cell interaction with bone marrow stromal cells, or would, by default, undergo apoptosis. This dependence on inducible cytokine secretion or vicinity to stromal cells allow for homeostasis of the blood cell composition. In response to leukaemia inhibitory factor (LIF), bone marrow stromal cells produce interleukins, IL-3 and IL-6, as well as granulocyte-macrophage colony-stimulating factor (GM-CSF), macrophage colony-stimulating factor (M-CSF) and granulocyte colony-stimulating factor (G-CSF) (Szilvassy *et al.*, 1996). Subsequently early haematopoietic progenitor cells stimulated with IL-3 and GM-CSF secrete IL-6, LIF and oncostatin M (OSM) (Yoshimura *et al.*, 1996). Multipotential progenitors can be stimulated by IL-3 and thrombopoietin (TPO) (Kaushansky, 1998) while IL7, IL-5, G-CSF, M-CSF and erythropoietin (EPO) stimulates lymphoid progenitors, eosinophils,

granulocytes, monocytes/macrophages and erythroblasts respectively. TPO also stimulates megakaryocyte proliferation and differentiation. Additionally, cytokines are produced by macrophages, mast cells and activated T-cells as part of the inflammatory response. Th1 helper T-cells secrete IL-2, tumor necrosis factor-β (TNFβ) and interferon-γ (IFNγ) while Th2 helper cells secrete IL-4, IL-5 and IL-10. Both Th1 and Th2 helper T-cells secrete IL-3 and GM-CSF and their own development is regulated by IL-12 and IL-4 respectively (Manetti *et al.*, 1993; Mosmann *et al.*, 2005; Takeda *et al.*, 1996; Thierfelder *et al.*, 1996). Cytokines appear to be pleiotropic and redundant therefore a considerable amount of studies have tried to decipher how they can initiate different signals.

Cytokines bind to their cognate receptor that are classified in five different subclasses. Most cytokine receptors consist of a specific ligand binding extracellular subunit and an intracellular signal transducing subunit that is common to the receptor of a given subclass (Taniguchi, 1995). They are devoid of intrinsic kinase activity and, like immunoreceptors, are dependant on cytoplasmic kinases for transduction of their signal (*Figure.I.16*).

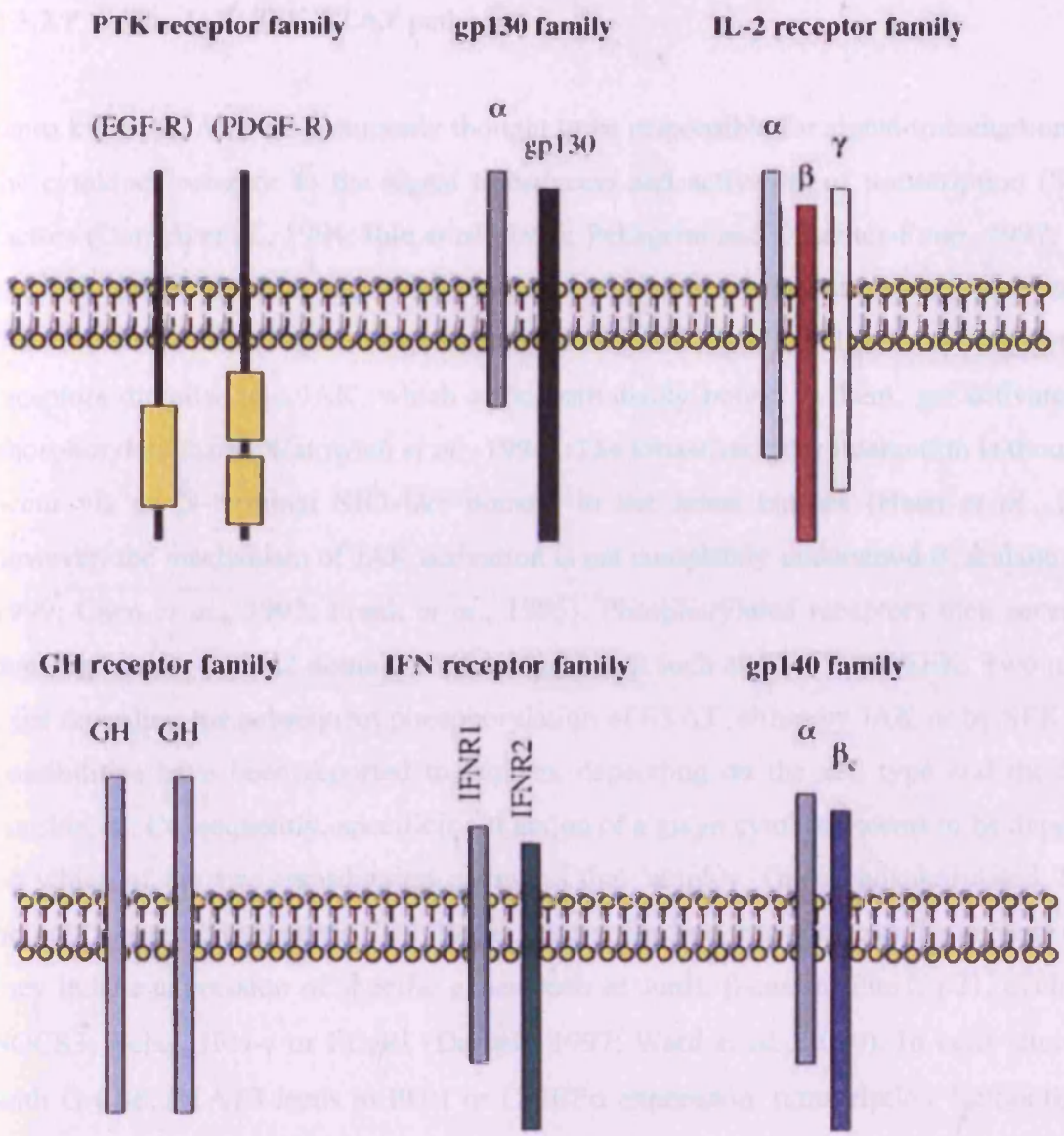


***Figure.I.16:*** ***Five subclasses of cytokine receptors (adapted from (Reddy et al., 2000).***

*Protein tyrosine kinase (PTK) receptor family is given as a counter example. The gp130 family signal through a common gp130 β-subunit and display a specific ligand binding α-subunit. The IL-2 receptor family signal through a common IL-2Rγ and a specific β-subunit; their ligand binds to a specific α-subunit. The GH family is structurally similar with a single subunit that homodimerises upon ligand binding. The IFN family is composed of paired signal transducing subunits that are structurally similar but distinct between the different members of the family. The gp140 family signal through a common gp140 β-subunit and possess a specific ligand binding α-subunit.*

#### 2.3.2.1 The JAK-SFK-STAT pathway

Janus kinases (JAK) are commonly thought to be responsible for signal transduction from the cytokines receptor to the signal transducers and activators of transcription (STAT) factors (Darnell *et al.*, 1994; Ihle *et al.*, 1995; Pellegrini and Dusanter-Fourt, 1997; Shuai and Liu, 2003; Ward *et al.*, 2000), but recent evidence implicate SFK in this axis of transduction as well (*Figure I.17;*(Rane and Reddy, 2002). Upon ligand binding, cytokine receptors dimerise and JAK, which are constitutively bound to them, get activated and phosphorylate them (Watowich *et al.*, 1994). The kinase/receptor interaction is thought to occur via an N-terminal SH2-like domain in the Janus kinases (Haan *et al.*, 2006), however, the mechanism of JAK activation is not completely understood (Cacalano *et al.*, 1999; Chen *et al.*, 1997; Frank *et al.*, 1995). Phosphorylated receptors then serve as a docking site for an SH2 domain containing protein such as STAT and SFK. Two models exist regarding the subsequent phosphorylation of STAT: either by JAK or by SFK. Both possibilities have been reported to happen, depending on the cell type and the STAT considered. Consequently, specificity of action of a given cytokine seems to be dependent on which of the two transduction pathways they employ. Once phosphorylated, STAT homo- or heterodimerise via SH2 domain interaction and translocate to the nucleus where they induce expression of specific genes such as JunB, β-casein, Pim1, p21, cyclin D1, SOCS3, $Bclx_L$, IFN-γ or FCγRI (Darnell, 1997; Ward *et al.*, 2000). In cells stimulated with G-CSF, STAT3 leads to PU.1 or C/EBPα expression, transcription factors that are essential for granulopoiesis (Numata *et al.*, 2005; Panopoulos *et al.*, 2002).

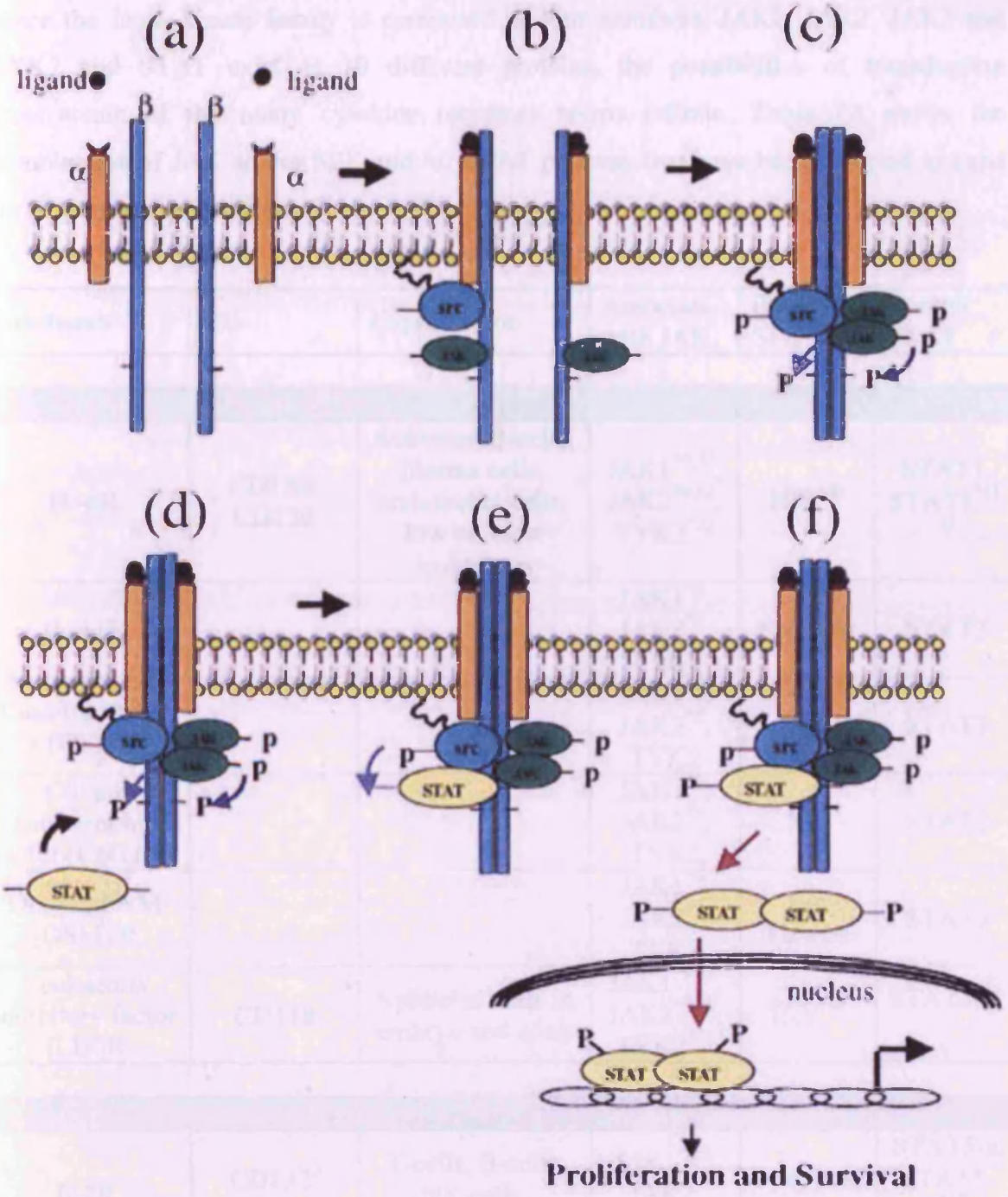


***Figure I.17:* The JAK-Src-STAT pathway (adapted from (Reddy et al., 2000).**

*Upon ligands binding, SFK are recruited to the cytokine receptors and phosphorylate the receptor in a JAK dependent or independent fashion, leading to STAT recruitment, phosphorylation and translocation into the nucleus.*

Since the Janus kinase family is composed of four members, JAK1, JAK2, JAK3 and TYK2 and STAT exist as 10 different proteins, the possibilities of transduction downstream of the many cytokine receptors seems infinite. *Table I.8* shows the combination of JAK and/or SFK and /or STAT pathway that have been reported to exist for each cytokine receptor.

| Subclasses | CD | Expressed on | Associate with JAK | Recruit SFK | Recruit STAT |
|---|---|---|---|---|---|
| | | | | | |
| **gp130 family** | | | | | |
| IL-6R | CD130/ CD126 | Activated B-cells, plasma cells, endothelial cells, low on most leukocytes | JAK1[*9,32], JAK2[*9,32], TYK2[*32] | Hck[*30] | STAT1, STAT3[*31, 32] |
| IL-11R | | | JAK1[*9], JAK2[*9], TYK2 | Src, Yes | STAT3 |
| Cardiotropin-1 (CT)R | | | JAK1[*9], JAK2[*9], TYK2 | ND | STAT3 |
| Ciliary neurotrophic factor (CNTF)R | | | JAK1[*9], JAK2[*9], TYK2 | ND | STAT3 |
| Oncostatin M (OSM) R | | | JAK1[*9], JAK2[*9], TYK2 | Src kinases | STAT3 |
| Leukaemia inhibitory factor (LIF)R | CD118 | Epithelial cells in embryo and adult | JAK1[*9,32], JAK2[*9,32], TYK2[*32] | Hck[*30] | STAT3[*31, 32] |
| | | | | | |
| **IL-2 receptor family** | | | | | |
| IL2R | CD132/ CD122 | T-cells, B-cells, NK cells, monocytes | JAK1[*1,2], JAK2, JAK3[*1,2] | Fyn, Lck, Hck | STAT5-a, STAT5-b[*17], STAT3 |
| IL-4R | CD132/ CD124 | Monocytes, haematopoietic precursors, epithelial cells, low on lymphocytes | JAK1[*1,2], JAK3[*1,2] | Lck | STAT6[*17] |
| IL-7R | CD132/ | T-cells, pro B- | JAK1[*1,2], | Lyn | STAT5-a, |

| | | | | | |
|---|---|---|---|---|---|
| | CD127 | cells | JAK3[*1,2] | | STAT5-b, STAT3 |
| IL-9R | CD132/ | | JAK3[*1,2] | ND | STAT5-a, STAT5-b, STAT3 |
| IL-15R | CD132/ | Activated monocytes | JAK1[*2], JAK3[*2] | Lck | STAT5-a, STAT5-b, STAT3 |
| | | | | | |
| Growth hormone family | | | | | |
| Growth hormone (GH)R | | | JAK2[*4,9] | Src kinases | STAT5-a, STAT5-b, STAT3 |
| Prolactin (PRL)R | | | JAK2[*10] | Src[*28] | STAT6, STAT5-a, STAT5-b, STAT3 |
| Erythropoietin (EPO)R | | | JAK2[*6,7,8, 9,24] | Src[*29], Lyn[*27,33] | STAT5-a, STAT5-b[*14,17,24,29, 33] |
| G-CSFR | CD114 | Myeloid progenitors, endothelial cells | JAK2, JAK3 | Lyn, Hck[*32] | STAT3, STAT5 |
| Thrombopoietin (TPO)R | CD110 | Megakaryocytes, platelets, some CD34low stem cells | TYK2, JAK2 | ND | STAT5-a, STAT5-b |
| | | | | | |
| Interferon family | | | | | |
| Interferon α receptor (IFNAR) | CD120a or b | Haematopoietic and non haematopoietic cells | JAK1, TYK2 | Lck | STAT1, STAT2 |
| Interferon γ receptor (IFNGR) | CDw119 | Macrophage, monocytes, B-cells, T-cells, NK cells neutrophils, endothelial cells | JAK1[*5], JAK2[*5] | Hck, Lyn | STAT1[*15, 16] |
| IL-10R | CDw210 | T-cells, B-cells, NK cells, monocytes, macrophages | JAK1, TYK2 | ND | STAT1, STAT3 |

| gp140 family | | | | | |
|---|---|---|---|---|---|
| IL-3R | CD131/ CDw123 | Lymphoid subset, basophils, haematopoietic progenitors, macrophages, DC cells, megakaryocytes | JAK2[*11] | Lyn, Hck[*25], Fyn | STAT5-a, STAT5-b[*17,18,23], STAT3 STAT6[*17] |
| IL-5R | CD131/ CDw125 | Eosinophils, basophils | JAK2[*13,19] | (Btk) | STAT1[*22], STAT5-a, STAT5-b[*19,23], STAT3[*21] |
| GM-CSFR | CD131/ CD116 | Monocytes, granulocytes, DCs, endothelial cells | JAK2[*3,12,20] | Lyn, Hck[*26] | STAT5-a, STAT5-b[*20,23] |

***Table I.8:*** ***JAK, SFK and STAT known to interact with each member of the five subclasses of cytokine receptors (adapted from (Rane and Reddy, 2002).***

*Compilation of references mentioning interactions between one or more of the JAK, SFK, STAT and/or cytokine receptors. *1 (Russell et al., 1994) *2(Russell et al., 1995) *3 (Zhao et al., 1995) *4(Frank et al., 1995) *5(Kohlhuber et al., 1997) *6(Watowich et al., 1994) *7(Witthuhn et al., 1993) *8(Miura et al., 1994) *9 (Tanner et al., 1995)*10(DaSilva et al., 1994) *11(Silvennoinen et al., 1993) *12(Quelle et al., 1994) *13(Takaki et al., 1994) *14(Barber et al., 2001) *15(Kovarik et al., 2001) *16(Kotenko et al., 1996) *17(Quelle et al., 1995) *18(Azam et al., 1995) *19(Kouro et al., 1996) *20(Matsuguchi et al., 1997) *21(Caldenhoven et al., 1995) *22(van der Bruggen et al., 1995) *23(Mui et al., 1995) *24(Wakao et al., 1995) *25(English, 1996) *26(Linnekin et al., 1994) *27(Chin et al., 1998) *28(Kazansky et al., 1999) *29(Okutani et al., 2001) *30(Ernst et al., 1999) *31 (Meyn et al., 2005) *32(Ernst et al., 1996) *32 (Ward et al., 1998) *33 (Ingley et al., 2005)*

When looking at JAK association per cytokine receptor subfamily, gp130 subfamily and gp140 subfamily each associates with a specific group of JAK. This selection is determined by motifs within the cytokine receptors (Jiang *et al.*, 1996; Narazaki *et al.*, 1994). Similarly, the type of STAT getting phosphorylated in a system is dependent on

binding sequences on the cytokine receptor and not on the type of JAK bound to the receptor, therefore the gp130 and IFN subfamilies never phosphorylate STAT5 isoforms, while the GH-R and IL-2R subfamilies never phosphorylate STAT1 (*Table I.8*). On the other hand, while most members of these two subclasses phosphorylate STAT3 and STAT5, the GH-R subclass uses JAK2 while the IL-2R subclass barely does. Differences in pattern of association between gp140 and GH-R subclasses are a priori more subtle to figure out. Activation pattern is probably also dependent on JAK availability since JAK3 expression is restricted to the haematopoietic system, while other JAK are ubiquitous. Transphosphorylation of JAK has been reported where stimulation and aggregation of one type of cytokine receptor triggers the activation of several JAK that are necessary for further signal transduction (Oakes *et al.*, 1996; Rodig *et al.*, 1998).

Most of the work linking SFK to the JAK-STAT pathway has been done in the IL-3 dependent murine 32Dcl3 cell line. This cell line undergoes apoptosis in the absence of IL-3, a phenomenon bypassed by overexpression of transforming v-Src (Kruger and Anderson, 1991). Furthermore, the v-Src infected cells lose their capacity to differentiate into mature granulocytes upon G-CSF stimulation, implicating an action of Src downstream of both the IL3 receptor and the G-CSF receptor in this model. Examination of the JAK phosphorylation status showed that they were not activated by v-Src while STAT1, STAT3 and STAT5 were. However, direct interaction could only be proven between v-Src and STAT3; STAT1 and STAT5 did not immunoprecipitate with Src (Chaturvedi *et al.*, 1997). Interdependence of the JAK and SFK is proven in IL-3 stimulated 32Dcl3 cells: in these cells, JAK1, JAK2 and Src are phosphorylated but a dominant negative mutant of JAK2 does not influence STAT3 phosphorylation, while a dominant negative mutant of Src prevents STAT3 phosphorylation (Chaturvedi *et al.*, 1998). Of note, v-Fgr does not abrogate 32Dcl3 cells' IL-3 dependence or capacity to terminally differentiate following G-CSF stimulation (Chaturvedi *et al.*, 1997). However, HCK overexpression lengthens 32Dcl3 cells' viability in absence of IL-3, without leading to independence and, surprisingly, blocks G-CSF induced granulocytic differentiation (English, 1996). Of note, another murine IL-3 dependent cell line, NFS-60, which proliferates rather than differentiates in the presence of G-CSF, shows activation of HCK

following G-CSF stimulation (32Dcl3 cell line does not express HCK) where HCK directly interacts and phosphorylates G-CSFR. In these two cell lines, activation of JAK1, JAK2, Tyk2, STAT1 and STAT3 is observed while it is not the case in terminally differentiated neutrophils also stimulated with G-CSF (Avalos *et al.*, 1997). In neutrophils, Lyn has been implicated in transmitting the G-CSF signal (Corey *et al.*, 1994). Thus, in overexpression systems, SFK differentially mediate the signal of a given cytokine receptor, probably via a SH2 and SH3 domains interaction based STAT recruitment and phosphorylation (Chaturvedi *et al.*, 1997).

Implication of HCK in the GM-CSF transduction pathway has been shown in neutrophils (Wei *et al.*, 1996) and in the AML FAB M2 HL-60 cell line, however HL60 cells required differentiating pretreatment with DMSO, retinoic acid (RA) or 1,25 dihydroxyvitamin D3 (Linnekin *et al.*, 1994). In G-CSF and GM-CSF studies, Lyn seemed to be constitutively associated with the cytokine receptor while HCK was only recruited upon cytokine stimulation.

Another example of linking SFK to STAT activation without requirement of JAK is found in BCR-ABL transduced cells. Indeed, Lyn and HCK have been shown to be phosphorylated in BCR-ABL transduced 32D cells (Danhauser-Riedl *et al.*, 1996) and HCK has been implicated in BCR-ABL induced IL-3 independence of the DAGM cell line. In these BCR-ABL transduced cells, cytokine independence was abolished by co-expression of a kinase dead mutant of HCK while co-expression of wild-type HCK only partially restrained the independence, suggesting the activation of several SFK for IL-3 independence (Lionberger *et al.*, 2000). In BCR-ABL expressing 32Dcl3 cells, HCK has been shown to directly interact with STAT5 and phosphorylate it while BCR-ABL itself is present in the immunocomplex but does not directly bind to STAT5 (Klejman *et al.*, 2002).

It is important to notice that all these studies implicating HCK have been done in BCR-ABL transduced cells and are also independent of any cytokine receptor stimulation. In cell lines derived from CML patients such as K562, STAT-5, JAK1, JAK2 (Chai *et al.*, 1997) and Lyn are constitutively phosphorylated while HCK is not (Donato *et al.*, 2003), (Danhauser-Riedl *et al.*, 1996). Other evidence of possible interaction of SFK with STAT comes from overexpression studies in insect cells (Schreiner *et al.*, 2002). In such studies,

proven direct interaction between SFK and STAT3 implicates the SFK SH3 domain but is not exactly physiological. Studies in murine embryonic stem cells (ES cells) indicate a direct interaction between HCK and the gp130 subunit which mediate LIF dependence for maintenance of self-renewal property (Ernst *et al.*, 1994). Further studies have also implicated JAK1, JAK2, TYK2 and STAT3 in this process, though JAK and SFK did not act through the same pathway (Ernst *et al.*, 1999; Ernst *et al.*, 1996; Meyn *et al.*, 2005). Moreover, overexpression of constitutively active HCK led to LIF independence for maintenance of undifferentiation, a phenotype shared by activated v-Ras (Ernst *et al.*, 1996). Studies in IL-3 dependent Baf-B03 cell lines transduced with an EpoR-gp130 chimaera confirmed interaction between HCK and the gp130 subunit that transduced a proliferation signal (Schaeffer *et al.*, 2001). Physiological interaction of SFK and gp130 has also been confirmed in multiple myeloma cell lines (Hallek *et al.*, 1997; Hausherr *et al.*, 2007). Of importance, studies using SFK inhibitors revealed that maintenance of an undifferentiated state was a matter of balance between different SFK expression and activation. It was observed that differentiating cells, following LIF withdrawal, naturally downregulated HCK and Lck, while, paradoxically, complete inhibition of all SFK led to LIF independence for maintenance of pluripotency (which is consistent with the previous HCK overexpression experiments). On the other hand, partial inhibition of some SFK led to ES cells differentiation despite the presence of LIF (Meyn *et al.*, 2005).

#### 2.3.2.2 Regulation of the JAK-Src-STAT pathway

Various phosphatases such as PTPeC, SH-PTP1, PTP1B and SHP-1, SHP-2 and CD45 have been shown to dephosphorylate at least one member of the JAK family in a cytokine receptor dependent fashion (Rane and Reddy, 2002), SHP-1 can also dephosphorylate cytokine receptors directly. Of note SHP-1, SHP-2 and CD45 have also been implicated in dephosphorylating SFK downstream of immunoreceptors (as described previously) but not yet downstream of cytokine receptors. The family of supressors of cytokine signalling (SOCS) is also involved in the JAK-STAT pathway regulation by either binding directly to JAK in their catalytic domain or by binding to cytokine receptors, where they compete with STAT, therefore inducing a downregulation of the signal transduction (*Figure I.18*).

Action of SOCS can also imply ubiquitination of JAK bound to cytokine receptors. Since STAT3 has been shown to induce gene transcription of at least SOCS3, SOCS regulation acts as an inducible feedback loop (Brender *et al.*, 2001; He *et al.*, 2003).

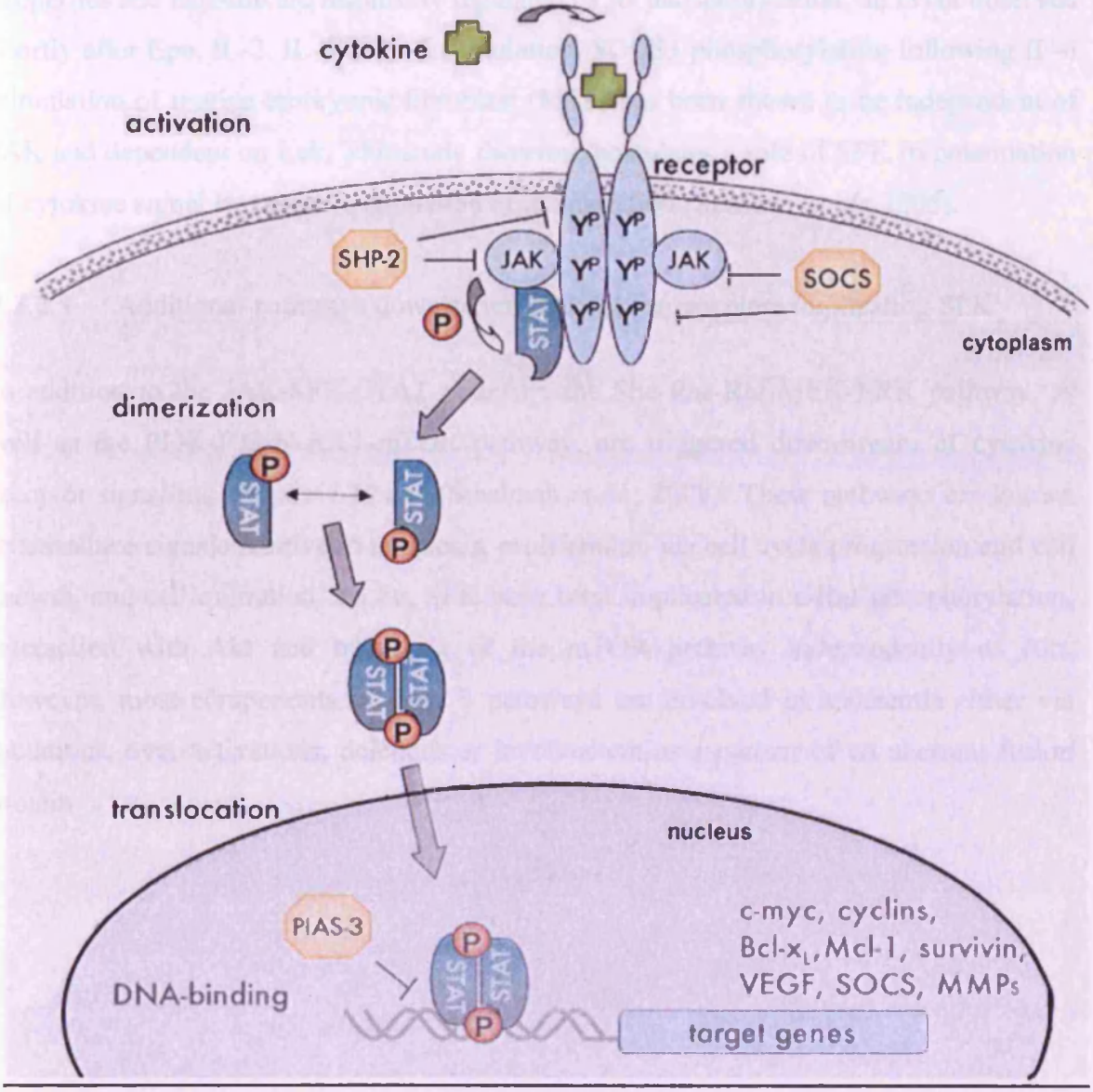


***Figure I.18:*** ***Regulation of the JAK-STAT pathway (adapted from (Desrivieres et al., 2006).***

*The JAK-STAT pathway is regulated at different levels by phosphatases, SOCS and PIAS.*

Additionally, the family of protein inhibitors of activated STAT (PIAS) offer further inhibition by directly binding specific phosphorylated STAT preventing them to bind DNA by SUMOylation (Wormald and Hilton, 2004). Of note, SOCS ubiquitination properties and half-life are negatively regulated by its phosphorylation, an event observed shortly after Epo, IL-2, IL-3 or IL-6 stimulation. SOCS3 phosphorylation following IL-6 stimulation of murine embryonic fibroblast (MEF) has been shown to be independent of JAK and dependent on Lck. This study therefore postulates a role of SFK in potentiation of cytokine signal by negative regulation of its inhibition (Sommer *et al.*, 2005).

#### 2.3.2.3 Additional pathways downstream of cytokine receptors implicating SFK

In addition to the JAK-SFK-STAT pathway, the Shc-Ras-Raf-MEK-ERK pathway, as well as the PI3K-PTEN-AKT-mTOR pathway, are triggered downstream of cytokine receptor signalling (*Figure I.19* and (Steelman *et al.*, 2008). These pathways are known to transduce signals relative to apoptosis, proliferation via cell cycle progression and cell growth, and cell migration. So far, SFK have been implicated in c-Raf phosphorylation, interaction with Akt and triggering of the mTOR pathway independently of Akt. However, most components of these 3 pathways are involved in leukaemia either via mutations, over-activations, deletions or involvement as a partner of an aberrant fusion protein.

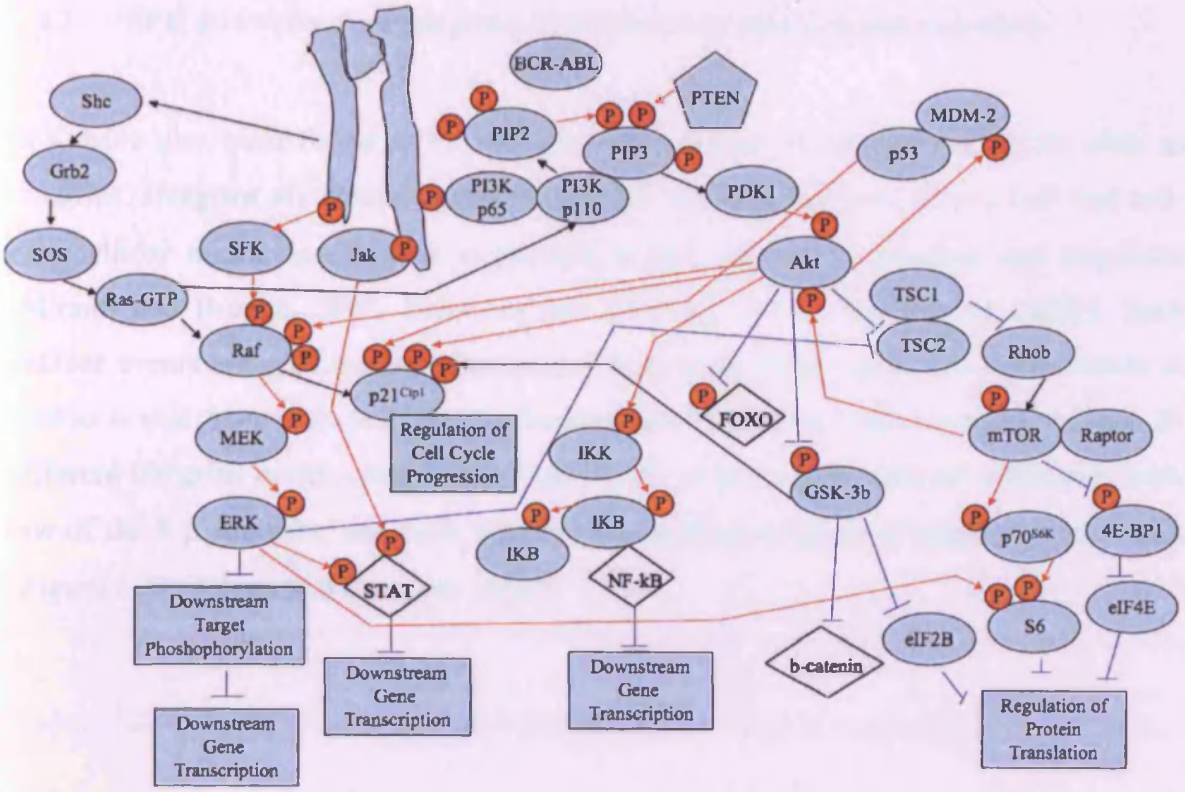


***Figure I.19:*** ***The JAK-SFK-STAT pathway, the Shc-Ras-Raf-MEK-ERK pathway and the PI3K-PTEN-AKT-mTOR pathway are triggered downstream of cytokine receptor signalling. (McCubrey et al., 2008).***

*Red arrows indicate phosphorylation. Blue arrows indicate inhibition. Black arrows indicate interaction. Diamonds indicate transcription factors. Circles indicate proteins. Boxes indicate action.*

### 2.3.3 SFK downstream of integrins: involvement in adhesion and migration

SFK have also been found to be activated downstream of adhesion receptors such as integrins. Integrins are heterodimers of α and β subunits involved in cell-cell and cell-extracellular matrix interactions implicated in cell adhesion, spreading and migration (Miranti and Brugge, 2002; Schwartz and Ginsberg, 2002; Webb *et al.*, 2002). Such cellular events are required in inflammatory responses, tissue repair and regeneration as well as in morphogenesis and can also be implicated in tumour cells invasion. At least 25 different integrins exists, composed of one of the 19 possible α subunits associated with one of the 8 β subunits, and each type is expressed on a subset of haematopoietic cells (*Figure I.20*)(Takagi and Springer, 2002).

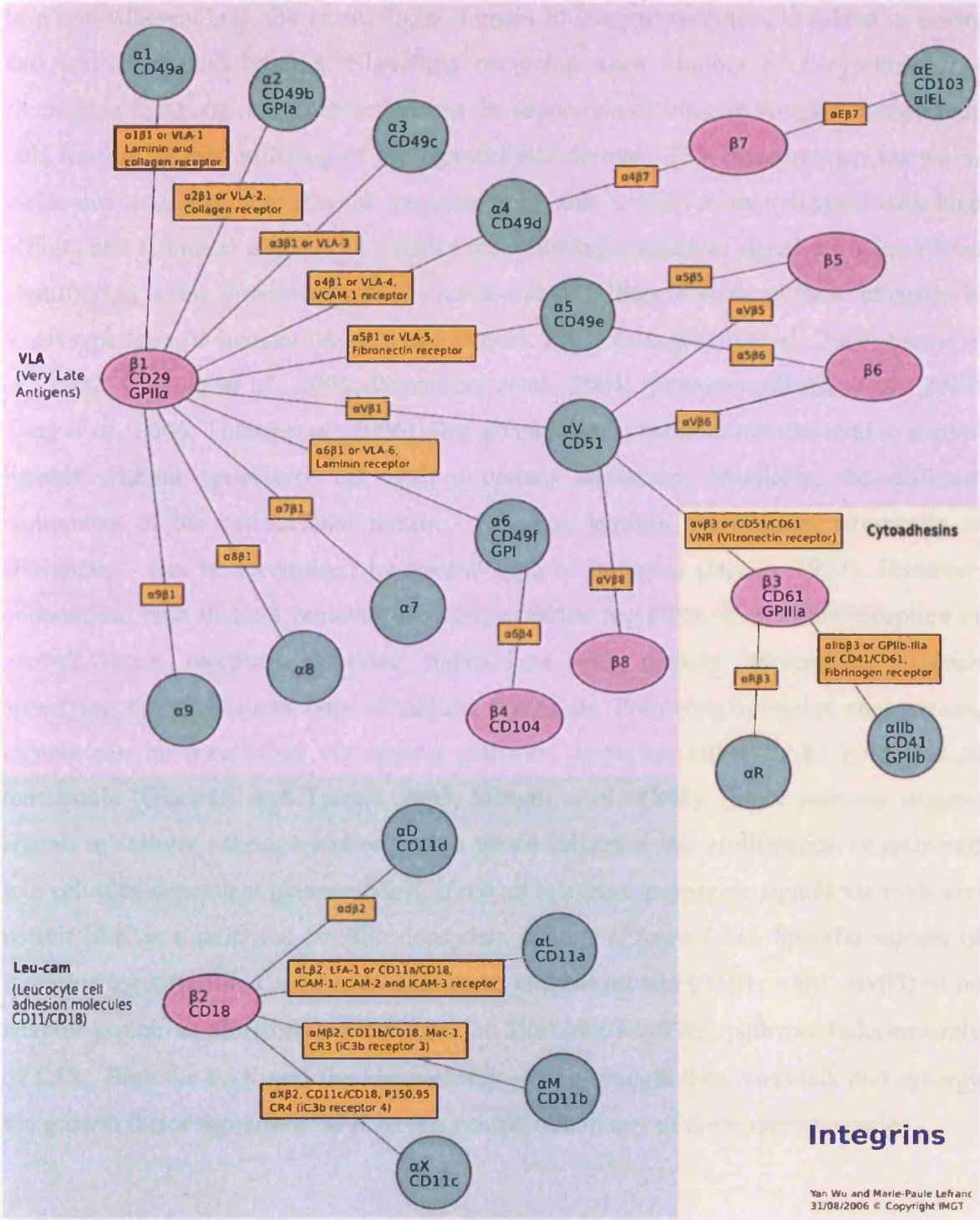


***Figure I.20:* The integrin family (http://imgt.cines.fr).**

*The integrin family is composed of 3 subfamilies: VLA, cytoadhesins and Leu-cam consisting of a specific mix and match of 19 possible α subunits associated with one of the 8 possible β subunits.*

In a non-adherent cell, the extracellular domain of integrin receptors is folded in a way that restricts ligand binding. Signalling occurring upon binding of a cytokine or a chemokine to its cognate receptor induces the separation of integrin receptor cytoplasmic tails leading to the unfolding of the extracellular domain. This phenomenon known as inside-out signalling activates the integrins to be able to bind to their ligands with high affinity and to cluster together to amplify the following outside-in signal. SFK have been identified as acting downstream of the inside-out signalling of some of these integrins in a cell type specific manner (Adachi and Suzuki, 2007; Evangelista *et al.*, 2007; Frame *et al.*, 2002; Giagulli *et al.*, 2006; Piccardoni *et al.*, 2004; Samayawardhena *et al.*, 2007; Tang *et al.*, 2006; Totani *et al.*, 2006). One given integrin heterodimer can bind to several ligands without specificity but with a certain selectivity. Similarly, the different component of the extracellular matrix - collagen, laminin, fibronectin, vitronectin or fibrinogen - can be recognised by several type of integrins (Hynes, 1992). However, cooperation with distinct immunoreceptors, cytokine receptors, chemokine receptors or growth factor receptors delineate interactions with distinct intracellular proteins specifying the subsequent type of cellular responses. Following integrins engagement, signals can be transduced via several pathways implying either FAK, Syk, Shc or tetraspanin (Giancotti and Tarone, 2003; Miranti *et al.*, 1998). Either pathway triggers signals of cellular adhesion and migration which influence cell proliferation or apoptosis in a cell type dependent manner. Most, if not all integrins, propagate signals via FAK and recruit SFK in a talin and paxillin dependent fashion (*Figure I.21*). Specific subsets of integrins use caveolin-1 instead of talin as an adaptor protein ($\alpha 1\beta 1$, $\alpha 5\beta 1$, $\alpha v\beta 3$) or no adaptor protein at all ($\alpha 6\beta 4$) and trigger the Shc/Grb2/Ras/ERK pathway independently of FAK. Both the FAK and the Shc pathway can be brought into cross-talk and synergy via growth factor signalling. SFK have a central role in any of these three scenarios.

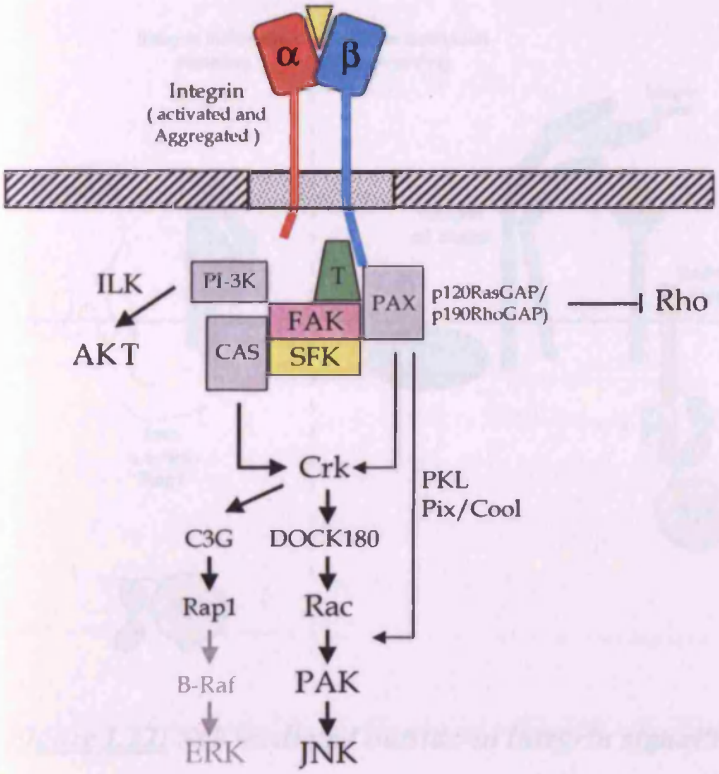


***Figure I.21:* Common outside-in β-subunit mediated integrin signalling (Giancotti and Tarone, 2003).**

*Most integrins (except α1β1, α5β1, αvβ3 and α6β4) propagate signals via FAK and recruit SFK in a talin and paxillin dependent fashion.*

Integrin signalling pathways implicating Syk are seen in haematopoietic cells such as leukocytes and platelets and transduce signals via the same intracytoplasmic proteins as the immunoreceptors (*Figure I.22*).

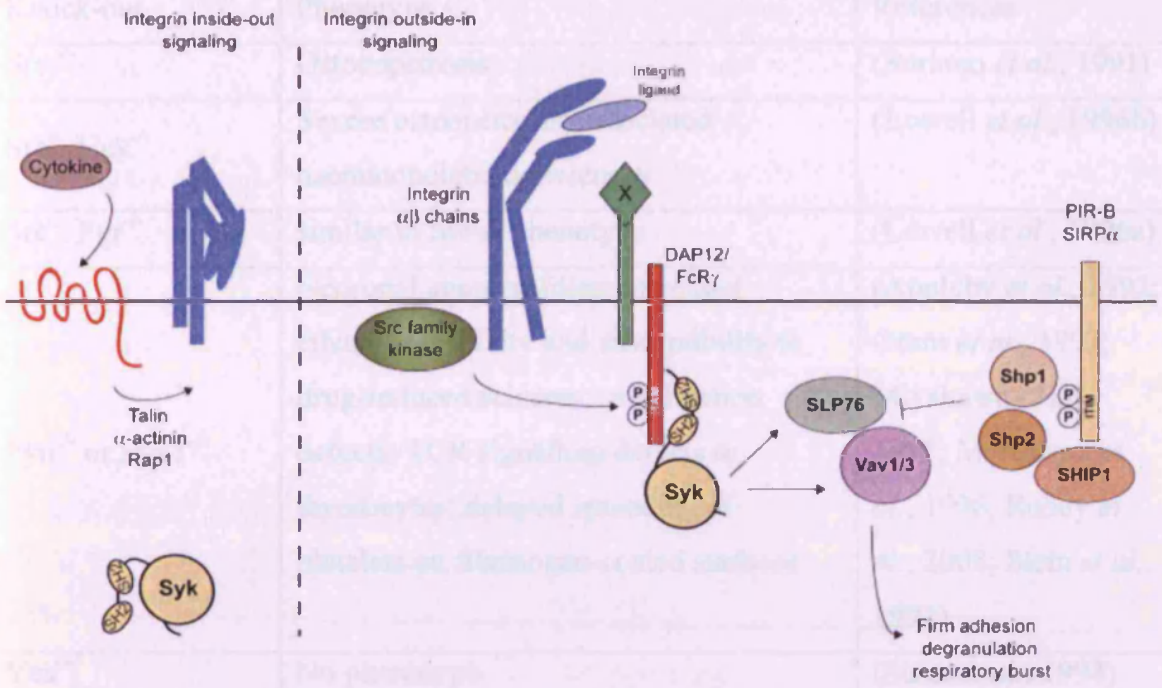


***Figure I.22:* Syk mediated outside-in integrin signalling (Abram and Lowell, 2007a).**
*Integrin signalling pathways implicating Syk are seen in haematopoietic cells such as leukocytes and platelets and transduce signals via the same intracytoplasmic proteins as the immunoreceptors.*

SFK involvement in integrin signalling and propagation of signals leading to cell adhesion and migration has clearly been established via phenotyping studies of various single, double and triple knock-out mice (*Table I.9*). However, detailed signalling distinguishing between each SFK needs further investigation.

HCK itself has not been reported to signal downstream of integrins via FAK or Shc. Its only known interaction with Shc is downstream of gp130 (Ernst *et al.*, 1996). HCK has been reported to specifically co-cap with Mac1/CD11b/CD18 but is not known to directly interact with any other integrin (Tang *et al.*, 2006). In a model of thrombohemorrhagic vasculitis, HCK has recently been reported to signal via Syk downstream of Mac-1 in neutrophils (Hirahashi *et al.*, 2006; Ley and Zarbock, 2006). The lack of knowledge about any other specific signalling pathway involving HCK is essentialy due to its high redundancy with Fgr and Lyn necessitating double or triple knock-out mice to reveal a phenotype

| Knock-out | Phenotype | References |
|---|---|---|
| Src $^{-/-}$ | Ostoeopetrosis | (Soriano *et al.*, 1991) |
| Src$^{-/-}$/Hck$^{-/-}$ | Severe osteopetrosis; associated haematopoietic deficiences | (Lowell *et al.*, 1996b) |
| Src$^{-/-}$/Fgr$^{-/-}$ | similar to Src-/- phenotype | (Lowell *et al.*, 1996a) |
| Fyn$^{-/-}$ or FynT$^{-/-}$ | Neuronal abnormalities; increased ethanol sensitivity and susceptibility to drug-induced seizures; myelination defects; TCR signalling defects in thymocytes; delayed spreading of platelets on fibrinogen-coated surfaces | (Appleby *et al.*, 1992; Grant *et al.*, 1992; Miyakawa *et al.*, 1997; Miyakawa *et al.*, 1996; Reddy *et al.*, 2008; Stein *et al.*, 1992) |
| Yes$^{-/-}$ | No phenotype | (Stein *et al.*, 1994) |
| Src$^{-/-}$/Yes$^{-/-}$ | Die perinatally | (Stein *et al.*, 1994) |
| Src$^{-/-}$/Fyn$^{-/-}$ | Die perinatally | (Stein *et al.*, 1994) |
| Fyn$^{-/-}$/Yes$^{-/-}$ | Autoimmune disease; renal malfunction | (Stein *et al.*, 1994) |
| Lck$^{-/-}$ | Defective TCR signalling and thymocyte maturation (low CD4+CD8+ T-cells); immune defects; retinal dysplasia | (Molina *et al.*, 1993; Molina *et al.*, 1992; Molina *et al.*, 1998) |
| Lck$^{-/-}$/Fyn$^{-/-}$ | No T-cells | (Groves *et al.*, 1996; van Oers *et al.*, 1996) |
| Lyn$^{-/-}$ | Defective BCR signalling and B-cell maturation; high level of serum IgM; autoimmune disease; age related splenomegaly and macrophage tumor, (mild myeloproliferative disease); defective FcR signalling and allergic response; neutrophils with enhanced respiratory burst and secondary granule release; hyperadhesive neutrophils and | (Harder *et al.*, 2001; Hibbs *et al.*, 1995; Nishizumi *et al.*, 1995; Pereira and Lowell, 2003) |

| | | |
|---|---|---|
| | macrophages | |
| $Lyn^{-/-}/Fyn^{-/-}$ | Severe autoimmune kidney disease | (Yu *et al.*, 2001) |
| $Lyn^{-/-}/Hck^{-/-}$ | Myeloproliferative disease (MPD), severe lung inflammation with extensive macrophage infiltration | (Xiao *et al.*, 2008) |
| $Hck^{-/-}$ | No obvious overall phenotype; slight delay in FcR mediated phagocytosis; do not develop thrombohemorrhagic vasculitis; reduced degranulation and cytokine production in FcεRI-stimulated hck(-/-) mast cells | (Hirahashi *et al.*, 2006; Hong *et al.*, 2007; Lowell *et al.*, 1994) |
| $Fgr^{-/-}$ | No obvious overall phenotype; decreased lung eosinophilia in allergic lung inflammation | (Lowell *et al.*, 1994; Vicentini *et al.*, 2002) |
| $Hck^{-/-}/Fgr^{-/-}$ | Extreme sensitivity to Listeria infection; resistant to LPS endotoxemia; defects in PML and macrophage responses (degranulation, respiratory burst); migration/adhesion defects; reduced neutrophils β2-integrin mediated spreading and adhesion; impaired polymorphonuclear leukocyte (PMN) capacity to adhere with activated platelets in suspension | (Evangelista *et al.*, 2007; Giagulli *et al.*, 2006; Lowell and Berton, 1998; Lowell *et al.*, 1996a; Lowell *et al.*, 1994; Mocsai *et al.*, 1999; Suen *et al.*, 1999) |
| $Hck^{-/-}/Fgr^{-/-}/Lyn^{-/-}$ (also named $SFK^{-/-}$ or HLF) | Impaired FcR induced signalling and phagocytosis; impaired polymorphonuclear leukocyte (PMN) capacity to adhere with activated platelets in suspension | (Evangelista *et al.*, 2007; Fitzer-Attas *et al.*, 2000) |

***Table I.9:*** ***Non-exhaustive phenotype of SFK single, double and triple available knock-out mice.***

Although knock-out mice did not allow to elucidate specific roles for HCK, overexpression studies of constitutively active HCK confirmed a role for HCK in adhesion/migration, phagocytosis and inflammation. Indeed, these mice showed a spontaneous lung inflammation with infiltration of macrophages and eosinophils and an excessive immune response to stimulating agents (Ernst *et al.*, 2002). An important body of work by Maridonneau-Parini's team, also using overexpression of constitutively active HCK but in fibroblasts (which do not express endogenous HCK), implicates p59HCK in the formation of membrane protusion in a Rac and Cdc42 dependent manner (Carreno *et al.*, 2002) and p61HCK in the formation of podosome rosettes in a Rac, Cdc42 and Rho dependent manner (Cougoule *et al.*, 2005). The formation of such structures has been confirmed to naturally occur in stimulated macrophages and in BCR-ABL positive CML cells, further stating a role for HCK in cellular adhesion (Poincloux *et al.*, 2006).

### 2.3.4 Role of SFK in primitive haematopoietic cells

Until recently, the role of SFK in primitive haematopoietic cells had not been examined. Using the background observation that patients with severe congenital neutropenia acquiring a G-CSFR truncating mutation have a high risk of developing AML, Mermel et al. examined the role of myeloid SFK in early granulopoiesis (Mermel *et al.*, 2006). This study revealed that even if single or triple myeloid SFK knock-out mice have a normal resting haematopoiesis, HCK specifically plays a role in regulating the G-CSF induced proliferation of granulocytic precursors, while Lyn controls the overall production of myeloid progenitors. None of these two SFK were shown to regulate the terminal granulocytic differentiation. Borneo J. et al. confirm an essential role of myeloid SFK following G-CSF stimulation by demonstrating their influence on HSC mobilisation both in an extrinsic and an instrinsic way (Borneo *et al.*, 2007). Although this study proposes a potential mechanism of action of myeloid SFK on the bone marrow environment in the context of HSC mobilisation, the influence of SFK on HSC intrinsic pathways in this same context remains to be fully explored. Additionally, SFK were shown to have a role in HSC self-renewal since triple knockout mice displayed a higher number of HSC in their bone marrow which have a decreased repopulating capacity. This HSC phenotype

was eventually attributed to the sole Lyn deficiency, confirming its role in both the HSC and myeloid progenitor production (Orschell *et al.*, 2008). While haematopoiesis in triple myeloid SFK knock-out mice proceed quite normally, surprisingly, double knock-out mice for both Lyn and HCK display a dramatic phenotype partially resembling Lyn single knock-out mice (developing mild MPD) and constitutively active Hck knock-in mice (developing severe lung inflammation) phenotypes (Xiao *et al.*, 2008). This phenotype is transplantable and has been shown to be STAT5 and SHIP dependent. Since all studies on SFK in HSC and haematopoietic progenitors have been done in mice and reveal intricate compensations between myeloid SFK, it remains to be established if the individual SFK play the same roles in human HSC.

## 3. Aim of this study

Acute myeloid leukaemia (AML) is characterised by an accumulation of immature blasts that fail to fully differentiate. Leukaemia is organised as a hierarchy, which is maintained by leukaemic stem cells (LSC). To identify molecular differences between normal haematopoietic stem cells (HSC) and LSC, we performed microarray analyses and found that haematopoietic cell kinase (HCK) is overexpressed in LSC in comparison to normal bone marrow and umbilical cord blood HSC.

By analysing various fractions of AML samples, we first assessed whether we could distinguish a specific pattern of HCK expression inbetween AML samples and in comparison to umbilical cord blood (UCB).

Then, in order to evaluate a potential role for HCK in leukaemogenesis, we used two different lentivirus based approaches to either (1) knock-down HCK in leukaemic cell lines (with the aim to ultimately work with patient sample fractions) or (2) to overexpress HCK in UCB stem cell enriched fractions.

# Chapter II

# II Materials and methods

## 1. Molecular biology

### 1.1 Quantitative real time PCR

#### 1.1.1 RNA extraction

RNA was extracted from sorted AML, normal bone marrow and umbilical cord blood samples using Trizol (Invitrogen). The RNeasy microkit (Qiagen) was used for extraction of RNA from cell lines according to manufacturer's instructions.

#### 1.1.2 RNA reverse transcription into cDNA

One hundred nanograms of RNA were added to the appropriate amount of RNAse and DNAse free water (Sigma) containing 1.2 µL of 10 µM oligo$T_{14\text{-}16}$ (Sigma) in a final volume of 13 µL. RNA was allowed to hybridise to oligodT by incubating the mix for 10 min at 65°C then on ice for 5 min. Seven microlitres of a master mix corresponding to 2 µL of 10x buffer, 2 µL of 10 µM dNTPs, 2 µL of 0.1 M DTT, 0.5 µL of RNase inhibitor and 0.5 µL of SuperScript III were added to each RNA sample and incubated at 50°C for 1h then at 70°C for 15min. If necessary, cDNA samples were stored at -20°C until ready to use for quantitative real time PCR.

#### 1.1.3 Quantitative real time PCR

A cDNA master mix of 20 µL of RNAse and DNAse free water and 2 µL of cDNA (corresponding to 5 ng of equivalent RNA for a duplicate reaction) was prepared for each

sample. Aliquots of 11 µL were pipetteted into a PCR 96 well plate. Aliquots of 11 µL of RNAse and DNAse free water only were also pipetteted as non-template controls (NTC). A master mix, corresponding to 25 µL of 2x SYBR® green PCR mix (Applied Biosystems), 1.5 µL of the appropriate 10 µM forward primer and 1.5 µL of the appropriate 10 µM reverse primer was prepared for each primer pair and 14 µL of the mix were added to each well of the PCR 96 well plate. The final volume of each duplicate reaction was 25 µL. Real-time PCR was performed using the ABI Prism 7700 Sequence Detector System (ABI/Perkin Elmer, Foster City, CA, USA). All the reactions were carried out in duplicate under the following conditions: an initial step at 50°C for 2 minutes and 95°C for 10 minutes, followed by 40 cycles of a two stage PCR, consisting of 95°C for 15 seconds and 60°C for one minute. GAPDH was used as an endogenous reference gene. Analysis was carried out using the software SDS provided with the ABI Prism 7700.

## 1.2 Cloning

### 1.2.1 shRNA cloning

#### 1.2.1.1 Hybridisation of shHCK4 oligonucleotides

Forward 5'-GATCCCCGCTTGCTGGACTTTCTGAATTCAAGAGATTCAGAAAGT CAGCAAGCTTTTTGGAAA-3' and reverse 5'-AGCTTTTCCAAAAAGCTTGCTGGA CTTTCTGAATCTCTTGAATTCAGAAAGTCCAGCAAGCGGG-3' shHCK4 encoding oligonucleotides were resuspended in RNAse and DNAse free water at a final concentration of 40 µM. 20 µL of each long oligonucletide were added to 10 µL of annealing buffer 5x (500 mM potassium acetate, 150 mM HEPES-KOH, pH 7.4, 10 mM magnesium acetate) and hybridised by incubating the 50 µL mix for 1 min at 95°C, 15 min at 37°C and overnight at RT.

#### 1.2.1.2 Verification of the integrity of the pH1-Xho shuttle vector

Two hundred nanograms of pH1-Xho plasmid DNA was digested in a mix of 2 µL of 10x *EcoRI* digestion buffer, 1 µL of *EcoRI* restriction enzyme and 1 µL of *BglII* restriction enzyme, topped up with water to a final volume of 20 µL (E/B digest) or in a mix of 2 µL of 10x buffer 2 digestion buffer, 1 µL of *XhoI* restriction enzyme and 2 µL of 10x BSA, topped up with water to a final volume of 20 µL (X digest). Digestion mixes were incubated for 4h30 at 37°C and loaded on an agarose gel to assess for successful digestion (See 'Agarose gel electrophoresis and visualisation' section). All reagents for restriction digests were from New England Biolabs, Hitchen, UK.

#### 1.2.1.3 Restriction digest of the pH1-Xho shuttle vector

Two hundred nanograms of pH1-Xho plasmid DNA was digested in a mix of 2 µL of 10x buffer 2 digestion buffer, 1 µL of *EcoRI* restriction enzyme and 1 µL of *HindIII* restriction enzyme, topped up with water to a final volume of 20 µL. Digestion mixes were incubated for 4h30 at 37°C and loaded on an agarose gel to assess for successful digestion and subsequent gel purification (See 'Agarose gel electrophoresis and visualisation' section). All reagents for restriction digests were from New England Biolabs, Hitchen, UK.

#### 1.2.1.4 Ligation of the hybridised shHCK4 oligonucleotides to the pH1-Xho shuttle vector

A ligation mix of 14 µL of hybridised oligonucleotides, 2 µL of *EcoRI/HindIII* restricted pH1-Xho plasmid DNA, 1 µL of T4 DNA ligase, 2 µL of 10x ligase buffer and 1 µL of RNAse and DNAse free water were left to incubate overnight at 16°C. DH5α bacteria were transformed with 2 µL of the ligation mix using Ampicillin as a selection antibiotic (see 'Bacterial transformation' section).

#### 1.2.1.5 Restriction of the shHCK4-pH1-Xho shuttle vector and the pRLL-SIN-cPPT-PGK-eGFP-WPRE lentiviral backbone/ Verification of cloning of pH1-shHCK4 into the lentiviral backbone

One microgram of lentiviral plasmid DNA or pH1-Xho plasmid DNA were digested in a mix of 5 µL of 10x buffer 2 digestion buffer, 1.5 µL of *XhoI* restriction enzyme and 5 µL of 10x BSA, topped up with water to a final volume of 50 µL. Digestion mixes were incubated for 4h at 37°C and loaded on an agarose gel to assess for successful digestion and subsequent gel purification. All reagents for restriction digests were from New England Biolabs, Hitchen, UK.

#### 1.2.1.6 Ligation of the pH1-shHCK4 fragment into the pRLL-SIN-cPPT-PGK-eGFP-WPRE lentiviral backbone

The *XhoI* restricted and gel purified pH1-shHCK4 fragment was serially diluted in RNAse and DNAse free water at dilution ratios 1:2, 1:10, 1:100 and 1:1000. One microlitre of either dilution was mixed to 1 µL of *XhoI* restricted, gel purified and dephosphorylated lentiviral plasmid DNA and the ligation mix was completed by adding 1 µL of T4 DNA ligase, 2 µL of 10x ligase buffer and 15 µL of RNAse and DNAse free water before being incubated overnight at 16°C. XL-Gold bacteria were transformed with 3 µL of the ligation mix using Ampicillin as a selection antibiotic (see 'Bacterial transformation' section).

### 1.2.2 miRNA cloning

#### 1.2.2.1 Hybridisation and dilution of miRNA oligonucleotides

Top strand of miRNA 604 (5'-TGCTGATCACTTCAGGGTTTGACATCGTTTTGGCC ACTGACTGACGATGTCAACCTGAAGTGAT-3'), miRNA 605 (5'-TGCTGTGTAGA AGTCATCCAGCACACGTTTTGGCCACTGACTGACGTGTGCTGTGACTTCTACA -3'), miRNA 606 (5'-TGCTGATACAGGGCAACCACGATGATGTTTTGGCCACTG

ACTGACATCATCGTTTGCCCTGTAT-3') and miRNA 607 (5'-TGCTGAAGAGTAG CTTCCTTTAGTGGGTTTTGGCCACTGACTGACCCACTAAAAAGCTACTCTT-3') and bottom strands (complementary sequence of the top strand) were resuspended as 200 µM solutions in RNAse and DNAse free water. Five microlitres of each given top strand were hybridised to 5 µL of their respective bottom strand by adding 2 µL of 10x Oligo Annealing Buffer (Invitrogen) and 8 µL of RNAse and DNAse free water. Each hybridisation mix was incubated for 4 min at 95°C then allowed to cool down at RT for 10 min. Each 50mM hybridised miRNA solution obtained was further serially diluted to a 500mM and a 10 nM solution in order to proceed to their ligation into the pcDNA$^{TM}$6.2GW/EmGFP-miR vector. Fifty micromolar stock solution and intermediate dilution solutions were frozen at -20°C.

#### 1.2.2.2 Ligation of the hybridised miRNA oligonucleotides to the pcDNA$^{TM}$6.2GW /EmGFP-miR vector

A ligation mix of 4 µL of hybridised miRNA oligonucleotides (miRNA 604, 605, 606 and 607), 2 µL of the linear pcDNA$^{TM}$6.2GW/EmGFP-miR vector plasmid, 1 µL of T4 DNA ligase (Invitrogen), 4 µL of 5x Ligation buffer (Invitrogen) and 9 µL of RNAse and DNAse free water was incubated 5 min at RT, then kept on ice until ready for transformation. TOP10 bacteria were transformed with 2 µL of the ligation mix using Spectinomycin as a selection antibiotic (see 'Bacterial transformation' section).

#### 1.2.2.3 Restriction digest of the pcDNA$^{TM}$6.2GW/EmGFP-miR-miRNA 604, 605, 606, 607 plasmids

One microgram of pcDNA$^{TM}$6.2GW /EmGFP-miR-miRNA 604, pcDNA$^{TM}$6.2GW /EmGFP-miR-miRNA 605, pcDNA$^{TM}$6.2GW /EmGFP-miR-miRNA 606 and pcDNA$^{TM}$6.2GW /EmGFP-miR-miRNA 607, to be used as 'backbone', were digested in a mix of 2 µL of 10x buffer 3 digestion buffer, 1 µL of *BglII* restriction enzyme, 1 µL of *XhoI* restriction enzyme and 2 µL of 10x BSA, topped up with water to a final volume of 20 µL. Three times 2 µg of pcDNA$^{TM}$6.2GW /EmGFP-miR-miRNA 604,

pcDNA$^{TM}$6.2GW /EmGFP-miR-miRNA 605, pcDNA$^{TM}$6.2GW /EmGFP-miR-miRNA 606 and pcDNA$^{TM}$6.2GW /EmGFP-miR-miRNA 607, to be used as 'insert', were digested in a mix of 2 µL of 10x buffer 3 digestion buffer, 1 µL of *BamHI* restriction enzyme, 1 µL of *XhoI* restriction enzyme and 2 µL of 10x BSA, topped up with water to a final volume of 20 µL. Digestion mixes were incubated for 4h at 37°C and loaded on an agarose gel to assess for successful digestion and subsequent gel purification. All reagents for restriction digests were from New England Biolabs, Hitchen, UK.

#### 1.2.2.4 Ligation of the pcDNA$^{TM}$6.2GW/EmGFP-miR-miRNA60.x 'backbones' to the miRNA60.x 'inserts'

'Backbone' pcDNA$^{TM}$6.2GW /EmGFP-miR-miRNA60.x was ligated to *BamHI/XhoI* digested miRNA604, 605, 606 and 607 inserts in a 1:3 ratio (where x represents the last digit of the miRNA name, 4, 5, 6 or 7). A ligation mix of 50 ng of the 5849 bp backbone, 3.94 µL of the 150 bp insert, 1 µL of T4 DNA ligase, 10 µL of 2x Ligation buffer, topped up to 20 µL with RNAse and DNAse free water, was incubated 5 min at RT then kept on ice until ready for transformation. TOP10 bacteria were transformed with 2 µL of either of the 12 ligation mixes using Spectinomycin as a selection antibiotic (see 'Bacterial transformation' section). pcDNA$^{TM}$6.2GW /EmGFP-miR-miRNA60**4** ligated to miRNA60**5** will be called mi**45**, pcDNA$^{TM}$6.2GW /EmGFP-miR-miRNA60**4** ligated to miRNA60**6** will be called mi**46**, pcDNA$^{TM}$6.2GW /EmGFP-miR-miRNA60**4** ligated to miRNA60**7** will be called mi**47**, pcDNA$^{TM}$6.2GW /EmGFP-miR-miRNA60**5** ligated to miRNA60**4** will be called mi**54**, pcDNA$^{TM}$6.2GW /EmGFP-miR-miRNA60**5** ligated to miRNA60**6** will be called mi**56**, etc.

#### 1.2.2.5 Restriction digest of the 12 pcDNA$^{TM}$6.2GW/EmGFP-miR-miRNA plasmids containing two miRNA sequences

One microgram of each of the 12 pcDNA$^{TM}$6.2GW /EmGFP-miR-miRNA 604-605, 604-606, 604-607 etc, generated previously, were digested in a mix of 2 µL of 10x buffer 3 digestion buffer, 1 µL of *BglII* restriction enzyme, 1 µL of *XhoI* restriction enzyme and 2

µL of 10x BSA, topped up with water to a final volume of 20 µL, to be used as 'backbone'. Digestion mixes were incubated for 4h at 37°C and loaded on an agarose gel to assess for successful digestion and subsequent gel purification. All reagents for restriction digests were from New England Biolabs, Hitchen, UK.

#### 1.2.2.6 Ligation of the pcDNA$^{TM}$6.2GW/EmGFP-miR-miRNA60.x-60.x 'backbones' to the miRNA60.x 'inserts'

Each of the 12 'backbone' pcDNA$^{TM}$6.2GW /EmGFP-miR-miRNA60.x-60.x was ligated to miRNA604, 605, 606 and 607 inserts in a 1:3 ratio. A ligation mix of 50 ng of the 6 kb backbone, 3.75 µL of the 150 bp insert, 1 µL of T4 DNA ligase, 10 µL of 2x Ligation buffer, topped up to 20 µL with RNAse and DNAse free water, was incubated 5 min at RT then kept on ice until ready for transformation. TOP10 bacteria were transformed with 2 µL of either of the 24 ligation mixes using Spectinomycin as a selection antibiotic (see 'Bacterial transformation' section). pcDNA$^{TM}$6.2GW /EmGFP-miR-miRNA60**4**-60**5** ligated to miRNA60**6** will be called mi**456**, pcDNA$^{TM}$6.2GW /EmGFP-miR-miRNA60**4**-60**5** ligated to miRNA607 will be called mi**457**, pcDNA$^{TM}$6.2GW /EmGFP-miR-miRNA60**4**-60**6** ligated to miRNA60**5** will be called mi**465**, pcDNA$^{TM}$6.2GW /EmGFP-miR-miRNA60**4**-60**6** ligated to miRNA607 will be called mi**467**, pcDNA$^{TM}$6.2GW /EmGFP-miR-miRNA60**4**-607 ligated to miRNA60**5** will be called mi**475**, etc.

### 1.2.3 p59HCK cDNA cloning

#### 1.2.3.1 Amplification of p59HCK cDNA

p59HCK cDNA was amplified from Mono-mac-6 cells' total cDNA using the forward primer 5'-ATGGGGTGCATGAAGTCCAAGT-3' and the reverse primer 5'-TCATGGC TGCTGTTGGTACTG-3'. Ideal annealing temperature was determined using a temperature gradient ranging from 57 to 63 °C. A master mix corresponding to 5 µL of 10x Takara buffer, 8 µL of Takara dNTPs, 0.1 µL of 100 µM forward primer, 0.1 µL of

100 µM reverse primer, 0.5 µL of Takara polymerase, 100 ng of equivalent RNA and 34.76 µL of RNAse and DNAse free water was prepared and 50 µL PCR mix was pipetteted into a PCR 96 well plate. PCR reactions were carried out in duplicate under the following conditions: an initial hot start step at 95°C for 1 minute, followed by 35 cycles of a four stage PCR, consisting of 100°C for 5 seconds, 98°C for 5 seconds, 1 min annealing at 57, 57.3, 57.9, 58.7, 59.8, 61.3 or 63°C and 2 min elongation at 68°C. A final elongation step at 72°C for 10 min completed the PCR, which was kept at 4°C until ready to run on an agarose gel. Ten microlitres of the PCR products were run on a 1% agarose gel (*Figure II.1*).

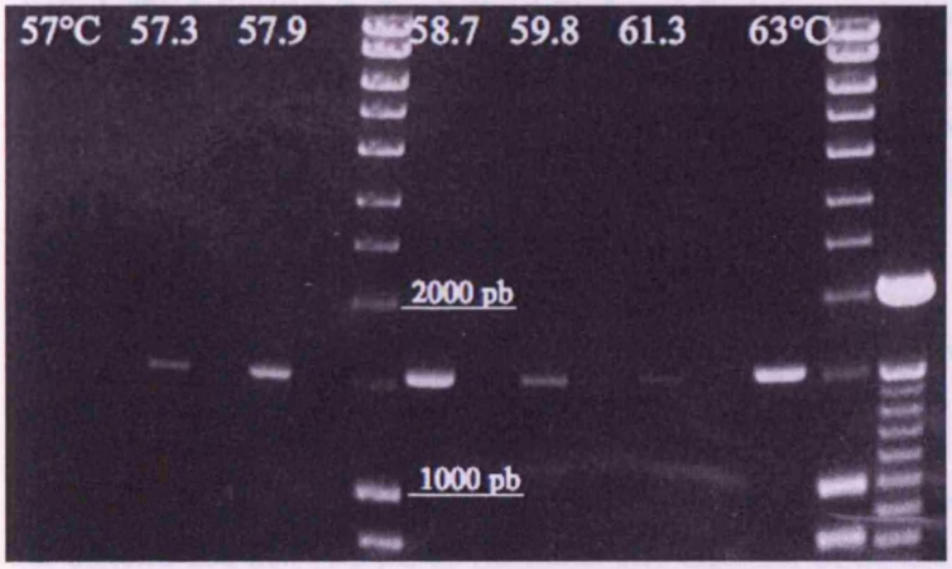


***Figure II.1: p59HCK PCR products.***
*p59HCK cDNA was amplified by PCR from Mono-mac-6 cells total cDNA using an annealing temperature gradient ranging from 57 to 63 °C.*

The 1.5 kb PCR product amplified at 63°C was cloned into the pCR® 2.1-TOPO vector by TA ligation.

1.2.3.2 TA ligation

The amplified p59HCK cDNA was cloned into the pCR® 2.1-TOPO vector by TA ligation (Invitrogen). This type of ligation takes advantage of the fact that the final PCR

extension step of 10 minutes at 72°C adds an A base overhang on PCR products. The linear pCR® 2.1-TOPO vector, provided by Invitrogen, contains T overhangs. Three or four microlitres of PCR product were ligated to 1 µL of pCR® 2.1-TOPO vector in saline conditions for 5 minutes at room temperature, according to the manufacturer's instructions (Invitrogen TOP bacteria were transformed with 1 µL of either ligation mix using Ampicillin as a selection antibiotic (see 'Bacterial transformation' section).

#### 1.2.3.3 Verification of cloning of p59HCK cDNA into the pCR® 2.1-TOPO vector

Two microlitres of each p59HCK-pCR® 2.1-TOPO vector were digested in a mix of 2 µL of 10x buffer 2 digestion buffer, 1 µL of *KpnI* restriction enzyme, 1 µL of *NotI* restriction enzyme and 2 µL of 10x BSA, topped up with water to a final volume of 20 µL. Digestion mixes were incubated for 2h at 37°C and loaded on an agarose gel to assess for successful digestion and subsequent gel purification. All reagents for restriction digests were from New England Biolabs, Hitchen, UK.

#### 1.2.3.4 Restriction of the pENTR1A-IRES-GFP shuttle vector and the p59HCK-pCR® 2.1-TOPO cloning vector

One microgram of pENTR1A-IRES-GFP plasmid or 1 µg of p59HCK-pCR® 2.1-TOPO was digested in a mix of 5 µL of 10x buffer Eco digestion buffer and 1.5 µL of *EcoRI* restriction enzyme, topped up with water to a final volume of 50 µL. Digestion mixes were incubated for 2h at 37°C and loaded on an agarose gel to assess for successful digestion and subsequent gel purification. All reagents for restriction digests were from New England Biolabs, Hitchen, UK.

#### 1.2.3.5 Ligation of the p59HCK fragment to the pENTR1A-IRES-GFP or pENTR1A-IRES-YFP shuttle vector

pENTR1A-IRES-GFP or pENTR1A-IRES-YFP shuttle vectors were ligated to the EcoRI restricted p59HCK fragment in a 1:1 and 1:2 molecular ratio. Ligation mixes of 50 ng of

the 3846 bp backbone, 50 ng or 100 ng of the 1580 bp insert, 1 µL of T4 DNA ligase, 10 µL of 2x Ligation buffer, topped up to 20 µL with RNAse and DNAse free water were incubated 5 min at RT then kept on ice until ready for transformation. DH5α bacteria were transformed with 2 µL of either ligation mix using Kanamycin as a selection antibiotic (see 'Bacterial transformation' section).

#### 1.2.3.6 Verification of cloning of p59HCK cDNA into the pENTR1A-IRES-GFP or the pENTR1A-IRES-YFP shuttle vectors

Two microlitres of each p59HCK-pENTR1A-IRES-GFP plasmid were digested in a mix of 2 µL of 10x buffer 4 digestion buffer, 1 µL of *XmaI* restriction enzyme and 2 µL of 10x BSA, topped up with water to a final volume of 20 µL. Digestion mixes were incubated for 2h at 37°C and loaded on an agarose gel to assess for successful digestion and subsequent gel purification. Two microlitres of each p59HCK-pENTR1A-IRES-YFP plasmid were digested in a mix of 2 µL of 10x buffer 3 digestion buffer and 1 µL of BstXI restriction enzyme, topped up with water to a final volume of 20 µL. Digestion mixes were incubated for 2h at 55°C and loaded on an agarose gel to assess for successful digestion and subsequent gel purification. All reagents for restriction digests were from New England Biolabs, Hitchen, UK.

#### 1.2.3.7 Gateway recombination of the pENTR1A-IRES-GFP or the pENTR1A-IRES-YFP plasmid with the LNT-Sffv-cddB-MCS lentiviral vector

p59HCK cDNA was transferred into the lentivirus vector LNT-Sffv-cddB-MCS, a kind gift from Dr Adrian Thrasher (Demaison et al., 2002), by the Gateway cloning system (Invitrogen) which uses site-specific recombination properties of the bacteriophage lambda. One hundred and fifty nanograms of destination vector (lentiviral vector) and 300 ng of the pENTR1A-HCK-IRES-GFP vector (or the pENTR1A-IRES-YFP vector) were incubated with 4 µL of 5x LR Clonase Reaction Buffer and 4 µL of LR Clonase Enzyme Mix in a final reaction volume of 20 µL. Reactions were incubated at 25°C for 1 hour. 2 µL of Proteinase K solution were added to terminate the reaction and incubated at

37°C for 10 min. XL-Gold bacteria were transformed with 2 µL of the recombination reaction using Ampicillin as a selection antibiotic (see 'Bacterial transformation' section).

#### 1.2.3.8 Verification of cloning of p59HCK cDNA into the LNT-Sffv-cddB-MCS lentiviral vector

One microgram of LNT-Sffv-p59HCK-IRES-GFP plasmid was digested in a mix of 2 µL of 10x buffer 4 digestion buffer, 1 µL of *SacII* restriction enzyme and 1 µL of *AgeI* restriction enzyme, topped up with water to a final volume of 20 µL. Digestion mixes were incubated for 2h at 37°C and loaded on an agarose gel to assess for successful digestion and subsequent gel purification. All reagents for restriction digests were from New England Biolabs, Hitchen, UK.

### 1.2.4 Agarose gel electrophoresis and visualisation

DNA fragments were separated by agarose gel electrophoresis, using Flowgen or Horizon 58 (Gibco) gel electrophoresis apparatus tank apparatus. Agarose gels were prepared by mixing 1 g - if looking at medium fragments (cloning into intermediary vectors) - or 2 g - if looking at small DNA fragments (cloning into lentiviral vectors) - of agarose powder (Life Technologies) to 1X Tris-Acetate-EDTA (TAE) buffer. The 1 or 2 % Agarose solution was brought to the boil by microwaving and allowed to cool down. Upon cooling, ethidium bromide solution was added at a final concentration of 0.5 µg/mL to allow for the subsequent visualisation of DNA fragment. The warm agarose solution was poured into an electrophoresis chamber and an appropriately sized comb was inserted to shape the loading wells prior to letting the agarose gel solidify. DNA samples diluted in 5x loading buffer and appropriate DNA size ladder (HyperLadder (Bioline) or 1kb ladder- Invitrogen) were loaded into the wells and gels were electrophoresed at 100V for the appropriate length of time. DNA was visualised by transillumination with ultraviolet light and photographed as a permanent record.

### 1.2.5 DNA fragment purification

#### 1.2.5.1 Agarose gel purification

Following agarose gel electrophoresis, restriction enzyme digest products of the appropriate size were excised using a clean scalpel with all efforts to keep exposure to UV light minimal. Qiagen Gel Purification Kit (Qiagen) was used to recover the digested DNA following manufacturer's protocol. Final elution volume was 30 µL of RNAse and DNAse free water.

#### 1.2.5.2 Column purification

One microgram of *EcoRI* restricted pENTR1A-IRES-GFP plasmid or the total volume of each dephosphorylation reaction was column purified according to manufacturer's instructions to remove enzymes (*EcoRI* or CIP) from the reaction mixes. The purified DNA fragments were eluted in 30 µL of RNAse and DNAse free water.

### 1.2.6 Calf intestinal phosphatase (CIP) treatment

To prevent vectors cut with a single restriction enzyme from self-ligating, the restricted and gel purified vector was treated with CIP enzyme (New England Biolabs, Hitchen, UK) to remove the phosphate group from the 5' overhangs. One unit of CIP/ µg of DNA was incubated with 1 µg of lentiviral vector DNA or 1 µg of pENTR1A-IRES-GFP for 1h30 at 25°C in 1x NEB buffer 3 in a final volume of 50 µL. CIP was inactivated by heating the mix to 70°C for 10 min. The dephosphorylated lentiviral backbone was subsequently column purified according to manufacturer's instructions.

### 1.2.7 Plasmid DNA sequencing

Each sequencing reaction was prepared by mixing 8 µL of BDT buffer containing

labelled dNTPs, 200 ng of DNA and 3.2 pg of primer topped up to a final volume of 20 µL. Amplification PCR was carried out using the progam described at the end of this paragraph at annealing temperature indicated in section 1.2.8, *Table II.1*. PCR products were purified using DyeEx 2.0 Spin Columns (Qiagen, Crawley, UK). Columns were vortexed to resuspend the matrix and then spun for 3 minutes at 750g. The sequencing PCR mix was then applied to the compacted column and again spun for 3 minutes at 750g. The purified samples were then dried using a vacuum centrifuge (DNA Speed Vac, DNA120; Savant). Samples were run on the Prism 3730 as a service provided by CRUK. Sequence analysis was carried out by using the 4Peaks program (http://mekentosj.com/4peaks/) and the BLAST online program, for verification of sequence identity and detection of false negative results. The CLUSTALW online program was used for sequence alignment. M13 forward and reverse primers were separately used to ensure the successful cloning of shHCK4 at an annealing temperature of 60°C. EmGFP forward sequencing primer was used to ensure the successful cloning and chaining of various combinations of miRNA 604, 605, 606 and 607 at an annealing temperature of 51°C.

Amplification PCR program for sequencing:

Step 1. Ramping by 2.5°C/sec to 96°C
Step 2. 96°C for 1min
Step 3. 96°C for 10 sec
Step 4.Ramping by 1°C/sec to annealing temperature
Step 5. Annealing temperature for 5 min
Step 6. Ramping by 1°C/sec to 60°C
Step 7. 60°C for 4 min
Go to step 3, 24 times
End step. 12°C for ever.

### 1.2.8 Primers used in this study

| Quantitative real-time PCR primers | |
|---|---|
| | |
| HCK F_RT | CATCATCGTGGTTGCCCTGTA |
| HCK R_RT | GCGGGCGACATAGTTGCTT |
| | |
| Fgr F_RT | GAGGAGCCCATCTACATCGTG |
| Fgr R_RT | CAGGGGTTGTACTCATCGTCC |
| | |
| Fyn F_RT | TGTGACCTCCATCCCCAACT |
| Fyn R_RT | AACTCAGGTCATCTTCTGTCCGT |
| | |
| Hck F2_RT | CATCATCGTGGTTGCCCTGTA |
| Hck R2_RT | GCGGGCGACATAGTTGCTT |
| | |
| Lck F_RT | CACGAAGGTGGCGGTGAAGA |
| Lck R_RT | GAAGGGGTCTTGAGAAAATCCA |
| | |
| Lyn F_RT | GAGGCTCTACGCTGTGGTCA |
| Lyn R_RT | GACTCGGAGACCAGAACATTAGC |
| | |
| Src F_RT | CAGTGTCTGACTTCGACAACGC |
| Src R_RT | CCATCGGCGTGTTTGGAGTA |
| | |
| Yes F_RT | GCTGCACTGTATGGTCGGTT |
| Yes R_RT | AGGGCACGGCATCCTGTATC |
| | |

| Sequencing primers | | Annealing temperature |
|---|---|---|
| | | |
| HCK-RTf2 | CATCATCGTGGTTGCCCTGTA | 61 |
| HCK-RTr2 | GCGGGCGACATAGTTGCTT | 64 |
| HCK_CTG | CTGGGGGGGCGCTCAAGC | 69 |
| hckGCbox_F | AGAGGCTTAGAGGCGAGTGG | 69 |
| HCKseq_1_F | TGGCAGTGAAGACGATGAAG | 61 |
| HCKseq_2_R | AAGTCAGCAATCTTACACAC | 51 |
| HCKseq_3_F | TGATGGAGATCGTCACCTACG | 62 |
| IRESseq_1_F | TGGCTCTCCTCAAGCGTATT | 61 |
| GFPseq_2_F | GAACTTCAGGGTCAGCTTGC | 61 |
| HCK_ATG | ATGGGGTGCATGAAGTCCAAGT | 66 |
| HCK_TCA | TCATGGCTGCTGTTGGTACTG | 63 |
| | | |
| EmGFP forward | GGCATGGACGAGCTGTACAA | 61 |

***Table II.1:*** ***Primers used for real-time quantitative PCR and sequencing PCR.***

## 1.3 Bacterial cultures

### 1.3.1 Bacterial transformation

Two microlitres of plasmid or ligation mix were transformed into 50 µL of chemically competent DH5α (Stratagene), XL-blue (Stratagene), XL-Gold (Stratagene) or TOP10 (Invitrogen) bacteria, according to manufacturer's protocol. Briefly, DNA was incubated with the bacteria on ice for 1h30; when dealing with XL-Gold bacteria, 2 µL β-mercaptoethanol was added per vial of cells and vials were tilted every 10 min during this 30 min incubation. Bacteria were then heat shocked at 42°C for 30 seconds and immediately put back on ice for 2 min. Three hundred microlitres of warm SOC media was added to the cells dropwise and mixed by tilting the vial. Bacterial solutions were incubated at 37°C for 1h at 220 rpm. Two hundred and fifty microlitres of bacteria solution were plated onto LB agar plates containing the appropriate antibiotic and incubated overnight at 37°C. If pCR® 2.1-TOPO vector plasmids, which contain the β-galactosidase reporter gene, were used, X -gal (20 mg/mL) was spread onto the LB agar plates 1h prior to bacteria plating, to allow for blue/white selection (white colonies are positive for the gene of interest). The next day, 10 colonies were picked from the plates and processed for adequately sized plasmid DNA preparation and glycerol stock preparation.

### 1.3.2 Plasmid preparation

Individual bacterial colonies were picked from LB agar plates using a 200/20 µL Gilson pipette non-filtered plastic tip and put to grow in 5 mL of LB broth supplemented with 50 µg/mL of either ampicillin, spectinomycin or kanamycin in a 37°C shaking incubator.

#### 1.3.2.1 Miniprep

Plasmid recovery from small amounts of bacterial culture (4 mL) was carried out using QIAprep Spin Miniprep Kit (Qiagen) following manufacturer's instructions. Final elution volume was 30 µL of RNAse and DNAse free water (Sigma). Alternatively minipreps were carried out on the Qiagen robot (miRNA chaining screening).

#### 1.3.2.2 Maxiprep

For purification of up to 500 µg of transfection grade plasmid DNA, Qiagen Plasmid Maxi Kit was used, following manufacturer's instructions.

#### 1.3.2.3 Megaprep – endotoxin free

For purification of up to 2.5 mg advanced transfection grade plasmid used in lentivirus production, Qiagen EndoFree Plasmid Mega Kit was used, following manufacturer's instructions.

### 1.3.3 Glycerol stocks

Bacteria were stored at -80°C in 15% glycerol.

## 2. Biochemistry

## 2.1 Western blotting

### 2.1.1 Protein isolation

Pelleted cells were resuspended in 100-200 µL of the appropriate cell lysis buffer and incubated on ice for 30 minutes (see below for composition of lysis buffers). The cell

lysate was cleared of cellular debris by centrifuging for 20 minutes at 20,000 g at 4°C. The supernatant containing the total proteins was collected and either frozen at -80°C or directly processed to measure protein concentration. Total protein concentration was determined using the Precision Red Advanced Protein Assay (Universal Biologicals, Cambridge) according to the manufacturer's instructions: a standard curve was made by serially diluting commercial lyophilised bovine serum albumin (BSA, NEB) to concentrations ranging from 0 to 50 μg/mL in PBS. Samples were appropriately diluted (usually 1:10) and 10 μL of the standard and unknown samples were pipetted into a flat-bottomed 96 well plate. After adding 300 μL of reagent to the 10 μL of samples, optical density was read at 600 nm and cell lysate protein concentrations were determined via reading against the BSA standard curve.

### 2.1.2 Immunoprecipitation

For each sample to be studied, 30 μL of 50% protein A-Sepharose bead slurry (Roche) were mixed with 0.5 mL ice cold PBS containing 1 μg of the appropriate antibody (mouse anti-HCK, rabbit anti-HCK, goat anti-phosphoHCK Y411 or isotype control antibodies) and left to bind for 1h at 4°C by tumbling the Eppendorf tubes end over end in a tube rotator set up at 8-10 rpm. In the meantime, each sample cell lysate was precleared by adding 30 μL of 50% protein A-Sepharose bead slurry (Roche) to a volume of cell lysate corresponding to 450 μg of total protein. Eppendorf tubes were tumbled end over end for 30 min at 4°C in a tube rotator set up at 8-10 rpm. In the meantime antibody-bound beads were washed three times by centrifuging the mix for 10 sec at 4°C at 16,000 g, aspirating the supernatant (containing unbound antibodies) using a P1000 tip connected to a vacuum aspirator, adding 1 mL of ice cold lysis buffer, inverting the Eppendorf tube three or four times and centrifuging the tubes again. When processing numerous samples, tubes were kept on ice all along the washing procedure. Eppendorf tubes containing the preclearing cell lysates were centrifuged for 5 min at 4°C at 16,000 g and supernatants were transferred to individual tubes containing antibody-bound beads and 20 μL of 5% BSA. The latter mixtures were allowed to immunoprecipitate overnight

by tumbling the Eppendorf tubes end over end at 4°C in a tube rotator set up at 8-10 rpm. Finally, immunoprecipitates were washed four times by centrifuging the mix for 10 sec at 4°C at 16,000 g, aspirating the supernatant (containing unbound proteins) using a P1000 tip connected to a vacuum aspirator, adding 1 mL of ice cold wash buffer, tumbling the Eppendorf tubes end over end in a tube rotator set up at 8-10 rpm for 5 min at 4°C by and centrifuging the tubes again. When processing numerous samples, tubes were kept on ice inbetween washing steps. The fourth wash was done in ice cold PBS instead of wash buffer and the final product of settled beads containing the bound antigen were boiled in 15 µL of 2x Lammeli sample buffer. Alternatively, the fourth and a fifth wash were done in 1x kinase buffer, keeping the beads in a final volume of 25 µL of kinase buffer to process into the *in vitro* non radioactive kinase assay.

### 2.1.3 SDS-PAGE

Thirty micrograms of total protein per sample were mixed with an equivalent volume of 2x sample loading buffer (see below for composition of the buffer) and proteins were denatured by boiling for 5 minutes at 95°C and then kept on ice until ready to load. Two Novex® Tris-Glycine 4-12% gels, 1 mm thick (Invitrogen), were assembled on an XCell SureLock® Mini-Cell system (Invitrogen) filled with running buffer (see below for composition of the buffer) according to the manufacturer's instructions. Once loaded, the gels were run at 125V and proteins were separated by electrophoresis for approximately 2.5 hours. Full-range Rainbow and Prestained broad range molecular weight markers (Amersham and New England Biolabs) were run alongside the samples, to allow for the identification of bands.

### 2.1.4 Western blotting

Proteins were transferred from the gel to a Hybond-C nitrocellulose membrane (Amersham) using a semi-dry transfer system (Biorad) in 1x transfer buffer (see below

for composition of the buffer) for 1.5h at 100 mA and 10V. The membranes were blocked with 30 mL 5% Marvel dry powder milk in TBST (see below for composition of the buffer) or for 5% BSA, 50 NM NaF in TBST when blocking for phospho specific detection, for 2 hours at room temperature, on a rocking shaker. Primary antibody was added at optimised dilutions to 15 mL blocking buffer and membranes were incubated overnight at 4°C on a rotating shaker. Rabbit anti-HCK antibody (N-30 Santa Cruz Biotechnology, Santa Cruz USA) and mouse anti-HCK antibody (clone 18 BD Bioscience) were used at 1:4,000 dilution. Goat anti-phospho-HCK antibody (Y411 Santa Cruz Biotechnology, Santa Cruz USA), rabbit anti-phospho-STAT5 Tyr694 antibody (C11C5 Cell Signalling Technology) and goat anti-phospho-STAT5 Tyr694 antibody (sc-11761 Santa Cruz Biotechnology, Santa Cruz USA) were used at 1:500 dilution. The membranes were washed 5 times for 5 minutes with fresh TBST. Secondary antibody (1:4,000 dilution; Pierce Biotechnology) conjugated to horse radish peroxidase was added to 15 mL blocking buffer and membranes were incubated for 2 hours at room temperature, on a rocking shaker. The membranes were washed 4 times for 5 minutes with fresh TBST, followed by a final wash in TBS buffer. Specific protein detection was achieved by incubating each membrane for 1 min with 5 mL of ECL Plus chemoluminescent substrate (Amersham) and exposing them to films (Kodak, Switzerland) for various lengths of time. Films were developed using a Hoeffman automatic developer.

## 2.2 Flow cytometry

### 2.2.1 Cell cycle analysis by DAPI internal staining

Half a million cells for cell lines or $0.25x10^6$ cells of $Lin^-/CD34^+/CD38^-$ were resuspended in 500 µL of PBS in a polystyrene 5 mL FACS tube (Falcon). 500 µL of 4% Paraformaldehyde (PFA; Sigma) equilibrated at room temperature was added to the cell suspension and cells were incubated for 10 minutes at RT (final concentration 2% PFA). Cells were washed by adding 4 mL of PBS and centrifuging them at 300 g for 7 minutes

(low brake speed). Supernatant was aspirated and cells were resuspended in 500 µL of PBS. 500 µL of 0.2% Triton-X100 was added to the cell suspension and cells were incubated at RT for 10 minutes (final concentration 0.1% Triton-X100). Cells were washed as described above with PBS 2% FCS and resuspended in 300 µL of PBS 2% FCS containing 1 µg/mL DAPI. After 20 min incubation in the dark, samples were processed for cell cycle analysis on LSRII analyser.

### 2.2.2 Apoptosis analysis by Annexin V external staining

Half a million cells were stained for Annexin V according to manufacturer's instructions (BD Biosciences). Briefly, cells were washed with ice cold PBS by centrifuging them at 300 g for 7 minutes (low brake speed). Cells were resuspended at $1x10^6$ cells/mL in 1x ice cold Binding Buffer provided by the manufacturer. Five microlitres of Annexin V-Alexa 647 conjugated antibody and 0.2 µg DAPI were added to each sample, which were then incubated in the dark for 15 min. Two hundred microlitres of ice cold Binding Buffer were added to each sample, which were analysed on an LSRII analyzer.

### 2.2.3 $HgCl_2$ treatment

Half a million cells were washed with PBS by centrifuging them at 300 g for 7 minutes (low brake speed) and resuspended in 1 mL of 0.5 mM $HgCl_2$. Cells were incubated for 5 min at 37°C in a 5% $CO_2$ incubator in a 5 mL polystyrene FACS tube. Cells were washed in PBS by centrifuging them at 300 g for 7 minutes (low brake speed). Pelleted cells were resuspended in 0.5 mL PBS and fixed by adding 0.5 mL of 4% Paraformaldehyde (PFA) dropwise and processed for staining for flow cytometry as described below. If cells were being treated for subsequent Western blot analysis, 3 million cells were washed with PBS by centrifuging them at 300 g for 7 minutes (low brake speed) and resuspended in 0.5 mL of pre-warmed culture medium. PP2 or SU6656 inhibitors were added to a final concentration of 5 or 10 µM and the cells were incubated for 1h at 37°C in a 5% $CO_2$

incubator in a 24 well plate (Falcon). Cells were pelleted by centrifuging them at 300 g for 7 minutes (low brake speed) and resuspended in 2x Lammeli sample buffer.

### 2.2.4 PP2 or SU6656 treatments

Half a million cells were washed with PBS by centrifuging them at 300 g for 7 minutes (low brake speed) and resuspended in 1 mL of pre-warmed culture medium. PP2 or SU6656 inhibitors were added at a final concentration of 5 or 10 μM and the cells were incubated for 1h at 37°C in a 5% $CO_2$ incubator in a 5 mL polystyrene FACS tube. Cells were fixed by adding 1 mL of 4% Paraformaldehyde (PFA) dropwise and processed for staining for flow cytometry as described below. If cells were being treated for subsequent Western blot analysis, 3 million cells were washed with PBS by centrifuging them at 300 g for 7 minutes (low brake) and resuspended in 0.5 mL of pre-warmed culture medium. PP2 or SU6656 inhibitors were added at a final concentration of 5 or 10 μM and the cells were incubated for 1h at 37°C in a 5% $CO_2$ incubator in 24 well plate (Falcon). Cells were pelleted by centrifuging them at 300 g for 7 minutes (low brake) and resuspended in 2x Lammeli sample buffer.

### 2.2.5 Intracellular staining for flow cytometry (non-phospho-specific)

Between 0.25 and $1x10^6$ cells (depending on the experiment) were resuspended in 500 μL of PBS in a polystyrene 5 mL FACS tube. 500 μL of 4% Paraformaldehyde (PFA) equilibrated at room temperature was added to the cell suspension and cells were incubated for 10 minutes at RT (final concentration 2% PFA). Cells were washed by adding 4 mL of PBS and centrifuging them at 300 g for 7 minutes (low brake). Supernatant was aspirated and cells were resuspended in 500 μL of PBS. 500 μL of 0.2% Triton-X100 was added to the cell suspension and cells were incubated at RT for 10 minutes (final concentration 0.1% Triton-X100). Cells were washed twice, as described above, with PBS 2% FCS and resuspended in PBS 2% FCS and aliquoted as 50 μL per

FACS tube (one tube per primary antibody needed). Primary antibody from a master mix was added to the cells to a final concentration of 1 µg /tube and incubated for 1 hour at RT. Cells were washed with PBS 2% FCS and resuspended in 50 µL 2% FCS. Secondary antibody conjugated to a fluorochrome diluted 1:50 was added the cells from a master mix (corresponding to 2 µL per tube) and incubated at RT for 45 minutes in the dark. Cells were washed with PBS 2% FCS, resuspended in 300 µL PBS 2% FCS 1 mg/mL DAPI and analysed by flow cytometry (LSRII, BD Biosciences).

### 2.2.6 Intracellular staining for flow cytometry (phospho-specific)

Cells were resuspended at a concentration of $1x10^6$/mL of OptiMEM 0.25% BSA in a polystyrene 5 mL FACS tube 15 min to 24h prior to staining. 1 mL of 4% Paraformaldehyde (PFA) equilibrated at 37°C was added dropwise, while vortexing, to the cell suspension and cells were incubated for 10 minutes at 37°C in a 5% CO2 incubator (final concentration 2% PFA). Cells were washed twice, first by centrifuging them at 300 g for 7 minutes (low brake) then by resuspending them in 1 mL PBS topped up to 5 mL and centrifuging at 300 g for 7 minutes (low brake). Supernatant was aspirated and cells were resuspended in 1 mL ice cold methanol added dropwise while vortexing. After 30 min incubation at 4°C, cells were washed twice, as described above, with PBS 5% BSA and resuspended in an appropriate volume of PBS 5% BSA, so that exactly 50 µL of cell suspension could be aliquoted per antibody needed. Fifty microlitres of primary antibody was added to the cells from a master mix to a final concentration of 1 µg/tube (or 3 µL of directly conjugated antibody/tube) and incubated for 1 hour at RT (protected from light for directly conjugated antibodies). Cells were washed with PBS 5% BSA and resuspended in 50 µL 5% BSA. If required, 50 µL of secondary antibody conjugated to a fluorochrome diluted 1:50 was added the cells from a master mix (corresponding to 2µL per tube) and incubated at RT for 45 minutes in the dark. Cells were washed with PBS 5% BSA, resuspended in 300 µL PBS 2% FCS 1 mg/mL DAPI and analysed by flow cytometry (LSRII, BD Biosciences).

### 2.2.7 PhosphoFACS: signal transduction by flow cytometry

Cells were resuspended at a concentration of $1x10^6$/mL of OptiMEM 0.25% BSA in a polystyrene 5 mL FACS tube 24h prior to proceeding for staining. Cells were stimulated with G-CSF, GM-CSF or IL-6 at a final concentration of 100 ng/mL for 30 min or 1h. Celles were fixed by adding 1 mL of 4% Paraformaldehyde (PFA) equilibrated at 37°C dropwise while vortexing and processed for intracellular staining for flow cytometry.

### 2.2.8 Extracellular staining for phenotyping

Half a million cells were washed with PBS and resuspended in 50 µL of PBS containing 2% FCS. Five microlitres of the appropriate directly conjugated antibodies were added to the 5 mL FACS tubes and the samples were incubated for 30 min at 4°C in the dark. Unbound antibodies were washed by centrifugation for 7 min at 300g, cells were resuspended in 300 µL PBS 2% FCS 1 mg/mL DAPI and analysed by flow cytometry (LSRII, BD Biosciences). Alternatively, cells were washed and processed for internal staining for flow cytometry. Flow cytometry analysis was conducted on a BD LSR II (BD Bioscience) using the Diva software (BD Biosciences). Subsequent analysis was performed with FlowJo software (Ashland USA). Lasers and bandpass filters required for analysis are listed in *Table II.2.* During analysis, the photomultiplier gains were set so that the background signal from the combined isotype control gave 1-5% positive cells in each collection channel. Compensation amounts were set according to the detected spectral overlap.

.

| Laser | Bandpass Filter | Fluorochrome |
|---|---|---|
| 488nm (blue) | 440/40 | DAPI |
| | 530/30 | FITC |
| | 575/26 | PE |
| | 660/20 | Topro-3 |
| | 695/40 | PerCP |
| | 780/60 | PE-Cy7 |
| 633nm (red) | 660/20 | APC |

***Table II.2:** Laser and bandpass filters used for flow cytometry analysis.*

2.2.9 Labelling of HCK antibody and mouse isotype control with Alexa 647 fluorochrome

Before proceeding to antibody labelling according to the manufacturer's instructions (Invitrogen), anti-HCK antibody was concentrated at 1 mg/mL using the iCON™ Concentrator 7 mL/20K column according to the manufacturer's instructions (Pierce). Briefly, 4 mL of Millipore treated water were added to the upper sample chamber and the column was pre-rinsed by centrifugation for 15 min at 2,000 g. The water was discarded and 1 mL of the appropriate antibody (mouse HCK sold by Santa Cruz at 250 µL/mL or mouse isotype control sold by BD) was added to the upper sample chamber. The column was centrifuged for 15 min at 2,000 g and the concentrated antibody was collected from the upper chamber. Antibody concentration was measured using a Nanodrop device and, if the concentration was near 1 mg/mL in a final volume of 100 µL, it was processed for Alexa 647 labelling.

A solution of 1M sodium bicarbonate was prepared according to manufacturer's instructions (Invitrogen) and 10 µL of this solution were added to the 100 µL of concentrated antibody solution. The latter mixture was transferred to a tube containing a reactive dye provided by the manufacturer and the dye was dissolved by inversion. The labelling reaction was allowed to occur by incubating the vial for 1h at room temperature, inverting it every 15 min. In the meantime, a resin bed was prepared for elution of the labelled antibody, by adding 1 mL of homogenised resin onto a spin column and allowing

it to settle. Resin was added until the volume bed reached 1.5 mL and the column was allowed to drain into a 5 mL FACS tube by gravity. The spin column was positioned onto a collection tube and centrifuged for 3 min at 1,100 g. The resin buffer was discarded and the 100 µL of labelling antibodies were loaded onto the resin bed dropwise. The antibody solution was allowed to absorb into the resin bed and the column was placed onto a fresh collection tube. The tube was centrifuged for 5 min at 1,100 g and the antibody concentration and degree of labelling were determined using a Nanodrop device. Labelled antibodies were stored protected from light at 4°C and a volume of antibody corresponding to 4 moles of Alexa 647 was used for subsequent FACS staining.

### 2.2.10 Absolute cell count using counting beads

Cells were washed with PBS and resuspended in 300 µL PBS 2% FCS 1 mg/mL DAPI. Fifty microlitres of counting beads were added to each tube shortly prior to analysis by flow cytometry (LSRII, BD Biosciences). Absolute number of cells originally present in the tube was calculated taking into account the original beads concentration indicated by the manufacturer (Invitrogen).

### 2.2.11 Antibodies used in this study

The following antibodies were used in external staining or internal staining for flow cytometry and for Western blots (*Table II.3*).

| Directely conjugated antibodies | | | |
|---|---|---|---|
| CD marker | Clone | Isotype | Conjugate |
| CD13 | WM15 | IgG1 κ | PE |
| CD13 | WM15 | IgG1 κ | APC |
| CD14 | M5E2 | IgG2a κ | APC |
| CD14 | M5E2 | IgG2a κ | PE-Cy7 |
| CD15 | HI98 | IgMκ | PE |
| CD15 | HI98 | IgMκ | APC |

| | | | |
|---|---|---|---|
| CD33 | WM53 | $IgG_1 \kappa$ | PE |
| CD33 | WM53 | $IgG_1 \kappa$ | APC |
| CD33 | P67.6 | $IgG_1 \kappa$ | PE-Cy7 |
| CD34 | 8G12 | $IgG_1 \kappa$ | PE |
| CD34 | 8G12 | $IgG_1 \kappa$ | PE-Cy7 |
| CD38 | HIT2 | $IgG_1 \kappa$ | PE |
| CD38 | HB7 | $IgG_1 \kappa$ | PE-Cy7 |
| Lineage cocktail (includes CD3, CD14, CD16, CD19, CD20, CD56) | Multiple | Multiple | FITC |
| | | | |
| Phospho-STAT5 Y694 | | | |
| Phospho-STAT3 Y705 | | | |
| Phospho-ERK | | | |
| Phospho-c-Raf | | | |
| | | | |
| Non-conjugated antibodies | | | |
| Mouse HCK | | | |
| Rabbit HCK* | | | |
| Phospho-HCK Y411* | | | |
| STAT5*** | | | |
| STAT5 | | | |
| | | | |
| Secondary antibodies | | | |
| Anti-mouse HRP* or Alexa 647** | | | |
| Anti-rabbit HRP* or Alexa 647** | | | |
| Anti-goat HRP* or Alexa 647** | | | |

***Table II.3:* Antibodies and fluorochromes used in this study.**
*All antibodies were purchased from Beckton Dickinson (BD) Biosciences, Cowley, Oxford except for antibodies marked with asterisks: . * Santa Cruz. ** Molecular probes, Invitrogen. *** Cell Signalling Technology. In addition, isotype controls were purchased from BD Biosciences. The fluorochromes used are FITC = fluorescein isothiocyanate, PE = phycoerythrin, APC = allophycocyanin, PE-Cy7 = phycoerythrin-cyanin 7.*

## 2.3 *In vitro* non-radioactive kinase assay

Final volume of each kinase assay reaction is 50 µL pipetted into a 384 well black plate, all pipetting was done at 4°C. An Antibody Beacon detection complex/substrate mix was prepared by mixing multiples of 18 µL of 1x kinase buffer (containing freshly added DTT at a final concentration of 2 µM), 0.5 µL of Oregon Green 488 ligand, 0.5 µL of anti-phosphotyrosine antibody P-Tyr-100 and 1 µL of tyrosine kinase substrate 1. ATP mix was prepared by mixing multiple of 15 µL of 1x kinase buffer and 0.74 µL of 100 mM ATP.

Duplicate control sample mixes consisted of (i): ligand only control: 1 µL of Oregon Green 488 ligand into 99 µL of 1x kinase buffer to split in two; (ii) phospho-peptide control: 1 µL of Oregon Green 488 ligand, 1 µL of anti-phosphotyrosine antibody P-Tyr-100, 5 µL of control phospho-peptide into 93 µL of kinase buffer to split in two; (iii) no kinase control: 40 µL of Antibody Beacon detection complex/substrate mix, 50 µL of kinase buffer to split in two replicates ultimately topped up by 5 µL 5 mM ATP; (iv) no ATP control: 1 µL recombinant HCK (25ng) into 60 µL kinase buffer and 40 µL of Antibody Beacon detection complex/substrate mix to split in two; (v) no substrate control: 1 µL recombinant HCK (25 ng), 1 µL of Oregon Green 488 ligand, 1 µL of anti-phosphotyrosine antibody P-Tyr-100 into 88 µL kinase buffer to split in two replicates, ultimately topped up by 5 µL 5 mM ATP. The recombinant kinase control scale was prepared by adding 1 µL of recombinant HCK (Active Motif) to 50 µL of kinase buffer and serially diluting it 5 times. Forty microlitres of Antibody Beacon detection complex/substrate mix were added to each well, which was split in two replicates ultimately topped up by 5 µL of 5 mM ATP. Twenty-five microlitres of each immunoprecipitate were pipetted into a well using a cut P20 tip, topped up with 20 µL of Antibody Beacon detection complex/substrate mix and 5 µL of 5 mM ATP. When appropriate, diluted Src kinase inhibitor or DMSO was added at room temperature prior to the addition of ATP. Plates were read in a microplate reader (Perkin Elmer), using a 485/530 nm filter, after a 45 or 50 min incubation period at room temperature in the chamber of the reader.

## 3. Cell biology

### 3.1 Cell culture

#### 3.1.1 Maintenance of adherent cells

SW28, JAR, 293T-HEK and HeLa cells were maintained in Dulbecco's Modified Eagle's Medium (DMEM, Gibco Invitrogen) high glucose, supplemented with 10% fetal calf serum (FCS, Gibco Invitrogen) and 1% penicillin/streptomycin (CRUK) in cell culture treated flasks (Falcon) in a 37°C 5% $CO_2$ incubator. Cells were passaged when reaching 80% confluency or whenever needed for performing experiments. To passage the cells, the media was removed from the cells by aspiration and the cells were washed with PBS. Trypsin (CRUK) was added to the cells and the flask was incubated for 5 minutes at 37°C. FCS was added to stop the trypsin activity and cells were centrifuged for 7 minutes at 300 g with high brake applied. Cells were resuspended in media and counted on a haemocytometer. An appropriate number of cells were perpetuated in fresh media.

#### 3.1.2 Maintenance of suspension cells

HL-60, NB4, Fujioka/P31, U937, THP1, K562, Jurkat, J6A, Kasumi-1 and KG1a cells were maintained in RPMI 1640 medium with Glutamax (Gibco Invitrogen), supplemented with 10% fetal calf serum (FCS, Gibco Invitrogen) and 1% penicillin/streptomycin (CRUK) in cell culture treated flasks (Falcon) in a 37°C 5% $CO_2$ incubator. Mono-mac-6 cells were maintained in the same medium additionally supplemented with 1% non-essential amino acids, 1 mM sodium pyruvate and 9 μg/ml human insulin. Cells were maintained as 300,000 cells/mL and numerated every 3 days using Trypan blue exclusion in order to generate their growth curve.

## 3.2 Stem cell enriched fraction purification

Stem cells were extracted from human umbilical cord blood. Informed consent was obtained from mothers awaiting caesarean section at the obstetric units of the Royal London Hospital, Whitechapel, London and the University College Hospital, Camden, London. Blood was extracted from the placenta and umbilical cords with a 20 mL syringe and immediately supplemented with heparin (Sigma Aldrich, Dorset, UK) to a final concentration of 1 mg/mL in 50 mL tubes. Tubes were transferred to the laboratory and stored overnight on a rocker at room temperature for extraction of stem cells on the next day.

### 3.2.1 Mononuclear cells preparation from umbilical cord blood by density centrifugation.

Fifteen mililitres of Ficoll-Paque Plus (Amersham Biosciences UK Ltd, Little Chalfont, Buckinghamshire) were distributed into 50 ml tubes (Corning). Umbilical cord blood was diluted with PBS (one volume of blood for three volumes of PBS) and 35 mL of diluted blood were slowly layered onto the Ficoll-Paque Plus. The tubes were centrifuged at 20°C for 30 minutes at 400 g with no brake applied. Pasteur pipettes (Fisher Scientific) were used to aspirate the mononuclear cells which form a layer at the interphase of serum and ficoll and mononuclear cells were pooled into fresh 50 mL tubes. The cells were diluted further with PBS (one volume of MNC for one volume of PBS) and centrifuged at 4°C for 7 minutes at 300 g to better wash off the Ficoll-Paque Plus. Recovered MNC were resuspended in 5 mL of PBS with 2% FCS and contaminating red cells were lysed by adding 40 mL of ammonium chloride (Stem Cell Technologies, Meylan, France) and incubated at 4°C for 5 minutes. Lysis was inactivated by addition of 5 mL of FCS. Cells were centrifuged at 4°C for 7 minutes at 300 g and MNC were numerated using a haematocytometer and the Trypan blue exclusion method for assessing their viability. If more than $2x10^8$ MNC were obtained, the cord blood sample was further processed by lineage depletion.

### 3.2.2 Lineage depletion of normal haematopoietic tissue

Mononuclear cells isolated from human cord blood were depleted of cells expressing mature lineage antigens using the StemSep column system from Stem Cell Technologies (Meylan, France). Mononuclear cells were resuspended in PBS with 2% FCS as $7x10^7$ cells/mL. StemSep Human Hematopoietic Progenitor Cell Enrichment Cocktail (Stem Cell Technologies, Vancouver, Canada) was added at a concentration of 100 uL of cocktail per mL of cells in solution. This antibody cocktail, consisting of anti-CD2, CD3, CD14, CD16, CD19, CD24, CD56, CD66b, and anti-glycophorin A antibodies, was supplemented with the anti-CD41 antibody at a concentration of 10 uL of CD41 per mL of cells in solution. After 30 minutes at 4°C, 60 µL of Magnetic Colloid (Stem Cell Technologies) per mL of cell suspension was added to the cell suspension. Cells were incubated for 30 minutes at 4°C. During this incuabation period, a StemSep Negative Selection Column (Stem Cell Technologies) was positioned within a magnetic field, primed with PBS and equilibrated with PBS with 2% FCS according to the manufacturer's instructions. The cell suspension labelled with colloid was pumped through the column and Lineage negative ($Lin^-$) cells were eluted into a fresh 50 mL tube by washing with PBS containing 2% FCS. Lineage marker expressing cells positively labelled with the colloid remain trapped within the column, as long as they stay within the magnetic field. $Lin^-$ cells were centrifuged at 4°C for 7 minutes at 300 g, counted and frozen in FCS supplemented with 10% dimethyl-sulphoxide (DMSO, Sigma). The column, containing the lineage positive cells, was washed with 2% FCS and the cells were either discarded, or frozen down and used as control cells in staining experiments.

## 3.3 siRNA electroporation

One millilitre of pre-warmed cell line culture medium was aliquoted in a 24 well plate and kept in a 37°C 5% $CO_2$ incubator until ready to use. The appropriate cell line was washed in PBS, numerated by Trypan blue exclusion and resuspended as $1x10^6$ cells/mL in pre-warmed growth medium. The cell solution was aliquoted in the appropriate

number of electroporation cuvette and 1 μg of the appropriate siRNA was added to the cell suspension. Electroporation was undergone at 300 millivolts and 125 millifarradays for 3.3 milliseconds and 500 μL of the pre-warmed culture medium previously aliquoted in the 24 well plate was added to the cuvette immediately after electroporation. The whole volume of electroporated cell suspension was transferred to one well of the 24 well plate (final volume 1.5 mL). Samples were incubated for the appropriate amount of time (as indicated in the text) at 37°C 5% $CO_2$ then assessed for HCK silencing.

### 3.4 siRNA or miRNA nucleofection

Half a millilitre of Supplement was mixed with 2.25 mL of Nucleofactor solution R, V or C according to the manufacturer's instructions (Amaxa) and was pre-warmed to 37°C. One millilitre of pre-warmed cell line culture medium was aliquoted in a 24 well plate and kept in a 37°C 5% $CO_2$ incubator until ready to use. The appropriate cell line was washed in PBS, numerated by Trypan blue exclusion and aliquoted as $1x10^6$ cells in 5 mL polystyrene FACS tubes. Each aliquot was centrifuged and processed one by one for nucleofection: one given aliquot of $1x10^6$ cells was resuspended in 100 μL of the appropriate Nucleofactor solution, 1 μg of the appropriate siRNA or miRNA encoding plasmid was added to the cell suspension and mixed by gently tilting the FACS tube. The whole volume of cell suspension was transferred to a fresh nucleofection cuvette. The appropriate Nucleofactor program was selected and the cuvette was positioned in the Nucleofector chamber. Immediately after nucleofection, 500 μL of pre-warmed culture medium was added to the cuvette and the whole volume of nucleofected cell suspension was transferred to one well of the 24 well plate using the thin plastic Pasteur pipette provided by the manufacturer. The Nucleofactor device was reset to start position and the next sample was processed for nucleofection. Samples were incubated for 48h at 37°C 5% $CO_2$ then assessed for HCK silencing (siRNA) or GFP expression (miRNA).

### 3.5 Transient transfection of 293T-HEK cells

700,000 293T-HEK cells per well were plated into a 6 well plate. Twenty-four hours later cells were transfected with either 3 μg of lentiviral mock plasmid encoding GFP or 3 μg of lentiviral mock plasmid encoding YFP or 3 μg of lentiviral plasmid encoding either p59HCK-GFP or p59HCK-YFP. PEI was used as a transfection agent at a 1:2 ratio (6 μg of PEI for 3 μg of DNA). Cells from one well were left as a non-transfected sample, but still incubated with PEI as a control for PEI toxicity and basal endogenous level of HCK. PEI was first mixed into Opti-MEM medium by vortexing, as a master mix for all reactions, and allowed to sit for 5 min at room temperature. Appropriate amount of DNA was mixed into Opti-MEM for each construct. 75 μL of PEI solution and 75 μL of DNA solution were mixed together by vortexing and allowed to sit for 20 min at room temperature. 150 μL of PEI-DNA complex solution was then added dropwise to 293T-HEK cells acclimatised into 3 mL of Opti-MEM medium. After 5h incubation at 37°C 5% $CO_2$, transfection reaction medium was changed for fresh culture medium and cells were incubated for 48h. GFP expression could be detected 24h post transduction under a fluorescence microscope. Forty-eight hours post transduction cells were trypsinised, fixed with 2% PFA and processed for HCK and phospho-HCK Y411 internal staining.

### 3.6 Overexpression/ silencing of HCK in 293T-HEK cells

The experimental design of this experiment is summarised in *Table II.4*. 700,000 293T-HEK cells per well were plated into a 6 well plate. Twenty-four hours later cells from 3 wells were transfected with 3 μg of lentiviral plasmid encoding p59HCK-YFP and cells from 2 wells were transfected with 3 μg of lentiviral mock plasmid encoding YFP. PEI was used as a transfection agent at a 1:2 ratio (6 μg of PEI for 3 μg of DNA). Cells from one well were left as a non-transfected sample, but still incubated with PEI as a control for PEI toxicity and basal endogenous level of HCK. PEI was first mixed with Opti-MEM medium by vortexing, as a master mix for all reactions, and allowed to sit for 5 min at room temperature. Appropriate amount of DNA was mixed with Opti-MEM, as

two master mixes for transfection, with either p59HCK-YFP or YFP. 75 µL of PEI solution and 75 µL of DNA solution were mixed together by vortexing and allowed to sit for 20 min at room temperature. 150 µL of PEI-DNA complex solution was then added dropwise to 293T-HEK cells acclimatised into 3 mL of Opti-MEM medium. After 5h incubation at 37°C 5% $CO_2$, transfection reaction medium was changed for fresh culture medium and cells were incubated overnight. For HCK silencing to occur, one of the 3 wells transfected with p59HCK-YFP was transduced with the pRLL-SIN-cPPT-shHCK4-PGK-eGFP-WPRE silencing lentivirus at MOI 10 (this combination will be called 'HCK sh'), one of the 3 wells was transduced with the pRLL-SIN-cPPT-PGK-eGFP-WPRE mock lentivirus at MOI 10 (this combination will be called 'HCK mock') and the last of the 3 wells transfected with p59HCK-YFP was left as a non-transduced control (this combination will be called 'HCK alone'). One of the 2 wells transfected with YFP was transduced with the pRLL-SIN-cPPT-PGK-eGFP-WPRE mock lentivirus at MOI 10 (this combination will be called 'YFP mock'). The other well was left as a non-transduced control (this combination will be called 'YFP alone'). Appropriate amount of virus was added to the 293T-HEK cells in 1 mL of fresh culture medium. GFP expression could be observed 24h post transduction under a fluorescence microscope. Forty-eight hours post transduction (i.e. 72h post-transfection) cells were numerated and 150,000 293T-HEK cells were lysed with 350 µL of RLT buffer and frozen at -80°C for further RNA extraction. Left over cells were lysed with RIPA buffer and cell lysates were frozen at -80°C for subsequent analysis by Western-blot.

| | Well 1 | Well 2 | Well 3 | Well 4 | Well 5 | Well 6 |
|---|---|---|---|---|---|---|
| Transfection | p59HCK-YFP | p59HCK-YFP | p59HCK-YFP | YFP | YFP | PEI only |
| Transduction | shHCK4-GFP | Mock GFP | --- | Mock GFP | --- | --- |
| Name of the combination | HCK sh | HCK mock | HCK alone | YFP mock | YFP alone | 293T |

***Table II.4:** Design of the transient HCK overexpression/stable shHCK4 transduction experiment in 293T-HEK cells.*

## 3.7 Lentivirus production

### 3.7.1 293T-HEK cells transfection and lentivirus production

Lentiviruses used to transduce leukaemic cell lines or lineage depleted umbilical cord blood cells were produced by transient transfection of three plasmids into 293T cells. These three plasmids were the self-inactivating transfer vector plasmid containing the gene or shRNA of interest, a multi-deleted packaging plasmid and pMD.G, which provides the viral envelope 139. Each plasmid was produced in an endotoxin free system (Qiagen EndoFree Plasmid Mega Kit for the self-inactivating transfer vector plasmid containing the gene or shRNA of interest, Plasmid Factory for the pMD.G and the multi-deleted packaging plasmid) .

Two million 293T-HEK cells per flask were seeded in twenty-four 175cm$^2$ flasks 4 days prior to transfection. A master mix corresponding to 100 μg of PEI per 5 mL of OptiMEM per flask was prepared, briefly vortexed and incubated for 5 min at RT. A master mix corresponding to 17.5 μg of the envelope plasmid, 32.5 μg of the packaging plasmid and 50 μg of the transfer vector plasmid in 5 mL OptiMEM per flask was prepared, added to the PEI suspension (final ratio 1:1), vortexed and incubated at room temperature for 20 minutes. Ten millilitres of the DNA plus PEI complexes were added to the cells, which were previously acclimatised in 15 mL of OptiMEM, resulting in a final volume of 25 mL. The cells were incubated at 37°C for 4 hours, after which the media was replaced with fresh supplemented DMEM culture medium. After 24 hours, the media was replaced with fresh media. Forty-eight hours post-transfection the medium was harvested and cleared of unattached cells and cellular debris by filtering through a 0.45 nm filter. Virus was concentrated by centrifuging for 4 hours at 19,000 g at 4°C in a Beckman ultracentrifuge. After centrifugation, the supernatant was removed and 100 μL StemSpan media (Stem Cell Technologies) was added to the pellet, which was left to dissolve on ice for 1 hour. The undissolved pellet was gently resuspended, taking great not to produce air bubbles, and the virus was aliquoted into 50 μL fractions, with 30 μL being saved for titration purposes. This harvesting and concentrating procedure was

repeated the next two days (72h and 96h post transfection).

### 3.7.2 Lentivirus titration

To titre the virus, 50,000 HeLa cells were plated into each well of a 12 well tissue culture treated plate (Falcon) in a volume of 1 mL normal growth media. Serial dilutions of the virus ranging from 1/100 to 1/100,000 for each day were prepared and added to the cells. Seventy two hours post-transduction the cells were trypsinised, resuspended in 300 µL PBS 2% FCS and analysed for GFP expression by flow cytometry on a FACSCalibur (BD Bioscience, San Jose USA) using TOPRO-3 as a live/dead cells discriminatory dye (2 µL/tube). Virus titre was calculated based on percentage of GFP positive HeLa cells.

## 3.8 Viral transduction

### 3.8.1 Transduction of leukaemic cell lines

Fujioka/P31, U937 and Mono-mac-6 cells were aliquoted into 12 well flat bottom tissue culture plates at a final concentration of $0.3x10^6$/mL (once the virus will be added) in their respective culture medium. Cells were transduced at multiplicity of infection (MOI) 80, meaning that 80 virus particles were added for every cell. Cells were left to transduce overnight in a 37°C 5% $CO_2$ incubator. The next day cells were washed by resuspending them in a final volume of 15 mL of growth medium and then resuspended in the same volume of fresh culture medium they were previously in.

### 3.8.2 Transduction of $Lin^-$ cells

Three wells of a flat bottom tissue culture 96 well plate were coated with 100 µL of retronectin (100 ng/mL, Takara) by incubating the plate 1h at 37°C. After washing the

wells twice with PBS, Lineage depleted cord blood mononuclear cells resuspended in StemSpan media (Stem Cell Technologies) supplemented with cytokines (50 ng/mL SCF, 50 ng/mL FLT3-L, 10 ng/mL IL -6, 20 ng/mL TPO; PeproTech) were aliquoted into the wells at a final concentration of $1x10^6$/mL (once the virus will be added). Lin$^-$ cells were aliquoted in triplicate for subsequent transduction with either (i) mock or (ii) silencing/overexpression lentivirus and for use as (iii) non-transduced control. Lin$^-$ cells were first left to activate at 37°C, 5% $CO_2$ for 4 hours then transduced at multiplicity of infection (MOI) 80, meaning that 80 virus particles were added for every Lin$^-$ cell, by simple addition of the appropriate volume of virus already resuspended in StemSpan. Cells were left to transduce overnight in a 37°C 5% $CO_2$ incubator. The next day cells were washed in PBS 2% FCS (washing each well with 5 volumes of 100 µL), counted and used immediately for *in vitro* assays.

### 3.9 XTT assay

Cells were plated at a density of 50,000 cells/100 µL in triplicate in four flat bottom 96 well plates and incubated at 37°C, 5% $CO_2$ for 24h, 48h or 96h. Fifty microlitres freshly mixed tetrazolium salt (XTT labelling reagent) and electron-coupling reagent were added to the wells of one plate 24h, 48h, 96h or immediately, after cell plating. XTT reagents containing plates were incubated for 2h at 37°C, 5% $CO_2$ and formazan salt production was determined by measuring absorbance at 450 and 650 nm. Cell proliferation was represented as absorbance at 450 nm corrected by absorbance at 650 nm over time.

### 3.10 Lin$^-$ *ex vivo* expansion

Equal numbers of mock transduced, shHCK4 transduced/ovHCK transduced or non-transduced Lin$^-$ cells were resuspended in a final volume of 100 µL of StemSpan containing either 300 ng/mL SCF, 300 ng/mL Flt3-L and 20 ng/mL TPO (medium1) or 100 ng/mL SCF, 100 ng/mL Flt3-L and 20 ng/mL IL-6 (medium 3). Lin$^-$ cells were numerated every 3 days on an LSRII analyser using counting beads, an appropriate number of cells were used for various *in vitro* assay and unused equal number of cells

were replated for each condition, adding fresh cytokines each time.

### 3.11 Myeloid differentiation culture

$Lin^-$ cells were resuspended in restricting myeloid differentiation medium (IMDM, 15% FCS, 20 ng/mL IL-3 and 20 ng/mL SCF (Barabe et al., 2007)) or in terminal granulocytic differentiation medium (IMDM, 20% FCS, 50 ng/mL G-CSF and 50 ng/mL SCF (Edvardsson et al., 2004)) at a final concentration of 20,000 cells/mL and seeded in triplicate. $Lin^-$ cells were maintained for 12 days, adding fresh cytokines every 3 days.

### 3.12 Erythroid differentiation culture

$Lin^-$ cells were resuspended in erythroid differentiation medium (100 ng/mL SCF, 5 ng/mL IL-3, 3 IU/mL EPO, 1% BSA, 120 μg/mL iron-saturated human transferrin, 900 ng/mL $FeSO_4$, 90 ng/mL $Fe(NO_3)_3$, 10 μg/mL insulin, $10^{-6}$ M hydrocortisone) (Giarratana et al., 2005) at a final concentration of 10,000 cells/mL and seeded in triplicate. $Lin^-$ cells were split 1:5 after 4 days in culture and cell differentiation was assessed by flow cytometry after 8 days in culture.

### 3.13 CFC assay

#### 3.13.1 CFC for leukaemic cell lines with and without cytokines

Four thousand virally transduced and mock Fujioka/P31, U937 or Mono-mac-6 cells were added to 4 mL of H4330 MethoCult media (Stem Cell Technologies) supplemented with 1% penicillin/streptomycin. Cells and media were vortexed gently to ensure even distribution of cells throughout the viscous media. 1 mL of methylcellulose and cells mixture was dispersed into a 35 mm cell culture plate (Falcon) using a 1 mL syringe and

blunt end needle. All samples were plated in triplicate and maintained in high humidity conditions. Plates were left for 14 days under normal growth conditions and then colonies were scored by visualisation under an inverted fluorescence microscope.

### 3.13.2 CFC for Lin$^-$ cells

Four thousand lentivirally transduced and control Lin$^-$ cells were added to 4 mL of H4434 MethoCult media (Stem Cell Technologies) supplemented with 1% penicillin/streptomycin. Cells and media were vortexed gently to ensure even distribution of cells throughout the viscous media. 1 mL of methylcellulose and cells mixture was dispersed into a 35 mm cell culture plate (Falcon) using a 1 mL syringe and blunt end needle. All samples were plated in triplicate and maintained in high humidity conditions. Plates were left for 14 days under normal growth conditions and then colonies were scored by visualisation under an inverted fluorescence microscope.
Methylcellulose assays only allow us to infer the cell of origin and are therefore retrospective in nature. By observing the type of colony present, the cell of origin can be determined. More primitive cells are able to give rise to larger colonies of mixed cell types. Colonies are categorised based on the morphology of the cells. They can be assembled into the following 6 categories, BFU-E, CFU-E, CFU-GEMM, CFU-GM, CFU-G and CFU-M.

## 3.14 Transwell migration assay

### 3.14.1 Migration towards FCS

An appropriate number of 8 μm inserts for 24 well plate (Thinsert, Greiner Bio One) were coated with 100 μL fibronectin (20 pg/mL) overnight at 4°C. The next day, each insert was washed 3 times with PBS and kept in PBS until ready to use. An appropriate number of wells from a 24 well plate were filled with 600 μL of pre-warmed IMDM

(Gibco) 0.25% BSA, adding 5% FCS (Gibco) when necessary. Triplicate wells were prepared for each sample and the plate was kept at 37°C, 5% $CO_2$ in an incubator until ready to use. Fujioka/P31, U937 or Mono-mac-6 cells transduced with mock or shHCK4 lentivirus or non-transduced were numerated and resuspended in pre-warmed serum free IMDM medium at a density of $6x10^5$ cells/mL. One millilitre of each cell solution was then kept at 37°C, 5% $CO_2$ in an incubator until ready to aliquot. One hundred and fifty microlitres of each cell solution were aliquoted in triplicate into an empty insert and the insert was transferred to a well containing serum free or serum supplemented IMDM, prepared previously. Plates were incubated for 4h30 at 37°C, 5% $CO_2$ and cell migration was determined by counting the number of cells at the bottom of the well using counting beads (Invitrogen). To do so, after the 4h30 incubation, the total volume of each well was transferred to a 5 mL polystyrene FACS tube (Falcon) and the well was washed with 1 mL PBS, also added to the tube. After centrifugation, the cells were resuspended in 300 µL of PBS containing DAPI and 50 µL of counting beads were added just before proceeding with reading on an LSR II analyser.

### 3.14.2 Cytokine pre-stimulation prior to migration assay towards FCS

Transmigration inserts were coated and 24 well plates were prepared as described above. Mono-mac-6 cells transduced with mock or shHCK4 lentivirus or non-transduced were numerated and resuspended in pre-warmed IMDM medium at a density of $6x10^5$ cells/mL. One millilitre of each cell solution was then aliquoted in triplicate and 1 µL of G-CSF or GM-CSF (PeproTech; final concentration 100 ng/mL) was added to two of the aliquots. Cells were incubated at 37°C, 5% $CO_2$ in the incubator for 15 min. The tubes were topped up with 4 mL PBS, centrifuged at room temperature for 7 minutes at 300g and pelleted cells were resuspended in pre-warmed serum free IMDM medium at a density of $6x10^5$ cells/mL. One hundred and fifty microlitres of each cell solution was aliquoted in triplicate into an empty insert and the insert was transferred to a well containing serum supplemented IMDM, prepared previously. Plates were incubated for 4h30 at 37°C, 5% $CO_2$ and cell migration was determined by counting the number of

cells at the bottom of the well using counting beads (Invitrogen).

### 3.14.3 Chemotaxis assay

Transmigration inserts were coated as described above. . An appropriate number of wells from a 24 well plate were filled with 600 µL of pre-warmed IMDM (Gibco) 0.25% BSA, containing G-CSF, GM-CSF or both cytokines at a final concentration of 100 ng/mL. IMDM containing 5% FCS (Gibco) was used as a control. Triplicate wells were prepared for each sample and the plate was kept at 37°C, 5% $CO_2$ in the incubator until ready to use. Mono-mac-6 cells were added in the upper part of the transwell, allowed to migrate and numerated as described above.

## 4. Storage of patient samples

Blood patient samples obtained by leukapheresis or venepuncture were collected with informed consent and stored in the Centre for Medical Oncology, John Vane Science Centre, Charterhouse Square, London. Samples arrived at the centre either in a solution of RPMI medium with heparin or in a solution of EDTA, to prevent clotting. Samples in EDTA were diluted with RPMI prior to processing. Whole mononuclear cells were enriched from the patient sample by density centrifugation. To this end, 5 mL of Lymphoprep (Axis-Shield PoC, Oslo, Norway) were added to 15 mL tubes (Corning, Sigma-Aldrich, Dorset, UK) and 10 mL of the patient blood sample were layered on top of the Lymphoprep with a plastic pipette. Tubes were then centrifuged at room temperature for 25 minutes at 400 g with no brake (using a Beckman GS6R centrifuge, Beckman Coulter, Fullerton, USA). The differentially centrifuged central layer of white blood cells was separated from the plasma and red blood cells by aspiration with a plastic Pasteur pipette. The collected white blood cells were further diluted with 10 mL of RPMI and the 15 mL collection tubes (Corning) were then centrifuged at 300 g for 10 minutes with high brake. The supernatant was discarded and the cells were resuspended in an appropriate amount of ice cold solution of RPMI and 10% DMSO added dropwise. Cells

suspension was aliquoted in cryovials and stored in liquid nitrogen.

## 5. Solutions and recipes

Analytical or equivalent grade chemicals were obtained from Sigma, UK or BDH, UK. All buffers and solutions used de -ionised water as the diluent and were sterilised by autoclaving or filtration as appropriate.

### 5.1 Electrophoresis

#### 5.1.1 10x TBE electrophoresis buffer (1L)

108g Tris base
55g boric acid
40mL 0.5 M EDTA, pH 8.0
Working stock = 1x

#### 5.1.2 Agarose gel electrophoresis loading buffer (10x)

25mM EDTA
50% glycerol (v/v)
0.25% bromophenol blue (w/v).

### 5.2 Western Blotting

#### 5.2.1 Modified RIPA buffer (200 mL)

50 mM TrisHCl buffer pH 7.5
150mM NaCl
1% Nonidet P40
1 mM EDTA

0.3 mM activated sodium orthovanadate ($Na_3VO_4$)

50 mM sodium fluoride (NaF)

Protease inhibitors (Sigma)

### 5.2.2 Buffer A (100 mL)

50 mM Tris buffer pH 7.5

1 mM EDTA

1 mM EGTA

0.5 mM activated sodium orthovanadate ($Na_3VO_4$)

10 mM sodium β-glycerophosphate

50 mM sodium fluoride (NaF)

5 mM sodium pyrophosphate

1% Triton X-100

0.1% β-mercaptoethanol

Protease inhibitors (Sigma)

### 5.2.3 10x Running Buffer (1L)

30g Trizma base

144g Glycine

10g SDS

120

pH to 8.5

Working stock = 1x

### 5.2.4 Transfer Buffer (2L)

22.5 g glycine

4.84 g Trizma base

400 mL methanol

5.2.5 10x TBS (1L)

24.2g Trizma base

80g sodium chloride

pH to 7.6

Working stock = 1x

5.2.6 TBST (2L)

200 mL 10x TBS

10 mL 10% Tween

5.2.7 Blocking Solution for non-phospho Western Blot

5% Marvel milk in TBST

5.2.8 Blocking Solution for phospho Western Blot

5% BSA, 50 mM NaF in TBST

## 5.3 Bacteria Culture

5.3.1 LB -Broth 1 litre (CRUK)

15 g bacto -agar

Melt then cool to 50°C prior to addition of antibiotics. Pour into petri dishes and leave to set at room temperature in a laminar airflow hood. Dry plates in 37°C incubator 2 -3 hours before use.

5.3.2 X -gal

Stock solution 20 mg/ml. 0.2 g dissolved in 10 ml of N,N -Dimethylformamide. Filter, sterilise through a 0.4 μm filter and store at -20 °C.

5.3.3 Ampicillin, Kanamycin and Spectinomycin

Stock solution 50 mg/ml. Filter, sterilise through a 0.4 μm filter and store at -20°C. Use at a final concentration of 0.05 mg/ml in media.

## 5.4 Miscellaneous

TE buffer pH 7.4 or pH 8.0

10 mM Tris -HCl (pH titrated with 10 M NaOH)

1 mM EDTA pH 8.0

# Chapter III

# III Microarrays LSC vs HSC

## 1. Preliminary work

### 1.1 Microarray set up

To try to understand what makes SCID-leukaemia initiating cells (SL-IC) different from SCID-repopulating cells (SRC) at the molecular level, a gene profiling study comparing $Lin^-/CD34^+/CD38^-$ leukaemic/normal stem cell fractions and $Lin^-/CD34^+/CD38^+$ leukaemic blast/early progenitor fractions using Affymetrix U133A oligonucleotide arrays was started. Fractions were sorted from (i) seven AML patient peripheral blood samples, (ii) three independent commercial normal bone marrow samples and (iii) two pooled umbilical cord blood (UCB) samples. Patients with a variety of karyotypes and FAB classes were intentionally chosen since the starting point of interest was to identify AML 'leukaemic stem cell features' regardless of the AML type (*Figure III.1*). $Lin^-/CD34^+/CD38^-$ and $Lin^-/CD34^+/CD38^+$ fractions from patients and commercial bone marrow were isolated by three way fluorescence activated cell sorting (FACS) using anti-Lineage cocktail, anti-CD34 and anti-CD38 antibodies. An additional Ficoll-Paque™ gradient isolation step was performed before FACS for UCB. mRNA was extracted using Trizol® and cDNA was generated following Affymetrix recommendations.

| Sample (MNC) | FAB | Karyotype |
|---|---|---|
| 1 | M1 | Normal karyotype |
| 2 | M2 | Normal karyotype |
| 3 | M4 | 3+, 10+ |
| 4 | M4 | Normal karyotype |
| 5 | M2 | Normal karyotype |
| 6 | M2-tAML | Complex |
| 7 | M2 | t (8,21) |

Controls:
- 2 (pooled) cord blood samples
- 3 independent commercial normal bone marrow samples

***Figure III.1: Samples used in microarray analysis.***

*FAB classification and karyotype of the AML patient samples used in the microarray study. Pooled umbilical cord blood and bone marrow samples were used as controls.*

After application of different statistical tests (t-test, etc…) and normalisations, microarray data could be studied in two different directions. Either by looking exclusively at AML data first, extracting genes differentially expressed between the available fractions and then comparing the expression of the identified genes to normal samples, or by comparing AML samples to normal samples fraction to fraction and then in between fractions.

## 1.2 First approach to microarray analysis

The first approach, taking into account only AML data (the 'normal sample data' were not available at that time), allowed the identification of 15 genes common to all leukaemic patients that were either up- or downregulated when comparing the leukaemic stem cell ($Lin^-CD34^+CD38^-$) to both the leukaemic blast ($Lin^-CD34^+CD38^+$) and the bulk

leukaemic mononuclear cell transcriptomes (*Table III.1*). The expression of these selected genes was not varying between leukaemic blasts and MNC, suggesting that their level of expression was specific to LSC. However, when the expression of these genes was checked on microarrays of normal stem cell and progenitor fraction (cord blood and/or bone marrow), it was not significantly different between normal and leukaemic stem cells.

| Genes exclusively upregulated in $Lin^-/CD34^+/CD38^-$ cells in comparison to MNC and $Lin^-/CD34^+/CD38^+$ cells in all patient samples | | | | | |
|---|---|---|---|---|---|
| | Patient 3 | Patient 4 | Patient 5 | Patient 6 | Patient 7 |
| TBC1D16 | 1.340 | 1.455 | 1.222 | 1.377 | 1.503 |
| DRD2 | 1.212 | 1.297 | 1.196 | 1.174 | 1.149 |
| NFKBIA | 1.649 | 1.520 | 1.346 | 1.301 | 2.098 |
| Genes exclusively downregulated in $Lin^-/CD34^+/CD38^-$ cells in comparison to MNC and $Lin^-/CD34^+/CD38^+$ cells in all patient samples | | | | | |
| | Patient 3 | Patient 4 | Patient 5 | Patient 6 | Patient 7 |
| RACGAP1 | -5.236 | -1.715 | -3.559 | -3.344 | -1.567 |
| FLJ20485 | -1.587 | -1.988 | -1.675 | -2.028 | -2.262 |
| NUSAP1 | -32.258 | -5.556 | -2.262 | -2.688 | -4.854 |
| DLEU2 | -1.828 | -1.267 | -2.141 | -1.751 | -1.351 |
| FLJ10719 | -2.732 | -2.101 | -2.183 | -1.543 | -1.890 |
| MAC30 | -4.132 | -2.793 | -1.527 | -1.299 | -1.553 |
| RRM2 | -5.076 | -1.786 | -3.774 | -1.996 | -2.770 |
| TXNDC7 | -3.425 | -2.232 | -1.610 | -1.748 | -1.876 |
| ANP32E | -1.905 | -2.336 | -1.692 | -2.433 | -2.451 |
| RRM2 | -5.102 | -3.984 | -6.098 | -2.584 | -6.024 |
| PCNA | -3.704 | -3.650 | -2.801 | -2.070 | -2.532 |
| FABP5 | -7.299 | -2.132 | -2.558 | -2.045 | -1.185 |
| PRC1 | -14.368 | -2.445 | -2.404 | -1.555 | -2.315 |

***Table III.1: Genes differentially expressed in $Lin^-/CD34^+/CD38^-$ in comparison to MNC and $Lin^-/CD34^+/CD38^+$ in all patient samples.***

*Genes exclusively upregulated or downregulated in $Lin^-/CD34^+/CD38^-$ cells in comparison to MNC and $Lin^-/CD34^+/CD38^+$ cells in all patient samples.*

## 2. Fraction to fraction microarray analysis

Lists of genes of interest were generated using the Genespring software by applying two different statistical strategies. In each strategy five lists were generated: List 1 comparing $Lin^-/CD34^+/CD38^-$ fraction from normal bone marrow (HSC) to $Lin^-/CD34^+/CD38^-$ fraction from AML patients (LSC); List 2 comparing $Lin^-/CD34^+/CD38^+$ fraction from normal bone marrow (early progenitors) to $Lin^-/CD34^+/CD38^+$ fraction from AML patients (leukaemic blasts). Each list contains genes differentially expressed between the two given populations by at least two fold up or down using t-test statistics (*Figure III.2 a*). Using Venn diagram analysis Lists 3, 4 and 5 were obtained. List 3 corresponds to genes common to List 1 and 2, List 4 to genes unique to List 1 (differentially expressed only at the stem cell level) and List 5 to genes unique to List 2 (differentially expressed only in the $Lin^-/CD34^+/CD38^+$ compartment).

In strategy 1, the $Lin^-/CD34^+/CD38^-$ fraction of either of the two bone marrow samples (BM1 and BM2) or the mean value of the two bone marrow samples (mean BM) was compared pairwise to each of the seven $Lin^-/CD34^+/CD38^-$ AML fractions. The genes common to each of these pairwise comparisons correspond to List 1. List 2 was obtained in the same way comparing $Lin^-/CD34^+/CD38^+$ fractions (*Figure III.2 b,* Strategy 1*)*. This strategy takes into account the variability introduced by the heterogeneity of the AML samples.

a

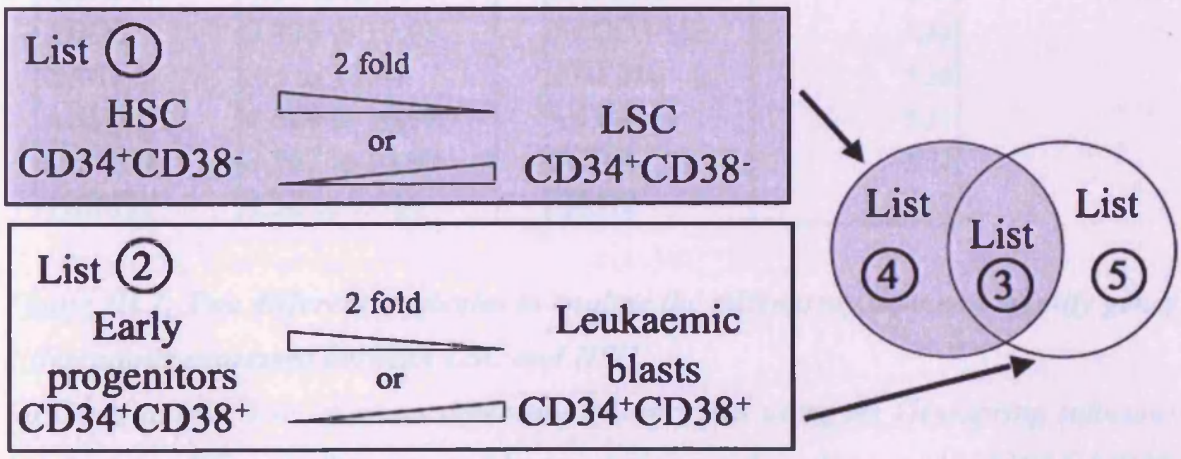

b

Strategy 1: comparing BM to each AML sample individually

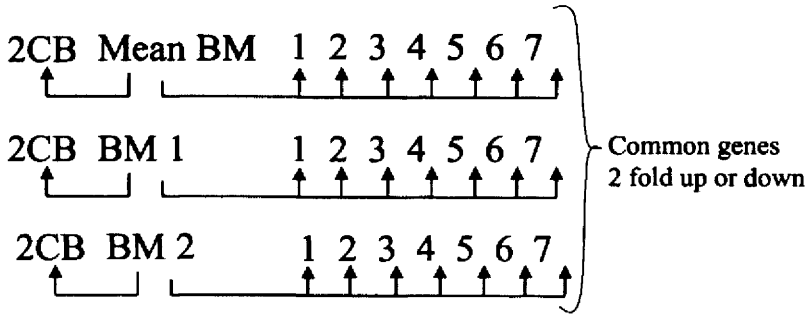


Strategy 2: comparing the mean value of BM to the mean value of the AML samples

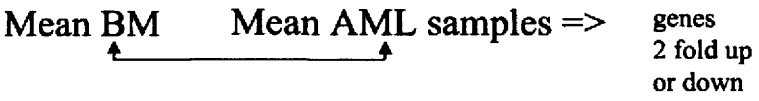


c

Top 12, List 4, Strategy 1

| | |
|---|---|
| HCK | 2.649 to 47.71 |
| CHS1 | 2.42 to 30.34 |
| AKAP13 | 6.226 to 27.3 |
| KYNU | 3.05 to 24.31 |
| MGC5395 | 4.278 to 16.77 |
| FYB | 2.206 to 17.78 |
| AKAP13 | 4.36 to12.51 |
| ADD3 | 3.805 to 12.05 |
| GAS7 | 2.3 to 11.85 |
| ANKRD12 | 4.608 to 10.99 |
| CAP350 | 3.567 to 10.90 |
| TRIM38 | 2.32 to 9.816 |

Top 12, List 4, Strategy 2

| | |
|---|---|
| HCK | 23.95 |
| GAS7 | 13.8 |
| TYROBP | 12.5 |
| NBS1 | 9.89 |
| unknown | 6.00 |
| NKTR | 5.59 |
| HIST2H2AA | 5.49 |
| SLCO3A1 | 5.43 |
| ZNF216 | 5.36 |
| UCP2 | 5.31 |
| ADD3 | 5.27 |
| BRD2 | 5.17 |

***Figure III.2: Two different strategies to analyse the microarray data and identify genes differentially expressed between LSC and HSC.***

*(a) Generation of lists of genes differentially expressed using the Genespring software: List 1: genes differentially expressed by two fold up or down between Lin$^-$/CD34$^+$/CD38$^-$*

*fraction from normal bone marrow (HSC) and Lin$^-$/CD34$^+$/CD38$^-$ fraction from AML patients (LSC); List 2: genes differentially expressed by two fold up or down between Lin$^-$/CD34$^+$/CD38$^+$ fraction from normal bone marrow and Lin$^-$/CD34$^+$/CD38$^+$ fraction from AML patients; List 3: genes common to List 1 and 2; List 4: genes unique to List 1; List 5: genes unique to List 2. (b) Two different statistical strategies to analyse the microarray data: Strategy 1, fraction (e.g. Lin$^-$/CD34$^+$/CD38$^-$ ) of either of the two bone marrow samples (BM1 and BM2) or the mean value of the two bone marrow samples (mean BM) was compared pairwise to each of the seven AML fractions using t-test statistics. Strategy 2, fraction (e.g. Lin$^-$/CD34$^+$/CD38$^-$ ) of the mean of the two bone marrow samples (mean BM) was compared to the mean value of the seven AML fractions (mean AML samples) using t-test statistics. (c) List of genes upregulated in Lin$^-$/CD34$^+$/CD38$^-$ AML fractions in comparison to normal bone marrow: top 12 of the genes upregulated in Lin$^-$/CD34$^+$/CD38$^-$ AML fractions generated by statistical strategies 1 or 2.*

In strategy 2, List 1 was generated comparing the Lin$^-$/CD34$^+$/CD38$^-$ fraction of the mean of the two bone marrow samples (mean BM) to the mean value of the seven Lin$^-$/CD34$^+$/CD38$^-$ AML fractions (mean AML samples). List 2 was generated comparing the Lin$^-$/CD34$^+$/CD38$^+$ fraction of the mean of the two bone marrow samples (mean BM) to the mean value of the seven Lin$^-$/CD34$^+$/CD38$^+$ AML fractions (mean AML samples) (*Figure III.2 b,* Strategy 2*)*. This strategy supports the search for leukaemic stem cell specific features independent of the AML subtype.

The two strategies show 50% genes in common, although not always falling in the same list (between Lists 3, 4 and 5). Nevertheless, by further investigating List 4 (genes differentially expressed between HSC and LSC only) from both strategies, we found that haematopoietic cell kinase (HCK) was the gene the most overexpressed in the Lin$^-$/CD34$^+$/CD38$^-$ fraction of the seven AML patients in comparison to normal bone marrow (*Figure III.2 c)*. We therefore decided to study a potential role for HCK in leukaemogenesis by either knocking it down in a leukaemic background (cell lines, then AML patient samples) or by overexpressing it in stem cells enriched Lin- umbilical cord blood cells.

### 3. Confirmation of microarray data in stem cell patient samples (qPCR)

Prior to manipulating HCK expression, we confirmed the microarray data for the $Lin^-/CD34^+/CD38^-$ and the $Lin^-/CD34^+/CD38^+$ fractions from six of the seven AML patients and the bone marrow samples used in the microarray analysis by quantitative real-time PCR using SYBR® green (*Figure III.3*). Leftover quantities of the mRNA used in the microarray were run in duplicate in this experiment. GAPDH was used to normalise the values of mRNA expression.

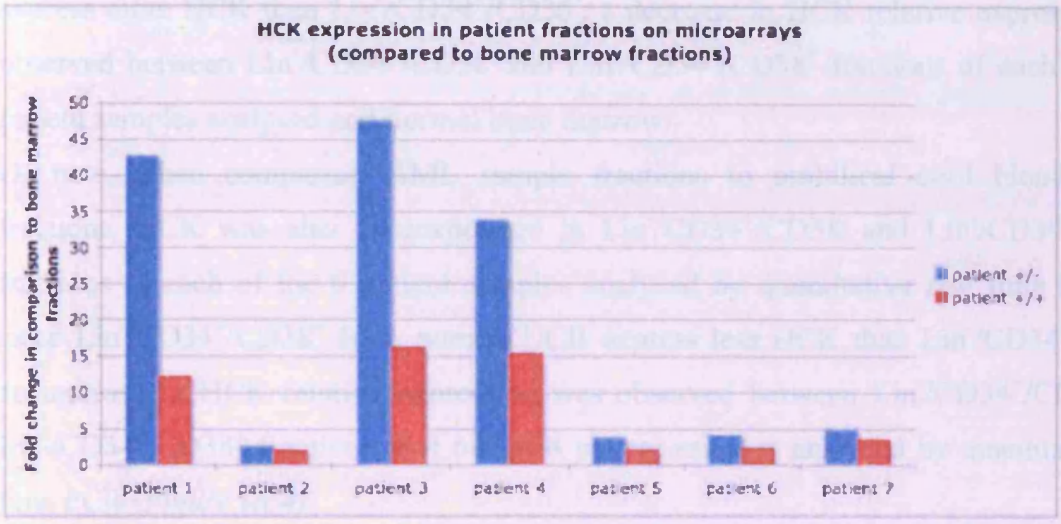


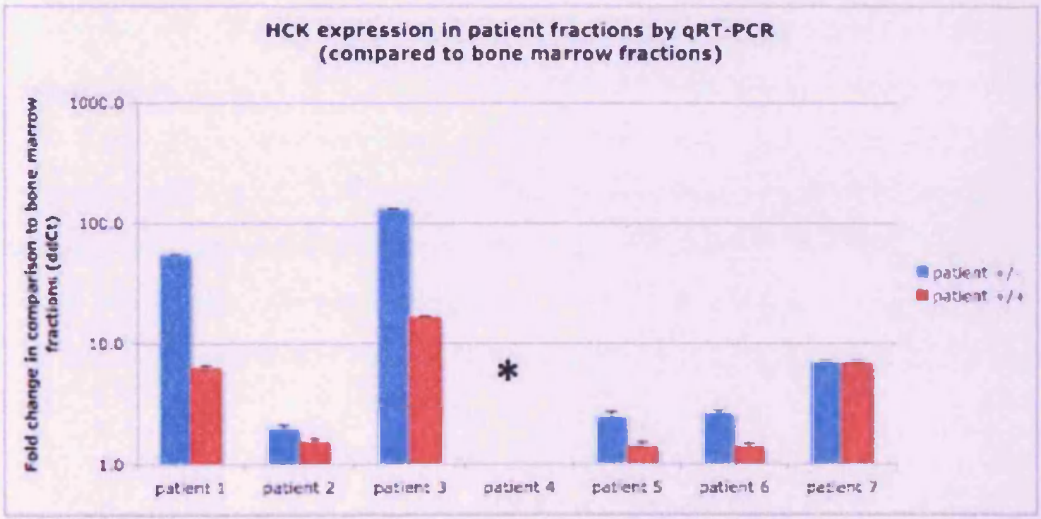


***Figure III.3: Confirmation of microarray data by quantitative real-time PCR.***

*Top panel: Microarray data displayed as a histogram. Bottom panel: Quantitative real-time PCR, using SYBR® green, run onto leftover RNA from the microarray experiment. GAPDH was used to normalise the values of mRNA expression. Stars indicate samples for which the PCR reaction was not run.*

Both microarray and quantitative real-time PCR analysis showed the same trend of HCK being overexpressed in $Lin^-/CD34^+/CD38^-$ of all 7 patient samples analysed, in comparison to normal bone marrow. HCK was also overexpressed in $Lin^-/CD34^+/CD38^+$ of all 7 patient samples analysed but since $Lin^-/CD34^+/CD38^+$ from normal bone marrow express more HCK than $Lin^-/CD34^+/CD38^-$, a decrease in HCK relative expression was observed between $Lin^-/CD34^+/CD38^-$ and $Lin^-/CD34^+/CD38^+$ fractions of each of the 7 patient samples analysed and normal bone marrow.

Of note, when comparing AML sample fractions to umbilical cord blood (UCB) fractions, HCK was also overexpressed in $Lin^-/CD34^+/CD38^-$ and $Lin^-/CD34^+/CD38^+$ fractions of each of the 6 patient samples analysed by quantitative real time PCR but since $Lin^-/CD34^+/CD38^+$ from normal UCB express less HCK than $Lin^-/CD34^+/CD38^-$, an increase in HCK relative expression was observed between $Lin^-/CD34^+/CD38^-$ and $Lin^-/CD34^+/CD38^+$ fractions in 4 out of 6 patient samples analysed by quantitative real time PCR (*Figure III.4)*.

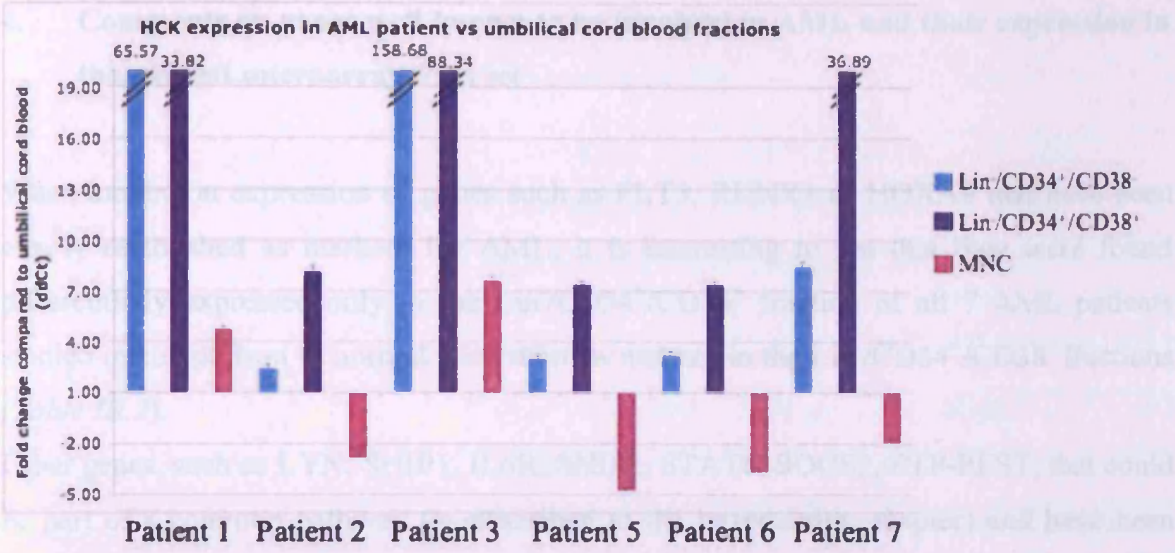


***Figure III.4: Comparison of HCK expression in patient sample fractions to HCK expression in UCB fractions by quantitative real-time PCR.***

*Quantitative real-time PCR, using SYBR® green, run onto leftover RNA from the microarray experiment. GAPDH was used to normalise the values of mRNA expression. PCR was not run for patient 4 due to lack of leftover RNA.*

When comparing HCK expression in bulk MNC of the same patient samples to UCB MNC, HCK expression was higher in leukaemic MNC than in UCB MNC for the 2 patients, patient 1 and patient 3, with very high expression of HCK in $Lin^-/CD34^+/CD38^-$ and $Lin^-/CD34^+/CD38^+$ fractions. HCK expression was lower in leukaemic MNC than in UCB MNC for all the other patient samples, which displayed 2 to 10 fold increased HCK expression in their $Lin^-/CD34^+/CD38^-$ fraction in comparison to UCB fraction.

Analysis by other members of the laboratory posterior to the beginning of this study suggest that patient patients 1 and 3 are $CD34^-$ AML patients whose $Lin^-/CD34^+/CD38^-$ most probably gives rise to normal multilineage engraftment (confirmed for patient 1).

## 4. Comments on genes well known to be involved in AML and their expression in the current microarray data set

When looking at expression of genes such as FLT3, RUNX1 or HOXA9 that have been clearly established as markers for AML, it is interesting to see that they were found differentially expressed only in the $Lin^-/CD34^+/CD38^+$ fraction of all 7 AML patients studied in comparison to normal bone marrow and not in the $Lin^-/CD34^+/CD38^-$ fractions (*Table III.2*).

Other genes, such as LYN, SHIP1, IL6R, SHIP2, STAT6, SOCS2, PTP-PEST, that could be part of a common pathway (as described in the introduction chapter) and have been implicated in AML or other leukaemias, are also found differentially expressed in the $Lin^-/CD34^+/CD38^+$ fraction and not in the $Lin^-/CD34^+/CD38^-$ fraction. PIAS1 that could belong to the same pathway is also differentially expressed, but has so far not been implicated in leukaemia. Genes such as FOXO3A, LEF1 and GATA1 have been implicated in leukaemia and related to FLT3 and are also found differentially expressed in $Lin^-/CD34^+/CD38^+$ and not in $Lin^-/CD34^+/CD38^-$ fractions.

| | Fold difference in $Lin^-/CD34^+/CD38^+$ | Implication in AML |
|---|---|---|
| LYN | 3.833 to 12.12 | (Dos Santos *et al.*, 2008; Okamoto *et al.*, 2007) |
| SHIP1 | 3.79 to 5.949 | (Biethahn *et al.*, 1999; Whitman *et al.*, 2008) |
| RUNX1 | 3.319 to 6.306 | (Satoh *et al.*, 2008; Takahashi *et al.*, 2005) |
| PIAS1 | 3.193 to 5.07 | |
| FOXO3A | 3.138 to 5.655 | (Brandts *et al.*, 2005) |
| FLT3 | 2.984 to 10.51 | (Birg *et al.*, 1992; Bullinger *et al.*, 2008) |
| IL6R | 2.335 to 6.194 | (Denizot, 2000; Graf *et al.*, 2004) |
| SHIP2 | 2.272 to 3.126 | (Bentires-Alj *et al.*, 2004; Konieczna *et al.*, 2008) |
| STAT6 | 2.004 to 2.972 | *(Bruns and Kaplan, 2006; Reddy et al., 2003)* |
| GATA1 | -3.086 to - 2.38 | *(Greene et al., 2003; Kawamura et al., 2008)* |
| HOXA9 | -9.433 to 5.209 | (Casas *et al.*, 2003; Kroon *et al.*, 2001) |
| SOCS2 | -10.152 to -2.544 | *(Puigdecanet et al., 2008)* |
| LEF1 | -10.152 to -7.518 | (Li *et al.*, 2004; Petropoulos *et al.*, 2008) |
| PTP-PEST | -10.548 to -2.267 | (Heinonen *et al.*, 2006) |

***Table III.2: Genes differentially expressed in AML $Lin^-/CD34^+/CD38^+$ fraction in comparison to normal bone marrow and not in the AML $Lin^-/CD34^+/CD38^-$ fraction in comparison to normal bone marrow belonging to the JAK-STAT pathway and related pathways.***

As mentioned in the introduction chapter, the $Lin^-/CD34^+/CD38^+$ fraction of normal UCB was initially thought to not contain HSC. However, this fraction has recently been reported to contain long-term engrafting cells when recipient mice are pre-treated with immunosuppressive anti-CD122 antibody when looking at either normal (McKenzie *et al.*, 2005) or leukaemic engraftment (Taussig *et al.*, 2008). When looking at normal cells, the $Lin^-/CD34^+/CD38^+$ fraction probably consists of progenitors with a restricted self-renewal capacity since it is incapable of giving rise to secondary transplants (Hogan et al., 2002). However such data on secondary engraftment are not yet available on AML samples. Since the engraftment of AML sample fractions seems to be highly variable from patient to patient, it would be interesting to test the quality of engraftment of the

$Lin^-/CD34^+/CD38^+$ fraction of the patient samples tested in this study with anti-CD122 conditioning and to then proceed to secondary transplantation. Such an experiment would allow for determining whether the LSC is located in the $Lin^-/CD34^+/CD38^-$ fraction or in the $Lin^-/CD34^+/CD38^+$ fraction of these patients. Of note, LSC could possibly present in both fractions for a few of the patients since they were found to cluster together when analysing the microarray data as non-oriented cluster analysis. In addition, microarray data presented in *Table III.2* show that a few hallmarks of AML, such as FLT3, HOXA9 and RUNX1, are overexpressed in the $Lin^-/CD34^+/CD38^+$ fraction reinforcing the idea that it could potentially be an LSC containing fraction for the patient samples studied here. An important amount of work on detailed patient sample engraftment quality therefore seems needed before being able to exploit the current microarray data set with certainty.

# Chapter IV

# IV Knocking-down HCK

As explained in the previous chapter, Haematopoietic cell kinase (HCK) was the gene found the most overexpressed in the $Lin^-/CD34^+/CD38^-$ fraction of the seven AML patient samples tested in our microarray data in comparison to normal bone marrow. We therefore decided to study a potential role for HCK in leukaemogenesis by either knocking it down in a leukaemic background or by overexpressing it in stem cells enriched $Lin^-$ umbilical cord blood cells. The approach we used to set up and study HCK knock-down will be described in this chapter.

## 1. HCK expression and activity in AML cell lines

### 1.1 HCK expression in various AML cell lines at the RNA level

Prior to knocking-down HCK, we needed to establish in which leukaemic cell line this kinase is expressed. Willman et al. described a high expression of the myeloid Src family kinases (SFK), HCK and FGR in FAB M4 and M5 AML blasts, a low expression of FGR and low expression or no expression of HCK in FAB M1 and M2 AML blasts and expression of only HCK in FAB M3 AML blasts (Willman *et al.*, 1991). Since the expression of HCK in that study was exclusively done by Nothern blot in patient samples, we were interested in knowing if we would obtain similar results by quantitative real-time PCR in AML cell lines. AML cell lines available in our laboratory correlated with the FAB classification and the haematopoietic tree are shown on *Figure IV.1*. This schematic is only approximate since the FAB classification is based on morphological criteria rather than on phenotypical features.

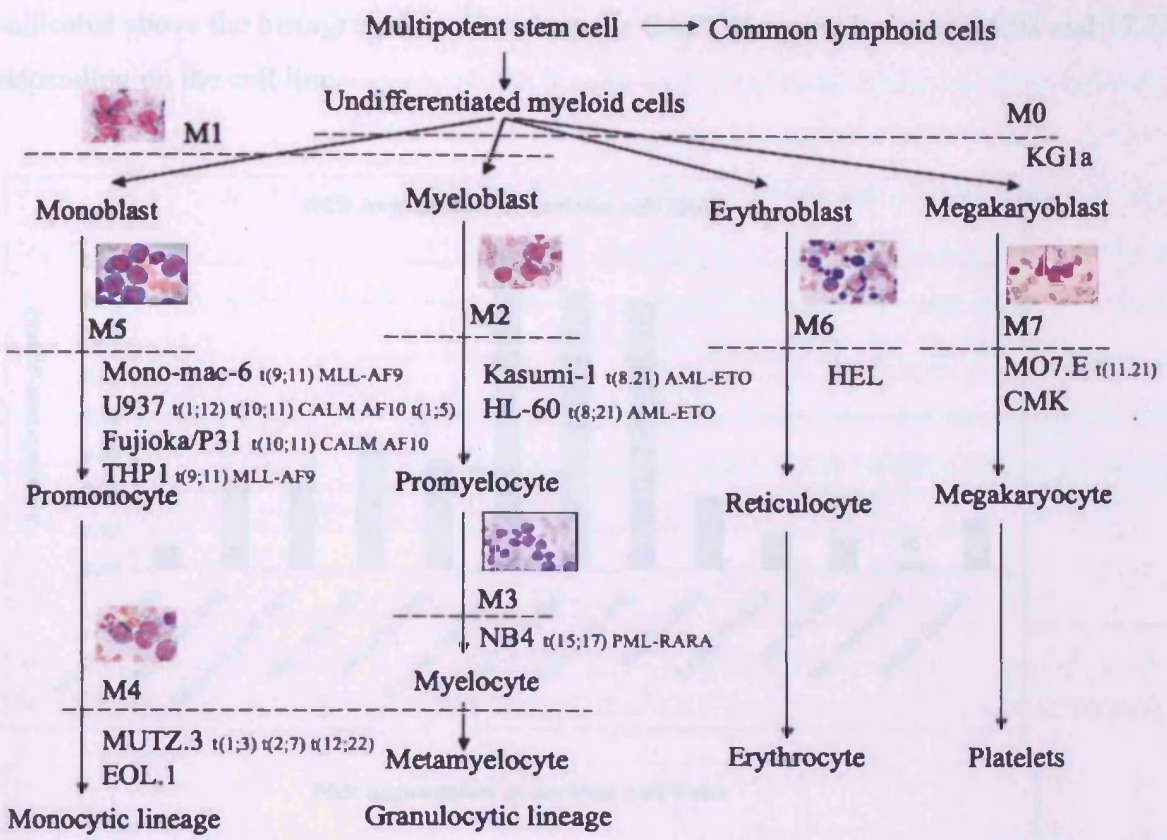


***Figure IV.1:* Correlation between the French-British-American (FAB) classification and the haematopoietic tree.**

*The FAB classification consists of 8 subclasses (M0 to M8). Based on their cell morphology, cell lines can be allocated to one of these classes.*

RNA was extracted from the HL-60, NB4, Fujioka/P31, U937, THP1, Kasumi-1, Mono-mac-6 and KG1a AML cell lines as well as from the K562 CML cell line, the Jurkat and J6A T-cell leukaemia cell lines and the SW28 (colon adenocarcinoma) and JAR (choriocarcinoma) cell lines as controls. HCK and FGR expression were assessed by quantitative real-time PCR using SYBR® green and each quantitative real-time PCR reaction has been run in duplicate (*Figure IV.2*). The experiment shown is representative of two distinct experiments. HCK or FGR expression were normalised to the expression of the housekeeping gene GAPDH and are expressed as $1/\Delta Ct$ for ease of visualisation. Cell lines for which the original Ct values for HCK or FGR is 40 (no expression) are

indicated above the histogram bar. Ct values for GAPDH varied between 16.08 and 17.77 depending on the cell line.

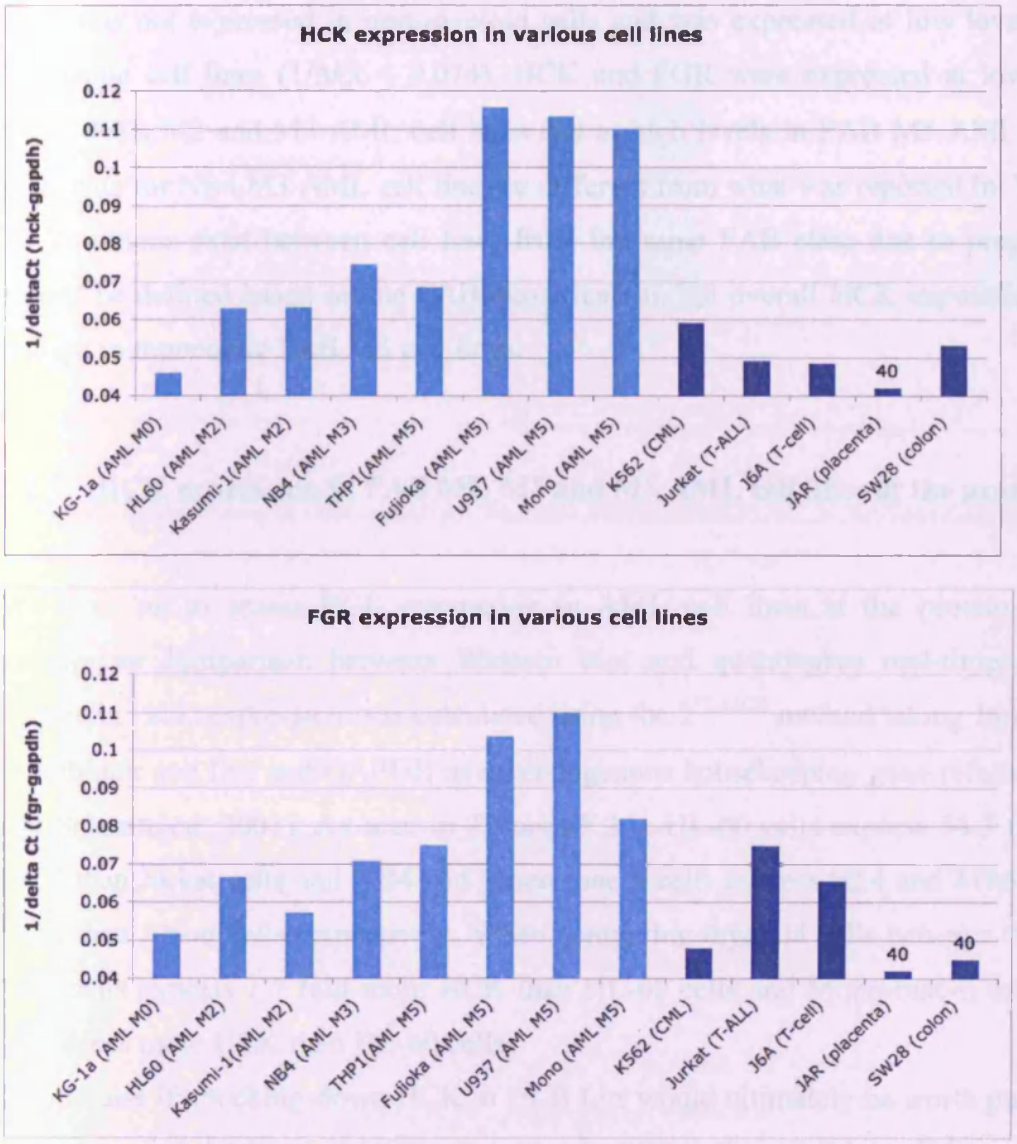


***Figure IV.2: HCK and FGR expression in leukaemic and non-leukaemic cell lines at the RNA level.***

*HCK expression (top panel) and FGR expression (bottom panel) were assessed by quantitative real-time PCR using SYBR® green. AML cell lines HL-60, NB4, Fujioka/P31, U937, THP1, Kasumi-1, Mono-mac-6 and KG1a are shown in blue histogram bars. K562, Jurkat, J6A, SW28 and JAR non-AML cell lines are shown in dark blue histogram bars.*

As expected, the expression of both HCK and FGR increased with cell differentiation. Non-myeloid cells and undifferentiated AML cells did not express HCK ($1/\Delta Ct < 0.051$). FGR was not expressed in non-myeloid cells and was expressed at low level in T-cell leukaemic cell lines ($1/\Delta Ct < 0.074$). HCK and FGR were expressed at low levels in CML, FAB M2 and M3 AML cell lines and at high levels in FAB M5 AML cell lines. FGR data for NB4 M3 AML cell line are different from what was reported by Willman et al. Variations exist between cell lines from the same FAB class due to properties that cannot be defined based on the FAB classification, but overall HCK expression was the highest in monocytic FAB M5 cell lines.

## 1.2 HCK expression in FAB M2, M3 and M5 AML cell lines at the protein level

We went on to assess HCK expression in AML cell lines at the protein level. For appropriate comparison between Western blot and quantitative real-time PCR, fold change in HCK expression was calculated using the $2^{\wedge(-\Delta\Delta Ct)}$ method taking Jurkat cells as a calibrator cell line and GAPDH as an endogenous housekeeping gene reference (Livak and Schmittgen, 2001). As seen in *Figure IV.3 a*, HL-60 cells express 54.3 times more HCK than Jurkat cells and NB4 and Mono-mac-6 cells express 92.4 and 4196 fold more HCK than Jurkat cells respectively. When comparing myeloid cells between themselves, NB4 cells express 1.7 fold more HCK than HL-60 cells and Mono-mac-6 cells express 77.3 times more HCK than HL-60 cells.

To appraise if knocking-down HCK in UCB $Lin^-$ would ultimately be worth pursuing, we also compared the level of HCK expression in $Lin^-$ to the potential cell lines to be used for setting up the knock-down. UCB Lin- expressed 667 fold more HCK than Jurkat cells what was considered a reasonable level to work with subsequently.

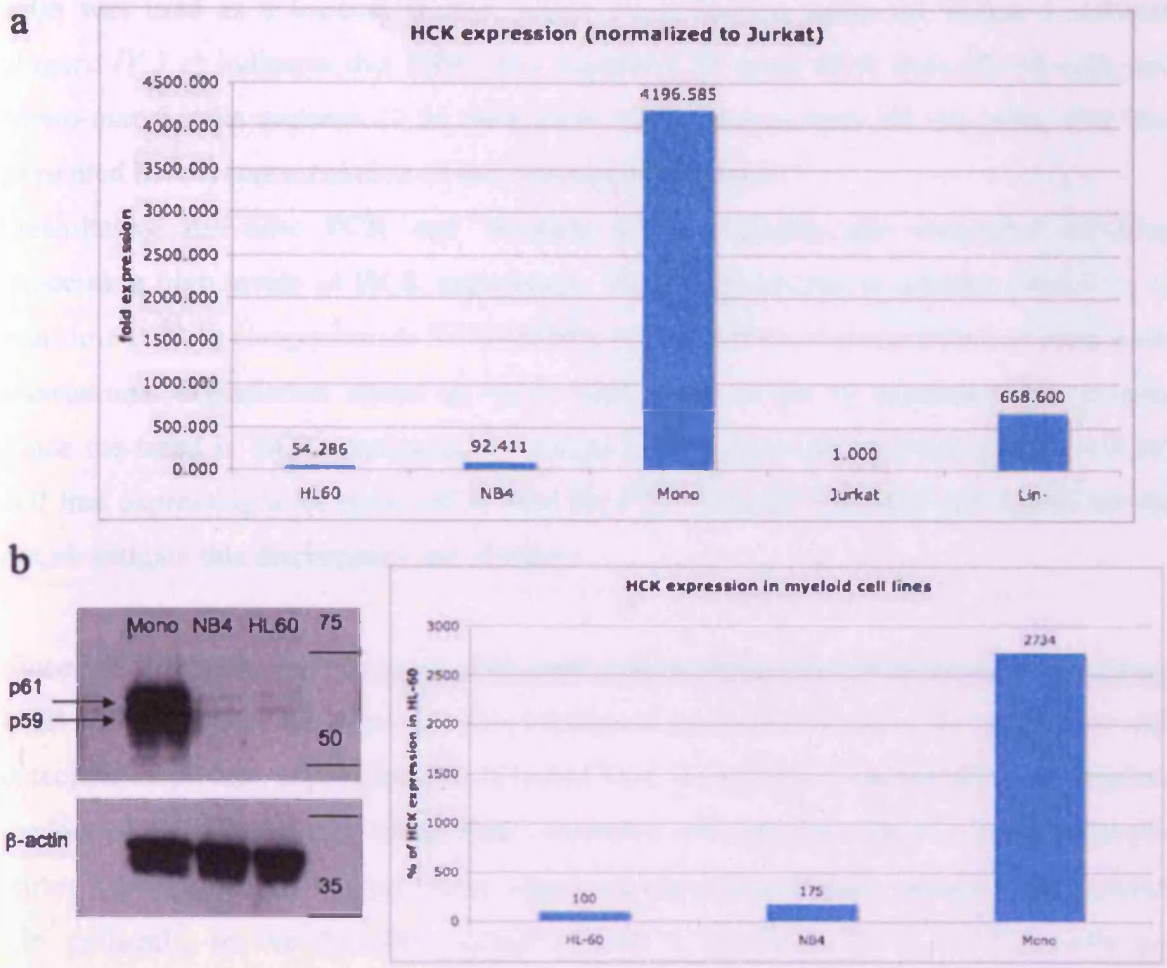


***Figure IV.3 : HCK expression in HL-60, NB4 and Mono-mac-6 by quantitative real time PCR and by Western blot.***

*(a) HCK expression in HL-60, NB4, Mono-mac-6, Jurkat and Lin⁻ cells, assessed by quantitative real-time PCR using SYBR® green, taking Jurkat cells as a calibrator cell line and GAPDH as an endogenous housekeeping gene reference. (b) HCK expression assessed by Western blot in HL-60, NB4, Mono-mac-6 cells. β-actin was used as a loading control. (c) Western blot band quantification using the Image J software expressed as percentage of HCK expression in HL-60 cells.*

To assess HCK expression in AML cell lines at the protein level, cells were lysed with RIPA buffer and proteins were separated by SDS-PAGE electrophoresis followed by Western blotting. *Figure IV.3 b* shows a faint expression of p61 and p59 HCK isoforms in HL-60 and NB4 cells while Mono-mac-6 cells highly express both HCK isoforms. β-

actin was used as a loading control. Band quantification using the Image J software (*Figure IV.3 c*) indicates that NB4 cells express 1.75 more HCK than HL-60 cells and Mono-mac-6 cells express 27.34 fold more HCK protein than HL-60 cells. The blot presented here is representative of two distinct experiments.

Quantitative real-time PCR and Western blotting results are somewhat differing concerning high levels of HCK expression. This might be due to a better sensitivity of real-time PCR in comparison to Western blot quantification or to the effect of some post-translational degradation where all HCK mRNA would not be translated into protein. Since the trend in HCK expression is similar between the two methods (with FAB M5 cell line expressing a lot more HCK than the FAB M2 and FAB M3 cell lines), we did not investigate this discrepancy any further.

Since we ultimately want to work with stem cells coming from UCB $Lin^-$ cells and each UCB collection does not allow for the isolation of a number of $Lin^-$ cells compatible with detection of protein expression via Western blot, we needed to establish an appropriate readout of HCK expression using flow cytometry. Of note, the size of a UCB collection varies between 60 and 100 mL from which we can approximately obtain 15,000-20,000 $Lin^-$ cells/mL, so we therefore usually obtain a maximun of $2x10^6$ $Lin^-$ cells per collection. $CD34^+/CD38^-$ HSC represent 5 to 10 % of $Lin^-$ cells, i.e 2,000 HSC/mL of UCB. HSC can thus only be phenotypically studied by flow cytometry.

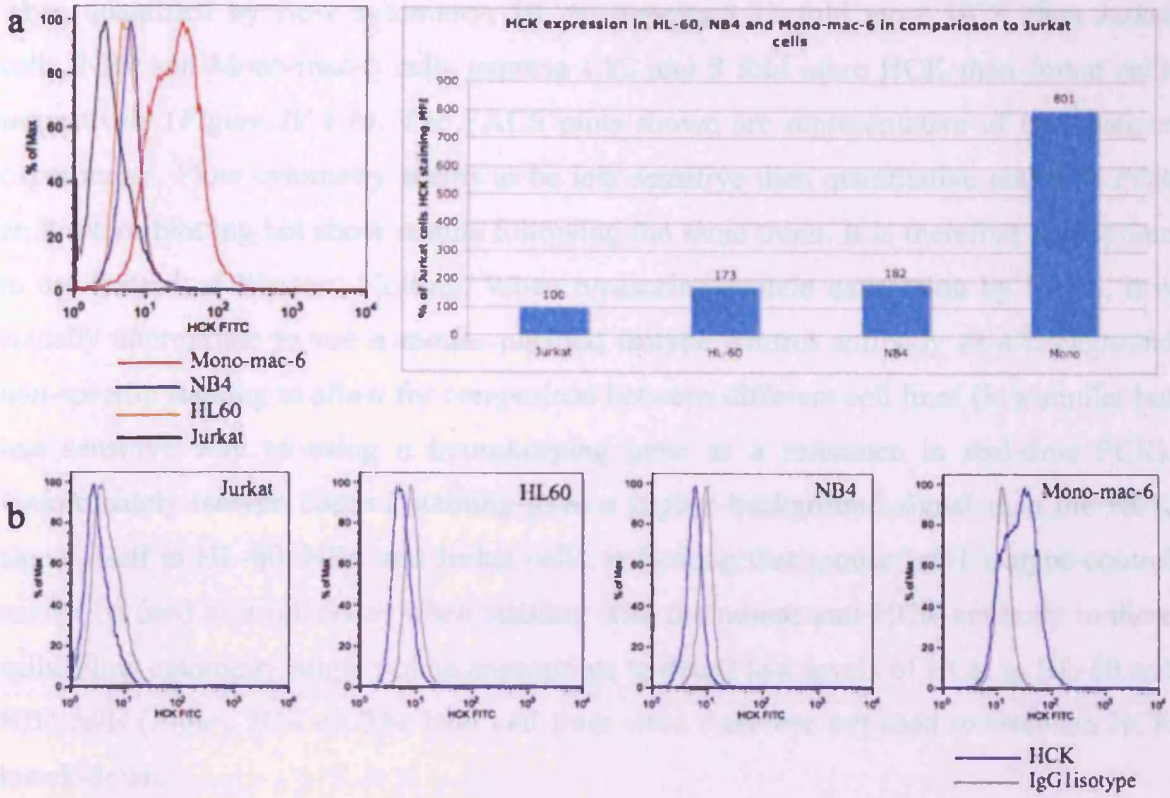


***Figure IV.4: HCK expression assessed by flow cytometry.***

*Cells were fixed, permeabilised and stained using the same mouse monoclonal antibody as the one used for Western blot, followed by secondary staining with a FITC-conjugated secondary antibody. (a) HCK expression in Jurkat (black histogram), HL-60 (orange histogram), NB4 (blue histogram) and Mono-mac-6 (red histogram) cells assessed by flow cytometry. (b) Quantification of the fluorescent signal expressed as percentage of the Jurkat cells signal's mean fluorescence intensity (MFI). (c) HCK expression in Jurkat, HL-60, NB4 and Mono-mac-6 cells (blue histogram) compared to a matching isotype control (grey histogram).*

HCK internal staining using the same mouse monoclonal antibody as the one used for Western blot, followed by secondary staining with a FITC-conjugated secondary antibody, successfully allowed the detection of HCK in HL-60, NB4 and Mono-mac-6 cells (*Figure IV.4 a*). However, when comparing the mean fluorescence intensity (MFI) of each of these three cell lines to the MFI of Jurkat cells, differences in HCK level of expression were very different from the ones measured by quantitative real time PCR:

when quantified by flow cytometry, HL-60 express 1.73 fold more HCK than Jurkat cells, NB4 and Mono-mac-6 cells express 1.82 and 8 fold more HCK than Jurkat cells respectively (*Figure IV.4 b*). The FACS plots shown are representative of two distinct experiments. Flow cytometry seems to be less sensitive than quantitative real-time PCR or Western blotting but show results following the same trend. It is therefore appropriate to use instead of Western blotting. When measuring protein expression by FACS, it is actually appropriate to use a mouse purified isotype control antibody as a background non-specific staining to allow for comparison between different cell lines (in a similar but less sensitive way to using a housekeeping gene as a reference in real-time PCR). Unfortunately isotype control staining gave a higher background signal than the HCK signal itself in HL-60, NB4 and Jurkat cells, indicating that mouse IgG1 isotype control cannot be used as a reference when staining with the mouse anti-HCK antibody in these cells. Flow cytometry might not be appropriate to detect low levels of HCK in HL-60 and NB4 cells (*Figure IV.4 c*). The later cell lines were therefore not used to establish HCK knock-down.

## 1.3 HCK activity in M5 AML cell lines

### 1.3.1 *In vitro* kinase assay

Once knowing that Mono-mac-6 or any FAB M5 AML cell lines can be a good cell line to establish HCK knock-down, we needed to validate a way of accessing any changes in HCK kinase activity. A classical way to detect changes in kinase activity is to proceed to an *in vitro* kinase assay. Such assays can be done based on the incorporation of radioactive ATP or based on the displacement and unquenching of a fluorescent ligand in a non-radioactive way. We decided to proceed with the latter method using the Antibody Beacon™ Tyrosine Kinase Assay Kit (Invitrogen). Since this kit is originally meant to work with recombinant kinases, we needed to validate it for HCK immunoprecipitated from cell lysate.

HCK was immunoprecipitated overnight from KG1a, Fujioka/P31, U937 and Mono-mac-6 cells lysed with buffer A, using either rabbit anti-HCK antibody (*Figure IV.5 a*) or a mouse anti-HCK antibody. Immunoprecipitation controls were also set up using a matching rabbit or mouse IgG1 isotype control and the KG1a cell line, not expressing HCK, was used as a negative control for the kinase assay. Cells need to be lysed in buffer A in order to proceed with the *in vitro* kinase assay in the kinase buffer provided in the kit (MOPS based). Immunoprecipitates were either resolved by Western blotting (*Figure IV.5 a*) or pipetted into a well of a black 394 well plate and subjected to kinase assay according to the manufacturer's instructions.

The Antibody Beacon™ Tyrosine Kinase Assay Kit is based on the following principle: when no phosphotyrosine containing specific sequence (specific phosphopeptide or tyrosine kinase specific phosphorylated substrate) is in the environment, the Oregon Green 488 ligand binds to the phospho-specific antibody provided in the kit and is quenched. When a phosphorylated substrate is in the environment it binds to the phospho-specific antibody with a higher affinity than the Oregon Green 488 ligand and displaces it. In this case, the Oregon Green 488 ligand is not quenched anymore and emits fluorescence that can be read at 530 nm. The intensity of fluorescence is proportional to the kinase activity (*Figure IV.5 b*).

a

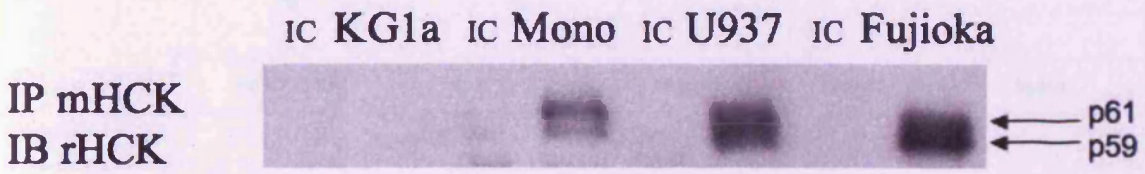

**b**

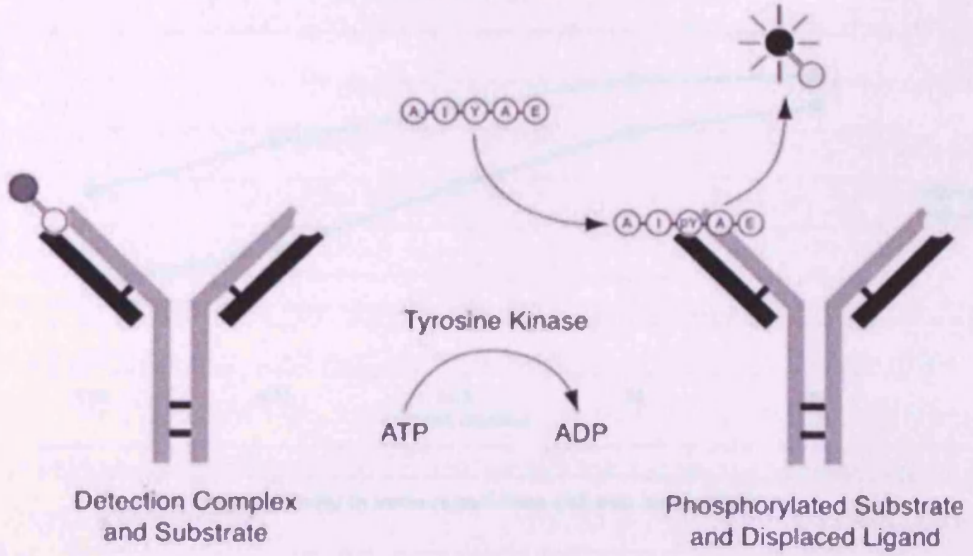
Tyrosine Kinase
ATP
ADP
Detection Complex
and Substrate
Phosphorylated Substrate
and Displaced Ligand

**c**

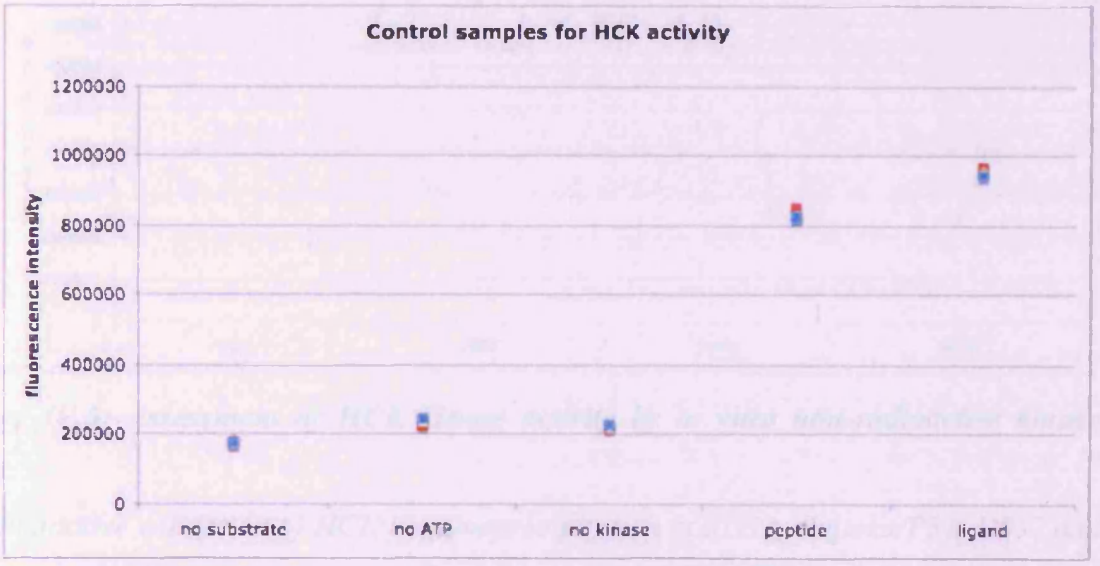
Control samples for HCK activity
fluorescence intensity
1200000
1000000
800000
600000
400000
200000
0
no substrate
no ATP
no kinase
peptide
ligand

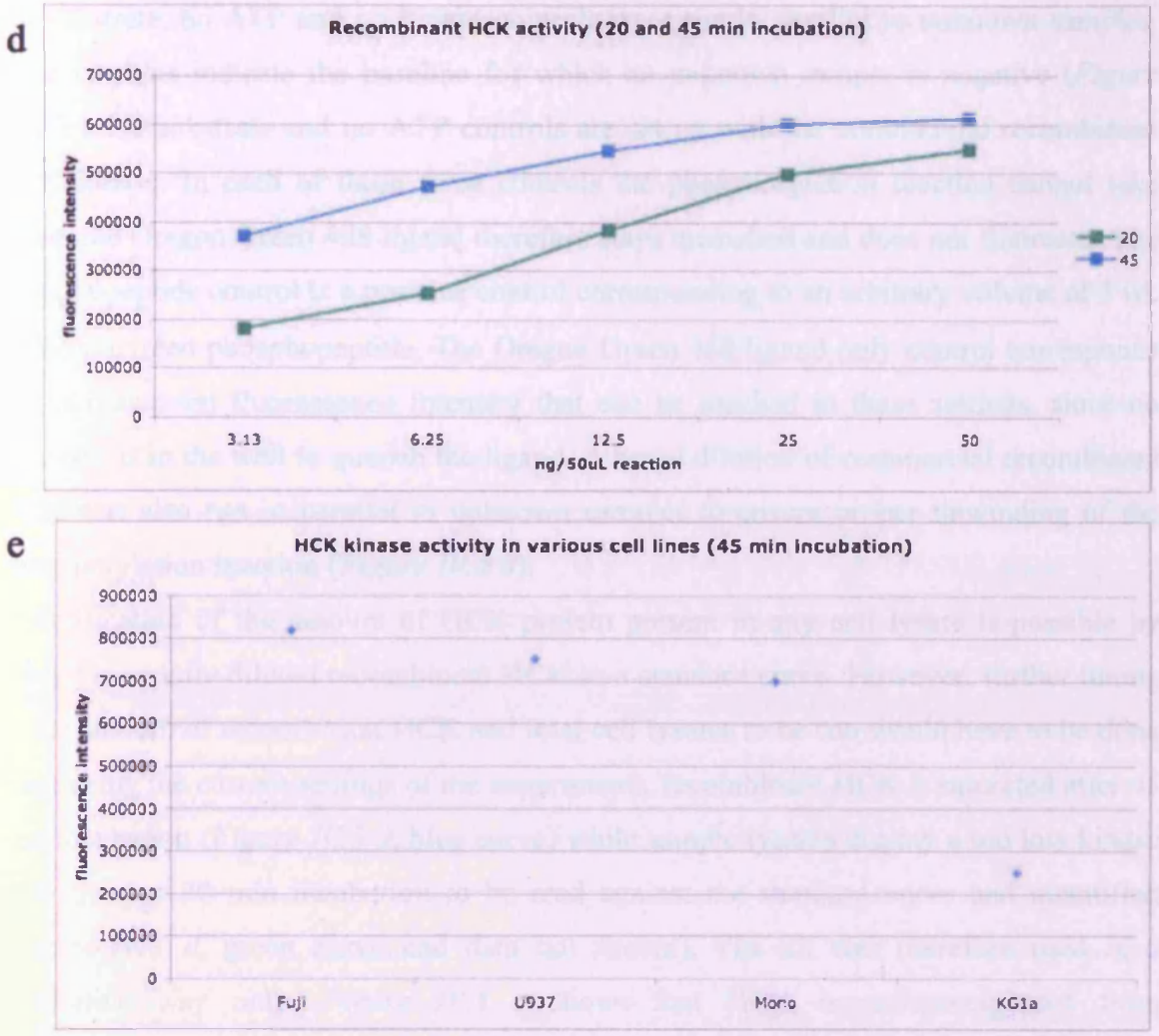


***Figure IV.5: Assessment of HCK kinase activity by in vitro non-radioactive kinase assay.***

*(a) Qualitative validation of HCK immunoprecipitation in KG1a, Fujioka/P31, U937 and Mono-mac-6 cell lines lysed with buffer A, using a rabbit anti-HCK antibody or matching rabbit isotype control for immunoprecipitation and a mouse anti-HCK antibody for immunoblotting. (b) Principle of action of the Antibody Beacon™ Tyrosine Kinase Assay Kit. (c) No substrate, no ATP, no kinase, phospho-peptide and Oregon Green 488 ligand only controls. (d) Serial dilution of commercial recombinant purified HCK used as control. The green curve shows the kinase activity after 20 minutes incubation at RT and the blue curve shows the kinase activity after 45 minutes incubation at RT. (e) Specific HCK activity corresponding to immunoprecipitation of 450 mg of total protein lysate.*

No substrate, no ATP and no kinase controls were run in parallel to unknown samples, these controls indicate the baseline for which an unknown sample is negative (*Figure IV.5 c*). No substrate and no ATP controls are set up with the commercial recombinant HCK kinase. In each of these three controls the phosphorylation reaction cannot take place, the Oregon Green 488 ligand therefore stays quenched and does not fluoresce. The phosphopeptide control is a positive control corresponding to an arbitrary volume of 3 µL of the provided phosphopeptide. The Oregon Green 488 ligand only control corresponds to the maximum fluorescence intensity that can be reached in these settings, since no antibody is in the well to quench the ligand. A serial dilution of commercial recombinant HCK was also run in parallel to unknown samples to ensure proper unwinding of the phosphorylation reaction (*Figure IV.5 d*).

Quantification of the amount of HCK protein present in any cell lysate is possible by using the serially diluted recombinant HCK as a standard curve. However, further tuning of the amount of recombinant HCK and total cell lysates to be run would have to be done since using the current settings of the experiments, recombinant HCK is saturated after 45 min incubation (*Figure IV.5 d*, blue curve) while sample lysates display a too low kinase activity after 20 min incubation to be read against the standard curve and quantified (*Figure IV.5 d*, green curve and data not shown). The kit was therefore used in a qualitative way only. *Figure IV.5 e* shows that HCK immunoprecipitated from Fujioka/P31, U937 or Mono-mac-6 cell lysates is active and validates the use of the Antibody Beacon™ Tyrosine Kinase Assay Kit with cell lysates. This experiment is representative of four distinct experiments where HCK was immunoprecipitated with either a mouse or a rabbit anti-HCK antibody. Both antibodies give similar results and do not give any non-specific signal in the HCK negative KG1a cell line.

### 1.3.2 Set up of phospho-specific flow cytometry using SFK inhibitors

Since we ultimately wanted to work with stem cells coming from UCB Lin$^-$ cells and limited number of cells does not allow for immunoprecipitation, we needed to establish

an appropriate readout for variation in HCK kinase activity in stem cells using flow cytometry.

As described previously in the introduction chapter, HCK is fully active when phosphorylated on the tyrosine Y411 in its activation loop. We therefore tried to set up an intracellular staining to detect phospho-HCK by flow cytometry. Mercuric chloride (HgCl2) which is known to activate SFK (Robbins *et al.*, 2000) was used as a positive control and 10 μM PP2, a SFK specific inhibitor, was used as a negative control. Since PP2 is resuspended in DMSO, DMSO was used as an internal control for the phospho-specific staining with anti-Y411 antibody (*Figure IV.6 a*). Quantification of the signal intensity using a matching goat isotype control and taking non-treated Mono-mac-6 cells as a reference shows a 1.8 fold increase in HCK Y411 phosphorylation upon HgCl2 treatment and a 2 fold decrease following PP2 treatment (*Figure IV.6 b*). However, no difference is seen between PP2 treated and DMSO treated cells, indicating the possibility of a non-specific signal. Although 10 μM is a commonly used dose of PP2 (Dos Santos *et al.*, 2008; Meyn *et al.*, 2005), we tried to assess if any other dose of PP2 could give a change in signal intensity. Although a certain dose effect was observed when incubating the cells with 5, 10 or 20 μM of PP2, the effect was once again the same when an equivalent volume of DMSO was added to the cells (*Figure IV.6 c*). We decided to test another SFK inhibitor with a broader spectrum, SU6656 (Blake *et al.*, 2000; Meyn *et al.*, 2005), however, a similar dose effect between SU6656 and DMSO was observed as well (*Figure IV.6 d*). Each experiment shown is representative of two experiments.

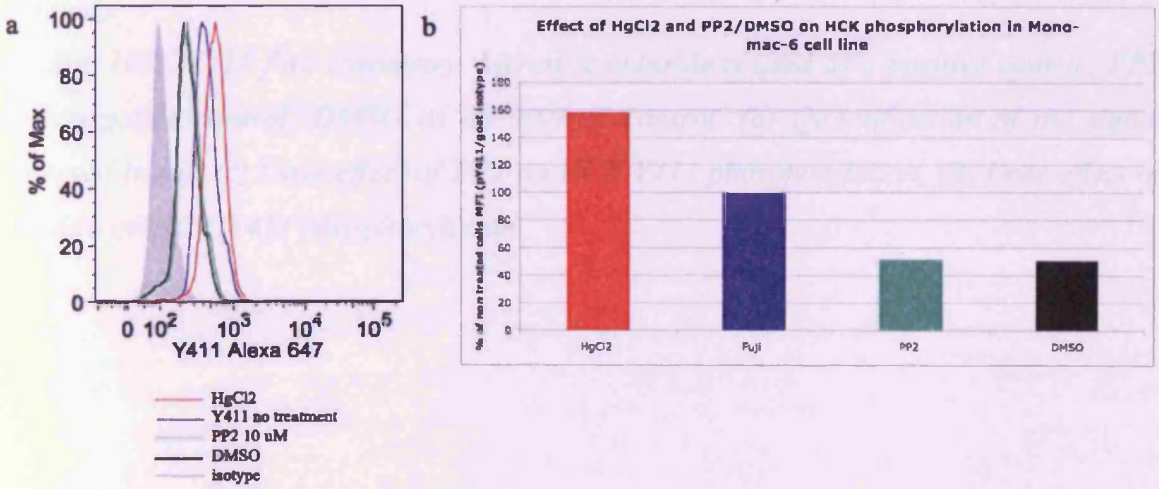

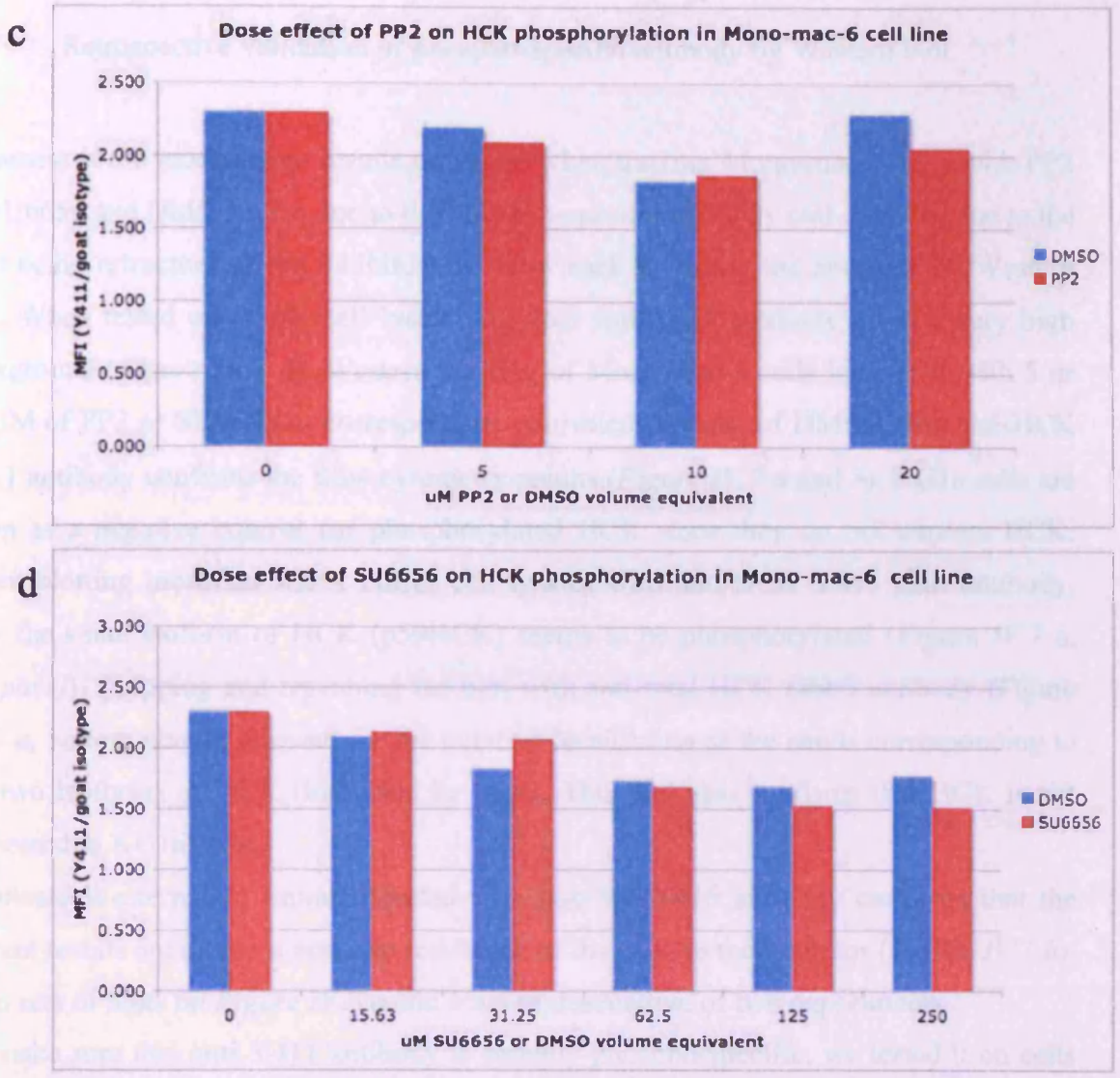


***Figure IV.6: Set up of phospho-specific flow cytometry using anti-HCK Y411 goat antibody.***

*(a) Anti HCK-Y411 flow cytometry. Mercuric chloride is used as a positive control, PP2 as a negative control, DMSO as an internal control. (b) Quantification of the signal observed in (a). (c) Dose effect of PP2 on HCK Y411 phosphorylation. (d) Dose effect of SU6656 on HCK Y411 phosphorylation.*

### 1.3.3 Retrospective validation of phospho-specific antibody by Western blot

To assess if the inconsistent results observed when treating Mono-mac-6 cells with PP2 or SU6656 and DMSO were due to the phospho-specific antibody anti-Y411 or due to the cells being refractory to the inhibitor, we went back to testing the antibody by Western blot. When tested on whole cell lysate, the goat anti-Y411 antibody gives a very high background (*Figure IV.7 a*). Western blotting of Mono-mac-6 cells incubated with 5 or 10 μM of PP2 or SU6656 or corresponding equivalent volume of DMSO with anti-HCK Y411 antibody confirms the flow cytometry results (*Figure IV.7 a* and *b*). KG1a cells are taken as a negative control for phosphorylated HCK since they do not express HCK. When blotting modified RIPA buffer cell lysates with anti-HCK Y411 goat antibody, only the small isoform of HCK (p59HCK) seems to be phosphorylated (*Figure IV.7 a, top panel*). Stripping and reprobing the blot with anti-total HCK rabbit antibody (Figure IV.7 *a, bottom panel*), allowed for the putative localisation of the bands corresponding to the two isoforms of HCK (indicated by stars). This blot also confirms that HCK is not expressed in KG1a cells.

Duplicate Western blot immunoblotted with pan-Src Y416 antibody confirms that the current results are due to a possible resistance of the cells to the inhibitor (*Figure IV.7 b*). Both sets of blots on *Figure IV.7 a* and *b* are representative of two experiments.

To make sure that anti-Y411 antibody is actually phospho-specific, we tested it on cells treated with shrimp alkaline phosphatase (SAP), taking $HgCl_2$ treated cells as a positive control, *Figure IV.7 c* confirms the phospho-specificity of anti-Y411. On this blot again only p59HCK seem to be phosphorylated. Since the cells have not been stimulated in any way, we can actually hypothesise that in Mono-mac-6 p59HCK is constitutively active while p61HCK is not and therefore not detected with the current settings. We can however not rule out that p61HCK in the cells is active but simply not in a fully active conformation where Y411 is phosphorylated and detectable by the antibody (see figure 2.5 in the introduction chapter for the different possible active conformation of HCK).

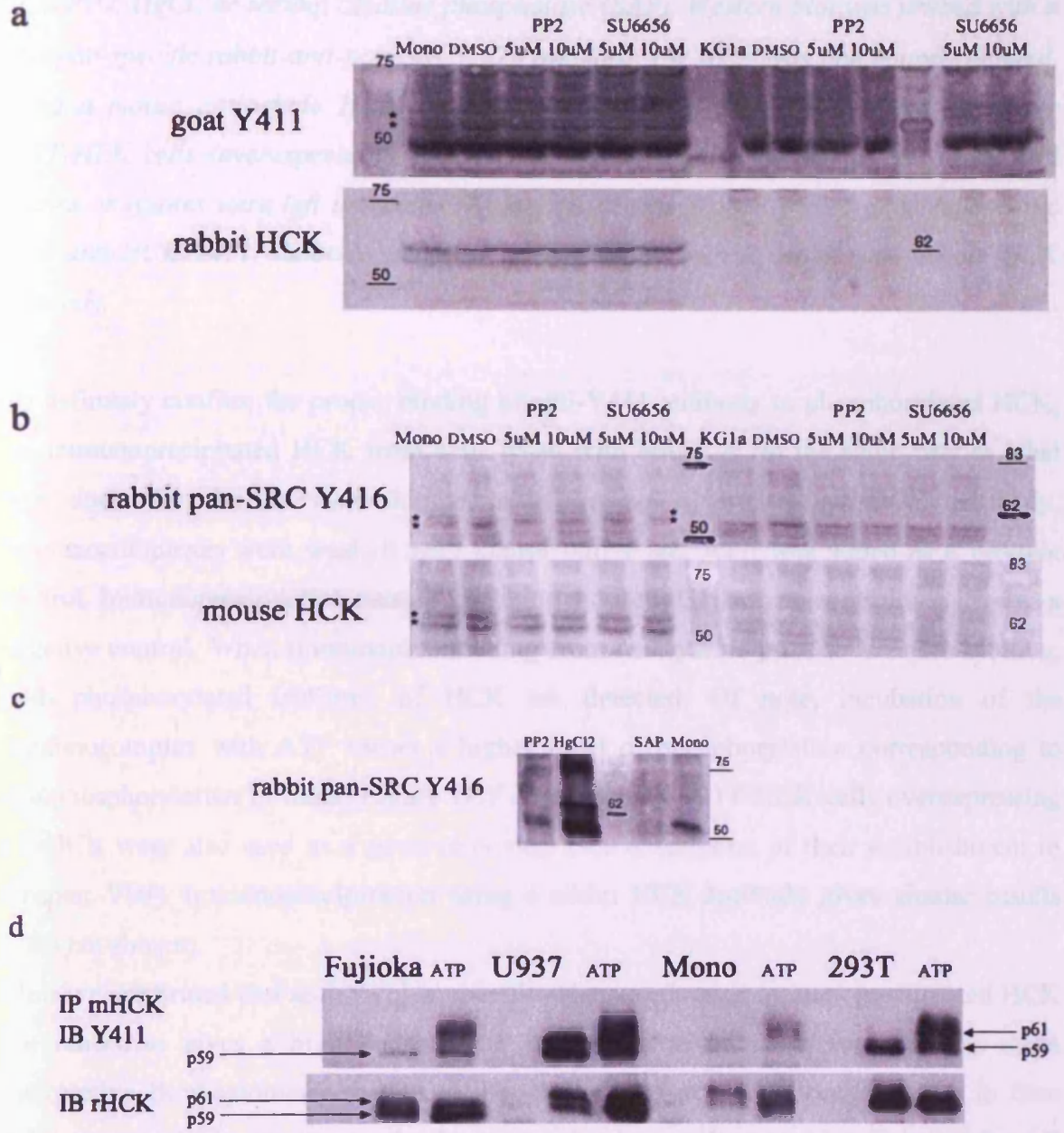


***Figure IV.7: Validation of the phospho-specific anti-HCK Y411 antibody by Western blot.***

*Mono-mac-6 and KG1a cells were treated with different doses of PP2 or SU6656 SFK inhibitor. (a) Whole cell lysate probed with a phospho-specific goat anti-HCK Y411 antibody, stripped and probed with a rabbit anti- whole HCK antibody. (b) Whole cell lysate probed with a phospho-specific rabbit anti-pan-SRC Y416 antibody, stripped and probed with a mouse anti-whole HCK antibody. (c) Mono-mac-6 cells were treated with*

*5μM PP2, $HgCl_2$ or shrimp alkaline phosphatase (SAP). Western blot was probed with a phospho-specific rabbit anti-pan-SRC Y416 antibody. (d) HCK was immunoprecipitated, using a mouse anti-whole HCK antibody, from Fujioka/P31, U937, Mono-mac-6 or 293T-HEK cells (overexpressing HCK) lysed in buffer A. ATP was added to the cell lysates or lysates were left untreated. Western blot was probed with a phospho-specific goat anti-HCK Y411 antibody, stripped and reprobed with a rabbit anti- whole HCK antibody.*

To definitely confirm the proper binding of anti-Y411 antibody to phosphorylated HCK, we immunoprecipitated HCK from cells lysed with buffer A (in the same way as what was done for the *in vitro* kinase assay) using a mouse anti-HCK antibody. Immunocomplexes were washed with kinase buffer and ATP was added as a positive control. Immunoprecipitation using a matching mouse IgG1 isotype control was used as a negative control. When immunoprecipitating from cell lysates prior to Western blotting, both phosphorylated isoforms of HCK are detected. Of note, incubation of the immunocomplex with ATP shows a higher level of phosphorylation corresponding to autophosphorylation in trans (*Figure IV.7 d*, top panel). 293T-HEK cells overexpressing p59HCK were also used as a positive control (see description of their establishment in Chapter VIII). Immunoprecipitation using a rabbit HCK antibody gives similar results (data not shown).

Thus we confirmed that anti-Y411 is specific when used on an immunoprecipitated HCK but otherwise gives a high background, which has to be taken into account when interpreting flow cytometry results. Although the background unspecific signal in flow cytometry might be similar to the background seen on Western blot from whole cell lysates, the HCK epitopes accessible to the anti-Y411 antibody in cells fixed and permeabilised in PFA and methanol are most probably in a different conformation from when the cells have been lysed and the protein lysate has been run on a Western blot.

### 1.3.4 Verification of the pharmacological activity of the PP2 inhibitor in use

To make sure that the PP2 inhibitor we were using had a pharmacological effect on HCK, we added 10 μM PP2 into the non-radioactive kinase just prior to the addition of ATP (*Figure IV.8*). Equivalent volume of DMSO was used as control and each reaction was run in duplicate.

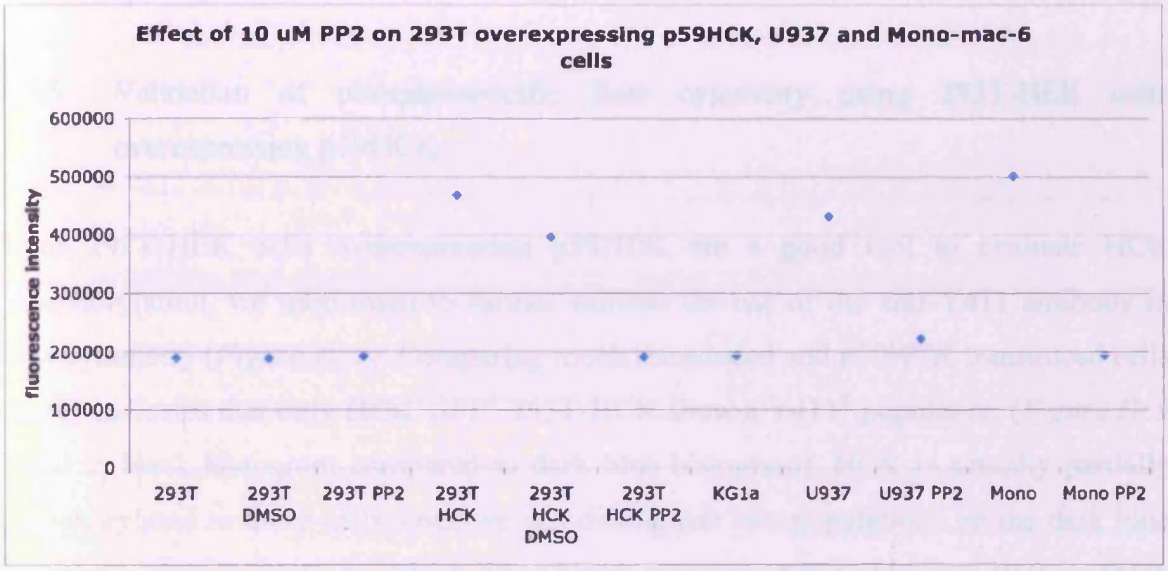


***Figure IV.8: Effect of PP2 on HCK activity in 293T-HEK cells overexpressing p59-HCK, U937 and Mono-mac-6 cells assessed by non-radioactive kinase assay.***

*293T-HEK cells, 293T-HEK cells overexpressing HCK, KG1a, U937 and Mono-mac-6 cells were lysed in buffer A and HCK was immunoprecipitated using a mouse anti-HCK antibody. An in vitro non radioactive kinase assay using the Antibody Beacon™ Tyrosine Kinase Assay Kit was set up in a 384 well black plate, 10 μM PP2 or equivalent DMSO volume was added to the well prior to addition of ATP and fluorescence was read at 530 nm after 45 min incubation. The fluorescence emitted is directly proportional to the kinase activity.*

As expected, no kinase activity was detected in 293T-HEK cell immunoprecipitates since 293T-HEK cells do not express HCK and addition of PP2 or DMSO to these samples does not influence the background signal. KG1a cells were taken as a negative control.

293T-HEK cells overexpressing p59-HCK, U937 and Mono-mac-6 highly express HCK and show kinase activity that is completely abolished by addition of PP2. Addition of DMSO to 293T-HEK cells overexpressing p59-HCK immunoprecipitate causes a 16% decrease in kinase activity. This experiment seems to indicate that PP2 is able to abolish HCK kinase activity when it is immobilised as an enzyme in an immunoprecipitate of a variety of cell lines, but does not have an effect when added to the growth medium of these same cell lines, possibly because it does not enter the cells.

### 1.3.5 Validation of phospho-specific flow cytometry using 293T-HEK cells overexpressing p59HCK

Since 293T-HEK cells overexpressing p59HCK are a good tool to evaluate HCK phosphorylation, we used them to further validate the use of the anti-Y411 antibody in flow cytometry (*Figure IV.9*). Comparing mock transduced and p59HCK transduced cells clearly indicates that only $HCK^{+}GFP^{+}$ 293T-HCK show a $Y411^{+}$ population (*Figure IV.9 c* and *d*, black histogram compared to dark blue histogram). HCK is actually partially phosphorylated in these cells since we can distinguish two populations on the dark blue histogram (*Figure IV.9 d*). Mock transduced cells are $Y411^{-}$ (*Figure IV.9 d*, black histogram) therefore setting the background level of the anti-Y411 staining. The FACS plots shown here are representative of two distinct experiments.

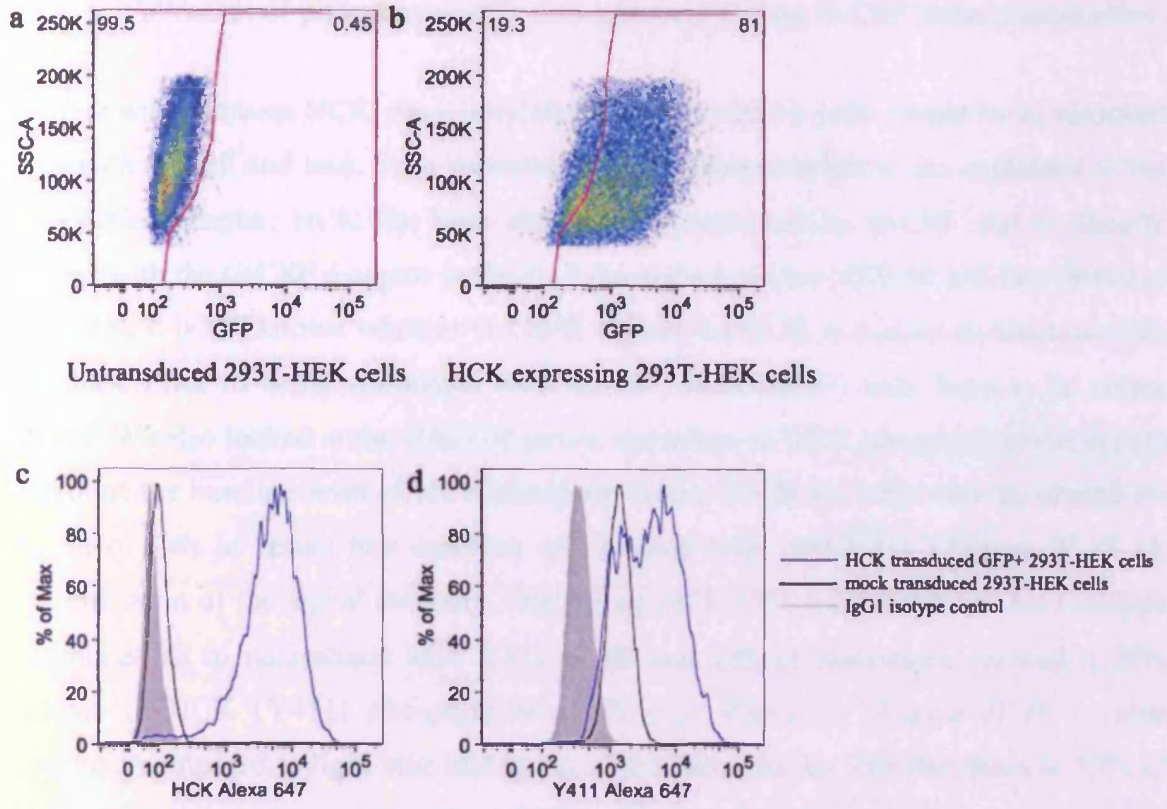


***Figure IV.9: HCK phosphorylation in 293T-HEK cells overexpressing p59HCK.***

*Top panel: GFP expression in p59HCK transduced 293T-HEK cells (b) and control non-transduced 293T-HEK cells (a). Bottom panel: (c) HCK expression: mock transduced 293T-HEK cells do not express HCK (black histogram), p59HCK transduced GFP positive 293T-HEK cells highly express HCK (dark blue histogram). A matching mouse IgG1 isotype control is used as a reference (solid grey histogram). (d) HCK phosphorylation (Y411 phosphorylation): mock transduced 293T-HEK cells are negative for anti-Y411 staining (black histogram), this staining gives a high background in comparison to the matching goat IgG1 isotype control (solid grey histogram). p59HCK transduced GFP positive 293T-HEK cells are partially phosphorylated (dark blue histogram, two populations).*

### 1.3.6 Validation of phospho-specific flow cytometry using G-CSF signal transduction

Another way to assess HCK phosphorylation in Mono-mac-6 cells would be to stimulate them with G-CSF and look for a variation in HCK phosphorylation. As explained in the introduction chapter, HCK has been shown to be activated by G-CSF and to directly interact with the G-CSF receptor in the IL-3 dependent murine NFS-60 cell line (Ward *et al.*, 1998). It is not known whether G-CSFR signals via HCK in human myelomonocytic cell lines. Prior to being stimulated with G-CSF, Mono-mac-6 cells have to be serum starved. We also looked at the effect of serum starvation on HCK phosphorylation to help determine the baseline level of HCK phosphorylation. To do so, cells were incubated for 1h, 4h or 24h in serum-free medium and stained with anti-Y411 (*Figure IV.10 a*). Quantification of the signal intensity, comparing MFI Y411 (normalised to MFI isotype control) at 1h to normalised MFI Y411 at 4h and 24h of starvation, showed a 29% increase in HCK (Y411) phosphorylation 4h post starvation (*Figure IV.10 a*, blue histogram compared to light blue histogram which decreases by 24h starvation to 33% of the initial value at 1h post starvation (*Figure IV.10 a*, dark blue histogram compared to light blue histogram).

We then took Y411 phosphorylation status 24h post starvation as a no stimulation control and compared it to starved Mono-mac-6 cells stimulated with G-CSF for 30 min. We observed that HCK phosphorylation increases by 27% upon G-CSF stimulation (*Figure IV.10 b*, red histogram compared to dark blue histogram), giving half the signal observed when cells are left to starve for 1h only (*Figure IV.10 b*, red histogram compared to light blue histogram). This experiment is representative of two distinct experiments.

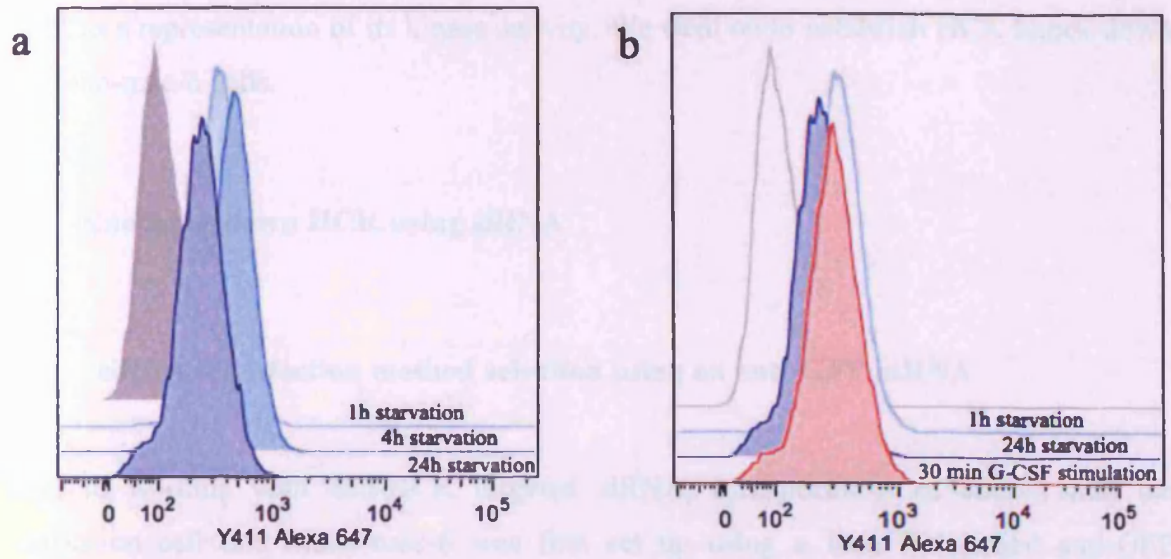


***Figure IV.10: Effect of serum starvation followed by G-CSF stimulation on HCK phosphorylation (Y411) in Mono-mac-6 cell line.***

*(a) Effect of serum starvation on HCK (Y411) phosphorylation over time. HCK phosphorylation level 1h post starvation (light blue histogram), 4h post starvation (blue histogram), 24h post starvation (dark blue histogram). Matching goat IgG1 isotype control is used as a reference for quantification of the signal (grey histogram). (b) Effect of G-CSF stimulation on HCK (Y411) phosphorylation. HCK phosphorylation level 1h post starvation (open light blue histogram), 24h post starvation (dark blue histogram), after 24h serum starvation followed by 30 min stimulation with G-CSF (red histogram).*

Thus, using 293T-HEK cells overexpressing p59HCK and Monomac-6 cells stimulated with G-CSF, we successfully prove that the phospho-specific Y411 antibody can be used in flow cytometry to detect activation of the protein kinase HCK. We can therefore use this staining to assess a change in HCK activity upon HCK knock-down in AML cell lines (see following section and Chapter V), to assess the activity status of HCK in AML samples (Chapter VI) or in UCB $Lin^-$ stem cell enriched fraction (Chapter VII and VIII). We also show that G-CSFR signals via HCK in Mono-mac-6 cell line.

Overall, we have shown in this first section of results that HCK is mostly expressed in AML FAB M5 myelomonocytic cell lines and that we can confidently use flow cytometry to measure its level of expression and its level of phosphorylation on tyrosine

Y411 as a representation of its kinase activity. We went on to establish HCK knock-down in Mono-mac-6 cells.

## 2. Knocking-down HCK using siRNA

### 2.1 siRNA transfection method selection using an anti-GFP siRNA

Prior to working with anti-HCK targeted siRNA, incorporation of siRNA into the suspension cell line Mono-mac-6 was first set up using a RedFP labelled anti-GFP siRNA. Several methods of co-transfection of a GFP plasmid and an anti-GFP siRNA using polyethylimine (PEI), Effectene or Transmessenger were unsuccessfully tested (data not shown). Another approach, first transducing Mono-mac-6 cells with a lentiviral vector carrying GFP under the PGK promoter, then followed by two rounds of electroporation at 300 millivolts and 125 millifarradays for 3.3 miliseconds, to transfect 1 μg of RedFP labelled anti-GFP, proved successful (*Figure IV.11 b)*. One round of electroporation under these conditions allowed the siRNA to enter the cells (as the Red-FP label is detected by FACS; *Figure IV.11 a)* but RNAi was observed only after two rounds of electroporation. In low GFP sorted cells RNAi leads to a 2.09 fold decrease in GFP expression, while in high GFP sorted cells the decrease reached 3.28 fold. Fold decreases are calculated by dividing the GFP MFI of the electroporated control without siRNA by the GFP MFI of the electroporated sample with anti-GFP siRNA. The RedFP-label cannot be clearly detected in silenced high GFP cells because of compensation issues. Data were collected 24, 48 and 72 hours post electroporation. Variations in GFP expression in live cells are shown for the 72h time point only.

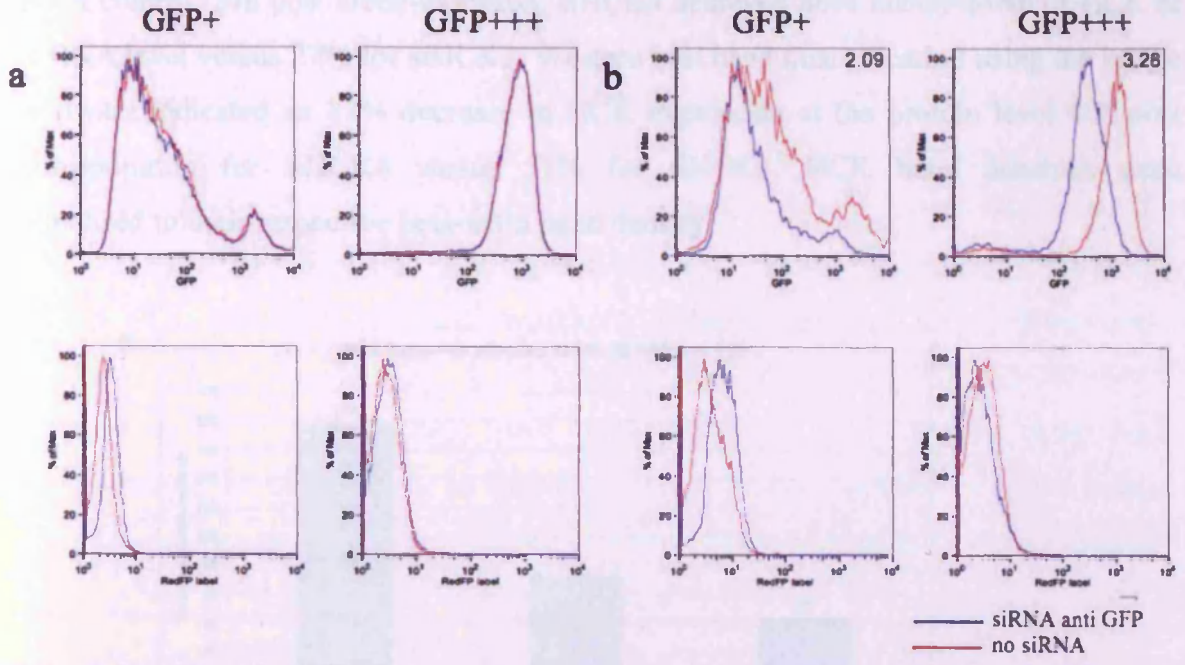


***Figure IV.11: Validation of electroporation as an siRNA transfection method into suspension cells.***

*Mono-mac-6 cells were transduced with a lentiviral vector carrying GFP under the PGK promoter and sorted as $GFP^{+}$ (low GFP sorted cells) and $GFP^{+++}$ (high GFP sorted cells). Mono-mac-6 cells then underwent (a) one round of electroporation or (b) two rounds of electroporation at 300 millivolts and 125 millifarradays for 3.3 miliseconds, to transfect 1 μg of RedFP labelled anti-GFP (blue histogram). Electroporated cells without addition of siRNA were taken as control (red histogram).*

## 2.2 Choice of anti-HCK siRNA sequence

Four different siRNA sequences targeting the coding sequence of HCK were ordered from Eurogentec and tested for RNA interference ability in the Monomac-6 cell line. One of the four siRNA sequences was labelled with Alexa 488 to allow checking for the efficiency of transfection. Two out of the four anti-HCK siRNA sequences were able to induce silencing of HCK at both the mRNA level (*Figure IV.12 a*) and the protein level (*Figure IV.12 b*). Monomac-6 cells electroporated with TE buffer were used as a no

siRNA control. 24h post electroporation, siHCK4 achieved 46% knock-down of HCK at the RNA level versus 27% for siHCK3. Western blot band quantification using the Image J software indicated an 82% decrease in HCK expression at the protein level 48h post electroporation for siHCK4 versus 51% for siHCK3. HCK band densities were normalised to their respective beta-actin band density.

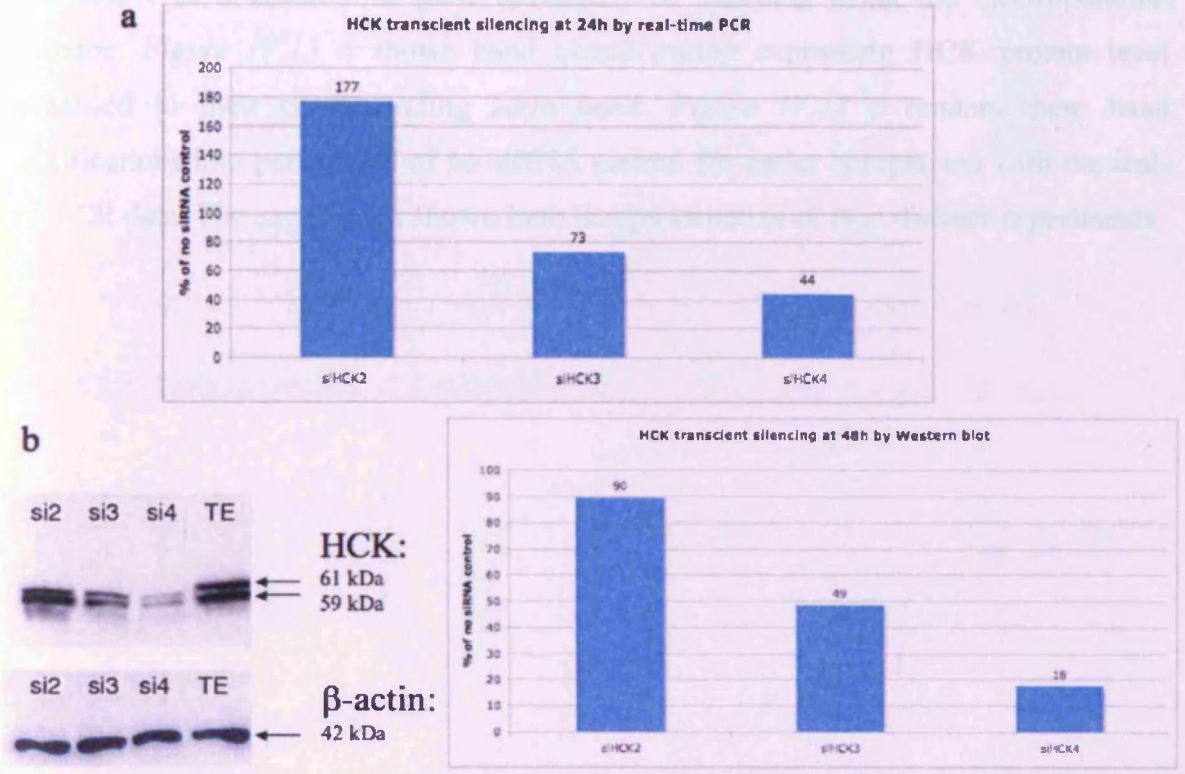


***Figure IV.12: Transient knock-down of HCK in Monomac-6 cells.***

*(a) Testing the knock-down of HCK by qRT-PCR: Silencing properties of four distinct siRNA sequences targeting the coding sequence of the HCK mRNA transcript were assessed by quantitative real-time PCR using SYBR® green. GAPDH was used to normalise the values of mRNA expression. (b) Testing the knock-down of HCK by Western blot: Silencing properties of four distinct siRNA sequences targeting the coding sequence of the HCK mRNA transcript were assessed by Western blotting. Beta-actin was used to normalise the intensities of protein expression. Results are expressed as percentage of expression in Monomac-6 cells electroporated with TE buffer and no siRNA.*

Duration of HCK transient knock-down in Mono-mac-6 was followed up over four days. As seen on *Figure IV.13 a* HCK silencing is not stable over 24h at the mRNA level. *Figure IV.13 b* and *c* show that HCK silencing at the protein level is delayed in comparison to the knock-down at the RNA level (24% less HCK expression at 24h for siHCK4 versus 53% decrease at 48h) and is not stable over 72h. In this experiment an additional non-coding scramble siRNA (scb on the graphs) was electroporated into Mono-mac-6 as a control for gene specificity of silencing using the electroporation technique. *Figure IV.13 b* shows band quantification expressing HCK protein level normalised to their corresponding actin band. *Figure IV.13 c* renders these band quantifications into percentage of no siRNA control for easier comparison with the real-time PCR data. The experiment shown here is representative of four distinct experiments.

a

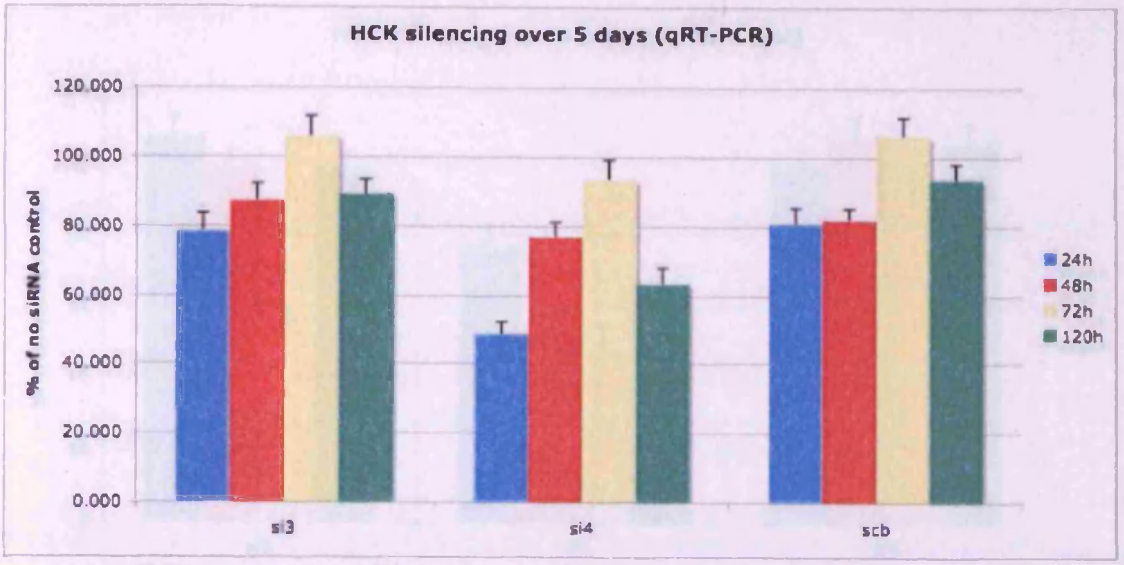
HCK silencing over 5 days (qRT-PCR)
% of no siRNA control
120.000
100.000
80.000
60.000
40.000
20.000
0.000
si3
si4
scb
24h
48h
72h
120h

b

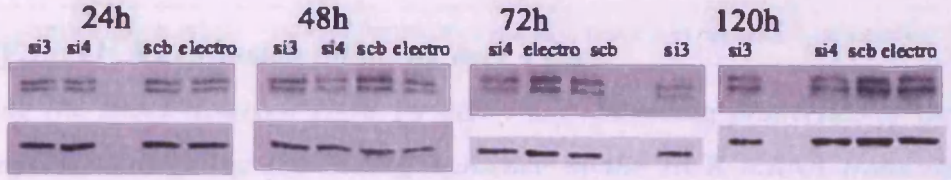
24h
si3 si4 scb electro
48h
si3 si4 scb electro
72h
si4 electro scb si3
120h
si3 si4 scb electro

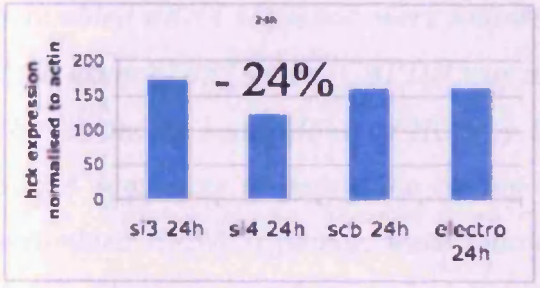
hck expression normalised to actin
200
150
100
50
0
- 24%
si3 24h
si4 24h
scb 24h
electro 24h

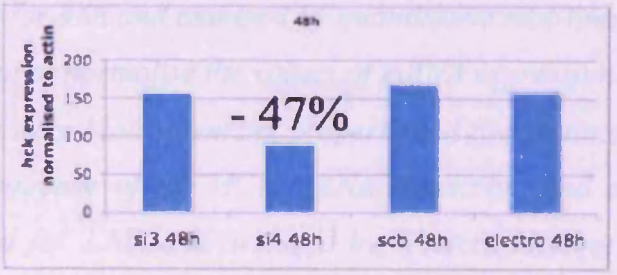
hck expression normalised to actin
200
150
100
50
0
- 47%
si3 48h
si4 48h
scb 48h
electro 48h

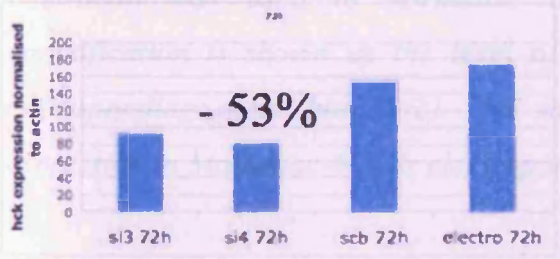
hck expression normalised to actin
- 53%
si3 72h
si4 72h
scb 72h
electro 72h

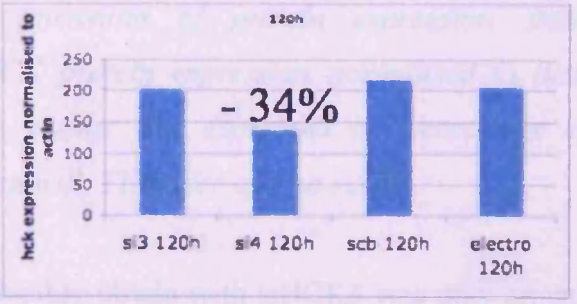
hck expression normalised to actin
250
200
150
100
50
0
- 34%
si3 120h
si4 120h
scb 120h
electro 120h

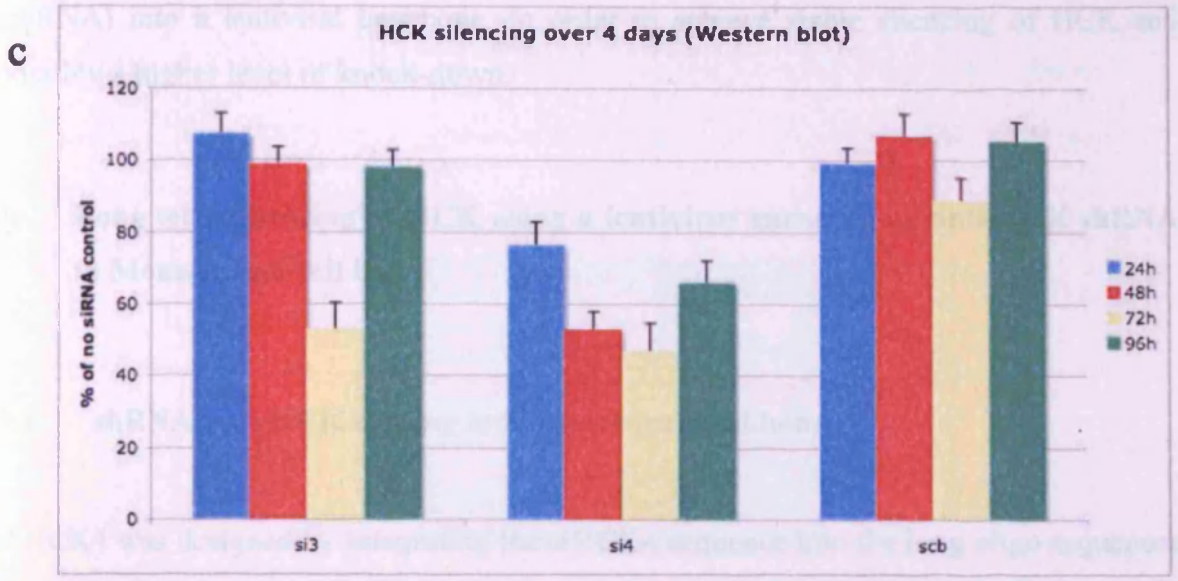


***Figure IV.13:* HCK expression follow up over 4 days.**

*(a) Testing the knock-down of HCK by qRT-PCR: Silencing properties of two distinct siRNA sequences targeting the coding sequence of the HCK mRNA transcript, and a scrambled siRNA sequence, were followed for 96h and assessed by quantitative real-time PCR using SYBR® green. GAPDH was used to normalise the values of mRNA expression. (b) Testing the knock-down of HCK by Western blot: Silencing properties of two distinct siRNA sequences targeting the coding sequence of the HCK mRNA transcript, and a scrambled siRNA sequence, were followed for 120h and assessed by Western blotting. Beta-actin was used to normalise the intensities of protein expression. Band quantification is shown as the level of HCK protein expression normalised to their corresponding actin band. (c) The same results are expressed as percentage of expression in Monomac-6 cells electroporated with TE buffer and no siRNA.*

Since the best knock-down we could reproducibly obtain with siHCK4 was only around 50%, we tested three additional anti-HCK siRNA sequences from Ambion and compared them to siHCK4 using nucleofection as a transfection method. Solution R and program U-001 from Amaxa proved to be the most appropriate to nucleofect Mono-mac-6 cells, but none of the new siRNA sequences tested lead to more than 50% HCK silencing (data not shown). We therefore went on to clone the siHCK4 sequence as a short hairpin RNA

(shRNA) into a lentiviral backbone, in order to achieve stable silencing of HCK and possibly a higher level of knock-down.

## 3. Long term silencing of HCK using a lentivirus encoding an anti-HCK shRNA in Mono-mac-6 cell line

### 3.1 shRNA anti-HCK cloning into a lentiviral backbone

shHCK4 was designed by integrating the siHCK4 sequence into the long oligo sequences represented in *Figure IV.14 a.* Prior to cloning the short hairpin into a 'pH1-Xho1' shuttle vector, the integrity of the latter was verified. As predicted from the map (*Figure IV.14 d*), a 260 base pair fragment is obtained when digesting the pH1-Xho1 shuttle vector with the *XhoI* restriction enzyme and a 221 base pair fragment is obtained when digesting pH1-Xho1 with the *EcoRI* and *BglII* (*Figure IV.14 b*). Oligos were annealed (*Figure IV.14 c*) and cloned in between the *BglII* and *HindIII* restriction sites of the pH1-Xho1 shuttle vector. This vector allows the positioning of the short hairpin under a RNA polymerase III specific promoter H1 (*Figure IV.14 d*).

a

Oligo forward gatcccc(N19SENS)ttcaagaga(N19ANTI-SENS)ttttggaaa

Oligo reverse agcttttccaaaaa(N19SENS)tctcttgaa(N19ANTI-SENS)ggg

b

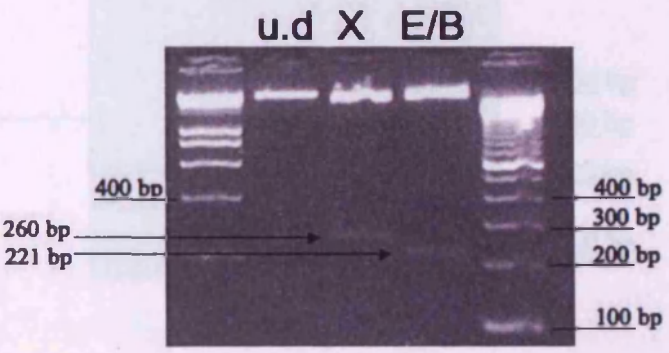


c

gatccccGCTTGCTGGACTTTCTGAAttcaagagaTTCAGAAAGTCCAGCAAGCtttttggaaa

gggCGAACGACCTGAAAGACTTaagttctctAAGTCTTTCAGGTCGTTCGaaaaaccttttcga

BglII loop HindIII

d

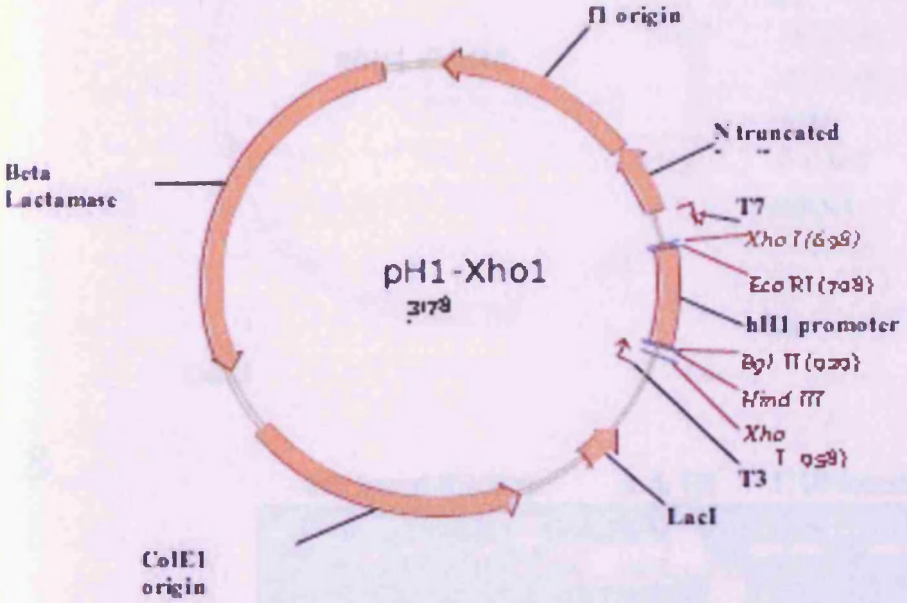

e

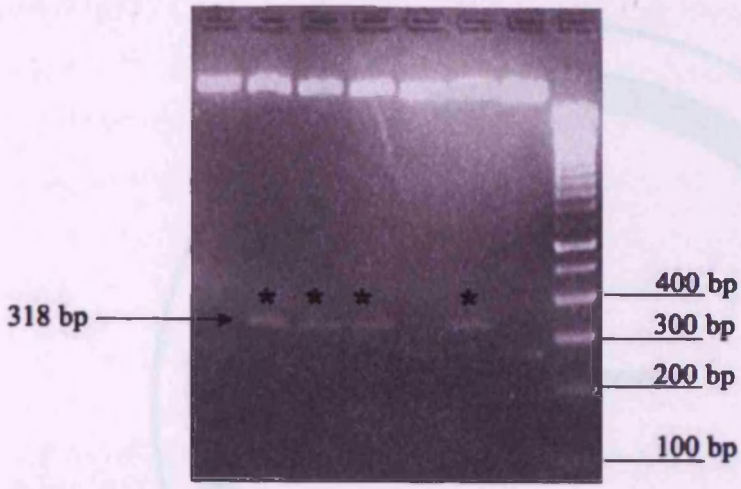
318 bp
400 bp
300 bp
200 bp
100 bp

f

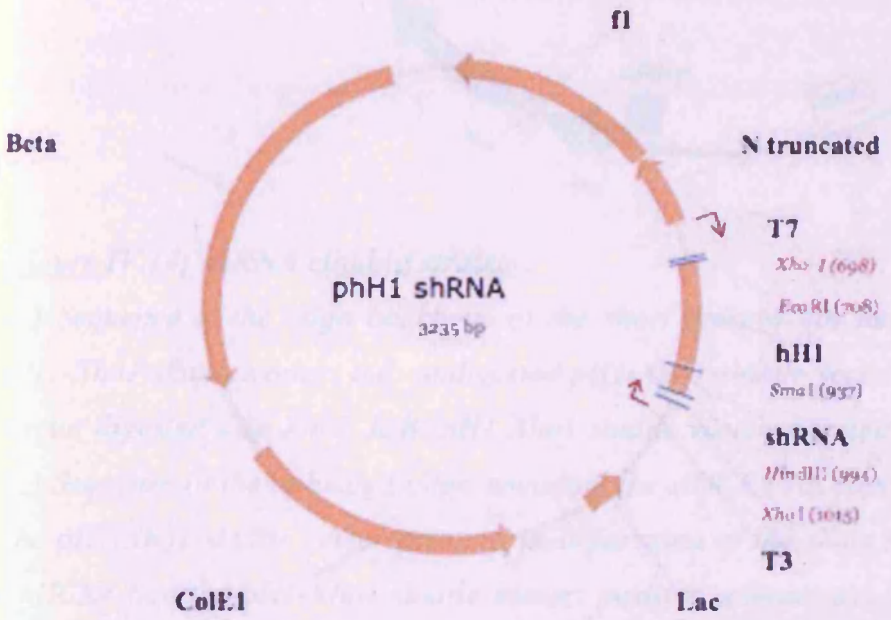
f1
Beta
N truncated
T7
Xho I (698)
EcoRI (708)
hH1
SmaI (957)
shRNA
HindIII (994)
XhoI (1015)
T3
phH1 shRNA
3235 bp
ColE1
Lac

g

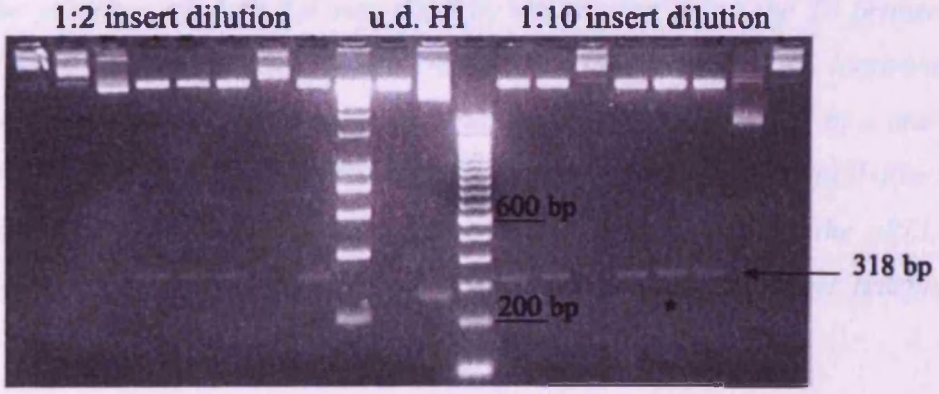
1:2 insert dilution
u.d. H1
1:10 insert dilution
600 bp
200 bp
318 bp

h

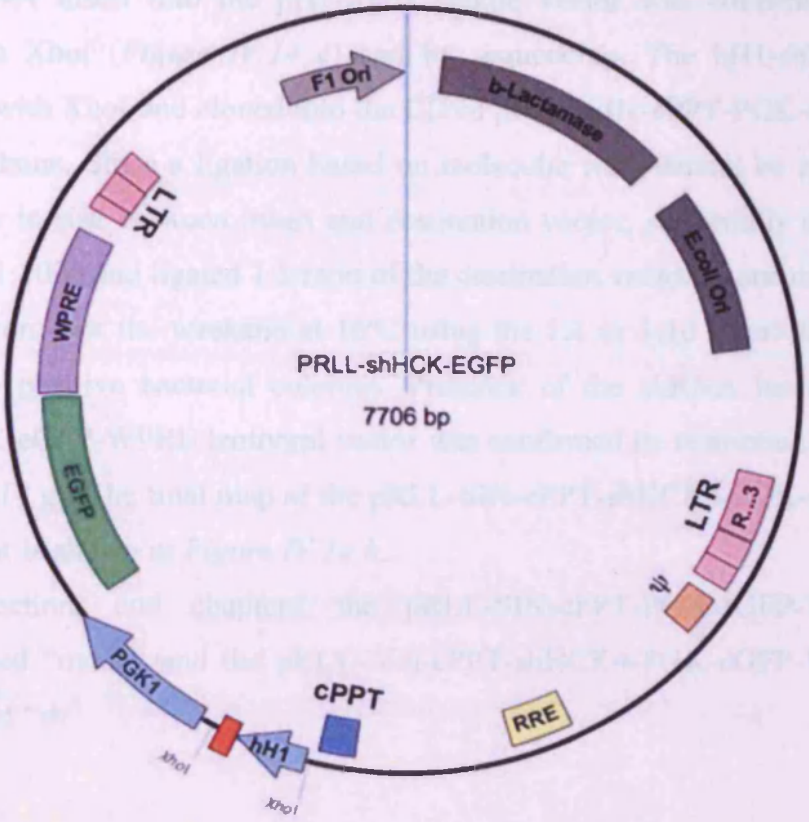


***Figure IV.14: shRNA cloning strategy.***

*(a) Sequence of the oligo backbone of the short hairpin. (b) Restriction profile of the pH1-Xho1 shuttle vector: u.d: undigested pH1-Xho1 shuttle vector; X: pH1-Xho1 shuttle vector digested with XhoI; E/B: pH1-Xho1 shuttle vector digested with EcoRI and BglII. (c) Sequence of the annealed oligo encoding the siHCK4 (in capital letters). (d) Map of the pH1-Xho1 shuttle vector prior to incorporation of the short hairpin. (e) Cloning of shHCK4 into the pH1-Xho1 shuttle vector: positive colonies are indicated by a star. (f) Map of the pH1-Xho1 shuttle vector after incorporation of the short hairpin. Confirmation of the presence of shHCK4 was done by sequencing using the T3 primer. (g) Cloning of shHCK4 into the pRLL-SIN-cPPT-shHCK4-PGK-eGFP-WPRE lentiviral vector: the positive colony subsequently used for virus production is indicated by a star. u.d: undigested pRLL-SIN-cPPT-shHCK4-PGK-eGFP-WPRE and H1: empty pH1-Xho1 shuttle vector digested with Xho1 are used as negative controls. (h) Map of the pRLL-SIN-cPPT-shHCK4-PGK-eGFP-WPRE vector after incorporation of the short hairpin anti-HCK.*

Presence of the shRNA insert into the pH1-Xho1 shuttle vector was confirmed by restriction digest with XhoI (*Figure IV.14 e*) and by sequencing. The hH1-shHCK4 fragment was cut out with XhoI and cloned into the CIPed pRLL-SIN-cPPT-PGK-eGFP-WPRE lentiviral backbone. Since a ligation based on molecular ratio cannot be applied with such a difference in size between insert and destination vector, we serially diluted the insert from 1:2 to 1:1000 and ligated 1:1 ratio of the destination vector to one of these insert dilutions. Ligation over the weekend at 16°C using the 1:2 or 1:10 insert dilution gave rise to shHCK4 positive bacterial colonies. Presence of the shRNA insert into pRLL-SIN-cPPT-PGK-eGFP-WPRE lentiviral vector was confirmed by restriction digest with XhoI (*Figure IV.14 g*). The final map of the pRLL-SIN-cPPT-shHCK4-PGK-eGFP-WPRE lentiviral vector is shown in *Figure IV.14 h.*

In the following sections and chapters, the pRLL-SIN-cPPT-PGK-eGFP-WPRE lentivirus will be called "mock" and the pRLL-SIN-cPPT-shHCK4-PGK-eGFP-WPRE lentivirus will be called "sh".

## 3.2 shRNA encoding lentivirus production and setup of efficient transduction

Highly concentrated mock and sh lentiviruses were produced using 293T-HEK cells as a packaging cell line as described in Chapter II. Mono-mac-6 transduction at multiplicity of infection (MOI) 5, 10 or 20 did not give any convincing HCK silencing (data not shown). These results could have three possible explanations: incapacity of the produced virus to knock-down HCK in a myelomonocytic cell line (Mono-mac-6 may have some reminiscent monocytic mechanisms for clearing out viral RNA), incapacity of the virus to enter a suspension cell line at this MOI or incapacity of the virus to knock-down native HCK due to the semi-silencing property of the siRNA sequence in a transient manner.

### 3.2.1 Validation of shRNA encoding lentivirus silencing function in 293T-HEK cells

To try to elucidate if any of these hypotheses could be validated, we performed a transient HCK overexpression/stable shHCK4 transduction experiment in 293T-HEK

cells. The design of this experiment is described in Chapter II and summarised in *Table IV.1.*

| Name on the graph | HCK sh | HCK mock | HCK alone | YFP mock | YFP alone | 293T |
|---|---|---|---|---|---|---|
| Transfection | p59HCK-YFP | p59HCK-YFP | p59HCK-YFP | YFP | YFP | PEI only |
| Transduction | shHCK4-GFP | Mock GFP | --- | Mock GFP | --- | --- |

***Table IV.1:** Design of the transient HCK overexpression/stable shHCK4 transduction experiment in 293T-HEK cells.*

*See Chapter II, section 3.6, for more detail.*

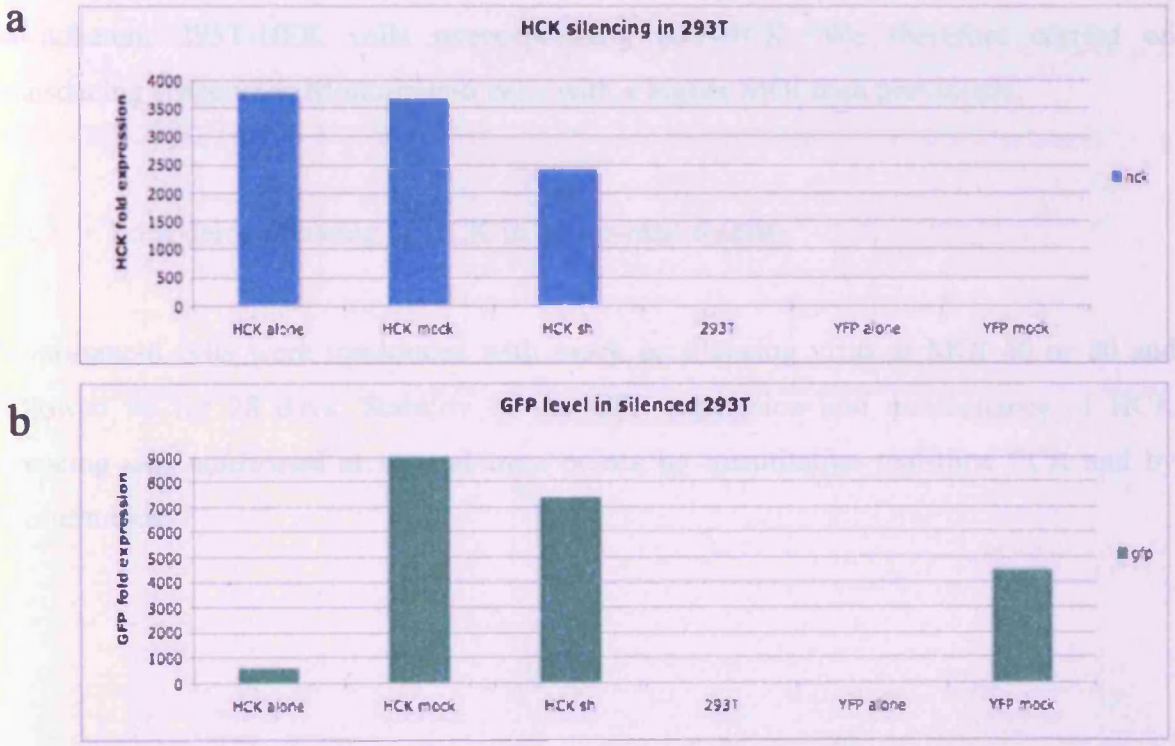


***Figure IV.15:** HCK silencing in 293T-HEK cells detected by quantitative real time PCR.*

*See Chapter II, section 3.6, for more detail.*

Taking untransfected and non-transduced 293T-HEK cells as a control ('293T'), we can see that both the YFP encoding overexpression vector and the GFP encoding silencing

vector entered the cells, since the GFP primers used in this experiment can amplify both GFP and YFP mRNA (*Figure IV.15 b*). 293T-HEK cells transduced with YFP only ('YFP alone') express it at a very low level that cannot be visualised with the Y-axis scale in use on *Figure IV.15 b.* In 293T-HEK cells transduced with p59HCK-YFP only ('HCK alone'), the YFP mRNA amplicon gives a signal 560 fold higher than the basal unspecific signal given by GFP primer dimers in control 293T-HEK cells (*Figure IV.15 b*, first histogram bar). Regarding HCK expression (*Figure IV.15 a*), shHCK4 encoding lentivirus induces a 35% decrease of HCK expression in 'HCK sh' cells in comparison to 'HCK mock' or 'HCK alone' cells transduced with GFP encoding mock vector or non-transduced cells respectively.

This experiment allows us to conclude that the silencing lentivirus produced is functional in adherent 293T-HEK cells overexpressing p59-HCK. We therefore carried on transducing suspension Mono-mac-6 cells with a higher MOI than previously.

### 3.2.2 Long-term silencing of HCK in Mono-mac-6 cells

Mono-mac-6 cells were transduced with mock or silencing virus at MOI 40 or 80 and followed up for 28 days. Stability of the GFP expression and maintenance of HCK silencing was confirmed at several time points by quantitative real-time PCR and by Western blot.

a

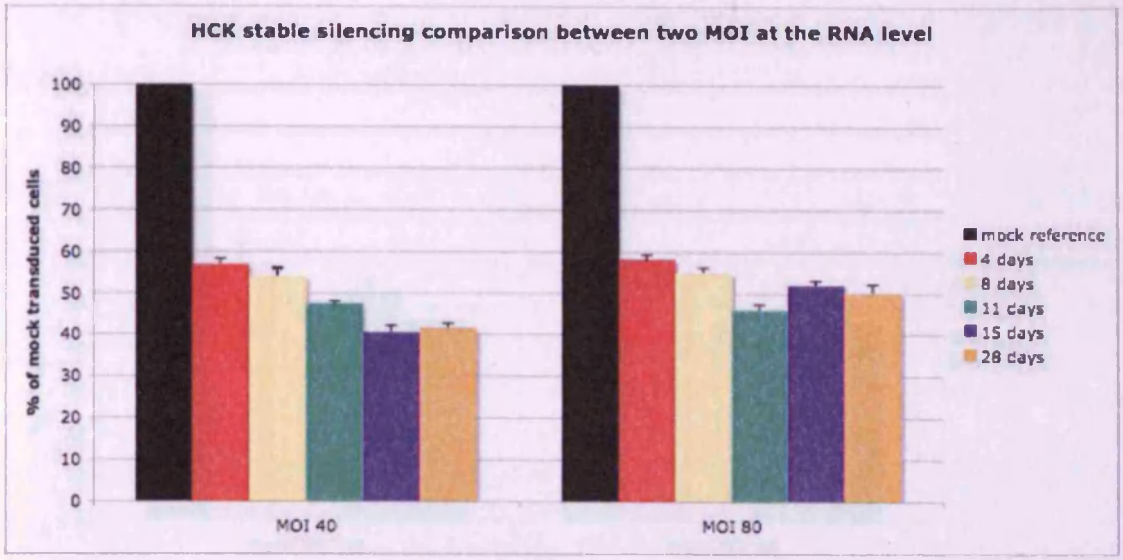
HCK stable silencing comparison between two MOI at the RNA level
% of mock transduced cells
100
90
80
70
60
50
40
30
20
10
0
MOI 40
MOI 80
mock reference
4 days
8 days
11 days
15 days
28 days

b

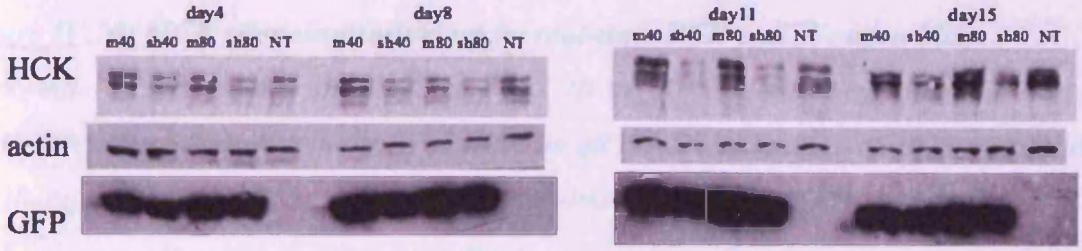
day4
day8
day11
day15
m40 sh40 m80 sh80 NT
HCK
actin
GFP

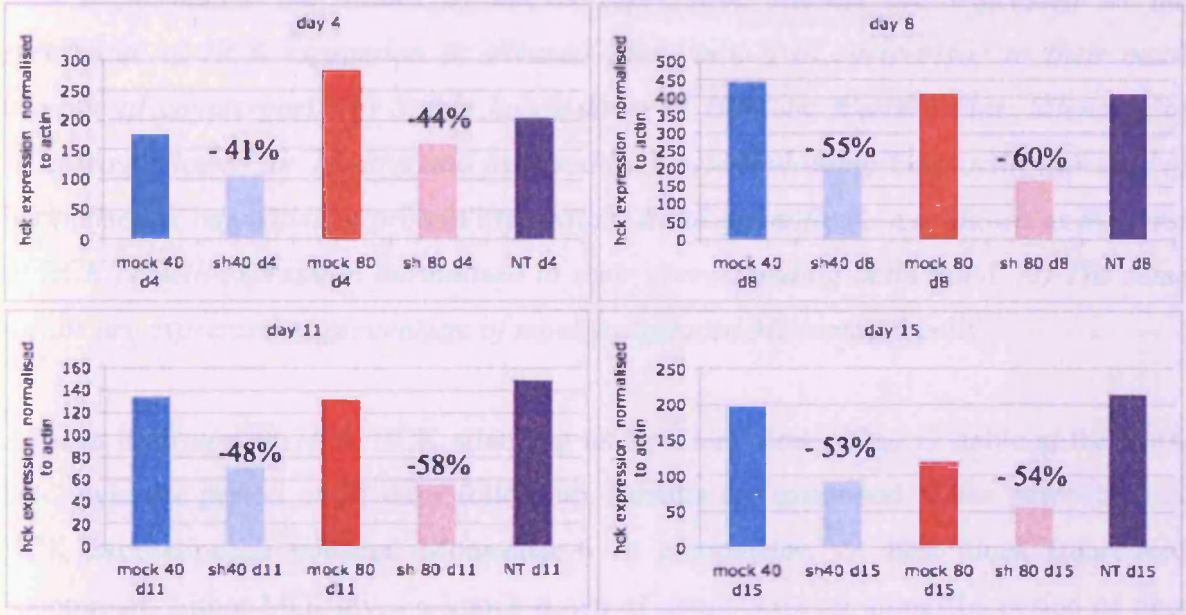
day 4
hck expression normalised to actin
- 41%
-44%
mock 40 d4
sh40 d4
mock 80 d4
sh 80 d4
NT d4
day 8
- 55%
- 60%
mock 40 d8
sh40 d8
mock 80 d8
sh 80 d8
NT d8
day 11
-48%
-58%
mock 40 d11
sh40 d11
mock 80 d11
sh 80 d11
NT d11
day 15
- 53%
- 54%
mock 40 d15
sh40 d15
mock 80 d15
sh 80 d15
NT d15

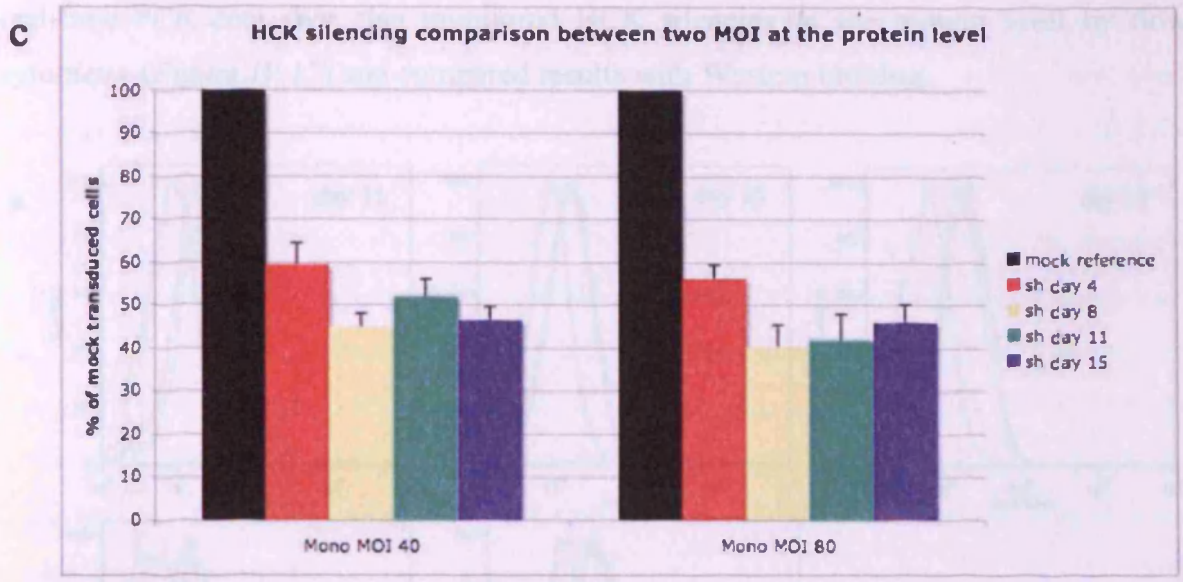


***Figure IV.16: HCK silencing follow up by real-time PCR and Western blot.***

*Mono-mac-6 cells were transduced at MOI 40 or 80 with mock or shHCK4 encoding lentiviruses. (a) Stable knock-down of HCK by qRT-PCR: Silencing of HCK was followed for 28 days and assessed by quantitative real-time PCR using SYBR® green. GAPDH was used to normalise the values of mRNA expression. Results are expressed as the percentage of HCK expression in silenced Mono-mac-6 in comparison to their mock transduced counterpart. (b) Stable knock-down of HCK by Western blot: Silencing of HCK was followed for 15 days and assessed by Western blotting. Beta-actin was used to normalise the intensities of protein expression. Band quantification is shown as the level of HCK protein expression normalised to their corresponding actin band. (c) The same results are expressed as percentage of mock transduced Monomac-6 cells.*

As seen in *Figure IV.16 a*, HCK silencing using a lentiviral vector is stable at the RNA level over the period of 28 days follow-up. Results are expressed as the percentage of HCK expression in silenced Mono-mac-6 in comparison to their mock transduced counterpart. Either MOI gives a knock-down of about 50% all along the period of time monitored. *Figure IV.16 b* and *c* show that HCK silencing is also stable around 50% at the protein level. *Figure IV.16 b* shows band quantification expressing HCK protein level normalised to their corresponding actin band. *Figure IV.16 c* renders these band quantifications into percentage of mock transduced control for easier comparison with the

real-time PCR data. We also monitored HCK silencing at the protein level by flow cytometry (*Figure IV.17*) and compared results with Western blotting.

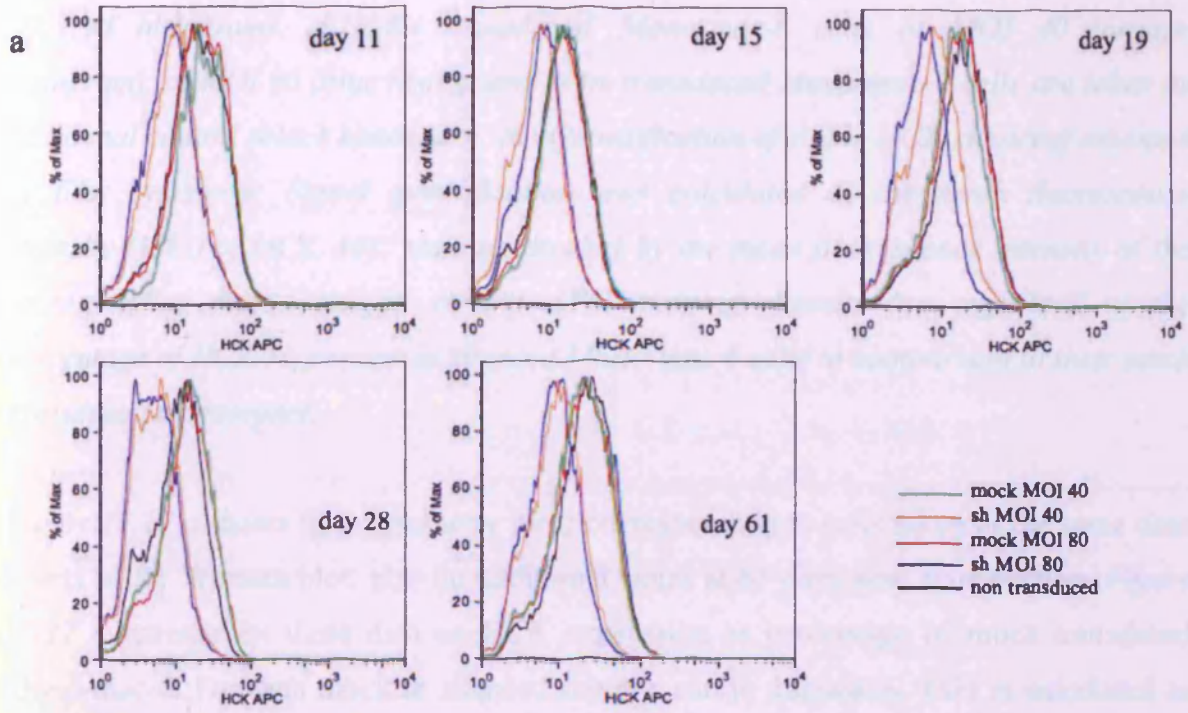


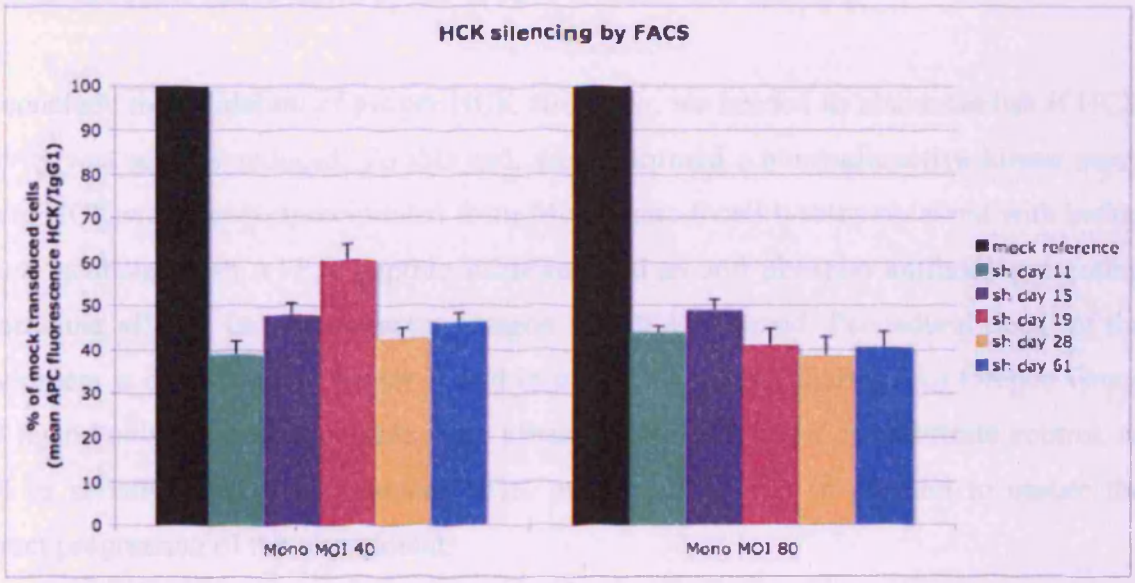


***Figure IV.17: HCK silencing assessed by flow cytometry.***

*Mono-mac-6 cells were transduced at MOI 40 or 80 with mock or shHCK4 encoding lentiviruses. (a) Flow cytometry plots showing the follow up of HCK stable knock-down for 61 days: Mock transduced Mono-mac-6 cells at MOI 40 (green histogram), at MOI 80 (red histogram). shHCK4 transduced Mono-mac-6 cells at MOI 40 (orange histogram), at MOI 80 (blue histogram). Non-transduced Mono-mac-6 cells are taken as additional control (black histogram). (b) Quantification of stable HCK silencing assessed by flow cytometry: Signal quantification was calculated as the mean fluorescence intensity (MFI) of HCK APC staining divided by the mean fluorescence intensity of the corresponding mouse isotype control APC staining. Results are expressed as the percentage of HCK expression in silenced Mono-mac-6 cells in comparison to their mock transduced counterpart.*

*Figure IV.17 a* shows flow cytometry plots corresponding to cells taken at the same time points as for Western blot, plus an additional point at 61 days post transduction. *Figure IV.17 b* summarises these data on HCK expression as percentage of mock transduced Mono-mac-6. For each mock or silenced sample, run in duplicates, MFI is calculated as the mean fluorescence intensity of HCK APC staining divided by the mean fluorescence intensity of the corresponding mouse isotype control APC staining. Flow cytometry data confirm that HCK knock-down by about 50% is stable over 61 days.

To conclude the validation of proper HCK silencing, we needed to also establish if HCK activity was actually reduced. To this end, we performed a non-radioactive kinase assay where HCK was immunoprecipitated from Mono-mac-6 cell lysates obtained with buffer A and incubated with ATP, a peptide substrate, and an anti-phospho antibody presenting a particular affinity for a fluorescent Oregon Green 488 ligand. Procedural detail of the experiment is described in Chapter II and in part 1.3.1 of this chapter. An Oregon Green 488 ligand only, a phosphopeptide, a no kinase, a no ATP and a no substrate control, as well as serially diluted recombinant HCK protein, were run in parallel to ensure the correct progression of the experiment.

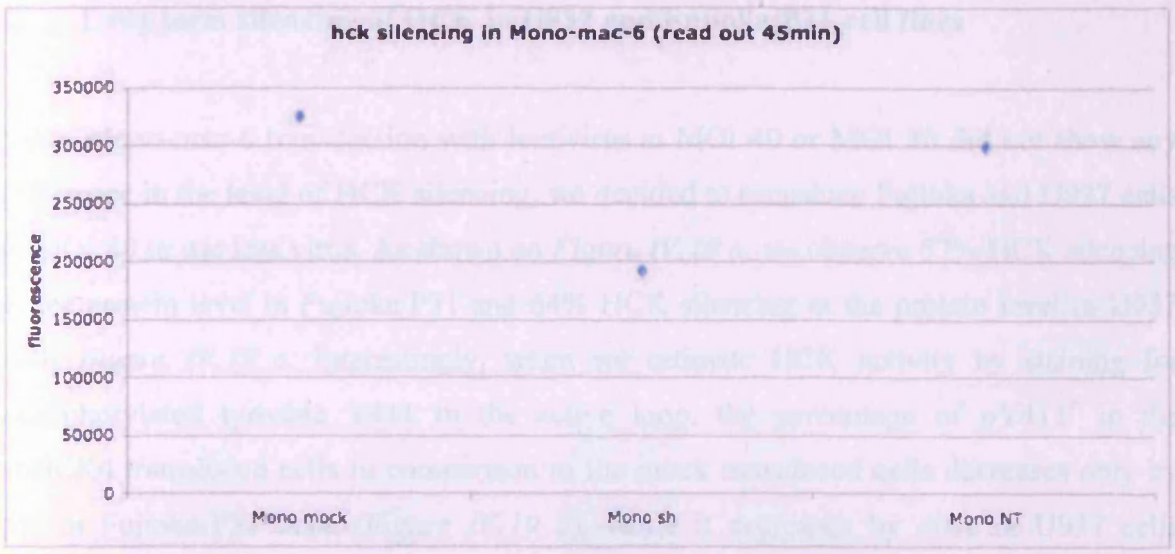


***Figure IV.18: HCK activity measured by non-radioactive kinase assay.***
*Mock transduced, shHCK4 transduced and non-transduced Mono-mac-6 cells were lysed in buffer A and HCK was immunoprecipitated using a mouse anti-HCK antibody. An in vitro non-radioactive kinase assay using the Antibody Beacon™ Tyrosine Kinase Assay Kit was set up in a 384 well black plate and fluorescence was read at 530 nm after 45 min incubation. The fluorescence emitted is directly proportional to the kinase activity.*

The non-radioactive kinase assay confirms that a 50% knock-down of HCK at the RNA and protein level in Mono-mac-6 cells corresponds to a 41% decrease in HCK activity *in vitro* (*Figure IV.18*). This experiment is representative of two independent experiments.

Since achieving 50% silencing of HCK in Mono-mac-6 cells was not completely satisfactory, we went on to try to see if we could obtain a better silencing in two different AML cell lines: U937 and Fujioka/P31. These two cell lines are also classified as M5 in the FAB classification, but are reported to be slightly more immature than Mono-mac-6 (Abrink *et al.*, 1994; Erl *et al.*, 1995; Ziegler-Heitbrock *et al.*, 1988). As quantified in part 1.1 of this chapter, they also highly express HCK.

## 4. Long term silencing of HCK in U937 and Fujioka/P31 cell lines

Since Mono-mac-6 transduction with lentivirus at MOI 40 or MOI 80 did not show any difference in the level of HCK silencing, we decided to transduce Fujioka and U937 cells at MOI 40 to use less virus. As shown on *Figure IV.19 a*, we observe 57% HCK silencing at the protein level in Fujioka/P31 and 64% HCK silencing at the protein level in U937 cells *Figure IV.19 c*. Interestingly, when we estimate HCK activity by staining for phosphorylated tyrosine Y411 in the active loop, the percentage of $pY411^{+}$ in the shHCK4 transduced cells in comparison to the mock transduced cells decreases only by 5% in Fujioka/P31 cells (*Figure IV.19 b*), while it decreases by 40% in U937 cells (*Figure IV.19 d*). *Figure IV.19 e* summarises these data on HCK silencing as percentage of mock transduced Fujioka/P31 or U937 cells for total HCK or phospho-HCK staining. For each mock or silenced sample, run in duplicates, MFI is calculated as the mean fluorescence intensity of HCK Alexa 647 staining divided by the mean fluorescence intensity of the corresponding mouse isotype control Alexa 647 staining. However, when estimating kinase activity by non-radioactive kinase assay, we could observe a decrease of 43% in kinase activity in Fujioka/P31 cells and of 38% in U937 cells. Mono-mac-6 cells were taken for comparison and show a 54% decrease in kinase activity when looking at 55 min incubation (*Figure IV.19 f*, n=6).

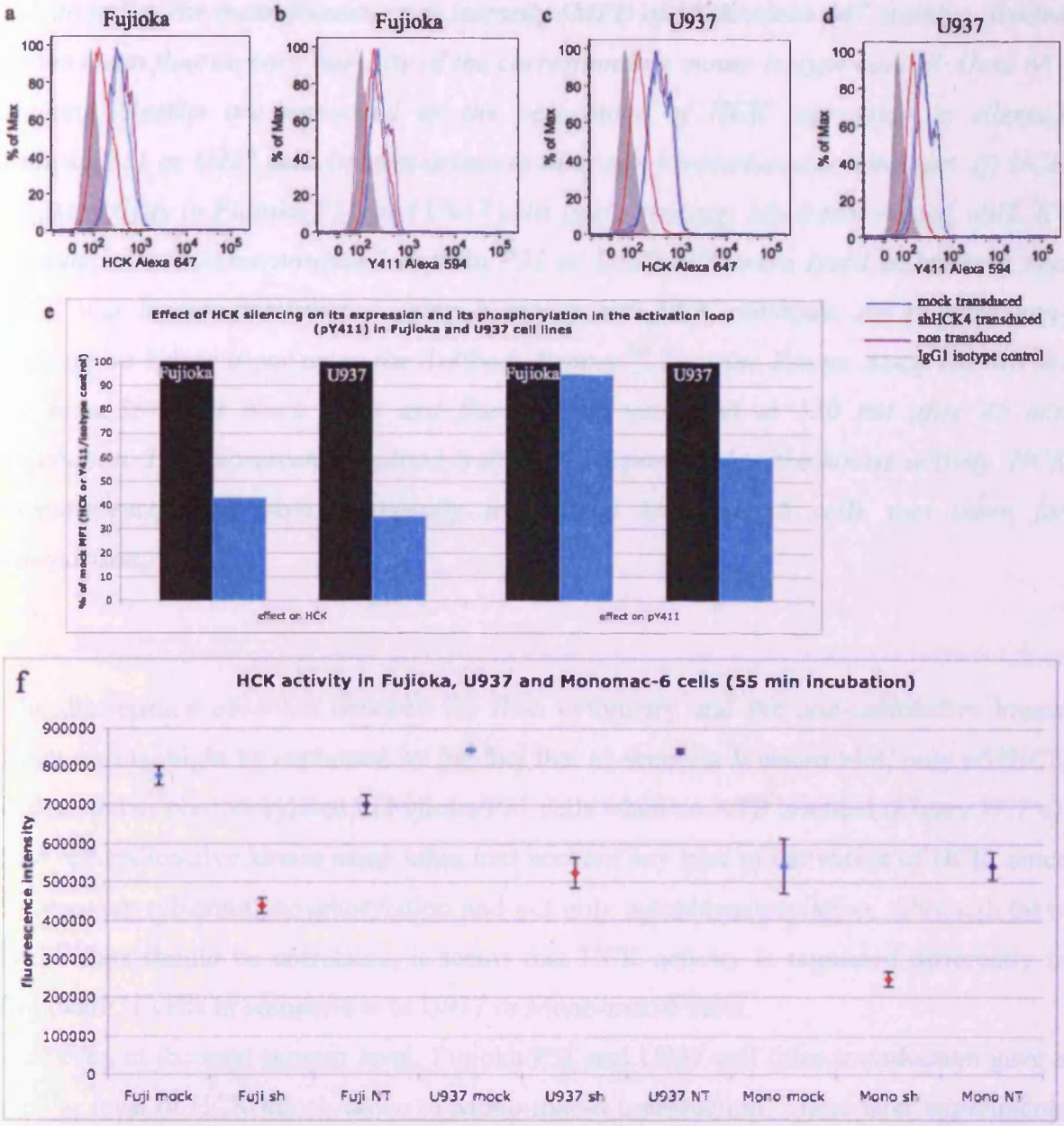


***Figure IV.19: HCK silencing in Fujioka/P31, U937 and Mono-mac-6 cell lines.***

*Fujioka/P31 and U937 cells were transduced with a mock (blue histogram) or shHCK4 (red histogram) lentivirus at MOI 40. Untransduced cells were taken as controls (puple histogram) (a) Fujioka/P31 cells staining for HCK. (b) Fujioka/P31 cells staining for phosphorylated HCK Y411. (c) U937 cells staining for HCK. (d) U937 cells staining for phosphorylated HCK Y411. Matching isotype controls were used to normalise each staining (grey histogram). (e) Quantification of HCK expression and HCK phosphorylation post silencing assessed by flow cytometry: Signal quantification was*

*calculated as the mean fluorescence intensity (MFI) of HCK Alexa 647 staining divided by the mean fluorescence intensity of the corresponding mouse isotype control Alexa 647 staining. Results are expressed as the percentage of HCK expression in silenced Fujioka/P31 or U937 cells in comparison to their mock transduced counterpart. (f) HCK kinase activity in Fujioka/P31 and U937 cells post silencing: Mock transduced, shHCK4 transduced and non-transduced Fujioka/P31 or U937 cells were lysed in buffer A and HCK was immunoprecipitated using a mouse anti-HCK antibody. An in vitro non-radioactive kinase assay using the Antibody Beacon™ Tyrosine Kinase Assay Kit was set up in a 384 well black plate and fluorescence was read at 530 nm after 45 min incubation. The fluorescence emitted is directly proportional to the kinase activity. HCK immunoprecipitated from lentivirally transduced Mono-mac-6 cells was taken for comparison.*

The discrepancy observed between the flow cytometry and the non-radioactive kinase assay results might be explained by the fact that as seen via Western blot, only p59HCK is detected as phosphorylated in Fujioka/P31 cells when no ATP is added (*Figure IV.7 d*). The non-radioactive kinase assay takes into account any type of activation of HCK, since it measures substrate phosphorylation and not only autophosphorylation. Although these two events should be correlated, it seems that HCK activity is regulated differently in Fujioka/P31 cells in comparison to U937 or Mono-mac-6 cells.

However, at the total protein level, Fujioka/P31 and U937 cell lines transduction gave a similar level of HCK knock-down to Mono-mac-6 transduction. These later experiments demonstrate that semi-silencing of HCK is a property intrinsic to the siRNA sequence in use and is independent of the cell line studied. To try to obtain a better level of HCK silencing, we decided to try using an miRNA based strategy that might give better results.

## 5. Attempt to knock-down HCK using an miRNA based strategy

miRNA present the advantage of being transcribed by the RNA polymerase II which is supposedly more efficient than the RNA polymerase III used to transcribe siRNA . They can also easily be chained into a vector, either as several different miRNA targeted towards the same gene or as miRNA targeted against different genes. We took advantage of the BLOCK-iT™ Pol II miR RNAi Expression Vector Kit commercialised by Invitrogen and ordered the package of 4 anti-HCK miRNA on offer.

### 5.1 miRNA anti-HCK cloning

Each of the 4 miRNA 604, 605, 606 and 607 were cloned into the pcDNA™6.2GW /EmGFP-miR plasmid according to the manufacturer's protocol and as described in Chapter II. Subsequently each miRNA was chained to each other as a combination of either 2 of each miRNA (12 constructs) and as a combination of either 3 of each miRNA (24 constructs) by digesting 'backbone' miRNA carrying vectors with *BglII* and *XhoI* and miRNA 'insert' with *BamHI* and *XhoI* (*Figure IV.20*).

a

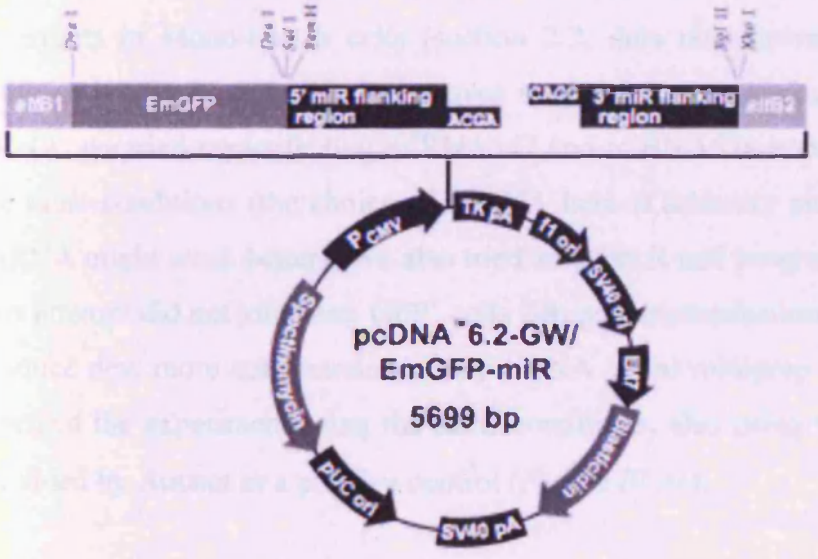

b

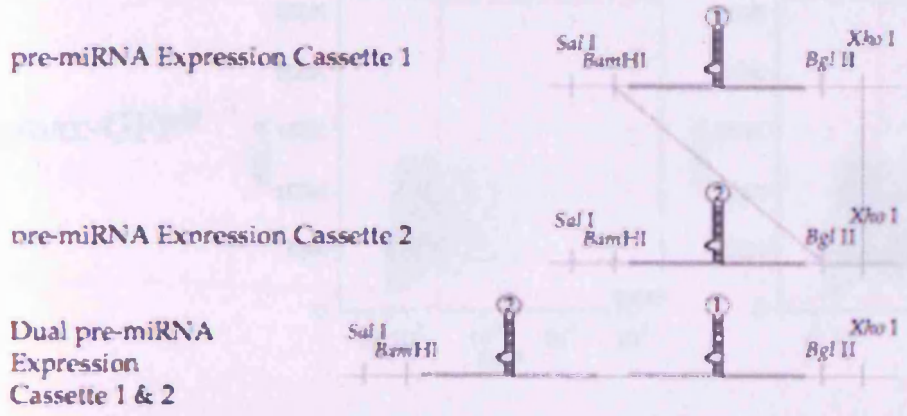


***Figure IV.20: miRNA cloning strategy.***

*(a) Map of the linearised pcDNA™6.2GW /EmGFP-miR plasmid. (b) Cloning strategy for chaining 2 miRNA expression cassettes combining restriction digests with BglII, BamHI and XhoI. See Chapter II for detail.*

## 5.2 Attempt of choosing the most efficient miRNA combination to silence HCK in Mono-mac-6 cells

Prior to cloning an miRNA or a combination of miRNA into a lentiviral vector, we tried to select for the most silencing miRNA condition by nucleofecting the produced constructs in Mono-mac-6 cells (section 2.2, data not shown). Since solution R and program U-001 from Amaxa had proven successful to nucleofect Mono-mac-6 cells with siRNA, we tried nucleofecting miRNA547 and miRNA574 into Mono-mac-6 cells using the same conditions (the choice of miRNA here is arbitrary and we assumed that triple miRNA might work better). We also tried solution R and program T-001 in parallel. This first attempt did not yield any $GFP^+$ cells 24h post nucleofection, we therefore went on to produce new more concentrated plasmid DNA (from midiprep instead of miniprep) and repeated the experiment using the same conditions, also using the pmax-GFP® plasmid provided by Amaxa as a positive control (*Figure IV.21*).

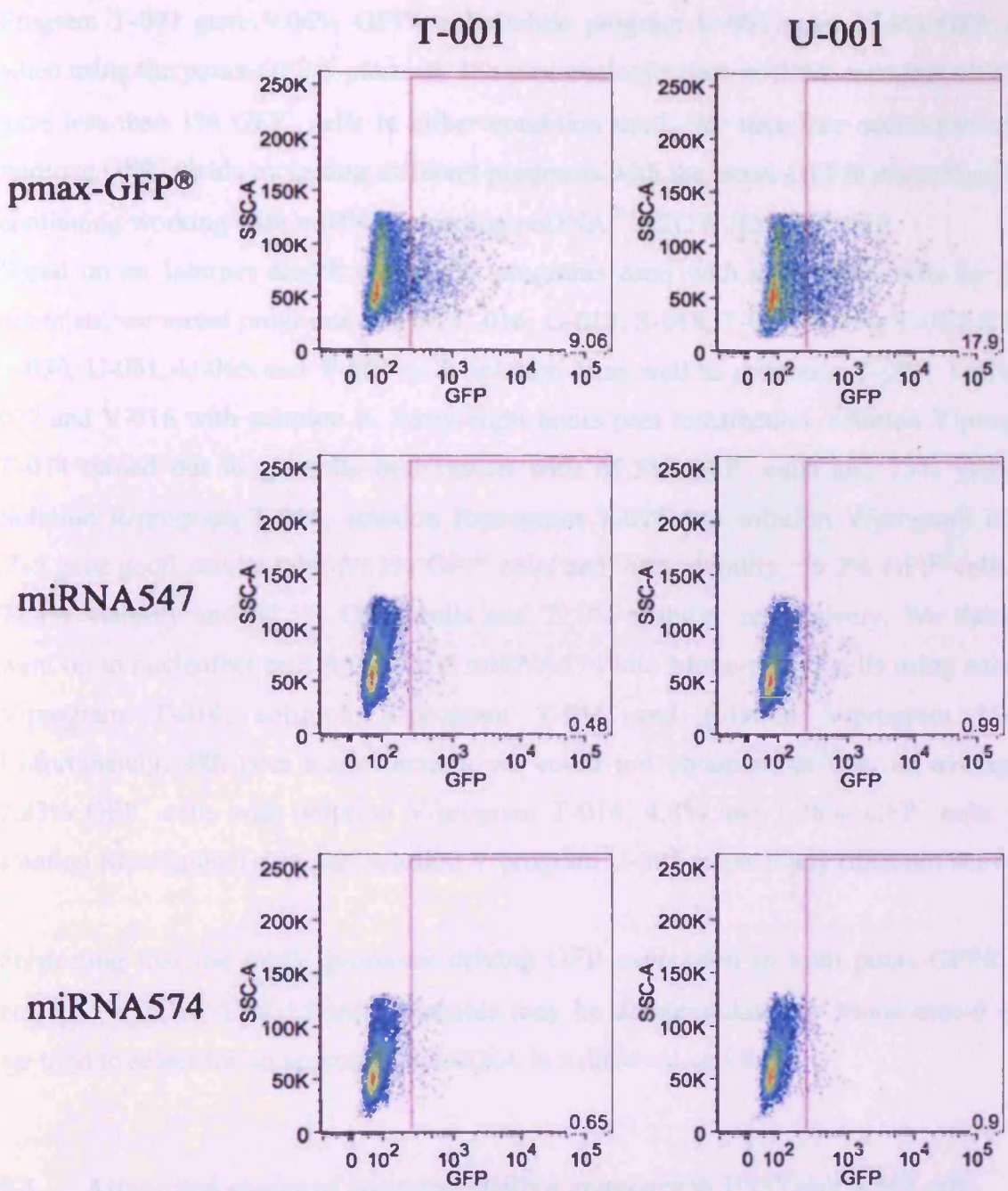


***Figure IV.21: Nucleofection test in Mono-mac-6 cell line using solution R, programs T-001 and U-001.***

*Top panel: GFP expression in Mono-mac-6 cells nucleofected with the control plasmid pmax-GFP®. Middle panel: GFP expression in Mono-mac-6 cells nucleofected with the miRNA547 expression cassette encoding pcDNA™6.2GW /EmGFP-miR plasmid. Bottom panel: GFP expression in Mono-mac-6 cells nucleofected with the miRNA574 expression cassette encoding pcDNA™6.2GW /EmGFP-miR plasmid.*

Program T-001 gave 9.06% GFP+ cells while program U-001 gave 17.9% GFP cells when using the pmax-GFP® plasmid, 48h post nucleofection. miRNA encoding plasmids gave less than 1% $GFP^+$ cells in either condition used. We therefore decided to try to improve $GFP^+$ yields by testing different programs with the pmax-GFP® plasmid prior to continuing working with miRNA encoding pcDNA$^{TM}$6.2GW /EmGFP-miR.
Based on an Internet search of Amaxa programs used with suspension cells by other scientists, we tested programs A-017, C-016, G-010, S-018, T-001, T-014, T-020, T-027, T-030, U-001, U-005 and V-001 with solution V as well as programs T-001, T-016, T-027 and V-016 with solution R. Forty-eight hours post transfection, solution V/program T-014 turned out to give the best results with 67.5% $GFP^+$ cells and 75% viability. Solution R/program T-016, solution R/program T-027 and solution V/program U-005 also gave good results with 60.3% $GFP^+$ cells and 70% viability, 59.2% $GFP^+$ cells and 72.1% viability and 57.5% $GFP^+$ cells and 72.9% viability respectively. We therefore went on to nucleofect miRNA547 and miRNA574 into Mono-mac-6 cells using solution V/program T-014, solution R/program T-016 and solution V/program U-005. Unfortunately, 48h post nucleofection, we could not obtain more than an average of 2.83% $GFP^+$ cells with solution V/program T-014, 4.8% and 1.58% $GFP^+$ cells with solution R/program T-016 and solution V/program U-005 respectively (data not shown).

Suspecting that the CMV promoter driving GFP expression in both pmax-GFP® and pcDNA$^{TM}$6.2GW /EmGFP-miR plasmids may be downregulated in Mono-mac-6 cells, we tried to select for an appropriate miRNA in a different cell line.

## 5.3 Attempted choice of silencing miRNA sequence in U937 and K562 cells

Amaxa having released a new kit for nucleofecting U937 cells, we made use of solution C/program W-001 and tried to nucleofect miRNA547 as well as single miRNA 604, 605, 606, 607 (in case unsuccessful transduction would be due to the chaining process). Having noticed from colleague's experiments that K562 cells can be successfully transduced with lentivirus at lower MOI than myelomonocytic cells (MOI 10 instead of 40) (Rangatia and Bonnet, 2006), we used K562 cells as a positive control for GFP

positivity and nucleofected them with solution V/program T-016, as recommended by Amaxa. Forty-eight hours post transfection in K562 cells, miRNA 605, 606 and 607 yield 44.2%, 62.3 % and 49.9% $GFP^+$ cells respectively and more than 86% cells were viable in every case (data not shown). In U937 cells, miRNA 604, 605, 606, 607 yield 3.09%, 10.1%, 7.9% and 2.25% $GFP^+$ cells respectively while the pmax-GFP® plasmid gave 23.6% GFP+ U937 cells (*Figure IV.22*). Of note, when transduced with the pmax-GFP® plasmid 61% of the U937 cells are viable, while 8.91%, 4.13 %, 10.3% and 68.7 cells are viable when transduced with miRNA 604, 605, 606, 607 respectively.

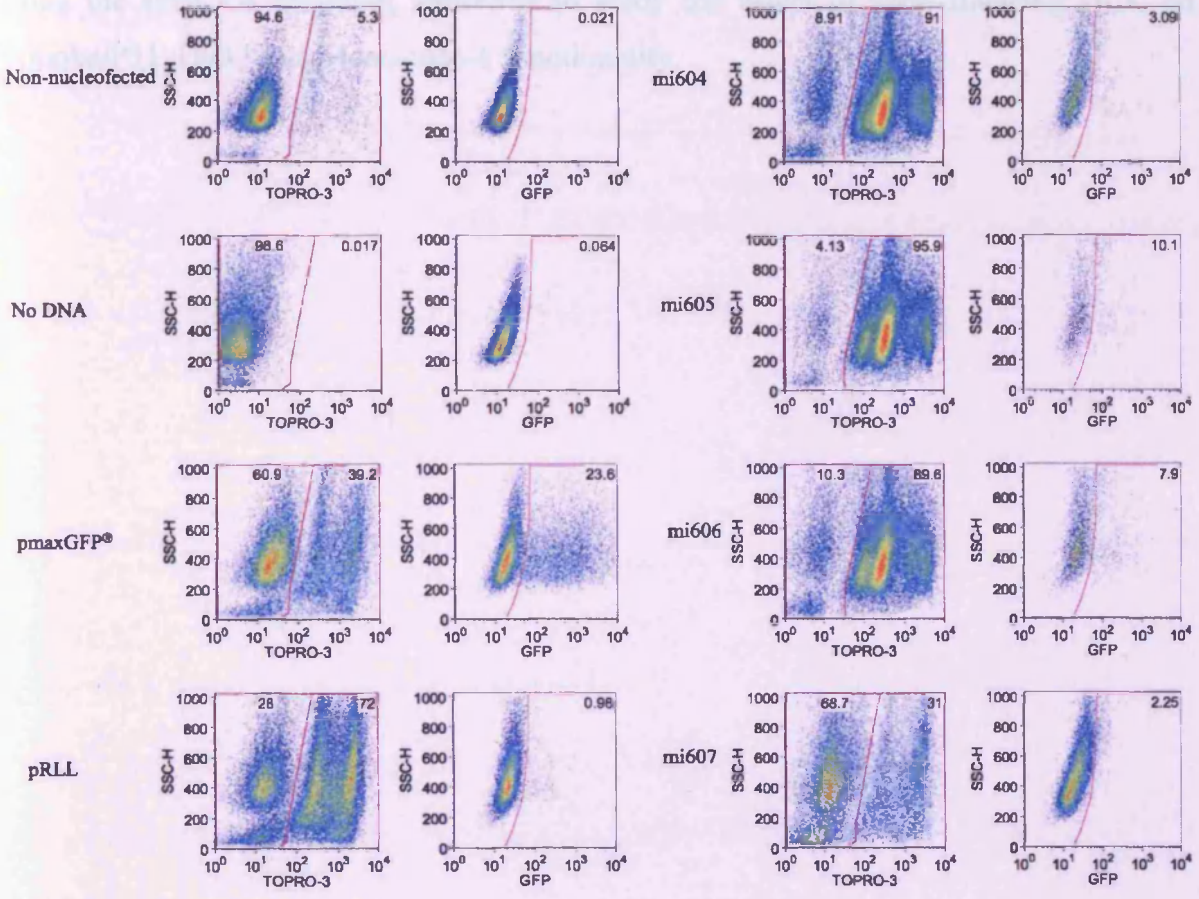


***Figure IV.22: Nucleofection test in U937 cell line using solution C, program W-001.***

*Percentage of live cells (TOPRO-3 negative cells) and GFP expression in non-nucleofected U937 cells, U937 cells nucleofected without addition of DNA, U937 cells nucleofected with the Control plasmid pmax-GFP®, the mock lentiviral backbone used in the shRNA study, the miRNA604, 605, 606, or 607 expression cassette encoding pcDNA™6.2GW /EmGFP-miR plasmid.*

This experiment confirms that the CMV promoter used to drive GFP expression is functional in K562 cells, but not in myelomonocytic cell lines. Since K562 cells do not express HCK, we could not investigate HCK silencing using miRNA any further in suspension cells.

## 6. Conclusion

Since the miRNA based system we tried to use did not prove helpful, we went back to using the shHCK4 encoding lentivirus to study the effect of semi-silencing HCK on Fujioka/P31, U937 and Mono-mac-6 functionality.

# Chapter V

# V Effect of HCK semi-silencing on AML cell lines

## 1. Effect of HCK semi-silencing on FAB M5 cell lines proliferation

### 1.1 XTT assay

We first looked at the metabolic activity of cell lines by the XTT assay. While Fujioka/P31 and U937 cell lines transduced with mock or silencing virus do not show any obvious change in metabolic activity that can be associated to proliferation (*Figure V.1, top and middle panel*), Mono-mac-6 cells transduced with shHCK4 encoding virus tend to proliferate faster than controls (*Figure V.1, bottom panel*) over 96h post transduction.

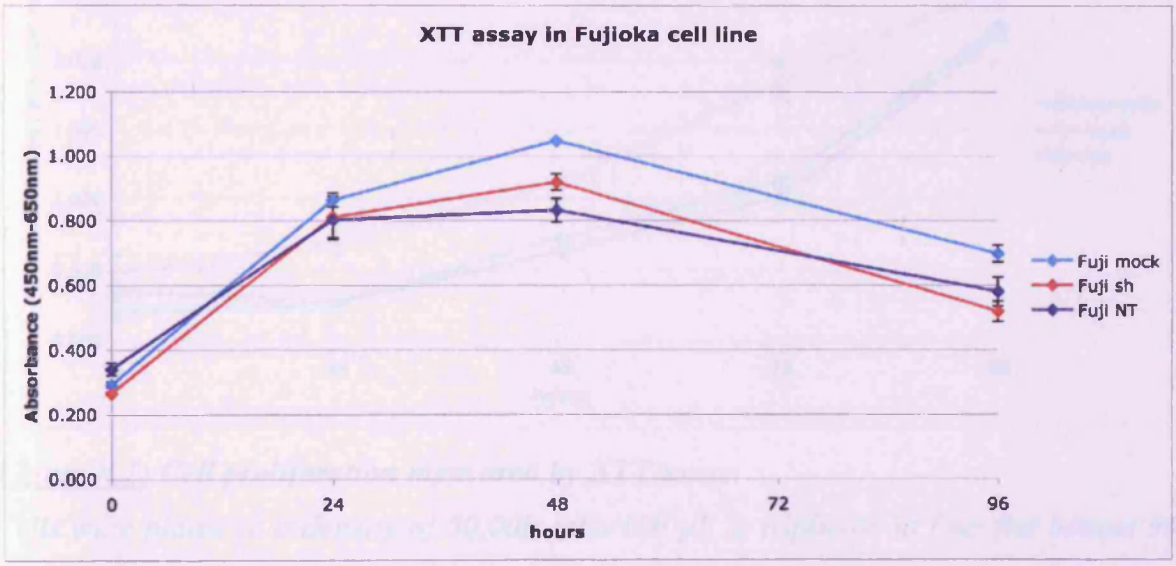

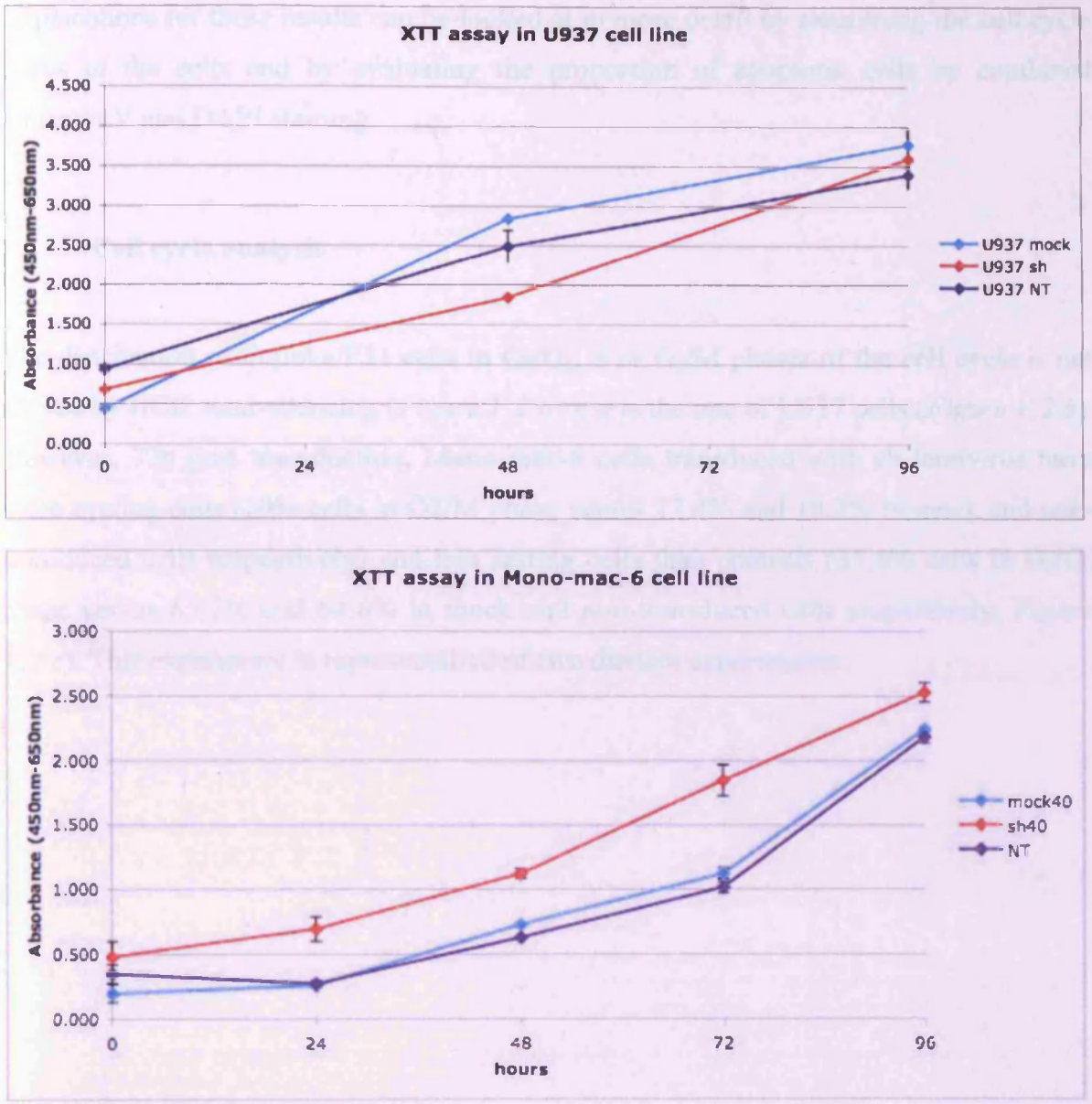


***Figure V.1:* Cell proliferation measured by XTT assay.**

*Cells were plated at a density of 50,000 cells/100 µL in triplicate in four flat bottom 96 well plates and incubated at 37°C, 5% $CO_2$ for 24h, 48h or 96h. Basal proliferation of the cells (time point zero) was determined by adding 50 µL of freshly mixed XTT reagents immediately after cell plating. After XTT reagents addition, plates were incubated 2h at 37°C, 5% $CO_2$ and cell proliferation was represented as absorbance at 450 nm corrected by absorbance at 650 nm over time.*

Explanations for these results can be looked at in more detail by examining the cell cycle status of the cells and by evaluating the proportion of apoptotic cells by combined Annexin V and DAPI staining.

### 1.2 Cell cycle analysis

The distribution of Fujioka/P31 cells in $G_0/G_1$, S or $G_2/M$ phases of the cell cycle is not altered by HCK semi-silencing (*Figure V.2 a*) nor is the one of U937 cells (*Figure V.2 b*). However, 72h post transduction, Mono-mac-6 cells transduced with sh lentivirus have more cycling cells (20% cells in G2/M phase versus 12.4% and 10.2% in mock and non-transduced cells respectively) and less resting cells than controls (57.4% cells in $G_0/G_1$ phase versus 65.7% and 64.6% in mock and non-transduced cells respectively; *Figure V.2 c*). This experiment is representative of two distinct experiments.

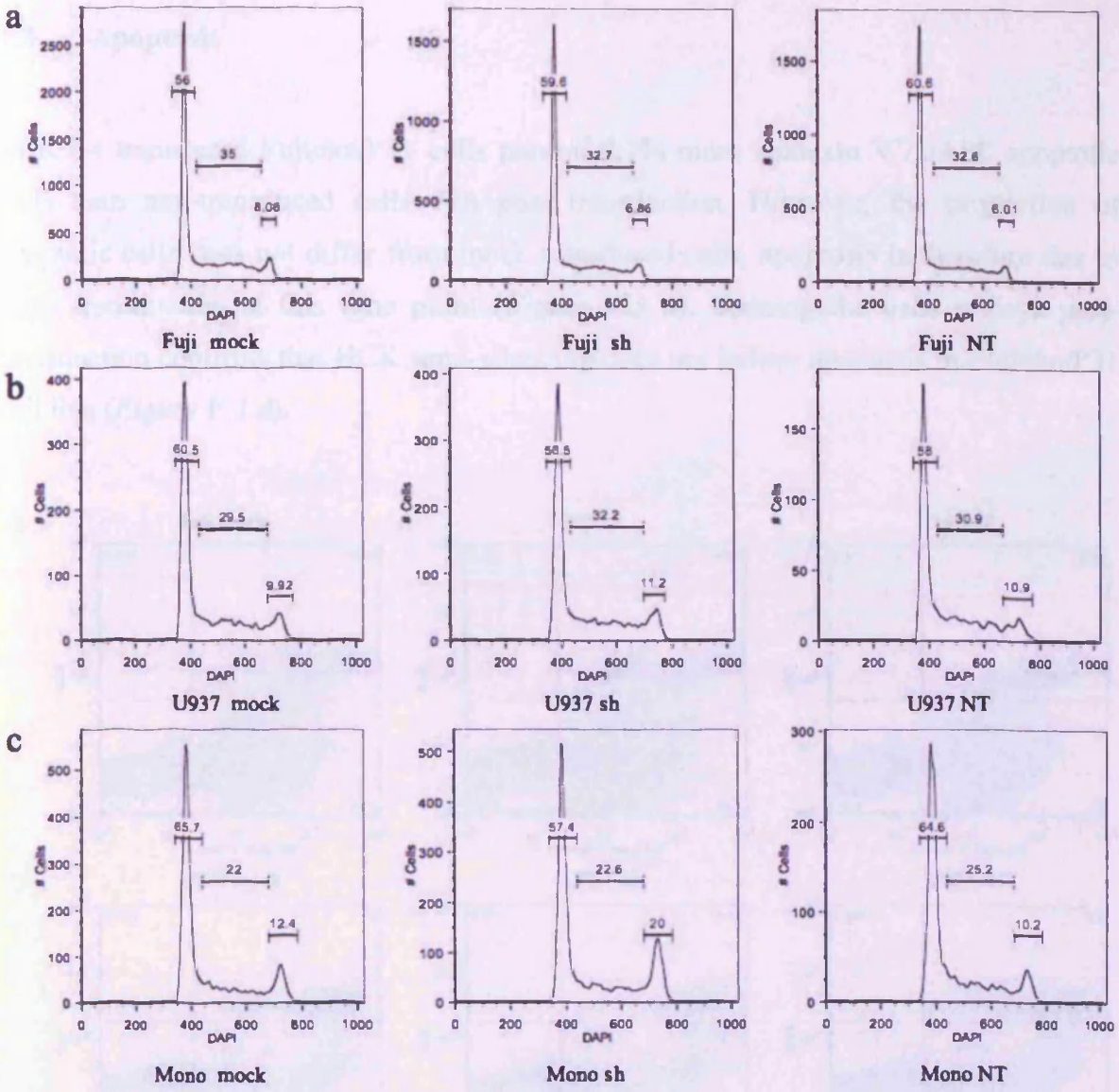


***Figure V.2:*** ***Cell cycle analysis in Fujioka/P31, U937 and Mono-mac-6 cell lines 72h post transduction.***

*Panel (a): Cell cycle analysis of mock transduced, shHCK4 transduced and non-transduced Fujioka/P31 cells. Panel (b): Cell cycle analysis of mock transduced, shHCK4 transduced and non-transduced U937 cells. Panel (c): Cell cycle analysis of mock transduced, shHCK4 transduced and non-transduced Mono-mac-6 cells.*

## 1.3 Apoptosis

shHCK4 transduced Fujioka/P31 cells present 8.7% more Annexin $V^+$/$DAPI^-$ apoptotic cells than non-transduced cells 72h post transduction. However, the proportion of apoptotic cells does not differ from mock transduced cells, apoptosis is therefore due to virus transduction at this time point (*Figure V.3 a*). Staining the cells 6 days post-transduction confirms that HCK semi-silencing does not induce apoptosis in Fujioka/P31 cell line (*Figure V.3 d*).

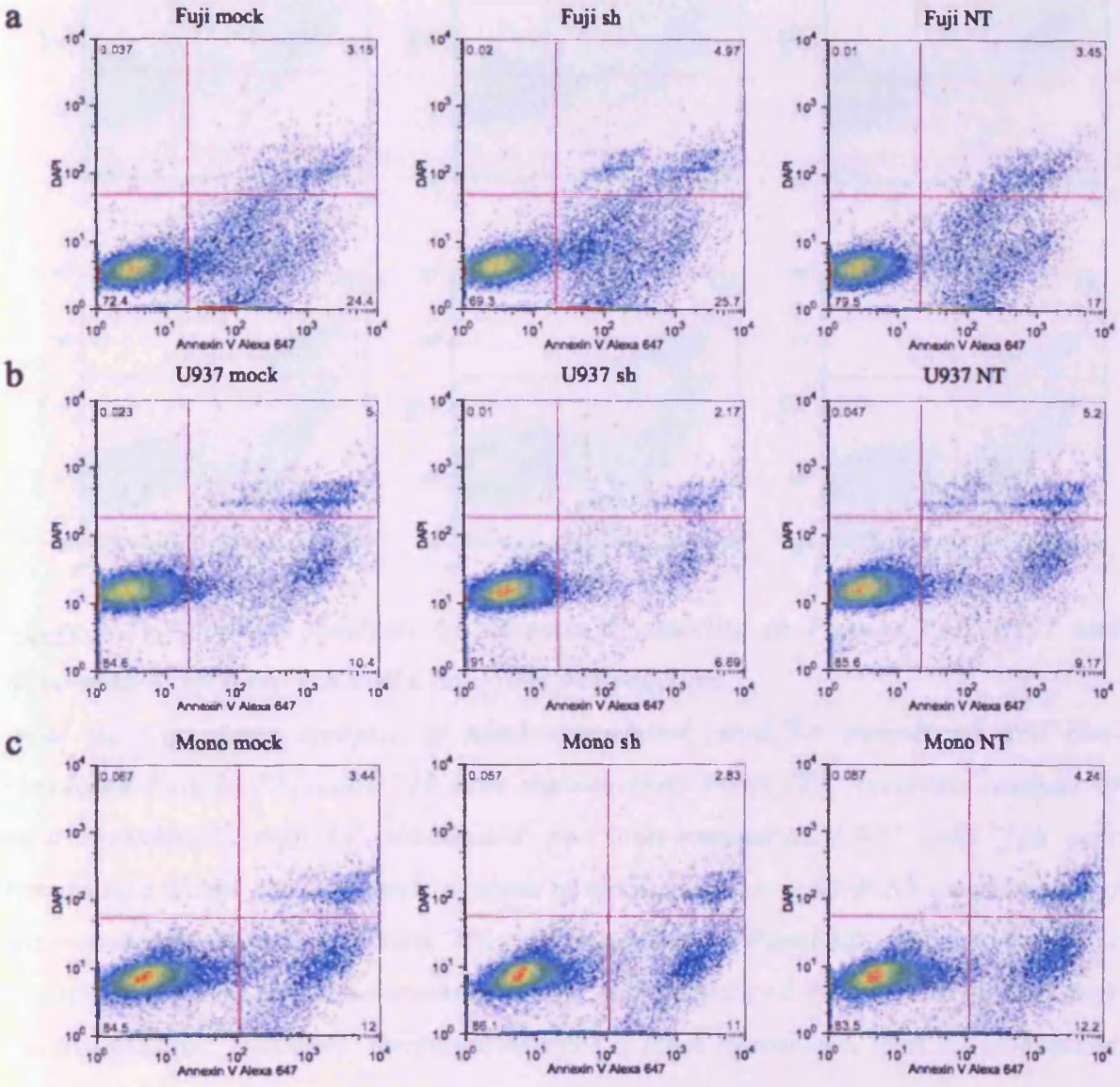

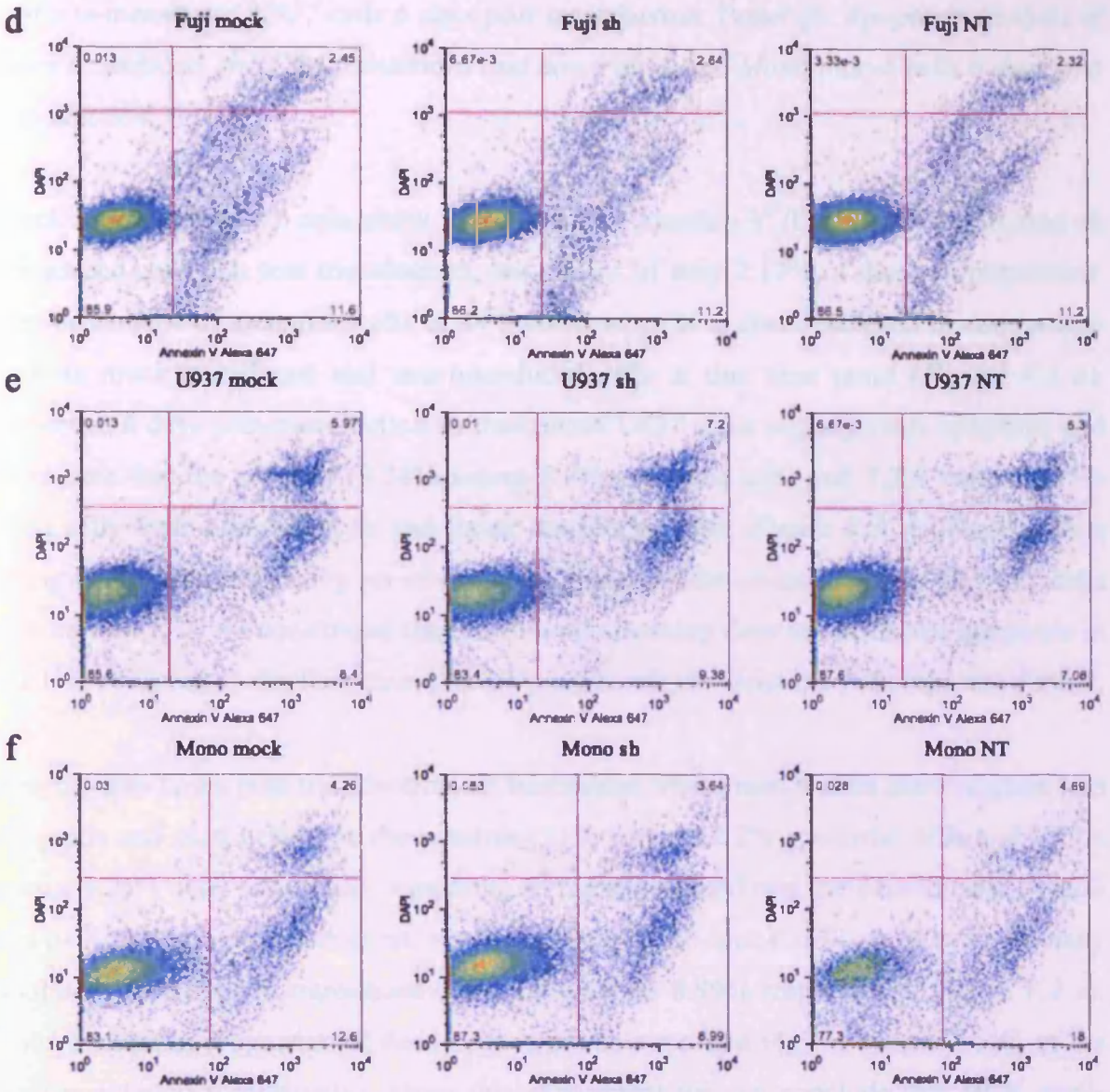


***Figure V.3: Apoptosis analysis by Annexin V staining in Fujioka/P31, U937 and Mono-mac-6 cell lines 72h and 6 days post transduction.***

*Panel (a): Apoptosis analysis of mock transduced, shHCK4 transduced and non-transduced Fujioka/P31 cells 72h post transduction. Panel (b): Apoptosis analysis of mock transduced, shHCK4 transduced and non-transduced U937 cells 72h post transduction. Panel (c): Apoptosis analysis of mock transduced, shHCK4 transduced and non-transduced Mono-mac-6 cells 72h post transduction. Panel (d): Apoptosis analysis of mock transduced, shHCK4 transduced and non-transduced Fujioka/P31 cells 6 days post transduction. Panel (e): Apoptosis analysis of mock transduced, shHCK4 transduced*

*and non-transduced U937 cells 6 days post transduction. Panel (f): Apoptosis analysis of mock transduced, shHCK4 transduced and non-transduced Mono-mac-6 cells 6 days post transduction.*

Mock transduced U937 cells show twice as many Annexin $V^+$/$DAPI^+$ dead cells than sh transduced cells 72h post transduction, but consist of only 2.17% of the total population. The percentage of apoptotic cells in sh transduced cells is also decreased in comparison to both mock transduced and non-transduced cells at this time point (*Figure V.3 b*). However, 6 days post-transduction sh transduced U937 show slightly more apoptotic and dead cells that the controls (9.38% versus 8.4% apoptotic cells and 7.2% versus 5.97% dead cells when comparing sh and mock transduced cells; *Figure V.3 e*). The variation being below 2% and seeing no obvious difference in the overall growth of U937 cells (see section 1.4), we considered that HCK semi-silencing does not influence apoptosis in the U937 cell line in the long term and did not investigate apoptotic pathways any further.

Seventy-two hours post transduction, sh transduced Mono-mac-6 cells show slightly less apoptotic and dead cells than the controls (11% versus 12.2% apoptotic cells and 2.83% versus 4.24% dead cells when comparing sh transduced and non transduced cells; *Figure V.3 c*). Six days post transduction, non-transduced Mono-mac-6 cells show twice as many apoptotic cells than sh transduced cells (18% versus 8.99% respectively; *Figure V.3 e*). The variation in proportion of dead cells is not as important (4.69% versus 3.64% of the total population respectively). From this experiment we can conclude that HCK semi-silencing may have a slight impact on Mono-mac-6 cells apoptosis, but cannot explain the increase in cell number observed associated with HCK silencing, as desribed below.

## 1.4 Growth curve

While growing the cells we followed their doublings generation over time. HCK semi-silencing does not seem to influence Fujioka/P31 or U937 doublings generation. However, sh transduced Mono-mac-6 cells tend to grow faster than mock transduced or non-transduced Mono-mac-6 cells (*Figure V.4*).

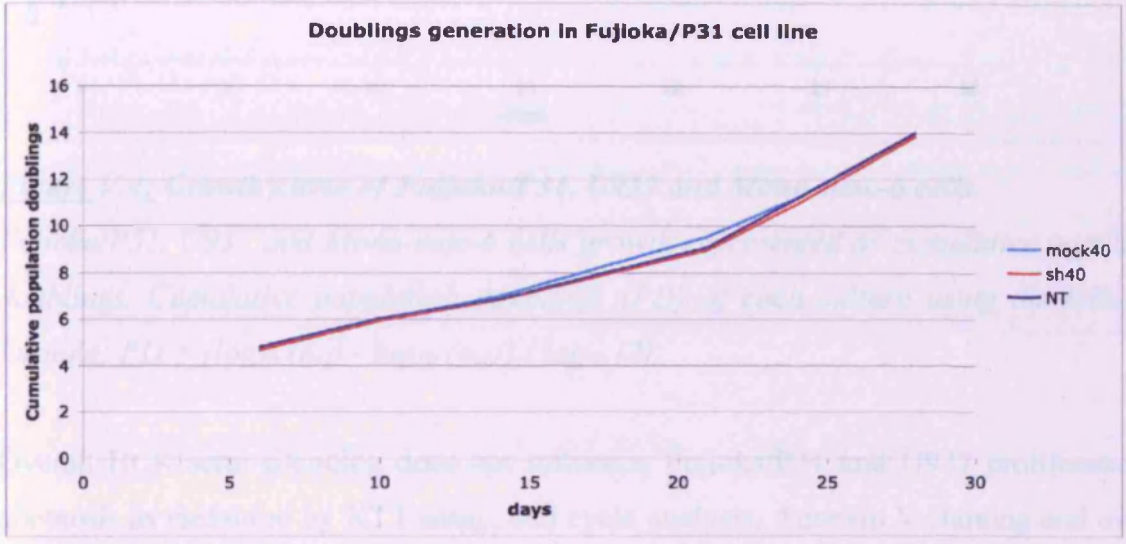


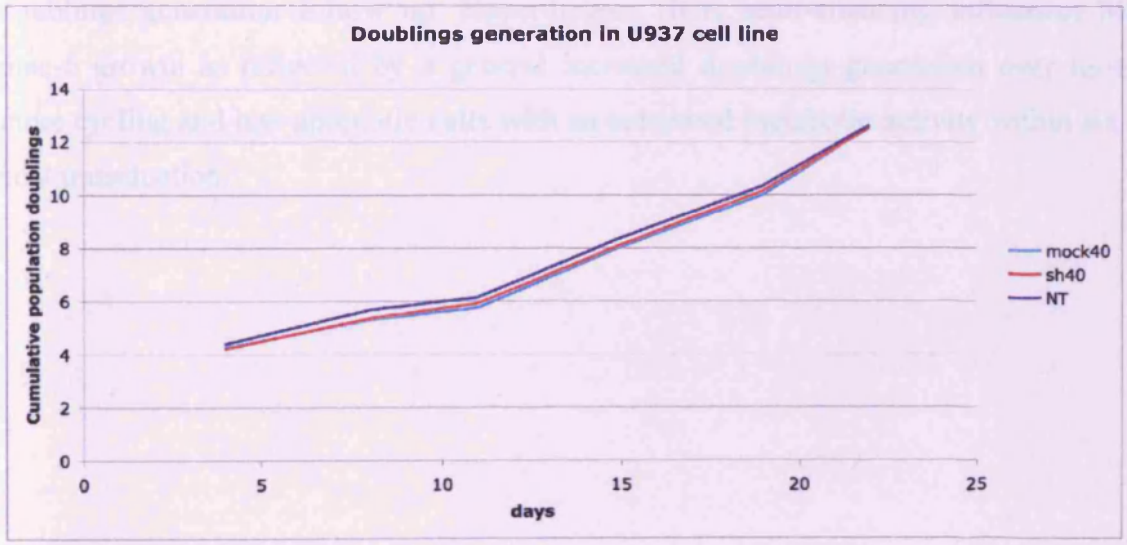

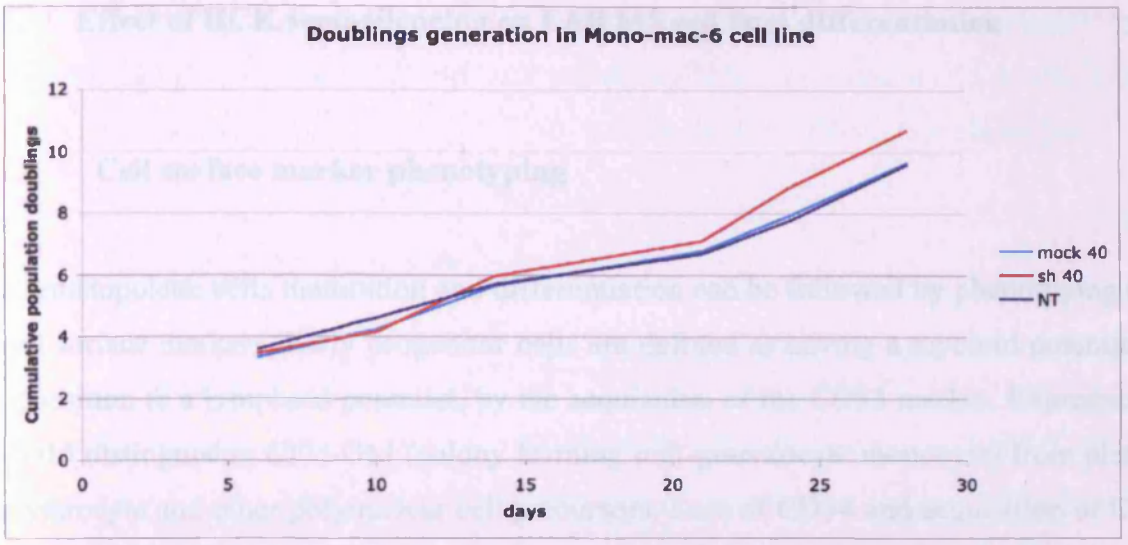


***Figure V.4: Growth curve of Fujioka/P31, U937 and Mono-mac-6 cells.***

*Fujioka/P31, U937 and Mono-mac-6 cells growth represented as cumulative population doublings. Cumulative population doublings (PD) of each culture using the following formula:* $PD = [\log_{10}(n_{t2}) - \log_{10}(n_{t1})] / \log_{10}(2)$.

Overall HCK semi-silencing does not influence Fujioka/P31 and U937 proliferation or apoptosis as measured by XTT assay, cell cycle analysis, Annexin V staining and overall doublings generation follow up. Nevertheless, HCK semi-silencing influences Mono-mac-6 growth as reflected by a general increased doublings generation over time and more cycling and less apoptotic cells with an enhanced metabolic activity within six days post transduction.

## 2. Effect of HCK semi-silencing on FAB M5 cell lines differentiation

### 2.1 Cell surface marker phenotyping

Haematopoietic cells maturation and differentiation can be followed by phenotyping their cell surface markers. Early progenitor cells are defined as having a myeloid potential, in opposition to a lymphoid potential, by the acquisition of the CD33 marker. Expression of CD15 distinguishes CFU-GM (colony forming unit-granulocyte monocyte) from platelet, erythrocyte and other polynuclear cell precursors. Loss of CD34 and acquisition of CD13 defines CFU-G (colony forming unit-granulocyte) that would eventually mature to granulocyte/neutrophils by among others losing CD13, acquiring CD11b and lowering their expression of CD33 (*Figure V.5*). Loss of CD34 and acquisition of CD13, CD14 and CD11b defines monoblasts that would mature to monocytes by losing CD15 (promonocyte stage) and then losing CD13. Monocytes get activated into macrophages upon migration via the blood stream towards damaged tissue.

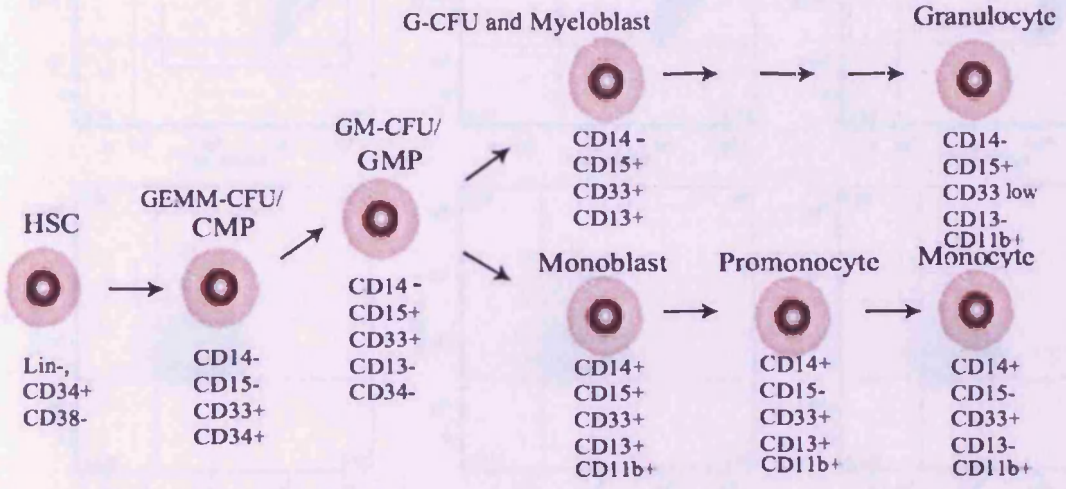


***Figure V.5: Cell surface marker expression along the haematopoietic tree (adapted from KEGG pathways; http://www.genome.jp/kegg/pathway/hsa/hsa04640.html).***

Although the expression of a given set of markers by a leukaemic cell might not be corresponding to the same normal cell physiologically, we intended to assess if HCK silencing would impair Fujioka/P31, U937 or Mono-mac-6 cell surface phenotype.

### 2.1.1 Phenotyping of Fujioka/P31 cell line

Plotting CD33 versus CD15 we can observe that all Fujioka/P31 cells are $CD33^{+}/CD15^{+}$, but with two populations: one is $CD33^{low}/CD15^{high}$, the other is $CD33^{high}/CD15^{low}$ (*Figure V.6 a, top panel*). Both populations express CD13 at a similar level (*Figure V.6 a, bottom panel*). To distinguish if the cells are monocytic or granulocytic, we need to look at CD14 expression.

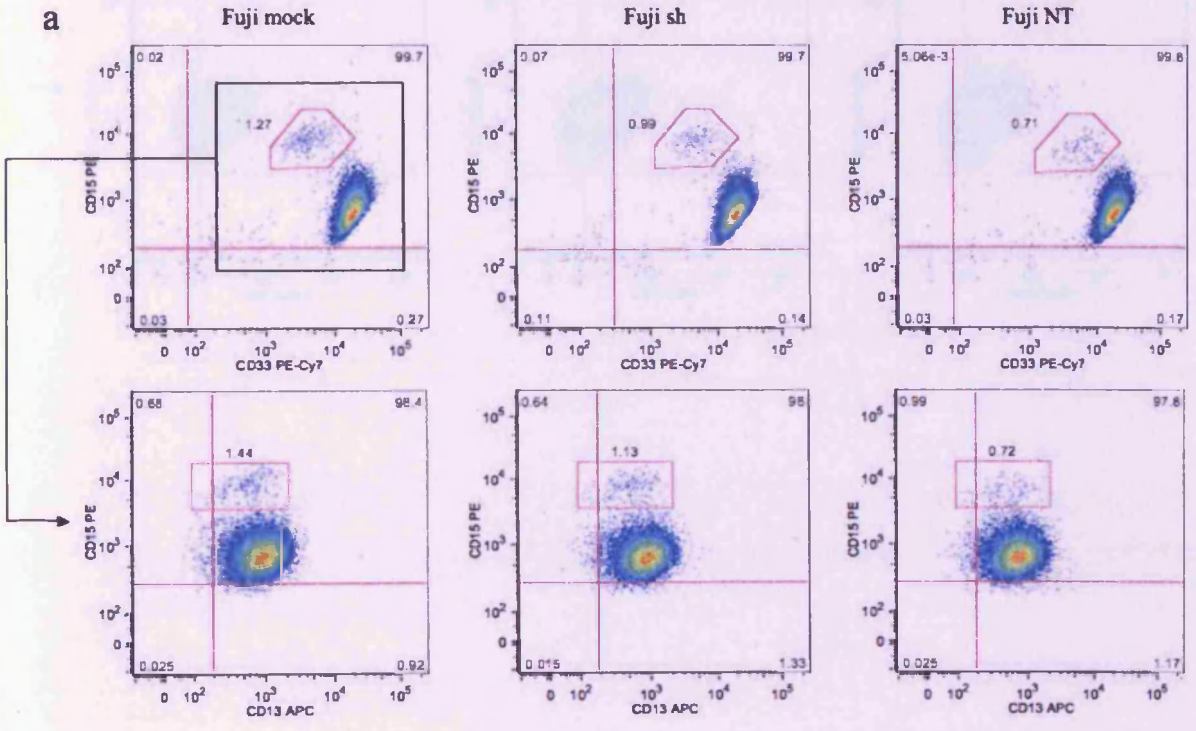

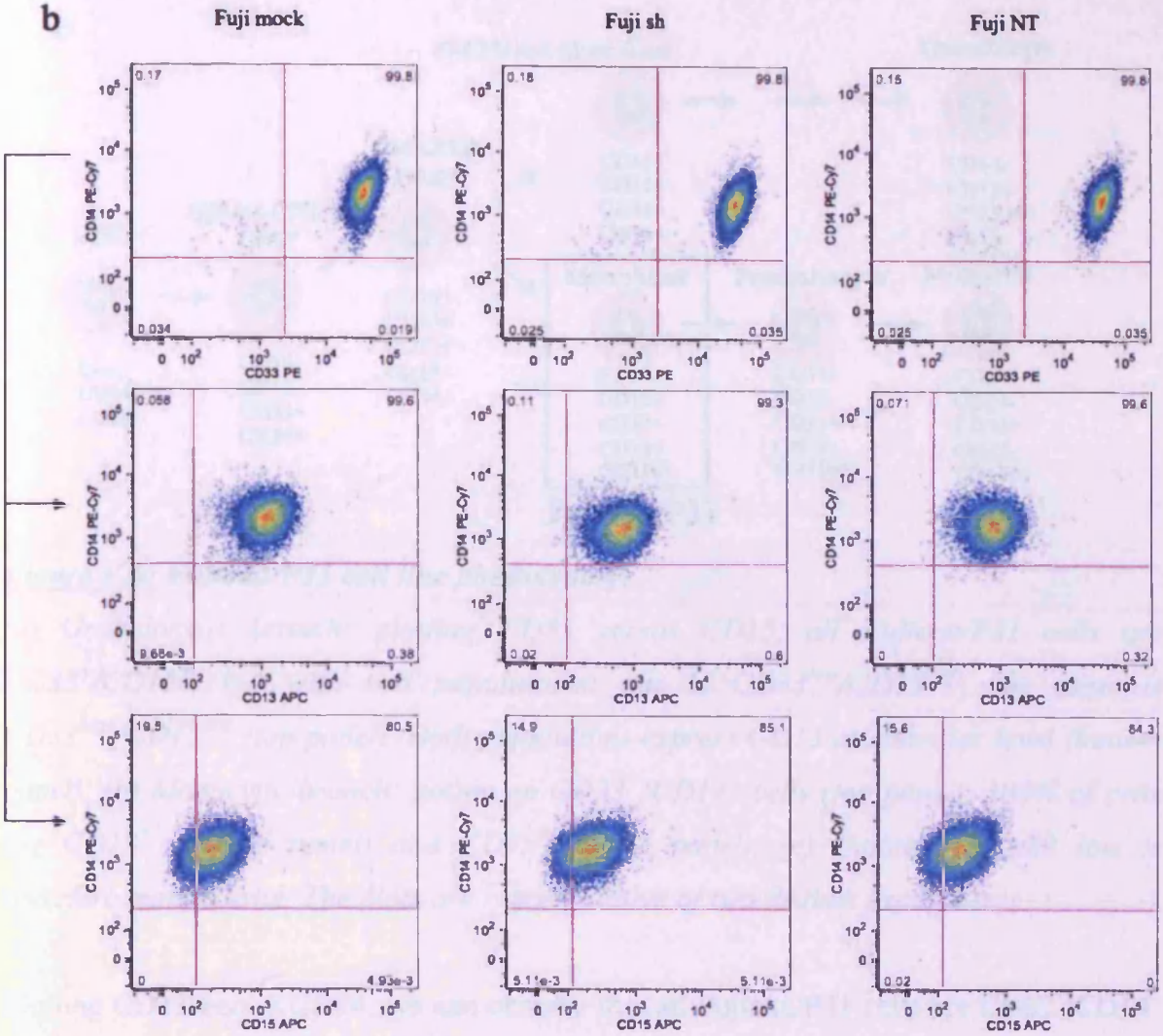
b
Fuji mock
Fuji sh
Fuji NT
CD14 PE-Cy7
CD33 PE
CD13 APC
CD15 APC
0.17
99.8
0.034
0.019
0.18
99.8
0.025
0.035
0.15
99.8
0.025
0.035
0.058
99.6
8.65e-3
0.38
0.11
99.3
0.02
0.6
0.071
99.6
0
0.32
19.5
80.5
0
4.93e-3
14.9
85.1
5.11e-3
5.11e-3
15.6
84.3
0.02
0

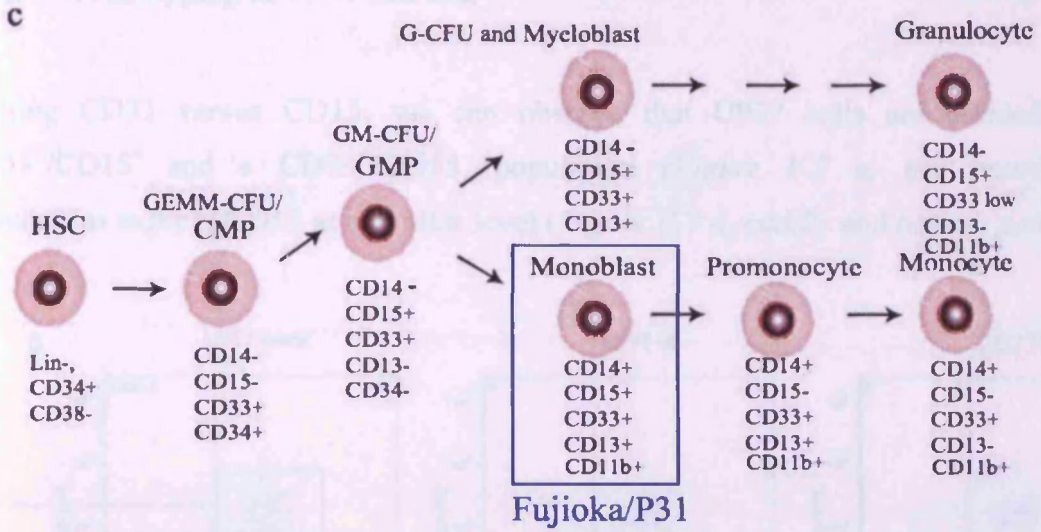


***Figure V.6: Fujioka/P31 cell line phenotyping.***

*(a) Granulocytic branch: plotting CD33 versus CD15, all Fujioka/P31 cells are $CD33^{+}/CD15^{+}$, but with two populations: one is $CD33^{low}/CD15^{high}$, the other is $CD33^{high}/CD15^{low}$ (top panel). Both populations express CD13 at a similar level (bottom panel). (b) Monocytic branch: gating on $CD33^{+}/CD14^{+}$ cells (top panel), 100% of cells are $CD13^{+}$ (middle panel) and $CD15^{+}$ (bottom panel). (c) Fujioka/P31 cell line is therefore monoblastic. The plots are representative of two distinct experiments.*

Plotting CD33 versus CD14, we can observe that all Fujioka/P31 cells are $CD33^{+}/CD14^{+}$ (*Figure V.6 b, top panel*). Gating on this $CD33^{+}/CD14^{+}$ population, we see that all the cells express CD13 (*Figure V.6 b, middle panel*) and CD15 (using the CD15 APC antibody we do not see a clearly distinct $CD15^{low}$ population anymore (*Figure V.6 b, bottom panel*)). Fujioka/P31 cells are $CD33^{+}/CD13^{+/}CD14^{+}/CD15^{+}$; they are therefore monoblastic (*Figure V.6 c)*. HCK semi-silencing does not seem to alter their phenotype when cells are grown in suspension.

### 2.1.2 Phenotyping of U937 cell line

Plotting CD33 versus CD15, we can observe that U937 cells are divided into a $CD33^{+}/CD15^{+}$ and a $CD33^{+}/CD15^{-}$ population (*Figure V.7 a, top panel*). Both populations express CD13 at a similar level (*Figure V.7 a, middle* and *bottom panels*).

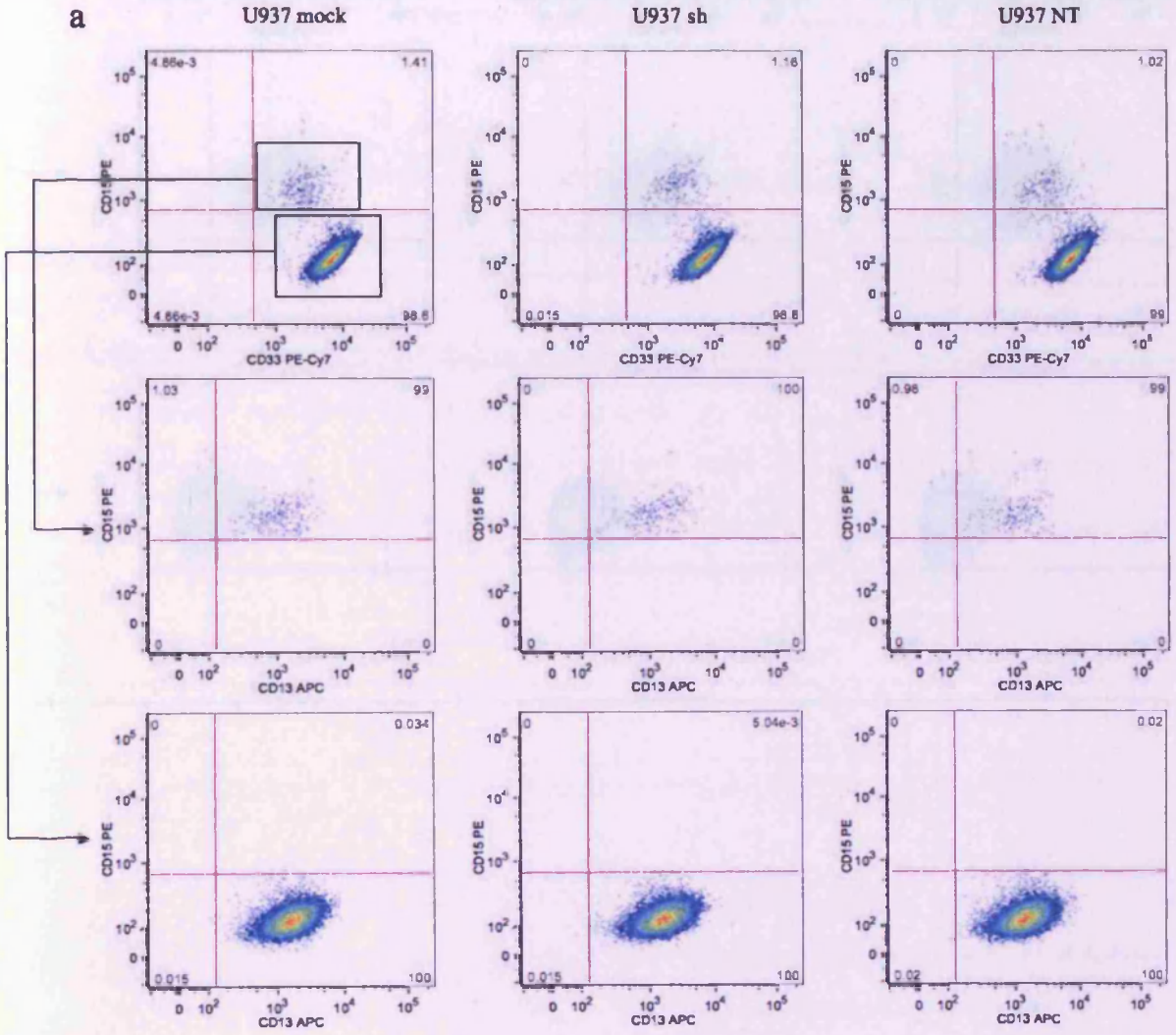

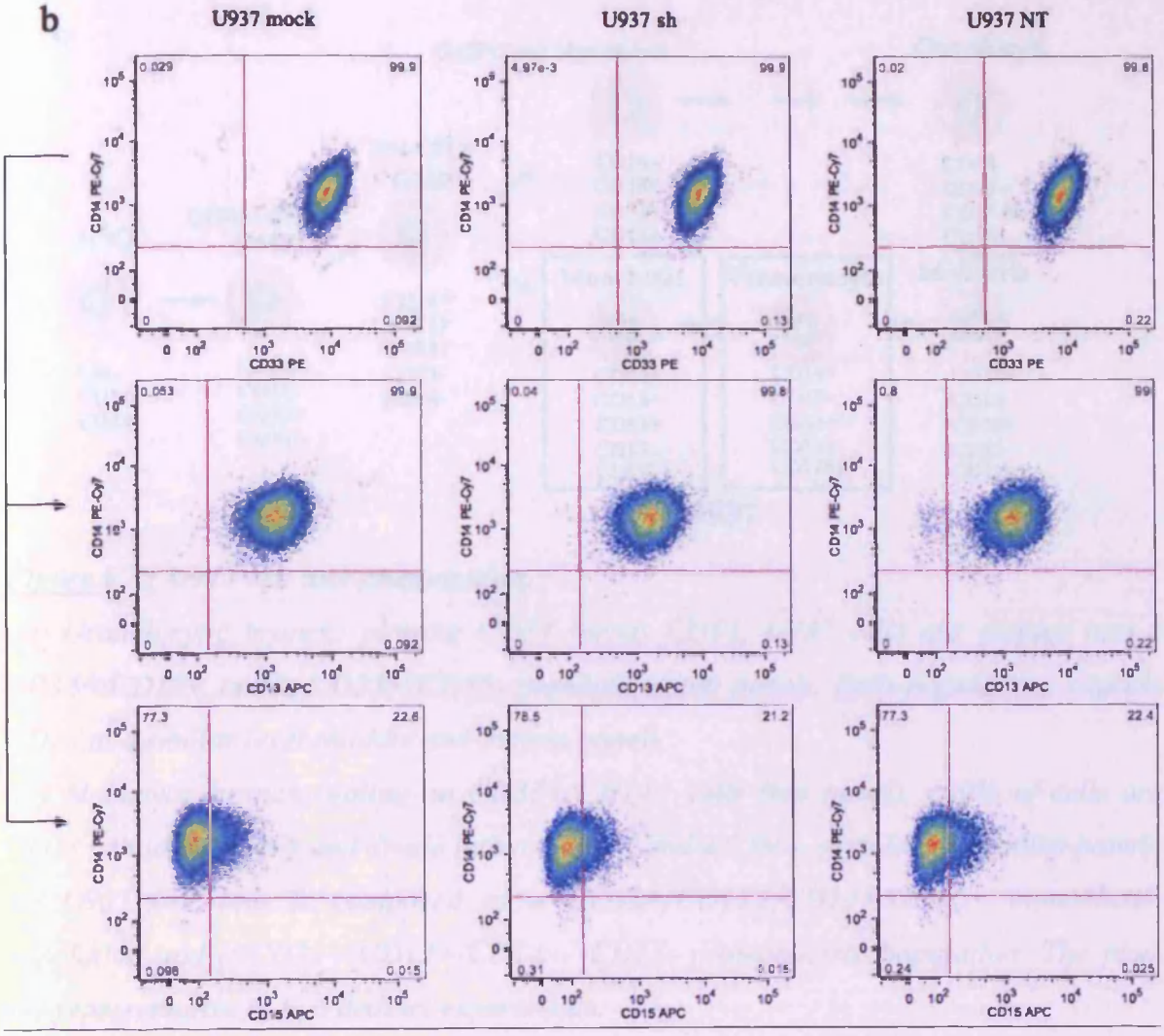
b
U937 mock
U937 sh
U937 NT
CD14 PE-Cy7
CD33 PE
CD13 APC
CD15 APC
0.029
99.9
0.092
4.97e-3
99.9
0.13
0.02
99.8
0.22
0.053
99.9
0.092
0.04
99.8
0.13
0.8
99
0.22
77.3
22.6
0.098
0.015
78.5
21.2
0.31
0.015
77.3
22.4
0.24
0.025

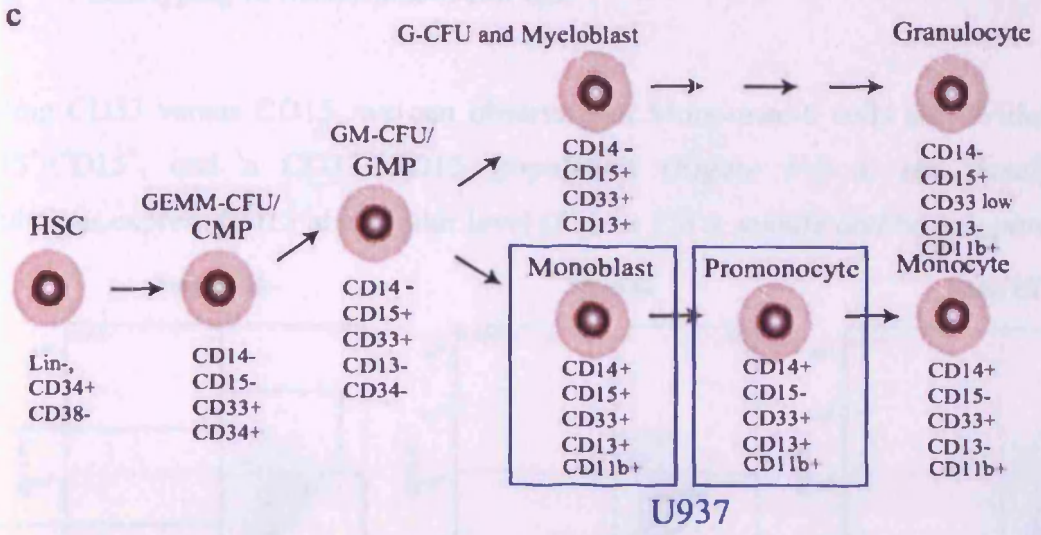


***Figure V.7: U937 cell line phenotyping.***

*(a) Granulocytic branch: plotting CD33 versus CD15, U937 cells are divided into a CD33+/CD15+ and a CD33+/CD15- population (top panel). Both populations express CD13 at a similar level (middle and bottom panel).*

*(b) Monocytic branch: gating on CD33+/CD14+ cells (top panel), 100% of cells are CD13+ (middle panel) and divide into a CD15+ and a CD15- population (bottom panel).*

*(c) U937 cell line is composed of a CD33+/CD13+/CD14+/CD15+ monoblastic population and a CD33+/CD13+/CD14+/ CD15- promonocytic population. The plots are representative of two distinct experiments.*

When plotting CD33 versus CD14, we can observe that all U937 cells are $CD33^+/CD14^+$ (*Figure V.7 b, top panel*). These cells all express CD13 at a similar level (*Figure V.7 b, middle panel*) and can still be separated into a $CD14^+/CD15^-$ population and a $CD14^+/CD15^+$ population (*Figure V.7 b, bottom panel*). U937 cell line is therefore heterogeneous with a $CD33^+/CD13^+/CD14^+/CD15^+$ monoblastic line and a $CD33^+/CD13^+/CD14^+/CD15^-$ promonocytic line (*Figure V.7 c*). HCK semi-silencing does not seem to alter its phenotype when cells are grown in suspension.

### 2.1.3 Phenotyping of Mono-mac-6 cell line

Plotting CD33 versus CD15, we can observe that Mono-mac-6 cells are divided into a $CD33^{+}/CD15^{+}$, and a $CD33^{+}/CD15^{-}$ population (*Figure V.8 a, top panel*). Both populations express CD13 at a similar level (*Figure V.8 a, middle and bottom panels*).

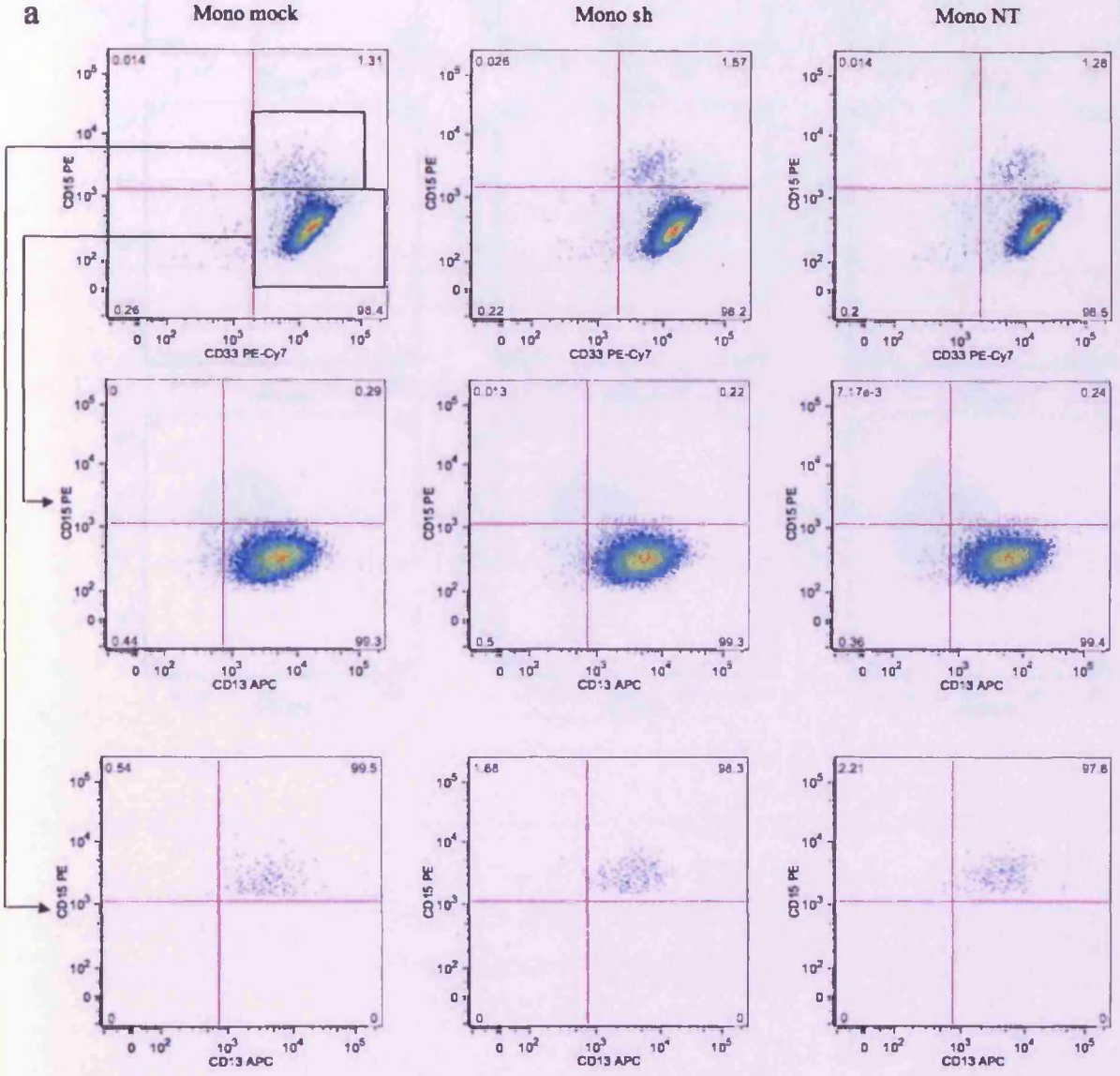

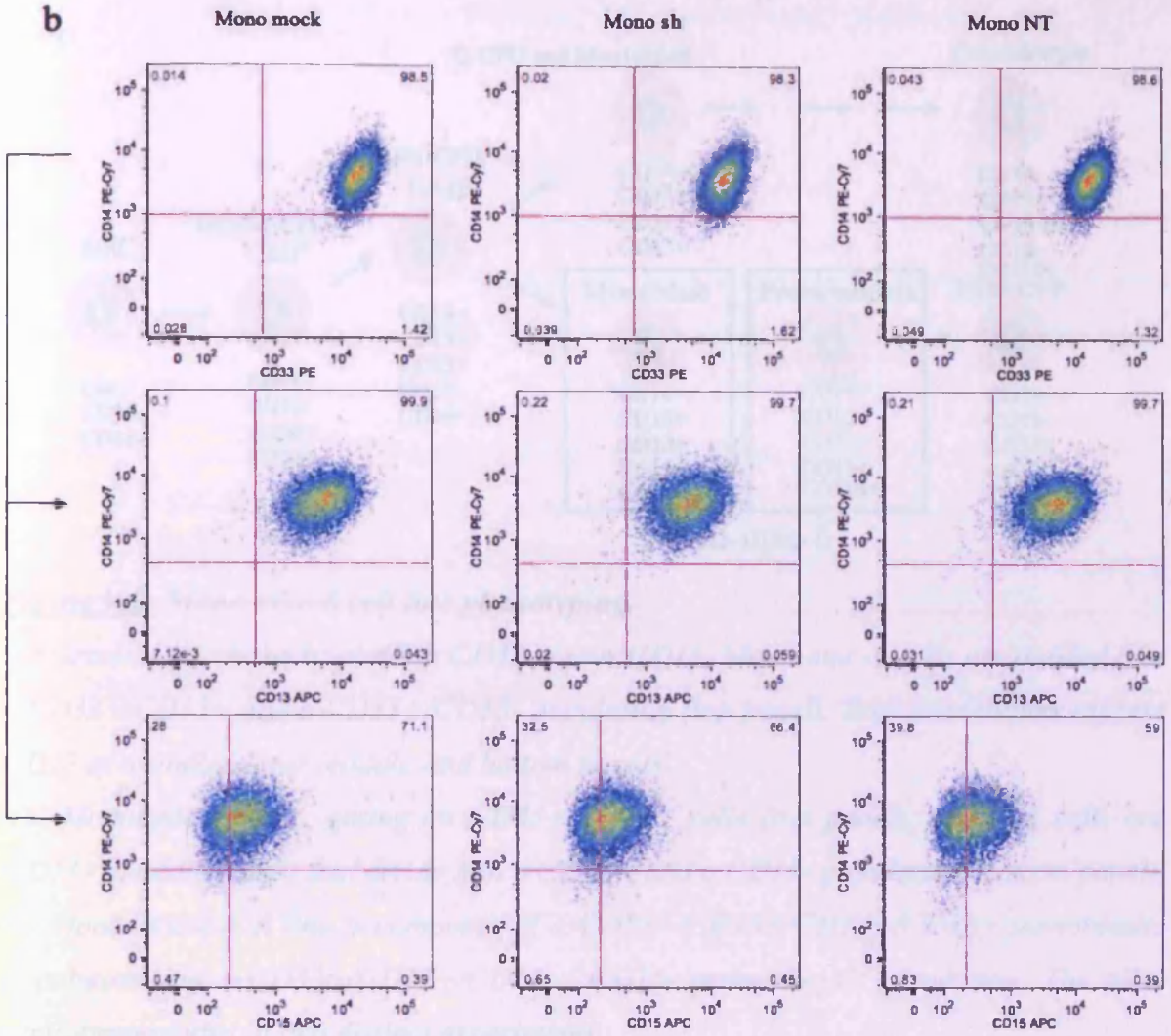
b
Mono mock
Mono sh
Mono NT
CD14 PE-Cy7
CD33 PE
CD13 APC
CD15 APC
0.014
98.5
0.028
1.42
0.02
98.3
0.039
1.62
0.043
98.6
0.049
1.32
0.1
99.9
7.12e-3
0.043
0.22
99.7
0.02
0.059
0.21
99.7
0.031
0.049
28
71.1
0.47
0.39
32.5
66.4
0.65
0.45
39.8
59
0.83
0.39

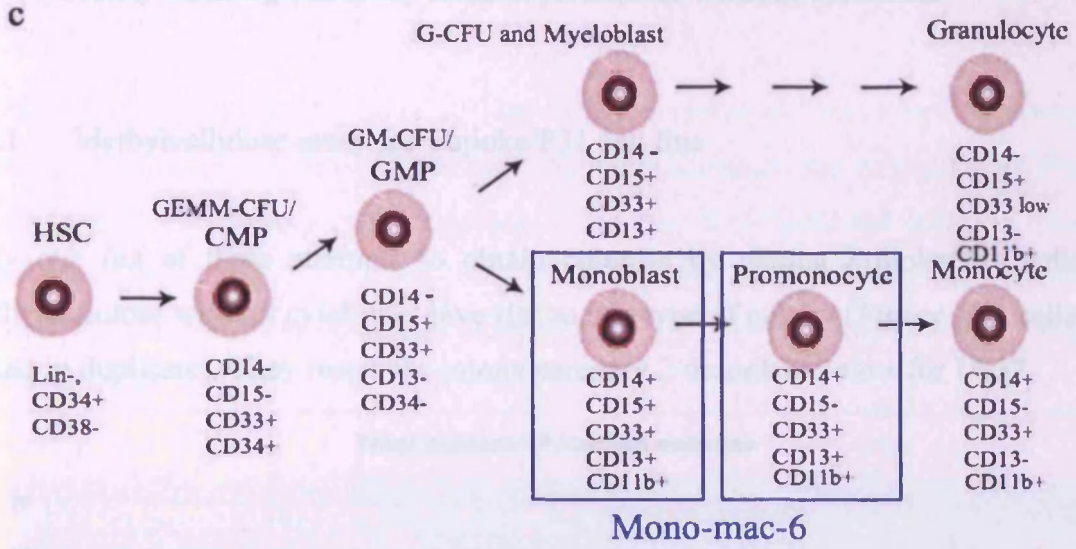


***Figure V.8:* Mono-mac-6 cell line phenotyping.**

*(a) Granulocytic branch: plotting CD33 versus CD15, Mono-mac-6 cells are divided into a CD33+/CD15+ and a CD33+/CD15- population (top panel). Both populations express CD13 at a similar level (middle and bottom panels).*

*(b) Monocytic branch: gating on CD33+/CD14+ cells (top panel), 100% of cells are CD13+ (middle panel) and divide into a CD15+ and a CD15- population (bottom panel).*

*(c) Mono-mac-6 cell line is composed of a CD33+/CD13+/CD14+/CD15+ monoblastic population and a CD33+/CD13+/CD14+/ CD15- promonocytic population. The plots are representative of two distinct experiments.*

When plotting CD33 versus CD14, we can observe that all Mono-mac-6 cells are $CD33^+/CD14^+$ (*Figure V.8 b, top panel*). These cells all express CD13 at a similar level (*Figure V.8 b, middle panel*) and can still be separated into a $CD14^+/CD15^-$ population and a $CD14^+/CD15^+$ population (*Figure V.8 b, bottom panel*). Mono-mac-6 cell line is therefore heterogeneous with a $CD33^+/CD13^+/CD14^+/CD15^+$ monoblastic line and a $CD33^+/CD13^+/ CD14^+/CD15^-$ promonocytic line (*Figure V.8 c*). HCK semi-silencing does not seem to alter Mono-mac-6 phenotype when cells are grown in suspension.

## 2.2 Colony forming cell assay in methylcellulose without cytokines

### 2.2.1 Methylcellulose assay for Fujioka/P31 cell line

Only one out of three attempts to obtain colonies by plating Fujioka/P31 cells into methylcellulose without cytokines gave rise to one type of colony (*Figure V.9*; cells were plated in duplicate). They resemble colony category 2 described below for U937.

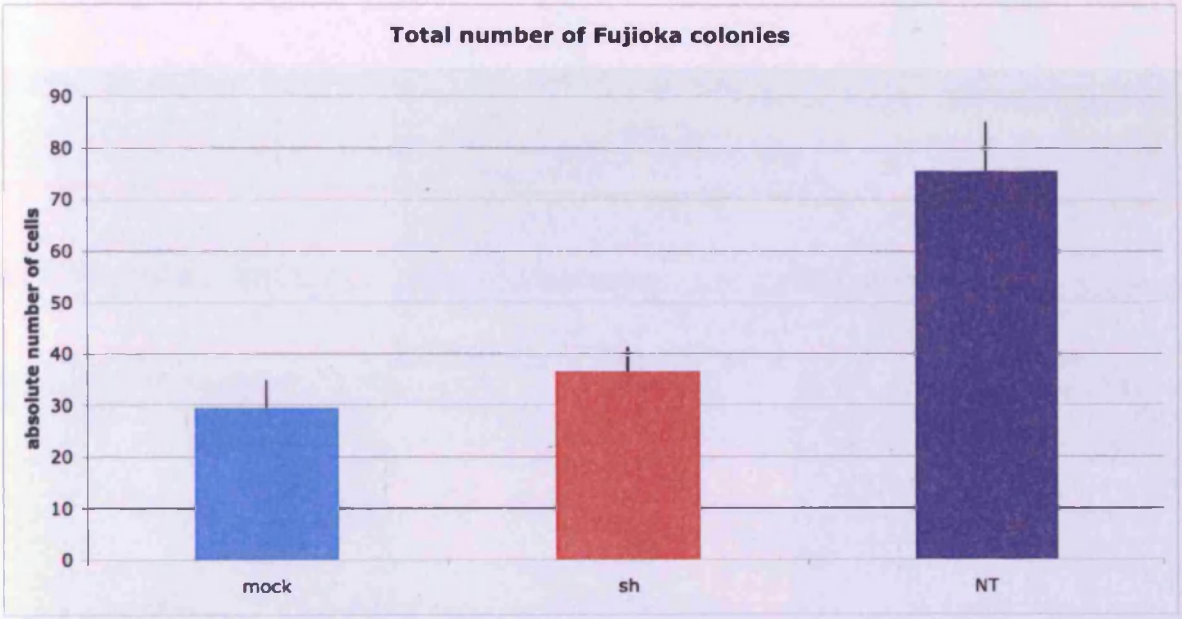


***Figure V.9: Spontaneous colony formation by Fujioka/P31 cells.***

*For each condition, 1,000 cells were plated in duplicate in H4330 MethoCult media (Stem Cell Technologies) and scored after 14 days (n=2).*

No major difference in number of colonies was found between sh and mock transduced Fujioka/P31 cells (*Figure V.9*). Non-transduced cells, however, give rise to nearly twice as many colonies as transduced cells. This result indicates a possible toxicity of the virus impairing colony formation.

### 2.2.2 Methylcellulose assay for U937 cell line

When plating U937 cells in methylcellulose without cytokines, we observed spontaneous formation of colonies with different sizes, all quite compact and resembling CFU-GM. As confirmed previously by phenotyping, U937 is a heterogeneous cell line. Colonies were scored according to their size (category 1 to 3) as exemplified on *Figure V.10*. All colonies are $GFP^+$ when U937 have been transduced with mock virus or with shHCK4 encoding virus.

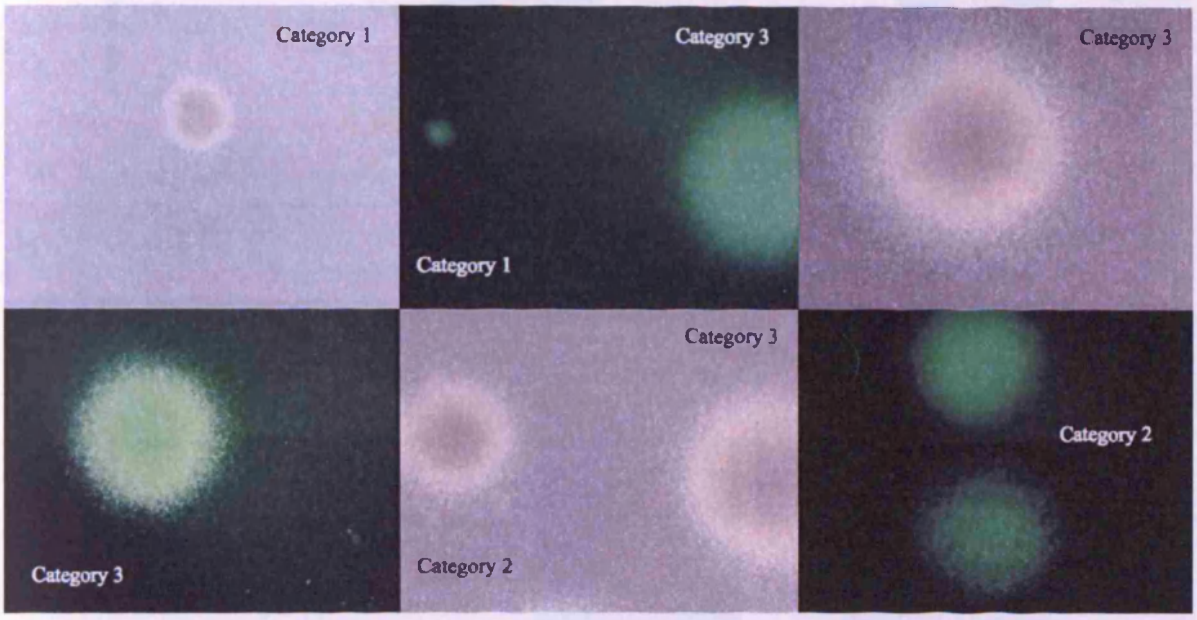


***Figure V.10: Types of colonies spontaneously formed by U937 cells in methylcellulose without cytokines.***

*Category 1 to 3 colonies spontaneously formed by U937 cells when plated in H4330 MethoCult media (Stem Cell Technologies) and scored after 14 days.*

As seen in *Figure V.11*, the U937 cell line forms, in general, more category 2 colonies than category 3 or category 1. U937 transduction with shHCK4 encoding virus does not seem to affect the number of colonies generated in each category. Since transduction with either mock or sh virus does not alter the total number of colonies produced, this trend is visible both when counting the absolute number of colonies arising (*Figure V.11 a*) or when assessing the percentage of colonies from the total colonies falling into the different

categories (*Figure V.11 b*). HCK semi-silencing does therefore not affect U937 differentiation when cells are grown in methylcellulose.

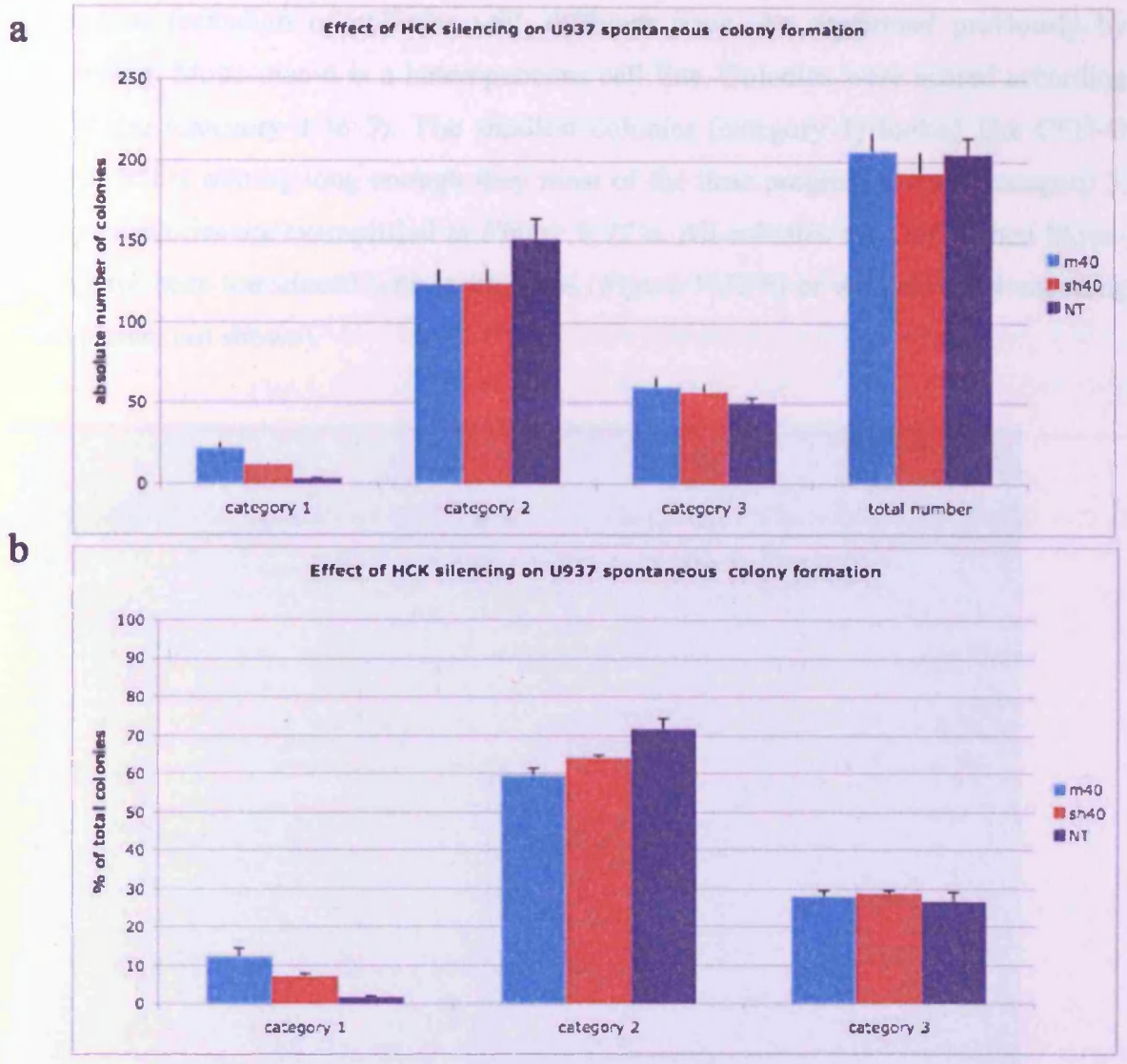


***Figure V.11: HCK silencing does not affect the size of the colonies formed by U937 cells.***

*For each condition, 1,000 cells were plated in duplicate or triplicate in H4330 MethoCult media (Stem Cell Technologies) and scored after 14 days (n=5).*

### 2.2.3 Methylcellulose assay for Mono-mac-6 cell line

When plating Mono-mac-6 in methylcellulose without cytokines, we observed spontaneous formation of colonies with different sizes. As confirmed previously by phenotyping, Mono-mac-6 is a heterogeneous cell line. Colonies were scored according to their size (category 1 to 3). The smallest colonies (category 1) looked like CFU-G colonies, but if waiting long enough they most of the time progress towards category 3. Colony categories are exemplified in *Figure V.12 a.* All colonies are $GFP^+$ when Mono-mac-6 have been transduced with mock virus (*Figure V.12 b*) or with shHCK4 encoding virus (picture not shown).

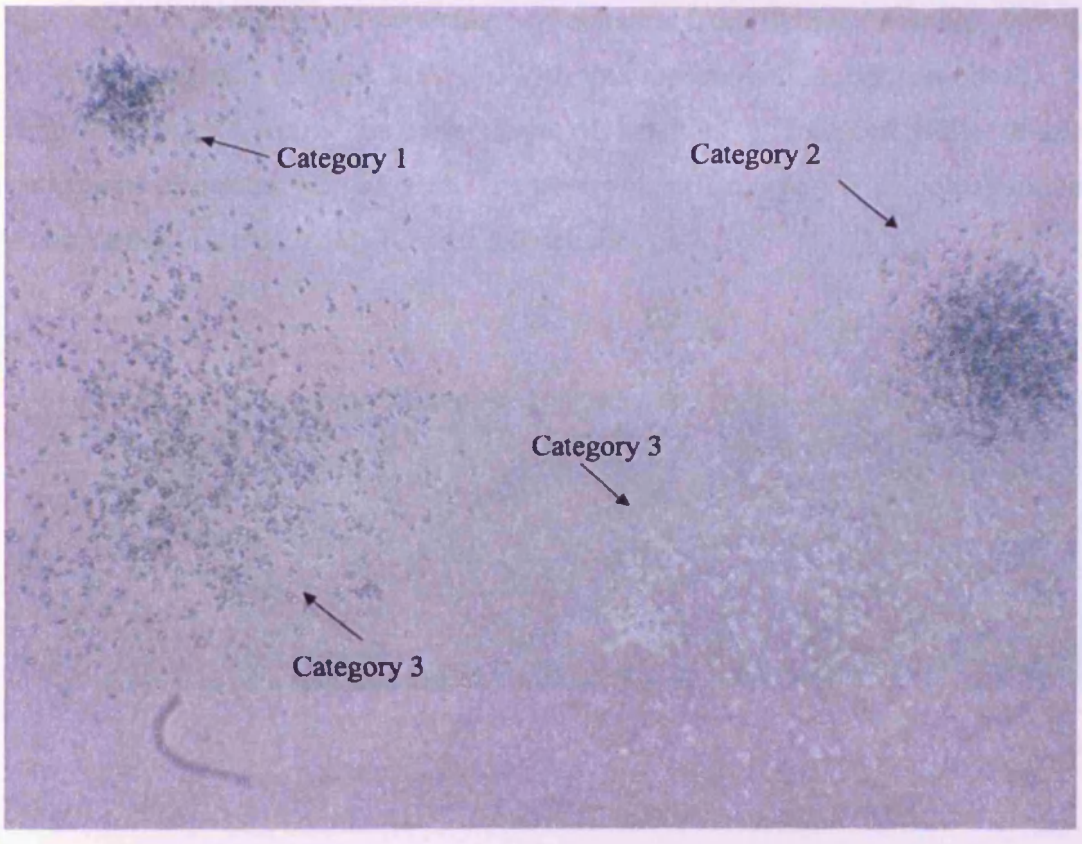


***Figure V.12: Types of colonies spontaneously formed by Mono-mac-6 cells in methylcellulose without cytokines.***

*Category 1 to 3 colonies spontaneously formed by Mono-mac-6 cells when plated in H4330 MethoCult media (Stem Cell Technologies) and scored after 14 days. All colonies were $GFP^+$.*

As seen in *Figure V.13 d*, Mono-mac-6 cell line give rise in general to more category 2 colonies than category 3 or category 1. However, Mono-mac-6 cells transduction with shHCK4 encoding virus significantly affects the number of total colonies generated in each category. As shown in *Figure V.13 b*, Mono-mac-6 cells transduced with shHCK4 virus produce smaller and more compact colonies than mock transduced or non-transduced controls (*Figure V.13 a* and *c* respectively). This is reflected in *Figure V.13 d* where we can see that HCK semi-silencing results in formation of more category 2 colonies than the controls and this effect is even more pronounced in category 1 colony formation. Category 3 colony formation does not seem affected by HCK silencing. Since transduction with sh virus also increases the total number of colonies arising, we needed to also assess the impact of HCK silencing on the production of these different type of colonies by calculating the percentage of colonies from the total colonies falling into the different categories (*Figure V.12 e*). With this representation, we can observe that HCK semi-silencing increases the percentage of category 1 colonies while decreasing the percentage of category 3 colonies. The percentage of category 2 colonies produced is not significantly affected by HCK semi-silencing.

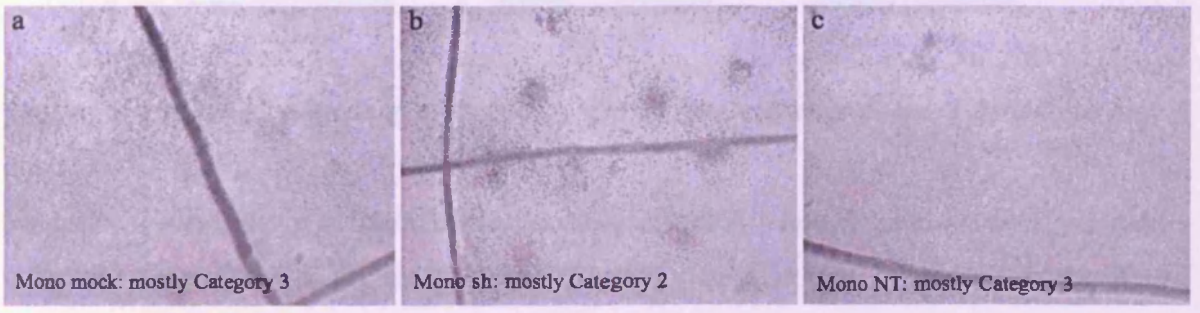

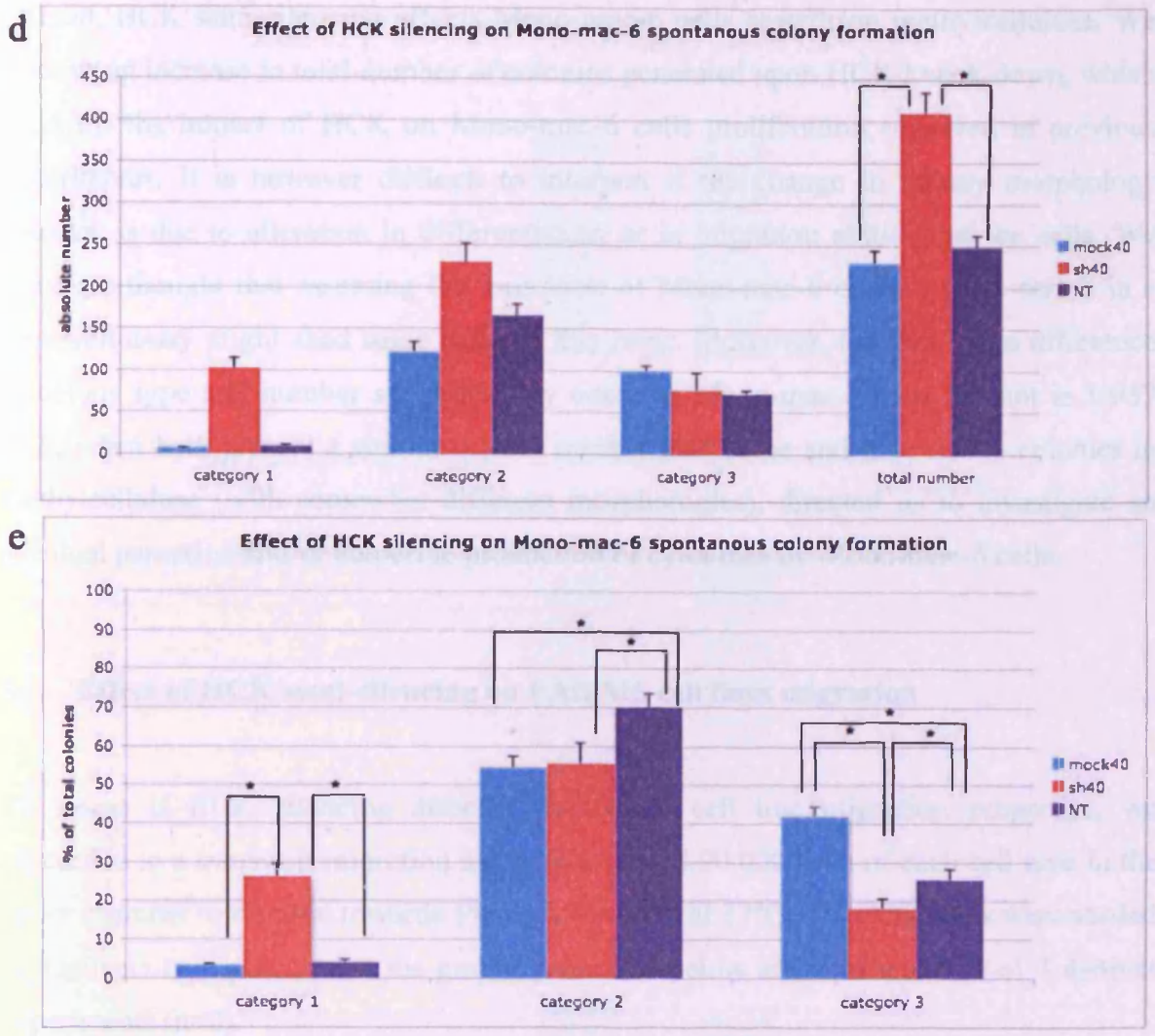


***Figure V.13: HCK silencing affects the size of the colonies formed by Mono-mac-6 cells.***

*(a) Overall view of the colonies spontaneously formed by mock transduced Mono-mac-6 cells. (b) Overall view of the colonies spontaneously formed by shHCK4 transduced Mono-mac-6 cells. (c) Overall view of the colonies spontaneously formed by non-transduced Mono-mac-6 cells. For each condition, 1,000 cells were plated in triplicates in H4330 MethoCult media (Stem Cell Technologies) and scored after 14 days (n=6). (d) Categories scoring of the colonies spontaneously formed by Mono-mac-6 cells represented as absolute number of colonies per plate. (e) Category scoring of the colonies spontaneously formed by Mono-mac-6 cells represented as percentage of total colonies per plate. Stars highlight statistically significant differences (p value <0.001).*

Overall, HCK semi-silencing affects Mono-mac-6 cells growth on methylcellulose. We observe an increase in total number of colonies generated upon HCK knock-down, which confirms the impact of HCK on Mono-mac-6 cells proliferation observed in previous experiments. It is however difficult to interpret if the change in colony morphology detected is due to alteration in differentiation or in migration abilities of the cells. We therefore thought that assessing the migration of Mono-mac-6 cells towards serum in a transwell assay might shed some light on this issue. Moreover, the fact that a difference in colony type and number spontaneously occur in Mono-mac-6 cells but not in U937 cells, when both present a similar surface marker phenotype and give rise to colonies in methylcellulose (with somewhat different morphologies), directed us to investigate an eventual paracrine and/or autocrine production of cytokines by Mono-mac-6 cells.

### 3. Effect of HCK semi-silencing on FAB M5 cell lines migration

To assess if HCK silencing affected monocytic cell line migration properties, we proceeded to a transwell migration assay. We seeded 90,000 cells of each cell type in the upper chamber to migrate towards 5% FCS for 4h30 at 37°C, 5% $CO_2$. Cells were seeded in duplicate or triplicate and the graphs presented below are representative of 3 distinct experiments (n=8).

We observed that in the absence of serum in the bottom chamber, Fujioka/P31 and U937 cells do not migrate (*Figure V.14 a* and *b* respectively) while Mono-mac-6 cells migrate transiently (*Figure V.14 c*). This transient migration is decreased by HCK silencing in a significant manner ($p < 0.01$). In the presence of serum, Fujioka/P31 cells migrate 1.5 fold more than non-transduced Mono-mac-6 cells and this cell migration is not affected by HCK silencing. Similarly, HCK silencing does not alter U937 cell migration. When looking at Mono-mac-6 migration, sh transduced cells migrate 1.43 fold less than mock transduced cells. Thus, HCK silencing significantly reduces Mono-mac-6 cells migration towards FCS.

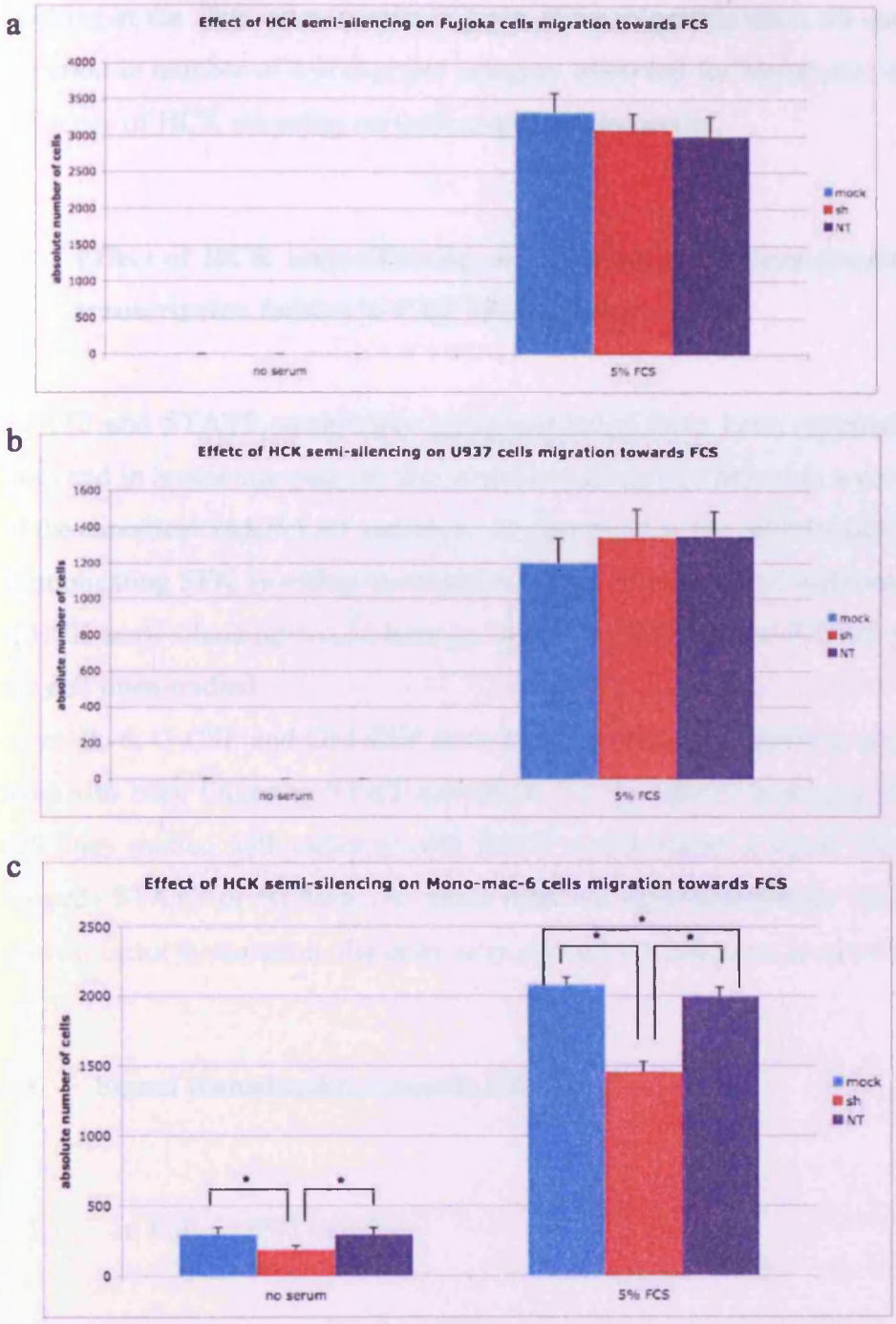


***Figure V.14:* Migration assay.**

*(a): Migration of mock transduced, shHCK4 transduced and non-transduced Fujioka/P31 cells towards 5% FCS after 4h30 incubation. (b): Migration of mock transduced, shHCK4 transduced and non-transduced U937 cells towards 5% FCS after 4h30 incubation. (c): Migration of mock transduced, shHCK4 transduced and non-transduced Mono-mac-6 cells towards 5% FCS after 4h30 incubation.*

Looking at the CFC assay results in light of the migration data, we can conclude that the variation in number of colonies per category observed for Mono-mac-6 cells is due to the influence of HCK silencing on their migration properties.

## 4. Effect of HCK semi-silencing on cytokine signal transduction towards STAT transcription factors in FAB M5 cell lines

STAT3 and STAT5 constitutive phosphorylation have been reported in leukaemic cell lines and in leukaemic patients that could not always be linked to a constitutive activation of the canonical JAK/STAT pathway. As described in the introduction, growing evidence is implicating SFK as acting upstream of STAT. We therefore were interested in knowing if HCK semi-silencing would have an impact on STAT3 and STAT5 phosphorylation on the cell lines studied.

Since IL-6, G-CSF and GM-CSF have been reported as signalling upstream of HCK and have also been linked to STAT activation, we thought of assessing if stimulation of the cell lines studied with either growth factor would trigger a signal transduction via HCK towards STAT3 or STAT5. To make sure we were specifically studying the effect of growth factor stimulation, the cells were starved for 24h prior to stimulation.

### 4.1 Signal transduction towards STAT3

#### 4.1.1 In Fujioka/P31 cell line

We first wanted to follow the effect of serum starvation on STAT3 phosphorylation status in the Fujioka/P31 cell line as a means to validate pSTAT3 staining and establish the level of background signal. The cells were therefore incubated for 1h, 4h or 24h in serum-free medium and stained with anti phospho-STAT3 antibody (Y705) (*Figure V.15, top panel*). Since the corresponding IgG2a isotype control gave a background signal higher than the phospho-STAT3 signal itself, we used unstained cells for normalisation

of the signal (solid grey histogram). FACS plots presented below are representative of two distinct experiments.

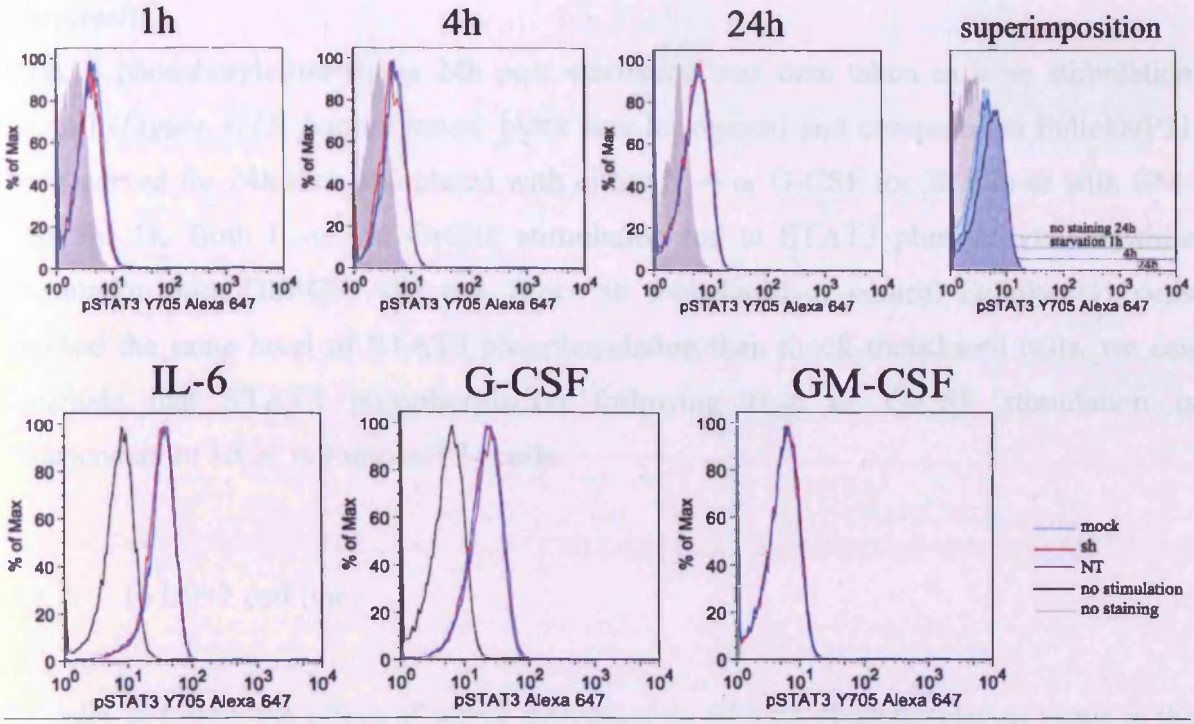


***Figure V.15: STAT3 phosphorylation in Fujioka/P31 cells.***

*Top panel: Effect of serum starvation on STAT3 phosphorylation. Cells were incubated for 1h, 4h or 24h in serum-free medium and stained with anti-phospho-STAT3 antibody (Y705). Since the corresponding IgG2a isotype control gave a background signal higher than the phospho-STAT3 signal itself, unstained cells were used for normalisation of the signal (solid grey histogram). Superimposition of the 1h, 4h and 24h starvation plots of a given sample (sh transduced cells) allows for a better visualisation of the control and sample histograms used to calculate MFI ratios for signal quantification and its variation over time. Indeed, with 24h starvation data being acquired on a different day, isotype histograms do not always superimpose with the 1h and 4h corresponding histograms and need to be used for correction. Bottom panel: Effect of cytokine stimulation on STAT3 phosphorylation. Cells were starved for 24h then stimulated with either IL-6 or G-CSF for 30 min or with GM-CSF for 1h or left unstimulated, as control.*

When comparing the normalised pSTAT3 MFI of the mock transduced sample 1h post starvation to the normalised pSTAT3 MFI of the other samples at different time points, no difference in signal intensity was seen over 24h of serum free incubation (*Figure V.15, top panel*).

STAT3 phosphorylation status 24h post starvation was then taken as a no stimulation control (*Figure V.15, bottom panel,* black line histogram) and compared to Fujioka/P31 cells starved for 24h then stimulated with either IL-6 or G-CSF for 30 min or with GM-CSF for 1h. Both IL-6 and G-CSF stimulation led to STAT3 phosphorylation while stimulation with GM-CSF did not. Since sh transduced or control Fujioka/P31 cells showed the same level of STAT3 phosphorylation than mock transduced cells, we can conclude that STAT3 phosphorylation following IL-6 or G-CSF stimulation is independent of HCK in Fujioka/P31 cells.

### 4.1.2 In U937 cell line

In order to follow the effect of serum starvation on STAT3 phosphorylation status in the U937 cell line, the cells were incubated for 1h, 4h or 24h in serum-free medium and stained with anti-phospho-STAT3 antibody (Y705) (*Figure V.16, top panel*). FACS plots presented below are representative of two distinct experiments.

Quantification of the signal intensity comparing normalised MFI pSTAT3 at 1h and at 24h of starvation showed a 45% increase in STAT3 phosphorylation 24h post starvation that is more visible upon the superimposition of the 1h, 4h and 24h starvation plots. This observation could correlate with data published by (Spiekermann *et al.*, 2001), reporting that STAT3 is constitutively active in U937 cells.

STAT3 phosphorylation status 24h post starvation was then taken as a no stimulation control (*Figure V.16, bottom panel,* black line histogram) and compared to U937 cells starved for 24h then stimulated with either IL-6 or G-CSF for 30 min or with GM-CSF for 1h. Both IL-6 and G-CSF stimulation led to STAT3 phosphorylation, independent of HCK level of expression. Here, again, GM-CSF did not signal towards STAT3.

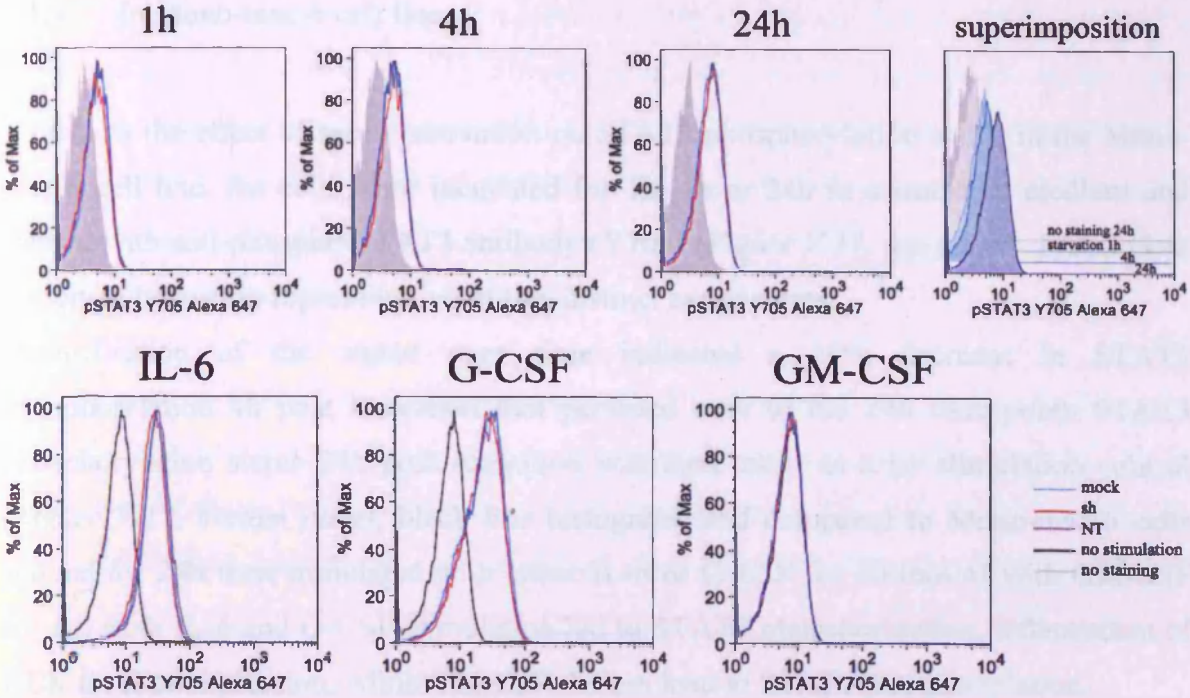


***Figure V.16: STAT3 phosphorylation in U937 cells.***

*Top panel: Effect of serum starvation on STAT3 phosphorylation. Cells were incubated for 1h, 4h or 24h in serum-free medium and stained with anti-phospho-STAT3 antibody (Y705). Since the corresponding IgG2a isotype control gave a background signal higher than the phospho-STAT3 signal itself, unstained cells were used for normalisation of the signal (solid grey histogram). Superimposition of the 1h, 4h and 24h starvation plots of a given sample (sh transduced cells) allows for a better visualisation of the control and sample histograms used to calculate MFI ratios for signal quantification and its variation over time. Indeed, with 24h starvation data being acquired on a different day, isotype histograms do not always superimpose with the 1h and 4h corresponding histograms and need to be used for correction. Bottom panel: Effect of cytokine stimulation on STAT3 phosphorylation. Cells were starved for 24h then stimulated with either IL-6 or G-CSF for 30 min or with GM-CSF for 1h or left unstimulated, as control.*

### 4.1.3 In Mono-mac-6 cell line

To follow the effect of serum starvation on STAT3 phosphorylation status in the Mono-mac-6 cell line, the cells were incubated for 1h, 4h or 24h in serum-free medium and stained with anti-phospho-STAT3 antibody (Y705) (*Figure V.17, top panel*). FACS plots presented below are representative of two distinct experiments.

Quantification of the signal over time indicated a 20% decrease in STAT3 phosphorylation 4h post starvation that persisted over to the 24h time point. STAT3 phosphorylation status 24h post starvation was then taken as a no stimulation control (*Figure V.17, bottom panel*, black line histogram) and compared to Mono-mac-6 cells starved for 24h then stimulated with either IL-6 or G-CSF for 30 min or with GM-CSF for 1h. Both IL-6 and G-CSF stimulation led to STAT3 phosphorylation, independent of HCK level of expression, while GM-CSF did not lead to STAT3 phosphorylation.

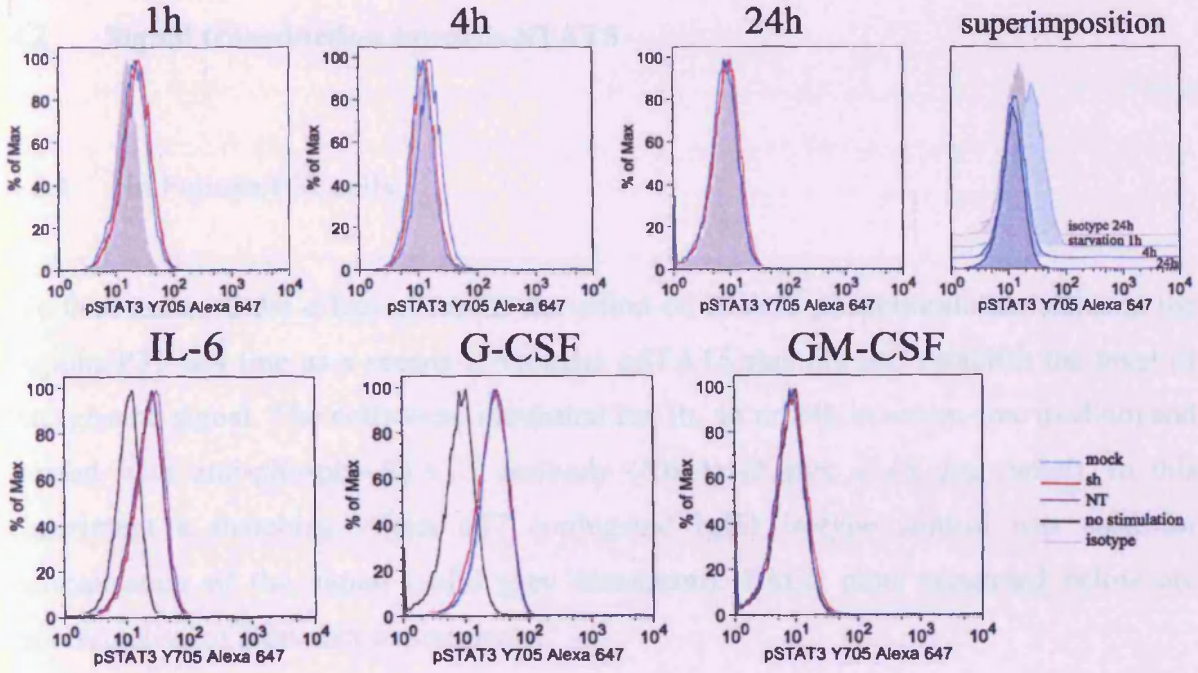


***Figure V.17: STAT3 phosphorylation in Mono-mac-6 cells.***

*Top panel: Effect of serum starvation on STAT3 phosphorylation. Cells were incubated for 1h, 4h or 24h in serum-free medium and stained with anti-phospho-STAT3 antibody (Y705). The corresponding IgG2a isotype control was used for normalisation of the*

*signal (solid grey histogram). Superimposition of the 1h, 4h and 24h starvation plots of a given sample (sh transduced cells) allows for a better visualisation of the control and sample histograms used to calculate MFI ratios for signal quantification and its variation over time. Bottom panel: Effect of cytokine stimulation on STAT3 phosphorylation. Cells were starved for 24h then stimulated with either IL-6 or G-CSF for 30 min or with GM-CSF for 1h or left unstimulated, as control.*

Thus, serum starvation led to an increase in STAT3 phosphorylation in U937 cells and a decrease in STAT3 phosphorylation in Mono-mac-6 cells, suggesting that STAT3 is active in a different way in these two cell types, while it is not phosphorylated in Fujioka/P31 cells. Moreover, we observed that GM-CSF does not lead to STAT3 phosphorylation in the 3 cell lines studied while IL-6 and G-CSF did induce STAT3 phosphorylation in the 3 cell lines studied in an HCK independent fashion.

## 4.2 Signal transduction towards STAT5

### 4.2.1 In Fujioka/P31 cells

We then assessed the effect of serum starvation on STAT5 phosphorylation status in the Fujioka/P31 cell line as a means to validate pSTAT5 staining and establish the level of background signal. The cells were incubated for 1h, 4h or 24h in serum-free medium and stained with anti-phospho-STAT5 antibody (Y654) (*Figure V.18, top panel*). In this experiment a matching Alexa 647 conjugated IgG1 isotype control was used for normalisation of the signal (solid grey histogram). FACS plots presented below are representative of 2 distinct experiments.

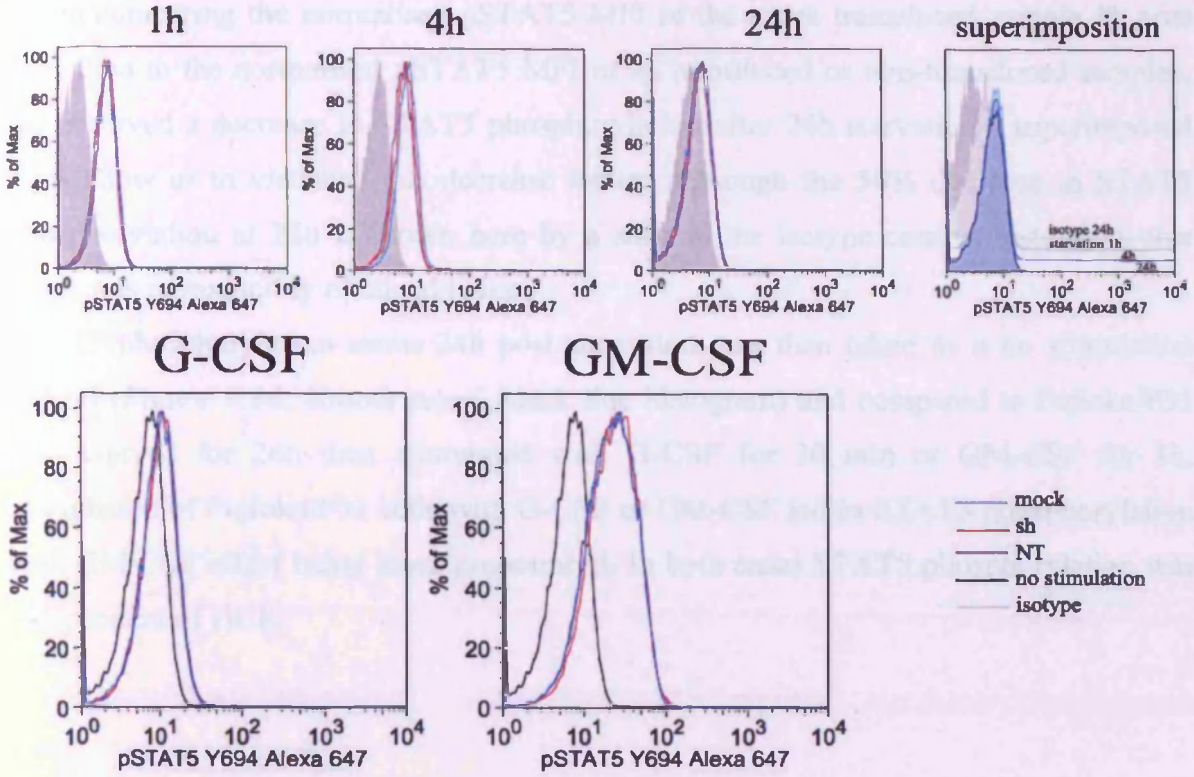


***Figure V.18: STAT5 phosphorylation in Fujioka/P31 cells.***

*Top panel: Effect of serum starvation on STAT5 phosphorylation. Cells were incubated for 1h, 4h or 24h in serum-free medium and stained with anti-phospho-STAT5 antibody (Y694). The corresponding IgG1 isotype was used for normalisation of the signal (solid grey histogram). Superimposition of the 1h, 4h and 24h starvation plots of a given sample (sh transduced cells) allows for a better visualisation of the control and sample histograms used to calculate MFI ratios for signal quantification and its variation over time. Indeed, with 24h starvation data being acquired on a different day, isotype histograms do not always superimpose with the 1h and 4h corresponding histogram and need to be used for correction. Bottom panel: Effect of cytokine stimulation on STAT5 phosphorylation. Cells were starved for 24h then stimulated with G-CSF for 30 min or with GM-CSF for 1h or left unstimulated, as control.*

When comparing the normalised pSTAT5 MFI of the mock transduced sample 1h post starvation to the normalised pSTAT5 MFI of sh transduced or non-transduced samples, we observed a decrease in STAT5 phosphorylation after 24h starvation - superimposed plots allow us to visualise this decrease better. Although the 50% decrease in STAT5 phosphorylation at 24h is shown here by a shift in the isotype control histogram, this result was reproducibly obtained twice.

STAT5 phosphorylation status 24h post starvation was then taken as a no stimulation control (*Figure V.18, bottom panel*, black line histogram) and compared to Fujioka/P31 cells starved for 24h then stimulated with G-CSF for 30 min or GM-CSF for 1h. Stimulation of Fujioka/P31 cells with G-CSF or GM-CSF led to STAT5 phosphorylation with GM-CSF effect being more pronounced. In both cases STAT5 phosphorylation was independent of HCK.

### 4.2.2 In U937 cell line

To assess the effect of serum starvation on STAT5 phosphorylation status in U937 cell line, the cells were incubated for 1h, 4h or 24h in serum-free medium and stained with anti-phospho-STAT5 antibody (Y654) (*Figure V.19, top panel*). FACS plots presented below are representative of two distinct experiments.

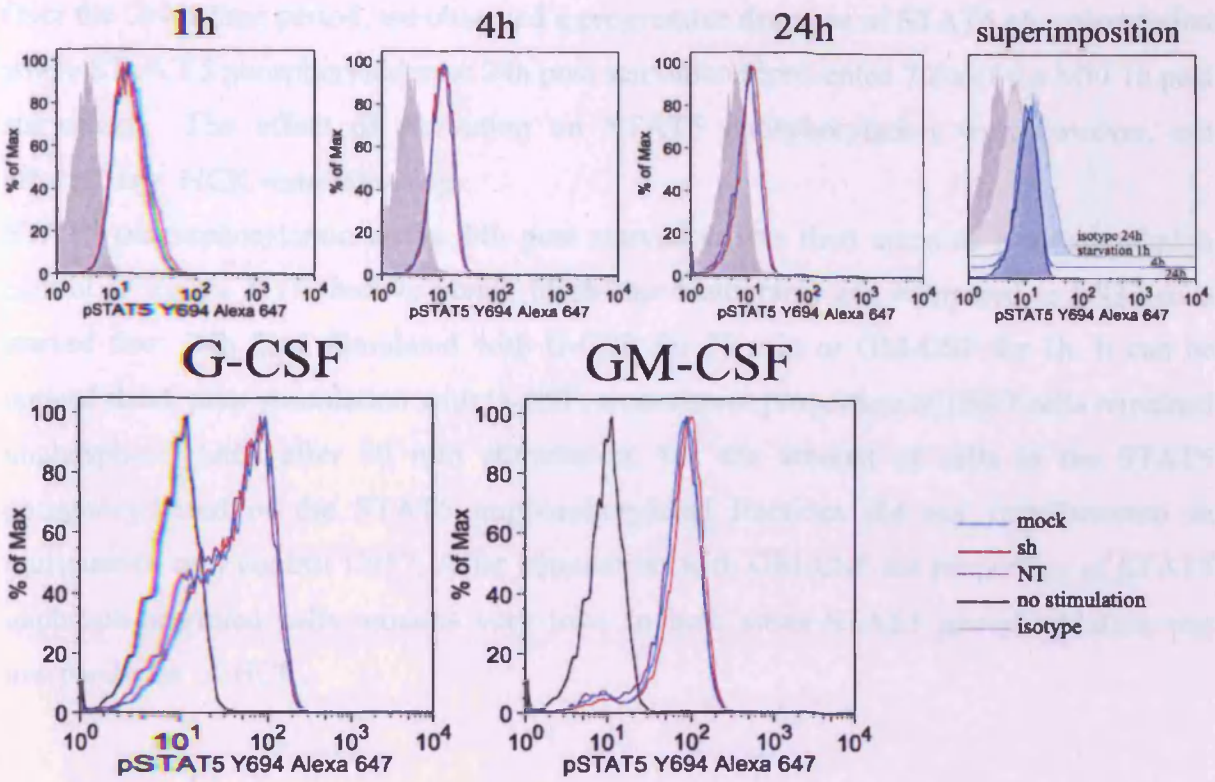


***Figure V.19: STAT5 phosphorylation in U937 cells.***

*Top panel: Effect of serum starvation on STAT5 phosphorylation. Cells were incubated for 1h, 4h or 24h in serum-free medium and stained with anti phospho-STAT5 antibody (Y694). The corresponding IgG1 isotype was used for normalisation of the signal (solid grey histogram). Superimposition of the 1h, 4h and 24h starvation plots of a given sample (sh transduced cells) allows for a better visualisation of the control and sample histograms used to calculate MFI ratios for signal quantification and its variation over time. Indeed, with 24h starvation data being acquired on a different day, isotype histograms do not always superimpose with the 1h and 4h corresponding histogram and need to be used for correction. Bottom panel: Effect of cytokine stimulation on STAT5 phosphorylation. Cells were starved for 24h then stimulated with G-CSF for 30 min or with GM-CSF for 1h or left unstimulated, as control.*

Over the 24h time period, we observed a progressive decrease of STAT5 phosphorylation where STAT5 phosphorylation at 24h post starvation represented 70% of the MFI 1h post starvation. The effect of starvation on STAT5 phosphorylation was, however, not affected by HCK semi-silencing.

STAT5 phosphorylation status 24h post starvation was then taken as a no stimulation control (*Figure V.19, bottom panel*, black line histogram) and compared to U937 cells starved for 24h then stimulated with G-CSF for 30 min or GM-CSF for 1h. It can be noticed that after stimulation with G-CSF, a consistent proportion of U937 cells remained unphosphorylated after 30 min stimulation, but the amount of cells in the STAT5 phosphorylated or the STAT5 unphosphorylated fractions did not vary between sh transduced and control U937. After stimulation with GM-CSF the proportion of STAT5 unphosphorylated cells remains very low. In both cases STAT5 phosphorylation was independent of HCK.

### 4.2.3 In Mono-mac-6 cell line

To assess the effect of serum starvation on STAT5 phosphorylation status in the Mono-mac-6 cell line, the cells were incubated for 1h, 4h or 24h in serum-free medium and stained with anti-phospho-STAT5 antibody (Y654) (*Figure V.20, top panel*). FACS plots presented below are representative of two distinct experiments.

One hour post starvation, we observed two distinct populations, one with phosphorylated STAT5 and one where STAT5 was not phosphorylated. The Mono-mac-6 population with phosphorylated STAT5 progressively disappeared over 24h of serum free starvation. Percentage of cells falling into phospho-STAT5 positive or negative populations did not differ between sh transduced and control Mono-mac-6 cells. The effect of starvation on STAT5 phosphorylation is therefore not affected by HCK semi-silencing.

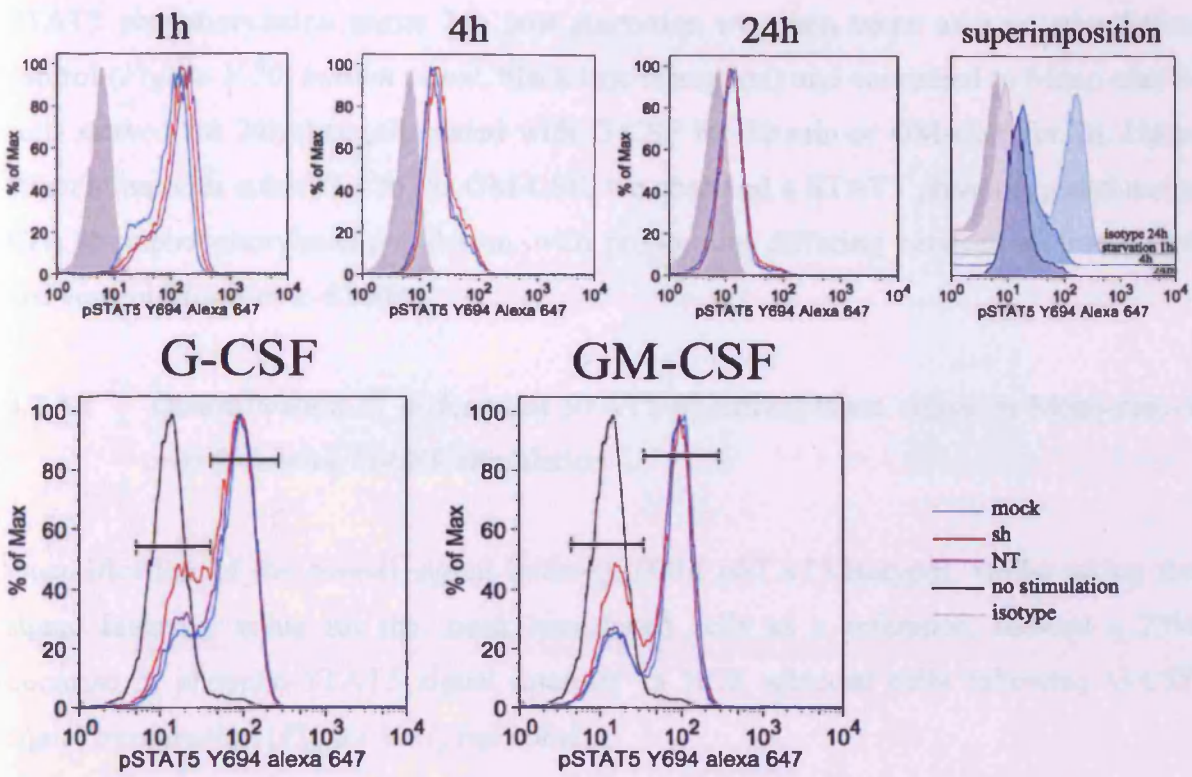


***Figure V.20: STAT5 phosphorylation in Mono-mac-6 cells.***

*Top panel: Effect of serum starvation on STAT5 phosphorylation. Cells were incubated for 1h, 4h or 24h in serum-free medium and stained with anti-phospho-STAT5 antibody (Y694). The corresponding IgG1 isotype was used for normalisation of the signal (solid grey histogram). Superimposition of the 1h, 4h and 24h starvation plots of a given sample (sh transduced cells) allows for a better visualisation of the control and sample histograms used to calculate MFI ratios for signal quantification and its variation over time. Indeed, with 24h starvation data being acquired on a different day, isotype histograms do not always superimpose with the 1h and 4h corresponding histogram and need to be used for correction. Bottom panel: Effect of cytokine stimulation on STAT5 phosphorylation. Cells were starved for 24h then stimulated with G-CSF for 30 min or with GM-CSF for 1h or left unstimulated, as control.*

STAT5 phosphorylation status 24h post starvation was then taken as a no stimulation control (*Figure V.20, bottom panel*, black line histogram) and compared to Mono-mac-6 cells starved for 24h then stimulated with G-CSF for 30 min or GM-CSF for 1h. Upon stimulation with either G-CSF or GM-CSF, we observed a STAT5 phosphorylated and a STAT5 unphosphorylated population, with proportions differing between sh transduced and control Mono-mac-6 cells.

#### 4.2.3.1 Quantification of differential STAT5 phosphorylation signal in Mono-mac-6 cells following G-CSF stimulation

Quantification of the overall signal intensity (MFI pSTAT5/isotype), whilst taking the signal intensity value for the mock transduced cells as a reference, showed a 23% decrease in phospho-STAT5 signal intensity in HCK silenced cells following G-CSF signal transduction (*Figure V.21, top panel*).

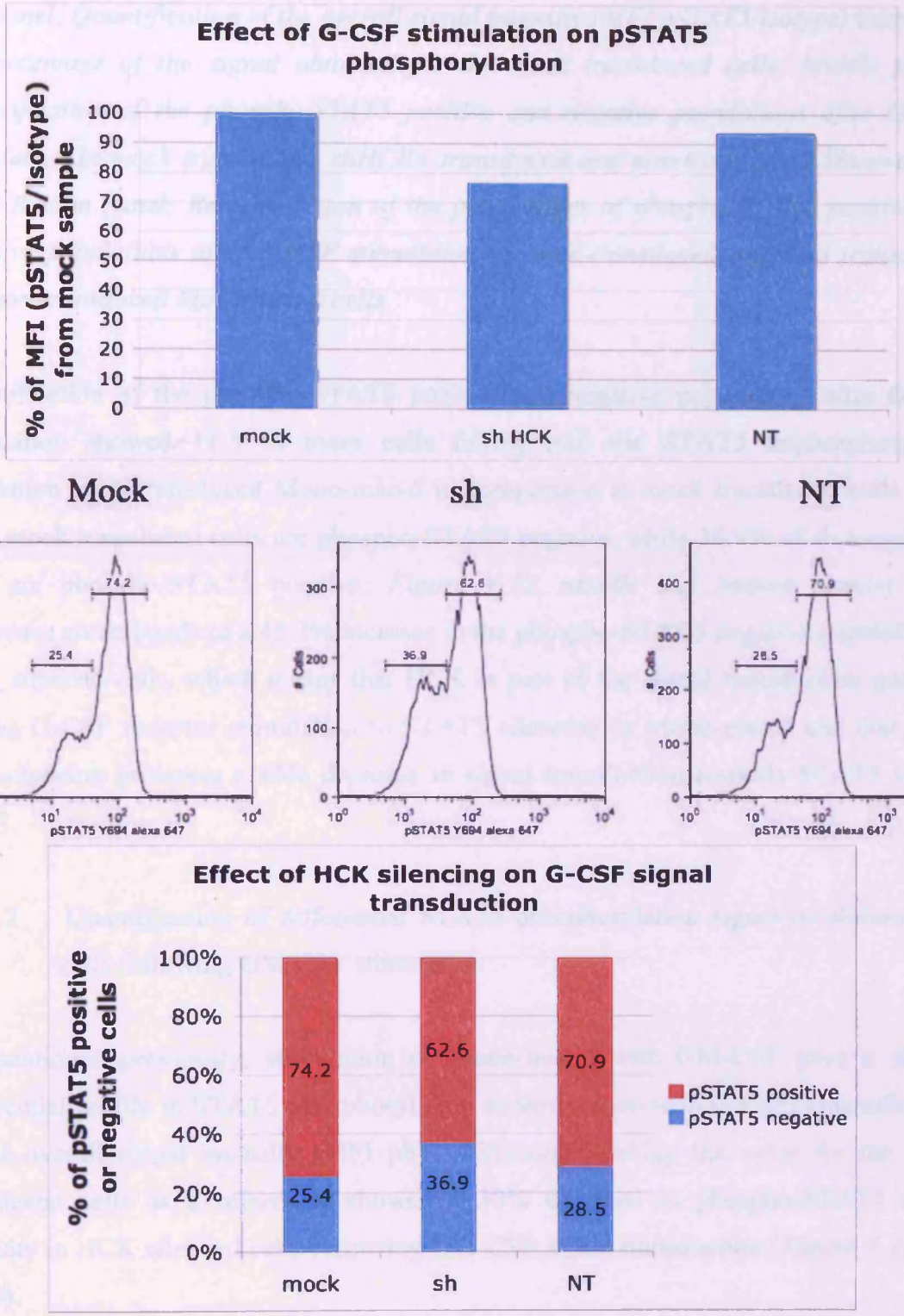


***Figure V.21: Quantification of STAT5 phosphorylation following G-CSF stimulation in Mono-mac-6 cells.***

*Top panel: Quantification of the overall signal intensity (MFI pSTAT5/isotype) expressed as percentage of the signal obtained for the mock transduced cells. Middle panel: Quantification of the phospho-STAT5 positive and negative populations after G-CSF stimulation in mock transduced, shHCK4 transduced and non-transduced Mono-mac-6 cells. Bottom panel: Representation of the percentages of phospho-STAT5 positive and negative populations after G-CSF stimulation in mock transduced, shHCK4 transduced and non-transduced Mono-mac-6 cells.*

Quantification of the phospho-STAT5 positive and negative populations after G-CSF stimulation showed 11.5 % more cells falling into the STAT5 unphosphorylated population in sh transduced Mono-mac-6 in comparison to mock transduced cells (25.4 % of mock transduced cells are phospho-STAT5 negative while 36.9% of sh transduced cells are phospho-STAT5 positive; *Figure V.21*, *middle* and *bottom panels*). This difference corresponds to a 45.3% increase in the phospho-STAT5 negative population in HCK silenced cells, which means that HCK is part of the signal transduction pathway linking G-CSF receptor stimulation to STAT5 silencing in Mono-mac-6 and that HCK semi-silencing provokes a 45% decrease in signal transduction towards STAT5 via G-CSFR.

#### 4.2.3.2 Quantification of differential STAT5 phosphorylation signal in Mono-mac-6 cells following GM-CSF stimulation

As mentioned previously, stimulation of Mono-mac-6 with GM-CSF gave a similar differential profile in STAT5 phosphorylation as stimulation with G-CSF. Quantification of the overall signal intensity (MFI pSTAT5/isotype), taking the value for the mock transduced cells as a reference, showed a 30% decrease in phospho-STAT5 signal intensity in HCK silenced cells following GM-CSF signal transduction (*Figure V.22, top panel*).

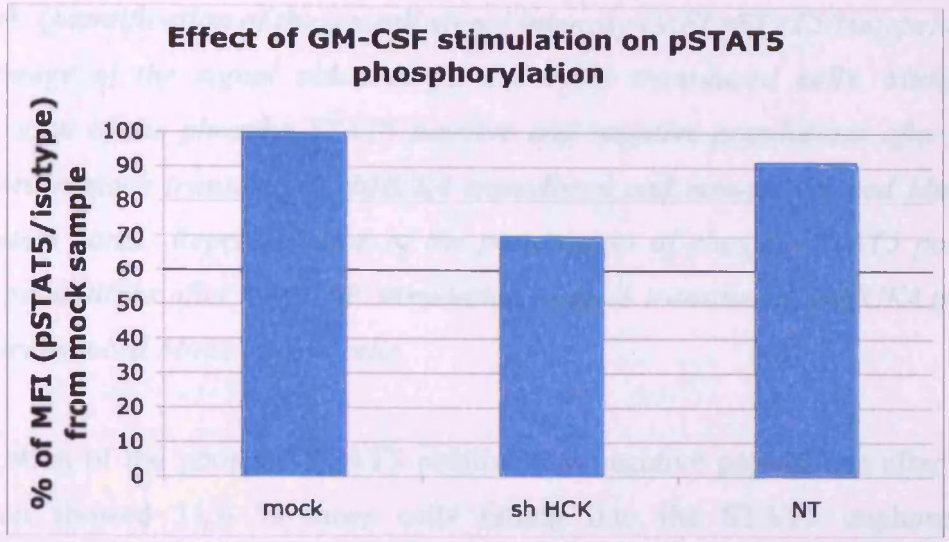


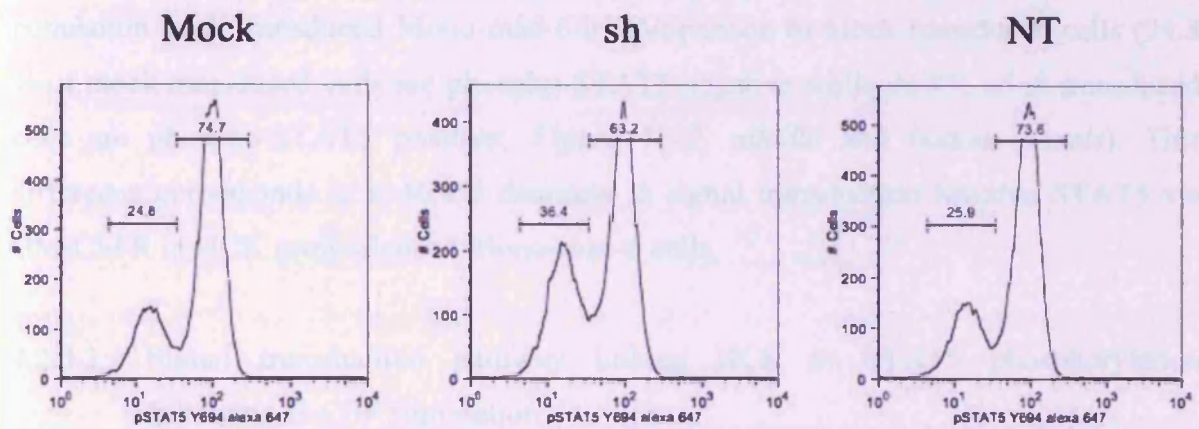


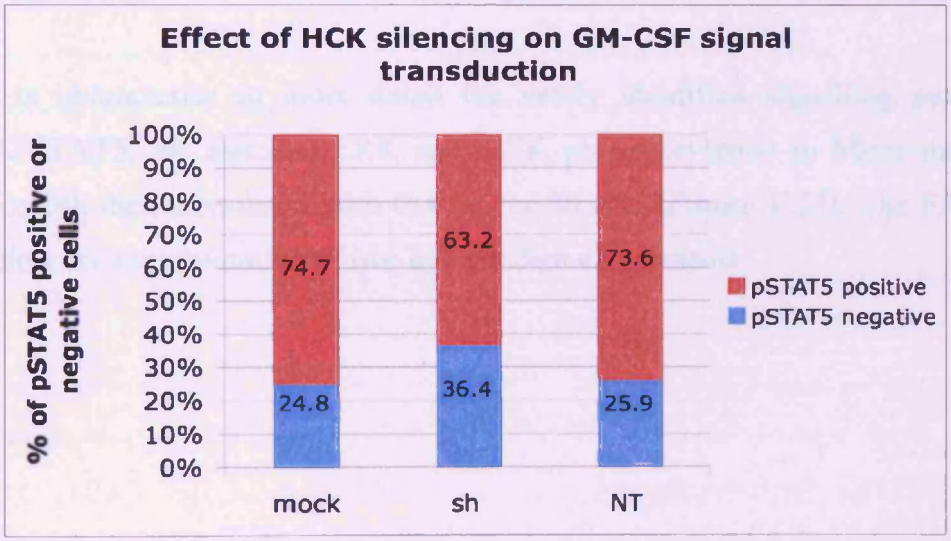


***Figure V.22: Quantification of STAT5 phosphorylation following G-CSF stimulation in Mono-mac-6 cells.***

*Top panel: Quantification of the overall signal intensity (MFI pSTAT5/isotype) expressed as percentage of the signal obtained for the mock transduced cells. Middle panel: Quantification of the phospho-STAT5 positive and negative populations after GM-CSF stimulation in mock transduced, shHCK4 transduced and non-transduced Mono-mac-6 cells. Bottom panel: Representation of the percentages of phospho-STAT5 positive and negative populations after GM-CSF stimulation in mock transduced, shHCK4 transduced and non-transduced Mono-mac-6 cells.*

Quantification of the phospho-STAT5 positive and negative populations after GM-CSF stimulation showed 11.6 % more cells falling into the STAT5 unphosphorylated population in sh transduced Mono-mac-6 in comparison to mock transduced cells (24.8 % of mock transduced cells are phospho-STAT5 negative while 36.4% of sh transduced cells are phospho-STAT5 positive; *Figure V.22*, *middle* and *bottom panels*). This difference corresponds to a 46.8% decrease in signal transduction towards STAT5 via GM-CSFR in HCK semi-silenced Mono-mac-6 cells.

#### 4.2.3.3 Signal transduction pathway linking HCK to STAT5 phosphorylation following G-CSF stimulation

In order to characterise in more detail the newly identified signalling pathway G-CSF/HCK/STAT5, we assessed ERK and MEK phosphorylation in Mono-mac-6 cells starved for 24h then stimulated with G-CSF for 30 min (*Figure V.23*). The FACS plots shown below are representative of two independent experiments.

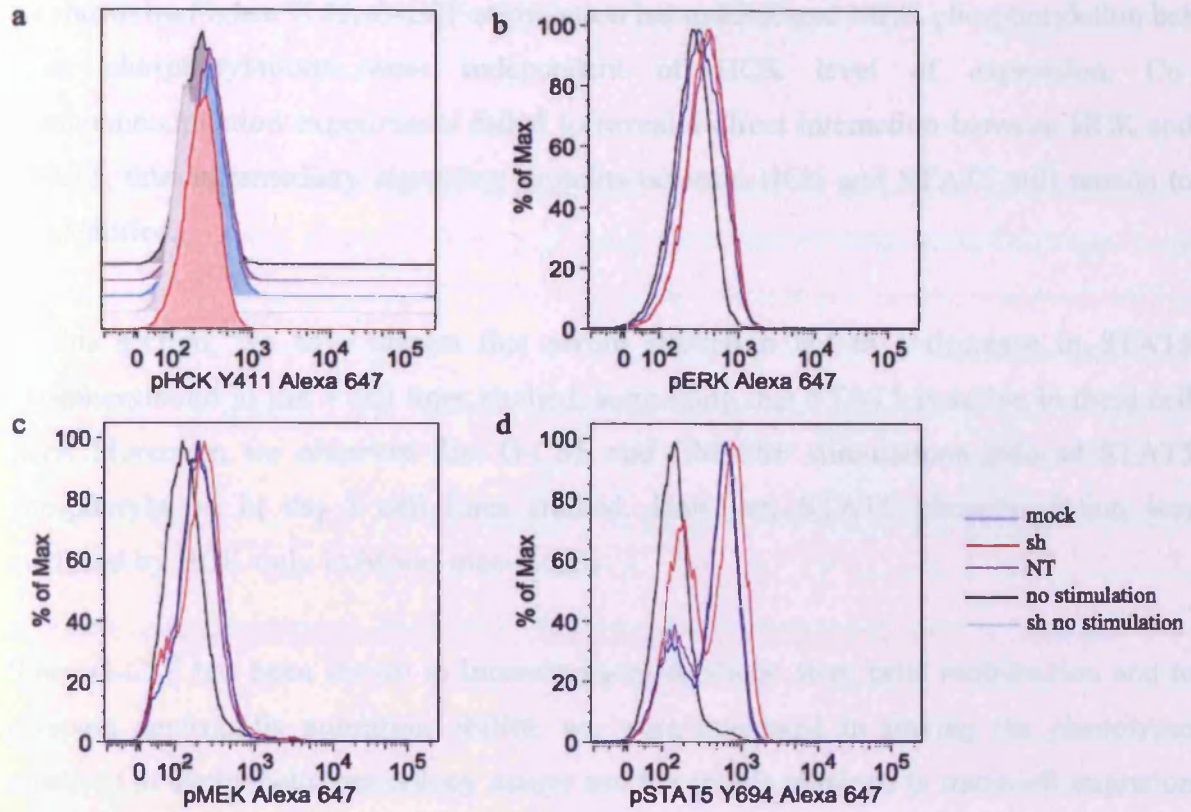


***Figure V.23: Phosphorylation of ERK and MEK in Mono-mac-6 cells upon HCK silencing.***

*(a) HCK Y411 phosphorylation in sh and mock transduced Mono-mac-6 cells upon G-CSF phosphorylation: mock and sh transduced Mono-mac-6 cells have a different level of background HCK phosphorylation after 24h starvation due to HCK silencing (black and grey histograms respectively). Upon G-CSF stimulation, HCK phosphorylation increases in both cell types. (b) ERK phosphorylation in sh and mock transduced Mono-mac-6 cells upon G-CSF phosphorylation: ERK is phosphorylated upon G-CSF stimulation, independently of HCK. (c) MEK phosphorylation in sh and mock transduced Mono-mac-6 cells upon G-CSF phosphorylation: MEK is phosphorylated upon G-CSF stimulation, independently of HCK. (d) STAT5 Y694 phosphorylation in sh and mock transduced Mono-mac-6 cells upon G-CSF phosphorylation: STAT5 is less phosphorylated upon G-CSF stimulation in sh transduced Mono-mac-6 cells than in mock transduced Mono-mac-6 cells.*

As shown on *Figure V.23*, G-CSF stimulation led to ERK and MEK phosphorylation but these phosphorylations were independent of HCK level of expression. Co-immunoprecipitation experiments failed to reveal a direct interaction between HCK and STAT5, thus intermediary signalling proteins between HCK and STAT5 still remain to be identified.

In this section, we have shown that serum starvation led to a decrease in STAT5 phosphorylation in the 3 cell lines studied, suggesting that STAT5 is active in these cell lines. Moreover, we observed that G-CSF and GM-CSF stimulations induced STAT5 phosphorylation in the 3 cell lines studied. However, STAT5 phosphorylation was mediated by HCK only in Mono-mac-6 cells.

Since G-CSF has been shown to increase haematopoietic stem cells mobilisation and to decrease neutrophils migration ability, we were interested in linking the phenotypes observed in methylcellulose colony assays and the results obtained in transwell migration assays to G-CSF or GM-CSF stimulation.

## 5. Correlation between G-CSF/GM-CSF stimulation and migration of semi-silenced Mono-mac-6 cells

Since G-CSF is a known chemoattractant and SFK can act differentially on inside-out or outside-in integrins signalling, we tried to separate the two possible effects by either pre-incubating Mono-mac-6 cells with G-CSF or GM-CSF for 15 min, then to have them migrating towards FCS in a transwell assay setting (inside-out signalling assessment) or by having the cells in serum free conditions and assessing their migration potential towards G-CSF, GM-CSF or both (outside-in signalling assessment).

## 5.1 Effect of HCK silencing on Mono-mac-6 cells migration following G-CSF or GM-CSF stimulation

Mono-mac-6 cells were incubated with G-CSF or GM-CSF at a final concentration of 100ng/mL for 15 min at 37°C, 5% $CO_2$ (*Figure V.24*). 90,000 cells of each cell type were then seeded in triplicate in the upper chamber of a fibronectin coated transwell system and allowed to migrate towards 5% FCS for 4h30 at 37°C, 5% $CO_2$. Unstimulated cells were taken as controls. The graphs presented below are representative of 3 distinct experiments (n=9).

As described previously, HCK silencing led to a 31% decrease of Mono-mac-6 migration towards FCS. Pre-stimulation of control cells with G-CSF or GM-CSF significantly diminished this migration (50% and 34% decrease respectively). However, in shHCK4 transduced cells, G-CSF prestimulation led to a 50% increase in Mono-mac-6 cells migration towards FCS, while GM-CSF prestimulation led to a 33% decrease in Mono-mac-6 cells migration towards FCS.

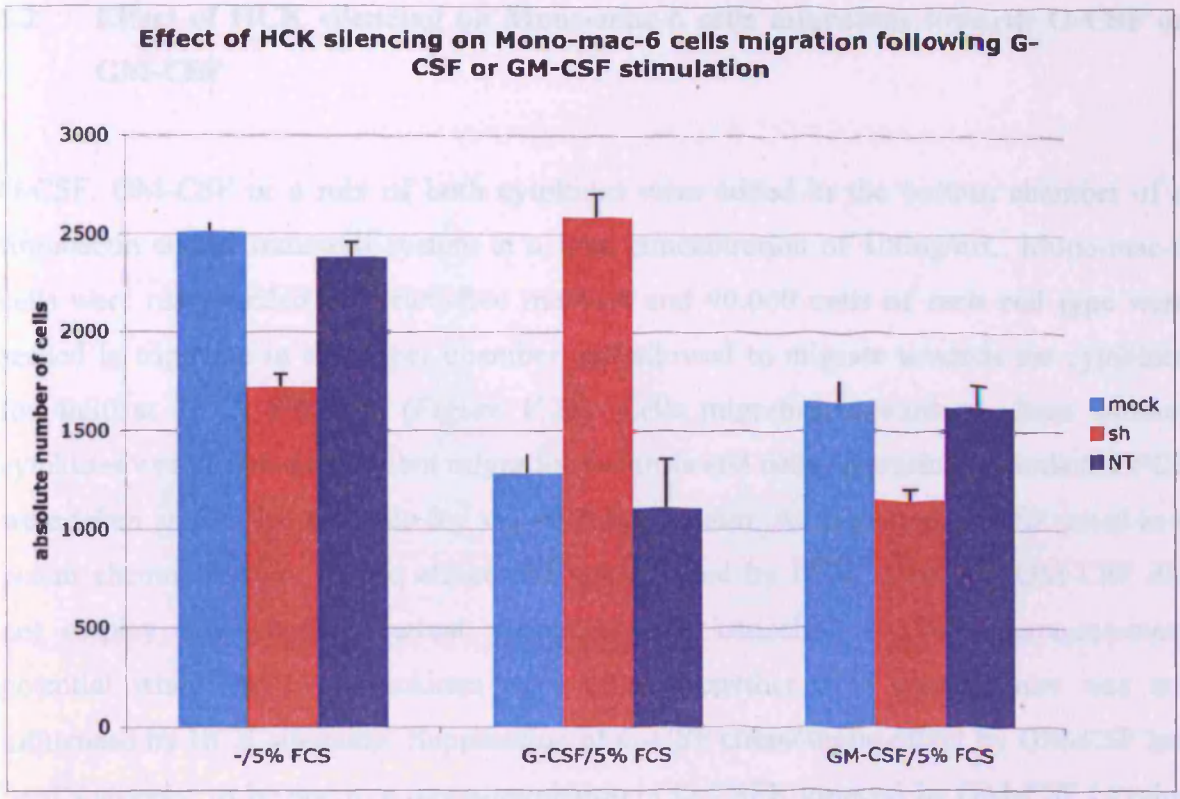


***Figure V.24: Effect of HCK silencing on Mono-mac-6 cells migration towards FCS following cytokine pre-stimulation.***

*Migration of mock transduced, shHCK4 transduced and non-transduced Mono-mac-6 cells, prestimulated for 15 min with G-CSF or GM-CSF, towards 5% FCS after 4h30 incubation.*

The differential effects of G-CSF and GM-CSF pre-stimulation observed in this migration assay suggest that cytokine stimulation triggered opposite inside-out signalling pathways involving engagement of integrin fibronectin receptors mediated by HCK. Integrins α5β1 and αVβ3 are the principal fibronectin receptor (Wu *et al.*, 1993), HCK has been shown to specifically associated with αMβ2 (Tang *et al.*, 2006) and α5β1and αMβ2 have been shown to differentially regulate neutrophils migration (Lishko *et al.*, 2003). It would therefore be interesting to assess integrins expression profile in sh or mock transduced Mono-mac-6 cells to try to understand the observed migration pattern in more details.

## 5.2 Effect of HCK silencing on Mono-mac-6 cells migration towards G-CSF or GM-CSF

G-CSF, GM-CSF or a mix of both cytokines were added in the bottom chamber of a fibronectin coated transwell system at a final concentration of 100ng/mL. Mono-mac-6 cells were resuspended in serum-free medium and 90,000 cells of each cell type were seeded in triplicate in the upper chamber and allowed to migrate towards the cytokines for 4h30 at 37°C, 5% $CO_2$ (*Figure V.25*). Cells migrating towards medium without cytokines were taken as transient migration controls and cells migrating towards 5% FCS were taken as positive controls for successful migration. As expected, G-CSF acted as a potent chemoattractant whose effect was not affected by HCK silencing. GM-CSF did not display any chemoattractant properties and cancelled G-CSF chemoattractant potential when the two cytokines were mixed together, this phenomenon was not influenced by HCK silencing. Suppression of G-CSF chemotactic effect by GM-CSF has been suggested to be due to a down-regulation of G-CSFR induced by GM-CSF (Avalos *et al.*, 1997; Nicola *et al.*, 1986), an aspect that HCK silencing does not modulate.

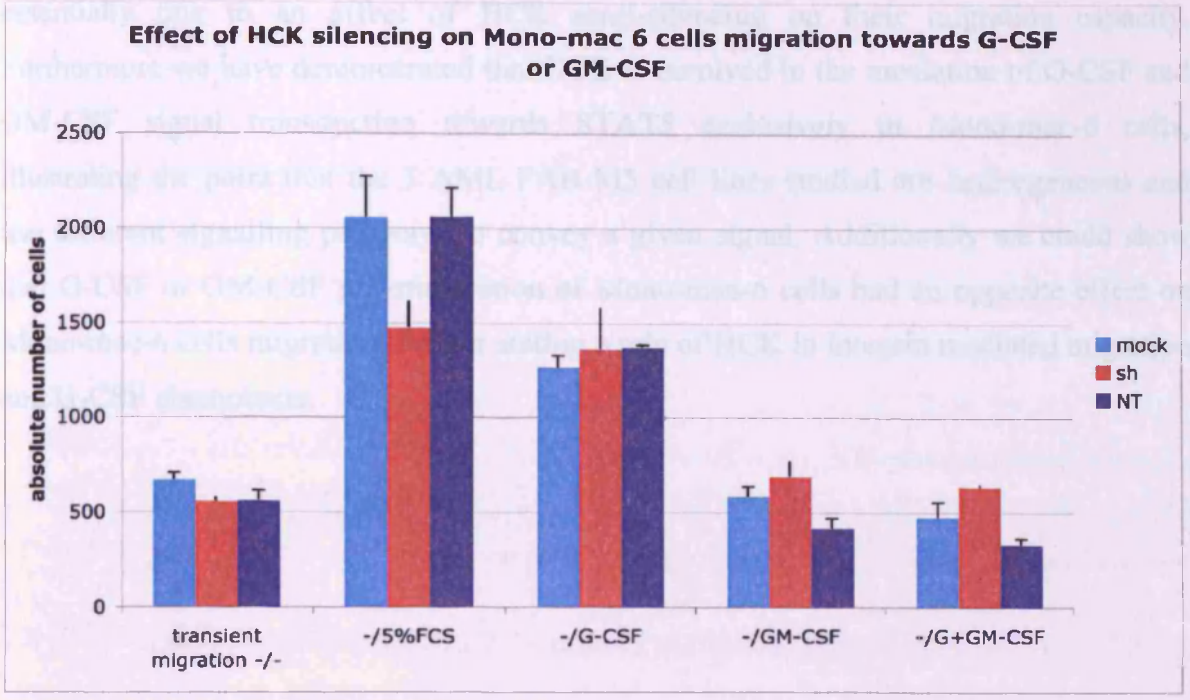


***Figure V.25: Effect of HCK silencing on Mono-mac-6 cells migration towards G-CSF or GM-CSF.***

*Migration of mock transduced, shHCK4 transduced and non-transduced Mono-mac-6 cells, towards G-CSF, GM-CSF or both cytokines. Cells migrating towards 5% FCS or towards serum-free medium were taken as controls. Migration was assessed after 4h30 incubation.*

Thus, we demonstrated that HCK mediates G-CSF and GM-CSF induced Mono-mac-6 cells migration in an opposite manner via mechanisms that still remain to be elucidated.

## 6. Conclusion

In this chapter, we have shown that HCK semi-silencing did not have any major effect on FAB M5 cell line proliferation, apoptosis or differentiation as shown by XTT assay, cell cycle analysis, Annexin V staining, population doublings calculation and specific cell surface marker staining respectively. However we observed that HCK knock-down had an influence on the spontaneous colony forming capacity of Mono-mac-6 cells that was

essentially due to an effect of HCK semi-silencing on their migration capacity. Furthermore we have demonstrated that HCK is involved in the mediation of G-CSF and GM-CSF signal transduction towards STAT5 exclusively in Mono-mac-6 cells, illustrating the point that the 3 AML FAB M5 cell lines studied are heterogeneous and use different signalling pathways to convey a given signal. Additionally we could show that G-CSF or GM-CSF pre-stimulation of Mono-mac-6 cells had an opposite effect on Mono-mac-6 cells migration, further stating a role of HCK in integrin mediated migration and G-CSF chemotaxis.

# Chapter VI

# VI Effect of HCK silencing on UCB Lin$^-$ cells

## 1. Effect of HCK silencing on *ex vivo* expanded Lin$^-$ growth

Equal numbers of mock transduced, shHCK4 transduced or non-transduced Lin$^-$ cells were resuspended in a final volume of 100 µL of StemSpan containing 300 ng/mL SCF, 300 ng/mL Flt3-L and 20 ng/mL TPO (Levac et al., 2005). Lin$^-$ cells were numerated every 3 days on an LSRII analyser using counting beads. An appropriate number of cells were used for various *in vitro* assays (CFC assay, cell cycle analysis, HCK expression by flow cytometry) and unused cells were replated, adding fresh cytokines each time.

### 1.1 Absolute number of cells

Transduced Lin$^-$ absolute numbers of cells were followed up for 11 days. As shown in *Figure VI.1*, HCK silencing led to an increase in absolute number of Lin$^-$ cells over time.

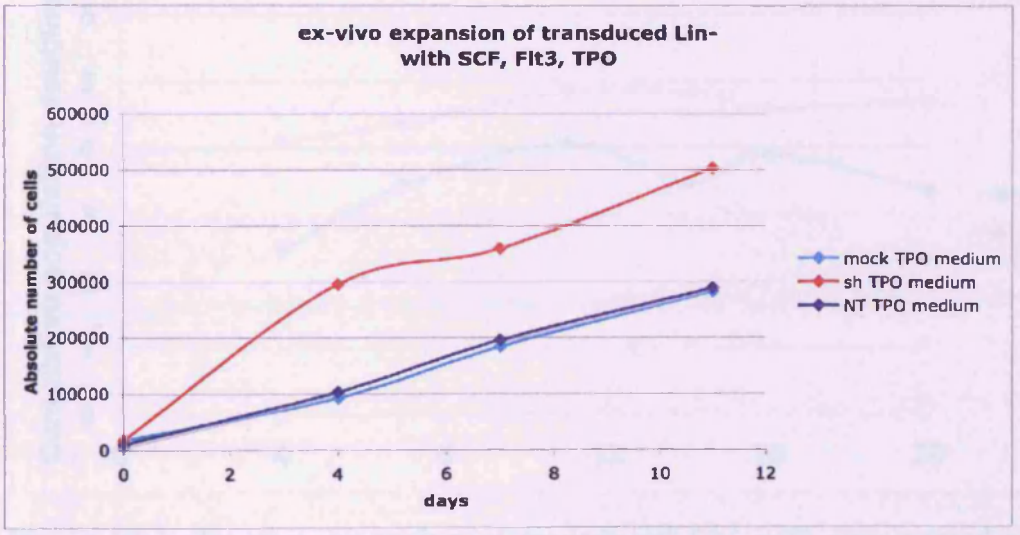


***Figure VI.1:* Ex vivo expansion of transduced Lin$^-$ cells.**
*Equal numbers of mock transduced, shHCK4 transduced or non-transduced Lin$^-$ cells were expanded in StemSpan containing 300 ng/mL SCF, 300 ng/mL Flt3-L and 20 ng/mL TPO. Lin$^-$ cells were numerated every 3 days on an LSRII analyser using counting beads.*

## 1.2 Population doublings

To have a more accurate representation of the population behaviour during expansion, we calculated the cumulative population doublings (PD) of each culture using the following formula: $PD = [\log_{10}(n_{t2}) - \log_{10}(n_{t1})] / \log_{10}(2)$ (Cristofalo et al., 1998). After 4 days in culture, shHCK4 transduced Lin$^-$ cells showed a 1.66 fold increase in population doubling in comparison to mock transduced Lin$^-$ (*Figure VI.2*). Past four days in culture, cumulative population doubling curves from both shHCK4 and mock transduced Lin$^-$ cells are growing parallel, indicating that both populations are not in an exponential growth phase anymore and proliferate at the same pace. The difference in PD observed initially suggests that HCK silencing could have an influence on the initial Lin$^-$ cells expansion capacity, but does not improve Lin$^-$ cells expansion beyond the classical 4 days window.

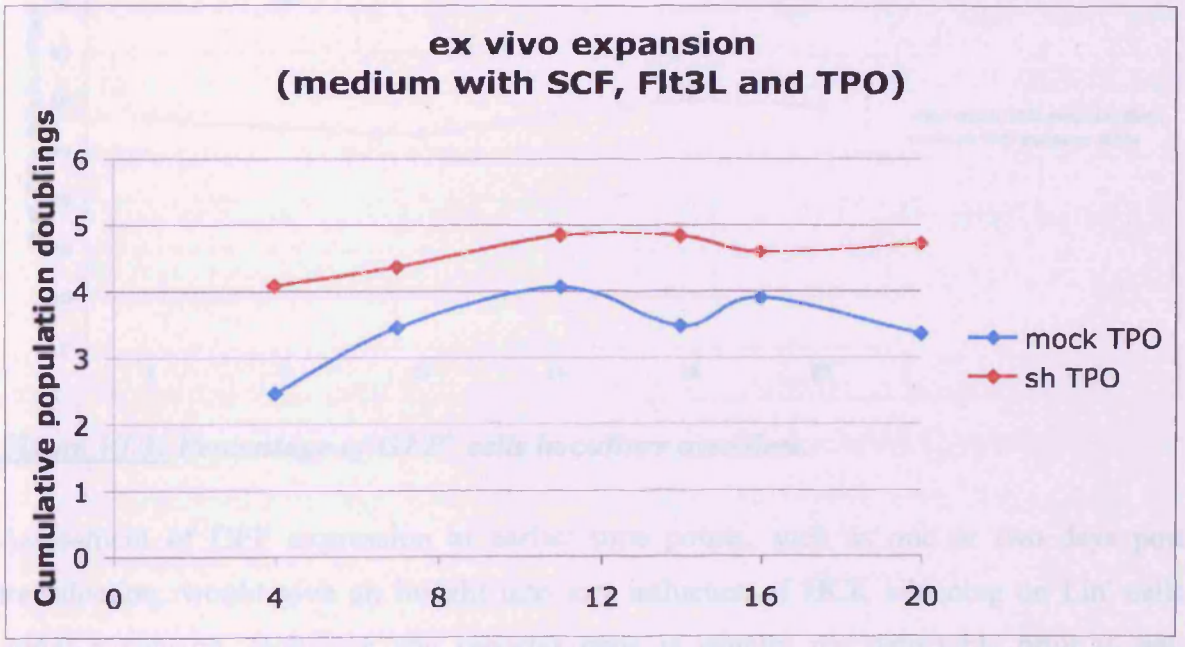


***Figure VI.2:*** ***Ex vivo expansion of transduced Lin$^-$ cells represented as cumulative population doublings.***
*Cumulative population doublings (PD) of each culture were calculated using the following formula: $PD = [\log_{10}(n_{t2}) - \log_{10}(n_{t1})] / \log_{10}(2)$.*

The use of mathematical formulae taking into account the non-exponential nature of stem cell growth as well as proportions of cycling or differentiating cells within the population would, however, allow a better representation of $Lin^-$ growth (Deasy et al., 2003).

### 1.3 $GFP^+$ population over time and cell cycle analysis

The data presented so far takes into account the bulk $Lin^-$ population. Following up the percentage of $GFP^+$ cells within the total $Lin^-$ population would allow us to see if HCK silencing gives any growth advantage to the shHCK4 transduced cells. Surprisingly, the percentage of $GFP^+$ cells remained constant over time (*Figure VI.3*).

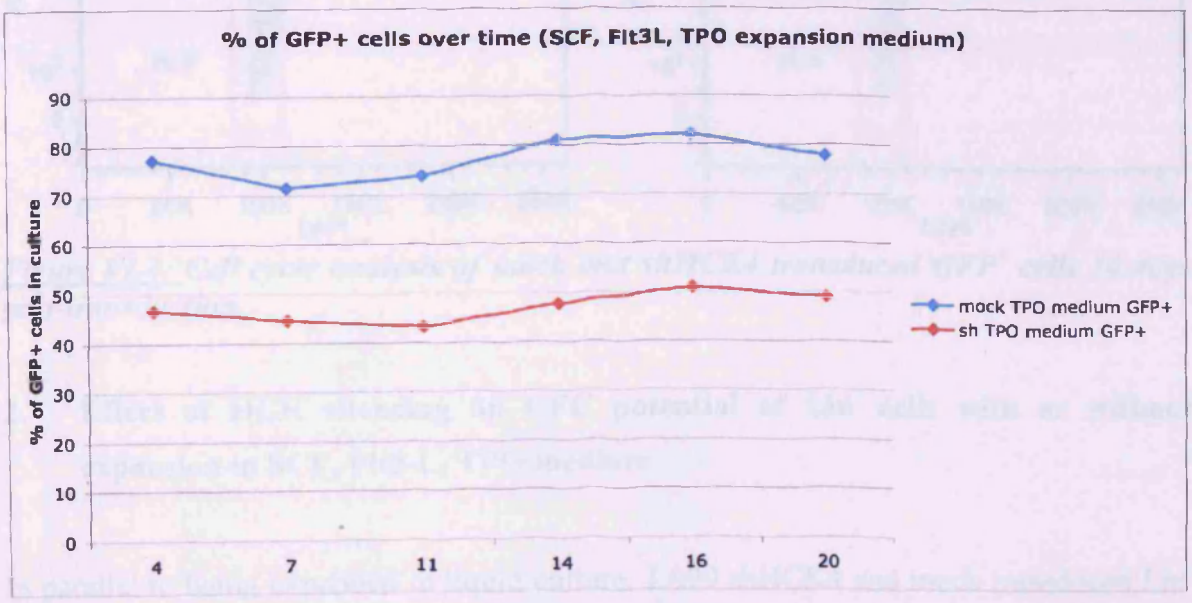


***Figure VI.3:* Percentage of $GFP^+$ cells in culture over time.**

Assessment of GFP expression at earlier time points, such as one or two days post transduction, would give an insight into any influence of HCK silencing on $Lin^-$ cells initial expansion. However, the reporter gene is usually not detectable prior to 48h making it technically unpractical to follow GFP expression within 4 days of transduction.

Cell cycle analysis using Ki67 as a marker of proliferation confirmed that shHCK4 and mock transduced GFP$^+$ cells had a similar cell cycle status 16 days post transfection when maintained in TPO containing medium (*Figure VI.4*).

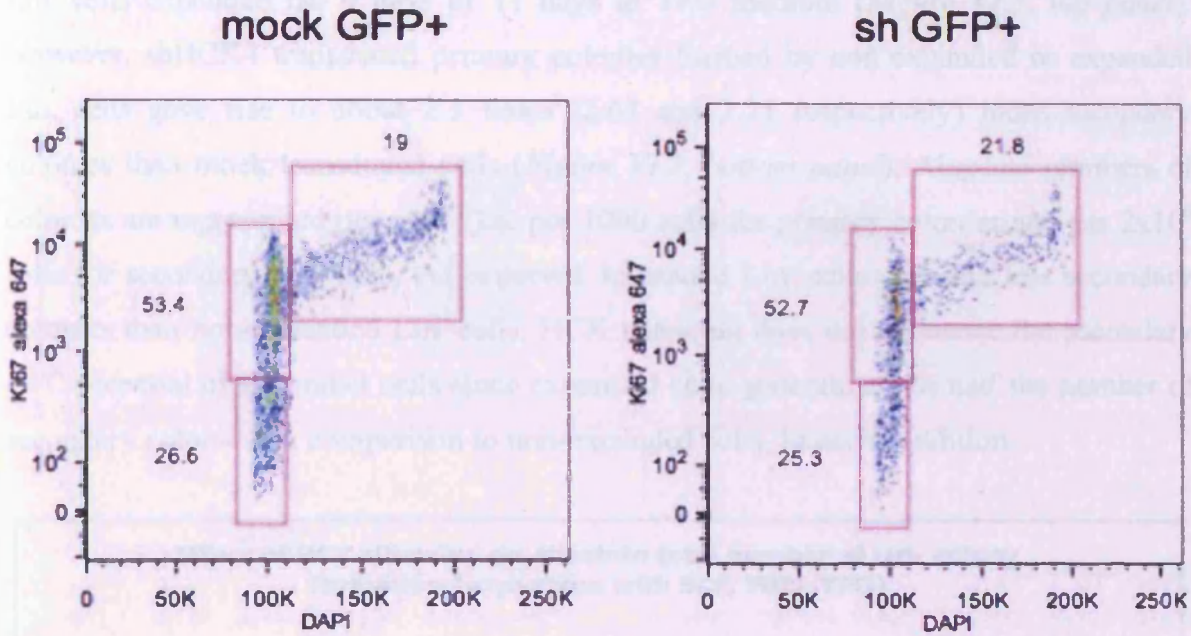


***Figure VI.4:** Cell cycle analysis of mock and shHCK4 transduced GFP$^+$ cells 16 days post-transduction.*

## 2. Effect of HCK silencing on CFC potential of Lin$^-$ cells with or without expansion in SCF, Flt3-L, TPO medium

In parallel to being expanded in liquid culture, 1,000 shHCK4 and mock transduced Lin$^-$ cells were plated in triplicate for CFC assay at day 1, day 4 and day 11 post-transfection. Two million cells from day 1 and day 4 primary CFC assays were also replated for secondary CFC assays.

## 2.1 Effect on absolute number of total primary and secondary colonies

HCK silencing did neither significantly influence the overall total number of colonies formed by non expanded Lin$^-$ cells nor the overall total number of colonies formed by Lin$^-$ cells expanded for 4 days or 11 days in TPO medium (*Figure VI.5, top panel*). However, shHCK4 transduced primary colonies formed by non expanded or expanded Lin$^-$ cells gave rise to about 2.5 times (2.63 and 2.21 respectively) more secondary colonies than mock transduced cells (*Figure VI.5, bottom panel*). Absolute numbers of colonies are represented per plate (i.e. per 1000 cells for primary colonies and per $2x10^6$ cells for secondary colonies). As expected, expanded Lin$^-$ cells generate less secondary colonies than non-expanded Lin$^-$ cells. HCK silencing does not influence the secondary CFC potential of expanded cells since expanded cells generate about half the number of secondary colonies, in comparison to non-expanded cells, in each condition.

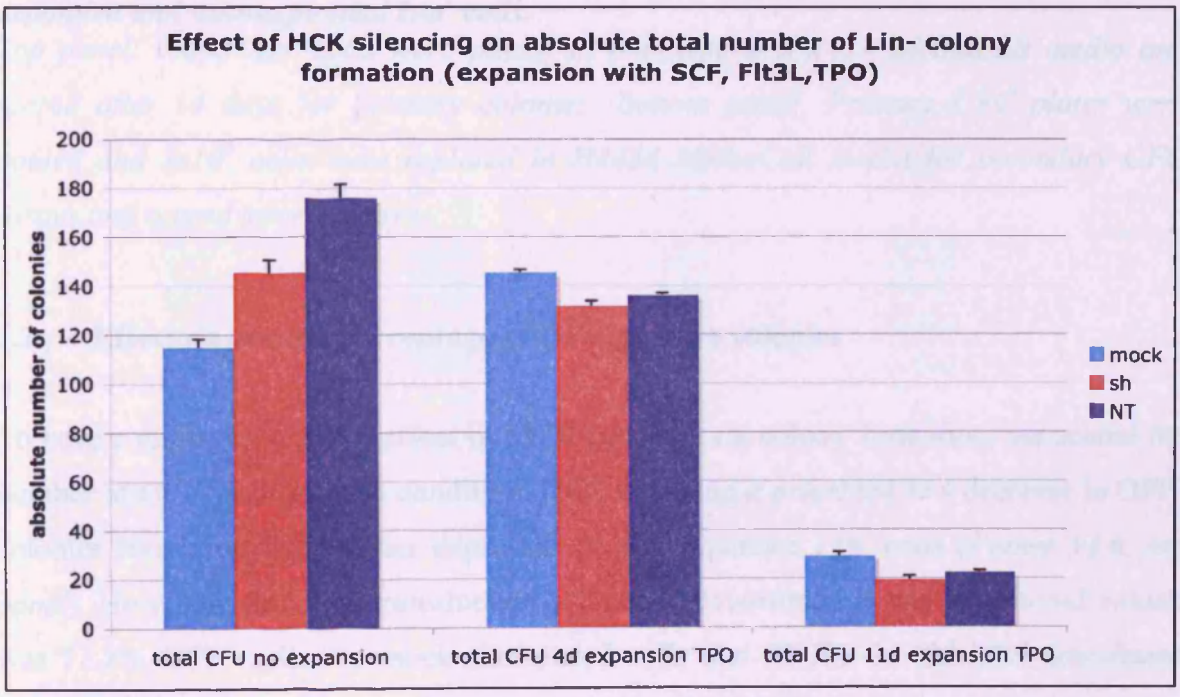

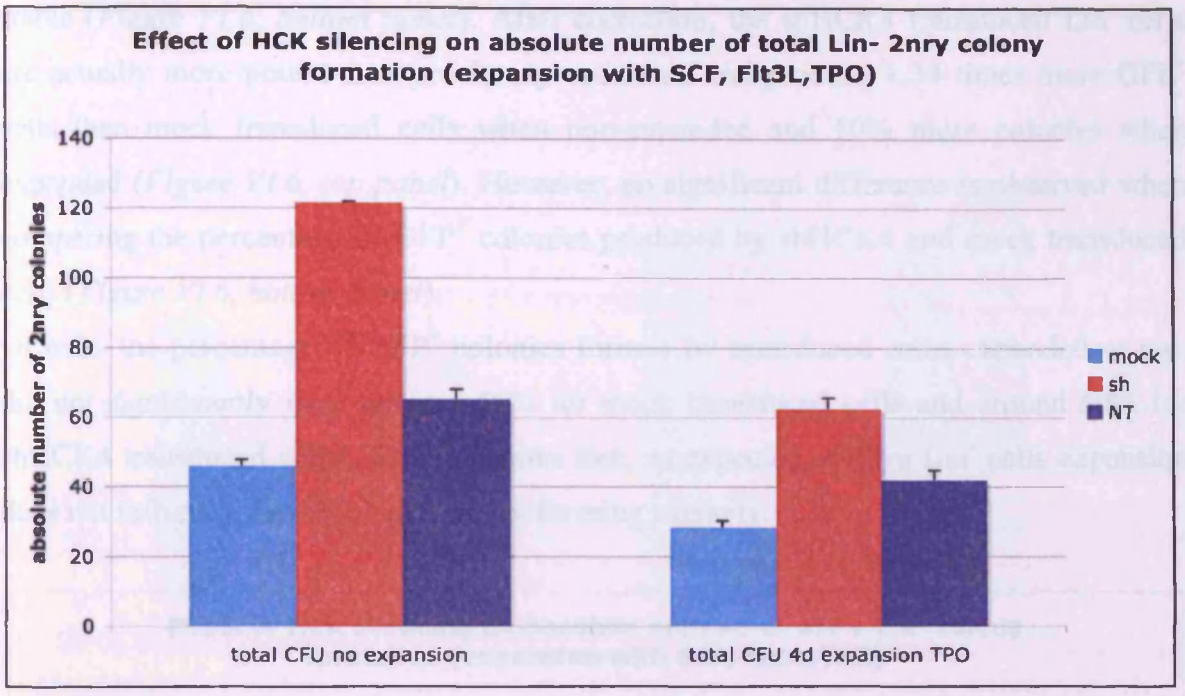


***Figure VI.5: Absolute number of total primary and secondary colonies generated by expanded and non-expanded Lin⁻ cells.***

*Top panel: 1,000 Lin⁻ cells were plated in triplicate in H4434 MethoCult media and scored after 14 days for primary colonies. Bottom panel: Primary CFC plates were pooled and $2x10^6$ cells were replated in H4434 MethoCult media for secondary CFC assays and scored after 12 days.*

## 2.2 Effect on overall percentage of GFP positive colonies

To have a closer look at the effect of HCK silencing on colony formation, we scored the number of $GFP^+$ cells in each condition. HCK silencing *a priori* led to a decrease in $GFP^+$ colonies formation from either expanded or non-expanded $Lin^-$ cells (*Figure VI.6, top panel*). However, since the transduction efficiency determined at day 4 in liquid culture was 77.2% $GFP^+$ cells for mock transduced cells and 46.7% for shHCK4 transduced cells, it was necessary to correct the number of $GFP^+$ colonies generated by the percentage of $GFP^+$ cells they are originating from (*Figure VI.6, top panel*). Although the original percentage of $GFP^+$ cells seeded for non-expanded $Lin^-$ cells cannot be determined at such an early time point, we extrapolated the correction based on the fact that the percentage of $GFP^+$ colonies generated by expanded or non-expanded cells was

stable (*Figure VI.6, bottom panel*). After correction, the shHCK4 transduced Lin$^-$ cells are actually more potent than previously estimated and produce 1.34 times more GFP$^+$ cells than mock transduced cells when non-expanded and 10% more colonies when expanded (*Figure VI.6, top panel*). However, no significant difference is observed when comparing the percentage of GFP$^+$ colonies produced by shHCK4 and mock transduced cells (*Figure VI.6, bottom panel*).

Of note, the percentage of GFP$^+$ colonies formed by transduced cells, expanded or not, did not significantly vary (around 50% for mock transduced cells and around 60% for shHCK4 transduced cells). This indicates that, as expected, 4 days Lin$^-$ cells expansion does not influence their intrinsic colony forming capacity.

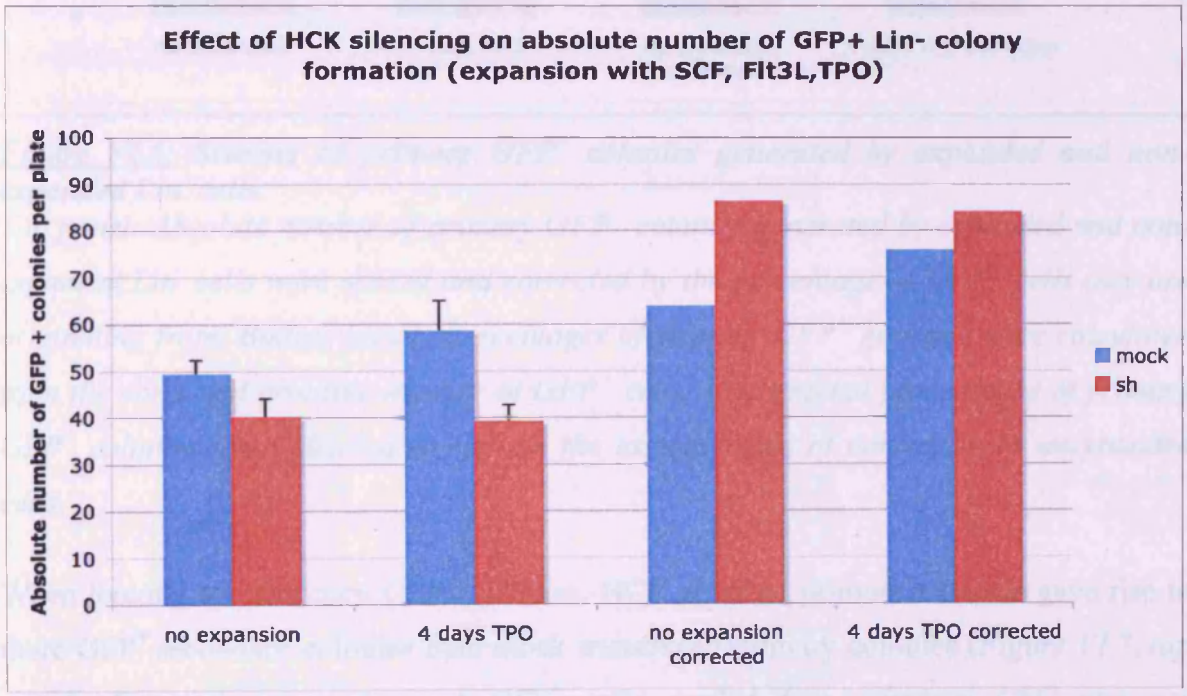

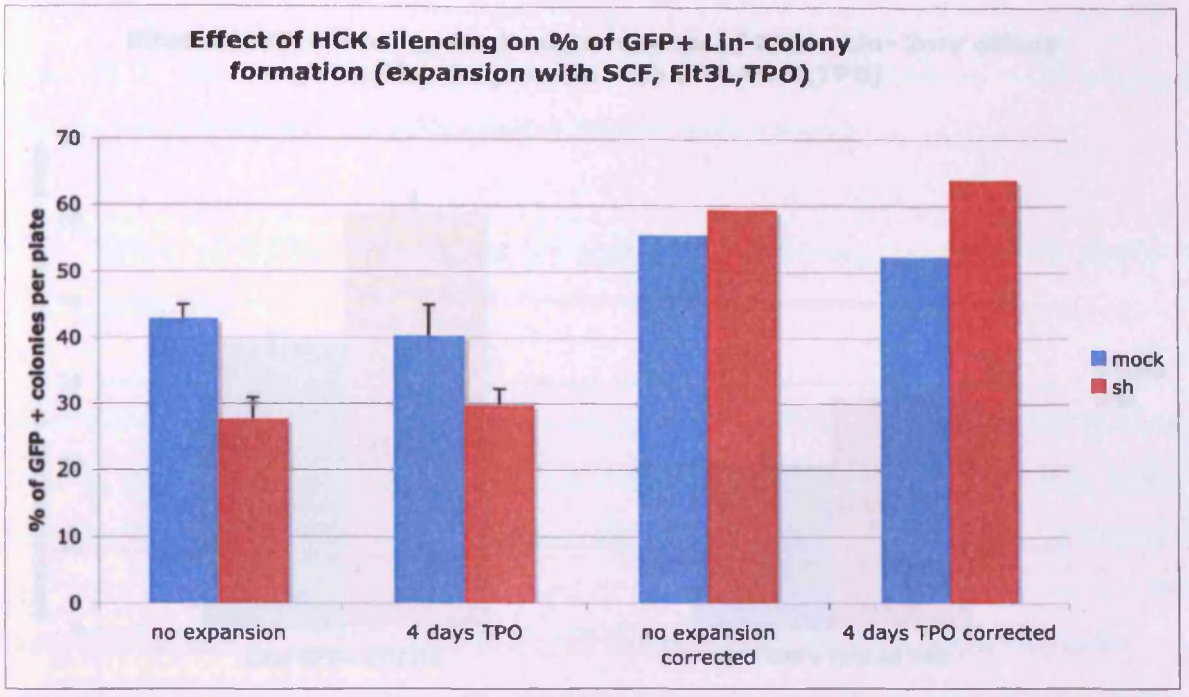


***Figure VI.6:*** ***Scoring of primary GFP$^+$ colonies generated by expanded and non-expanded Lin$^-$ cells.***
*Top panel: Absolute number of primary GFP$^+$ colonies generated by expanded and non-expanded Lin$^-$ cells were scored and corrected by the percentage of GFP$^+$ cells they are originating from. Bottom panel: Percentages of primary GFP$^+$ colonies were calculated from the corrected absolute number of GFP$^+$ cells. Uncorrected percentages of primary GFP$^+$ colonies are indicated to explain the extrapolation of correction to unexpanded cells.*

When looking at secondary GFP$^+$ colonies, HCK silenced primary colonies gave rise to more GFP$^+$ secondary colonies than mock transduced primary colonies (*Figure VI.7, top panel*). Since the percentage of GFP$^+$ cells seeded for secondary CFC was not determined, no correction can be applied to this graphical representation. However, when looking at uncorrected percentages of GFP$^+$ cells, we can conclude that although shHCK4 transduced primary colonies gave rise to more total secondary colonies than mock transduced Lin$^-$ colonies, they contain a constant proportion of GFP$^+$ colonies, indicating that HCK silencing does not confer any advantage to the shHCK4 transduced cells.

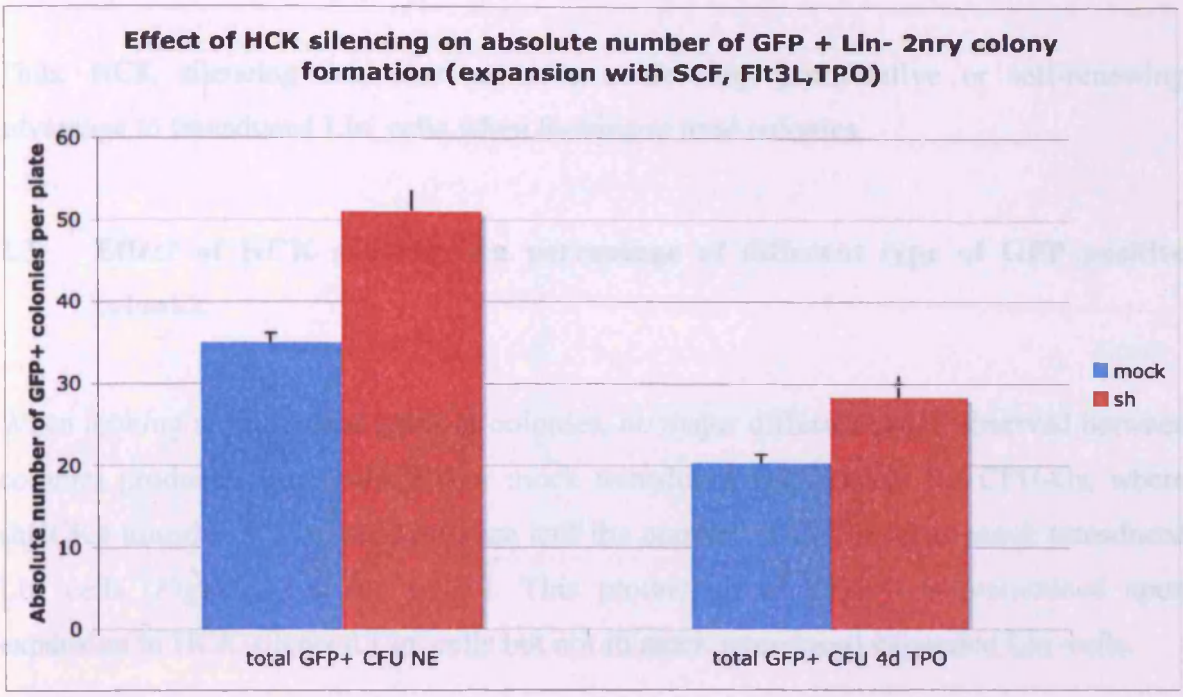


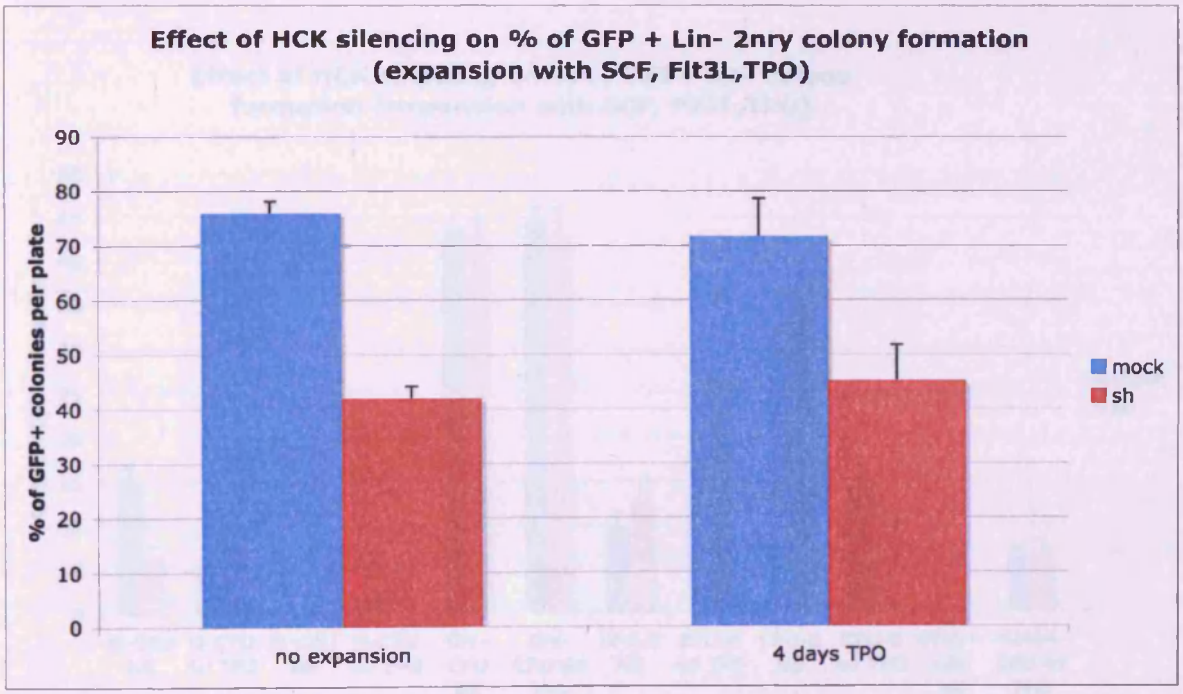


***Figure VI.7:* Scoring of secondary $GFP^+$ colonies generated by expanded and non-expanded $Lin^-$ cells.**

*Top panel: Absolute number of secondary $GFP^+$ colonies generated by expanded and non-expanded $Lin^-$ cells were scored 12 days after replating. Bottom panel: Percentages of secondary $GFP^+$ colonies were calculated from the total number of secondary colonies and the uncorrected absolute number of $GFP^+$ cells.*

Thus, HCK silencing does not seem to confer any proliferative or self-renewing advantage to transduced Lin$^-$ cells when looking at total colonies.

## 2.3 Effect of HCK silencing on percentage of different type of GFP positive colonies

When looking at individual types of colonies, no major differences are observed between colonies produced from shHCK4 or mock transduced cells except for CFU-Gs, where shHCK4 transduced Lin$^-$ cells produce half the number of CFU-G than mock transduced Lin$^-$ cells (*Figure VI.8, top panel*). This production of CFU-G is maintained upon expansion in HCK silenced Lin$^-$ cells but not in mock transduced expanded Lin$^-$ cells.

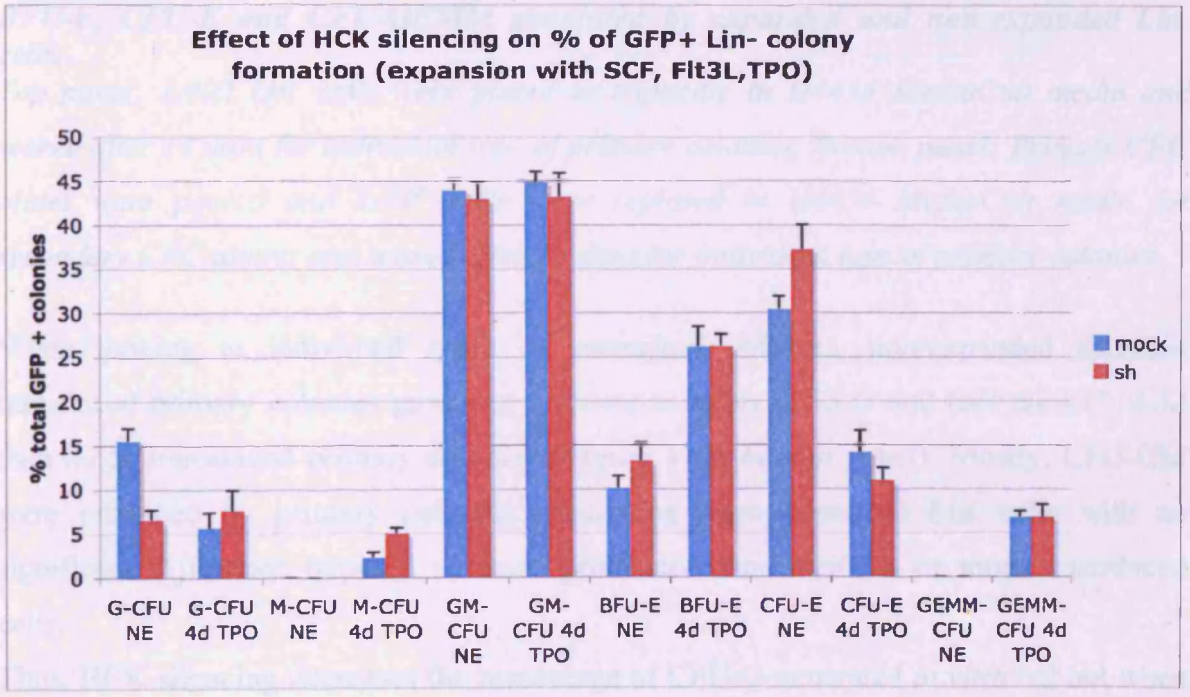

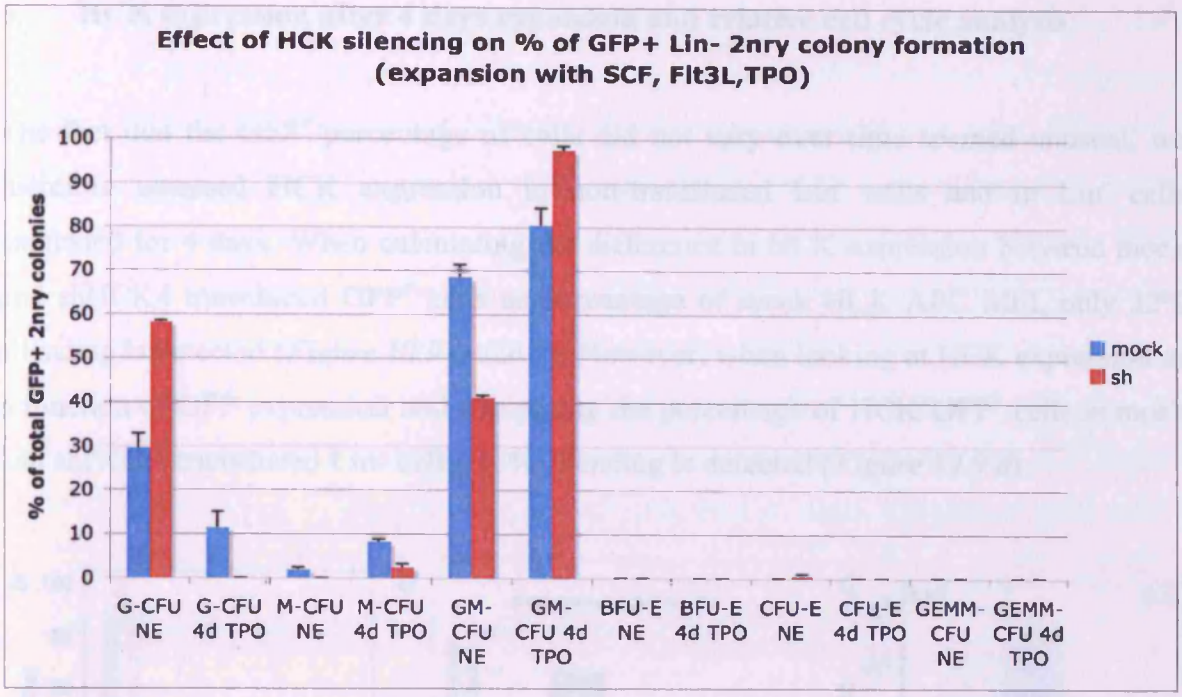


***Figure VI.8:** Percentage of primary and secondary GFP$^+$ CFU-G, CFU-GM, CFU-M, BFU-E, CFU-E and CFU-GEMM generated by expanded and non-expanded Lin$^-$ cells.*

*Top panel: 1,000 Lin$^-$ cells were plated in triplicate in H4434 MethoCult media and scored after 14 days for individual type of primary colonies. Bottom panel: Primary CFC plates were pooled and 2x10$^6$ cells were replated in H4434 MethoCult media for secondary CFC assays and scored after 12 days for individual type of primary colonies.*

When looking at individual types of secondary colonies, non-expanded shHCK4 transduced primary colonies gave rise to twice as many CFU-G and half the CFU-GM than mock transduced primary colonies (*Figure VI.8, bottom panel*). Mostly, CFU-GM were produced by primary colonies originating from expanded Lin$^-$ cells with no significant difference between colonies produced from shHCK4 or mock transduced cells.

Thus, HCK silencing decreases the percentage of CFU-G generated *in vitro* but not when Lin$^-$ cells have previously been expanded in culture. This observation should however be verified in an LTC-IC assay.

### 3. HCK expression after 4 days expansion and relative cell cycle analysis

The fact that the $GFP^+$ percentage of cells did not vary over time seemed unusual, we therefore assessed HCK expression in non-transduced $Lin^-$ cells and in $Lin^-$ cells expanded for 4 days. When calculating the difference in HCK expression between mock and shHCK4 transduced $GFP^+$ cells as percentage of mock HCK APC MFI, only 32% silencing is detected (*Figure VI.9 a* and *b*). However, when looking at HCK expression as a function of GFP expression and comparing the percentage of $HCK^+GFP^+$ cells in mock and shHCK4 transduced Lin- cells, 61% silencing is detected (*Figure VI.9 d*).

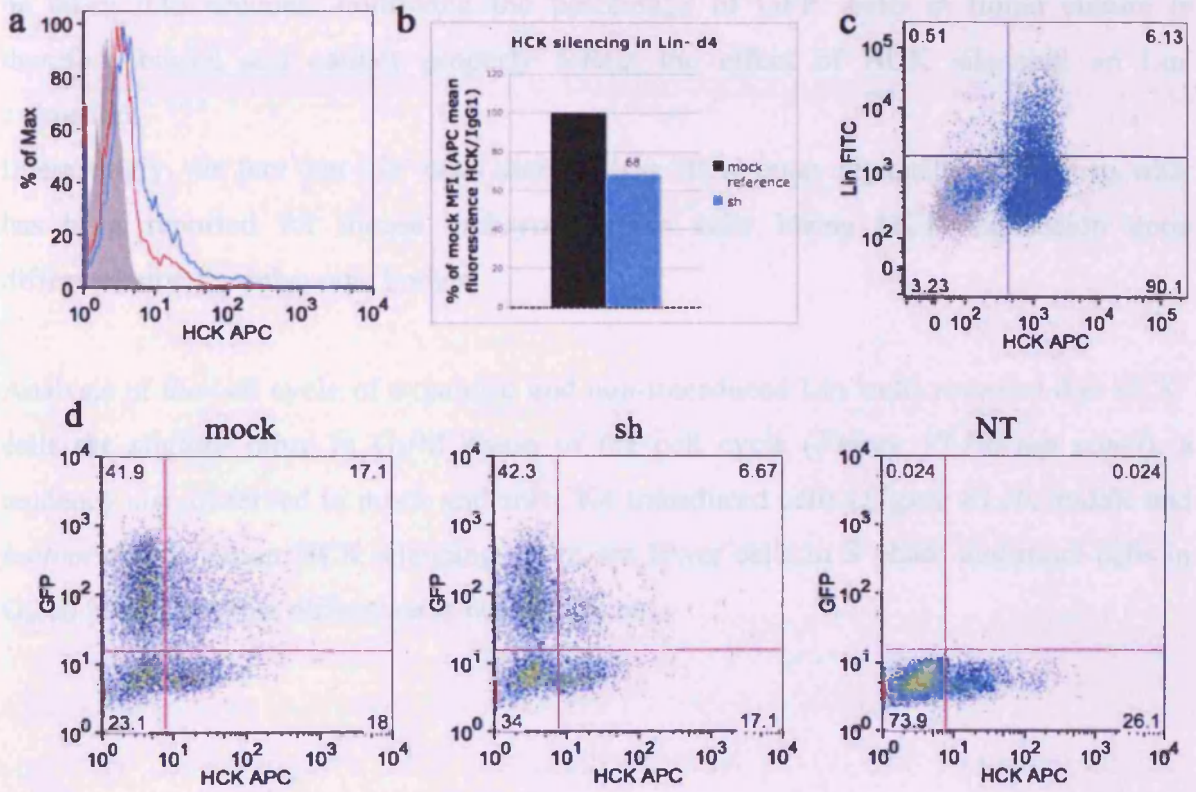


***Figure VI.9: HCK expression in GFP⁺ cells after 4 days expansion.***
*(a) HCK expression in mock and shHCK4 transduced $GFP^+$ cells. (b) HCK expression in mock and shHCK4 transduced $GFP^+$ cells represented as percentage of mock HCK APC MFI. (c) HCK expression as a function of Lin expression in non-expanded $Lin^-$ enriched UCB. (d) HCK expression as a function of GFP expression in mock transduced, shHCK4 transduced and non-transduced $Lin^-$ cells.*

Of note, after 4 days expansion only 26% of non-transduced cells (NT) were $HCK^+$ while staining of unmanipulated $Lin^-$ cells showed that more than 95% of $Lin^-$ cells originally express HCK at the protein level (*Figure VI.9 c*). In mock transduced cells, 18% of the cells express HCK but were left non-transduced ($HCK^+GFP^-$), a percentage that did not vary in shHCK4 transduced cells. Moreover, 42% of mock transduced cells were $GFP^+$ but did not express HCK (in this experiment 50% for both mock and shHCK4 transduced $Lin^-$ cells, as detected by flow cytometry prior to fixation). Thus, the fact that the percentage of $GFP^+$ cells in *ex vivo* expansion liquid culture comprises cells that are $GFP^+$ and have lost HCK expression upon expansion, as well as cells that still express HCK at a lower level in shHCK4 transduced cells than in mock transduced cells, has to be taken into account. Following the percentage of $GFP^+$ cells in liquid culture is therefore biased and cannot properly reflect the effect of HCK silencing on $Lin^-$ expansion.

Interestingly, the fact that $Lin^-$ cells seem to lose HCK upon expansion reminds us what has been reported for mouse embryonic stem cells losing HCK expression upon differentiation to embryonic bodies.

Analysis of the cell cycle of expanded and non-transduced $Lin^-$ cells revealed that $HCK^+$ cells are slightly more in $G_2$/M phase of the cell cycle (*Figure VI.10, top panel*), a tendency also observed in mock and shHCK4 transduced cells (*Figure VI.10, middle* and *bottom panel*). Upon HCK silencing, there are fewer cells in S phase and more cells in $G_0/G_1$ phase, but this difference is not significant.

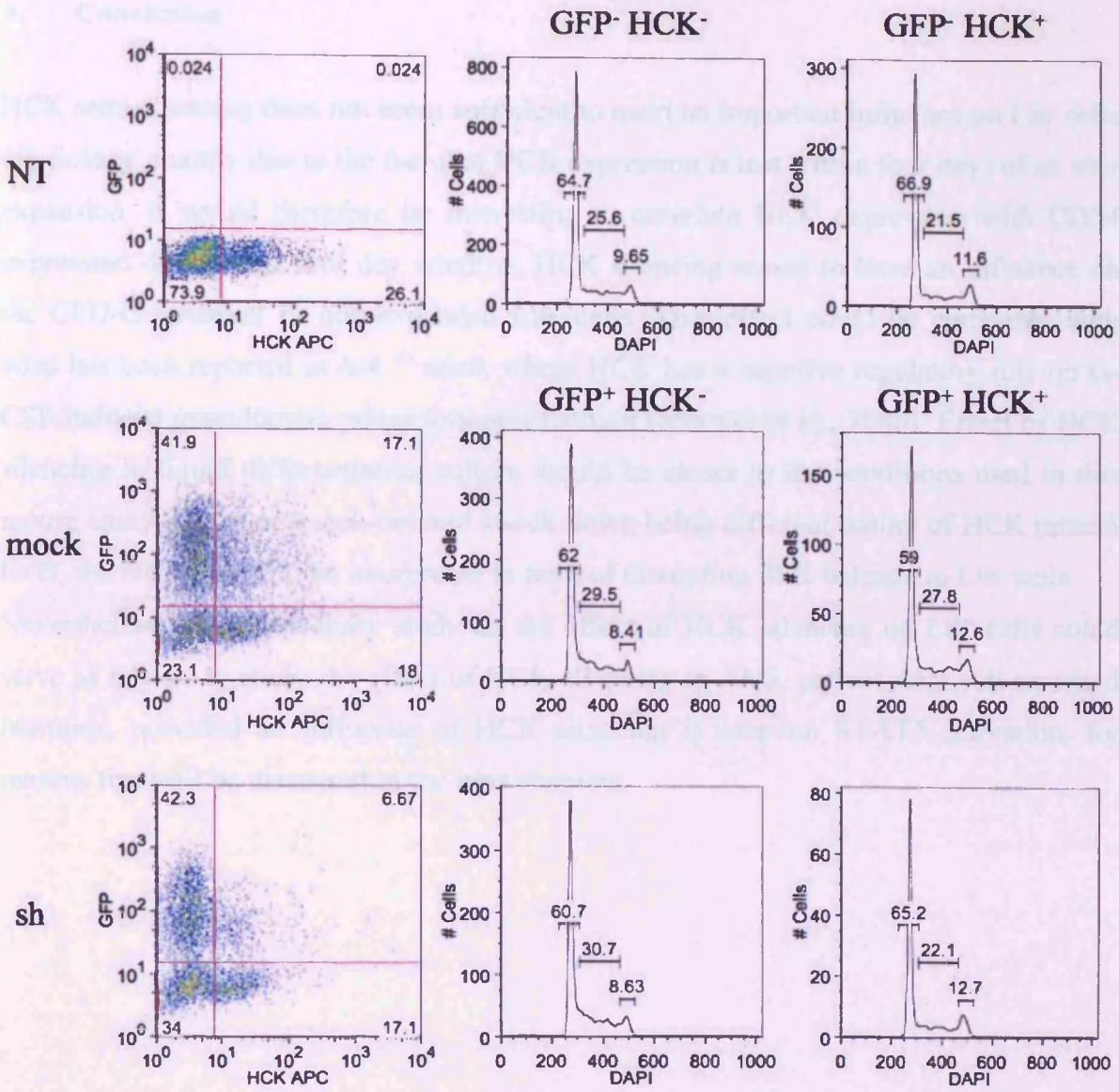


***Figure VI.10:*** ***Cell cycle analysis in HCK⁻ and HCK⁺ cells after 4 days expansion.***
*Top panel: Cell cycle analysis of HCK⁻ and HCK⁺ non-transduced cells. Middle panel: Cell cycle analysis of GFP⁺ HCK⁻ and GFP⁺ HCK⁺ mock transduced cells. Bottom panel: Cell cycle analysis of GFP⁺ HCK⁻ and GFP⁺ HCK⁺ shHCK4 transduced cells.*

## 4. Conclusion

HCK semi-silencing does not seem sufficient to exert an important influence on $Lin^-$ cells physiology, mainly due to the fact that HCK expression is lost within four days of *ex vivo* expansion. It would therefore be interesting to correlate HCK expression with CD34 expression during this four day window. HCK silencing seems to have an influence on the CFU-G potential of non-expanded $Lin^-$ cells. This effect could be correlated with what has been reported in *hck* $^{-/-}$ mice, where HCK has a negative regulatory role on G-CSF induced granulocytic precursors proliferation (Mermel et al., 2006). Effect of HCK silencing in liquid differentiation culture would be closer to the conditions used in this mouse study, however knock-out and knock-down being different tuning of HCK protein level, the results have to be interpreted in term of disrupting SFK balance in $Lin^-$ cells. Nevertheless, this preliminary study on the effect of HCK silencing on $Lin^-$ cells could serve as a basis to study the effect of HCK silencing in AML patient stem cell enriched fractions, provided an influence of HCK silencing is seen on STAT5 activation, for reasons that will be discussed in the next chapters.

# Chapter VII

# VII HCK expression in patient samples

Blood patient samples obtained by leukapheresis or venepuncture were collected with informed consent and stored in the Centre for Medical Oncology, John Vane Science Centre, Charterhouse Square, London. Whole mononuclear cells were enriched from the patient sample by density centrifugation as described in Chapter II. Mononuclear cells from 34 patient samples were used to produce the results presented below. These samples were processed for RNA extraction, Western blot or flow cytometry analysis.

## 1. Karyotype, FAB class and NPM11 mutation status of the AML patients used in this study

AML patient samples used in this chapter are summarised in *Table VII.1*, organised according to their FAB class (M1 to M5).

| Patient | Karyotype | FAB class | NPM11 mutation |
|---|---|---|---|
| 23 | -5q | M1 | ND |
| 17 | +8 | M1 | ND |
| 1 | NK | M1 | Yes |
| 12 | NK | M1 | Yes |
| 24 | +13 | M1 | ND |
| 13 | t(6,11), +9 | M1 t-AML | ND |
| 18 | del5,der12,ins12(q22) | M1 tAML | No |
| 25 | ND | M1 | ND |
| 26 | +12, +21 | M2 | ND |
| 14 | +11, +13 | M2 | No |
| 6 | Complex | M2-tAML | No |
| 27 | t(8,21)+8, -5q | M2 | No |
| 7 | t(8;21) | M2 | No |
| 28 | t(8,21) | M2 | No |
| 2 | NK | M2 | ND |
| 5 | NK | M2 | ND |
| 19 | NK | M2eo | No |
| 20 | NK | M2eo | ND |
| 3 | +3, +10 | M4 | Yes |
| 29 | NK | M4 | Yes |
| 15 | NK | M4 | No |
| 21 | NK | M4 | ND |
| 4 | NK | M4 | ND |
| 30 | ins (6;11) | M4 | ND |
| 31 | inv(16) | M4eo | ND |
| 16 | (3-9) del | M5 | No |
| 32 | NK | M5a | ND |
| 33 | t(11,19) | M5a | No |
| 34 | inv(3),-7 | ND | No |
| 35 | +13 | ND | ND |
| 36 | t(3;14) | ND | ND |
| 37 | inv(16) | ND | ND |
| 38 | NK | ND | Yes |
| 22 | ND | ND | ND |

***Table VII.1:** Karyotype, FAB class and nucleophosmin (NPM11) mutation status of the AML patient samples used in this study.*

## 2. HCK expression in MNC at the RNA level

Since we could successfully relate HCK expression and FAB classification in AML cell lines, we assessed if the same would be true for MNC from patient samples. We could however not find any correlation between FAB class and HCK expression, all patient samples were expressing HCK at levels superior to that of Mono-mac-6 cells (one of the cell lines tested expressing the highest level of HCK) (*Figure VII.1*). Two individual UCB MNC samples and one pool UCB MNC sample, used for comparison, also express higher levels of HCK than Mono-mac-6 cells, probably due to their high content in macrophages and granulocytes known to highly express HCK.

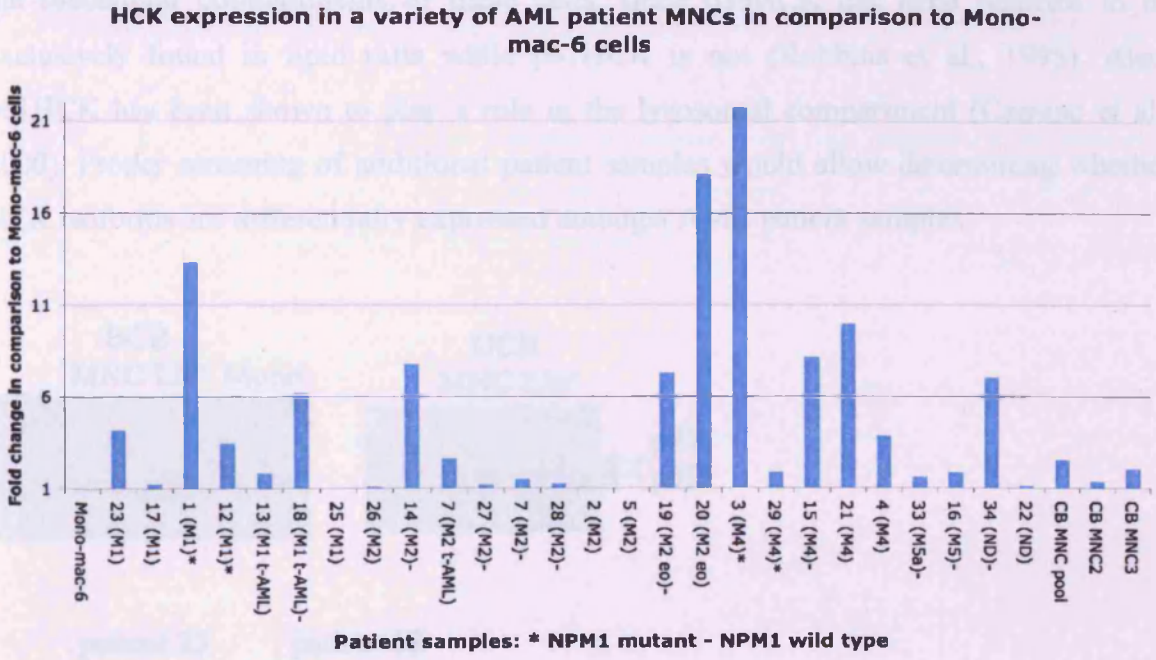


***Figure VII.1:* HCK expression in mononuclear cells from 26 AML patient samples.** *HCK expression was assessed by quantitative real-time PCR using SYBR® green. GAPDH was used to normalise the values of mRNA expression. Results are expressed as fold change in comparison to the Mono-mac-6 cell line.*

### 3. HCK expression in MNC at the protein level assessed by Western Blot

We went on to look at HCK isoforms expression by Western blot in two AML samples and two UCB pools (*Figure VII.2*). We could observe that p59HCK is preferentially expressed in UCB in comparison to p61HCK. Both isoforms seem to be expressed in similar quantities in patient sample 12 in either fraction tested while in patient 25, HCK isoforms expression seems to be similar to what was observed in UCB. Relative quantitation data between $Lin^-$, $Lin^+$ and bulk MNC fractions cannot be extracted from the blots since less total protein seems to have been loaded in the MNC lane according to the β-actin loading controls. However, the difference in isoforms expressed by MNC from UCB or patient samples might reflect a difference in maturation and functionality of the subcellular compartments of these cells, since p59HCK has been reported to be exclusively found in lipid rafts while p61HCK is not (Robbins et al., 1995). Also, p61HCK has been shown to play a role in the lysosomal compartment (Carreno et al., 2000). Proper screening of additional patient samples would allow determining whether HCK isoforms are differentially expressed amongst AML patient samples.

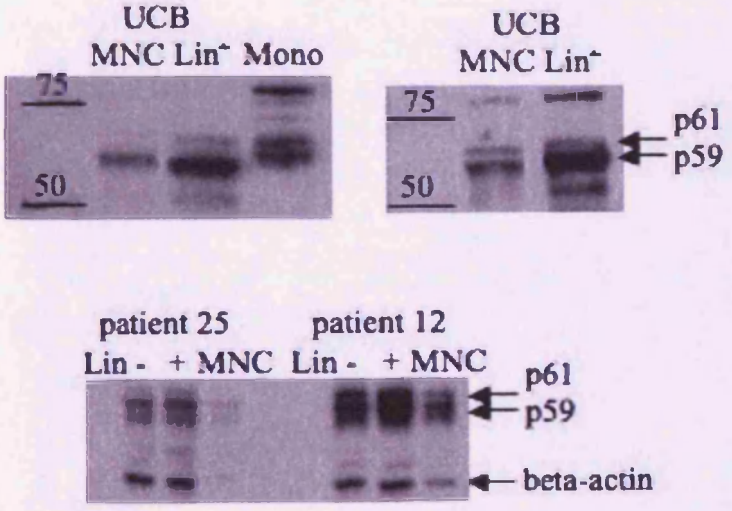


***Figure VII.2:* HCK expression in $Lin^-$, $Lin^+$ and bulk mononuclear cells from two AML samples and from umbilical cord blood.**
*Top panel: HCK expression in UCB bulk MNC and $Lin^+$ cells from 2 independent UCB pool. Mono-mac-6 cells were taken as control. Bottom panel: HCK expression in $Lin^-$, $Lin^+$ and bulk MNC from 2 AML patient samples (patient 25 and patient 12). $Lin^-$ and*

*$Lin^+$cells were separated by magnetic separation using a colloid labelled Lineage antibody cocktail.*

## 4. HCK expression in MNC at the protein level assessed by flow cytometry

We also assessed, by flow cytometry, if HCK was expressed uniformly within MNC from 8 AML patient samples and whether we could fractionate subpopulations expressing different levels of HCK (*Figure VII.3*). Umbilical cord blood MNC pools were used as a reference and gave rise to 3 distinct populations expressing various levels of HCK (*Figure VII.3 a*) that could also be separated into two distinct populations according to HCK phosphorylation level (*Figure VII.3 b*). Levels of HCK expression were variable between the patient samples tested and cells could be separated into 2 to 3 distinct subpopulations, according to their level of HCK expression, in 7/8 cases (*Figure VII.3 c, e, g, I, k, m, o*; except for patient 25 where only one population is observed *Figure VII.3 q*). HCK was found constitutively activated in 4/7 cases, as shown by staining for phosphorylated HCK Y411 (*Figure VII.3 d, f, h, j, l, p, r*; except for patient 30 where the Y411 staining is not reliable *Figure VII.3 n*).

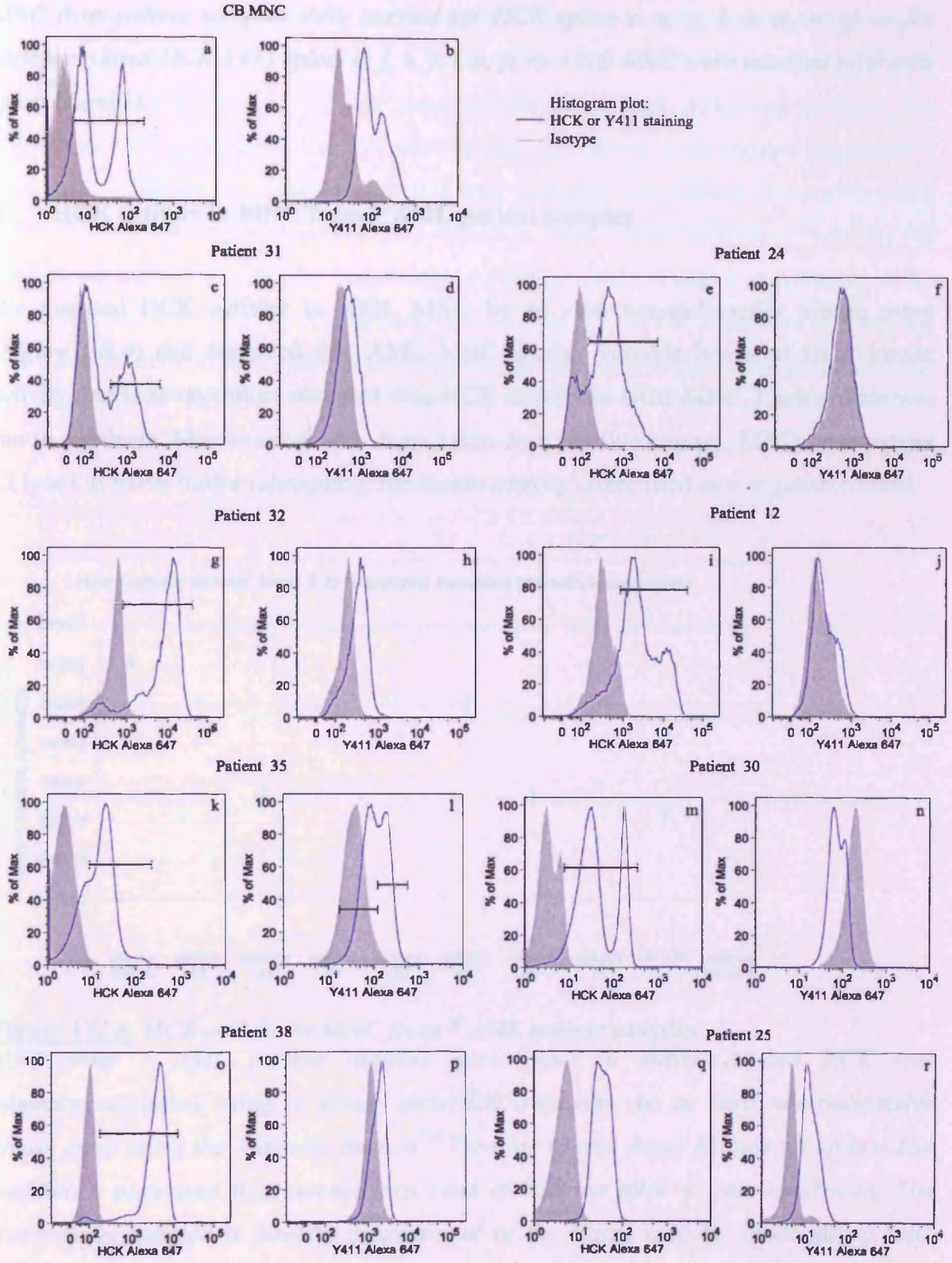


***Figure VII.3:*** ***HCK expression and phosphorylation status in MNC from 8 AML patient samples.***

*MNC from patient samples were stained for HCK (plots c, e, g, i, k, m, o, q) or for phosphorylated HCK Y411 (plots d, f, h, j, l, n, p, r). UCB MNC were taken as reference (plots a and b).*

## 5. HCK activity in MNC from 7 AML patient samples

We assessed HCK activity in AML MNC by *in vitro* non-radioactive kinase assay (*Figure VII.4*) and observed that AML MNC display variable levels of HCK kinase activity that is always more elevated than HCK activity in UCB MNC. Each sample was run in duplicate. Mono-mac-6 cells were taken as a positive control. MNC from patient 12 lysed in RIPA buffer (abrogating the kinase activity) were used as a negative control.

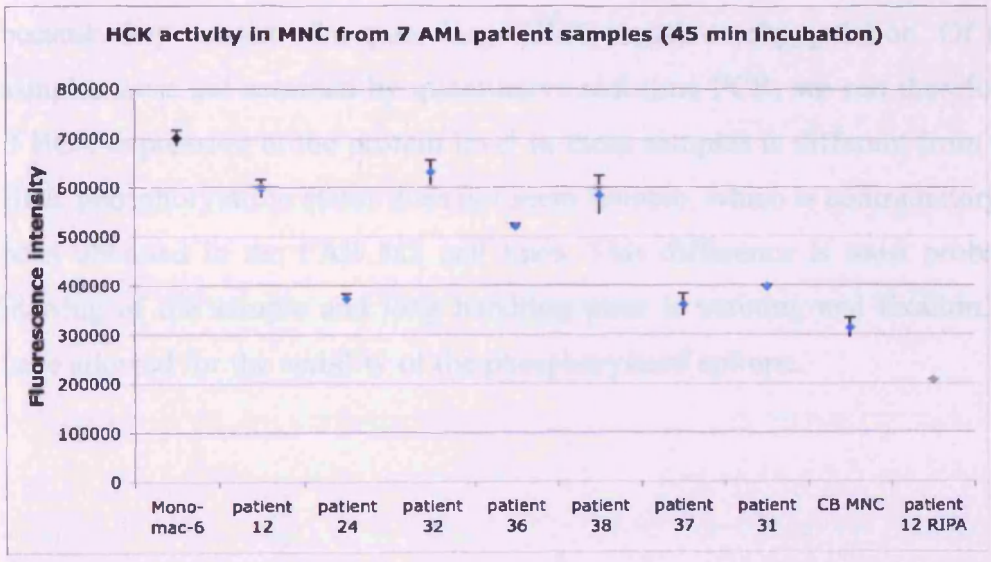


***Figure VII.4: HCK activity in MNC from 7 AML patient samples.***
*MNC from 7 AML patient samples were lysed in buffer A and HCK was immunoprecipitated using a mouse anti-HCK antibody. An in vitro non-radioactive kinase assay using the Antibody Beacon™ Tyrosine Kinase Assay Kit was set up in a 384 well black plate and fluorescence was read at 530 nm after 45 min incubation. The fluorescence emitted is directly proportional to the kinase activity. Mono-mac-6 cells were taken as a positive control. MNC from patient 12 lysed in RIPA buffer were used as a negative control.*

We then compared *in vitro* HCK activity to HCK expression and phosphorylation levels measured by FACS (*Table VII.2*). Fold differences in HCK expression, HCK phosphorylation and HCK activity were calculated as fold difference between the normalised MFI of the HCK positive population(s) of a given AML sample (as indicated by a gate on the flow cytometry plots in *Figure VII.3*) in comparison to the normalised MFI of the HCK positive populations of UCB MNC; fold difference between the normalised MFI of the Y411 population(s) of a given AML sample in comparison to the normalised MFI of the Y411 populations of UCB MNC and fold difference between the fluorescence intensity of a given AML sample in comparison to the fluorescence intensity of UCB MNC.

HCK expression and HCK activity show the same trend for each sample studied, e.g. samples with the highest levels of HCK expression have also the highest HCK *in vitro* activity. Patients 31 and 24 are shown to overall express less HCK than UCB MNC because they consist of a quite large HCK negative subpopulation. Of note, these two samples were not assessed by quantitative real-time PCR, we can therefore not establish if HCK expression at the protein level in these samples is different from the RNA level. HCK phosphorylation status does not seem reliable, which is contradictory with what has been obtained in the FAB M5 cell lines. This difference is most probably due to the thawing of the sample and long handling prior to staining and fixation, that might not have allowed for the stability of the phosphorylated epitope.

| Patient / Fold change | 12 | 31 | 24 | 32 | 30 | 38 | 25 | 35 | 36 | 37 |
|---|---|---|---|---|---|---|---|---|---|---|
| HCK | + | -- | - | ++ | + | ++ | = | + | ND | ND |
| Y411 | -- | -- | -- | -- | -- | -- | - | - | ND | ND |
| HCK activity | + | + | + | ++ | ND | + | ND | ND | + | + |

***Table VII.2:* Comparison between HCK expression, HCK Y411 phosphorylation measured by flow cytometry and HCK activity measured by non-radioactive in vitro kinase assay in MNC from AML patient samples.**

*'++' indicates a two fold increase (or higher), '+' indicates less than two fold increase, '--' indicates a two fold decrease (or lower), '-' indicates less than two fold decrease. Fold differences in HCK expression, HCK phosphorylation and HCK activity were calculated as fold difference between the normalised MFI of the HCK positive population(s) of a given AML sample (as indicated by a gate on the flow cytometry plots on Figure VII.3) in comparison to the normalised MFI of the HCK positive populations of UCB MNC; fold difference between the normalised MFI of the Y411 population(s) of a given AML sample in comparison to the normalised MFI of the Y411 populations of UCB MNC and fold difference between the fluorescence intensity of a given AML sample in comparison to the fluorescence intensity of UCB MNC.*

## 6. HCK expression in the stem cell compartment assessed by flow cytometry

Ultimately we were interested in knowing if the HCK overexpression in the AML sample $Lin^-/CD34^+/CD38^-$ fractions observed in the microarray at the RNA level, in comparison to normal bone marrow and UCB, could also be detected at the protein level and, more importantly, to determine if this overexpression was reflecting an increase in HCK activity. For this purpose, we established a protocol for external cell surface marker staining (i.e. Lineage) combined with an internal staining for HCK or phospho-HCK Y411. CD34 and CD38 antigens could not be used to successfully fractionate MNC, due to technical difficulties, we therefore went on to quantify HCK expression and phosphorylation in $Lin^-$ versus $Lin^+$ populations in 3 patient and 2 UCB samples (*Figure VII.5*).

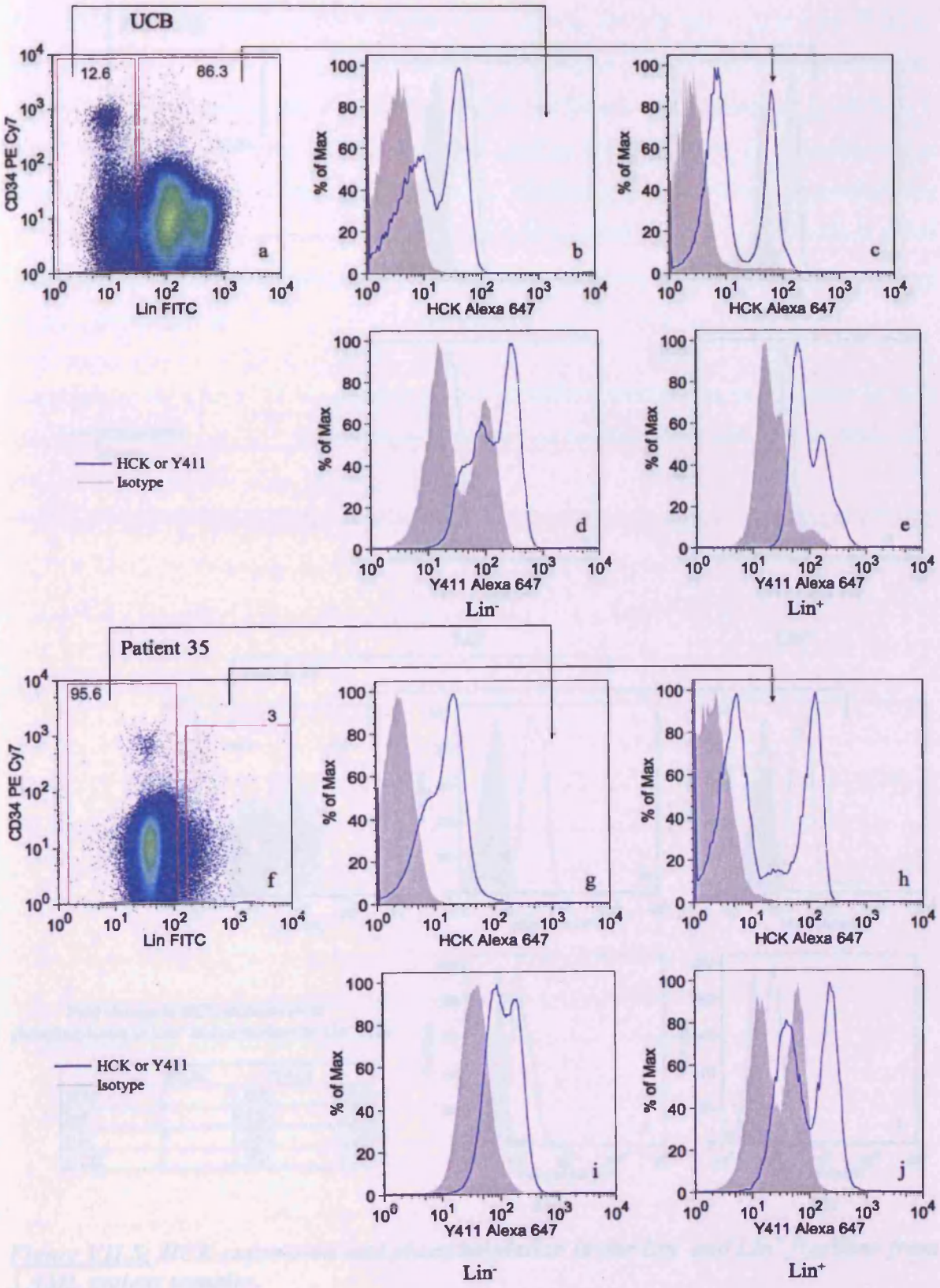
UCB
12.6
86.3
CD34 PE Cy7
Lin FITC
a
% of Max
HCK Alexa 647
b
c
HCK or Y411
Isotype
Y411 Alexa 647
d
e
Lin-
Lin+
Patient 35
95.6
3
f
g
h
i
j

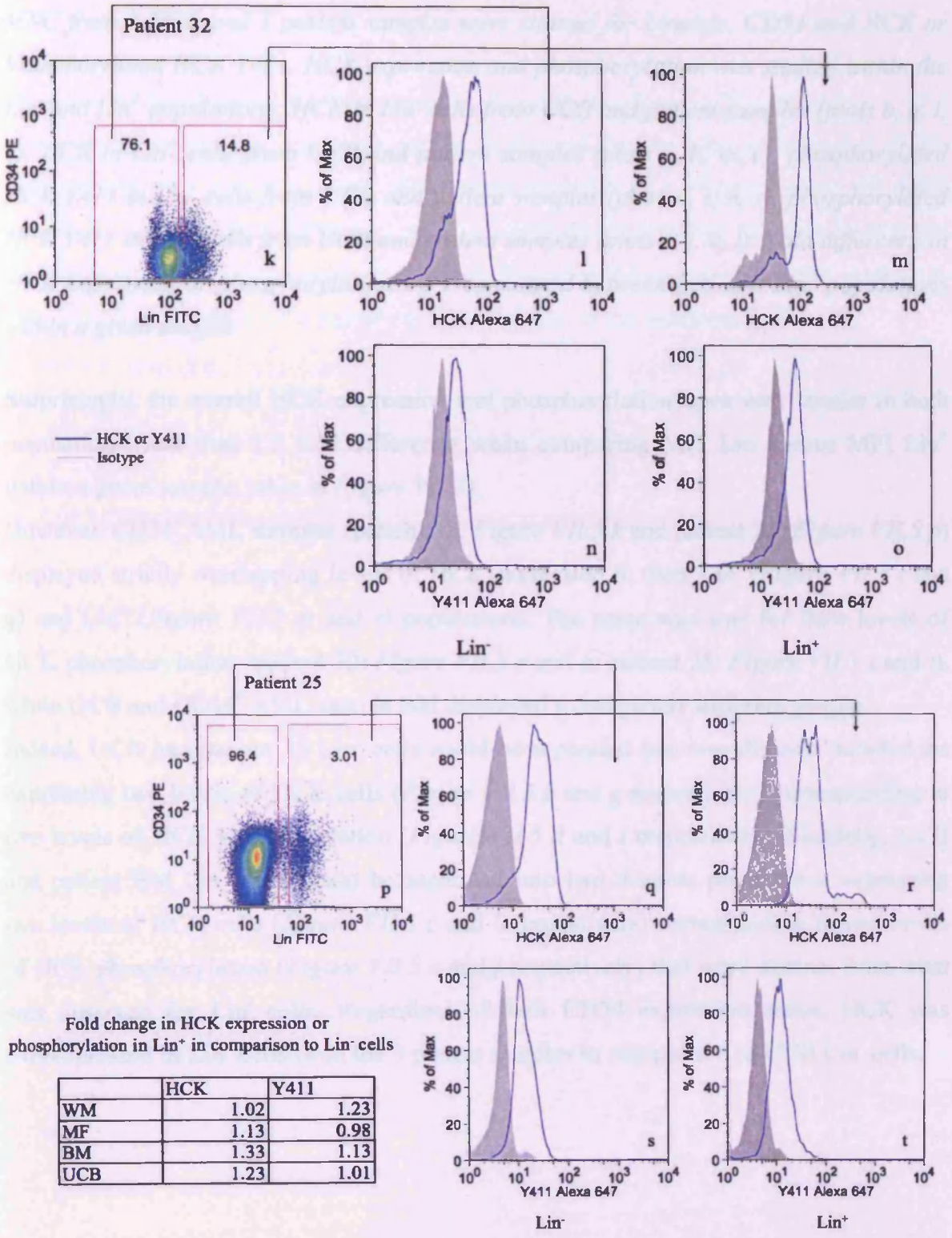


Fold change in HCK expression or phosphorylation in Lin$^+$ in comparison to Lin$^-$ cells

| | HCK | Y411 |
|---|---|---|
| WM | 1.02 | 1.23 |
| MF | 1.13 | 0.98 |
| BM | 1.33 | 1.13 |
| UCB | 1.23 | 1.01 |

***Figure VII.5:** HCK expression and phosphorylation in the Lin$^-$ and Lin$^+$ fractions from 3 AML patient samples.*

*MNC from 2 UCB and 3 patient samples were stained for Lineage, CD34 and HCK or phosphorylated HCK Y411. HCK expression and phosphorylation was studied within the Lin$^-$ and Lin$^+$ populations: HCK in Lin$^-$ cells from UCB and patient samples (plots b, g, l, q), HCK in Lin$^+$ cells from UCB and patient samples (plots c, h, m, r), phosphorylated HCK Y411 in Lin$^-$ cells from UCB and patient samples (plots d, i, n, s), phosphorylated HCK Y411 in Lin$^+$ cells from UCB and patient samples (plots e, j, o, t). Fold difference in HCK expression or phosphorylation were calculated between Lin$^-$ and Lin$^+$ populations within a given sample.*

Surprisingly, the overall HCK expression and phosphorylation were very similar in both populations (less than 1.5 fold difference when comparing MFI Lin$^-$ versus MFI Lin$^+$ within a given sample, table in *Figure VII.5*).

However, CD34$^-$ AML samples (patient 32: *Figure VII.5 k* and patient 25: *Figure VII.5 p*) displayed strictly overlapping levels of HCK expression in their Lin$^-$ (*Figure VII.5 l* and *q*) and Lin$^+$ (*Figure VII.5 m* and *r*) populations. The same was true for their levels of HCK phosphorylation (patient 32: *Figure VII.5 n* and *o;* patient 25: *Figure VII.5 s* and *t*), while UCB and CD34$^+$ AML sample BM displayed a completely different profile.

Indeed, UCB and patient 35 Lin$^-$ cells could be separated into two discrete populations expressing two levels of HCK cells (*Figure VII.5 b* and *g* respectively) corresponding to two levels of HCK phosphorylation (*Figure VII.5 d* and *i* respectively). Similarly, UCB and patient BM Lin$^+$ cells could be separated into two discrete populations expressing two levels of HCK cells (*Figure VII.5 c* and *h* respectively) corresponding to two levels of HCK phosphorylation (*Figure VII.5 e* and *j* respectively) that were distinct from what was observed for Lin$^-$ cells. Regardless of their CD34 expression status, HCK was overexpressed in Lin$^-$ cells from the 3 patient samples in comparison to UCB Lin$^-$ cells.

## 7. Conclusion

Thus, staining $Lin^-$ and $Lin^+$ AML populations for HCK expression (and phosphorylation) reveals a complex pattern of expression. Managing staining that allows fractionation of $Lin^-$ cells, could allow distinguishing of a clearer pattern of HCK expression. Screening of additional AML samples and correlating the data to Western blot data on HCK isoforms expression might allow determining whether HCK expression specifically correlates with a degree of differentiation of the primitive cells.

# Chapter VIII

# VIII Effect of HCK overexpression on UCB Lin$^-$ cells

Since in our microarray analysis, we found HCK overexpressed in the Lin$^-$/CD34$^+$/CD38$^-$ fraction from AML samples in comparison to normal bone marrow and UCB, we decided to also try to study a potential role for HCK in leukaemogenesis by overexpressing it in stem cells enriched Lin- umbilical cord blood cells. In order to ultimately work with HSC, the HCK cDNA had to be cloned into a lentiviral vector.

## 1. HCK cloning

### 1.1 Cloning of p59HCK cDNA into the pENTR1A-IRES-GFP shuttle vector

RNA was extracted from Mono-mac-6 cells and reverse transcribed into cDNA as described in Chapter II. Since we found p59HCK preferentially expressed in leukaemic MNC and this HCK isoform is known to be the one responsible for signalling in lipid raft, p59HCK cDNA was amplified by PCR using the Takara polymerase and the PCR product was cloned into the pCR® 2.1-TOPO vector by TA ligation, according to the manufacturer's instructions (Invitrogen). Presence of the p59HCK cDNA insert into the pCR® 2.1-TOPO vector was assessed by restriction digest with KpnI and NotI and four clones were sequenced using the M13 forward and reverse primer to verify the orientation of the cDNA sequence (*Figure VIII.1 a*).

p59HCK was further cloned into the pENTR1A-IRES-GFP or pENTR1A-IRES-YFP shuttle vectors to allow for subsequent Gateway crossover into a lentiviral backbone. The p59HCK fragment was cut out of the pCR® 2.1-TOPO vector with the *EcoRI* restriction enzyme and cloned into a linearised and CIPed pENTR1A-IRES-GFP or pENTR1A-IRES-YFP shuttle vector. After ligation, presence of the p59HCK insert into the pENTR1A-IRES vectors was confirmed by restriction digest with *XmaI* for pENTR1A-IRES-GFP and *BstXI* for pENTR1A-IRES-YFP. The final map of the pENTR1A-IRES-GFP shuttle vector is shown in *Figure VIII.1 b.*

a

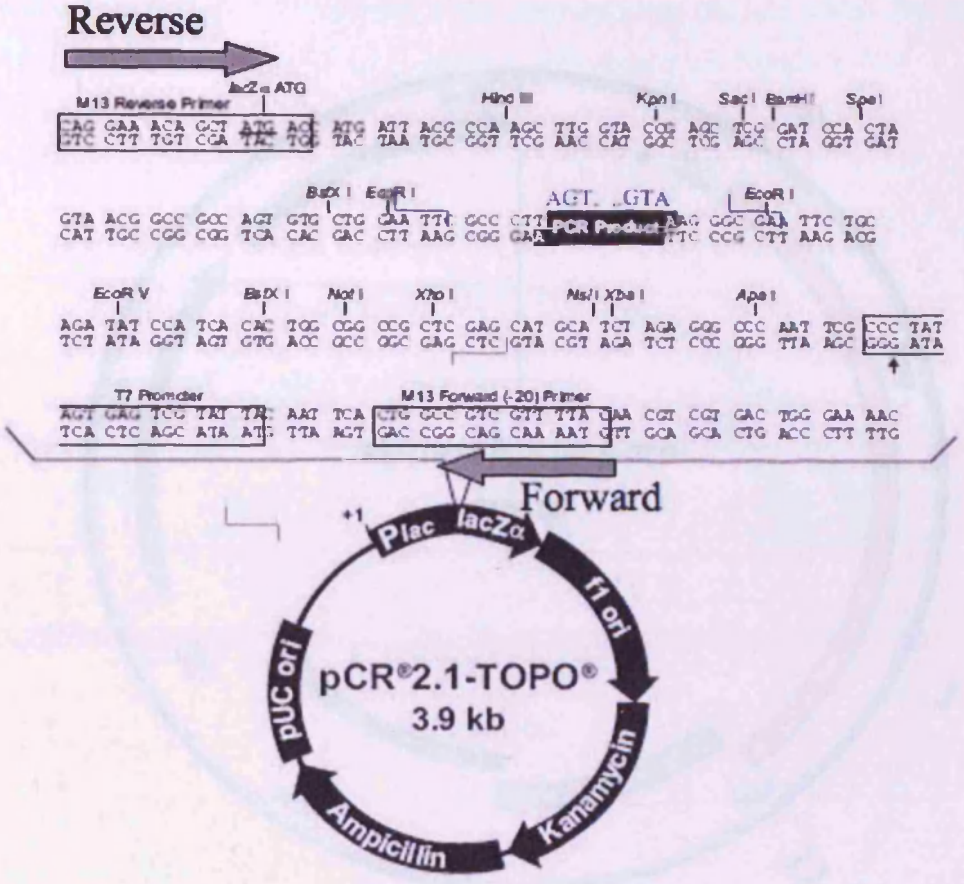
Reverse
M13 Reverse Primer
lacZ α ATG
Hind III
Kpn I
Sac I
BamH I
Spe I
BstX I
EcoR I
AGT ..GTA
PCR Product
EcoR I
EcoR V
BstX I
Not I
Xho I
Nsi I
Xba I
Ape I
T7 Promoter
M13 Forward (-20) Primer
Forward
+1
Plac
lacZα
f1 ori
pUC ori
pCR®2.1-TOPO®
3.9 kb
Ampicillin
Kanamycin

b

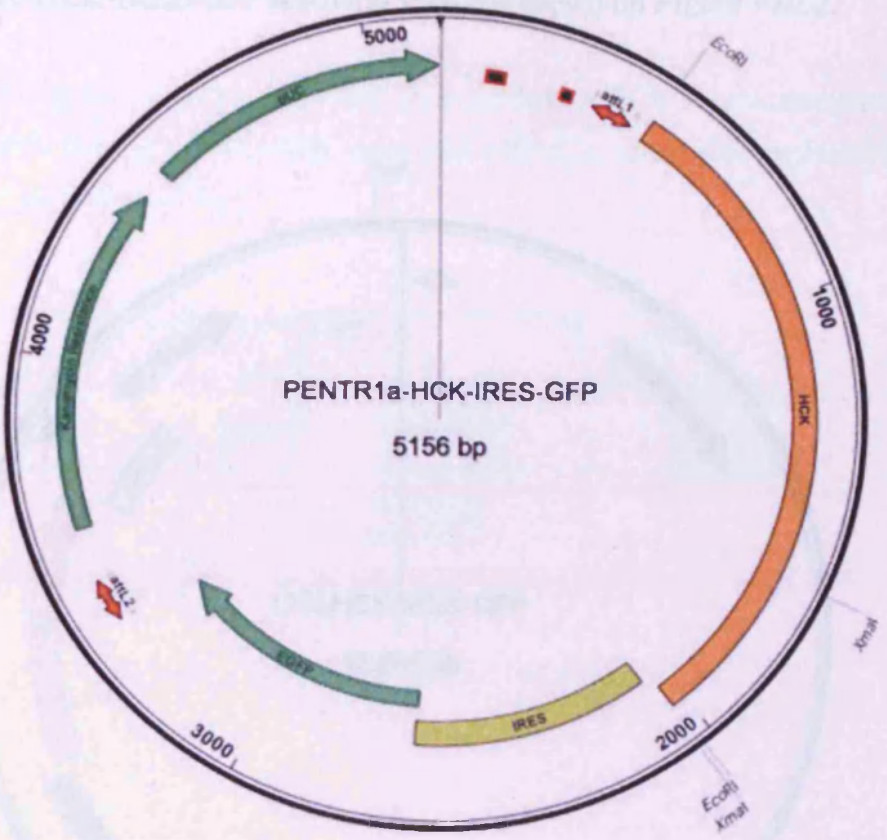


***Figure VIII.1:*** ***Cloning of p59HCK cDNA into the pENTR1A-IRES-GFP shuttle vector.***

*(a) pCR® 2.1-TOPO vector multiple cloning site (MCS) map and localisation of the primers used to assess proper cloning of p59HCK cDNA. (b) Map of the pENTR1A-HCK-IRES-GFP plasmid.*

## 1.2 Cloning of p59HCK cDNA into the LNT-Sffv-cddB-MCS lentiviral backbone

pHCK59–IRES-GFP was recombined with the LNT-Sffv-cddB-MCS lentiviral vector using the Gateway recombination technology (Invitrogen). Presence of the p59HCK-IRES-GFP insert into the lentiviral backbone was confirmed by restriction digest with *SacII* and *Age I*, which would give a 4 kb and a 8 kb fragment when HCK-IRES-GFP is

inserted and a 4 kb and a 5 kb fragment when the crossover did not occur. The final map of the LNT-Sffv-HCK-IRES-GFP lentiviral vector is shown on *Figure VIII.2*.

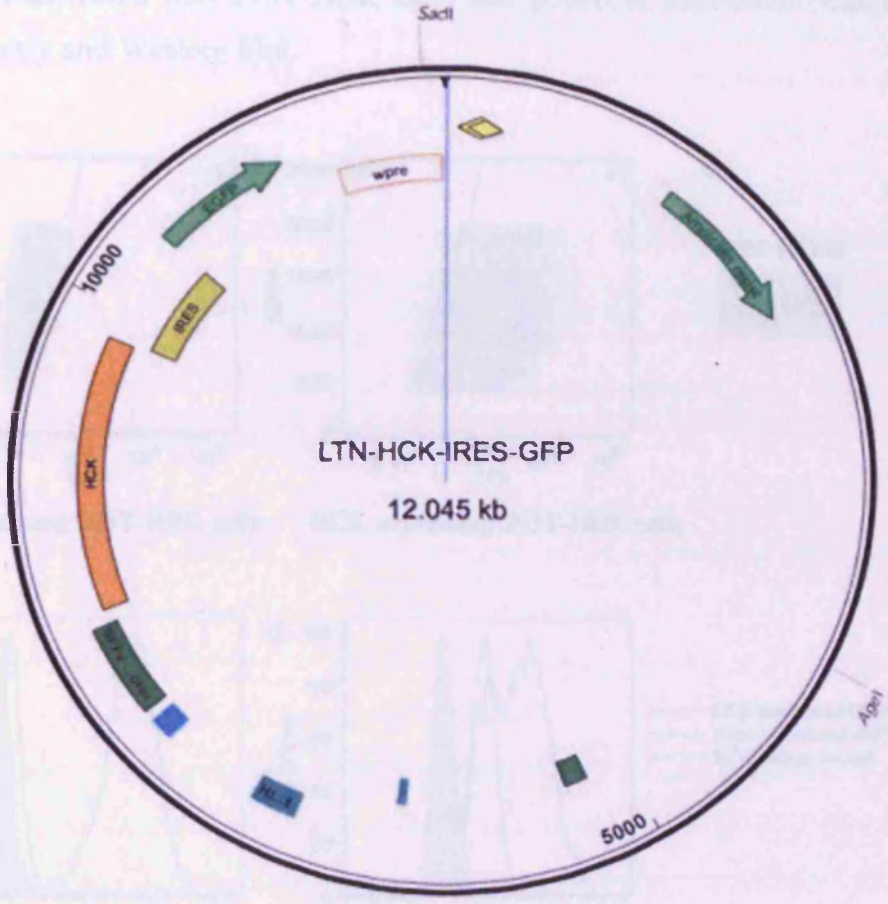


***Figure VIII.2:*** ***Cloning of p59HCK cDNA into the LNT-Sffv-cddB-MCS lentiviral backbone.***

*Map of the LNT-Sffv-HCK-IRES-GFP plasmid.*

## 1.3 Assessment of p59HCK overexpression in 293T-HEK cells

The lentiviral backbone encoding p59HCK (also termed ovHCK in this manuscript) was transiently transfected into 293T-HEK cells and p59HCK expression was assessed by flow cytometry and Western blot.

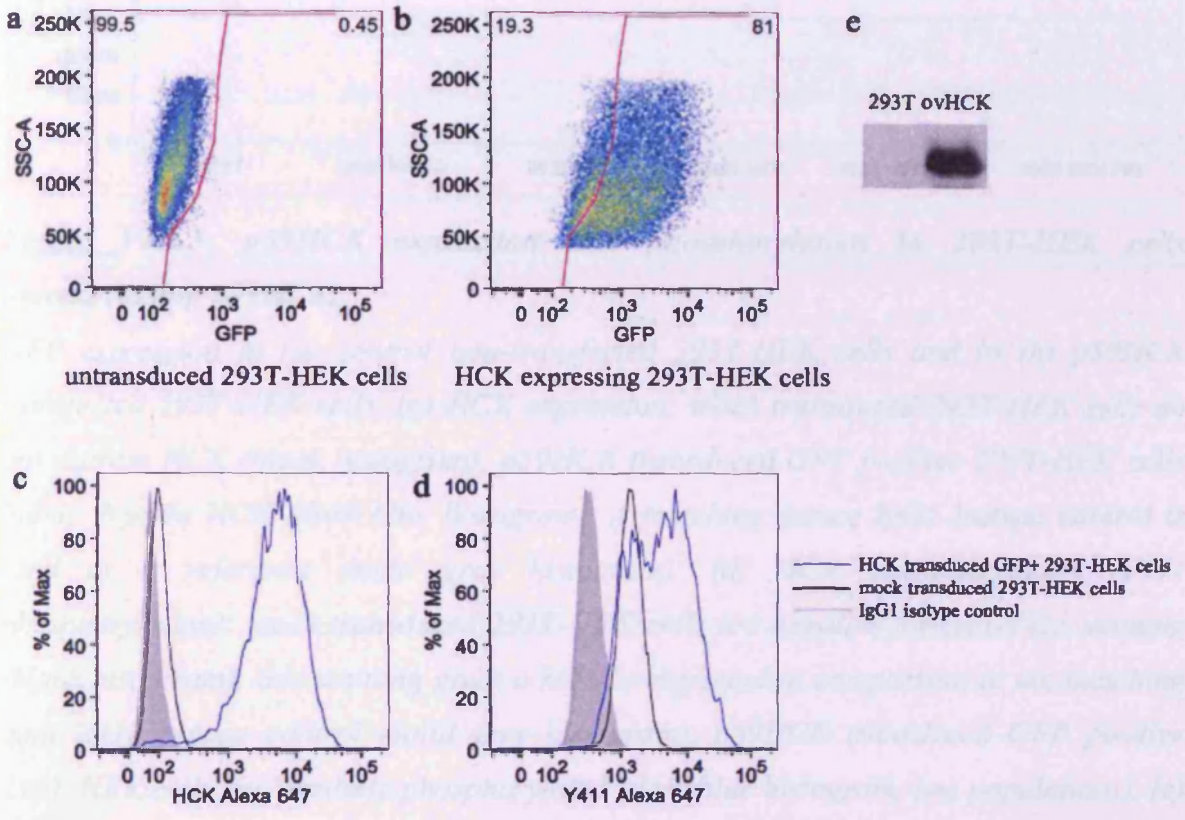


f

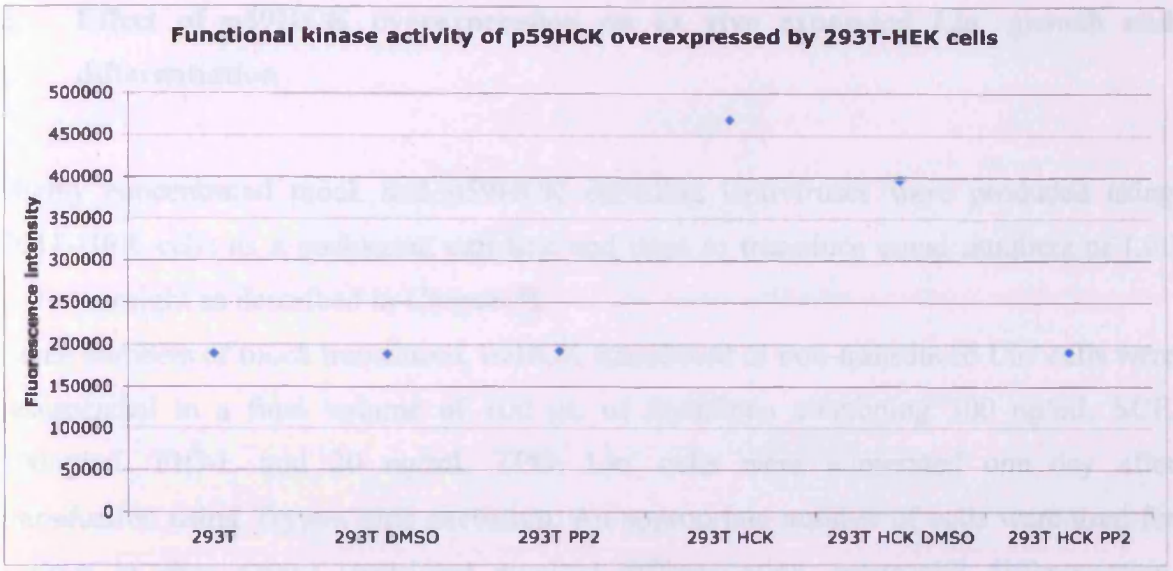


***Figure VIII.3: p59HCK expression and phosphorylation in 293T-HEK cells overexpressing p59HCK.***

*GFP expression in (a) control non-transfected 293T-HEK cells and in (b) p59HCK transfected 293T-HEK cells. (c) HCK expression: mock transduced 293T-HEK cells do not express HCK (black histogram), p59HCK transduced GFP positive 293T-HEK cells highly express HCK (dark blue histogram). A matching mouse IgG1 isotype control is used as a reference (solid grey histogram). (d) HCK phosphorylation (Y411 phosphorylation): mock transduced 293T-HEK cells are negative for anti-Y411 staining (black histogram), this staining gives a high background in comparison to the matching goat IgG1 isotype control (solid grey histogram). p59HCK transduced GFP positive 293T-HEK cells are partially phosphorylated (dark blue histogram, two populations). (e) p59HCK expression by Western blot. (f) HCK functional kinase activity: HCK antibody immunoprecipitate from non-transduced 293T-HEK does not display any kinase activity, while immunoprecipitate from 293T-HEK cells overexpressing p59HCK shows a (specific) kinase activity that can be successfully abrogated by the addition of the SFK inhibitor PP2 to the kinase assay reaction.*

## 2. Effect of p59HCK overexpression on ex vivo expanded Lin$^-$ growth and differentiation

Highly concentrated mock and p59HCK encoding lentiviruses were produced using 293T-HEK cells as a packaging cell line and used to transduce equal numbers of Lin$^-$ cells overnight as described in Chapter II.

Equal numbers of mock transduced, ovHCK transduced or non-transduced Lin$^-$ cells were resuspended in a final volume of 100 µL of StemSpan containing 300 ng/mL SCF, 300ng/mL Flt3-L and 20 ng/mL TPO. Lin$^-$ cells were numerated one day after transduction using Trypan blue exclusion. An appropriate number of cells were used for various *in vitro* assays (restricted myeloid differentiation, neutrophil differentiation, erythroid differentiation, CFC assay, signalling pathway analysis by flow cytometry) and unused equal numbers of cells were replated for each condition, adding fresh cytokines every 3 days.

### 2.1 Cell cycle analysis

To assess if HCK overexpression had any influence on Lin$^-$ proliferation, we analysed the cell cycle status of GFP$^+$/Lin$^-$ after 4 days expansion using Ki67 as a marker of proliferation (*Figure VIII.4*). HCK overexpression did not influence Lin$^-$ cell cycle status. Of note, the percentage of GFP$^+$/Lin$^-$ overexpressing HCK cells was quite low (10% versus 45% in mock transduced cells) therefore not allowing the acquisition of GFP$^+$ events in the FACS plots pictured below. These FACS plots represented below are representative of two independent experiments.

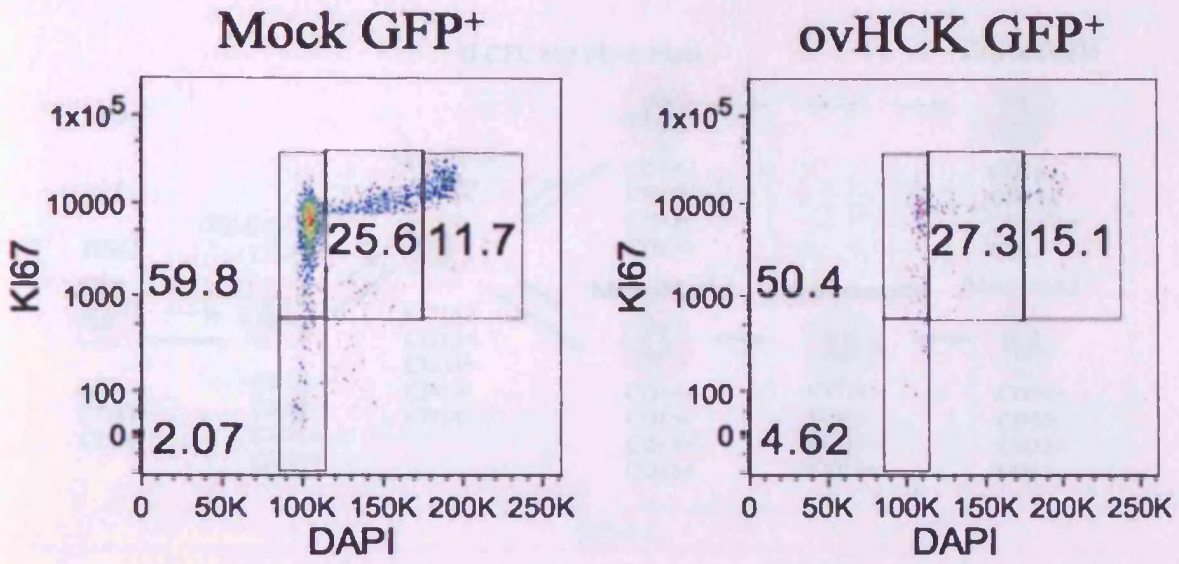


***Figure VIII.4: Cell cycle analysis of Lin⁻ overexpressing p59HCK 4 days after transduction.***

## 2.2 Influence of p59HCK overexpression on myeloid differentiation in liquid culture

To assess the effect of HCK overexpression on the myeloid differentiation potential of Lin⁻ cells, 20,000 Lin⁻ cells/mL were seeded in triplicate and maintained for 12 days in restricting myeloid differentiation medium (IMDM, 15% FCS, 20 ng/mL IL-3 and 20 ng/mL SCF (Barabe *et al.*, 2007)) or in terminal granulocytic differentiation medium (IMDM, 20% FCS, 50 ng/mL G-CSF and 50 ng/mL SCF (Edvardsson *et al.*, 2004)). Fresh cytokines were added to the cells every 3 days. *Figure VIII.5* indicates the different types of cells produced in either differentiation conditions.

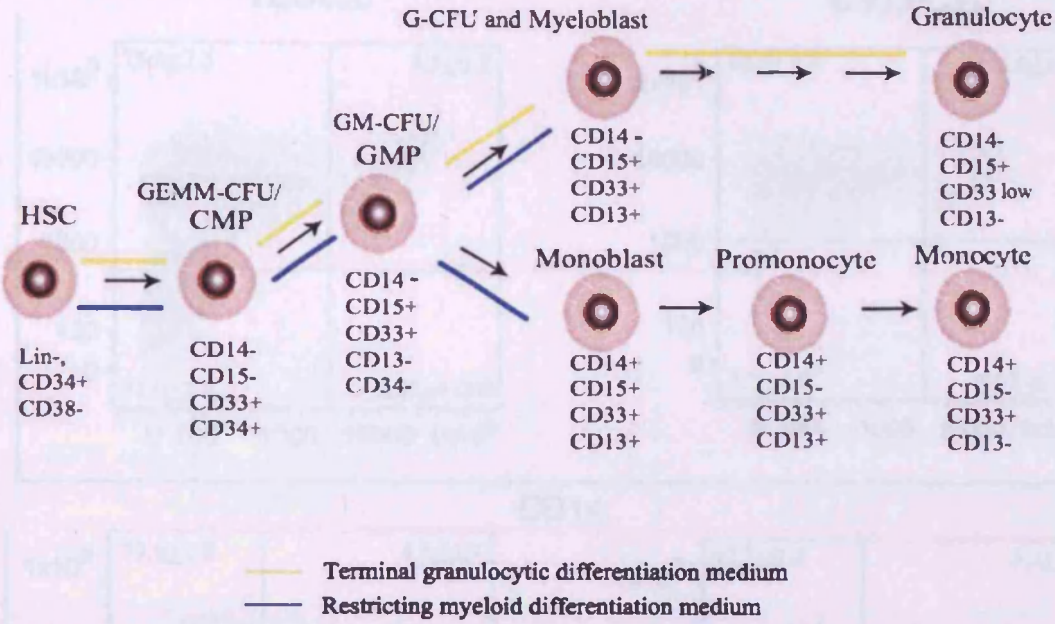


***Figure VIII.5: Schematic representation of myeloid differentiation (adapted from KEGG pathways; http://www.genome.jp/kegg/pathway/hsa/hsa04640.html)***

After 12 days in culture with restricting myeloid differentiation medium, 21% of mock transduced cells have not yet entered the myeloid pathway since they are $CD33^-$ (*Figure VIII.6*). About 75% of them are myeloid progenitors that are $CD33^+/CD14^-/CD15^-$ and about 4% of them are myeloblast or monoblast that are $CD33^+/CD14^-/CD15^+$ or $CD33^+/CD14^+/CD15^+$ respectively. No differentiated promonocytes ($CD33^+/CD14^+/CD15^-$ cells) or granulocytes ($CD33^+/CD14^-/CD15^+$ cells) are detectable in this differentiation condition, since the medium in use does not promote further differentiation. Interestingly, after 12 days in culture in the same conditions 90% of HCK overexpressing $Lin^-$ cells became $CD33^+/CD14^-/CD15^-$ progenitors and, similarly to mock transduced cells, about 4.5% of Lin- cells have differentiated to myeloblasts or monoblasts (*Figure VIII.6*).

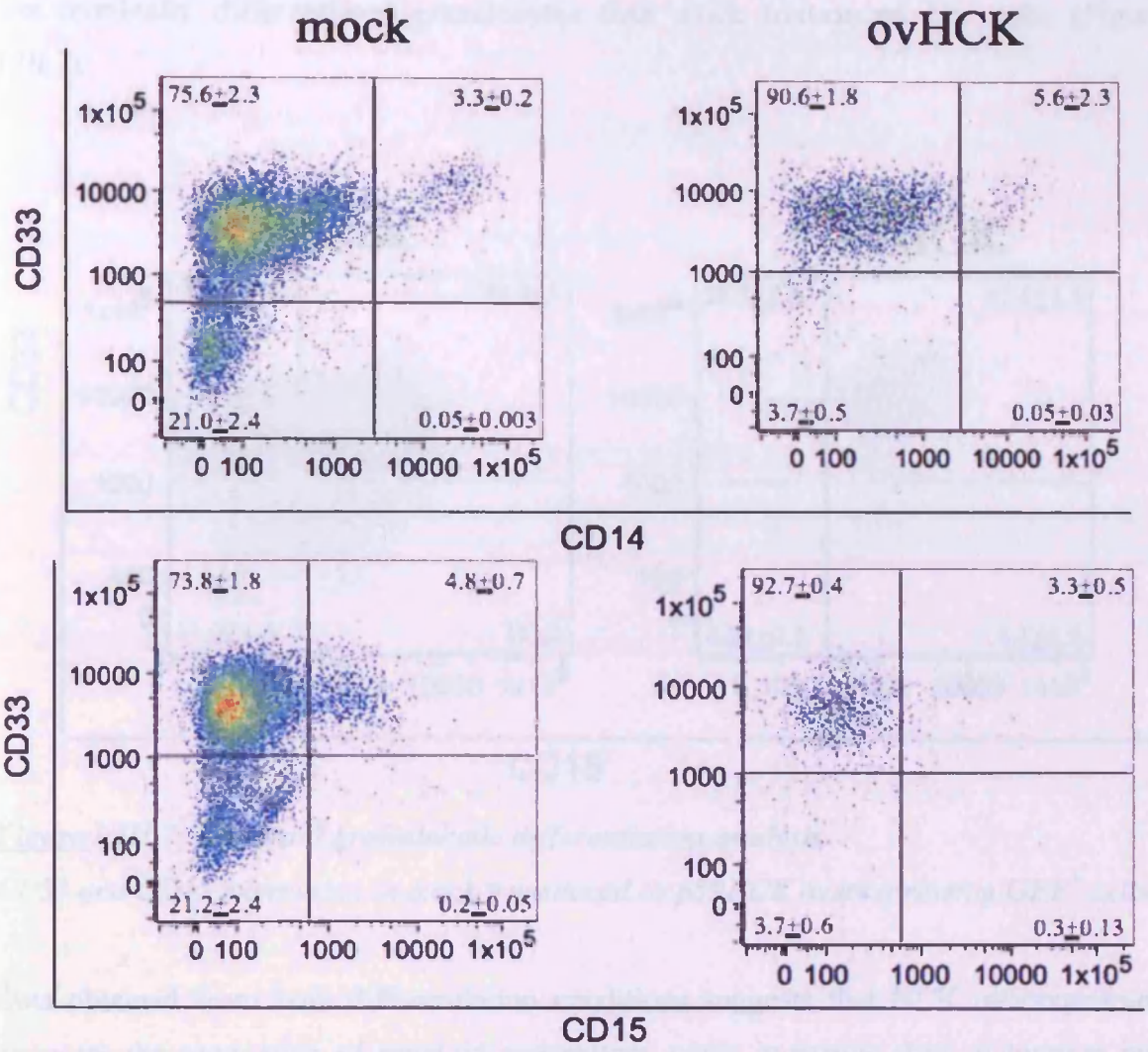


***Figure VIII.6: Restricted myeloid differentiation analysis.***

*Top panel: CD33 and CD14 expression in mock transduced or p59HCK overexpressing GFP$^+$ cells. Bottom panel: CD33 and CD15 expression in mock transduced or p59HCK overexpressing GFP$^+$ cells.*

After 12 days in culture with terminal granulocytic differentiation medium, 11% of mock transduced cells have not yet entered the myeloid pathway since they are CD33$^-$ (*Figure VIII.7*). About 30% of them are myeloid progenitors (CD33$^+$/CD15$^-$ cells), 44.5% are myeloblasts (CD33$^+$/CD15$^+$ cells) and 15% are granulocytes (CD33$^{low}$/CD15$^+$ cells). Interestingly, after 12 days in culture in the same conditions, HCK overexpressing Lin$^-$ cells all entered the myeloid pathway, mostly giving rise to myeloblasts and to four times

less terminally differentiated granulocytes than mock transduced Lin$^-$ cells (*Figure VIII.7*).

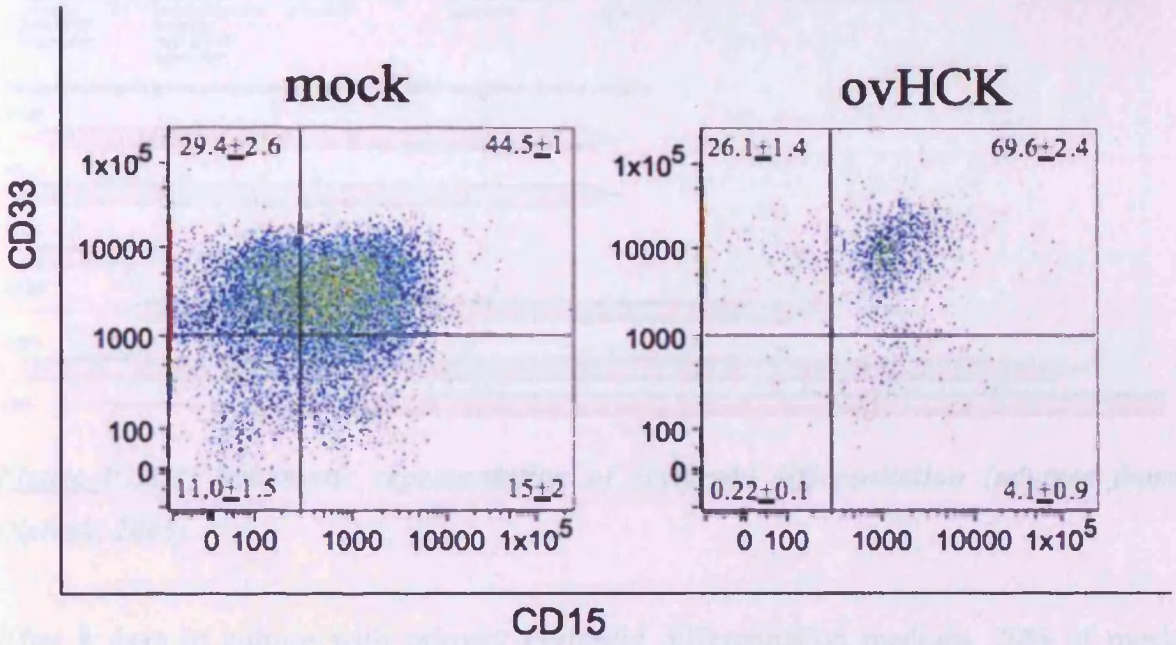


***Figure VIII.7: Terminal granulocytic differentiation analysis.***
*CD33 and CD15 expression in mock transduced or p59HCK overexpressing GFP$^+$ cells.*

Data obtained from both differentiation conditions suggests that HCK overexpression promotes the production of myeloid progenitors, while impairing their maturation into neutrophils.

## 2.3 Influence of p59HCK overexpression on erythroid differentiation in liquid culture

To assess the effect of HCK overexpression on the erythroid differentiation potential of Lin$^-$ cells, 10,000 Lin$^-$ cells/mL were seeded in triplicate and maintained for 8 days in primary erythroid differentiation medium (Giarratana *et al.*, 2005). Cells were split 1:5 after 4 days and supplemented with fresh cytokines. *Figure VIII.8* illustrates the different types of cells produced in these differentiation conditions.

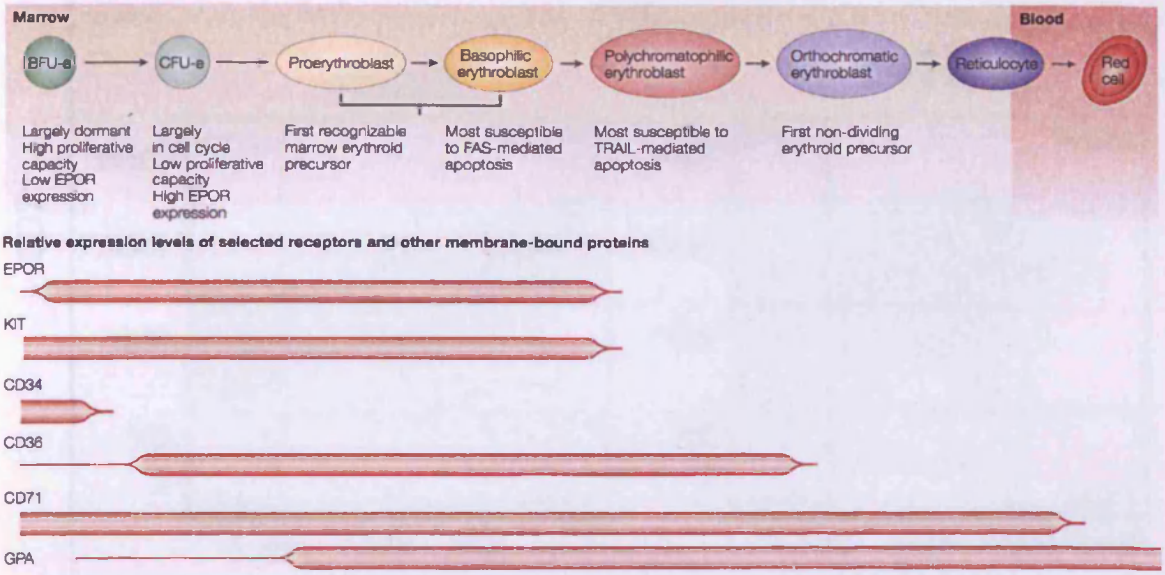


***Figure VIII.8: Schematic representation of erythroid differentiation (adapted from (Spivak, 2005).***

After 8 days in culture with primary erythroid differentiation medium, 20% of mock transduced Lin- cells became erythroid progenitors that are $CD71^{+}$/Glycophorin-$A^{-}$, 67% became erythroblasts that are $CD71^{+}$/Glycophorin-$A^{+}$ and 12.5% became reticulocytes that are $CD71^{-}$/Glycophorin-$A^{+}$ (*Figure VIII.9*). After 8 days in culture in the same conditions, HCK overexpressing $Lin^{-}$ cells seem to have a delay in the erythroid differentiation process since 38% of HCK overexpressing $Lin^{-}$ cells became erythroid progenitors, 57% became erythroblasts and 4% became reticulocytes.

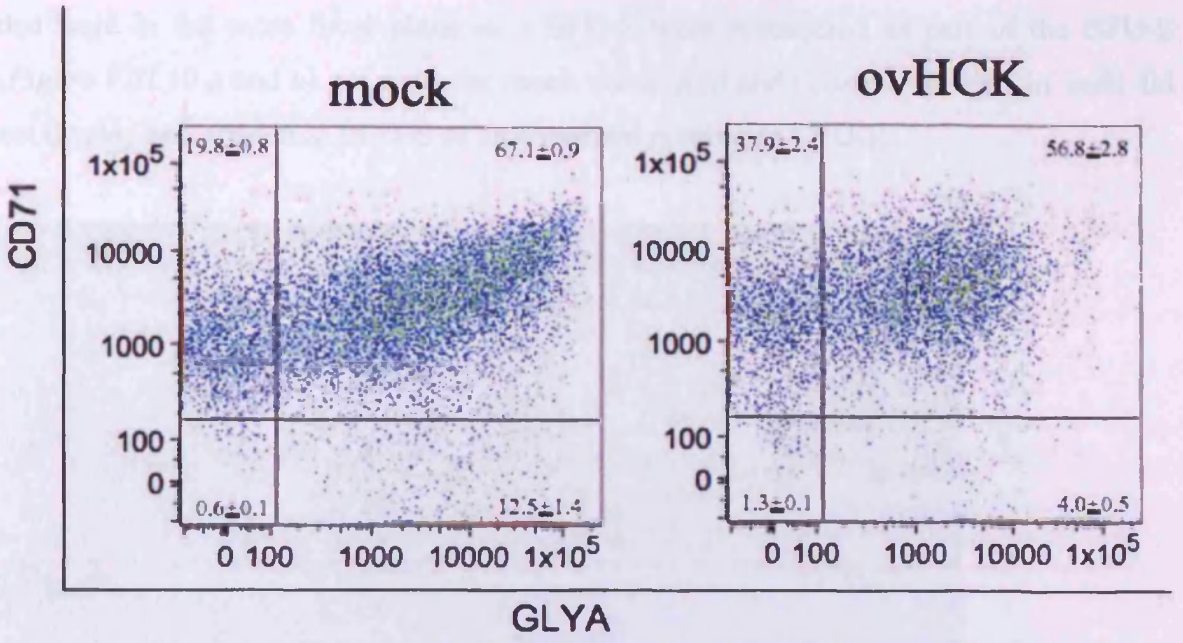


***Figure VIII.9: Primary erythroid differentiation analysis.***

*CD71 and Glycophorin A (GLYA) expression in mock transduced or p59HCK overexpressing GFP$^+$ cells.*

## 2.4 Influence of p59HCK overexpression on CFC potential of Lin$^-$ cells

In parallel to being expanded in liquid culture, 1000 ovHCK and mock transduced Lin$^-$ cells were plated in triplicate for CFC assay at day 1 and day 4 post-transduction.

### 2.4.1 Influence of HCK overexpression on the morphology of erythroid colonies

Upon p59HCK overexpression Lin$^-$ cells gave rise to small GFP$^+$ structures which, most of the time, surrounded a BFU-E, as pointed out by an arrow in *Figure VIII.10*. The small GFP$^+$ structures were mainly in a different focal plane than the central BFU-E they surrounded, which were often GFP$^-$ confirming a distinct origin (*Figure VIII.10 d*). We therefore scored the small structures that were not in the same focal plane as any surrounding BFU-E as individual CFU-Es (*Figure VIII.10 c*), while the small structures

that were in the same focal plane as a BFU-E were considered as part of the BFU-E (*Figure VIII.10 a* and *b*). Of note, the mock transduced and non-transduced $Lin^-$ cells did not display any abnormal BFU-E or an abnormal number of CFU-E.

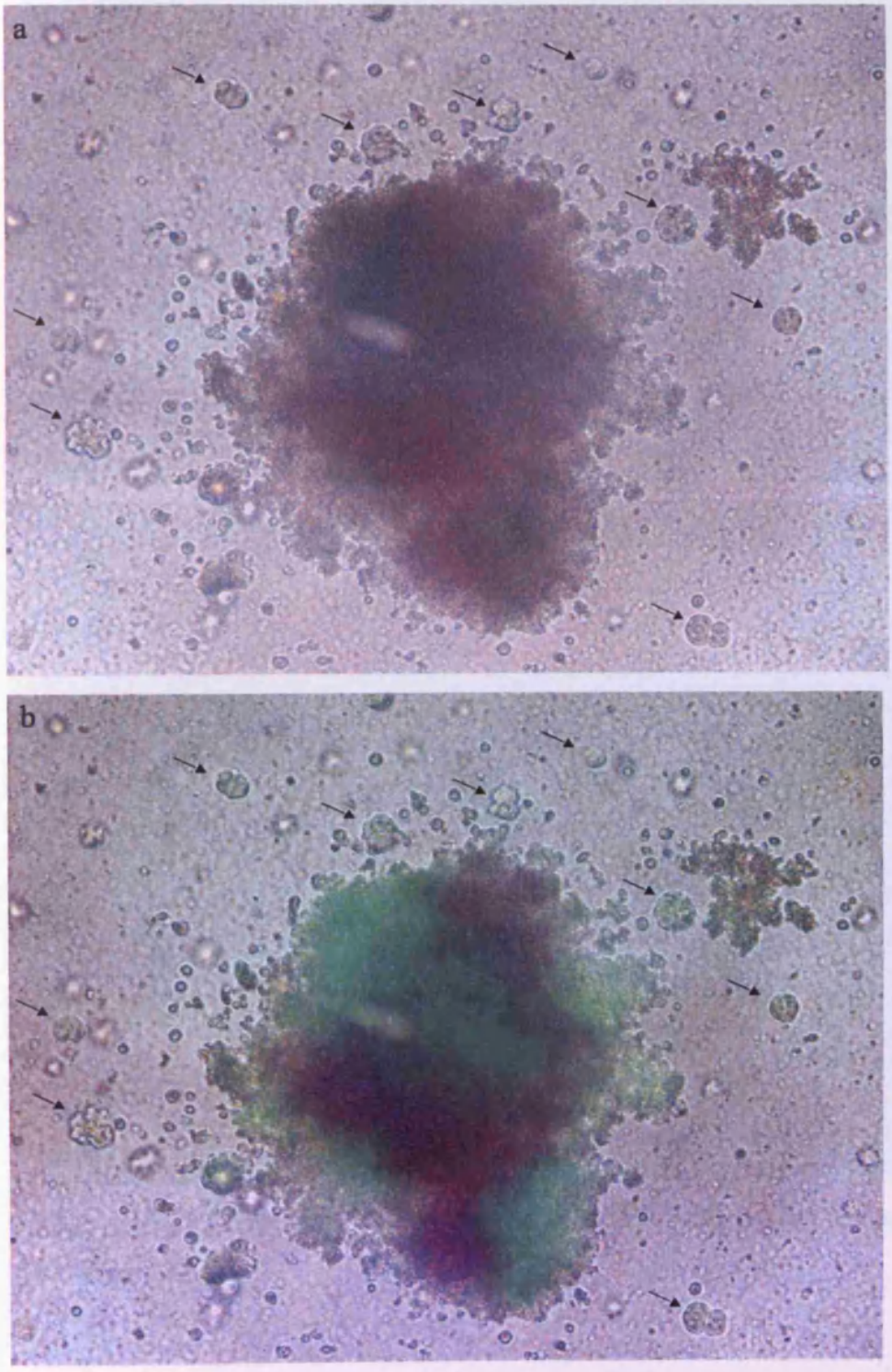

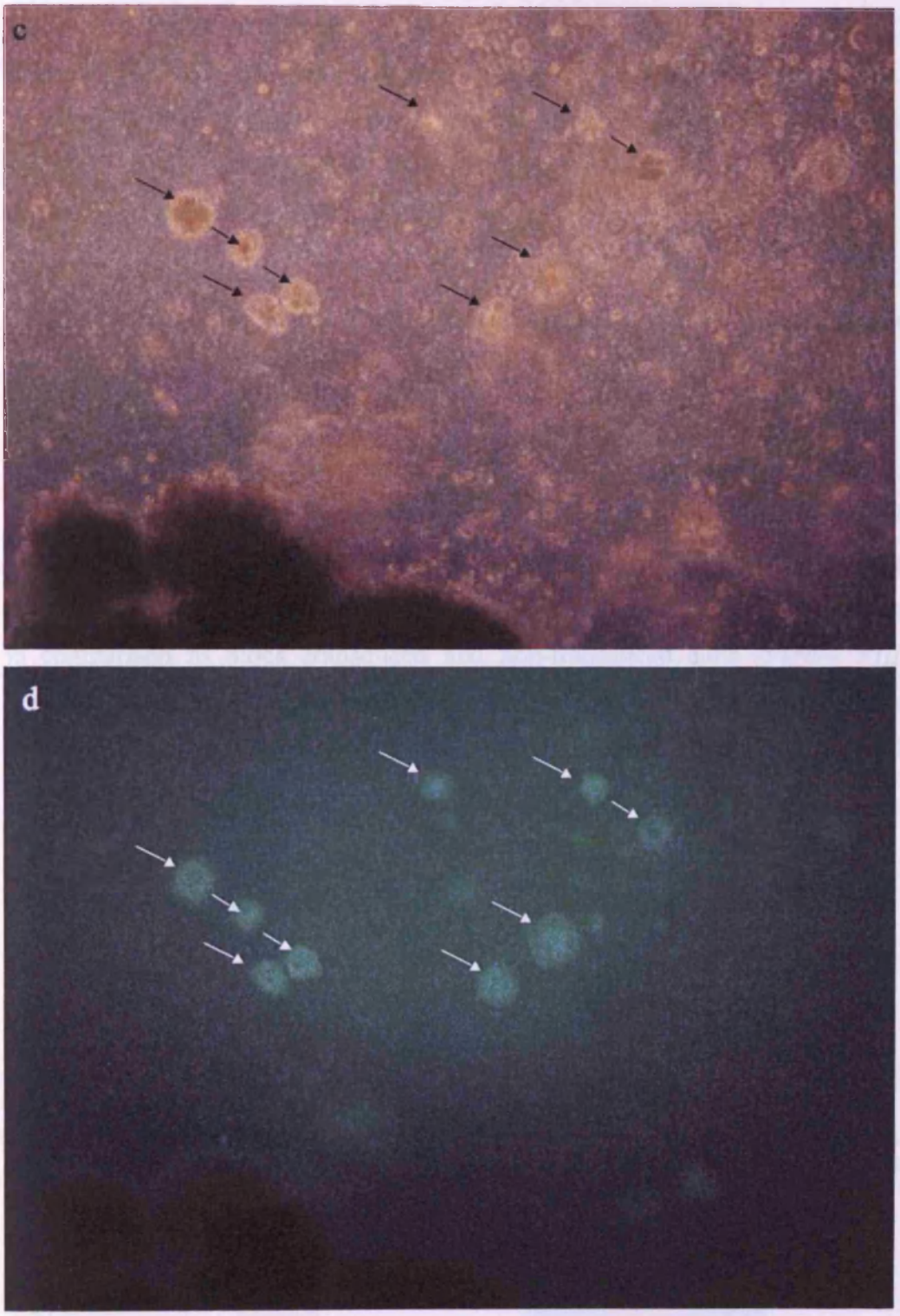


***Figure VIII.10:*** ***Erythroid colonies formed by Lin⁻ cells overexpressing p59HCK in CFC assay (14 days).***

*(a) Phase contrast picture of a BFU-E formed by Lin⁻ overexpressing p59HCK. (b) The same BFU-E as in (a) under UV light of a fluorescent inverted microscope. (c) Phase contrast picture of a BFU-E and several CFU-Es formed by Lin⁻ overexpressing p59HCK. (d) The same BFU-E and CFU-Es as in (c) under UV light of a fluorescent inverted microscope. Only the CFU-Es are GFP⁺.*

### 2.4.2 Influence of p59HCK overexpression on the type of colonies formed by Lin⁻ cells

Since the Lin⁻ cells overexpressing p59HCK displayed a very high number of CFU-E (132 fold higher than mock transduced cells), the overall total number of CFU formed by these cells was 4.6 fold higher than in control cells (*Figure VIII.11 a*). Consequently, percentages of other CFU types appeared very low in Lin⁻ cells overexpressing p59HCK in comparison to mock transduced and non-transduced cells (*Figure VIII.11 c*), we therefore show the absolute number of each type of CFU numerated in each condition to be able to consider if formation of CFU-G, CFU-GM, BFU-E and CFU-GEMM occurred normally upon HCK overexpression (*Figure VIII.11 b*).

a

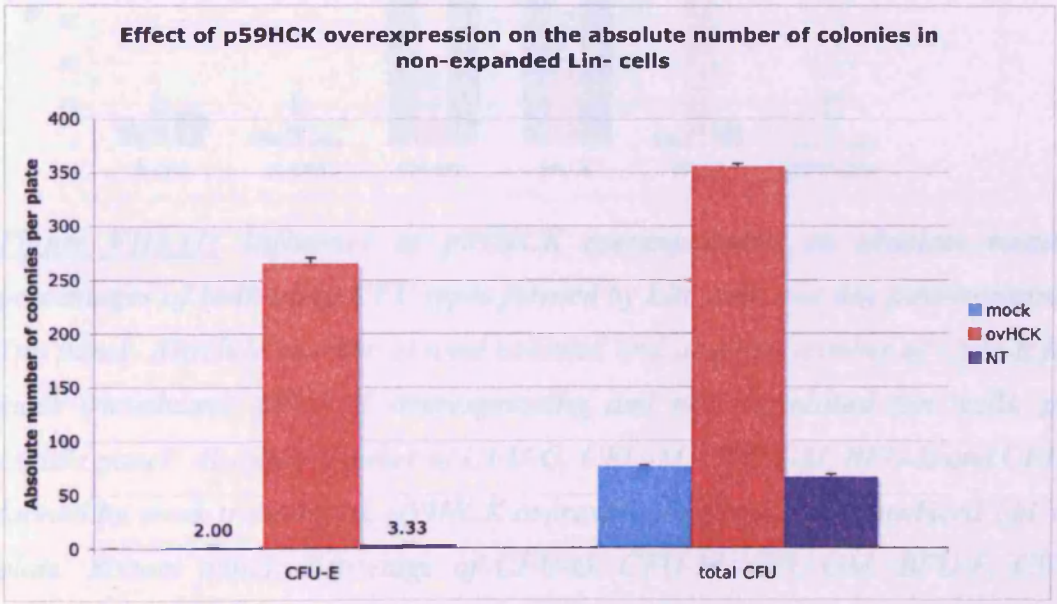

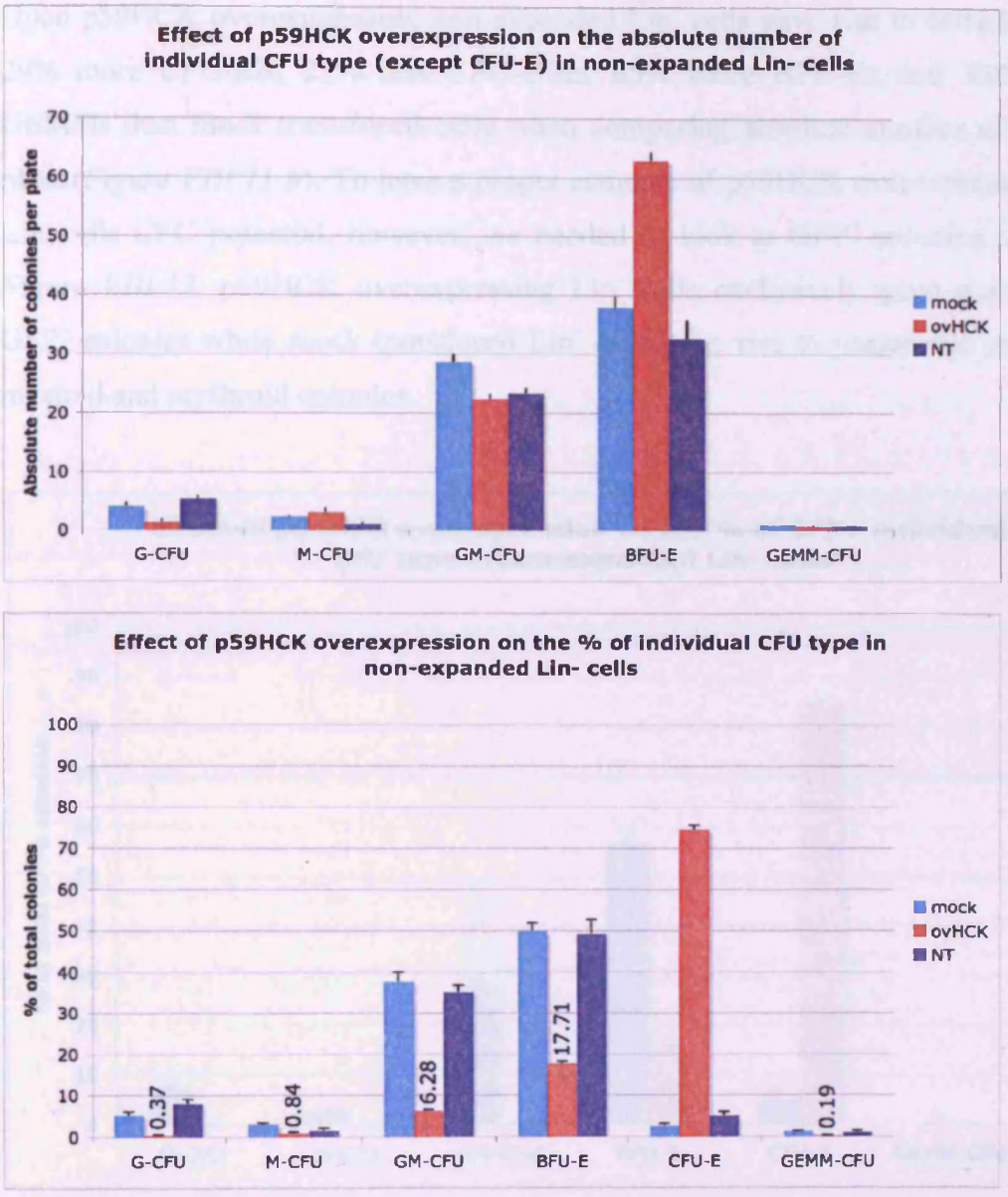


***Figure VIII.11:*** ***Influence of p59HCK overexpression on absolute numbers and percentages of individual CFU types formed by Lin⁻ cells one day post-transduction.***
*Top panel: Absolute number of total colonies and absolute number of CFU-E formed by mock transduced, p59HCK overexpressing and non-transduced Lin⁻ cells, per plate. Middle panel: Absolute number of CFU-G, CFU-M, CFU-GM, BFU-E and CFU-GEMM formed by mock transduced, p59HCK overexpressing and non-transduced Lin⁻ cells, per plate. Bottom panel: Percentge of CFU-G, CFU-M, CFU-GM, BFU-E, CFU-E and CFU-GEMM formed by mock transduced, p59HCK overexpressing and non-transduced Lin⁻ cells, per plate.*

Upon p59HCK overexpression, non-expanded Lin$^-$ cells gave rise to 66% less CFU-Gs, 29% more CFU-Ms, 22% less CFU-GMs, 65% more BFU-Es and 33% less CFU-GEMMs than mock transduced cells when comparing absolute number of colonies per plate (*Figure VIII.11 b*). To have a proper estimate of p59HCK overexpression effect on Lin$^-$ cells CFC potential, however, we needed to look at GFP$^+$ colonies. As shown in *Figure VIII.12*, p59HCK overexpressing Lin$^-$ cells exclusively gave rise to erythroid GFP$^+$ colonies while mock transduced Lin$^-$ cells gave rise to reasonable percentages of myeloid and erythroid colonies.

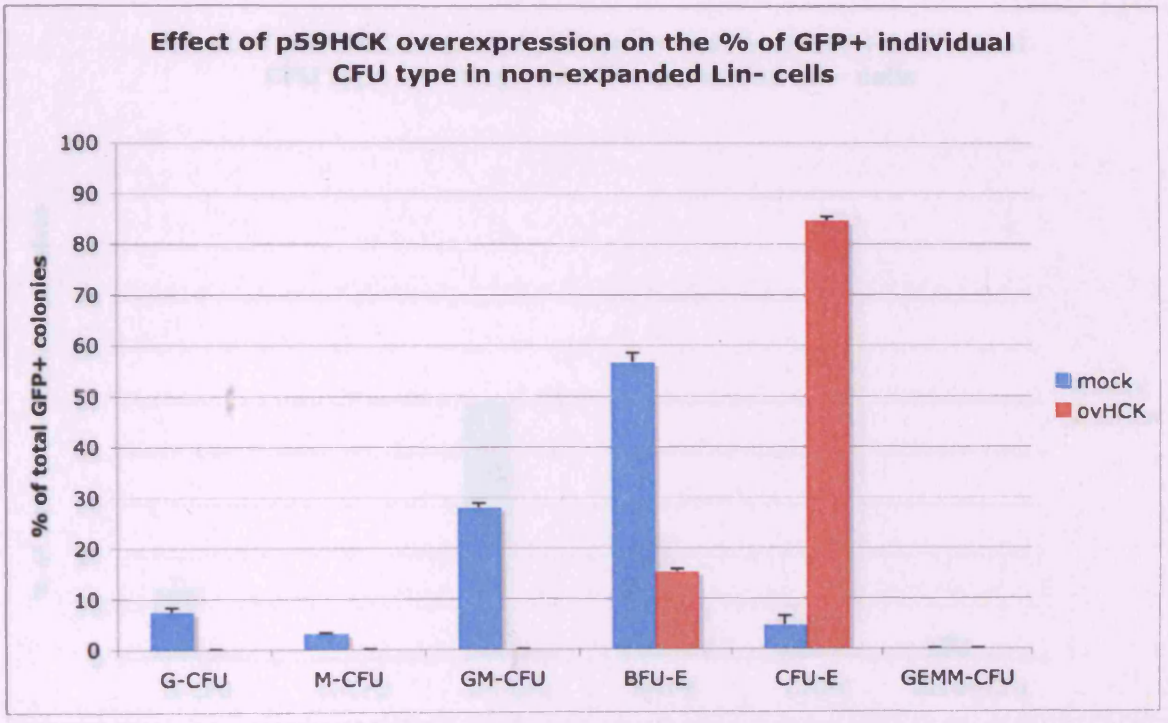


***Figure VIII.12: Influence of p59HCK overexpression on GFP$^+$ colony formation by non-expanded Lin$^-$ cells.***

*Percentage of GFP$^+$ CFU-G, CFU-M, CFU-GM, BFU-E, CFU-E and CFU-GEMM formed by mock transduced and p59HCK overexpressing non-expanded Lin$^-$ cells, per plate.*

To determine whether the results obtained in CFC assay could be modulated by expanding the Lin$^-$ cells, *in vitro*, prior to proceeding with the CFC assay, Lin$^-$ cells were cultured for 4 days in StemSpan containing 300 ng/mL SCF, 300ng/mL Flt3-L and 20

ng/mL TPO (*Figure VIII.13*). Expanded Lin$^-$ cells overexpressing HCK gave rise to 27 fold less GFP$^+$ CFU-G, 29 fold less GFP$^+$ CFU-GM, 2.24 fold less GFP$^+$ BFU-E, 10 fold more GFP$^+$ CFU-E and 16 fold less GFP$^+$ CFU-GEMM than mock transduced cells (*Figure VIII.13*). Once again, most HCK overexpressing GFP$^+$ colonies were CFU-E. Since we could detect myeloid GFP$^+$ colonies in CFC assay from expanded Lin$^-$ cells overexpressing p59HCK, we can conclude that p59HCK overexpression does not completely abrogate myeloid differentiation but rather skew Lin$^-$ cells differentiation towards the erythroid lineage.

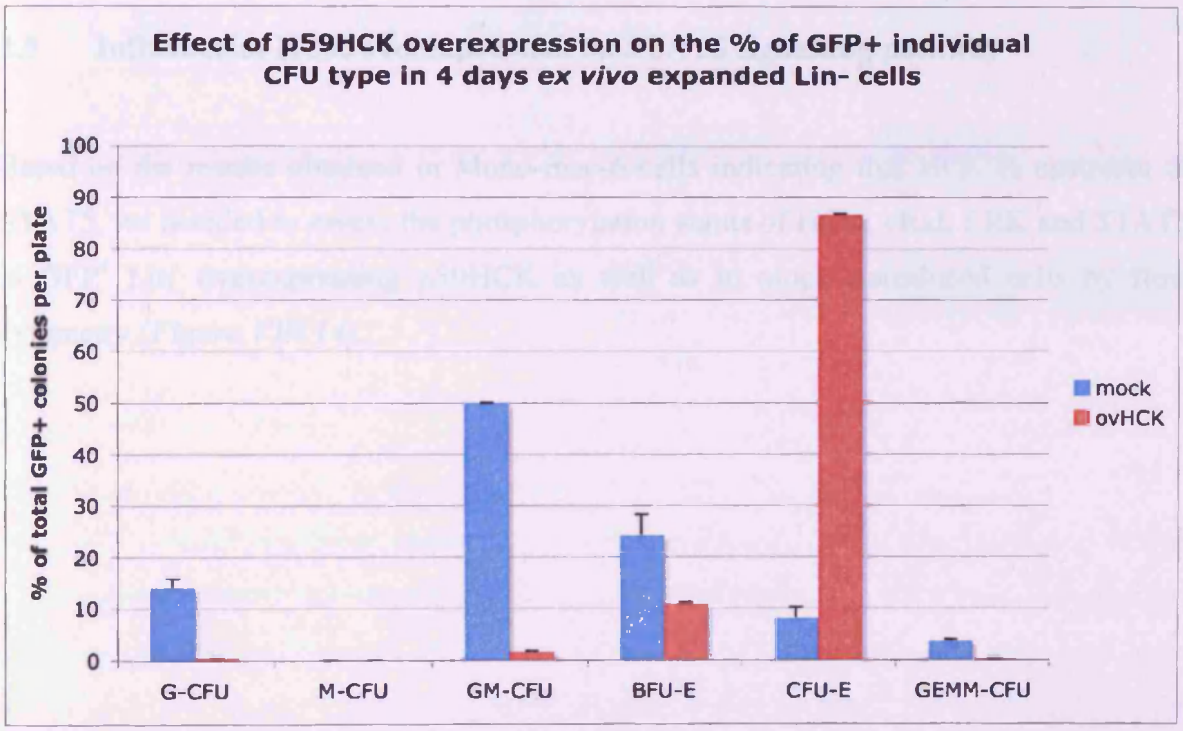


***Figure VIII.13: Influence of p59HCK overexpression on GFP$^+$ colony formation by Lin$^-$ cells 4 days post-transduction.***

*Percentage of GFP$^+$ CFU-G, CFU-M, CFU-GM, BFU-E, CFU-E and CFU-GEMM formed by mock transduced and p59HCK overexpressing expanded Lin$^-$ cells, per plate.*

Thus, in a CFC assay supporting both myeloid and erythroid growth simultaneously, p59HCK overexpression led to a block in production of myeloid colonies while increasing the production of CFU-E by 10 fold.

Although the identity of the colonies specifically produced by $Lin^-$ cells overexpressing p59HCK that we scored as CFU-E were difficult to establish, both liquid cultures, supporting either myeloid or erythroid differentiation, and CFC assays, supporting both differentiation simultaneously, provide evidence to conclude that p59HCK overexpression impairs myeloid differentiation while promoting erythroid differentiation.

## 2.5 Influence of HCK overexpression on STAT5 signalling pathway

Based on the results obtained in Mono-mac-6 cells indicating that HCK is upstream of STAT5, we decided to assess the phosphorylation status of HCK, cRaf, ERK and STAT5 in $GFP^+$ $Lin^-$ overexpressing p59HCK as well as in mock transduced cells by flow cytometry (*Figure VIII.14*).

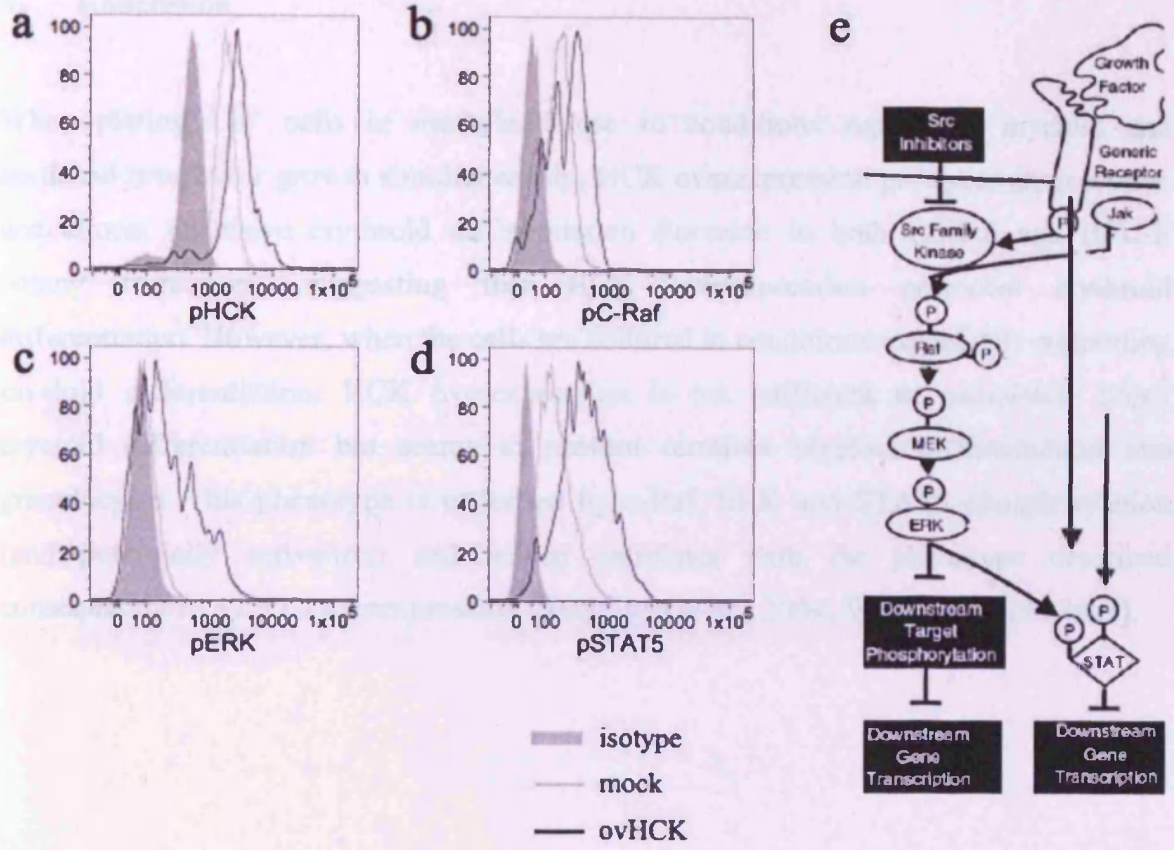


***Figure VIII.14: Phosphorylation status of HCK, cRaf, ERK and STAT5 in Lin⁻ overexpressing p59HCK analysed by flow cytometry.***

*(a) HCK phosphorylation status in mock transduced (grey histogram), p59HCK overexpressing (black histogram) and non-transduced (solid grey istogram) Lin⁻ cells. (b) c-Raf status phosphorylation in mock transduced, p59HCK overexpressing and non-transduced Lin⁻ cells. (c) ERK phosphorylation status in mock transduced, p59HCK overexpressing and non-transduced Lin⁻ cells. (d) STAT5 phosphorylation status in mock transduced, p59HCK overexpressing and non-transduced Lin⁻ cells. (e) Schematic representation of the pathways linking SFK, c-Raf, ERK and STAT5 adapted from (McCubrey et al., 2008).*

We found out that overexpression of p59HCK in Lin⁻ cells induces c-Raf, ERK and STAT5 phosphorylations, while this pathway is not active in mock transduced Lin⁻ cells. The FACS plots displayed are representative of two independent experiments.

## 3. Conclusion

When plating $Lin^-$ cells in methylcellulose in conditions supporting myeloid and erythroid progenitor growth simultaneously, HCK overexpression provokes an excessive and almost exclusive erythroid differentiation (increase in both CFU-E and BFU-E colony formation), suggesting that HCK overexpression promotes erythroid differentiation. However, when the cells are cultured in conditions exclusively supporting myeloid differentiation, HCK overexpression is not sufficient to completely block myeloid differentiation but seems to prevent terminal myeloid differentiation into granulocytes. This phenotype is underlied by c-Raf, ERK and STAT5 phosphorylation (and potentially activation) and indeed correlates with the phenotype described consequently to STAT5 overexpression (Schuringa *et al.*, 2004; Wierenga *et al.*, 2008).

# Chapter IX

## IX Discussion

AML is a clonal, malignant proliferation of undifferentiated haematopoietic cells that is morphologically, genetically and therapeutically heterogeneous. AML mostly consists of a bulk of leukaemic blasts with low proliferative potential that are maintained by a rare population of LSC responsible for propagating the disease. Elucidating the identity of the LSC and the mechanisms underlying its ability to self-renew is of great interest and LSC have been proposed to reside in the $CD34^+/CD38^-$ (Bonnet and Dick, 1997), $CD34^+/CD38^+$ (Taussig *et al.*, 2008) or the $CD34^-$ (Blair *et al.*, 1997) compartment, depending on the AML sample studied.

In an attempt to identify genes differentially expressed between the $Lin^-/CD34^+/CD38^-$ and $Lin^-/CD34^+/CD38^+$ potential leukaemic stem cell compartments and their normal counterparts, microarray analyses were carried out in our laboratory. Haematopoietic cell kinase (HCK) was identified as the gene most overexpressed in the $Lin^-/CD34^+/CD38^-$ fraction from 7 AML patients in comparison to normal bone marrow. HCK was also overexpressed in the $Lin^-/CD34^+/CD38^+$ fraction from these 7 AML patients in comparison to normal bone marrow. Although a decrease in HCK expression was observed when comparing $Lin^-/CD34^+/CD38^-$ and $Lin^-/CD34^+/CD38^+$ data from leukaemic samples, HCK was still overexpressed by at least two folds in all leukaemic subfractions studied in comparison to normal bone marrow.

In order to elucidate if HCK could have a part in leukaemogenesis, we decided to study its role in haematopoietic cells by either downregulating it in leukaemic cells or overexpressing it in normal stem cells. Since STAT have been shown to be constitutively active in leukaemic AML patient samples (Gouilleux-Gruart *et al.*, 1996; Xia *et al.*, 1998) and this phenomenon could not be exclusively explained by the disruption of the canonical JAK-STAT pathway (Biethahn *et al.*, 1999; Steensma *et al.*, 2006), and since a parallel role for HCK or at least SFK in STAT5 or STAT3 activation was emerging from various publications using various cell type background (Ernst *et al.*, 1996; Klejman *et al.*, 2002), we were also interested in establishing if a link between HCK level of

expression and STAT activation was existing in normal HSC and/or in AML cells.

In this study we demonstrated that HCK acts upstream of STAT5 and that the pathways engaged in this axis of signal transduction are highly cell type dependent, therefore leading to very distinct phenotypes within leukaemic cell lines and in stem cell enriched cell fractions.

## 1. HCK is involved in G-CSF and GM-CSF signal transduction and is implicated in the migration of the 'mature' myelomonocytic cell line Mono-mac-6

We first confirmed that HCK expression could be correlated to the FAB class of the leukaemic cell lines tested and that AML FAB M5 cell lines were the AML cell lines expressing the most HCK. We then showed that a similar correlation could not be established between the FAB class of MNC from primary leukaemic samples and HCK expression; all samples tested were expressing HCK at higher level than AML FAB M5 cell lines at the RNA level. After showing that the two isoforms of HCK, p59 and p61, were expressed at similar levels in the 3 AML FAB M5 cell lines tested, Fujioka/P31, U937 and Mono-mac-6, we noticed that only p59 seemed to be autophosphorylated in Fujioka/P31, while both p59 and p61 were autophosphorylated in U937 and Mono-mac-6 cells, as shown by phospho-specific Western blotting. However, the kinases had a similar catalytic activity when tested in an *in vitro* non-radioactive kinase assay that measured substrate phosphorylation rather than autophosphorylation. We also showed that UCB MNC expressed more p59 than p61 HCK and that MNC from UCB and various patient samples had variable levels of HCK activity.

Since we showed by surface marker phenotyping that U937 and Mono-mac-6 cells are more mature than Fujioka/P31 cells and since p61HCK has been reported to be exclusively associated with lysosomes (Carreno *et al.*, 2000), the differential expression of the HCK isoforms in the 3 cell lines studied might be reflecting their degree of maturation, which is most likely associated with a distinct organisation and functionality of their subcellular compartments.

Primarily in leukaemic cell lines, but later in normal or leukaemic stem cells, we wanted to knock-down HCK using RNA interference (RNAi). To do so we tested two different strategies of RNAi: testing several siRNA sequences and also trying to establish knock-down using an miRNA based system. We could only achieve 50% knock-down of HCK using an shRNA expressing lentiviral system. The relative efficiency of the knock-down turned out to be sequence inherent and independent of the cell line (293T-HEK overexpressing HCK, Fujioka/P31, U937 or Mono-mac-6 cell lines) or way of silencing used (transient by electroporation, nucleofection or PEI mediated transfection, or stable by lentiviral transduction). We, however, decided to further study HCK semi-silencing assuming that 50% HCK knock-down, representing a disruption in the balance of SFK expression as a whole, might be sufficient to trigger a distinct phenotype.

In myelomonocytic cell lines, we showed that HCK semi-silencing did not have any major effect on their proliferation, apoptosis or differentiation as shown by XTT assay, cell cycle analysis, Annexin V staining, population doublings calculation and specific cell surface marker staining respectively. However, we observed that HCK knock-down had an influence on the spontaneous colony forming capacity of Mono-mac-6 cells that was essentially due to an effect of HCK semi-silencing on their migration capacity. Furthermore we could demonstrate that HCK is involved in the mediation of G-CSF and GM-CSF signal transduction towards STAT5 exclusively in Mono-mac-6 cells, illustrating the point that the 3 AML FAB M5 cell lines studied are heterogeneous and use different signalling pathways to convey a given signal. Additionally we could show that G-CSF or GM-CSF pre-stimulation of Mono-mac-6 cells had an opposite effect on Mono-mac-6 cells migration, further stating a role of HCK in integrin mediated migration and G-CSF chemotaxis. These results are in accordance with the reduced *in vitro* motility observed for macrophages taken from $Hck^{-/-}/Fgr^{-/-}$ knock-out mice (Suen *et al.*, 1999), however such a phenotype was not reported for $Hck^{-/-}$ knock-out mice (Lowell *et al.*, 1994). Additionally, evidence for a role of HCK in adhesion of human cells has only been reported in one overexpression study in human fibroblasts and activated macrophages (Carreno *et al.*, 2002). Thus it would be of interest to study in more detail

the link between G-CSF stimulation, integrin engagement, HCK activation and cell migration.

It would especially be interesting to study the relationship between G-CSF stimulation, integrin engagement, HCK activation and cell migration in a stem cell context since SFK have recently been implicated in G-CSF mediated HSC mobilisation (Borneo *et al.*, 2007), as well as in G-protein-coupled receptors signalling in a cell type dependent manner (Vichalkovski *et al.*, 2005). Moreover, ectopic expression of HCK in Jurkat cells lacking LCK has recently been shown to restore responsiveness to SDF1 induced chemotaxis of the mutant Jurkat cells, suggesting a potential role for HCK in the SDF1/CXCR4 signalling pathway. It would therefore be interesting to assess if modulation of HCK expression would affect human HSC migration towards SDF-1 and/or mobilisation *in vivo* by disrupting the SFK expression balance.

## 2. HCK semi-silencing does not alter Lin$^-$ CFC capacity

HCK semi-silencing of the stem cell enriched Lin$^-$ fraction did not impair their differentiation capacity as shown in CFC assays. We observed a significant increase in total cell numbers after 4 days *ex vivo* expansion but could not be linked it to any change in cell cycle status of the cells. Since it was observed that 75% of normal Lin$^-$ cells lose HCK expression within 4 days of *ex vivo* expansion, it was concluded that 50% HCK silencing would not affect Lin$^-$ physiology beyond this natural HCK downregulation with differentiation and thus studying the effect of HCK silencing in this ex vivo expansion assay was impractical. However, it would be worth assessing whether the level of STAT5 activation is decreased upon HCK semi-silencing in Lin$^-$ cells and, if it is, to study the effect of HCK semi-silencing on stem cell enriched fractions in LTC-IC assays.

Indeed, recent studies by Schuring and Vellanga's group showed that intermediate levels of STAT5 activity had the maximal effect on increasing HSC self-renewal capacity *in vitro* (Wierenga *et al.*, 2008), while silencing of STAT5 was leading to a decrease in LTC-IC frequency and progenitor numbers in CFAC assay (Schepers *et al.*, 2007). It is therefore likely that HCK semi-silencing would have an effect on HSC self-renewal

capacity only if it is sufficient to down-regulate STAT5 activity. However, LYN activity has been shown to increase upon HCK knock-out in mice (Lowell *et al.*, 1994), LYN has also been linked to STAT5 signalling (Karur *et al.*, 2006; Xiao *et al.*, 2008) and *Lyn*$^{-/-}$ knock-out mice display an increased number of HSC with an impaired repopulating capacity (Orschell *et al.*, 2008). Endogenous LYN expression (and activity) may then counterbalance the effect of HCK silencing on STAT5 activation. Achievement of a stronger HCK knock-down might therefore be necessary to trigger a proper phenotype and if proven successful could eventually be used to study the effect of HCK silencing in AML patient samples.

Indeed, Schepers' study also showed that silencing STAT5 in leukaemic CD34$^+$ cells displaying a constitutive STAT5 activity led to a decrease in expansion of the leukaemic cells grown in stromal culture (Schepers *et al.*, 2007). Hence, it would be interesting to see if HCK plays a role in such a phenotype by sorting patient samples according to their level of STAT5 activity and HCK expression prior to silencing HCK.

### 3. HCK overexpression promotes erythroid differentiation at the expense of myeloid differentiation in Lin$^-$ cells

HCK overexpression in Lin$^-$ cells exhibited a clear phenotype of enhanced erythroid differentiation at the expense of myeloid differentiation underlined by the activation of c-Raf, ERK and STAT5. Liquid culture exclusively supporting myeloid differentiation indicated a delay in myeloid differentiation and a block in terminal differentiation upon HCK overexpression, while liquid culture exclusively supporting primitive erythroid differentiation indicated a delay in erythroid differentiation. However, CFC assays supporting both myeloid and erythroid progenitor differentiation simultaneously showed a skew in differentiation towards erythropoiesis. Interestingly this later phenotype correlates with phenotypes observed upon overexpression of constitutively active STAT5 or mutant Flt3-ITD in UCB CD34$^+$ cells by CAFC assays (Chung *et al.*, 2005; Moore *et al.*, 2007; Schuringa *et al.*, 2004). Since erythropoietin (EPO) independence and enhanced self-renewal have also been observed in the later studies, it could be interesting

to test if HCK is also involved in such phenotypes by conducting CFC assays in the absence of EPO, performing colony replating and assaying for repopulating capacity *in vivo* using the NOD/SCID model. Additionally, since intermediary levels of STAT5 overexpression have been reported to positively impact on LTC-IC frequency (Wierenga *et al.*, 2008), the use of an inducible system to modulate HCK overexpression could yield more insight into the implication of HCK in STAT5 activation regulation.

Although it can appear contradictory that we observed HCK overexpression in $Lin^-/CD34^+/CD38^-$ cells from leukaemic patients and that overexpression of HCK in $Lin^-$ cells led to the increase formation of CFU-E accompanied by a decrease in myeloid colony formation, these results have to be looked at in light of the following studies. First of all, it is interesting to see that $Lyn^{-/-}$ mice display a block in erythropoiesis, as early-stage erythroblasts fail to expand upon EPO and SCF stimulation (Karur *et al.*, 2006). It could therefore be of interest to see if LYN silencing in human $Lin^-$ cells would give rise to a similar phenotype to the one observed in murine HSC, suggesting an opposite role for HCK and LYN in erythroid cell expansion at different stages of erythropoiesis. In addition, it would be interesting to see what happens upon LYN overexpression. Moreover, $Lyn^{-/-}/Hck^{-/-}$ mice display a STAT5 dependent skewed differentiation towards macrophages that evolves into mild MPD (Xiao *et al.*, 2008). It is intriguing to observe that LYN knock-out led to a decrease in STAT5 activation in $Lyn^{-/-}$ erythroblasts, while $Lyn^{-/-}/Hck^{-/-}$ mouse HSC and macrophages displayed an increased STAT5 activation. It would therefore be important to confirm whether HCK silencing in $Lin^-$ cells leads to a decrease in STAT5 activity and to establish whether LYN silencing in human cells also results in decreased STAT5 activity, in order to clarify if the regulatory relationships between HCK and LYN that have been established in mouse studies are exactly the same in humans.

In light of these intricate mechanisms of STAT5 activity regulation, it has to be remembered that we found LYN as well as HCK overexpressed in the $Lin^-/CD34^+/CD38^+$ AML fraction in comparison to normal bone marrow in our microarray data, while only HCK was overexpressed in the $Lin^-/CD34^+/CD38^-$ AML fraction in comparison to normal bone marrow. Thus, modulating HCK expression in $Lin^-/CD34^+/CD38^-$ or $Lin^-$

/$CD34^+$/$CD38^+$ subset might have a different impact on their differentiation and self-renewal capacity. When working with AML patients, screening for the expression (and activity) of different SFK, or at least HCK and LYN, as well as STAT5 and STAT3 activity prior to manipulating them might allow to stratify normal karyotype patient samples and could also be looked at in correlation to FLT3 or SHIP1 mutation status. Indeed these different proteins are all involved in the same signalling pathway that culminates in the modulation of differentiation specific transcription factors such as CEBPα, PU.1 and GATA1 (Choudhary *et al.*, 2007; Ingley *et al.*, 2005; Olthof *et al.*, 2008; Rimmele *et al.*, 2007; Wierenga *et al.*, 2006) and are also implicated in leukaemogenesis involving chromosomal translocations. Ultimately such studies would help to understand which critical transducer of this signalling pathway should be specifically targeted in order to induce differentiation of AML blasts and/or abrogate their maintenance by LSC.

## References

Abram C. L. and Lowell C. A. (2007a) Convergence of immunoreceptor and integrin signaling. *Immunol Rev* **218**, 29-44.

Abram C. L. and Lowell C. A. (2007b) The expanding role for ITAM-based signaling pathways in immune cells. *Sci STKE* **2007**, re2.

Abrink M., Gobl A. E., Huang R., Nilsson K. and Hellman L. (1994) Human cell lines U-937, THP-1 and Mono Mac 6 represent relatively immature cells of the monocyte-macrophage cell lineage. *Leukemia* **8**, 1579-84.

Achuthan A., Elsegood C., Masendycz P., Hamilton J. A. and Scholz G. M. (2006) CpG DNA enhances macrophage cell spreading by promoting the Src-family kinase-mediated phosphorylation of paxillin. *Cell Signal* **18**, 2252-61.

Adachi R. and Suzuki K. (2007) Lyn, one of the Src-family tyrosine kinases expressed in phagocytes, plays an important role in beta2 integrin-signalling pathways in opsonized zymosan-activated macrophage-like U937 cells. *Cell Biochem Funct* **25**, 323-33.

Al-Hajj M., Wicha M. S., Benito-Hernandez A., Morrison S. J. and Clarke M. F. (2003) Prospective identification of tumorigenic breast cancer cells. *Proc Natl Acad Sci U S A* **100**, 3983-8.

Appelbaum F. R., Rowe J. M., Radich J. and Dick J. E. (2001) Acute myeloid leukemia. *Hematology Am Soc Hematol Educ Program*, 62-86.

Appleby M. W., Gross J. A., Cooke M. P., Levin S. D., Qian X. and Perlmutter R. M. (1992) Defective T cell receptor signaling in mice lacking the thymic isoform of p59fyn. *Cell* **70**, 751-63.

Avalos B. R., Parker J. M., Ware D. A., Hunter M. G., Sibert K. A. and Druker B. J. (1997) Dissociation of the Jak kinase pathway from G-CSF receptor signaling in neutrophils. *Exp Hematol* **25**, 160-8.

Azam M., Erdjument-Bromage H., Kreider B. L., Xia M., Quelle F., Basu R., Saris C., Tempst P., Ihle J. N. and Schindler C. (1995) Interleukin-3 signals through multiple isoforms of Stat5. *Embo J* **14**, 1402-11.

Banavali N. K. and Roux B. (2008) Flexibility and charge asymmetry in the activation loop of Src tyrosine kinases. *Proteins*.

Barabe F., Kennedy J. A., Hope K. J. and Dick J. E. (2007) Modeling the initiation and progression of human acute leukemia in mice. *Science* **316**, 600-4.

Barber D. L., Beattie B. K., Mason J. M., Nguyen M. H., Yoakim M., Neel B. G., D'Andrea A. D. and Frank D. A. (2001) A common epitope is shared by activated signal transducer and activator of transcription-5 (STAT5) and the phosphorylated erythropoietin receptor: implications for the docking model of STAT activation. *Blood* **97**, 2230-7.

Barjesteh van Waalwijk van Doorn-Khosrovani S., Erpelinck C., Meijer J., van Oosterhoud S., van Putten W. L., Valk P. J., Berna Beverloo H., Tenen D. G., Lowenberg B. and Delwel R. (2003) Biallelic mutations in the CEBPA gene and low CEBPA expression levels as prognostic markers in intermediate-risk AML. *Hematol J* **4**, 31-40.

Beghini A., Peterlongo P., Ripamonti C. B., Larizza L., Cairoli R., Morra E. and Mecucci C. (2000) C-kit mutations in core binding factor leukemias. *Blood* **95**, 726-7.

Benati D. and Baldari C. T. (2008) SRC family kinases as potential therapeutic targets for malignancies and immunological disorders. *Curr Med Chem* **15**, 1154-65.

Bentires-Alj M., Paez J. G., David F. S., Keilhack H., Halmos B., Naoki K., Maris J. M., Richardson A., Bardelli A., Sugarbaker D. J., Richards W. G., Du J., Girard L., Minna J. D., Loh M. L., Fisher D. E., Velculescu V. E., Vogelstein B., Meyerson M., Sellers W. R. and Neel B. G. (2004) Activating mutations of the noonan syndrome-associated SHP2/PTPN11 gene in human solid tumors and adult acute myelogenous leukemia. *Cancer Res* **64**, 8816-20.

Bergmann L., Maurer U. and Weidmann E. (1997) Wilms tumor gene expression in acute myeloid leukemias. *Leuk Lymphoma* **25**, 435-43.

Bhatia M., Bonnet D., Murdoch B., Gan O. I. and Dick J. E. (1998) A newly discovered class of human hematopoietic cells with SCID-repopulating activity. *Nat Med* **4**, 1038-45.

Bhatia M., Wang J. C., Kapp U., Bonnet D. and Dick J. E. (1997) Purification of primitive human hematopoietic cells capable of repopulating immune-deficient mice. *Proc Natl Acad Sci U S A* **94**, 5320-5.

Bibbins K. B., Boeuf H. and Varmus H. E. (1993) Binding of the Src SH2 domain to phosphopeptides is determined by residues in both the SH2 domain and the phosphopeptides. *Mol Cell Biol* **13**, 7278-87.

Bienz M., Ludwig M., Leibundgut E. O., Mueller B. U., Ratschiller D., Solenthaler M., Fey M. F. and Pabst T. (2005) Risk assessment in patients with acute myeloid leukemia and a normal karyotype. *Clin Cancer Res* **11**, 1416-24.

Biethahn S., Alves F., Wilde S., Hiddemann W. and Spiekermann K. (1999) Expression of granulocyte colony-stimulating factor- and granulocyte-macrophage colony-stimulating factor-associated signal transduction proteins of the JAK/STAT pathway in normal granulopoiesis and in blast cells of acute myelogenous leukemia. *Exp Hematol* **27**, 885-94.

Birg F., Courcoul M., Rosnet O., Bardin F., Pebusque M. J., Marchetto S., Tabilio A., Mannoni P. and Birnbaum D. (1992) Expression of the FMS/KIT-like gene FLT3 in human acute leukemias of the myeloid and lymphoid lineages. *Blood* **80**, 2584-93.

Bjorge J. D., Jakymiw A. and Fujita D. J. (2000) Selected glimpses into the activation and function of Src kinase. *Oncogene* **19**, 5620-35.

Blair A., Hogge D. E., Ailles L. E., Lansdorp P. M. and Sutherland H. J. (1997) Lack of expression of Thy-1 (CD90) on acute myeloid leukemia cells with long-term proliferative ability in vitro and in vivo. *Blood* **89**, 3104-12.

Blake R. A., Broome M. A., Liu X., Wu J., Gishizky M., Sun L. and Courtneidge S. A. (2000) SU6656, a selective src family kinase inhibitor, used to probe growth factor signaling. *Mol Cell Biol* **20**, 9018-27.

Boissel N., Renneville A., Biggio V., Philippe N., Thomas X., Cayuela J. M., Terre C., Tigaud I., Castaigne S., Raffoux E., De Botton S., Fenaux P., Dombret H. and Preudhomme C. (2005) Prevalence, clinical profile, and prognosis of NPM1 mutations in AML with normal karyotype. *Blood* **106**, 3618-20.

Bonnet D. and Dick J. E. (1997) Human acute myeloid leukemia is organized as a hierarchy that originates from a primitive hematopoietic cell. *Nat Med* **3**, 730-7.

Borneo J., Munugalavadla V., Sims E. C., Vemula S., Orschell C. M., Yoder M. and Kapur R. (2007) Src family kinase-mediated negative regulation of hematopoietic stem cell mobilization involves both intrinsic and microenvironmental factors. *Exp Hematol* **35**, 1026-37.

Brandts C. H., Sargin B., Rode M., Biermann C., Lindtner B., Schwable J., Buerger H., Muller-Tidow C., Choudhary C., McMahon M., Berdel W. E. and Serve H. (2005) Constitutive activation of Akt by Flt3 internal tandem duplications is necessary for increased survival, proliferation, and myeloid transformation. *Cancer Res* **65**, 9643-50.

Breems D. A., Blokland E. A., Neben S. and Ploemacher R. E. (1994) Frequency analysis of human primitive haematopoietic stem cell subsets using a cobblestone area forming cell assay. *Leukemia* **8**, 1095-104.

Brender C., Nielsen M., Kaltoft K., Mikkelsen G., Zhang Q., Wasik M., Billestrup N. and Odum N. (2001) STAT3-mediated constitutive expression of SOCS-3 in cutaneous T-cell lymphoma. *Blood* **97**, 1056-62.

Briggs S. D., Bryant S. S., Jove R., Sanderson S. D. and Smithgall T. E. (1995) The Ras GTPase-activating protein (GAP) is an SH3 domain-binding protein and substrate for the Src-related tyrosine kinase, Hck. *J Biol Chem* **270**, 14718-24.

Briggs S. D., Sharkey M., Stevenson M. and Smithgall T. E. (1997) SH3-mediated Hck tyrosine kinase activation and fibroblast transformation by the Nef protein of HIV-1. *J Biol Chem* **272**, 17899-902.

Broome M. A. and Hunter T. (1997) The PDGF receptor phosphorylates Tyr 138 in the c-Src SH3 domain in vivo reducing peptide ligand binding. *Oncogene* **14**, 17-34.

Brown M. T. and Cooper J. A. (1996) Regulation, substrates and functions of src. *Biochim Biophys Acta* **1287**, 121-49.

Brugge J. S., Cotton P. C., Queral A. E., Barrett J. N., Nonner D. and Keane R. W. (1985) Neurones express high levels of a structurally modified, activated form of pp60c-src. *Nature* **316**, 554-7.

Bruns H. A. and Kaplan M. H. (2006) The role of constitutively active Stat6 in leukemia and lymphoma. *Crit Rev Oncol Hematol* **57**, 245-53.

Bullinger L., Dohner K., Kranz R., Stirner C., Frohling S., Scholl C., Kim Y. H., Schlenk R. F., Tibshirani R., Dohner H. and Pollack J. R. (2008) An FLT3 gene-expression signature predicts clinical outcome in normal karyotype AML. *Blood* **111**, 4490-5.

Buss J. E., Kamps M. P. and Sefton B. M. (1984) Myristic acid is attached to the transforming protein of Rous sarcoma virus during or immediately after synthesis and is present in both soluble and membrane-bound forms of the protein. *Mol Cell Biol* **4**, 2697-704.

Byrd J. C., Mrozek K., Dodge R. K., Carroll A. J., Edwards C. G., Arthur D. C., Pettenati M. J., Patil S. R., Rao K. W., Watson M. S., Koduru P. R., Moore J. O., Stone R. M., Mayer R. J., Feldman E. J., Davey F. R., Schiffer C. A., Larson R. A. and Bloomfield C. D. (2002) Pretreatment cytogenetic abnormalities are predictive of induction success, cumulative incidence of relapse, and overall survival in adult

patients with de novo acute myeloid leukemia: results from Cancer and Leukemia Group B (CALGB 8461). *Blood* **100**, 4325-36.

Cacalano N. A., Migone T. S., Bazan F., Hanson E. P., Chen M., Candotti F., O'Shea J. J. and Johnston J. A. (1999) Autosomal SCID caused by a point mutation in the N-terminus of Jak3: mapping of the Jak3-receptor interaction domain. *Embo J* **18**, 1549-58.

Caldenhoven E., van Dijk T., Raaijmakers J. A., Lammers J. W., Koenderman L. and De Groot R. P. (1995) Activation of the STAT3/acute phase response factor transcription factor by interleukin-5. *J Biol Chem* **270**, 25778-84.

Caligiuri M. A., Strout M. P., Lawrence D., Arthur D. C., Baer M. R., Yu F., Knuutila S., Mrozek K., Oberkircher A. R., Marcucci G., de la Chapelle A., Elonen E., Block A. W., Rao P. N., Herzig G. P., Powell B. L., Ruutu T., Schiffer C. A. and Bloomfield C. D. (1998) Rearrangement of ALL1 (MLL) in acute myeloid leukemia with normal cytogenetics. *Cancer Res* **58**, 55-9.

Carreno S., Caron E., Cougoule C., Emorine L. J. and Maridonneau-Parini I. (2002) p59Hck isoform induces F-actin reorganization to form protrusions of the plasma membrane in a Cdc42- and Rac-dependent manner. *J Biol Chem* **277**, 21007-16.

Carreno S., Gouze M. E., Schaak S., Emorine L. J. and Maridonneau-Parini I. (2000) Lack of palmitoylation redirects p59Hck from the plasma membrane to p61Hck-positive lysosomes. *J Biol Chem* **275**, 36223-9.

Casas S., Nagy B., Elonen E., Aventin A., Larramendy M. L., Sierra J., Ruutu T. and Knuutila S. (2003) Aberrant expression of HOXA9, DEK, CBL and CSF1R in acute myeloid leukemia. *Leuk Lymphoma* **44**, 1935-41.

Cashman J. D., Lapidot T., Wang J. C., Doedens M., Shultz L. D., Lansdorp P., Dick J. E. and Eaves C. J. (1997) Kinetic evidence of the regeneration of multilineage hematopoiesis from primitive cells in normal human bone marrow transplanted into immunodeficient mice. *Blood* **89**, 4307-16.

Chai S. K., Nichols G. L. and Rothman P. (1997) Constitutive activation of JAK and STAT in BCR-Abl-expressing cell lines and peripheral blood cells derived from leukemic patients. *J Immunol* **159**, 4720-8.

Chang C. M., Shu H. K. and Kung H. J. (1995) Disease specificity of kinase domains: the src-encoded catalytic domain converts erbB into a sarcoma oncogene. *Proc Natl Acad Sci U S A* **92**, 3928-32.

Chaturvedi P., Reddy M. V. and Reddy E. P. (1998) Src kinases and not JAK activate STAT during IL-3 induced myeloid cell proliferation. *Oncogene* **16**, 1749-58.

Chaturvedi P., Sharma S. and Reddy E. P. (1997) Abrogation of interleukin-3 dependence of myeloid cells by the v-src oncogene requires SH2 and SH3 domains which specify activation of STAT. *Mol Cell Biol* **17**, 3295-304.

Cheadle C., Ivashchenko Y., South V., Searfoss G. H., French S., Howk R., Ricca G. A. and Jaye M. (1994) Identification of a Src SH3 domain binding motif by screening a random phage display library. *J Biol Chem* **269**, 24034-9.

Chen M., Cheng A., Chen Y. Q., Hymel A., Hanson E. P., Kimmel L., Minami Y., Taniguchi T., Changelian P. S. and O'Shea J. J. (1997) The amino terminus of JAK3 is necessary and sufficient for binding to the common gamma chain and confers the ability to transmit interleukin 2-mediated signals. *Proc Natl Acad Sci U S A* **94**, 6910-5.

Chen W., Rassidakis G. Z. and Medeiros L. J. (2006) Nucleophosmin gene mutations in acute myeloid leukemia. *Arch Pathol Lab Med* **130**, 1687-92.

Chin H., Arai A., Wakao H., Kamiyama R., Miyasaka N. and Miura O. (1998) Lyn physically associates with the erythropoietin receptor and may play a role in activation of the Stat5 pathway. *Blood* **91**, 3734-45.

Chong Y. P., Ia K. K., Mulhern T. D. and Cheng H. C. (2005) Endogenous and synthetic inhibitors of the Src-family protein tyrosine kinases. *Biochim Biophys Acta* **1754**, 210-20.

Choudhary C., Brandts C., Schwable J., Tickenbrock L., Sargin B., Ueker A., Bohmer F. D., Berdel W. E., Muller-Tidow C. and Serve H. (2007) Activation mechanisms of STAT5 by oncogenic Flt3-ITD. *Blood* **110**, 370-4.

Chung K. Y., Morrone G., Schuringa J. J., Wong B., Dorn D. C. and Moore M. A. (2005) Enforced expression of an Flt3 internal tandem duplication in human CD34+ cells confers properties of self-renewal and enhanced erythropoiesis. *Blood* **105**, 77-84.

Collins A. T., Berry P. A., Hyde C., Stower M. J. and Maitland N. J. (2005) Prospective identification of tumorigenic prostate cancer stem cells. *Cancer Res* **65**, 10946-51.

Cooper J. A. and Howell B. (1993) The when and how of Src regulation. *Cell* **73**, 1051-4.

Corey S. J. and Anderson S. M. (1999) Src-related protein tyrosine kinases in hematopoiesis. *Blood* **93**, 1-14.

Corey S. J., Burkhardt A. L., Bolen J. B., Geahlen R. L., Tkatch L. S. and Tweardy D. J. (1994) Granulocyte colony-stimulating factor receptor signaling involves the formation of a three-component complex with Lyn and Syk protein-tyrosine kinases. *Proc Natl Acad Sci U S A* **91**, 4683-7.

Cougoule C., Carreno S., Castandet J., Labrousse A., Astarie-Dequeker C., Poincloux R., Le Cabec V. and Maridonneau-Parini I. (2005) Activation of the lysosome-associated p61Hck isoform triggers the biogenesis of podosomes. *Traffic* **6**, 682-94.

Cristofalo V. J., Allen R. G., Pignolo R. J., Martin B. G. and Beck J. C. (1998) Relationship between donor age and the replicative lifespan of human cells in culture: a reevaluation. *Proc Natl Acad Sci U S A* **95**, 10614-9.

Cuenco G. M. and Ren R. (2004) Both AML1 and EVI1 oncogenic components are required for the cooperation of AML1/MDS1/EVI1 with BCR/ABL in the induction of acute myelogenous leukemia in mice. *Oncogene* **23**, 569-79.

Dalerba P., Dylla S. J., Park I. K., Liu R., Wang X., Cho R. W., Hoey T., Gurney A., Huang E. H., Simeone D. M., Shelton A. A., Parmiani G., Castelli C. and Clarke M. F. (2007) Phenotypic characterization of human colorectal cancer stem cells. *Proc Natl Acad Sci U S A* **104**, 10158-63.

Danhauser-Riedl S., Warmuth M., Druker B. J., Emmerich B. and Hallek M. (1996) Activation of Src kinases p53/56lyn and p59hck by p210bcr/abl in myeloid cells. *Cancer Res* **56**, 3589-96.

Darnell J. E., Jr. (1997) STAT and gene regulation. *Science* **277**, 1630-5.

Darnell J. E., Jr., Kerr I. M. and Stark G. R. (1994) Jak-STAT pathways and transcriptional activation in response to IFNs and other extracellular signaling proteins. *Science* **264**, 1415-21.

Dash A. and Gilliland D. G. (2001) Molecular genetics of acute myeloid leukaemia. *Best Pract Res Clin Haematol* **14**, 49-64.

DaSilva L., Howard O. M., Rui H., Kirken R. A. and Farrar W. L. (1994) Growth signaling and JAK2 association mediated by membrane-proximal cytoplasmic regions of prolactin receptors. *J Biol Chem* **269**, 18267-70.

Davidson D., Chow L. M., Fournel M. and Veillette A. (1992) Differential regulation of T cell antigen responsiveness by isoforms of the src-related tyrosine protein kinase p59fyn. *J Exp Med* **175**, 1483-92.

Deasy B. M., Jankowski R. J., Payne T. R., Cao B., Goff J. P., Greenberger J. S. and Huard J. (2003) Modeling stem cell population growth: incorporating terms for proliferative heterogeneity. *Stem Cells* **21**, 536-45.

Demaison C., Parsley K., Brouns G., Scherr M., Battmer K., Kinnon C., Grez M. and Thrasher A. J. (2002) High-level transduction and gene expression in hematopoietic repopulating cells using a human immunodeficiency [correction of imunodeficiency] virus type 1-based lentiviral vector containing an internal spleen focus forming virus promoter. *Hum Gene Ther* **13**, 803-13.

Denizot Y. (2000) Soluble IL-6 receptor levels in AML patients. *Cytokine* **12**, 422.

Desrivieres S., Kunz C., Barash I., Vafaizadeh V., Borghouts C. and Groner B. (2006) The biological functions of the versatile transcription factors STAT3 and STAT5 and new strategies for their targeted inhibition. *J Mammary Gland Biol Neoplasia* **11**, 75-87.

Dick J. E., Bhatia M., Gan O., Kapp U. and Wang J. C. (1997) Assay of human stem cells by repopulation of NOD/SCID mice. *Stem Cells* **15 Suppl 1**, 199-203; discussion 204-7.

Dohner K., Schlenk R. F., Habdank M., Scholl C., Rucker F. G., Corbacioglu A., Bullinger L., Frohling S. and Dohner H. (2005) Mutant nucleophosmin (NPM11) predicts favorable prognosis in younger adults with acute myeloid leukemia and normal cytogenetics: interaction with other gene mutations. *Blood* **106**, 3740-6.

Dohner K., Tobis K., Ulrich R., Frohling S., Benner A., Schlenk R. F. and Dohner H. (2002) Prognostic significance of partial tandem duplications of the MLL gene in adult patients 16 to 60 years old with acute myeloid leukemia and normal cytogenetics: a study of the Acute Myeloid Leukemia Study Group Ulm. *J Clin Oncol* **20**, 3254-61.

Donato N. J., Wu J. Y., Stapley J., Gallick G., Lin H., Arlinghaus R. and Talpaz M. (2003) BCR-ABL independence and LYN kinase overexpression in chronic myelogenous leukemia cells selected for resistance to STI571. *Blood* **101**, 690-8.

Dos Santos C., Demur C., Bardet V., Prade-Houdellier N., Payrastre B. and Recher C. (2008) A critical role for Lyn in acute myeloid leukemia. *Blood* **111**, 2269-79.

Drynan L. F., Pannell R., Forster A., Chan N. M., Cano F., Daser A. and Rabbitts T. H. (2005) Mll fusions generated by Cre-loxP-mediated de novo translocations can induce lineage reassignment in tumorigenesis. *Embo J* **24**, 3136-46.

Dutartre H., Harris M., Olive D. and Collette Y. (1998) The human immunodeficiency virus type 1 Nef protein binds the Src-related tyrosine kinase Lck SH2 domain through a novel phosphotyrosine independent mechanism. *Virology* **247**, 200-11.

Edvardsson L., Dykes J., Olsson M. L. and Olofsson T. (2004) Clonogenicity, gene expression and phenotype during neutrophil versus erythroid differentiation of cytokine-stimulated CD34+ human marrow cells in vitro. *Br J Haematol* **127**, 451-63.

English B. K. (1996) Expression of the activated (Y501-F501) hck tyrosine kinase in 32Dcl3 myeloid cells prolongs survival in the absence of IL-3 and blocks granulocytic differentiation in response to G-CSF. *J Leukoc Biol* **60**, 667-73.

Erl W., Weber C., Wardemann C. and Weber P. C. (1995) Adhesion properties of Mono Mac 6, a monocytic cell line with characteristics of mature human monocytes. *Atherosclerosis* **113**, 99-107.

Ernst M., Gearing D. P. and Dunn A. R. (1994) Functional and biochemical association of Hck with the LIF/IL-6 receptor signal transducing subunit gp130 in embryonic stem cells. *Embo J* **13**, 1574-84.

Ernst M., Inglese M., Scholz G. M., Harder K. W., Clay F. J., Bozinovski S., Waring P., Darwiche R., Kay T., Sly P., Collins R., Turner D., Hibbs M. L., Anderson G. P. and Dunn A. R. (2002) Constitutive activation of the SRC family kinase Hck results in spontaneous pulmonary inflammation and an enhanced innate immune response. *J Exp Med* **196**, 589-604.

Ernst M., Novak U., Nicholson S. E., Layton J. E. and Dunn A. R. (1999) The carboxyl-terminal domains of gp130-related cytokine receptors are necessary for suppressing embryonic stem cell differentiation. Involvement of STAT3. *J Biol Chem* **274**, 9729-37.

Ernst M., Oates A. and Dunn A. R. (1996) Gp130-mediated signal transduction in embryonic stem cells involves activation of Jak and Ras/mitogen-activated protein kinase pathways. *J Biol Chem* **271**, 30136-43.

Erpel T., Superti-Furga G. and Courtneidge S. A. (1995) Mutational analysis of the Src SH3 domain: the same residues of the ligand binding surface are important for intra- and intermolecular interactions. *Embo J* **14**, 963-75.

Evangelista V., Pamuklar Z., Piccoli A., Manarini S., Dell'elba G., Pecce R., Martelli N., Federico L., Rojas M., Berton G., Lowell C. A., Totani L. and Smyth S. S. (2007) Src family kinases mediate neutrophil adhesion to adherent platelets. *Blood* **109**, 2461-9.

Fang D., Nguyen T. K., Leishear K., Finko R., Kulp A. N., Hotz S., Van Belle P. A., Xu X., Elder D. E. and Herlyn M. (2005) A tumorigenic subpopulation with stem cell properties in melanomas. *Cancer Res* **65**, 9328-37.

Ferracini R. and Brugge J. (1990) Analysis of mutant forms of the c-src gene product containing a phenylalanine substitution for tyrosine 416. *Oncogene Res* **5**, 205-19.

Fitzer-Attas C. J., Lowry M., Crowley M. T., Finn A. J., Meng F., DeFranco A. L. and Lowell C. A. (2000) Fcgamma receptor-mediated phagocytosis in macrophages lacking the Src family tyrosine kinases Hck, Fgr, and Lyn. *J Exp Med* **191**, 669-82.

Ford A. M., Bennett C. A., Price C. M., Bruin M. C., Van Wering E. R. and Greaves M. (1998) Fetal origins of the TEL-AML1 fusion gene in identical twins with leukemia. *Proc Natl Acad Sci U S A* **95**, 4584-8.

Frame M. C., Fincham V. J., Carragher N. O. and Wyke J. A. (2002) v-Src's hold over actin and cell adhesions. *Nat Rev Mol Cell Biol* **3**, 233-45.

Frank S. J., Yi W., Zhao Y., Goldsmith J. F., Gilliland G., Jiang J., Sakai I. and Kraft A. S. (1995) Regions of the JAK2 tyrosine kinase required for coupling to the growth hormone receptor. *J Biol Chem* **270**, 14776-85.

Frohling S., Schlenk R. F., Stolze I., Bihlmayr J., Benner A., Kreitmeier S., Tobis K., Dohner H. and Dohner K. (2004) CEBPA mutations in younger adults with acute myeloid leukemia and normal cytogenetics: prognostic relevance and analysis of cooperating mutations. *J Clin Oncol* **22**, 624-33.

Gassmann M., Guttinger M., Amrein K. E. and Burn P. (1992) Protein tyrosine kinase p59fyn is associated with the T cell receptor-CD3 complex in functional human lymphocytes. *Eur J Immunol* **22**, 283-6.

Giagulli C., Ottoboni L., Caveggion E., Rossi B., Lowell C., Constantin G., Laudanna C. and Berton G. (2006) The Src family kinases Hck and Fgr are dispensable for inside-out, chemoattractant-induced signaling regulating beta 2 integrin affinity and valency in neutrophils, but are required for beta 2 integrin-mediated outside-in signaling involved in sustained adhesion. *J Immunol* **177**, 604-11.

Giancotti F. G. and Tarone G. (2003) Positional control of cell fate through joint integrin/receptor protein kinase signaling. *Annu Rev Cell Dev Biol* **19**, 173-206.

Giarratana M. C., Kobari L., Lapillonne H., Chalmers D., Kiger L., Cynober T., Marden M. C., Wajcman H. and Douay L. (2005) Ex vivo generation of fully mature human red blood cells from hematopoietic stem cells. *Nat Biotechnol* **23**, 69-74.

Gilliland D. G. (2001) Hematologic malignancies. *Curr Opin Hematol* **8**, 189-91.

Gouilleux-Gruart V., Gouilleux F., Desaint C., Claisse J. F., Capiod J. C., Delobel J., Weber-Nordt R., Dusanter-Fourt I., Dreyfus F., Groner B. and Prin L. (1996) STAT-related transcription factors are constitutively activated in peripheral blood cells from acute leukemia patients. *Blood* **87**, 1692-7.

Graf M., Hecht K., Reif S., Pelka-Fleischer R., Pfister K. and Schmetzer H. (2004) Expression and prognostic value of hemopoietic cytokine receptors in acute myeloid leukemia (AML): implications for future therapeutical strategies. *Eur J Haematol* **72**, 89-106.

Grant S. G., O'Dell T. J., Karl K. A., Stein P. L., Soriano P. and Kandel E. R. (1992) Impaired long-term potentiation, spatial learning, and hippocampal development in fyn mutant mice. *Science* **258**, 1903-10.

Greene M. E., Mundschau G., Wechsler J., McDevitt M., Gamis A., Karp J., Gurbuxani S., Arceci R. and Crispino J. D. (2003) Mutations in GATA1 in both transient myeloproliferative disorder and acute megakaryoblastic leukemia of Down syndrome. *Blood Cells Mol Dis* **31**, 351-6.

Grimwade D., Walker H., Oliver F., Wheatley K., Harrison C., Harrison G., Rees J., Hann I., Stevens R., Burnett A. and Goldstone A. (1998) The importance of diagnostic cytogenetics on outcome in AML: analysis of 1,612 patients entered into the MRC AML 10 trial. The Medical Research Council Adult and Children's Leukaemia Working Parties. *Blood* **92**, 2322-33.

Grisendi S., Bernardi R., Rossi M., Cheng K., Khandker L., Manova K. and Pandolfi P. P. (2005) Role of nucleophosmin in embryonic development and tumorigenesis. *Nature* **437**, 147-53.

Groves T., Smiley P., Cooke M. P., Forbush K., Perlmutter R. M. and Guidos C. J. (1996) Fyn can partially substitute for Lck in T lymphocyte development. *Immunity* **5**, 417-28.

Guan Y., Gerhard B. and Hogge D. E. (2003) Detection, isolation, and stimulation of quiescent primitive leukemic progenitor cells from patients with acute myeloid leukemia (AML). *Blood* **101**, 3142-9.

Haan C., Kreis S., Margue C. and Behrmann I. (2006) JAK and cytokine receptors--an intimate relationship. *Biochem Pharmacol* **72**, 1538-46.

Hallek M., Neumann C., Schaffer M., Danhauser-Riedl S., von Bubnoff N., de Vos G., Druker B. J., Yasukawa K., Griffin J. D. and Emmerich B. (1997) Signal transduction of interleukin-6 involves tyrosine phosphorylation of multiple cytosolic proteins and activation of Src-family kinases Fyn, Hck, and Lyn in multiple myeloma cell lines. *Exp Hematol* **25**, 1367-77.

Hamerman J. A. and Lanier L. L. (2006) Inhibition of immune responses by ITAM-bearing receptors. *Sci STKE* **2006**, re1.

Hao Q. L., Smogorzewska E. M., Barsky L. W. and Crooks G. M. (1998) In vitro identification of single CD34+CD38- cells with both lymphoid and myeloid potential. *Blood* **91**, 4145-51.

Harder K. W., Parsons L. M., Armes J., Evans N., Kountouri N., Clark R., Quilici C., Grail D., Hodgson G. S., Dunn A. R. and Hibbs M. L. (2001) Gain- and loss-of-function Lyn mutant mice define a critical inhibitory role for Lyn in the myeloid lineage. *Immunity* **15**, 603-15.

Harris N. L., Jaffe E. S., Diebold J., Flandrin G., Muller-Hermelink H. K., Vardiman J., Lister T. A. and Bloomfield C. D. (1999) World Health Organization classification of neoplastic diseases of the hematopoietic and lymphoid tissues: report of the Clinical Advisory Committee meeting-Airlie House, Virginia, November 1997. *J Clin Oncol* **17**, 3835-49.

Hausherr A., Tavares R., Schaffer M., Obermeier A., Miksch C., Mitina O., Ellwart J., Hallek M. and Krause G. (2007) Inhibition of IL-6-dependent growth of myeloma cells by an acidic peptide repressing the gp130-mediated activation of Src family kinases. *Oncogene* **26**, 4987-98.

He B., You L., Uematsu K., Matsangou M., Xu Z., He M., McCormick F. and Jablons D. M. (2003) Cloning and characterization of a functional promoter of the human SOCS-3 gene. *Biochem Biophys Res Commun* **301**, 386-91.

Heinonen K. M., Dube N., Bourdeau A., Lapp W. S. and Tremblay M. L. (2006) Protein tyrosine phosphatase 1B negatively regulates macrophage development through CSF-1 signaling. *Proc Natl Acad Sci U S A* **103**, 2776-81.

Hethcote H. W. and Knudson A. G., Jr. (1978) Model for the incidence of embryonal cancers: application to retinoblastoma. *Proc Natl Acad Sci U S A* **75**, 2453-7.

Hibbs M. L., Tarlinton D. M., Armes J., Grail D., Hodgson G., Maglitto R., Stacker S. A. and Dunn A. R. (1995) Multiple defects in the immune system of Lyn-deficient mice, culminating in autoimmune disease. *Cell* **83**, 301-11.

Hiddemann W., Spiekermann K., Buske C., Feuring-Buske M., Braess J., Haferlach T., Schoch C., Kern W., Schnittger S., Berdel W., Wormann B., Heinecke A., Sauerland C. and Buchner T. (2005) Towards a pathogenesis-oriented therapy of acute myeloid leukemia. *Crit Rev Oncol Hematol* **56**, 235-45.

Hirahashi J., Mekala D., Van Ziffle J., Xiao L., Saffaripour S., Wagner D. D., Shapiro S. D., Lowell C. and Mayadas T. N. (2006) Mac-1 signaling via Src-family and Syk

kinases results in elastase-dependent thrombohemorrhagic vasculopathy. *Immunity* **25**, 271-83.

Hirai H. and Varmus H. E. (1990a) Mutations in src homology regions 2 and 3 of activated chicken c-src that result in preferential transformation of mouse or chicken cells. *Proc Natl Acad Sci U S A* **87**, 8592-6.

Hirai H. and Varmus H. E. (1990b) Site-directed mutagenesis of the SH2- and SH3-coding domains of c-src produces varied phenotypes, including oncogenic activation of p60c-src. *Mol Cell Biol* **10**, 1307-18.

Ho A. D. (2005) Kinetics and symmetry of divisions of hematopoietic stem cells. *Exp Hematol* **33**, 1-8.

Hogan C. J., Shpall E. J., McNulty O., McNiece I., Dick J. E., Shultz L. D. and Keller G. (1997) Engraftment and development of human CD34(+)-enriched cells from umbilical cord blood in NOD/LtSz-scid/scid mice. *Blood* **90**, 85-96.

Hong D., Gupta R., Ancliff P., Atzberger A., Brown J., Soneji S., Green J., Colman S., Piacibello W., Buckle V., Tsuzuki S., Greaves M. and Enver T. (2008) Initiating and cancer-propagating cells in TEL-AML1-associated childhood leukemia. *Science* **319**, 336-9.

Hong H., Kitaura J., Xiao W., Horejsi V., Ra C., Lowell C. A., Kawakami Y. and Kawakami T. (2007) The Src family kinase Hck regulates mast cell activation by suppressing an inhibitory Src family kinase Lyn. *Blood* **110**, 2511-9.

Horowitz M. M., Gale R. P., Sondel P. M., Goldman J. M., Kersey J., Kolb H. J., Rimm A. A., Ringden O., Rozman C., Speck B. and et al. (1990) Graft-versus-leukemia reactions after bone marrow transplantation. *Blood* **75**, 555-62.

Howlett C. J., Bisson S. A., Resek M. E., Tigley A. W. and Robbins S. M. (1999) The proto-oncogene p120(Cbl) is a downstream substrate of the Hck protein-tyrosine kinase. *Biochem Biophys Res Commun* **257**, 129-38.

Hunter T. (1989) Protein modification: phosphorylation on tyrosine residues. *Curr Opin Cell Biol* **1**, 1168-81.

Hunter T. and Cooper J. A. (1985) Protein-tyrosine kinases. *Annu Rev Biochem* **54**, 897-930.

Hunter T. and Sefton B. M. (1980) Transforming gene product of Rous sarcoma virus phosphorylates tyrosine. *Proc Natl Acad Sci U S A* **77**, 1311-5.

Hynes R. O. (1992) Integrins: versatility, modulation, and signaling in cell adhesion. *Cell* **69**, 11-25.

Ihle J. N., Witthuhn B. A., Quelle F. W., Yamamoto K. and Silvennoinen O. (1995) Signaling through the hematopoietic cytokine receptors. *Annu Rev Immunol* **13**, 369-98.

Ilangumaran S., He H. T. and Hoessli D. C. (2000) Microdomains in lymphocyte signalling: beyond GPI-anchored proteins. *Immunol Today* **21**, 2-7.

Ingley E., McCarthy D. J., Pore J. R., Sarna M. K., Adenan A. S., Wright M. J., Erber W., Tilbrook P. A. and Klinken S. P. (2005) Lyn deficiency reduces GATA-1, EKLF and STAT5, and induces extramedullary stress erythropoiesis. *Oncogene* **24**, 336-43.

Irby R. B., Mao W., Coppola D., Kang J., Loubeau J. M., Trudeau W., Karl R., Fujita D. J., Jove R. and Yeatman T. J. (1999) Activating SRC mutation in a subset of advanced human colon cancers. *Nat Genet* **21**, 187-90.

Irby R. B. and Yeatman T. J. (2000) Role of Src expression and activation in human cancer. *Oncogene* **19**, 5636-42.

Ito M., Hiramatsu H., Kobayashi K., Suzue K., Kawahata M., Hioki K., Ueyama Y., Koyanagi Y., Sugamura K., Tsuji K., Heike T. and Nakahata T. (2002) NOD/SCID/gamma(c)(null) mouse: an excellent recipient mouse model for engraftment of human cells. *Blood* **100**, 3175-82.

Jiang N., He T. C., Miyajima A. and Wojchowski D. M. (1996) The box1 domain of the erythropoietin receptor specifies Janus kinase 2 activation and functions mitogenically within an interleukin 2 beta-receptor chimera. *J Biol Chem* **271**, 16472-6.

Joung I., Strominger J. L. and Shin J. (1996) Molecular cloning of a phosphotyrosine-independent ligand of the p56lck SH2 domain. *Proc Natl Acad Sci U S A* **93**, 5991-5.

Kaplan J. M., Mardon G., Bishop J. M. and Varmus H. E. (1988) The first seven amino acids encoded by the v-src oncogene act as a myristylation signal: lysine 7 is a critical determinant. *Mol Cell Biol* **8**, 2435-41.

Karur V. G., Lowell C. A., Besmer P., Agosti V. and Wojchowski D. M. (2006) Lyn kinase promotes erythroblast expansion and late-stage development. *Blood* **108**, 1524-32.

Katagiri K., Katagiri T., Koyama Y., Morikawa M., Yamamoto T. and Yoshida T. (1991) Expression of src family genes during monocytic differentiation of HL-60 cells. *J Immunol* **146**, 701-7.

Kaushansky K. (1998) Thrombopoietin and the hematopoietic stem cell. *Blood* **92**, 1-3.

Kawamura M., Kaku H., Taketani T., Taki T., Shimada A. and Hayashi Y. (2008) Mutations of GATA1, FLT3, MLL-partial tandem duplication, NRAS, and RUNX1 genes are not found in a 7-year-old Down syndrome patient with acute myeloid leukemia (FAB-M2) having a good prognosis. *Cancer Genet Cytogenet* **180**, 74-8.

Kazansky A. V., Kabotyanski E. B., Wyszomierski S. L., Mancini M. A. and Rosen J. M. (1999) Differential effects of prolactin and src/abl kinases on the nuclear translocation of STAT5B and STAT5A. *J Biol Chem* **274**, 22484-92.

Kelly L. M., Kutok J. L., Williams I. R., Boulton C. L., Amaral S. M., Curley D. P., Ley T. J. and Gilliland D. G. (2002) PML/RARalpha and FLT3-ITD induce an APL-like disease in a mouse model. *Proc Natl Acad Sci U S A* **99**, 8283-8.

Klejman A., Schreiner S. J., Nieborowska-Skorska M., Slupianek A., Wilson M., Smithgall T. E. and Skorski T. (2002) The Src family kinase Hck couples BCR/ABL to STAT5 activation in myeloid leukemia cells. *Embo J* **21**, 5766-74.

Knudson A. G. (2001) Two genetic hits (more or less) to cancer. *Nat Rev Cancer* **1**, 157-62.

Kohlhuber F., Rogers N. C., Watling D., Feng J., Guschin D., Briscoe J., Witthuhn B. A., Kotenko S. V., Pestka S., Stark G. R., Ihle J. N. and Kerr I. M. (1997) A JAK1/JAK2 chimera can sustain alpha and gamma interferon responses. *Mol Cell Biol* **17**, 695-706.

Kollet O., Peled A., Byk T., Ben-Hur H., Greiner D., Shultz L. and Lapidot T. (2000) beta2 microglobulin-deficient (B2m(null)) NOD/SCID mice are excellent recipients for studying human stem cell function. *Blood* **95**, 3102-5.

Kondo M., Wagers A. J., Manz M. G., Prohaska S. S., Scherer D. C., Beilhack G. F., Shizuru J. A. and Weissman I. L. (2003) Biology of hematopoietic stem cells and progenitors: implications for clinical application. *Annu Rev Immunol* **21**, 759-806.

Konieczna I., Horvath E., Wang H., Lindsey S., Saberwal G., Bei L., Huang W., Platanias L. and Eklund E. A. (2008) Constitutive activation of SHP2 in mice cooperates with ICSBP deficiency to accelerate progression to acute myeloid leukemia. *J Clin Invest* **118**, 853-67.

Kotenko S. V., Izotova L. S., Pollack B. P., Muthukumaran G., Paukku K., Silvennoinen O., Ihle J. N. and Pestka S. (1996) Other kinases can substitute for Jak2 in signal transduction by interferon-gamma. *J Biol Chem* **271**, 17174-82.

Kouro T., Kikuchi Y., Kanazawa H., Hirokawa K., Harada N., Shiiba M., Wakao H., Takaki S. and Takatsu K. (1996) Critical proline residues of the cytoplasmic domain of the IL-5 receptor alpha chain and its function in IL-5-mediated activation of JAK kinase and STAT5. *Int Immunol* **8**, 237-45.

Kouroku Y., Soyama A., Fujita E., Urase K., Tsukahara T. and Momoi T. (1998) RA70 is a src kinase-associated protein expressed ubiquitously. *Biochem Biophys Res Commun* **252**, 738-42.

Kovarik P., Mangold M., Ramsauer K., Heidari H., Steinborn R., Zotter A., Levy D. E., Muller M. and Decker T. (2001) Specificity of signaling by STAT1 depends on SH2 and C-terminal domains that regulate Ser727 phosphorylation, differentially affecting specific target gene expression. *Embo J* **20**, 91-100.

Kroon E., Thorsteinsdottir U., Mayotte N., Nakamura T. and Sauvageau G. (2001) NUP98-HOXA9 expression in hemopoietic stem cells induces chronic and acute myeloid leukemias in mice. *Embo J* **20**, 350-61.

Kruger A. and Anderson S. M. (1991) The v-src oncogene blocks the differentiation of a murine myeloid progenitor cell line and induces a tumorigenic phenotype. *Oncogene* **6**, 245-56.

Laham L. E., Mukhopadhyay N. and Roberts T. M. (2000) The activation loop in Lck regulates oncogenic potential by inhibiting basal kinase activity and restricting substrate specificity. *Oncogene* **19**, 3961-70.

Lapidot T., Pflumio F., Doedens M., Murdoch B., Williams D. E. and Dick J. E. (1992) Cytokine stimulation of multilineage hematopoiesis from immature human cells engrafted in SCID mice. *Science* **255**, 1137-41.

Lapidot T., Sirard C., Vormoor J., Murdoch B., Hoang T., Caceres-Cortes J., Minden M., Paterson B., Caligiuri M. A. and Dick J. E. (1994) A cell initiating human acute myeloid leukaemia after transplantation into SCID mice. *Nature* **367**, 645-8.

Larochelle A., Vormoor J., Hanenberg H., Wang J. C., Bhatia M., Lapidot T., Moritz T., Murdoch B., Xiao X. L., Kato I., Williams D. A. and Dick J. E. (1996) Identification of primitive human hematopoietic cells capable of repopulating NOD/SCID mouse bone marrow: implications for gene therapy. *Nat Med* **2**, 1329-37.

Latour S. and Veillette A. (2001) Proximal protein tyrosine kinases in immunoreceptor signaling. *Curr Opin Immunol* **13**, 299-306.

Lerner E. C. and Smithgall T. E. (2002) SH3-dependent stimulation of Src-family kinase autophosphorylation without tail release from the SH2 domain in vivo. *Nat Struct Biol* **9**, 365-9.

Levac K., Karanu F. and Bhatia M. (2005) Identification of growth factor conditions that reduce ex vivo cord blood progenitor expansion but do not alter human repopulating cell function in vivo. *Haematologica* **90**, 166-72.

Levinson A. D., Courtneidge S. A. and Bishop J. M. (1981) Structural and functional domains of the Rous sarcoma virus transforming protein (pp60src). *Proc Natl Acad Sci U S A* **78**, 1624-8.

Levy J. B. and Brugge J. S. (1989) Biological and biochemical properties of the c-src+ gene product overexpressed in chicken embryo fibroblasts. *Mol Cell Biol* **9**, 3332-41.

Ley K. and Zarbock A. (2006) Hold on to your endothelium: postarrest steps of the leukocyte adhesion cascade. *Immunity* **25**, 185-7.

Li C., Heidt D. G., Dalerba P., Burant C. F., Zhang L., Adsay V., Wicha M., Clarke M. F. and Simeone D. M. (2007) Identification of pancreatic cancer stem cells. *Cancer Res* **67**, 1030-7.

Li F. Q., Person R. E., Takemaru K., Williams K., Meade-White K., Ozsahin A. H., Gungor T., Moon R. T. and Horwitz M. (2004) Lymphoid enhancer factor-1 links two hereditary leukemia syndromes through core-binding factor alpha regulation of ELA2. *J Biol Chem* **279**, 2873-84.

Liang X., Lu Y., Wilkes M., Neubert T. A. and Resh M. D. (2004) The N-terminal SH4 region of the Src family kinase Fyn is modified by methylation and heterogeneous fatty acylation: role in membrane targeting, cell adhesion, and spreading. *J Biol Chem* **279**, 8133-9.

Linder M. E. and Deschenes R. J. (2003) New insights into the mechanisms of protein palmitoylation. *Biochemistry* **42**, 4311-20.

Linnekin D., Howard O. M., Park L., Farrar W., Ferris D. and Longo D. L. (1994) Hck expression correlates with granulocyte-macrophage colony-stimulating factor-induced proliferation in HL-60 cells. *Blood* **84**, 94-103.

Lionberger J. M., Wilson M. B. and Smithgall T. E. (2000) Transformation of myeloid leukemia cells to cytokine independence by Bcr-Abl is suppressed by kinase-defective Hck. *J Biol Chem* **275**, 18581-5.

Lishko V. K., Yakubenko V. P. and Ugarova T. P. (2003) The interplay between integrins alphaMbeta2 and alpha5beta1 during cell migration to fibronectin. *Exp Cell Res* **283**, 116-26.

Liu Yin J. A., Wheatley K., Rees J. K. and Burnett A. K. (2001) Comparison of 'sequential' versus 'standard' chemotherapy as re-induction treatment, with or without cyclosporine, in refractory/relapsed acute myeloid leukaemia (AML): results of the UK Medical Research Council AML-R trial. *Br J Haematol* **113**, 713-26.

Livak K. J. and Schmittgen T. D. (2001) Analysis of relative gene expression data using real-time quantitative PCR and the 2(-Delta Delta C(T)) Method. *Methods* **25**, 402-8.

Lock P., Ralph S., Stanley E., Boulet I., Ramsay R. and Dunn A. R. (1991) Two isoforms of murine hck, generated by utilization of alternative translational initiation codons, exhibit different patterns of subcellular localization. *Mol Cell Biol* **11**, 4363-70.

Lowell C. A. and Berton G. (1998) Resistance to endotoxic shock and reduced neutrophil migration in mice deficient for the Src-family kinases Hck and Fgr. *Proc Natl Acad Sci U S A* **95**, 7580-4.

Lowell C. A., Fumagalli L. and Berton G. (1996a) Deficiency of Src family kinases p59/61hck and p58c-fgr results in defective adhesion-dependent neutrophil functions. *J Cell Biol* **133**, 895-910.

Lowell C. A., Niwa M., Soriano P. and Varmus H. E. (1996b) Deficiency of the Hck and Src tyrosine kinases results in extreme levels of extramedullary hematopoiesis. *Blood* **87**, 1780-92.

Lowell C. A., Soriano P. and Varmus H. E. (1994) Functional overlap in the src gene family: inactivation of hck and fgr impairs natural immunity. *Genes Dev* **8**, 387-98.

Manetti R., Parronchi P., Giudizi M. G., Piccinni M. P., Maggi E., Trinchieri G. and Romagnani S. (1993) Natural killer cell stimulatory factor (interleukin 12 [IL-12]) induces T helper type 1 (Th1)-specific immune responses and inhibits the development of IL-4-producing Th cells. *J Exp Med* **177**, 1199-204.

Marcucci G., Baldus C. D., Ruppert A. S., Radmacher M. D., Mrozek K., Whitman S. P., Kolitz J. E., Edwards C. G., Vardiman J. W., Powell B. L., Baer M. R., Moore J. O., Perrotti D., Caligiuri M. A., Carroll A. J., Larson R. A., de la Chapelle A. and Bloomfield C. D. (2005a) Overexpression of the ETS-related gene, ERG, predicts a worse outcome in acute myeloid leukemia with normal karyotype: a Cancer and Leukemia Group B study. *J Clin Oncol* **23**, 9234-42.

Marcucci G., Mrozek K. and Bloomfield C. D. (2005b) Molecular heterogeneity and prognostic biomarkers in adults with acute myeloid leukemia and normal cytogenetics. *Curr Opin Hematol* **12**, 68-75.

Martinez R., Mathey-Prevot B., Bernards A. and Baltimore D. (1987) Neuronal pp60c-src contains a six-amino acid insertion relative to its non-neuronal counterpart. *Science* **237**, 411-5.

Matsuguchi T., Zhao Y., Lilly M. B. and Kraft A. S. (1997) The cytoplasmic domain of granulocyte-macrophage colony-stimulating factor (GM-CSF) receptor alpha subunit is essential for both GM-CSF-mediated growth and differentiation. *J Biol Chem* **272**, 17450-9.

Matsui W., Huff C. A., Wang Q., Malehorn M. T., Barber J., Tanhehco Y., Smith B. D., Civin C. I. and Jones R. J. (2004) Characterization of clonogenic multiple myeloma cells. *Blood* **103**, 2332-6.

McCormack E., Bruserud O. and Gjertsen B. T. (2008) Review: genetic models of acute myeloid leukaemia. *Oncogene* **27**, 3765-79.

McCubrey J. A., Milella M., Tafuri A., Martelli A. M., Lunghi P., Bonati A., Cervello M., Lee J. T. and Steelman L. S. (2008) Targeting the Raf/MEK/ERK pathway with small-molecule inhibitors. *Curr Opin Investig Drugs* **9**, 614-30.

McKenzie J. L., Gan O. I., Doedens M. and Dick J. E. (2005) Human short-term repopulating stem cells are efficiently detected following intrafemoral transplantation into NOD/SCID recipients depleted of CD122+ cells. *Blood* **106**, 1259-61.

Melo J. V. (1996) The molecular biology of chronic myeloid leukaemia. *Leukemia* **10**, 751-6.

Mermel C. H., McLemore M. L., Liu F., Pereira S., Woloszynek J., Lowell C. A. and Link D. C. (2006) Src family kinases are important negative regulators of G-CSF-dependent granulopoiesis. *Blood* **108**, 2562-8.

Meyn M. A., 3rd, Schreiner S. J., Dumitrescu T. P., Nau G. J. and Smithgall T. E. (2005) SRC family kinase activity is required for murine embryonic stem cell growth and differentiation. *Mol Pharmacol* **68**, 1320-30.

Miller J. S., McCullar V., Punzel M., Lemischka I. R. and Moore K. A. (1999) Single adult human CD34(+)/Lin-/CD38(-) progenitors give rise to natural killer cells, B-lineage cells, dendritic cells, and myeloid cells. *Blood* **93**, 96-106.

Miranti C. K. and Brugge J. S. (2002) Sensing the environment: a historical perspective on integrin signal transduction. *Nat Cell Biol* **4**, E83-90.

Miranti C. K., Leng L., Maschberger P., Brugge J. S. and Shattil S. J. (1998) Identification of a novel integrin signaling pathway involving the kinase Syk and the guanine nucleotide exchange factor Vav1. *Curr Biol* **8**, 1289-99.

Mitelman F., Johansson B. and Mertens F. (2007) The impact of translocations and gene fusions on cancer causation. *Nat Rev Cancer* **7**, 233-45.

Mitelman F., Johansson B. and Mertens F. (2008) Mitelman Database of Chromosome Aberrations in Cancer http://cgap.nci.nih.gov/Chromosomes/Mitelman".

Mitina O., Warmuth M., Krause G., Hallek M. and Obermeier A. (2007) Src family tyrosine kinases phosphorylate Flt3 on juxtamembrane tyrosines and interfere with receptor maturation in a kinase-dependent manner. *Ann Hematol* **86**, 777-85.

Mitterbauer-Hohendanner G. and Mannhalter C. (2004) The biological and clinical significance of MLL abnormalities in haematological malignancies. *Eur J Clin Invest* **34 Suppl 2**, 12-24.

Miura O., Nakamura N., Quelle F. W., Witthuhn B. A., Ihle J. N. and Aoki N. (1994) Erythropoietin induces association of the JAK2 protein tyrosine kinase with the erythropoietin receptor in vivo. *Blood* **84**, 1501-7.

Miyakawa T., Yagi T., Kitazawa H., Yasuda M., Kawai N., Tsuboi K. and Niki H. (1997) Fyn-kinase as a determinant of ethanol sensitivity: relation to NMDA-receptor function. *Science* **278**, 698-701.

Miyakawa T., Yagi T., Tateishi K. and Niki H. (1996) Susceptibility to drug-induced seizures of Fyn tyrosine kinase-deficient mice. *Neuroreport* **7**, 2723-6.

Moarefi I., LaFevre-Bernt M., Sicheri F., Huse M., Lee C. H., Kuriyan J. and Miller W. T. (1997) Activation of the Src-family tyrosine kinase Hck by SH3 domain displacement. *Nature* **385**, 650-3.

Mocsai A., Ligeti E., Lowell C. A. and Berton G. (1999) Adhesion-dependent degranulation of neutrophils requires the Src family kinases Fgr and Hck. *J Immunol* **162**, 1120-6.

Modafferi E. F. and Black D. L. (1999) Combinatorial control of a neuron-specific exon. *Rna* **5**, 687-706.

Molina T. J., Bachmann M. F., Kundig T. M., Zinkernagel R. M. and Mak T. W. (1993) Peripheral T cells in mice lacking p56lck do not express significant antiviral effector functions. *J Immunol* **151**, 699-706.

Molina T. J., Kishihara K., Siderovski D. P., van Ewijk W., Narendran A., Timms E., Wakeham A., Paige C. J., Hartmann K. U., Veillette A. and et al. (1992) Profound block in thymocyte development in mice lacking p56lck. *Nature* **357**, 161-4.

Molina T. J., Perrot J. Y., Penninger J., Ramos A., Audouin J., Briand P., Mak T. W. and Diebold J. (1998) Differential requirement for p56lck in fetal and adult thymopoiesis. *J Immunol* **160**, 3828-34.

Mongiovi A. M., Romano P. R., Panni S., Mendoza M., Wong W. T., Musacchio A., Cesareni G. and Di Fiore P. P. (1999) A novel peptide-SH3 interaction. *Embo J* **18**, 5300-9.

Moore M. A., Dorn D. C., Schuringa J. J., Chung K. Y. and Morrone G. (2007) Constitutive activation of Flt3 and STAT5A enhances self-renewal and alters differentiation of hematopoietic stem cells. *Exp Hematol* **35**, 105-16.

Morgan M. A. and Reuter C. W. (2006) Molecularly targeted therapies in myelodysplastic syndromes and acute myeloid leukemias. *Ann Hematol* **85**, 139-63.

Morrison S. J. and Weissman I. L. (1994) The long-term repopulating subset of hematopoietic stem cells is deterministic and isolatable by phenotype. *Immunity* **1**, 661-73.

Mosmann T. R., Cherwinski H., Bond M. W., Giedlin M. A. and Coffman R. L. (2005) Two types of murine helper T cell clone. I. Definition according to profiles of lymphokine activities and secreted proteins. 1986. *J Immunol* **175**, 5-14.

Mrozek K. and Bloomfield C. D. (2008) Clinical significance of the most common chromosome translocations in adult acute myeloid leukemia. *J Natl Cancer Inst Monogr*, 52-7.

Mrozek K., Dohner H. and Bloomfield C. D. (2007a) Influence of new molecular prognostic markers in patients with karyotypically normal acute myeloid leukemia: recent advances. *Curr Opin Hematol* **14**, 106-14.

Mrozek K., Marcucci G., Paschka P., Whitman S. P. and Bloomfield C. D. (2007b) Clinical relevance of mutations and gene-expression changes in adult acute myeloid leukemia with normal cytogenetics: are we ready for a prognostically prioritized molecular classification? *Blood* **109**, 431-48.

Mui A. L., Wakao H., O'Farrell A. M., Harada N. and Miyajima A. (1995) Interleukin-3, granulocyte-macrophage colony stimulating factor and interleukin-5 transduce signals through two STAT5 homologs. *Embo J* **14**, 1166-75.

Musacchio A. (2002) How SH3 domains recognize proline. *Adv Protein Chem* **61**, 211-68.

Naharro G., Dunn C. Y. and Robbins K. C. (1983) Analysis of the primary translational product and integrated DNA of a new feline sarcoma virus, GR-FeSV. *Virology* **125**, 502-7.

Nair S. A., Kim M. H., Warren S. D., Choi S., Songyang Z., Cantley L. C. and Hangauer D. G. (1995) Identification of efficient pentapeptide substrates for the tyrosine kinase pp60c-src. *J Med Chem* **38**, 4276-83.

Narazaki M., Witthuhn B. A., Yoshida K., Silvennoinen O., Yasukawa K., Ihle J. N., Kishimoto T. and Taga T. (1994) Activation of JAK2 kinase mediated by the interleukin 6 signal transducer gp130. *Proc Natl Acad Sci U S A* **91**, 2285-9.

Nicola N. A., Vadas M. A. and Lopez A. F. (1986) Down-modulation of receptors for granulocyte colony-stimulating factor on human neutrophils by granulocyte-activating agents. *J Cell Physiol* **128**, 501-9.

Nishizumi H., Taniuchi I., Yamanashi Y., Kitamura D., Ilic D., Mori S., Watanabe T. and Yamamoto T. (1995) Impaired proliferation of peripheral B cells and indication of autoimmune disease in lyn-deficient mice. *Immunity* **3**, 549-60.

Numata A., Shimoda K., Kamezaki K., Haro T., Kakumitsu H., Shide K., Kato K., Miyamoto T., Yamashita Y., Oshima Y., Nakajima H., Iwama A., Aoki K., Takase K., Gondo H., Mano H. and Harada M. (2005) Signal transducers and activators of transcription 3 augments the transcriptional activity of CCAAT/enhancer-binding protein alpha in granulocyte colony-stimulating factor signaling pathway. *J Biol Chem* **280**, 12621-9.

O'Brien C. A., Pollett A., Gallinger S. and Dick J. E. (2007) A human colon cancer cell capable of initiating tumour growth in immunodeficient mice. *Nature* **445**, 106-10.

O'Brien M. C., Fukui Y. and Hanafusa H. (1990) Activation of the proto-oncogene p60c-src by point mutations in the SH2 domain. *Mol Cell Biol* **10**, 2855-62.

Oakes S. A., Candotti F., Johnston J. A., Chen Y. Q., Ryan J. J., Taylor N., Liu X., Hennighausen L., Notarangelo L. D., Paul W. E., Blaese R. M. and O'Shea J. J. (1996) Signaling via IL-2 and IL-4 in JAK3-deficient severe combined immunodeficiency lymphocytes: JAK3-dependent and independent pathways. *Immunity* **5**, 605-15.

Okada M., Howell B. W., Broome M. A. and Cooper J. A. (1993) Deletion of the SH3 domain of Src interferes with regulation by the phosphorylated carboxyl-terminal tyrosine. *J Biol Chem* **268**, 18070-5.

Okamoto M., Hayakawa F., Miyata Y., Watamoto K., Emi N., Abe A., Kiyoi H., Towatari M. and Naoe T. (2007) Lyn is an important component of the signal transduction pathway specific to FLT3/ITD and can be a therapeutic target in the treatment of AML with FLT3/ITD. *Leukemia* **21**, 403-10.

Okutani Y., Kitanaka A., Tanaka T., Kamano H., Ohnishi H., Kubota Y., Ishida T. and Takahara J. (2001) Src directly tyrosine-phosphorylates STAT5 on its activation site and is involved in erythropoietin-induced signaling pathway. *Oncogene* **20**, 6643-50.

Olthof S. G., Fatrai S., Drayer A. L., Tyl M. R., Vellenga E. and Schuringa J. J. (2008) Downregulation of signal transducer and activator of transcription 5 (STAT5) in CD34+ cells promotes megakaryocytic development, whereas activation of STAT5 drives erythropoiesis. *Stem Cells* **26**, 1732-42.

Orschell C. M., Borneo J., Munugalavadla V., Ma P., Sims E., Ramdas B., Yoder M. C. and Kapur R. (2008) Deficiency of Src family kinases compromises the repopulating ability of hematopoietic stem cells. *Exp Hematol* **36**, 655-66.

Osawa M., Nakamura K., Nishi N., Takahasi N., Tokuomoto Y., Inoue H. and Nakauchi H. (1996) In vivo self-renewal of c-Kit+ Sca-1+ Lin(low/-) hemopoietic stem cells. *J Immunol* **156**, 3207-14.

Paliwal P., Radha V. and Swarup G. (2007) Regulation of p73 by Hck through kinase-dependent and independent mechanisms. *BMC Mol Biol* **8**, 45.

Pandolfi P. P. (2001) Oncogenes and tumor suppressors in the molecular pathogenesis of acute promyelocytic leukemia. *Hum Mol Genet* **10**, 769-75.

Panopoulos A. D., Bartos D., Zhang L. and Watowich S. S. (2002) Control of myeloid-specific integrin alpha Mbeta 2 (CD11b/CD18) expression by cytokines is regulated by Stat3-dependent activation of PU.1. *J Biol Chem* **277**, 19001-7.

Park I., Chung J., Walsh C. T., Yun Y., Strominger J. L. and Shin J. (1995) Phosphotyrosine-independent binding of a 62-kDa protein to the src homology 2 (SH2) domain of p56lck and its regulation by phosphorylation of Ser-59 in the lck unique N-terminal region. *Proc Natl Acad Sci U S A* **92**, 12338-42.

Pawson T., Gish G. D. and Nash P. (2001) SH2 domains, interaction modules and cellular wiring. *Trends Cell Biol* **11**, 504-11.

Pellegrini S. and Dusanter-Fourt I. (1997) The structure, regulation and function of the Janus kinases (JAK) and the signal transducers and activators of transcription (STAT). *Eur J Biochem* **248**, 615-33.

Pellman D., Garber E. A., Cross F. R. and Hanafusa H. (1985) An N-terminal peptide from p60src can direct myristylation and plasma membrane localization when fused to heterologous proteins. *Nature* **314**, 374-7.

Pereira S. and Lowell C. (2003) The Lyn tyrosine kinase negatively regulates neutrophil integrin signaling. *J Immunol* **171**, 1319-27.

Petropoulos K., Arseni N., Schessl C., Stadler C. R., Rawat V. P., Deshpande A. J., Heilmeier B., Hiddemann W., Quintanilla-Martinez L., Bohlander S. K., Feuring-Buske M. and Buske C. (2008) A novel role for Lef-1, a central transcription mediator of Wnt signaling, in leukemogenesis. *J Exp Med* **205**, 515-22.

Picard C., Gilles A., Pontarotti P., Olive D. and Collette Y. (2002) Cutting edge: recruitment of the ancestral fyn gene during emergence of the adaptive immune system. *J Immunol* **168**, 2595-8.

Piccardoni P., Manarini S., Federico L., Bagoly Z., Pecce R., Martelli N., Piccoli A., Totani L., Cerletti C. and Evangelista V. (2004) SRC-dependent outside-in signalling is a key step in the process of autoregulation of beta2 integrins in polymorphonuclear cells. *Biochem J* **380**, 57-65.

Pinheiro R. F., Moreira Ede S., Silva M. R., Greggio B., Alberto F. L. and Chauffaille Mde L. (2007) FLT3 mutation and AML/ETO in a case of Myelodysplastic syndrome in transformation corroborates the two hit model of leukemogenesis. *Leuk Res* **31**, 1015-8.

Ploemacher R. E., van der Sluijs J. P., Voerman J. S. and Brons N. H. (1989) An in vitro limiting-dilution assay of long-term repopulating hematopoietic stem cells in the mouse. *Blood* **74**, 2755-63.

Poghosyan Z., Robbins S. M., Houslay M. D., Webster A., Murphy G. and Edwards D. R. (2002) Phosphorylation-dependent interactions between ADAM15 cytoplasmic domain and Src family protein-tyrosine kinases. *J Biol Chem* **277**, 4999-5007.

Poincloux R., Vincent C., Labrousse A., Castandet J., Rigo M., Cougoule C., Bordier C., Le Cabec V. and Maridonneau-Parini I. (2006) Re-arrangements of podosome structures are observed when Hck is activated in myeloid cells. *Eur J Cell Biol* **85**, 327-32.

Porter M., Schindler T., Kuriyan J. and Miller W. T. (2000) Reciprocal regulation of Hck activity by phosphorylation of Tyr(527) and Tyr(416). Effect of introducing a high affinity intramolecular SH2 ligand. *J Biol Chem* **275**, 2721-6.

Preudhomme C., Sagot C., Boissel N., Cayuela J. M., Tigaud I., de Botton S., Thomas X., Raffoux E., Lamandin C., Castaigne S., Fenaux P. and Dombret H. (2002) Favorable prognostic significance of CEBPA mutations in patients with de novo acute myeloid leukemia: a study from the Acute Leukemia French Association (ALFA). *Blood* **100**, 2717-23.

Preudhomme C., Warot-Loze D., Roumier C., Grardel-Duflos N., Garand R., Lai J. L., Dastugue N., Macintyre E., Denis C., Bauters F., Kerckaert J. P., Cosson A. and Fenaux P. (2000) High incidence of biallelic point mutations in the Runt domain of the AML1/PEBP2 alpha B gene in Mo acute myeloid leukemia and in myeloid malignancies with acquired trisomy 21. *Blood* **96**, 2862-9.

Prince M. E., Sivanandan R., Kaczorowski A., Wolf G. T., Kaplan M. J., Dalerba P., Weissman I. L., Clarke M. F. and Ailles L. E. (2007) Identification of a subpopulation of cells with cancer stem cell properties in head and neck squamous cell carcinoma. *Proc Natl Acad Sci U S A* **104**, 973-8.

Puigdecanet E., Espinet B., Lozano J. J., Sumoy L., Bellosillo B., Arenillas L., Alvarez-Larran A., Sole F., Serrano S., Besses C. and Florensa L. (2008) Gene expression profiling distinguishes JAK2V617F-negative from JAK2V617F-positive patients in essential thrombocythemia. *Leukemia* **22**, 1368-76.

Quelle F. W., Sato N., Witthuhn B. A., Inhorn R. C., Eder M., Miyajima A., Griffin J. D. and Ihle J. N. (1994) JAK2 associates with the beta c chain of the receptor for granulocyte-macrophage colony-stimulating factor, and its activation requires the membrane-proximal region. *Mol Cell Biol* **14**, 4335-41.

Quelle F. W., Shimoda K., Thierfelder W., Fischer C., Kim A., Ruben S. M., Cleveland J. L., Pierce J. H., Keegan A. D., Nelms K. and et al. (1995) Cloning of murine Stat6 and human Stat6, Stat proteins that are tyrosine phosphorylated in responses to IL-4 and IL-3 but are not required for mitogenesis. *Mol Cell Biol* **15**, 3336-43.

Quintrell N., Lebo R., Varmus H., Bishop J. M., Pettenati M. J., Le Beau M. M., Diaz M. O. and Rowley J. D. (1987) Identification of a human gene (HCK) that encodes a protein-tyrosine kinase and is expressed in hemopoietic cells. *Mol Cell Biol* **7**, 2267-75.

Rabbitts T. H., Appert A., Chung G., Collins E. C., Drynan L., Forster A., Lobato M. N., McCormack M. P., Pannell R., Spandidos A., Stocks M. R., Tanaka T. and Tse E. (2001) Mouse models of human chromosomal translocations and approaches to cancer therapy. *Blood Cells Mol Dis* **27**, 249-59.

Rane S. G. and Reddy E. P. (2002) JAK, STAT and Src kinases in hematopoiesis. *Oncogene* **21**, 3334-58.

Rangatia J. and Bonnet D. (2006) Transient or long-term silencing of BCR-ABL alone induces cell cycle and proliferation arrest, apoptosis and differentiation. *Leukemia* **20**, 68-76.

Ravetch J. V. and Lanier L. L. (2000) Immune inhibitory receptors. *Science* **290**, 84-9.

Reddy E. P., Korapati A., Chaturvedi P. and Rane S. (2000) IL-3 signaling and the role of Src kinases, JAK and STAT: a covert liaison unveiled. *Oncogene* **19**, 2532-47.

Reddy K. B., Smith D. M. and Plow E. F. (2008) Analysis of Fyn function in hemostasis and alphaIIbbeta3-integrin signaling. *J Cell Sci* **121**, 1641-8.

Reddy P., Teshima T., Hildebrandt G., Williams D. L., Liu C., Cooke K. R. and Ferrara J. L. (2003) Pretreatment of donors with interleukin-18 attenuates acute graft-

versus-host disease via STAT6 and preserves graft-versus-leukemia effects. *Blood* **101**, 2877-85.

Renneville A., Roumier C., Biggio V., Nibourel O., Boissel N., Fenaux P. and Preudhomme C. (2008) Cooperating gene mutations in acute myeloid leukemia: a review of the literature. *Leukemia* **22**, 915-31.

Resh M. D. (1996) Regulation of cellular signalling by fatty acid acylation and prenylation of signal transduction proteins. *Cell Signal* **8**, 403-12.

Reynolds P. J., Hurley T. R. and Sefton B. M. (1992) Functional analysis of the SH2 and SH3 domains of the lck tyrosine protein kinase. *Oncogene* **7**, 1949-55.

Ricci-Vitiani L., Lombardi D. G., Pilozzi E., Biffoni M., Todaro M., Peschle C. and De Maria R. (2007) Identification and expansion of human colon-cancer-initiating cells. *Nature* **445**, 111-5.

Rickles R. J., Botfield M. C., Weng Z., Taylor J. A., Green O. M., Brugge J. S. and Zoller M. J. (1994) Identification of Src, Fyn, Lyn, PI3K and Abl SH3 domain ligands using phage display libraries. *Embo J* **13**, 5598-604.

Rickles R. J., Botfield M. C., Zhou X. M., Henry P. A., Brugge J. S. and Zoller M. J. (1995) Phage display selection of ligand residues important for Src homology 3 domain binding specificity. *Proc Natl Acad Sci U S A* **92**, 10909-13.

Rimmele P., Kosmider O., Mayeux P., Moreau-Gachelin F. and Guillouf C. (2007) Spi-1/PU.1 participates in erythroleukemogenesis by inhibiting apoptosis in cooperation with Epo signaling and by blocking erythroid differentiation. *Blood* **109**, 3007-14.

Robbins S. M., Quintrell N. A. and Bishop J. M. (1995) Myristoylation and differential palmitoylation of the HCK protein-tyrosine kinases govern their attachment to membranes and association with caveolae. *Mol Cell Biol* **15**, 3507-15.

Robbins S. M., Quintrell N. A. and Bishop J. M. (2000) Mercuric chloride activates the Src-family protein tyrosine kinase, Hck in myelomonocytic cells. *Eur J Biochem* **267**, 7201-8.

Rodig S. J., Meraz M. A., White J. M., Lampe P. A., Riley J. K., Arthur C. D., King K. L., Sheehan K. C., Yin L., Pennica D., Johnson E. M., Jr. and Schreiber R. D. (1998) Disruption of the Jak1 gene demonstrates obligatory and nonredundant roles of the JAK in cytokine-induced biologic responses. *Cell* **93**, 373-83.

Rous P. A. (1911a) A sarcoma of the fowl transmissible by an agent separable from the tumor cells. *Journal of Experimental Medicine* **13**, 397-411.

Rous P. A. (1911b) Transmission of a malignant new growth by means of a cell-free lysate. *Journal of American Medicine Association*, 198.

Rudd C. E., Janssen O., Prasad K. V., Raab M., da Silva A., Telfer J. C. and Yamamoto M. (1993) src-related protein tyrosine kinases and their surface receptors. *Biochim Biophys Acta* **1155**, 239-66.

Russell S. M., Johnston J. A., Noguchi M., Kawamura M., Bacon C. M., Friedmann M., Berg M., McVicar D. W., Witthuhn B. A., Silvennoinen O. and et al. (1994) Interaction of IL-2R beta and gamma c chains with Jak1 and Jak3: implications for XSCID and XCID. *Science* **266**, 1042-5.

Russell S. M., Tayebi N., Nakajima H., Riedy M. C., Roberts J. L., Aman M. J., Migone T. S., Noguchi M., Markert M. L., Buckley R. H., O'Shea J. J. and Leonard W. J.

(1995) Mutation of Jak3 in a patient with SCID: essential role of Jak3 in lymphoid development. *Science* **270**, 797-800.

Sabe H., Okada M., Nakagawa H. and Hanafusa H. (1992) Activation of c-Src in cells bearing v-Crk and its suppression by Csk. *Mol Cell Biol* **12**, 4706-13.

Saksela K., Cheng G. and Baltimore D. (1995) Proline-rich (PxxP) motifs in HIV-1 Nef bind to SH3 domains of a subset of Src kinases and are required for the enhanced growth of Nef+ viruses but not for down-regulation of CD4. *Embo J* **14**, 484-91.

Samayawardhena L. A., Kapur R. and Craig A. W. (2007) Involvement of Fyn kinase in Kit and integrin-mediated Rac activation, cytoskeletal reorganization, and chemotaxis of mast cells. *Blood* **109**, 3679-86.

Satoh Y., Matsumura I., Tanaka H., Ezoe S., Fukushima K., Tokunaga M., Yasumi M., Shibayama H., Mizuki M., Era T., Okuda T. and Kanakura Y. (2008) AML1/runx1 works as a negative regulator of C-MPL in hematopoietic stem cells. *J Biol Chem.*

Schaeffer M., Schneiderbauer M., Weidler S., Tavares R., Warmuth M., de Vos G. and Hallek M. (2001) Signaling through a novel domain of gp130 mediates cell proliferation and activation of Hck and Erk kinases. *Mol Cell Biol* **21**, 8068-81.

Schepers H., van Gosliga D., Wierenga A. T., Eggen B. J., Schuringa J. J. and Vellenga E. (2007) STAT5 is required for long-term maintenance of normal and leukemic human stem/progenitor cells. *Blood* **110**, 2880-8.

Schindler T., Sicheri F., Pico A., Gazit A., Levitzki A. and Kuriyan J. (1999) Crystal structure of Hck in complex with a Src family-selective tyrosine kinase inhibitor. *Mol Cell* **3**, 639-48.

Schmitz R., Baumann G. and Gram H. (1996) Catalytic specificity of phosphotyrosine kinases Blk, Lyn, c-Src and Syk as assessed by phage display. *J Mol Biol* **260**, 664-77.

Schnittger S., Schoch C., Kern W., Mecucci C., Tschulik C., Martelli M. F., Haferlach T., Hiddemann W. and Falini B. (2005) Nucleophosmin gene mutations are predictors of favorable prognosis in acute myelogenous leukemia with a normal karyotype. *Blood* **106**, 3733-9.

Schreiner S. J., Schiavone A. P. and Smithgall T. E. (2002) Activation of STAT3 by the Src family kinase Hck requires a functional SH3 domain. *J Biol Chem* **277**, 45680-7.

Schuringa J. J., Chung K. Y., Morrone G. and Moore M. A. (2004) Constitutive activation of STAT5A promotes human hematopoietic stem cell self-renewal and erythroid differentiation. *J Exp Med* **200**, 623-35.

Schwartz M. A. and Ginsberg M. H. (2002) Networks and crosstalk: integrin signalling spreads. *Nat Cell Biol* **4**, E65-8.

Scott M. P., Zappacosta F., Kim E. Y., Annan R. S. and Miller W. T. (2002) Identification of novel SH3 domain ligands for the Src family kinase Hck. Wiskott-Aldrich syndrome protein (WASP), WASP-interacting protein (WIP), and ELMO1. *J Biol Chem* **277**, 28238-46.

Sefton B. M., Hunter T., Beemon K. and Eckhart W. (1980) Evidence that the phosphorylation of tyrosine is essential for cellular transformation by Rous sarcoma virus. *Cell* **20**, 807-16.

Seidel-Dugan C., Meyer B. E., Thomas S. M. and Brugge J. S. (1992) Effects of SH2 and SH3 deletions on the functional activities of wild-type and transforming variants of c-Src. *Mol Cell Biol* **12**, 1835-45.

Shalloway D., Zelenetz A. D. and Cooper G. M. (1981) Molecular cloning and characterization of the chicken gene homologous to the transforming gene of Rous sarcoma virus. *Cell* **24**, 531-41.

Shaw A. S., Amrein K. E., Hammond C., Stern D. F., Sefton B. M. and Rose J. K. (1989) The lck tyrosine protein kinase interacts with the cytoplasmic tail of the CD4 glycoprotein through its unique amino-terminal domain. *Cell* **59**, 627-36.

Shenoy-Scaria A. M., Dietzen D. J., Kwong J., Link D. C. and Lublin D. M. (1994) Cysteine3 of Src family protein tyrosine kinase determines palmitoylation and localization in caveolae. *J Cell Biol* **126**, 353-63.

Shivakrupa R., Radha V., Sudhakar C. and Swarup G. (2003) Physical and functional interaction between Hck tyrosine kinase and guanine nucleotide exchange factor C3G results in apoptosis, which is independent of C3G catalytic domain. *J Biol Chem* **278**, 52188-94.

Shuai K. and Liu B. (2003) Regulation of JAK-STAT signalling in the immune system. *Nat Rev Immunol* **3**, 900-11.

Shultz L. D., Schweitzer P. A., Christianson S. W., Gott B., Schweitzer I. B., Tennent B., McKenna S., Mobraaten L., Rajan T. V., Greiner D. L. and et al. (1995) Multiple defects in innate and adaptive immunologic function in NOD/LtSz-scid mice. *J Immunol* **154**, 180-91.

Sicheri F. and Kuriyan J. (1997) Structures of Src-family tyrosine kinases. *Curr Opin Struct Biol* **7**, 777-85.

Sicheri F., Moarefi I. and Kuriyan J. (1997) Crystal structure of the Src family tyrosine kinase Hck. *Nature* **385**, 602-9.

Silvennoinen O., Witthuhn B. A., Quelle F. W., Cleveland J. L., Yi T. and Ihle J. N. (1993) Structure of the murine Jak2 protein-tyrosine kinase and its role in interleukin 3 signal transduction. *Proc Natl Acad Sci U S A* **90**, 8429-33.

Silverman L., Sudol M. and Resh M. D. (1993) Members of the src family of nonreceptor tyrosine kinases share a common mechanism for membrane binding. *Cell Growth Differ* **4**, 475-82.

Singh S. K., Hawkins C., Clarke I. D., Squire J. A., Bayani J., Hide T., Henkelman R. M., Cusimano M. D. and Dirks P. B. (2004) Identification of human brain tumour initiating cells. *Nature* **432**, 396-401.

Skorski T. (2008) BCR/ABL, DNA damage and DNA repair: implications for new treatment concepts. *Leuk Lymphoma* **49**, 610-4.

Small D. (2006) FLT3 mutations: biology and treatment. *Hematology Am Soc Hematol Educ Program*, 178-84.

So C. W. and Cleary M. L. (2004) Dimerization: a versatile switch for oncogenesis. *Blood* **104**, 919-22.

So C. W., Karsunky H., Passegue E., Cozzio A., Weissman I. L. and Cleary M. L. (2003) MLL-GAS7 transforms multipotent hematopoietic progenitors and induces mixed lineage leukemias in mice. *Cancer Cell* **3**, 161-71.

Sommer U., Schmid C., Sobota R. M., Lehmann U., Stevenson N. J., Johnston J. A., Schaper F., Heinrich P. C. and Haan S. (2005) Mechanisms of SOCS3

phosphorylation upon interleukin-6 stimulation. Contributions of Src- and receptor-tyrosine kinases. *J Biol Chem* **280**, 31478-88.

Songyang Z. and Cantley L. C. (1995) Recognition and specificity in protein tyrosine kinase-mediated signalling. *Trends Biochem Sci* **20**, 470-5.

Songyang Z., Carraway K. L., 3rd, Eck M. J., Harrison S. C., Feldman R. A., Mohammadi M., Schlessinger J., Hubbard S. R., Smith D. P., Eng C. and et al. (1995a) Catalytic specificity of protein-tyrosine kinases is critical for selective signalling. *Nature* **373**, 536-9.

Songyang Z., Gish G., Mbamalu G., Pawson T. and Cantley L. C. (1995b) A single point mutation switches the specificity of group III Src homology (SH) 2 domains to that of group I SH2 domains. *J Biol Chem* **270**, 26029-32.

Songyang Z., Shoelson S. E., Chaudhuri M., Gish G., Pawson T., Haser W. G., King F., Roberts T., Ratnofsky S., Lechleider R. J. and et al. (1993) SH2 domains recognize specific phosphopeptide sequences. *Cell* **72**, 767-78.

Soriano P., Montgomery C., Geske R. and Bradley A. (1991) Targeted disruption of the c-src proto-oncogene leads to osteopetrosis in mice. *Cell* **64**, 693-702.

Spangrude G. J., Heimfeld S. and Weissman I. L. (1988) Purification and characterization of mouse hematopoietic stem cells. *Science* **241**, 58-62.

Spiekermann K., Biethahn S., Wilde S., Hiddemann W. and Alves F. (2001) Constitutive activation of STAT transcription factors in acute myelogenous leukemia. *Eur J Haematol* **67**, 63-71.

Spivak J. L. (2005) The anaemia of cancer: death by a thousand cuts. *Nat Rev Cancer* **5**, 543-55.

Stanglmaier M., Warmuth M., Kleinlein I., Reis S. and Hallek M. (2003) The interaction of the Bcr-Abl tyrosine kinase with the Src kinase Hck is mediated by multiple binding domains. *Leukemia* **17**, 283-9.

Steelman L. S., Abrams S. L., Whelan J., Bertrand F. E., Ludwig D. E., Basecke J., Libra M., Stivala F., Milella M., Tafuri A., Lunghi P., Bonati A., Martelli A. M. and McCubrey J. A. (2008) Contributions of the Raf/MEK/ERK, PI3K/PTEN/Akt/mTOR and Jak/STAT pathways to leukemia. *Leukemia* **22**, 686-707.

Steensma D. P., McClure R. F., Karp J. E., Tefferi A., Lasho T. L., Powell H. L., DeWald G. W. and Kaufmann S. H. (2006) JAK2 V617F is a rare finding in de novo acute myeloid leukemia, but STAT3 activation is common and remains unexplained. *Leukemia* **20**, 971-8.

Stehelin D., Varmus H. E., Bishop J. M. and Vogt P. K. (1976) DNA related to the transforming gene(s) of avian sarcoma viruses is present in normal avian DNA. *Nature* **260**, 170-3.

Stein P. L., Lee H. M., Rich S. and Soriano P. (1992) pp59fyn mutant mice display differential signaling in thymocytes and peripheral T cells. *Cell* **70**, 741-50.

Stein P. L., Vogel H. and Soriano P. (1994) Combined deficiencies of Src, Fyn, and Yes tyrosine kinases in mutant mice. *Genes Dev* **8**, 1999-2007.

Stirewalt D. L., Kopecky K. J., Meshinchi S., Appelbaum F. R., Slovak M. L., Willman C. L. and Radich J. P. (2001) FLT3, RAS, and TP53 mutations in elderly patients with acute myeloid leukemia. *Blood* **97**, 3589-95.

Stirewalt D. L., Kopecky K. J., Meshinchi S., Engel J. H., Pogosova-Agadjanyan E. L., Linsley J., Slovak M. L., Willman C. L. and Radich J. P. (2006) Size of FLT3 internal tandem duplication has prognostic significance in patients with acute myeloid leukemia. *Blood* **107**, 3724-6.

Stirewalt D. L. and Radich J. P. (2003) The role of FLT3 in haematopoietic malignancies. *Nat Rev Cancer* **3**, 650-65.

Stone R. M., O'Donnell M. R. and Sekeres M. A. (2004) Acute myeloid leukemia. *Hematology Am Soc Hematol Educ Program*, 98-117.

Sudol M., Greulich H., Newman L., Sarkar A., Sukegawa J. and Yamamoto T. (1993) A novel Yes-related kinase, Yrk, is expressed at elevated levels in neural and hematopoietic tissues. *Oncogene* **8**, 823-31.

Suen P. W., Ilic D., Caveggion E., Berton G., Damsky C. H. and Lowell C. A. (1999) Impaired integrin-mediated signal transduction, altered cytoskeletal structure and reduced motility in Hck/Fgr deficient macrophages. *J Cell Sci* **112 ( Pt 22)**, 4067-78.

Summy J. M. and Gallick G. E. (2003) Src family kinases in tumor progression and metastasis. *Cancer Metastasis Rev* **22**, 337-58.

Superti-Furga G., Fumagalli S., Koegl M., Courtneidge S. A. and Draetta G. (1993) Csk inhibition of c-Src activity requires both the SH2 and SH3 domains of Src. *Embo J* **12**, 2625-34.

Sutherland H. J., Eaves C. J., Eaves A. C., Dragowska W. and Lansdorp P. M. (1989) Characterization and partial purification of human marrow cells capable of initiating long-term hematopoiesis in vitro. *Blood* **74**, 1563-70.

Suzuki T., Kiyoi H., Ozeki K., Tomita A., Yamaji S., Suzuki R., Kodera Y., Miyawaki S., Asou N., Kuriyama K., Yagasaki F., Shimazaki C., Akiyama H., Nishimura M., Motoji T., Shinagawa K., Takeshita A., Ueda R., Kinoshita T., Emi N. and Naoe T. (2005) Clinical characteristics and prognostic implications of NPM11 mutations in acute myeloid leukemia. *Blood* **106**, 2854-61.

Szilvassy S. J., Weller K. P., Lin W., Sharma A. K., Ho A. S., Tsukamoto A., Hoffman R., Leiby K. R. and Gearing D. P. (1996) Leukemia inhibitory factor upregulates cytokine expression by a murine stromal cell line enabling the maintenance of highly enriched competitive repopulating stem cells. *Blood* **87**, 4618-28.

Taguchi T., Kiyokawa N., Sato N., Saito M. and Fujimoto J. (2000) Characteristic expression of Hck in human B-cell precursors. *Exp Hematol* **28**, 55-64.

Takagi J. and Springer T. A. (2002) Integrin activation and structural rearrangement. *Immunol Rev* **186**, 141-63.

Takahashi S., Harigae H., Kameoka J., Sasaki T. and Kaku M. (2005) AML1B transcriptional repressor function is impaired by the Flt3-internal tandem duplication. *Br J Haematol* **130**, 428-36.

Takaki S., Kanazawa H., Shiiba M. and Takatsu K. (1994) A critical cytoplasmic domain of the interleukin-5 (IL-5) receptor alpha chain and its function in IL-5-mediated growth signal transduction. *Mol Cell Biol* **14**, 7404-13.

Takata M., Sabe H., Hata A., Inazu T., Homma Y., Nukada T., Yamamura H. and Kurosaki T. (1994) Tyrosine kinases Lyn and Syk regulate B cell receptor-coupled Ca2+ mobilization through distinct pathways. *Embo J* **13**, 1341-9.

Takeda K., Tanaka T., Shi W., Matsumoto M., Minami M., Kashiwamura S., Nakanishi K., Yoshida N., Kishimoto T. and Akira S. (1996) Essential role of Stat6 in IL-4 signalling. *Nature* **380**, 627-30.

Takeya T., Feldman R. A. and Hanafusa H. (1982) DNA sequence of the viral and cellular src gene of chickens. 1. Complete nucleotide sequence of an EcoRI fragment of recovered avian sarcoma virus which codes for gp37 and pp60src. *J Virol* **44**, 1-11.

Takeya T., Hanafusa H., Junghans R. P., Ju G. and Skalka A. M. (1981) Comparison between the viral transforming gene (src) of recovered avian sarcoma virus and its cellular homolog. *Mol Cell Biol* **1**, 1024-37.

Tang R. H., Law S. K. and Tan S. M. (2006) Selective recruitment of src family kinase Hck by leukocyte integrin alphaMbeta2 but not alphaLbeta2 or alphaXbeta2. *FEBS Lett* **580**, 4435-42.

Taniguchi T. (1995) Cytokine signaling through nonreceptor protein tyrosine kinases. *Science* **268**, 251-5.

Tanner J. W., Chen W., Young R. L., Longmore G. D. and Shaw A. S. (1995) The conserved box 1 motif of cytokine receptors is required for association with JAK kinases. *J Biol Chem* **270**, 6523-30.

Taussig D. C., Miraki-Moud F., Anjos-Afonso F., Pearce D. J., Allen K., Ridler C., Lillington D., Oakervee H., Cavenagh J., Agrawal S. G., Lister T. A., Gribben J. G. and Bonnet D. (2008) Anti-CD38 antibody-mediated clearance of human repopulating cells masks the heterogeneity of leukemia-initiating cells. *Blood* **112**, 568-75.

Taylor S. S., Knighton D. R., Zheng J., Sowadski J. M., Gibbs C. S. and Zoller M. J. (1993) A template for the protein kinase family. *Trends Biochem Sci* **18**, 84-9.

Thierfelder W. E., van Deursen J. M., Yamamoto K., Tripp R. A., Sarawar S. R., Carson R. T., Sangster M. Y., Vignali D. A., Doherty P. C., Grosveld G. C. and Ihle J. N. (1996) Requirement for Stat4 in interleukin-12-mediated responses of natural killer and T cells. *Nature* **382**, 171-4.

Thomas S. M. and Brugge J. S. (1997) Cellular functions regulated by Src family kinases. *Annu Rev Cell Dev Biol* **13**, 513-609.

Timson Gauen L. K., Kong A. N., Samelson L. E. and Shaw A. S. (1992) p59fyn tyrosine kinase associates with multiple T-cell receptor subunits through its unique amino-terminal domain. *Mol Cell Biol* **12**, 5438-46.

Totani L., Piccoli A., Manarini S., Federico L., Pecce R., Martelli N., Cerletti C., Piccardoni P., Lowell C. A., Smyth S. S., Berton G. and Evangelista V. (2006) Src-family kinases mediate an outside-in signal necessary for beta2 integrins to achieve full activation and sustain firm adhesion of polymorphonuclear leucocytes tethered on E-selectin. *Biochem J* **396**, 89-98.

van der Bruggen T., Caldenhoven E., Kanters D., Coffer P., Raaijmakers J. A., Lammers J. W. and Koenderman L. (1995) Interleukin-5 signaling in human eosinophils involves JAK2 tyrosine kinase and Stat1 alpha. *Blood* **85**, 1442-8.

van Oers N. S., Lowin-Kropf B., Finlay D., Connolly K. and Weiss A. (1996) alpha beta T cell development is abolished in mice lacking both Lck and Fyn protein tyrosine kinases. *Immunity* **5**, 429-36.

Varmus H. E. and Lowell C. A. (1994) Cancer genes and hematopoiesis. *Blood* **83**, 5-9.

Veillette A., Bookman M. A., Horak E. M. and Bolen J. B. (1988) The CD4 and CD8 T cell surface antigens are associated with the internal membrane tyrosine-protein kinase p56lck. *Cell* **55**, 301-8.

Veillette A., Caron L., Fournel M. and Pawson T. (1992) Regulation of the enzymatic function of the lymphocyte-specific tyrosine protein kinase p56lck by the non-catalytic SH2 and SH3 domains. *Oncogene* **7**, 971-80.

Vicentini L., Mazzi P., Caveggion E., Continolo S., Fumagalli L., Lapinet-Vera J. A., Lowell C. A. and Berton G. (2002) Fgr deficiency results in defective eosinophil recruitment to the lung during allergic airway inflammation. *J Immunol* **168**, 6446-54.

Vichalkovski A., Baltensperger K., Thomann D. and Porzig H. (2005) Two different pathways link G-protein-coupled receptors with tyrosine kinases for the modulation of growth and survival in human hematopoietic progenitor cells. *Cell Signal* **17**, 447-59.

Visani G., Bernasconi P., Boni M., Castoldi G. L., Ciolli S., Clavio M., Cox M. C., Cuneo A., Del Poeta G., Dini D., Falzetti D., Fanin R., Gobbi M., Isidori A., Leoni F., Liso V., Malagola M., Martinelli G., Mecucci C., Piccaluga P. P., Petti M. C., Rondelli R., Russo D., Sessarego M., Specchia G., Testoni N., Torelli G., Mandelli F. and Tura S. (2001) The prognostic value of cytogenetics is reinforced by the kind of induction/consolidation therapy in influencing the outcome of acute myeloid leukemia--analysis of 848 patients. *Leukemia* **15**, 903-9.

Wakao H., Harada N., Kitamura T., Mui A. L. and Miyajima A. (1995) Interleukin 2 and erythropoietin activate STAT5/MGF via distinct pathways. *Embo J* **14**, 2527-35.

Ward A. C., Monkhouse J. L., Csar X. F., Touw I. P. and Bello P. A. (1998) The Src-like tyrosine kinase Hck is activated by granulocyte colony-stimulating factor (G-CSF) and docks to the activated G-CSF receptor. *Biochem Biophys Res Commun* **251**, 117-23.

Ward A. C., Touw I. and Yoshimura A. (2000) The Jak-Stat pathway in normal and perturbed hematopoiesis. *Blood* **95**, 19-29.

Warrell R. P., Jr., Frankel S. R., Miller W. H., Jr., Scheinberg D. A., Itri L. M., Hittelman W. N., Vyas R., Andreeff M., Tafuri A., Jakubowski A. and et al. (1991) Differentiation therapy of acute promyelocytic leukemia with tretinoin (all-trans-retinoic acid). *N Engl J Med* **324**, 1385-93.

Watowich S. S., Hilton D. J. and Lodish H. F. (1994) Activation and inhibition of erythropoietin receptor function: role of receptor dimerization. *Mol Cell Biol* **14**, 3535-49.

Webb D. J., Parsons J. T. and Horwitz A. F. (2002) Adhesion assembly, disassembly and turnover in migrating cells -- over and over and over again. *Nat Cell Biol* **4**, E97-100.

Wei S., Liu J. H., Epling-Burnette P. K., Gamero A. M., Ussery D., Pearson E. W., Elkabani M. E., Diaz J. I. and Djeu J. Y. (1996) Critical role of Lyn kinase in inhibition of neutrophil apoptosis by granulocyte-macrophage colony-stimulating factor. *J Immunol* **157**, 5155-62.

Whitman S. P., Archer K. J., Feng L., Baldus C., Becknell B., Carlson B. D., Carroll A. J., Mrozek K., Vardiman J. W., George S. L., Kolitz J. E., Larson R. A., Bloomfield C. D. and Caligiuri M. A. (2001) Absence of the wild-type allele

predicts poor prognosis in adult de novo acute myeloid leukemia with normal cytogenetics and the internal tandem duplication of FLT3: a cancer and leukemia group B study. *Cancer Res* **61**, 7233-9.

Whitman S. P., Ruppert A. S., Radmacher M. D., Mrozek K., Paschka P., Langer C., Baldus C. D., Wen J., Racke F., Powell B. L., Kolitz J. E., Larson R. A., Caligiuri M. A., Marcucci G. and Bloomfield C. D. (2008) FLT3 D835/I836 mutations are associated with poor disease-free survival and a distinct gene-expression signature among younger adults with de novo cytogenetically normal acute myeloid leukemia lacking FLT3 internal tandem duplications. *Blood* **111**, 1552-9.

Wierenga A. T., Schepers H., Moore M. A., Vellenga E. and Schuringa J. J. (2006) STAT5-induced self-renewal and impaired myelopoiesis of human hematopoietic stem/progenitor cells involves down-modulation of C/EBPalpha. *Blood* **107**, 4326-33.

Wierenga A. T., Vellenga E. and Schuringa J. J. (2008) Maximal STAT5-induced proliferation and self-renewal at intermediate STAT5 activity levels. *Mol Cell Biol.*

Willman C. L., Stewart C. C., Longacre T. L., Head D. R., Habbersett R., Ziegler S. F. and Perlmutter R. M. (1991) Expression of the c-fgr and hck protein-tyrosine kinases in acute myeloid leukemic blasts is associated with early commitment and differentiation events in the monocytic and granulocytic lineages. *Blood* **77**, 726-34.

Witthuhn B. A., Quelle F. W., Silvennoinen O., Yi T., Tang B., Miura O. and Ihle J. N. (1993) JAK2 associates with the erythropoietin receptor and is tyrosine phosphorylated and activated following stimulation with erythropoietin. *Cell* **74**, 227-36.

Wognum A. W., Eaves A. C. and Thomas T. E. (2003) Identification and isolation of hematopoietic stem cells. *Arch Med Res* **34**, 461-75.

Wormald S. and Hilton D. J. (2004) Inhibitors of cytokine signal transduction. *J Biol Chem* **279**, 821-4.

Wu C., Bauer J. S., Juliano R. L. and McDonald J. A. (1993) The alpha 5 beta 1 integrin fibronectin receptor, but not the alpha 5 cytoplasmic domain, functions in an early and essential step in fibronectin matrix assembly. *J Biol Chem* **268**, 21883-8.

Wu Y., Spencer S. D. and Lasky L. A. (1998) Tyrosine phosphorylation regulates the SH3-mediated binding of the Wiskott-Aldrich syndrome protein to PSTPIP, a cytoskeletal-associated protein. *J Biol Chem* **273**, 5765-70.

Xavier R. and Seed B. (1999) Membrane compartmentation and the response to antigen. *Curr Opin Immunol* **11**, 265-9.

Xia Z., Baer M. R., Block A. W., Baumann H. and Wetzler M. (1998) Expression of signal transducers and activators of transcription proteins in acute myeloid leukemia blasts. *Cancer Res* **58**, 3173-80.

Xiao W., Hong H., Kawakami Y., Lowell C. A. and Kawakami T. (2008) Regulation of myeloproliferation and M2 macrophage programming in mice by Lyn/Hck, SHIP, and Stat5. *J Clin Invest.*

Xu W., Harrison S. C. and Eck M. J. (1997) Three-dimensional structure of the tyrosine kinase c-Src. *Nature* **385**, 595-602.

Yamaguchi H. and Hendrickson W. A. (1996) Structural basis for activation of human lymphocyte kinase Lck upon tyrosine phosphorylation. *Nature* **384**, 484-9.

Yi T. L., Bolen J. B. and Ihle J. N. (1991) Hematopoietic cells express two forms of lyn kinase differing by 21 amino acids in the amino terminus. *Mol Cell Biol* **11**, 2391-8.

Yokoyama N. and Miller W. T. (2003) Biochemical properties of the Cdc42-associated tyrosine kinase ACK1. Substrate specificity, authphosphorylation, and interaction with Hck. *J Biol Chem* **278**, 47713-23.

Yoshimura A., Ichihara M., Kinjyo I., Moriyama M., Copeland N. G., Gilbert D. J., Jenkins N. A., Hara T. and Miyajima A. (1996) Mouse oncostatin M: an immediate early gene induced by multiple cytokines through the JAK-STAT5 pathway. *Embo J* **15**, 1055-63.

Young M. A., Gonfloni S., Superti-Furga G., Roux B. and Kuriyan J. (2001) Dynamic coupling between the SH2 and SH3 domains of c-Src and Hck underlies their inactivation by C-terminal tyrosine phosphorylation. *Cell* **105**, 115-26.

Yu C. C., Yen T. S., Lowell C. A. and DeFranco A. L. (2001) Lupus-like kidney disease in mice deficient in the Src family tyrosine kinases Lyn and Fyn. *Curr Biol* **11**, 34-8.

Yu H., Chen J. K., Feng S., Dalgarno D. C., Brauer A. W. and Schreiber S. L. (1994) Structural basis for the binding of proline-rich peptides to SH3 domains. *Cell* **76**, 933-45.

Zajchowski L. D. and Robbins S. M. (2002) Lipid rafts and little caves. Compartmentalized signalling in membrane microdomains. *Eur J Biochem* **269**, 737-52.

Zhao Y., Wagner F., Frank S. J. and Kraft A. S. (1995) The amino-terminal portion of the JAK2 protein kinase is necessary for binding and phosphorylation of the granulocyte-macrophage colony-stimulating factor receptor beta c chain. *J Biol Chem* **270**, 13814-8.

Ziegler-Heitbrock H. W., Thiel E., Futterer A., Herzog V., Wirtz A. and Riethmuller G. (1988) Establishment of a human cell line (Mono Mac 6) with characteristics of mature monocytes. *Int J Cancer* **41**, 456-61.